Brownell, L. E. (Lloyd Earl), 1915-

MANUAL FOR AEC-NSF INSTITUTE

RADIOISOTOPE TECHNOLOGY

by

Lloyd E. Brownell

June, 1961

enm

UMRC624

PREFACE

Chapters 1-5 of this manuscript were originally written for possible use in the text "Radiation Uses in Industry and Science", prepared for AEC by L. E. Brownell and published by the US Government Printing Office, June, 1961. Chapters 1 and 2 of this manuscript were originally combined for use in the above mentioned text but were not used because revisions and up-dating to include 1961 maximum permissible radiation doses could not be completed in sufficient time to meet the publication schedule. Chapters 3-5 of this manuscript were not included in the above mentioned text because the subject material in these chapters was considered to be too technical. These first five chapters mentioned above have been revised and printed at the University of Michigan for special use in teaching the AEC-NSF 1961 Summer Institute in Radioisotope Technology and as a supplement to the text "Radiation Uses in Industry and Science". The remaining chapters are based on the laboratory work conducted at the University of Michigan during the Summer Institute.

The author wishes to acknowledge the extensive assistance received by many co-workers in preparing the material in this manuscript. Dr. John Nehemias, former health physicist at the Fission Products Laboratory, and Dr. Ardath Emmons, former Supervisor of the Michigan Memorial Phoenix Project Laboratories, were major contributors to the original version of Chapters 1 and 2, respectively. Chapter 1 was reviewed and up-dated with assistance from Messrs. Lowell Yemin and John Jones, Health Physicists, Radiation Control Service, University of Michigan. Chapters 3 and 4 were revised by Messrs. N.E. Kothary and J.E. Sickles, respectively, of the Graduate School. Chapter 5 was prepared using lecture notes of Professor W. Kerr, Department of Nuclear Engineering and class notes of J.V. Nehemias.

Chapter 6, "Experimental Techniques in Nuclear Tracer Studies" was prepared by Professor Adon Gordus, of the Department of Chemistry, the University of Michigan. Chapter 7, "Experiments in Radioisotope Technology" was prepared by Professor Lloyd Brownell and Messrs. R. Borcherts and J.Sickles of the Department of Nuclear Engineering, the University of Michigan. Chapter 8 "Nuclear Radiation Detection and Measurement", was prepared by Professor Geza Gyorey and Mr. Philip Pluto also of the Department of Nuclear Engineering, the University of Michigan. The reader should recognize that these three chapters are in major part a reproduction of class notes and were not prepared using the same format used in the first five chapters.

Thanks is given to many other individuals who helped in various ways and to authors and publishers for permission to reproduce tables and figures used in this manuscript.

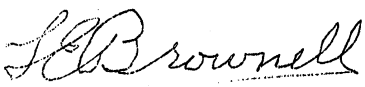

L. E. Brownell
Professor of Nuclear and
Chemical Engineering

June 16, 1961

TABLE OF CONTENTS

TABLE OF CONTENTS (CON'T)

TABLE OF CONTENTS (CON'T)

TABLE OF CONTENTS (CON'T)

TABLE OF CONTENTS (CON'T)

TABLE OF CONTENTS (CON'T)

LIST OF FIGURE CAPTIONS

LIST OF FIGURE CAPTIONS (CON'T)

LIST OF FIGURE CAPTIONS (CON'T)

LIST OF FUGURE CAPTIONS (CON'T)

LIST OF FIGURE CAPTIONS (CON'T)

LIST OF FIGURE CAPTIONS (CON'T)

LIST OF FIGURE CAPTIONS (CON'T)

Chapter 1

Safety in Work With Radioisotopes

The problem of safety when working ionizing radiation is unique in that in almost all cases the human senses provide no warning of dangerous levels of radiation. Safety in work with radioactive material requires an understanding of potential hazards associated with its use plus an understanding of the methods of evaluating the hazard.

This chapter briefly discusses qualitatively the problem of radiation hazards and the biological effects of radiation exposure. The quantitative aspects of the problem, units of radiation dosage, tolerances, permissible exposure levels, and safety rules are then considered.

1.1 Early history of radiation exposure

The animal body has a variety of defenses against most natural dangers, but it has no means of instantaneously detecting ionizing radiation which cannot be seen, felt, heard, smelled or tasted. The odor of ozone may be detected in air exposed to intense ionizing radiation, but the radiation level required to produce this detectable quantity of ozone is tremendously higher than minimum danger levels. Thus it is necessary to depend on instruments for the detection of radiation.

The early history of work with radiation is marred by many cases of serious overexposure to external radiation (1-6). Within thirty days of the discovery of X-rays by Roentgen in 1896, one of his co-workers reported hand dermatitis so acute that medical aid was required (4).

Another radiation injury occurred to Henri Becquerel (5). Several years after his discovery of radioactivity, he carried a glass tube containing a radium compound in his vest pocket for six days. An ugly red ulcer developed on his body, which healed in a few months but which left a permanent scar.

Pierre Curie voluntarily exposed his arm for several hours to the action of radium. A lesion resulted, resembling a burn, which required several months to heal (6).

In the early days, the hazards of radiation exposure were not considered important by public health authorities. Relatively few workers were ever exposed to ionizing radiation and these were considered to be highly competent, skilled technicians. In spite of early accidents resulting from faulty equipment and ignorance of the hazards involved, radiation control was left largely to the individual radiation worker (78).

During the first World War the use of paints containing traces of radium for dial illumination and related applications became widespread. No radiation protection measures were observed. Some of the dial painters habitually pointed their brushes on their tongues. A number of the women employed in this industry have developed bone sarcoma and other radiation injuries. The first clinical symptons exhibited by these women appeared from 10 to 30 years after exposure to radium handling had terminated (9,10).

1.2 Recent developments

The development of the X-ray machine with its world-wide installation in medical and dental centers, and the advent of nuclear energy with the widespread use of many types of radiation, have increased the hazards of radiation injuries by many orders of magnitude. Yet the serious overexposures that have occurred since December 1942 (when the first nuclear reactor was completed) have involved a much smaller percentage of those working with radiation. One lethal injury occurred when a scientist studying criticality of a fissionable mass was obliged to reach in and quickly separate reacting components in order to avoid a catastrophe (11).

An operating nuclear reactor presents a unique combination of various radiation hazards. The reacting core is an intense cource of neutron, gamma, and beta radiation. The beta-particles are absorbed in the reactor core but neutrons and gamma photons are very penetrating. Personnel working in the vicinity of the reactor must be protected against these latter two types of radiation. Because different shielding materials provide optimum protection for these two types of radiation, reactor shielding calculations and design must be twofold. A further hazard is presented by the radioactivity induced in any material, experimental, structural, or otherwise, which has been exposed to the neutron flux at or near the core. Any material removed from the reactor is itself an additional radiation hazard and must be treated as such. Also, as fission proceeds, fission products are formed which are intensely radioactive. Removal, manipulation, and reprocessing of spent reactor fuel elements must be performed under strict radiation control. Figure 1.1 shows an irradiated sample being removed from a reactor into a portable lead tunnel, in which it can be moved safely to the site of the experiment. The radiation level is being read and recorded.

1.3 Safety in the atomic energy industry

The remarkably small number of radiation injuries occurring in the atomic energy program to date demonstrates the efficiency of safety procedures in protecting personnel of this new industry from the unique hazards of radiation. During the operation of the Manhattan Project from 1942 to 1946 there were only two accidents that involved radiation injury to personnel. The same high standard of safety has been maintained since the transfer of this project to the AEC. Tables 1.1, 1.2, and 1.3 summarize the experience of the 32 major AEC operating contractors in routine operation. In addition, between August 1, 1945, and July 3, 1956, there were 16 radiation accidents in which 69 persons were overexposed of which two died and 19 suffered radiation burns (12).

Table 1.1 shows that the average exposure per worker was only a small percentage of the yearly maximum permissible dose. From 1947 to 1955 only 0.34% received over 5 rem (roentgen equivalent man) in routine operations. The permissible dose during this period was 15 rem/year (the present permissible dose is 5 rem/year). This attention to radiation safety has also resulted in a remarkably low rate of accidents of all types and the overall safety records of plants in the atomic energy program are considerably better than those of the average industrial plant. The atomic energy industry is one of the safest industries in which to work, as is indicated by Table 1.4 (13).

Table 1.1

Exposure of Personnel Working for AEC Contractors (12)(*)
External Radiation

	1947-1955		1955 only		1958 only	
Annual Total Amount	Number of Workers	Per Cent of Total	Number of Workers	Per Cent of Total	Number of Workers	Per Cent of Total
0-1rem	186,836	95.34	56,708	94.21	59,316	90
1-5	8.468	4.32	3,157	5.24	6,393	9.7
5-15	642	0.33	326	0.54	181	0.2
7-15	19	0.01	3	0.005	12	0.018

(*) Major Activities in the Atomic Energy Programs
Jan.-Dec. 1959. USAEC Jan. 1960

Table 1.2

Highest Accumulated Yearly Exposure in Rem to Individual Employees of AEC Contractors During Routine Operations (12) (Does not include accidents)

	1947	1948	1949	1950	1951	1952	1953	1954	1955
ıest Dose	23.5	20.3	13.6	9.0	7.1	15.7	12.9	27.8	17.9
ːage of Highest Doses (a)	7.4	7.8	4.0	3.9	2.8	5.0	4.9	6.5	5.8
ːage of 10 Highest Doses (b)	5.2	4.2	2.6	2.2	1.8	2.9	3.4	3.9	4.1

Indicates average of single highest exposures which occurred each year.

Indicates average of 10 highest annual exposures.

Table 1.3

Fraction of Permissible Body Burden of Aec Contractor Employees by Isotope. January 1947 - June 1956. Figures are for Maximum values obtained for each person in each year (12).

Percent of Permissible Body Burden	Uranium (a)	Fission Prod'ts + Other Isotopes	Plutonium	Polonium	Strontium	Fission Prod'ts	Tritium	Ruthenium	Cesium	Americium	Total
Less than 10	14,481	10,037	6,394	4,584	4,537	1,598	102	28	5	0	41,766
10-50	15,564	3	25	475	47	1	8	0	0	0	16,123
50-100	8,177	0	5	129	9	0	1	0	0	2	8,323
More than 100	4,844	0	5	59	1	0	1	0	0	0	4,910

(a) Based on chemical toxicity of uranium which is greater than its radiation hazard.

Table 1.4

Injuries per Million Man Hours (13)

	1948	1949
Lumbering Industry	49.04	47.72
Air Transport	15.05	12.97
Shipbuilding	10.14	8.86
Automobile	8.47	6.35
Steel	5.86	4.96
All Chemical Industries	7.51	5.72
All Industries	11.49	10.14
Oak Ridge National Laboratory	2.03	1.28

The excellent record of Oak Ridge National Laboratory illustrated in Table 1.4, and of other national laboratories, is the result of careful, competent safety work in all fields and particularly in the new field of "health physics." The Hanford Atomic plant in the state of Washington has had an excellent record with no deaths or permanent injuries as a result of work with radiative materials. Earlier workers in the field of radiation had a much poorer safety record.

1.4 Health Physics

The new field termed "health physics" has appeared as a direct result of the birth and rapid development of the atomic energy industry. Health Physics may be defined as the science and art of radiation protection. It is a science devoted to the study, evaluation, and control of ionizing radiation. The health physicist's responsibility is the protection of personnel from radiation injury which may result from ignorance of radiation hazards or from preoccupation with other duties which preclude adequate attention to these hazards. The health physicist must be thoroughly trained in working with radioactive materials and familiar with the nature of the hazards and the means of measurement and protection. Among his duties are:

1. Protecting personnel from radiation, and, in those instances where some exposure is unavoidable, maintaining exposure levels below the maximum permissible tolerance values set by the Atomic Energy Commission.

3. Requiring that appropriate protective clothing, such as gloves and respirators, be worn in potentially dangerous radiocontaminated areas.

Figure 1.2 shows two laboratory workers at the Hanford Atomic plant wearing protective clothing and filter type masks in a contaminated atmosphere while checking some contaminated waste.

4. Establishing and supervising adequate shielding procedures, decontamination, indicating radiation danger areas, radioactive monitoring of areas, laboratories, and personnel, and maintaining records of radiation and exposure levels.

Figure 1.3 shows the entrance to a high-level radiation area at Hanford marked for protection of personnel. In this area specially designed clothing for use in contaminated areas and radiation detection equipment are used.

5. Providing surveillance and coordination on over-all aspects of radiation protection and notifying laboratory supervisors immediately of all violations of good health practice.

Figure 1.4 shows two types of devices used to measure the cumulative external exposure that an individual may receive while working with sources of ionizing radiation. One of these "pencil" devices is the "pocket chamber" which is actually a pocket sized ionization chamber charged to approximately 150 volts prior to use. An electrometer is needed to read the risidual charge on the chamber after a period of use. The electrometer is calibrated so that the scale reads directly in milliroentgens. A similar "pencil" device, but perhaps more useful in certain instances, is the self reading pocket electroscope. This instrument, in addition to the pocket air condenser chamber contains its own electroscope calibrated in milliroentgens, enabling a person to keep constant check on his cumulated exposure during the course of an experiment. The pocket chamber devices are seldon used as the sole record of a person's exposure because of technical difficulties inherent in this type of device. If a chamber is inadvertantly dropped or bumped against an object, it may be discharged thereby indicating a high reading. Also, a chamber capable of measuring the maximum permissible dose of radiation (to man) will not measure extremely high doses.

The badge shown in Figure 1.4 serves both for identification ans as a record of radiation exposure. It contains two films sensitive to X-ray, beta-particle, and gamma radiation. One film is very sensitive to low levels of radiation and the other is sensitive to high levels. The badge also contains various filters which may be made of copper, lead, or cadmium. These filters permit identification of the degree of penetration of the radiation used in the exposure. Thus, beta-particle radiation may be distinguised from

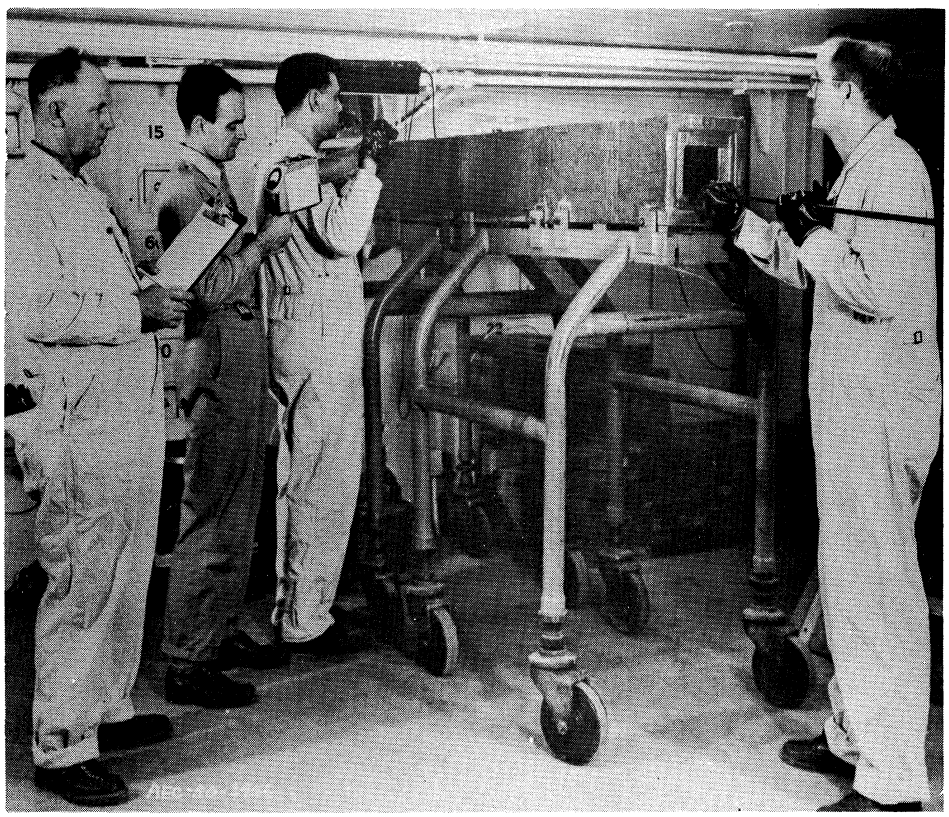

Figure 1.1 Withdrawing irradiated material from reactor core (Courtesy Oak Ridge National Laboratory (7)

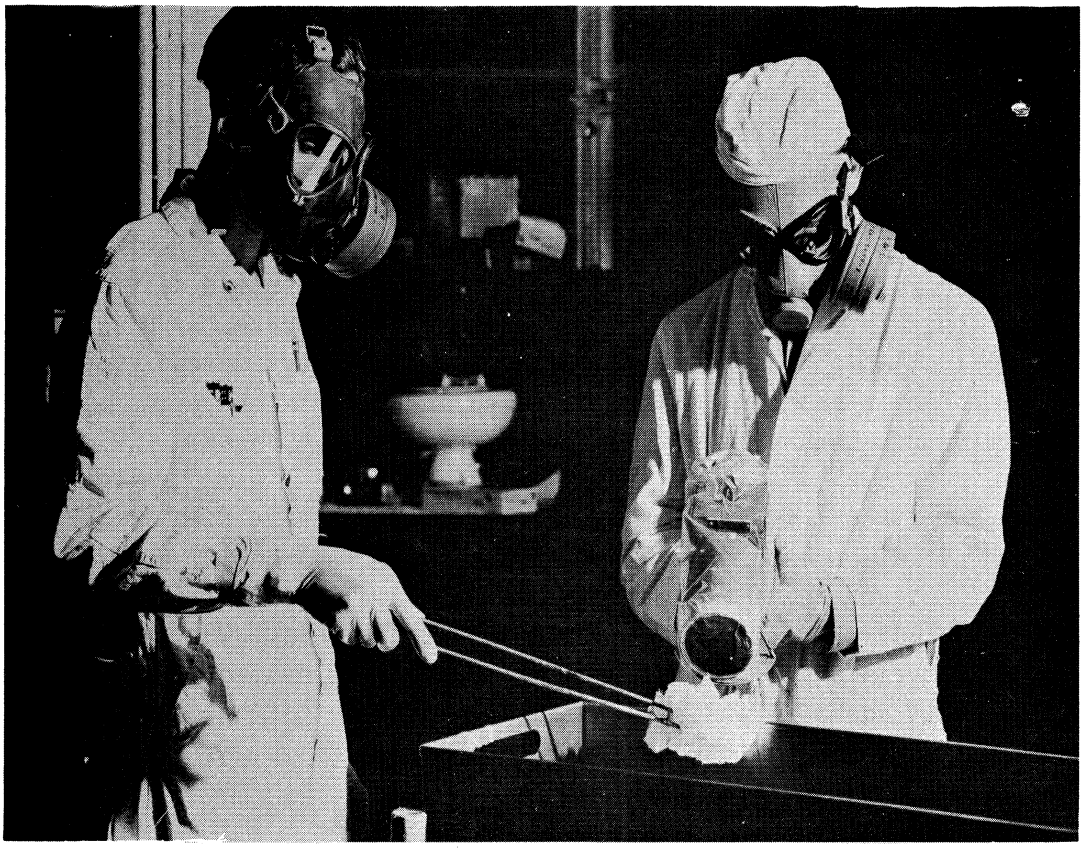

Figure 1.2 Filter type masks and protective clothing (Courtesy of General Electric Co.)

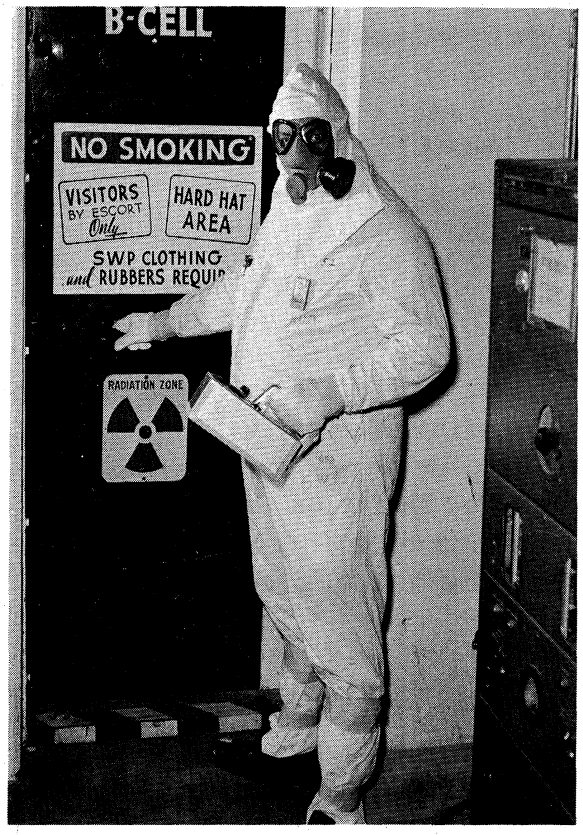

Figure 1.3 High level radiation area at the Hanford Atomic Products Operation marked for protection of personnel (Courtesy of General Electric Co.)

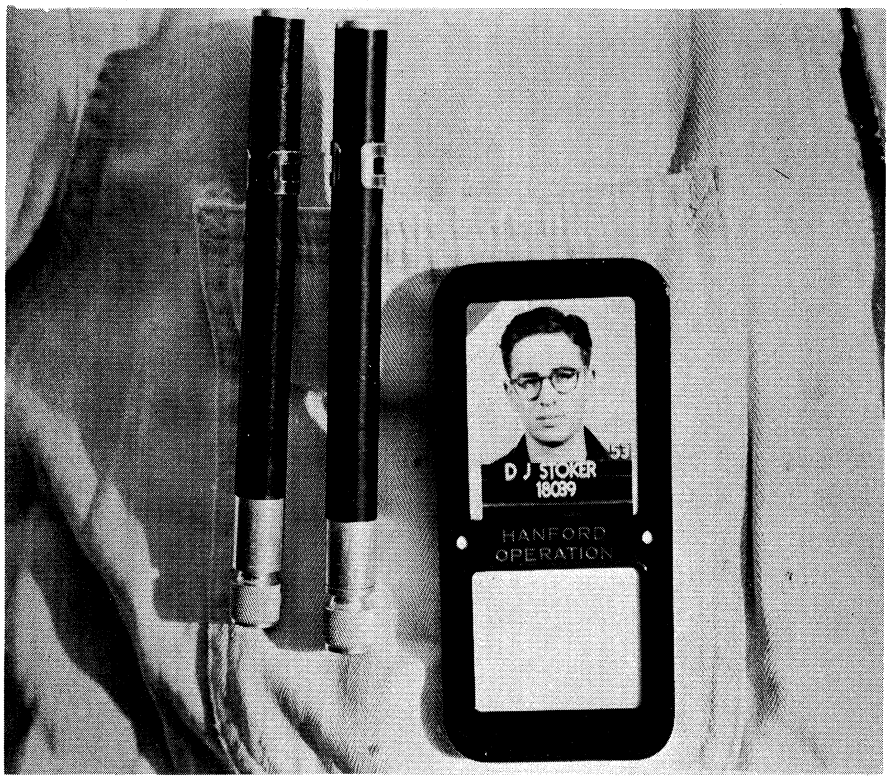

Figure 1.4 Pencils and badges worn to obtain records of radiation exposure (Courtesy of General Electric Co.)

electromagnetic (X or gamma) radiation, and the approximate energy of the latter also may be evaluated. The developed film is read in a densitometer, and the amount of fogging is related to the amount of external radiation to which a person has been exposed. Sometimes a special film that will record neutron tracks in the emulsion is used to indicate exposure to neutrons. This film is usually placed inside the same badge that contains the beta-gamma film. (See Chapter 3 for additional information on film badges.)

To obtain a better understanding of safety in working with radiation, the units of radiation as applied to health physics are discussed in the next section.

1.5 Radiological Units

Various units of radiation dosage are employed in health physics, the most important of which are defined as follows.

Roentgen The first unit of radiation was the roentgen, developed for X-ray measurements. It is a unit of energy absorption in air and defined for X- or gamma radiation only. The following equivalents should serve to clarify its significance:

$$\begin{aligned} 1 \text{ roentgen} &= 1 \text{ ESU per c.c. of air (at STP)} \\ &= 2.083 \times 10^{9} \text{ ion pairs per c.c. of air} \\ &= 6.95 \times 10^{4} \text{ Mev.per c.c. of air} \\ &= 5.40 \times 10^{7} \text{ Mev.per gram of air} \\ &= 86 \text{ ergs per gram of air} \end{aligned}$$

The roentgen is now the unit of exposure dose for X- and gamma radiation and is officially defined as "that quantity of X- or gamma radiation such that the associated corpuscular emission per 0.001293 gram of air produces in air one electrostatic unit quantity of electricity of either sign." (14)

Rep (roentgen equivalent physical). The rep was the first attempt to extend the concept of absorbed dose to tissue. Several definitions of the rep have been proposed, but the most widely accepted one is that it is a dose in tissue of 93 ergs of ionizing radiation absorbed per gram of soft tissue. The rep is no longer in active use, having been replaced by the more general unit, the rad.

Rad The rad is the present standard unit of absorbed energy. It is a measure of the dose of any ionizing radiation in terms of the energy absorbed per unit mass of the absorber. One rad is equal to 100 ergs of energy absorbed per gram of absorber. It should be noted that the rad may be used with any material such as tissue, metals, chemicals, etc. that have very different absorption characteristics.

Rem The rem is the dose of any ionizing radiation to body tissue in terms of its estimated biological effect equivalent to the dose in tissue of one rad of X-radiation having a linear energy transfer to water of 3.5 Kev per micron. The relation of the rem to other dose units depends upon the biological effect under consideration and upon the conditions of irradiation. For purposes of comparison, any of the following may be considered as equivalent to a dose of one rem:

(1) A tissue dose resulting from 1 r due to X- or gamma radiation;

(2) A tissue dose from 1 rad due to X-, gamma, or beta radiation;

(3) A tissue dose from 0.1 rad due to neutrons or high energy protons;

(4) A dose in tissue of 0.05 rad due to particles heavier than protons and with sufficient energy to reach the lens of the eye.

However, it should be born in mind that any exact relationship between the roentgen, the rad, and the rem is very difficult to express for several reasons.

(1) The biological damage is nearly always basically different for the several kinds of radiation. Therefore, the rem should never be used to express results of biological experiments.

(2) The rep and rad units are defined as absorbed energy in any gram of matter whereas the roentgen is defined in terms of ion pairs produced per unit volume of air by the secondary electrons.

(3) It is not known whether or not damage to tissue is proportional to the number of ion pairs produced or if the damage is proportional to the energy expended in the tissue.

Figure 1.5 illustrates schematically the greater local tissue damage caused by "softer" radiation such as alpha particles, beta particles and soft X-rays.

Dosages resulting from neutrons are more conveniently measured and expressed in terms of the neutron flux than in rads or rems. For rough estimates one rem of neutron dosage may be assumed to be equivalent to the exposure of the body to 14 million neutrons per square centimeter. If the approximate energy distribution of the neutrons is known, a more precise determination of dosage is possible with the use of Table 1.5. Table 1.5 gives both the number of neutrons per square centimeter equivalent to a dose of one rem and the average flux (neutrons) required to deliver 100 millirem in 40 hours as a function of neutron energy.

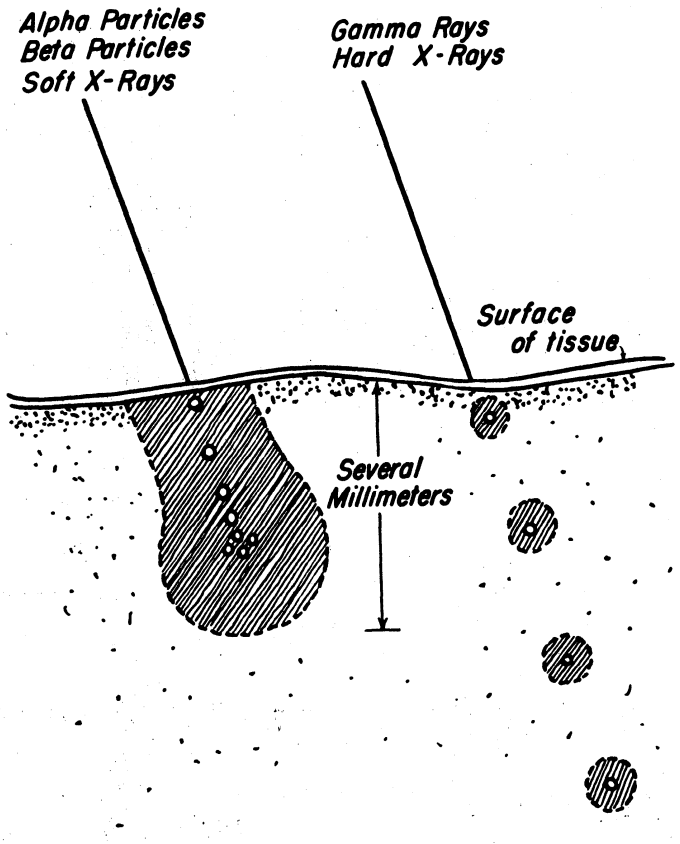

Figure 1.5 Effect of different types of radiation on tissue (15)

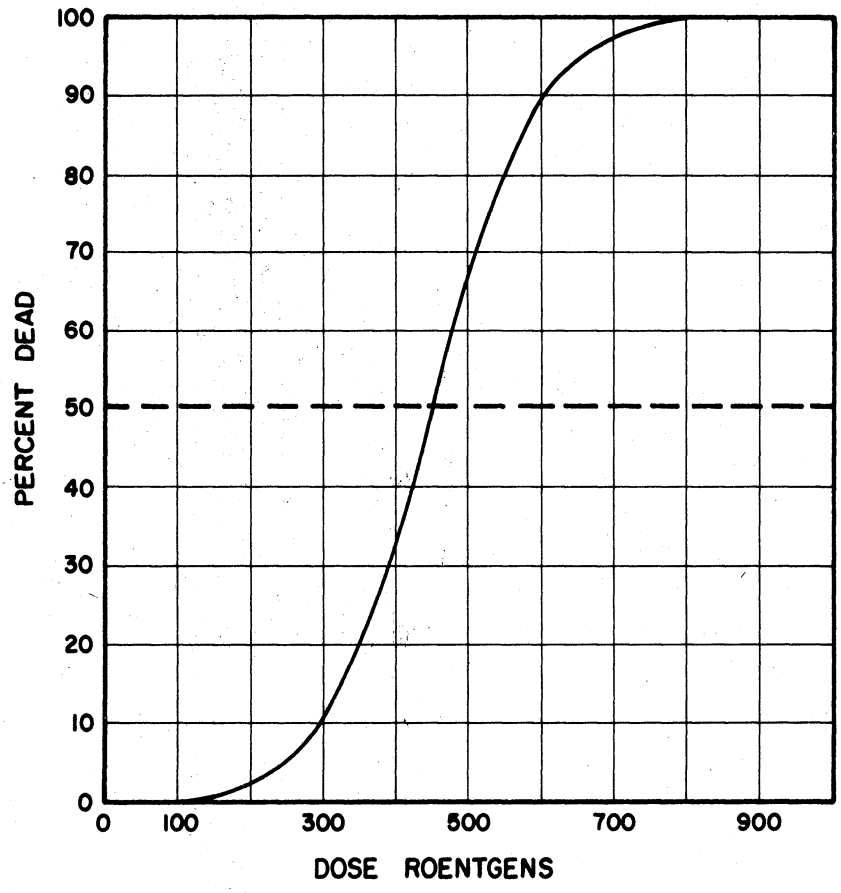

Figure 1.6 Typical "S"-Curve for radiation-induced death with L-D 50 of 450 roentgens (for man)

Table 1.5

Neutron Flux Dose Equivalents (16)

Neutron Energy Mev	Number of Neutrons per $cm.^2$ Equivalent to a Dose of 1 Rem (neutrons/$cm.^2$)X 10^6	Average Flux to Deliver 100 Millirems in 40 Hours (neutrons/$cm.^2$ per sec.)
Thermal	970	670
0.0001	720	500
0.005	820	570
0.02	400	280
0.1	120	80
0.5	43	30
1.0	26	18
2.5	29	20
5.0	26	18
7.5	24	17
10.0	24	17
10 to 30	14	10

The foregoing definitions serve to identify quantities of radiation effects, either as ionization in air, energy in tissue, or biological damage. It is further of interest to define a unit of quantity of radioactive material.

Curie One curie is a quantity of a radioactive nuclide in which the number of disintegrations per second is 3.700×10^{10}.

This unit is entirely independent of decay scheme or type of radiation emitted. The radiation level to be expected in the vicinity of a curie of radioactive material will depend only on the type and energy of radiation emitted in addition to external factors.

Through the years it has been convenient to speak of a gram of radium, or the amount of radioactivity associated with a gram of radium. This amount of radioactivity has been defined as a curie, in recognition of the fundamental contributions of Marie Curie in the field of radioactivity.

More and more precision has been applied to the experimental determination of the number of disintegrations per second from one gram of radium. Recent measurements vary from 3.4 to 3.7×10^{10}. To eliminate this uncertainty and specify the unit of radioactivity, the value given above is now in general use.

1.6 Biological effects of radiation

The absorption of ionizing radiation by living tissue results in damage to individual living cells. This damage is followed by malfunction or death of the irradiated cells and may subsequently cause the death of the organism. However, no pain or discomfort is experienced by the victim at the time of the exposure until doses much greater than a lethal dose are received. Death does not follow immediately after whole body exposure to lethal doses of radiation. Destruction of vital cells, build-up of degenerative toxins, and lowered resistance to trauma and infection occur. Death results from secondary effects (19, 20).

1.7 Radiation syndrome

The clinical manifestations produced by excessive exposure to ionizing radiation, often referred to as the "radiation syndrome", have four phases. The first phase, including the early symptons of nausea and vomiting, followed by general lassitude, is the "radiation sickness" of patients receiving intense radiation therapy.

The second period may last from a few days after severe exposures to several weeks following lesser exposures and is a period of general well-being. This is followed by the third and crucial period in which the body reaction reaches a maximum. The patient loses appetite and weight and experiences general prostration, palpitation of the heart, bleeding of the gums, loss of hair, and severe diarrhea. In mild cases this phase may last only days, but in severe cases it may last weeks or become progressively worse until the patient succumbs. If the patient survives the third stage, a period of convalescence, which is the fourth stage, follows.

In spite of the patient's apparently complete recovery from the radiation syndrome following massive sublethal radiation exposures, some permanent physiological impairment may be sustained. Extensive animal irradiation experiments, as well as follow-up data on the survivors in Hiroshima and Nagaski, indicate two aspects of this long-term hazard.

Morgan (1) listed five factors which determine radiation damage to man:

(1) Total accumulation of exposure.

(2) Area or volume of tissue irradiated.

(3) Radio-sensitivity of body tissue involved.

(4) Rate of irradiation.

(5) Specific ionization of the radiation.

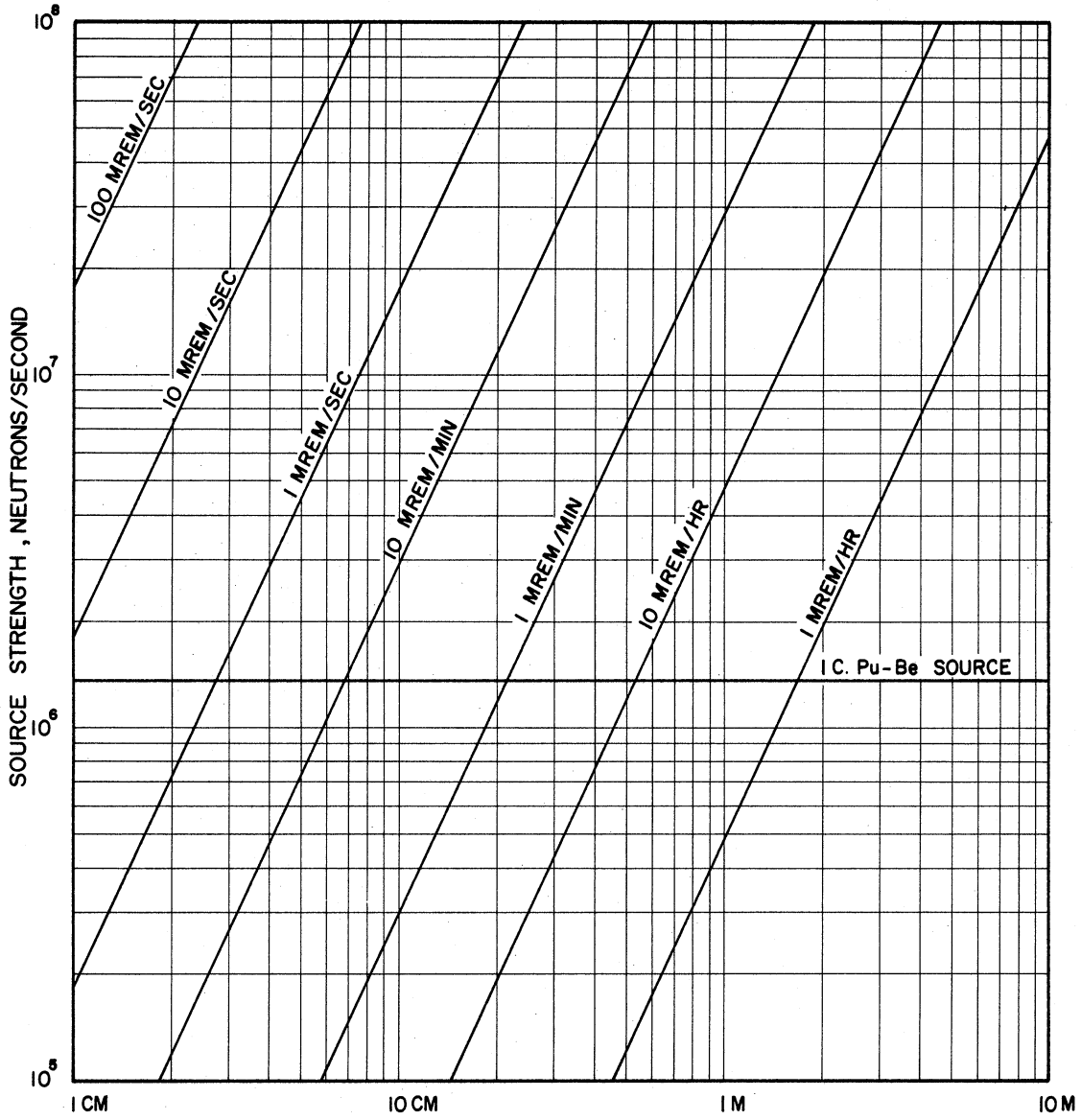

Fig. 1.6a Radiation dose rates due to an unshielded point isotopic source of fast (10 to 30 Mev) neutrons.

Prepared by
G.L. Gyorey

The total X- or gamma ray exposure required to kill 50 per cent of a group of humans has been estimated to be between 400 and 500 roentgens. This estimate is based on animal experiments and a few large human exposures (19). The biological effects of various doses of total body exposure and local exposure are summarized in Table 1.6 (20). For additional information on the biological effects of radiation exposure see references 21 to 89.

Table 1.6

Radiation Dosimetry and Biological Response (18)

Dosimetry			
Dose r	Dose Rate	Exposure*	Biological Response
0.3	Weekly	T	Probably none (permissible dose)
1	Daily (for years)	T	Leukopenia
1.5	Weekly	L	Probably none (permissible dose for hands and fingers)
25	Single dose	L	Chromosome break in tumor cells (tissue culture)
50-100	In accumulated small dose	L	Gene mutations to double spontaneous rate per generation
60	Single dose	L	Depression of phosphate activity
200	Single dose	T	Nausea
300	Single dose	L	Erythema dose for 100 kv (small field)
300-500	Single dose	T	LD_{50} for man
300-600	Single dose	L (ovaries)	Sterilization in female
400	Single dose	L	Reversible epilation
400-500	10-50 r/day	T	Clinical recovery
500	Single dose	L	Erythema dose for 200 kv (small field)
600-800	Single dose	L (testes)	Sterilization in male
600-900	300 r/day or small doses	L	Radiation cataract
1000	Single dose	L	Erythema dose for radium
1000-1500	200-300 r/day	L	Epiphyseal retardation
1000-2500	200-300 r/day	L	Response of markedly radiosensitive cancer
1500	200-300 r/day	L (ovaries)	Castration in female
1500-2000	200-300 r/day	L	Cessation of salivary glandular functions
1800-2000	200-300 r/day	L (stomach)	Archlorhydria
2000	Single dose	L	Erythema dose for 2 Mev
2000-3000	200-300 r/day	L (kidney)	Radiation nephritis

Table 1.6 cont.

2500-6000	200-300 r/day	L	Response of moderately radiosensitive cancer
2700-3000	Single dose	L	Moist desquamation, but healing of skin; 100-kv radiation (small field)
3600-5000	200-300 r/day	L	Limits of skin (single portal, 200 kv, 5 x 5-cm field)
4000-5000	200-300 r/day	L	Moist desquamation, but healing of skin (single portal 2000 to 3000-kv radiation, 10 x 10-cm field)
50,000	10-100 r/day	L	Carcinogenic

* T = total body; L = local.

1.8 Effect on cancer incidence

One of the most feared aspects of radiation is the possible increase in cancer incidence. Several cases of skin cancer developed following radiation injury to the skin of early X-ray technicians. Increased rates of cancer incidence in animals exposed to ionizing radiation have been reported by many laboratories. Lawrence and Hamilton have reviewed the field and report a summary of carcinogenic effects of local and whole body irradiation as well as of internally administered radioelements. (21)

Equally important in this regard, but less obvious, is the observed increased incidence of leukemia following radiation exposure in experimental animals. The death rate from leukemia among physicians has also been found to be twice that of the total adult male population (22), and the death rate among radiologists to be ten times that found among physicians in general. These two figures are commensurate with the portion of physicians working in radiology (23). Although these data are not direct proof that leukemia in humans is induced by radiation, the existence of an increased incidence, which is well above statistical deviations, among persons exposed to ionizing radiation is clearly indicated. References 24-29 give additional information on carcinogenesis and leukogenesis.

1.9 Effect on life span

Another aspect of long-term physiological hazard associated with radiation exposure has to do with a possible shortening of the life span. Because the plot of the incidence of death against radiation dose is an S-curve as shown in Figure 1.6 (for man), the 50 per cent point is well defined, but lower and higher mortality rates are not. For comparison of experiments, therefore, the 50 per cent fatality point is generally used.

When a particular strain of mice were exposed to 400 r, 50 per cent of the irradiated animals died within 30 days (30). Thus, 400 would be called the L.D.-50/30). With further fractionation, the number of deaths directly resulting from the same total exposure were reduced to zero. However, the life spans of these irradiated animals were found to be significantly less than those of nonirradiated animals. The percentage reduction in survival time was found to be proportional to the size of the daily exposure in the range from 5 to 25 r per day. Yockey (31) suggests that this induced aging might serve as a well-defined measure of radiation damage.

1.10 Radiosensitivity of different tissues

The variation in the radiosensitivity of body tissue may influence the extent of radiation damage. As early as 1913 the concept of tissue sensitivity depending on the rate of metabolism or rate of cell division was advanced (32). The available data on radiation damage support such a concept. Numbered among the more radiosensitive tissues of the body are the lymphocytes, gonads, bone marrow and the gastrointestinal tract, while nerve, muscle and heart tissues are less radiosensitive. A number of interesting experiments illustrative of this principle of radiosensitivity appear in the literature. Jacobson (33) gave the following data (Table 1.7) to illustrate the increased survival rate of rats when the spleen was shielded from radiation damage. References 34-43 give additional information on the effects of radiation on special tissues.

Table 1.7

The Sensitivity of Spleen in Albino Rats to Radiation Damage (33)

Dose	Survival of Nonshielded Controls	Survival of Spleen Shielded
600 r	50.0%	100%
1025	1.2	86.0
1100	0	55.0
1200	0	14.3
1300	0	3.0

1.11 Effect of rate of irradiation

Morgan (13) gives as a fourth factor of radiation damage the rate of dose delivery. Again one can illustrate this phenomenon with techniques employed by radiologists. The radiologist "fractionates" his X-ray therapy doses to prevent overwhelming the body's recuperative powers and also because certain tissues with high reproductive capacity are more affected by repeated doses. Kaplan (44) has illustrated the effect of dose fractionation on the 30-day L.D.-50 in mice. He found the L.D.-50 for a single dose to be 510 roentgens, for two equal daily fractions the L.D.-50 was 585 r, for four equal daily doses it was 720 r and for eight it increased to 850 roentgens. He then tried equal fractionated doses four days apart and found the L.D.-50 increased even more.

1.12 The influence of the nature of the radiation

A fifth factor influencing radiation damage to man is that of specific ionization of the radiation. It is known, for example, that low-energy X-radiation is more effective than high-energy X- or gamma radiation in producing local damage in tissue (see Figure 1.5).

Although the characteristic cellular destruction caused by ionizing radiation is basically the same for all known types of ionizing radiation, the severity and degree of localization of the injury vary according to the rate of absorption of the type of radiation in question. External alpha radiation, for instance, is totally absorbed in the horny surface layer of dead epithelial tissue. As a result, significant injury to living tissue from external alpha radiation is extremely unlikely.

Beta radiation, on the other hand, can penetrate several millimeters of tissue. Severe blistering and burns, which heal very slowly, result from local overexposure to external beta radiation. Gross total body damage from external beta radiation occurs only if the dose has been very large.

The tissue damage resulting from an X-ray or gamma-ray exposure arises from the production of secondary electrons. The ionization density along the path of the secondary electron is a function of the electron energy, which depends on the incident photon energy. The effects of gamma radiation, because of its highly penetrating nature, are produced throughout the body rather than locally. Gross metabolic effects, such as reduction in white blood-cell levels, result from severe overexposure.

The neutron, though not an ionizing particle, produces recoil protons which give rise to dense ionization tracks in tissue. There is evidence which seems to indicate that certain organs and tissues in the body are especially sensitive to neutron exposures (45-47).

Exposure to neutrons introduces a different type of effect in addition to the dense ionization tracks which occur at points of interaction between the neutron and atomic nuclei. Under certain conditions a neutron is absorbed by the nucleus, resulting in the production of an "excited" or radioactive nucleus. This phenomenon presents a two-fold hazard. First, additional radiation exposure results from this induced radioactivity. Second, the nucleus in question is transmuted to an element higher in the periodic table. If the atom is part of a molecule which plays an important role in cellular metabolism, it may be anticipated that cellular function will be impaired.

Table 1.8 summarizes the health-physics characteristics of various types of nuclear radiations. References 48-73 give additional information on whole body irradiation.

Table 1.8

Health-Physics Characteristics of Various Nuclear Radiations

	Alpha	Beta	Gamma	Neutrons
Tissue Penetration	Surface of Skin	A Few Millimeters	Many Centimeters	Many Centimeters
External Injury	None	Severe Burn	Gross Radiation Effects	Gross Radiation Effects
External Shielding Required	None	1/4" Lucite	Lead as Required	High Cross-section Material as Required
Internal Injury	Cell Destruction and Tumor Production	Cell Destruction and Tumor Production	Gross Radiation Effects	Gross Radiation Effects

1.13 Internal hazard

When a radioactive element enters the body it is distributed throughout the body, metabolized and utilized in the same manner as it would be if it were non-radioactive (74). When these processes lead to incorporation into the body structure by deposition in the bones or other vital organs, localized internal radiation damage may ensue (75). As in the case of external radiation injury, no immediate pain or discomfort is experienced by the victim, sometimes not for several years. This time lag between the exposure and the first clinically observable symptoms renders the tasks of diagnosing the initial cause of the injury and evaluating potential damage from an exposure exceedingly difficult.

Radioactive material, when injested, presents a greater hazard than when the body is exposed to external sources.

The reasons are as follows:

(1) Radioactive nuclides within the body are in intimate contact with the surrounding tissue. Thus, alpha and beta radiations can dissipate all of the energy in a small volume of tissue.

(2) It is extremely difficult to determine the amount of material in the body precisely.

(3) The body is irradiated continuously until the substance is eliminated.
(for example: 10 μc Ra^{226} injested would result in an average dose rate to the bone of 56 rem/wh or about 151,000 rem assuming a 50 year life after injestion)

(4) It is impossible at the present time to satisfactorily remove injested radioactive material by artificial means. Therefore, it is very important that persons working with radioactive material avoid any possibility of injestion of radioactive material. Significantly the amount of radium in the preceeding example would weigh 0.00001 grams. Not all radioactive materials however, are as hazardous to handle as radium since some nuclides have an extremely short physical half life and others have a short biological half life in addition to other factors. Even so, a person should always avoid needless injestion of any radioactive material because any amount of exposure to radiation may do some harm.

1.14 Possible effect of radiation on subsequent generations

In a sexually reproducing species, such as man, the transmission of all

hereditary characteristics from generation to generation is maintained through one cell from each parent. These two cells fuse and develop to form the new individual. Radiation damage to these sex cells, or to the cells responsible for their production, may produce abnormalities in the new individual which can be transmitted to the next generation. Such changes are called mutations. As a mutation is a permenent hereditary change, and may be caused by a single ionizing event, the total number produced in an individual will depend on the total dose received. Russell (83) has indicated, however, that there is some dependence on the dose rate, the mutation frequency being lower at the lower dose rates.

The mechanism of inheritance is one of the most radiosensitive biological functions. The "Digest of Findings and Recommendations" of the National Academy of Sciences states that any quantity of radiation, however small, may cause mutations (84). The most recent report by this group states that genetic effects per unit of dose rate may be less than previously estimated. However, there is still considerable question as to what extent mutations are increased by chronic exposure to radiation.

All individuals are exposed to background radiation, which causes an unavoidable background mutation rate. The number of mutations present in an individual is cumulative and builds up as the total radiation exposure increases from the time of conception of the individual until conception of his last child. Mutant genes can survive until the inheritance line in which they are carried dies out. If the mutation involves a serious loss of function, the line may cease after the first filial generation. If the mutation effect is slight, it may be carried through hundreds of generations before elimination.

Radiation-induced mutations are not new genetic changes, but constitute an increased rate of occurrence of normally occurring mutations. Favorable mutations have been absorbed into the population and unfavorable mutations eliminated through natural selection. Most new mutations are likely to be deleterious to the individual born with them.

About 50 per cent of all children are born to parents under 30 years of age and about 90 per cent to parents under 40 years of age. It has been estimated that a typical individual at the age of 30 would have received a cumulative radiation dose of 4.3 rem from background; 3 rem from X-radiation and fluoroscopy; and .02 and 0.5 rem from fall-out from atomic weapon tests.

1.15 Shortening of life span

There is increasing evidence that radiation in large dose may lead to shortening of the life span of an individual aside from the result of damage to a specific tissue such as development of skin cancer, leukemia, etc. It is also thought by many pathologists that there is no "threshold effect" for this shortening of the life span. Thus, presumably any dose of radiation, however small, may shorten expected life by some small fraction. It is believed however, that the levels of radiation as recommended by the NCRP and the ICRP are such that any shortening of normal expected life span will be insignificant. One may well expect greater effect from air polution or any number of other environmental factors.

1.16 Significance of radiation effects

The immediate reaction of the popular press in 1957 to the report "The Biological Effects of Atomic Radiation" by the National Academy of Sciences was that of apprehension (100).

The reaction of persons familiar with the situation, on the other hand, was favorable to the report and definitely not apprehensive (101). It is felt that the report notably documents and assembles already existing information about radiation effects, and that sufficient time remains before the nuclear power industry reaches its anticipated large size to evaluate, verify and prepare intelligently for the degree of radiation hazard to be expected. In 1958 Russell et al. (83) reviewed the effect of dose rate on mutation frequency. Additional information on radiation hazards are in References 84 to 99.

The nuclear industry has been so conservative since its inception that the average exposure of the personnel working in the present atomic energy industry has been much less than the internationally accepted maximum permissible levels in use since the discovery of fission. Thus, downward revisions of these levels should not cause undue concern.

Perhaps the most important recommendations of the report were that total exposure to medical X-rays be reduced by all means possible to the minimum consistant with medical necessity, and that records of all important medical exposures be maintained in addition to records already maintained for exposure to nuclear radiations.

1.17 Maximum permissible exposure levels

Maximum permissible radiation exposure levels are based on an intensive study of the biological data now available, although according to one theory, any dose of ionizing radiation may cause some somatic or genetic damage. The levels set are considered to entail a risk no greater than is

presently accepted in other industries.

In the early days of work with radiation, when the possibility of injury from radiation exposure was becoming evident, any safety measures that existed were self-imposed. One prominent worker in the field monitored his exposures by clipping a piece of photographic film to his lapel with a paper clip. If a certain radiological procedure resulted in the appearance of a photographic image of the paper clip, he would revise the procedure to reduce future exposures. His early "tolerance" dose was, therefore, any amount of radiation which would not produce a photographic image of a paper clip.

As industrial, medical, and laboratory uses of radiation expanded, a growing recognition of the radiation hazard occurred. During the 1920's and 1930's local standards of radiation tolerance were slowly established. These local standards provided valuable guidance to medical and health-physics people when they faced the tremendous radiation problems associated with the Manhattan Project.

As radiation intensity decreased with the square of the distance from a radiation source and with the amount of shielding material between the source and the observer, sufficient distance or shielding thickness can reduce the radiation from a particular source to any desired level. In the practical case, space and monetary limitations impose some lower limit on the minimum attainable radiation level. It is impossible, of course, to reduce radiation levels below the level due to cosmic rays and the presence of natural radioactivity in everyday materials.

It was important, therefore, to define a rate of radiation exposure which could be tolerated by an individual for any given period or for a lifetime with no observable ill effects. Such a "tolerable" dose has come to be called a "tolerance dose."

The National Committee on Radiation Protection adopted the limit for external radiation of 0.1 r for an 8-hour day in 1936. The permissible radiation exposures in Britain and Canada during the same interval were 0.2 and 0.05 r per day, respectively. These values have since been lowered several times.

Table 1.9 shows how the "tolerance dose" for individuals who work with radium or X rays, or in the atomic energy industry has been modified since 1902.

Table 1.9

Historical Development of "Tolerance Dose" (102)

Author	Date	Calculated r/day
Rollins	1902	10
Mutscheller	1925	0.2
Sievert	1925	0.2
Solomon	1926	2.0
Dutch Board	1927	0.04
Bayclay and Cox	1928	0.17
Kaye	1928	0.12
Failla (rays)	1932	(2) 0.1
Stenstrom	1932	0.16
ICRP (3)	1934	0.2
NCRP (4)	1936	0.1
NCRP	1949	(5) 0.075
ICRP	1950	(5) 0.075
ICRP	1958	0.025
NCRP	1959	0.025

(1) Photographic; (2) Established by ray erythema = 1,800 r; other calculations or erythema = 600 r; (3) International Commission on Radiological Protection, then known as International X-ray and Radium Protection Commission; (4) National Committee on Radiation Protection and Measurements, then known as Advisory Committee on X-ray and Radium Protection; (5) Based on a weekly irradiation of 0.3 r in air.

The fact that the "tolerance" level has been steadily lowered gives no assurance that a lower limit has finally been reached. Future revisions could be even lower.

The concept of "maximum permissible" dose rather than a so called "tolerance dose" was first applied in handbook 59 of the National Bureau of Standards.(117) This new terminology was used instead of the older term because "tolerance" indicates an assumption that if the dose is lower than a certain value no injury results. Since recent investigations show there is no "threshold" dose for gene mutations or somatic damage, the term "maximum permissible" dose has been accepted implying there is some finite risk involved yet so small that the risk will be readily acceptable.

The International Commission on Radiological Protection (ICRP) and the National Committee on Radiation Protection (NCRP) in 1958 published virtually identical recommendations regarding maximum permissible limits for external and internal radiation exposures. (103-106)

The following is a reproduction of part of the addendum to handbook 59 and is a summary of the recommendations as regards external exposure. (106)

1.18 Accumulated dose (radiation workers) (106)

A. External exposure to critical organs

Whole body, head and trunk, active blood-forming organs, or gonads: The maximum permissible dose (MPD), to the most critical organs, accumulated at any age, shall not exceed 5 rems multiplied by the number of years beyond age 18, and the dose in any 13 consecutive weeks shall not exceed 3 rems.*

Thus the accumulated MPD = (N-18)X 5 rems, where N is the age in years and is greater than 18.

Comment: This applies to radiation of sufficient penetrating power to affect a significant fraction of the critical tissue.

B. External exposure to other organs

Skin of whole body: MPD = 10 (N-18) rems, and the dose in any 13 consecutive weeks shall not exceed 6 rems.**

Comment: This rule applies to radiation of low penetrating power. See figure 2, H59.

Lens of the eyes: The dose to the lens of the eyes shall be limited by the dose to the head and trunk (A, above).

Hands and forearms, feet, and ankles: MPD = 75 rems/year, and the dose in any 13 consecutive weeks shall not exceed 25 rems.***

C. Internal exposures

The permissible levels from internal emitters will be consistent as far as possible with the age-proration principles above. Control of the internal dose will be achieved by limiting the body burden of radioisotopes. This will generally be accomplished by control of the average concentration of radioactive materials in the air, water, or food taken into the body.

---

* The quarterly limitation of 3 rems in 13 weeks is basically the same as in H59 except that it is no longer related to the old weekly dose limit. The yearly limitation is 12 rems instead of the 15 rems as given in the NCRP preliminary recommendations of January 8, 1957.

** This is similar to the 1954 (H59) recommendations in that the permissible skin dose is double the whole-body dose. H59 made no statement regarding a 13-week limitation.

*** This is basically the same as the 1954 (H59) recommendations except for the 13-week limitation.

Since it would be impractical to set different MPC values for air, water, and food for radiation workers as a function of age, the MPC values are selected in such a manner that they conform to the above-stated limits when applied to the most restrictive case, viz., they are set to be applicable to radiation workers of age 18. Thus, the values are conservative and are applicable to radiation workers of any age (assuming there is no occupational exposure to radiation permitted at age less than 18).

The maximum permissible average concentrations of radionuclides in air and water are determined from biological data whenever such data are available, or are calculated on the basis of an averaged annual dose of 15 rems for most individual organs of the body,* 30 rems when the critical organ is the thyroid or skin, and 5 rems when the gonads or the whole body is the critical organ. For bone seekers the maximum permissible limit is based on the distribution of the deposit, the RBE, and a comparison of the energy release in the bone with the energy release delivered by a manimum permissible body burden of 0.1 μg Ra^{226} plus daughters.

1.19 Emergency dose (radiation workers) (106)

An accidental or emergency dose of 25 rems to the whole body or a major portion thereof, occurring only once in the lifetime of the person, need not be included in the determination of the radiation exposure status of that person (see p. 69, H59).**

1.20 Medical dose (radiation workers) (106)

Radiation exposures resulting from necessary medical and dental procedures need not be included in the determination of the radiation exposure status of the person concerned.**

1.21 Dose to persons outside of controlled areas (106)

The radiation or radioactive material outside a controlled area, attributable to normal operations within the controlled area, shall be such that it is improbable that any individual will receive a dose of more than 0.5 rem in any 1 year from external radiation.

The maximum permissible average body burden of radionuclides in persons outside of the controlled area and attributable to the operations within the controlled area shall not exceed one-tenth of that for radiation workers.***

* This is basically the same as the 1953 (H59) recommendations (117)
** This is the same as the 1954 (H59) recommendations (117)
*** This is basically the same as the recommendations of January 8, 1957 (105)

This will normally entail control of the average concentrations in air or water at the point of intake, or rate of intake to the body in foodstuffs, to levels not exceeding one-tenth of the maximum permissible concentrations allowed in air, water, and foodstuffs for occupational exposure. The body burden and concentrations of radionuclides may be averaged over periods up to 1 year.

The maximum permissible dose and the maximum permissible concentrations of radionuclides as recommended above are primarily for the purpose of keeping the average dose to the whole population as low as reasonably possible, and not because of specific injury to the individual.

Comment: Occupancy-factor guides will be needed by several of the subcommittees. It will be important that these do not differ markedly between different handbooks. The Executive Committee will endeavor to establish a set of uniform occupancy-factor guides.

1.22 Operational and administrative guides

The maximum dose of 12 rems in any 1 year as governed by the 13 week limitation, should be allowed only when adequate past and current exposure records exist. The allowance of a dose of 12 rems in any 1 year should not be encouraged as a part of routine operations; it should be regarded as an allowable but unusual condition. The records of previous exposures must show that the addition of such a dose will not cause the individual to exceed his age-prorated allowance.

The full 3-rem dose should not be allowed to be taken within a short time interval under routine or ordinary circumstances (however, see paragraph 2 on Emergency Dose above.) Desirably, it should be distributed in time as uniformly as possible and in any case the dose should not be greater than 3 rems in any 13 consecutive weeks. When the individual is not personally monitored and/or personal exposure records are not maintained, the exposure of 12 rems in a year should not be allowed; the yearly allowance under these circumstances should be 5 rems, provided area surveys indicate an adequate margin of safety.

When any person accepts employment in radiation work, it shall be assumed that he has received his age-prorated dose up to that time unless (1) satisfactory records from prior radiation employment show the contrary, or (2) it can be satisfactorily demonstrated that he has not been employed in radiation work. This is not to imply that such an individual should be expected to routinely accept exposures at radiation levels approaching the yearly maximum of 12 rems up to the time he reaches his age-prorated limit. Application of these principles will serve to minimize abuse.

The new MPD standards stated above are not intended to be applied retroactively to individuals exposed under previously accepted standards.

It is implicit in the establishment of the basic protection rules that at present it is neither possible nor prudent to administer a suitably safe radiation protection plan on the basis of yearly monitoring only. It is also implicit that at the low permissible dose levels now being recommended, there is fairly wide latitude in the rate of delivery of this dose to an individual so long as the dose remains within the age-prorated limits specified above. In spite of a lack of clear evidence of harm due to irradiation at dose rates in excess of some specified level, it is prudent to set some reasonable upper limit to the rate at which an occupational exposure may be delivered. Therefore, it has been agreed that the dose to a radiation worker should not exceed 3 rems in any 13 consecutive weeks.

The latitude that may appropriately be applied in the operational and administrative control of occupational exposure will be dictated by two major factors (a) the type of risk involved and the likelihood of the occurrence of over-exposures and (b) the monitoring methods, equipment, and the dose recording procedures available to the radiation users. Where the hazards are minimal and hot likely to change from day to day or where there are auxiliary controls to insure that the 13-week limitation will not be exceeded, the integration may be carried out over periods up to 3 months. Where the hazards are significant and where the exposure experience indicates unpredictability as to exposure levels, the doses should be determined more frequently, such as weekly, daily, hourly, or oftener, as may be required to limit the exposure to permissible values.

For the vast majority of installations (medical and industrial), operation is more or less routine and reasonably predictable and it may be expected that their monitoring procedures will be minimal. For such installations the protection design should be adequate to insure that over-exposures will not occur--otherwise frequent sampling tests should be specified. Where film badges are used for monitoring, it is preferable that they be worn for 4 weeks or longer, since otherwise the inaccuracy of the readings may unduly prejudice the radiation history of the individual. Where operations are not routine or are subject to unpredictable variations that may be hazardous, self-reading pocket dosimeters, pocket chambers, or other such devices should also be worn and should be read daily or more often as circumstances dictate.

Except for planning, convenience of calculation, design, or administrative guides, the NCRP will discontinue the use of a weekly MPDor MPC.*

The Committee has deliberately omitted the discussion of future exposure forfeiture for exposures exceeding the MPD on the grounds that any such statements might lend encouragement to the unnecessary use of forfeiture provisions.

---

*This represents a minor change from the NCRP recommendations of January 8, 1957, but no change in the basic MPD.

The maximum permissible body burdens and maximum permissible concentrations of radionuclides as specified by the Rules and Regulations from Title 10, Part 20 of the Federal Register are given in Table 1.10 (107).

Table 1.10

Maximum Permissible Concentrations for Radioisotopes

in Air and Water Above Natural Background (107)

Element (atomic number)	Isotope [1]		Table I		Table II	
			Column 1 Air (μc/ml)	Column 2 Water (μc/ml)	Column 1 Air (μc/ml)	Column 2 Water (μc/ml)
Actinium (89)	Ac 227	S	2×10^{-12}	6×10^{-8}	8×10^{-14}	2×10^{-6}
		I	3×10^{-11}	9×10^{-8}	9×10^{-13}	3×10^{-6}
	Ac 228	S	8×10^{-8}	3×10^{-5}	3×10^{-9}	9×10^{-8}
		I	2×10^{-8}	3×10^{-5}	6×10^{-10}	9×10^{-8}
Americium (95)	Am 241	S	6×10^{-13}	1×10^{-4}	2×10^{-13}	4×10^{-6}
		I	1×10^{-10}	8×10^{-4}	4×10^{-12}	2×10^{-5}
	Am 243	S	6×10^{-13}	1×10^{-4}	2×10^{-13}	4×10^{-6}
		I	1×10^{-10}	8×10^{-4}	4×10^{-12}	3×10^{-5}
Antimony (51)	Sb 122	S	2×10^{-7}	8×10^{-4}	6×10^{-9}	3×10^{-5}
		I	1×10^{-7}	8×10^{-4}	5×10^{-9}	3×10^{-5}
	Sb 124	S	2×10^{-7}	7×10^{-4}	5×10^{-9}	2×10^{-5}
		I	2×10^{-8}	7×10^{-4}	7×10^{-10}	2×10^{-5}
	Sb 125	S	5×10^{-7}	3×10^{-5}	2×10^{-8}	1×10^{-4}
		I	3×10^{-8}	3×10^{-5}	9×10^{-10}	1×10^{-4}
Argon (18)	A 37	Sub [2]	6×10^{-3}	----------	1×10^{-4}	----------
	A 41	Sub	2×10^{-6}	----------	4×10^{-8}	----------
Arsenic (33)	As 73	S	2×10^{-6}	1×10^{-3}	7×10^{-8}	5×10^{-4}
		I	4×10^{-7}	1×10^{-3}	1×10^{-8}	5×10^{-4}
	As 74	S	3×10^{-7}	2×10^{-3}	1×10^{-8}	5×10^{-5}
		I	1×10^{-7}	2×10^{-3}	4×10^{-9}	5×10^{-5}
	As 76	S	1×10^{-7}	6×10^{-4}	4×10^{-9}	2×10^{-5}
		I	1×10^{-7}	6×10^{-4}	3×10^{-9}	2×10^{-5}
	As 77	S	5×10^{-7}	2×10^{-3}	2×10^{-8}	8×10^{-5}
		I	4×10^{-7}	2×10^{-3}	1×10^{-8}	8×10^{-5}
Astatine (85)	At 211	S	7×10^{-9}	5×10^{-5}	2×10^{-10}	2×10^{-6}
		I	3×10^{-8}	2×10^{-3}	1×10^{-9}	7×10^{-5}
Barium (56)	Ba 131	S	1×10^{-6}	5×10^{-3}	4×10^{-8}	2×10^{-4}
		I	4×10^{-7}	5×10^{-3}	1×10^{-8}	2×10^{-4}
	Ba 140	S	1×10^{-7}	8×10^{-4}	4×10^{-9}	3×10^{-5}
		I	4×10^{-8}	7×10^{-4}	1×10^{-9}	2×10^{-5}
Berkelium (97)	Bk 249	S	9×10^{-10}	2×10^{-3}	3×10^{-11}	6×10^{-4}
		I	1×10^{-7}	2×10^{-3}	4×10^{-9}	6×10^{-4}
Beryllium (4)	Be 7	S	6×10^{-6}	5×10^{-3}	2×10^{-7}	2×10^{-3}
		I	1×10^{-6}	5×10^{-3}	4×10^{-8}	2×10^{-3}
Bismuth (83)	Bi 206	S	2×10^{-7}	1×10^{-3}	6×10^{-9}	4×10^{-4}
		I	1×10^{-7}	1×10^{-3}	5×10^{-9}	4×10^{-4}
	Bi 207	S	2×10^{-7}	2×10^{-3}	6×10^{-9}	6×10^{-5}
		I	1×10^{-7}	2×10^{-3}	5×10^{-10}	6×10^{-5}
	Bi 210	S	6×10^{-9}	1×10^{-3}	2×10^{-10}	4×10^{-5}
		I	6×10^{-9}	1×10^{-3}	2×10^{-10}	4×10^{-5}
	Bi 212	S	1×10^{-7}	1×10^{-3}	3×10^{-9}	4×10^{-4}
		I	2×10^{-7}	1×10^{-3}	7×10^{-9}	4×10^{-4}
Bromine (35)	Br 82	S	1×10^{-6}	8×10^{-3}	4×10^{-8}	3×10^{-4}
		I	2×10^{-7}	1×10^{-3}	6×10^{-9}	4×10^{-5}
Cadmium (48)	Cd 109	S	5×10^{-8}	5×10^{-3}	2×10^{-9}	2×10^{-4}
		I	7×10^{-8}	5×10^{-3}	3×10^{-9}	2×10^{-4}
	Cd 115m	S	4×10^{-8}	7×10^{-4}	1×10^{-9}	3×10^{-5}
		I	4×10^{-8}	7×10^{-4}	1×10^{-9}	3×10^{-5}
	Cd 115	S	2×10^{-7}	1×10^{-3}	8×10^{-9}	3×10^{-5}
		I	2×10^{-7}	1×10^{-3}	6×10^{-9}	4×10^{-5}
Calcium (20)	Ca 45	S	3×10^{-8}	3×10^{-4}	1×10^{-9}	9×10^{-6}
		I	1×10^{-7}	5×10^{-3}	4×10^{-9}	2×10^{-4}
	Ca 47	S	2×10^{-7}	1×10^{-3}	6×10^{-9}	5×10^{-5}
		I	2×10^{-7}	1×10^{-3}	6×10^{-9}	3×10^{-5}
Californium (98)	Cf 249	S	2×10^{-13}	1×10^{-4}	5×10^{-14}	4×10^{-6}
		I	1×10^{-10}	7×10^{-4}	3×10^{-12}	2×10^{-5}
	Cf 250	S	5×10^{-12}	4×10^{-4}	2×10^{-13}	1×10^{-5}
		I	1×10^{-10}	7×10^{-4}	3×10^{-12}	3×10^{-5}
	Cf 252	S	2×10^{-11}	7×10^{-4}	7×10^{-13}	2×10^{-5}
		I	1×10^{-10}	7×10^{-4}	4×10^{-12}	2×10^{-5}
Carbon (6)	C 14	S	4×10^{-6}	2×10^{-3}	1×10^{-7}	8×10^{-4}
	(CO_2)	Sub	5×10^{-5}	----------	1×10^{-6}	----------
Cerium (58)	Ce 141	S	4×10^{-7}	3×10^{-3}	2×10^{-8}	9×10^{-5}
		I	2×10^{-7}	3×10^{-3}	5×10^{-9}	9×10^{-5}
	Ce 143	S	3×10^{-7}	1×10^{-3}	9×10^{-9}	4×10^{-5}
		I	2×10^{-7}	1×10^{-3}	7×10^{-9}	4×10^{-5}
	Ce 144	S	1×10^{-8}	3×10^{-4}	3×10^{-10}	1×10^{-5}
		I	6×10^{-9}	3×10^{-4}	2×10^{-10}	1×10^{-5}

See footnotes at end of table.

Table 1.10 Contd.

Element (atomic number)	Isotope [1]	Table I		Table II	
		Column 1 Air (μc/ml)	Column 2 Water (μc/ml)	Column 1 Air (μc/ml)	Column 2 Water (μc/ml)
Cesium (55)	Cs 131	1×10^{-5}	7×10^{-2}	4×10^{-7}	2×10^{-3}
	Cs 134m	3×10^{-6}	3×10^{-2}	1×10^{-7}	9×10^{-4}
	Cs 134	4×10^{-5}	2×10^{-1}	1×10^{-6}	6×10^{-3}
	Cs 135	6×10^{-6}	3×10^{-2}	2×10^{-7}	1×10^{-3}
	Cs 136	4×10^{-6}	3×10^{-4}	1×10^{-9}	9×10^{-6}
	Cs 137	1×10^{-5}	1×10^{-3}	4×10^{-10}	4×10^{-5}
Chlorine (17)	Cl 36	5×10^{-7}	3×10^{-3}	2×10^{-8}	1×10^{-4}
	Cl 38	9×10^{-5}	7×10^{-3}	3×10^{-9}	2×10^{-4}
Chromium (24)	Cr 51	4×10^{-7}	2×10^{-3}	1×10^{-8}	9×10^{-6}
Cobalt (27)	Co 57	2×10^{-7}	2×10^{-3}	6×10^{-9}	6×10^{-5}
	Co 58m	6×10^{-8}	4×10^{-4}	2×10^{-9}	2×10^{-5}
	Co 58	1×10^{-8}	1×10^{-3}	5×10^{-10}	4×10^{-6}
	Co 60	4×10^{-7}	2×10^{-3}	1×10^{-8}	8×10^{-5}
Copper (29)	Cu 64	2×10^{-8}	2×10^{-3}	8×10^{-10}	6×10^{-5}
Curium (96)	Cm 242	3×10^{-6}	1×10^{-2}	9×10^{-8}	4×10^{-4}
	Cm 243	2×10^{-6}	1×10^{-2}	7×10^{-8}	4×10^{-4}
	Cm 244α	1×10^{-5}	5×10^{-2}	4×10^{-7}	2×10^{-3}
	Cm 245	2×10^{-6}	5×10^{-2}	8×10^{-8}	2×10^{-3}
	Cm 246	3×10^{-6}	2×10^{-2}	1×10^{-7}	5×10^{-4}
Dysprosium (66)	Dy 165	2×10^{-7}	1×10^{-2}	6×10^{-9}	4×10^{-4}
	Dy 166	2×10^{-5}	8×10^{-2}	6×10^{-7}	3×10^{-3}
Erbium (68)	Er 169	9×10^{-6}	6×10^{-2}	3×10^{-7}	2×10^{-3}
	Er 171	8×10^{-7}	4×10^{-3}	3×10^{-8}	1×10^{-4}
Europium (63)	Eu 152 (T/2=9.2 hrs)	5×10^{-8}	3×10^{-3}	2×10^{-9}	9×10^{-5}
	Eu 152 (T/2=13 yrs)	3×10^{-7}	1×10^{-3}	1×10^{-8}	5×10^{-5}
	Eu 154	9×10^{-9}	1×10^{-3}	3×10^{-10}	3×10^{-5}
	Eu 155	2×10^{-6}	1×10^{-2}	7×10^{-8}	3×10^{-4}
Fluorine (9)	F 18	1×10^{-6}	6×10^{-3}	4×10^{-8}	2×10^{-4}
Gadolinium (64)	Gd 153	1×10^{-10}	7×10^{-4}	4×10^{-12}	2×10^{-5}
	Gd 159	2×10^{-10}	7×10^{-4}	6×10^{-12}	3×10^{-5}
Gallium (31)	Ga 72	6×10^{-12}	1×10^{-4}	2×10^{-13}	5×10^{-6}
Germanium (32)	Ge 71	1×10^{-10}	7×10^{-4}	3×10^{-12}	2×10^{-5}
Gold (79)	Au 196	9×10^{-12}	2×10^{-4}	3×10^{-13}	7×10^{-6}
	Au 198	1×10^{-10}	8×10^{-4}	3×10^{-12}	3×10^{-5}
		5×10^{-12}	1×10^{-4}	2×10^{-13}	4×10^{-6}
		1×10^{-10}	8×10^{-4}	4×10^{-12}	3×10^{-5}
		5×10^{-12}	1×10^{-4}	2×10^{-13}	4×10^{-6}
		1×10^{-10}	8×10^{-4}	4×10^{-12}	3×10^{-5}
		3×10^{-6}	1×10^{-2}	9×10^{-8}	4×10^{-4}
		2×10^{-6}	1×10^{-2}	7×10^{-8}	4×10^{-4}
		2×10^{-7}	1×10^{-3}	8×10^{-9}	4×10^{-5}
		2×10^{-7}	1×10^{-3}	7×10^{-9}	4×10^{-5}
		6×10^{-7}	3×10^{-3}	2×10^{-8}	9×10^{-5}
		4×10^{-7}	3×10^{-3}	1×10^{-8}	9×10^{-5}
		7×10^{-7}	3×10^{-3}	2×10^{-8}	1×10^{-4}
		6×10^{-7}	3×10^{-3}	2×10^{-8}	1×10^{-4}
		4×10^{-7}	2×10^{-3}	1×10^{-8}	6×10^{-5}
		3×10^{-7}	2×10^{-3}	1×10^{-8}	6×10^{-5}
		1×10^{-9}	2×10^{-3}	4×10^{-10}	8×10^{-5}
		2×10^{-9}	2×10^{-3}	6×10^{-10}	8×10^{-5}
		4×10^{-9}	6×10^{-4}	1×10^{-10}	2×10^{-5}
		7×10^{-9}	6×10^{-4}	2×10^{-10}	2×10^{-5}
		9×10^{-8}	6×10^{-3}	3×10^{-9}	2×10^{-4}
		7×10^{-8}	6×10^{-3}	3×10^{-9}	2×10^{-4}
		5×10^{-6}	2×10^{-2}	2×10^{-7}	8×10^{-4}
		3×10^{-6}	1×10^{-2}	9×10^{-8}	5×10^{-4}
		2×10^{-7}	6×10^{-3}	8×10^{-9}	2×10^{-4}
		9×10^{-8}	6×10^{-3}	3×10^{-9}	2×10^{-4}
		5×10^{-7}	2×10^{-3}	2×10^{-8}	8×10^{-5}
		4×10^{-7}	2×10^{-3}	1×10^{-8}	8×10^{-5}
		2×10^{-7}	1×10^{-3}	8×10^{-9}	4×10^{-5}
		2×10^{-7}	1×10^{-3}	6×10^{-9}	4×10^{-5}
		1×10^{-8}	5×10^{-2}	4×10^{-7}	2×10^{-3}
		6×10^{-6}	5×10^{-2}	2×10^{-7}	2×10^{-3}
		1×10^{-6}	5×10^{-3}	4×10^{-8}	2×10^{-3}
		6×10^{-7}	4×10^{-3}	2×10^{-8}	2×10^{-4}
		3×10^{-7}	2×10^{-3}	1×10^{-8}	1×10^{-4}
		2×10^{-7}	1×10^{-3}	8×10^{-9}	5×10^{-5}
					5×10^{-5}

Table 1.10 Contd.

Element (atomic number)	Isotope [1]		Table I Column 1 Air (μc/ml)	Table I Column 2 Water (μc/ml)	Table II Column 1 Air (μc/ml)	Table II Column 2 Water (μc/ml)
Gold (79)	Au 199	S	1×10^{-6}	5×10^{-3}	4×10^{-8}	2×10^{-4}
		I	8×10^{-7}	4×10^{-3}	3×10^{-8}	2×10^{-4}
Hafnium (72)	Hf 181	S	4×10^{-8}	2×10^{-3}	1×10^{-9}	7×10^{-5}
		I	7×10^{-8}	2×10^{-3}	3×10^{-9}	7×10^{-5}
Holmium (67)	Ho 166	S	2×10^{-7}	9×10^{-4}	7×10^{-9}	3×10^{-5}
		I	2×10^{-7}	9×10^{-4}	6×10^{-9}	3×10^{-5}
Hydrogen (1)	H3	S	5×10^{-6}	1×10^{-1}	2×10^{-7}	3×10^{-3}
		Sub	2×10^{-3}		4×10^{-5}	
Indium (49)	In 113m	S	8×10^{-6}	4×10^{-2}	3×10^{-7}	1×10^{-3}
		I	7×10^{-6}	4×10^{-2}	2×10^{-7}	1×10^{-3}
	In 114m	S	1×10^{-7}	5×10^{-4}	4×10^{-9}	2×10^{-5}
		I	2×10^{-8}	5×10^{-4}	7×10^{-10}	2×10^{-5}
	In 115m	S	2×10^{-6}	1×10^{-2}	8×10^{-8}	4×10^{-4}
		I	2×10^{-6}	1×10^{-2}	6×10^{-8}	4×10^{-4}
	In 115	S	2×10^{-7}	3×10^{-3}	9×10^{-9}	9×10^{-5}
		I	3×10^{-8}	3×10^{-3}	1×10^{-9}	9×10^{-5}
Iodine (53)	I 126	S	8×10^{-6}	5×10^{-5}	3×10^{-10}	2×10^{-6}
		I	3×10^{-7}	3×10^{-3}	1×10^{-8}	9×10^{-5}
	I 129	S	2×10^{-9}	1×10^{-5}	6×10^{-11}	4×10^{-7}
		I	7×10^{-8}	6×10^{-3}	2×10^{-9}	2×10^{-4}
	I 131	S	9×10^{-9}	6×10^{-5}	3×10^{-10}	2×10^{-6}
		I	3×10^{-7}	2×10^{-3}	1×10^{-8}	6×10^{-5}
	I 132	S	2×10^{-7}	2×10^{-3}	8×10^{-9}	6×10^{-5}
		I	9×10^{-7}	5×10^{-3}	3×10^{-8}	2×10^{-4}
	I 133	S	3×10^{-8}	2×10^{-4}	1×10^{-9}	7×10^{-6}
		I	2×10^{-7}	1×10^{-3}	7×10^{-9}	4×10^{-5}
	I 134	S	5×10^{-7}	4×10^{-3}	2×10^{-8}	1×10^{-4}
		I	3×10^{-6}	2×10^{-2}	1×10^{-7}	6×10^{-4}
	I 135	S	1×10^{-7}	7×10^{-4}	4×10^{-9}	2×10^{-5}
		I	4×10^{-7}	2×10^{-3}	1×10^{-8}	7×10^{-5}
Iridium (77)	Ir 190	S	1×10^{-6}	6×10^{-3}	4×10^{-8}	2×10^{-4}
		I	4×10^{-7}	5×10^{-3}	1×10^{-8}	2×10^{-4}
	Ir 192	S	1×10^{-7}	1×10^{-3}	4×10^{-9}	4×10^{-5}
		I	3×10^{-8}	1×10^{-3}	9×10^{-10}	4×10^{-5}
	Ir 194	S	2×10^{-7}	1×10^{-3}	8×10^{-9}	3×10^{-5}
		I	2×10^{-7}	9×10^{-4}	5×10^{-9}	3×10^{-5}
Iron (26)	Fe 55	S	9×10^{-7}	2×10^{-2}	3×10^{-8}	8×10^{-4}
		I	1×10^{-6}	7×10^{-2}	3×10^{-8}	2×10^{-3}
	Fe 59	S	1×10^{-7}	2×10^{-3}	5×10^{-9}	6×10^{-5}
		I	5×10^{-8}	2×10^{-3}	2×10^{-9}	5×10^{-5}
Krypton [2] (36)	Kr 85m	Sub	6×10^{-6}		1×10^{-7}	
	Kr 85	Sub	1×10^{-5}		3×10^{-7}	
	Kr 87	Sub	1×10^{-6}		2×10^{-8}	
Lanthanum (57)	La 140	S	2×10^{-7}	7×10^{-4}	5×10^{-9}	2×10^{-5}
		I	1×10^{-7}	7×10^{-4}	4×10^{-9}	2×10^{-5}
Lead (82)	Pb 203	S	3×10^{-6}	1×10^{-2}	9×10^{-8}	4×10^{-4}
		I	2×10^{-6}	1×10^{-2}	6×10^{-8}	4×10^{-4}
	Pb 210	S	1×10^{-10}	4×10^{-6}	4×10^{-12}	1×10^{-7}
		I	2×10^{-10}	5×10^{-3}	8×10^{-12}	2×10^{-4}
	Pb 212	S	2×10^{-8}	6×10^{-4}	6×10^{-10}	2×10^{-5}
		I	2×10^{-8}	5×10^{-4}	7×10^{-10}	2×10^{-5}
Lutetium (71)	Lu 177	S	6×10^{-7}	3×10^{-3}	2×10^{-8}	1×10^{-4}
		I	5×10^{-7}	3×10^{-3}	2×10^{-8}	1×10^{-4}
Manganese (25)	Mn 52	S	2×10^{-7}	1×10^{-3}	7×10^{-9}	3×10^{-5}
		I	1×10^{-7}	9×10^{-4}	5×10^{-9}	3×10^{-5}
	Mn 54	S	4×10^{-7}	4×10^{-3}	1×10^{-9}	1×10^{-4}
		I	4×10^{-8}	3×10^{-3}	1×10^{-9}	1×10^{-4}
	Mn 56	S	8×10^{-7}	4×10^{-3}	3×10^{-8}	1×10^{-4}
		I	5×10^{-7}	3×10^{-3}	2×10^{-8}	1×10^{-4}
Mercury (80)	Hg 197m	S	7×10^{-7}	6×10^{-3}	3×10^{-8}	2×10^{-4}
		I	8×10^{-7}	5×10^{-3}	3×10^{-8}	2×10^{-4}
	Hg 197	S	1×10^{-6}	9×10^{-3}	4×10^{-8}	3×10^{-4}
		I	3×10^{-6}	1×10^{-2}	9×10^{-8}	5×10^{-4}
	Hg 203	S	7×10^{-8}	5×10^{-4}	2×10^{-9}	2×10^{-5}
		I	1×10^{-7}	3×10^{-3}	4×10^{-9}	1×10^{-4}
Molybdenum (42)	Mo 99	S	7×10^{-7}	5×10^{-3}	3×10^{-8}	2×10^{-4}
		I	2×10^{-7}	1×10^{-3}	7×10^{-9}	4×10^{-5}
Neodymium (60)	Nd 144	S	8×10^{-11}	2×10^{-3}	3×10^{-12}	7×10^{-5}
		I	3×10^{-10}	2×10^{-3}	1×10^{-11}	8×10^{-5}

See footnotes at end of table.

Table 1.10 Contd.

Element (atomic number)	Isotope [1]		Table I		Table II	
			Column 1 Air (μc/ml)	Column 2 Water (μc/ml)	Column 1 Air (μc/ml)	Column 2 Water (μc/ml)
Neodymium (60)	Nd 147	S	4×10^{-7}	2×10^{-3}	1×10^{-8}	6×10^{-5}
		I	2×10^{-7}	2×10^{-3}	8×10^{-9}	6×10^{-5}
	Nd 149	S	2×10^{-6}	8×10^{-3}	6×10^{-8}	3×10^{-4}
		I	1×10^{-6}	8×10^{-3}	5×10^{-8}	3×10^{-4}
Neptunium (93)	Np 237	S	4×10^{-12}	9×10^{-5}	1×10^{-13}	3×10^{-6}
		I	1×10^{-10}	9×10^{-4}	4×10^{-12}	3×10^{-5}
	Np 239	S	8×10^{-7}	4×10^{-3}	3×10^{-8}	1×10^{-4}
		I	7×10^{-7}	4×10^{-3}	2×10^{-8}	1×10^{-4}
Nickel (28)	Ni 59	S	5×10^{-7}	6×10^{-3}	2×10^{-8}	2×10^{-4}
		I	8×10^{-7}	6×10^{-2}	3×10^{-8}	2×10^{-3}
	Ni 63	S	6×10^{-6}	8×10^{-4}	2×10^{-9}	3×10^{-5}
		I	3×10^{-7}	2×10^{-2}	1×10^{-8}	7×10^{-4}
	Ni 65	S	9×10^{-7}	4×10^{-3}	3×10^{-8}	1×10^{-4}
		I	5×10^{-7}	3×10^{-3}	2×10^{-8}	1×10^{-4}
Niobium (Columbium) (41)	Nb 93m	S	1×10^{-7}	1×10^{-2}	4×10^{-9}	4×10^{-4}
		I	2×10^{-7}	1×10^{-2}	5×10^{-9}	4×10^{-4}
	Nb 95	S	5×10^{-7}	3×10^{-3}	2×10^{-8}	1×10^{-4}
		I	1×10^{-7}	3×10^{-3}	3×10^{-9}	1×10^{-4}
	Nb 97	S	6×10^{-6}	3×10^{-2}	2×10^{-7}	9×10^{-4}
		I	5×10^{-6}	3×10^{-2}	2×10^{-7}	9×10^{-4}
Osmium (ó)	Os 185	S	5×10^{-7}	2×10^{-3}	2×10^{-8}	7×10^{-5}
		I	5×10^{-8}	2×10^{-3}	2×10^{-9}	7×10^{-5}
	Os 191m	S	2×10^{-5}	7×10^{-2}	6×10^{-7}	3×10^{-3}
		I	9×10^{-6}	7×10^{-2}	3×10^{-7}	2×10^{-3}
	Os 191	S	1×10^{-6}	5×10^{-3}	4×10^{-8}	2×10^{-4}
		I	4×10^{-7}	5×10^{-3}	1×10^{-8}	2×10^{-4}
	Os 193	S	4×10^{-7}	2×10^{-3}	1×10^{-8}	6×10^{-5}
		I	3×10^{-7}	2×10^{-3}	9×10^{-9}	5×10^{-5}
Palladium (46)	Pd 103	S	1×10^{-6}	1×10^{-2}	5×10^{-8}	3×10^{-4}
		I	7×10^{-7}	8×10^{-3}	3×10^{-8}	3×10^{-4}
	Pd 109	S	6×10^{-7}	3×10^{-3}	2×10^{-8}	9×10^{-5}
		I	4×10^{-7}	2×10^{-3}	1×10^{-8}	7×10^{-5}
Phosphorus (15)	P 32	S	7×10^{-8}	5×10^{-4}	2×10^{-9}	2×10^{-5}
		I	8×10^{-8}	7×10^{-4}	3×10^{-9}	2×10^{-5}
Platinum (78)	Pt 191	S	8×10^{-7}	4×10^{-3}	3×10^{-8}	1×10^{-4}
		I	6×10^{-7}	3×10^{-3}	2×10^{-8}	1×10^{-4}
	Pt 193m	S	7×10^{-6}	3×10^{-2}	2×10^{-7}	1×10^{-3}
		I	5×10^{-6}	3×10^{-2}	2×10^{-7}	1×10^{-3}
	Pt 197m	S	6×10^{-6}	3×10^{-2}	2×10^{-7}	1×10^{-3}
		I	5×10^{-6}	3×10^{-2}	2×10^{-7}	9×10^{-4}
	Pt 197	S	8×10^{-7}	4×10^{-3}	3×10^{-8}	1×10^{-4}
		I	6×10^{-7}	3×10^{-3}	2×10^{-8}	1×10^{-4}
Plutonium (94)	Pu 238	S	2×10^{-12}	1×10^{-4}	7×10^{-14}	5×10^{-6}
		I	3×10^{-11}	8×10^{-4}	1×10^{-12}	3×10^{-5}
	Pu 239	S	2×10^{-12}	1×10^{-4}	6×10^{-14}	5×10^{-6}
		I	4×10^{-11}	8×10^{-4}	1×10^{-12}	3×10^{-5}
	Pu 240	S	2×10^{-12}	1×10^{-4}	6×10^{-14}	5×10^{-6}
		I	4×10^{-11}	8×10^{-4}	1×10^{-12}	3×10^{-5}
	Pu 241	S	9×10^{-11}	7×10^{-3}	3×10^{-12}	2×10^{-4}
		I	4×10^{-8}	4×10^{-2}	1×10^{-9}	1×10^{-3}
	Pu 242	S	2×10^{-12}	1×10^{-4}	6×10^{-14}	5×10^{-6}
		I	4×10^{-11}	9×10^{-4}	1×10^{-12}	3×10^{-5}
Polonium (84)	Po 210	S	5×10^{-10}	2×10^{-5}	2×10^{-11}	7×10^{-7}
		I	2×10^{-10}	8×10^{-4}	7×10^{-12}	3×10^{-5}
Potassium (19)	K42	S	2×10^{-6}	9×10^{-3}	7×10^{-8}	3×10^{-4}
		I	1×10^{-7}	6×10^{-4}	4×10^{-9}	2×10^{-5}
Praseodymium (59)	Pr 142	S	2×10^{-7}	9×10^{-4}	7×10^{-9}	3×10^{-5}
		I	2×10^{-7}	9×10^{-4}	5×10^{-9}	3×10^{-5}
	Pr 143	S	3×10^{-7}	1×10^{-3}	1×10^{-8}	5×10^{-5}
		I	2×10^{-7}	1×10^{-3}	6×10^{-9}	5×10^{-5}
Promethium (61)	Pm 147	S	6×10^{-8}	6×10^{-3}	2×10^{-9}	2×10^{-4}
		I	1×10^{-7}	6×10^{-3}	3×10^{-9}	2×10^{-4}
	Pm 149	S	3×10^{-7}	1×10^{-3}	1×10^{-8}	4×10^{-5}
		I	2×10^{-7}	1×10^{-3}	8×10^{-9}	4×10^{-5}
Protoactinium (91)	Pa 230	S	2×10^{-9}	7×10^{-3}	6×10^{-11}	2×10^{-4}
		I	8×10^{-10}	7×10^{-3}	3×10^{-11}	2×10^{-4}
	Pa 231	S	1×10^{-12}	3×10^{-5}	4×10^{-14}	9×10^{-7}
		I	1×10^{-10}	8×10^{-4}	4×10^{-12}	2×10^{-5}

Table 1.10 Contd.

Element (atomic number)	Isotope [1]		Table I Column 1 Air (μc/ml)	Table I Column 2 Water (μc/ml)	Table II Column 1 Air (μc/ml)	Table II Column 2 Water (μc/ml)
Protoactinium (91)	Pa 233	S	6×10^{-7}	4×10^{-3}	2×10^{-8}	1×10^{-4}
		I	2×10^{-7}	3×10^{-3}	6×10^{-9}	1×10^{-4}
Radium (88)	Ra 223	S	2×10^{-9}	2×10^{-5}	6×10^{-11}	7×10^{-7}
		I	2×10^{-10}	1×10^{-4}	8×10^{-12}	4×10^{-6}
	Ra 224	S	5×10^{-9}	7×10^{-5}	2×10^{-10}	2×10^{-6}
		I	7×10^{-10}	2×10^{-4}	2×10^{-11}	5×10^{-6}
	Ra 226	S	3×10^{-11}	4×10^{-7}	1×10^{-12}	1×10^{-8}
		I	5×10^{-11}	9×10^{-4}	2×10^{-12}	3×10^{-5}
	Ra 228	S	7×10^{-11}	8×10^{-7}	2×10^{-12}	3×10^{-8}
		I	4×10^{-11}	7×10^{-4}	1×10^{-12}	3×10^{-5}
Radon (86)	Rn 220	S	3×10^{-7}	----------	1×10^{-8}	----------
		I	----------	----------	----------	----------
	Rn 222	S	1×10^{-7}	----------	3×10^{-9}	----------
Rhenium (75)	Re 183	S	3×10^{-6}	2×10^{-2}	9×10^{-8}	6×10^{-4}
		I	2×10^{-7}	8×10^{-3}	5×10^{-9}	3×10^{-4}
	Re 186	S	6×10^{-7}	3×10^{-3}	2×10^{-8}	9×10^{-5}
		I	2×10^{-7}	1×10^{-3}	8×10^{-9}	5×10^{-5}
	Re 187	S	9×10^{-6}	7×10^{-2}	3×10^{-7}	3×10^{-3}
		I	5×10^{-7}	4×10^{-2}	2×10^{-8}	2×10^{-3}
	Re 188	S	4×10^{-7}	2×10^{-3}	1×10^{-8}	6×10^{-5}
		I	2×10^{-7}	9×10^{-4}	6×10^{-9}	3×10^{-5}
Rhodium (45)	Rh 103m	S	8×10^{-5}	4×10^{-1}	3×10^{-6}	1×10^{-2}
		I	6×10^{-5}	3×10^{-1}	2×10^{-6}	1×10^{-2}
	Rh 105	S	8×10^{-7}	4×10^{-3}	3×10^{-8}	1×10^{-4}
		I	5×10^{-7}	3×10^{-3}	2×10^{-8}	1×10^{-4}
Rubidium (37)	Rb 86	S	3×10^{-7}	2×10^{-3}	1×10^{-8}	7×10^{-5}
		I	7×10^{-8}	7×10^{-4}	2×10^{-9}	2×10^{-5}
	Rb 87	S	5×10^{-7}	3×10^{-3}	2×10^{-8}	1×10^{-4}
		I	7×10^{-8}	5×10^{-3}	2×10^{-9}	2×10^{-4}
Ruthenium (44)	Ru 97	S	2×10^{-6}	1×10^{-2}	8×10^{-8}	4×10^{-4}
		I	2×10^{-6}	1×10^{-2}	6×10^{-8}	3×10^{-4}
	Ru 103	S	5×10^{-7}	2×10^{-3}	2×10^{-8}	8×10^{-5}
		I	8×10^{-8}	2×10^{-3}	3×10^{-9}	8×10^{-5}
	Ru 105	S	7×10^{-7}	3×10^{-3}	2×10^{-8}	1×10^{-4}
		I	5×10^{-7}	3×10^{-3}	2×10^{-8}	1×10^{-4}
	Ru 106	S	8×10^{-8}	4×10^{-4}	3×10^{-9}	1×10^{-5}
		I	6×10^{-9}	3×10^{-4}	2×10^{-10}	1×10^{-5}
Samarium (62)	Sm 147	S	7×10^{-11}	2×10^{-3}	2×10^{-12}	6×10^{-5}
		I	3×10^{-10}	2×10^{-3}	9×10^{-12}	7×10^{-5}
	Sm 151	S	6×10^{-8}	1×10^{-2}	2×10^{-9}	4×10^{-4}
		I	1×10^{-7}	1×10^{-2}	5×10^{-9}	4×10^{-4}
	Sm 153	S	5×10^{-7}	2×10^{-3}	2×10^{-8}	8×10^{-5}
		I	4×10^{-7}	2×10^{-3}	1×10^{-8}	8×10^{-5}
Scandium (21)	Sc 46	S	2×10^{-7}	1×10^{-3}	8×10^{-9}	4×10^{-5}
		I	2×10^{-8}	1×10^{-3}	8×10^{-10}	4×10^{-5}
	Sc 47	S	6×10^{-7}	3×10^{-3}	2×10^{-8}	9×10^{-5}
		I	5×10^{-7}	3×10^{-3}	2×10^{-8}	9×10^{-5}
	Sc 48	S	2×10^{-7}	8×10^{-4}	6×10^{-9}	3×10^{-5}
		I	1×10^{-7}	8×10^{-4}	5×10^{-9}	3×10^{-5}
Selenium (34)	Se 75	S	1×10^{-6}	9×10^{-3}	4×10^{-8}	3×10^{-4}
		I	1×10^{-7}	8×10^{-3}	4×10^{-9}	3×10^{-4}
Silicon (14)	Si 31	S	6×10^{-6}	3×10^{-2}	2×10^{-7}	9×10^{-4}
		I	1×10^{-6}	6×10^{-3}	3×10^{-8}	2×10^{-4}
Silver (47)	Ag 105	S	6×10^{-7}	3×10^{-3}	2×10^{-8}	1×10^{-4}
		I	8×10^{-9}	3×10^{-3}	3×10^{-9}	1×10^{-4}
	Ag 110m	S	2×10^{-7}	9×10^{-4}	7×10^{-9}	3×10^{-5}
		I	1×10^{-8}	9×10^{-4}	3×10^{-10}	3×10^{-5}
	Ag 111	S	3×10^{-7}	1×10^{-3}	1×10^{-8}	4×10^{-5}
		I	2×10^{-7}	1×10^{-3}	8×10^{-9}	4×10^{-5}
Sodium (11)	Na 22	S	2×10^{-7}	1×10^{-3}	6×10^{-9}	4×10^{-5}
		I	9×10^{-9}	9×10^{-4}	3×10^{-10}	3×10^{-5}
	Na 24	S	1×10^{-6}	6×10^{-3}	4×10^{-8}	2×10^{-4}
		I	1×10^{-7}	8×10^{-4}	5×10^{-9}	3×10^{-5}
Strontium (38)	Sr 85m	S	4×10^{-5}	2×10^{-1}	1×10^{-6}	7×10^{-3}
		I	3×10^{-5}	2×10^{-1}	1×10^{-6}	7×10^{-3}
	Sr 85	S	2×10^{-7}	3×10^{-3}	8×10^{-9}	1×10^{-4}
		I	1×10^{-7}	5×10^{-3}	4×10^{-9}	2×10^{-4}
	Sr 89	S	3×10^{-8}	3×10^{-4}	1×10^{-9}	1×10^{-5}
		I	4×10^{-8}	8×10^{-4}	1×10^{-9}	3×10^{-5}

See footnotes at end of table.

Table 1.10 Contd.

Element (atomic number)	Isotope [1]		Table I		Table II	
			Column 1 Air (μc/ml)	Column 2 Water (μc/ml)	Column 1 Air (μc/ml)	Column 2 Water (μc/ml)
Strontium (38)	Sr 90	S	3×10^{-10}	4×10^{-6}	1×10^{-11}	1×10^{-7}
		I	5×10^{-9}	1×10^{-3}	2×10^{-10}	4×10^{-6}
	Sr 91	S	4×10^{-7}	2×10^{-3}	2×10^{-8}	7×10^{-5}
		I	3×10^{-7}	1×10^{-3}	9×10^{-9}	5×10^{-6}
	Sr 92	S	4×10^{-7}	2×10^{-3}	2×10^{-8}	7×10^{-5}
		I	3×10^{-7}	2×10^{-3}	1×10^{-8}	6×10^{-5}
Sulfur (16)	S 35	S	3×10^{-7}	2×10^{-3}	9×10^{-9}	6×10^{-6}
		I	3×10^{-7}	8×10^{-3}	9×10^{-9}	3×10^{-4}
Tantalum (73)	Ta 182	S	4×10^{-8}	1×10^{-3}	1×10^{-9}	4×10^{-6}
		I	2×10^{-8}	1×10^{-3}	7×10^{-10}	4×10^{-6}
Technetium (43)	Tc 96m	S	8×10^{-5}	4×10^{-1}	3×10^{-6}	1×10^{-2}
		I	3×10^{-5}	3×10^{-1}	1×10^{-6}	1×10^{-2}
	Tc 96	S	6×10^{-7}	3×10^{-3}	2×10^{-8}	1×10^{-4}
		I	2×10^{-7}	1×10^{-3}	8×10^{-9}	5×10^{-5}
	Tc 97m	S	2×10^{-6}	1×10^{-2}	8×10^{-8}	4×10^{-4}
		I	2×10^{-7}	5×10^{-3}	5×10^{-9}	2×10^{-4}
	Tc 97	S	1×10^{-5}	5×10^{-2}	4×10^{-7}	2×10^{-3}
		I	3×10^{-7}	2×10^{-2}	1×10^{-8}	8×10^{-4}
	Tc 99m	S	4×10^{-5}	2×10^{-1}	1×10^{-6}	6×10^{-3}
		I	1×10^{-5}	8×10^{-2}	5×10^{-7}	3×10^{-3}
	Tc 99	S	2×10^{-6}	1×10^{-2}	7×10^{-8}	3×10^{-4}
		I	6×10^{-8}	5×10^{-3}	2×10^{-9}	2×10^{-4}
Tellurium (52)	Te 125m	S	4×10^{-7}	5×10^{-3}	1×10^{-8}	2×10^{-4}
		I	1×10^{-7}	3×10^{-3}	4×10^{-9}	1×10^{-4}
	Te 127m	S	1×10^{-7}	2×10^{-3}	5×10^{-9}	6×10^{-5}
		I	4×10^{-8}	2×10^{-3}	1×10^{-9}	5×10^{-6}
	Te 127	S	2×10^{-6}	8×10^{-3}	6×10^{-8}	3×10^{-4}
		I	9×10^{-7}	5×10^{-3}	3×10^{-8}	2×10^{-4}
	Te 129m	S	8×10^{-8}	1×10^{-3}	3×10^{-9}	3×10^{-5}
		I	3×10^{-8}	6×10^{-4}	1×10^{-9}	2×10^{-5}
	Te 129	S	5×10^{-6}	2×10^{-2}	2×10^{-7}	8×10^{-4}
		I	4×10^{-6}	2×10^{-2}	1×10^{-7}	8×10^{-4}
	Te 131m	S	4×10^{-7}	2×10^{-3}	1×10^{-8}	6×10^{-5}
		I	2×10^{-7}	1×10^{-3}	6×10^{-9}	4×10^{-5}
	Te 132	S	2×10^{-7}	9×10^{-4}	7×10^{-9}	3×10^{-5}
		I	1×10^{-7}	6×10^{-4}	4×10^{-9}	2×10^{-5}
Terbium (65)	Tb 160	S	1×10^{-7}	1×10^{-3}	3×10^{-9}	4×10^{-5}
		I	3×10^{-8}	1×10^{-3}	1×10^{-9}	4×10^{-5}
Thallium (81)	Tl 200	S	3×10^{-6}	1×10^{-2}	9×10^{-8}	4×10^{-4}
		I	1×10^{-6}	7×10^{-3}	4×10^{-8}	2×10^{-4}
	Tl 201	S	2×10^{-6}	9×10^{-3}	7×10^{-8}	3×10^{-4}
		I	9×10^{-7}	5×10^{-3}	3×10^{-8}	2×10^{-4}
	Tl 202	S	8×10^{-7}	4×10^{-3}	3×10^{-8}	1×10^{-4}
		I	2×10^{-7}	2×10^{-3}	8×10^{-9}	7×10^{-5}
	Tl 204	S	6×10^{-7}	3×10^{-3}	2×10^{-8}	1×10^{-4}
		I	3×10^{-8}	2×10^{-3}	9×10^{-10}	6×10^{-5}
Thorium (90)	Th 228	S	9×10^{-12}	2×10^{-4}	3×10^{-13}	7×10^{-6}
		I	6×10^{-12}	4×10^{-4}	2×10^{-13}	10^{-5}
	Th 230	S	2×10^{-12}	5×10^{-5}	8×10^{-14}	2×10^{-6}
		I	10^{-11}	9×10^{-4}	3×10^{-13}	3×10^{-5}
	Th 232	S	3×10^{-11}	5×10^{-5}	10^{-12}	2×10^{-6}
		I	3×10^{-11}	10^{-3}	10^{-12}	4×10^{-5}
	Th natural	S	3×10^{-11}	3×10^{-5}	10^{-12}	10^{-6}
		I	3×10^{-11}	3×10^{-4}	10^{-12}	10^{-5}
	Th 234	S	6×10^{-8}	5×10^{-4}	2×10^{-9}	2×10^{-5}
		I	3×10^{-8}	5×10^{-4}	10^{-9}	2×10^{-5}
Thulium (69)	Tm 170	S	4×10^{-8}	1×10^{-3}	1×10^{-9}	5×10^{-5}
		I	3×10^{-8}	1×10^{-3}	1×10^{-9}	5×10^{-5}
	Tm 171	S	1×10^{-7}	1×10^{-2}	4×10^{-9}	5×10^{-4}
		I	2×10^{-7}	1×10^{-2}	8×10^{-9}	5×10^{-4}
Tin (50)	Sn 113	S	4×10^{-7}	2×10^{-3}	1×10^{-8}	9×10^{-5}
		I	5×10^{-8}	2×10^{-3}	2×10^{-9}	8×10^{-5}
	Sn 125	S	1×10^{-7}	5×10^{-4}	4×10^{-9}	2×10^{-5}
		I	8×10^{-8}	5×10^{-4}	3×10^{-9}	2×10^{-5}
Tungsten (Wolfram) (74)	W 181	S	2×10^{-6}	1×10^{-2}	8×10^{-8}	4×10^{-4}
		I	1×10^{-7}	1×10^{-2}	4×10^{-9}	3×10^{-4}
	W 185	S	8×10^{-7}	4×10^{-3}	3×10^{-8}	1×10^{-4}
		I	1×10^{-7}	3×10^{-3}	4×10^{-9}	1×10^{-4}

Table 1.10 Contd.

Element (atomic number)	Isotope [1]		Table I Column 1 Air (μc/ml)	Table I Column 2 Water (μc/ml)	Table II Column 1 Air (μc/ml)	Table II Column 2 Water (μc/ml)
Tungsten (Wolfram) (74)	W 187	S	4×10^{-7}	2×10^{-3}	2×10^{-8}	7×10^{-5}
		I	3×10^{-7}	2×10^{-3}	1×10^{-8}	6×10^{-5}
Uranium (92)	U 230	S	3×10^{-10}	1×10^{-4}	1×10^{-11}	5×10^{-6}
		I	1×10^{-10}	1×10^{-4}	4×10^{-12}	5×10^{-6}
	U 232	S	1×10^{-10}	8×10^{-4}	3×10^{-12}	3×10^{-5}
		I	3×10^{-11}	8×10^{-4}	9×10^{-13}	3×10^{-5}
	U 233	S	5×10^{-10}	9×10^{-4}	2×10^{-11}	3×10^{-5}
		I	1×10^{-10}	9×10^{-4}	4×10^{-12}	3×10^{-5}
	U 234	S	6×10^{-10}	9×10^{-4}	2×10^{-11}	3×10^{-5}
		I	1×10^{-10}	9×10^{-4}	4×10^{-12}	3×10^{-5}
	U 235	S	5×10^{-10}	8×10^{-4}	2×10^{-11}	3×10^{-5}
		I	1×10^{-10}	8×10^{-4}	4×10^{-12}	3×10^{-5}
	U 236	S	6×10^{-10}	1×10^{-3}	2×10^{-11}	3×10^{-5}
		I	1×10^{-10}	1×10^{-3}	4×10^{-12}	3×10^{-5}
	U 238	S	7×10^{-11}	1×10^{-3}	3×10^{-12}	4×10^{-5}
		I	1×10^{-10}	1×10^{-3}	5×10^{-12}	4×10^{-5}
	U-natural	S	7×10^{-11}	5×10^{-4}	3×10^{-12}	2×10^{-5}
		I	6×10^{-11}	5×10^{-4}	2×10^{-12}	2×10^{-5}
Vanadium (23)	V 48	S	2×10^{-7}	9×10^{-4}	6×10^{-9}	3×10^{-5}
		I	6×10^{-8}	8×10^{-4}	2×10^{-9}	3×10^{-5}
Xenon (54)	Xe 131m	Sub	2×10^{-5}	----------	4×10^{-7}	----------
	Xe 133	Sub	1×10^{-5}	----------	3×10^{-7}	----------
	Xe 135	Sub	4×10^{-6}	----------	1×10^{-7}	----------
Ytterbium (70)	Yb 175	S	7×10^{-7}	3×10^{-3}	2×10^{-8}	1×10^{-4}
		I	6×10^{-7}	3×10^{-3}	2×10^{-8}	1×10^{-4}
Yttrium (39)	Y 90	S	1×10^{-7}	6×10^{-4}	4×10^{-9}	2×10^{-5}
		I	1×10^{-7}	6×10^{-4}	3×10^{-9}	2×10^{-5}
	Y 91m	S	2×10^{-5}	1×10^{-1}	8×10^{-7}	3×10^{-3}
		I	2×10^{-5}	1×10^{-1}	6×10^{-7}	3×10^{-3}
	Y 91	S	4×10^{-5}	8×10^{-4}	1×10^{-9}	3×10^{-5}
		I	3×10^{-8}	8×10^{-4}	1×10^{-9}	3×10^{-5}
	Y 92	S	4×10^{-7}	2×10^{-3}	1×10^{-8}	6×10^{-5}
		I	3×10^{-7}	2×10^{-3}	1×10^{-8}	6×10^{-5}
	Y 93	S	2×10^{-7}	8×10^{-4}	6×10^{-9}	3×10^{-5}
		I	1×10^{-7}	8×10^{-4}	5×10^{-9}	3×10^{-5}
Zinc (30)	Zn 65	S	1×10^{-7}	3×10^{-3}	4×10^{-9}	1×10^{-4}
		I	6×10^{-8}	5×10^{-3}	2×10^{-9}	2×10^{-4}
	Zn 69m	S	4×10^{-7}	2×10^{-3}	1×10^{-8}	7×10^{-5}
		I	3×10^{-7}	2×10^{-3}	1×10^{-8}	6×10^{-5}
	Zn 69	S	7×10^{-6}	5×10^{-2}	2×10^{-7}	2×10^{-3}
		I	9×10^{-6}	5×10^{-2}	3×10^{-7}	2×10^{-3}
Zirconium (40)	Zr 93	S	1×10^{-7}	2×10^{-2}	4×10^{-9}	8×10^{-4}
		I	3×10^{-7}	2×10^{-2}	1×10^{-8}	8×10^{-4}
	Zr 95	S	1×10^{-7}	2×10^{-3}	4×10^{-9}	6×10^{-5}
		I	3×10^{-8}	2×10^{-3}	1×10^{-9}	6×10^{-5}
	Zr 97	S	1×10^{-7}	5×10^{-4}	4×10^{-9}	2×10^{-5}
		I	9×10^{-8}	5×10^{-4}	3×10^{-9}	2×10^{-5}

[1] Soluble (S); Insoluble (I).

[2] "Sub" means that values given are for submersion in an infinite cloud of gaseous material.

NOTE: In any case where there is a mixture in air or water of more than one radionuclide, the limiting values for purposes of this Appendix should be determined as follows:

1. If the identity and concentration of each radionuclide in the mixture are known, the limiting values should be derived as follows: Determine, for each radionuclide in the mixture, the ratio between the quantity present in the mixture and the limit otherwise established in Appendix B for the specific radionuclide when not in a mixture. The sum of such ratios for all the radionuclides in the mixture may not exceed "1" (i.e., "unity").

EXAMPLE: If radionuclides A, B, and C are present in concentrations C_A, C_B, and C_C, and if the applicable MPC's, are MPC_A, and MPC_B, and MPC_C respectively, then the concentrations shall be limited so that the following relationship exists:

$$\frac{C_A}{MPC_A}+\frac{C_B}{MPC_B}+\frac{C_C}{MPC_C}\leq 1$$

2. If either the identity or the concentration of any radionuclide in the mixture is not known, the limiting values for purposes of Appendix B shall be:

a. For purposes of Table I, Col. 1—1×10^{-12}
b. For purposes of Table I, Col. 2—3×10^{-7}
c. For purposes of Table II, Col. 1—4×10^{-14}
d. For purposes of Table II, Col. 2—1×10^{-8}

3. If the conditions specified below are met, the corresponding values specified below may be used in lieu of those specified in paragraph 2 above.

As of January 1, 1961 revised AEC regulations went into effect (107). These new regulations differ only slightly from the NCRP and ICRP recommendations, but for purposes of comparison will be discussed in the next section. It should be noted that while the ICRP and NCRP may make recommendations, these organizations have no legal authority in so far as regulation and control of radioactive substances is concerned.

In summary, the men responsible for the recommendations made by ICRP are experts in physics, biology, genetics and radiation protection. They have made conservative and intelligent estimates of permissible dosages, based upon sparse data on human radiation injury, and extrapolation from extensive animal experimentation. As more detailed information about radiation effects is accumulated, it may be anticipated that these permissible levels will be further altered.

1.23 Regulation and control by AEC

Before 1946 all regulation and control of radioactive material where it existed was based on local and state regulations, and to a lesser extent, the federal government in so far as interstate commerce was concerned. In 1946, however, the Atomic Energy Act (Public Law 703, 83rd. Cong., 2nd. Sess., 60 Stat. 919) was passed. This was followed by the Atomic Energy Act of 1954, which was an amendment to the original act. The act as summarized by the McMahon Committee was to initiate the following:

(1) An Atomic Energy Commission whose members should be appointed by the President, with the advice and consent of the Senate.

(2) Control by the Commission over all atomic energy installations, with the authority to acquire source materials, i.e. uranium ores, and other property needed in the development of atomic energy

(3) Encouragement by the Commission of research, development, and exploitation in the field of atomic energy with the power to license property and facilities for these purposes.

(4) A prohibition on the export or import of source materials except under the direction of the Commission.

(5) Security regulations and penalties for their violation to be prescribed by the Commission.

The AEC thus was given in the act (among other things) the duty to issue licenses to individuals and organizations for the use of byproduct material. Byproduct material is any radioactive material (except special nuclear material) produced by a nuclear reactor. The AEC, therefore, has

control only in so far as issuance of licenses are concerned. In actual practice, however, this control covers practically all of non-naturally occurring radioactive material since there are few nuclear accelerators large enough to produce large amounts of active material.

In order to maintain a license, once it has been issued by the AEC, the licensee must comply with the regulations as written in the Federal Register (Title 10, Part 20). (107)

The regulations are in general a restatement of the recommendations of the ICRP and the NCRP with a few exceptions. The most important differences are given in the following section.

1.24 Differences between AEC regulations and ICRP recommendations

(1) The AEC regulations do not apply to x-radiation as produced by any mechanical device not containing byproduct radioactive material. X-ray machines are in general licensed by the state or local governments.

(2) The AEC regulations do not apply to any naturally occurring radioactive nuclides such as radium and its daughters if the substance was not produced in a nuclear reactor.

(3) The AEC regulations state the appropriate radiation signs and symbols to be used in radiation areas and in regard to labeling source and byproduct material.

(4) The AEC regualtions describe what records must be kept and detail when a licensee must make reports to the AEC regarding radiation incidents.

(5) The AEC regulations have set the following exposure limits for individuals in restricted areas:

A. No individual shall possess, use, or transfer radioactive material in such a manner as to cause any person in any period of one calendar quarter to receive a dose in excess of the limits specified in Table 1.11.

Table 1.11

Maximum Permissible Doses in Rems per Calendar Quarter (107)

1. Whole body; head and trunk; active blood-forming organs; lens of eyes; or gonads----------1 1/4

2. Hands and forearms; feet and ankles----------18 3/4

3. Skin of whole body----------7 1/2

B. An individual may receive a dose to the whole body greater than that permitted in paragraph (1) A provided:

(i) That during any calendar quarter the dose to the whole body does not exceed 3 rems; and

(ii) That the dose to the whole body when added to the accumulated lifetime dose does not exceed 5 (N-18) rems, where "N" equals the individual's age in years; and

(iii) That "dose to the whole body" shall include any dose to the whole body, gonads, active blood-forming organs, head and trunk, or lens of the eye.

(6) Exposure of minors--The regulations prohibit a licensee from causing an individual within a restricted area, who is under 18 years of age, to receive a dose in excess of 10 per cent of the limits specified in (5) above.

1.25 Practical limits-comparison with "background"

Sufficiently sensitive radiation detection apparatus invariably records the presence of radiation, even in the total absence of known radiation sources. This omnipresent radiation level, which may exhibit rather wide fluctuations with time and differs significantly from place to place, is called "background radiation."

Because every living organism is subjected to this radiation throughout life, an evaluation of the dosage received and its likely effects upon existing species is essential to an intelligent selection of maximum permissible radiation exposure levels.

The major portion of total background radiation levels (roughly 70 per cent at sea level) can be shown to be due to the bombardment of the earth by high-energy particles from outer space. These particles are considered to be

predominately protons and are called "cosmic rays." This radiation is known to remain fairly constant at any one location, but to demonstrate systematic variations with altitude and latidude.

The remaining fraction of total background radiation levels, which demonstrates wide local fluctuations with time and location, is due to naturally occurring radioactive substances. In addition to the four radioactive series of heavy elements (the uranium, thorium, actinium, and neptunium series) seven other radioactive isotopes occur in nature. These are listed in Table 1.12. (88)

Table 1.12

Natural Radioisotopes Other than Heavy Elements (88)

Isotope	% of natural element	Half life	Radiation		
			alpha	beta	gamma
K^{40}	.0119	1.3×10^{9} y		x	x
Rb^{87}	27.2	6.3×10^{10} y		x	x
Sn^{124}	6.0	6×10^{13} y		x	
Nd^{154}		1×10^{12} y		x	
Sm^{159}	26.6	2×10^{11} y	x		
Lu^{176}	2.5	2.4×10^{10} y		x	x
Re^{187}	62.9	4×10^{12} y		x	

The naturally radioactive materials are present in the soil, air and water and are present in measurable quantity in the human body. For example, a layer of typical soil, one foot thick and one square mile in area, contains 6 tons of uranium and 12 tons of thorium.

Among the decay products of the uranium and thorium in the ground is the radioactive gases radon and thoron. Radon and thoron decay, in turn, to a radioactive charged particles which for the most part attache to dust particles. It is the radon and thoron always present in the air which contributes to the wide, nonstatistical variations of background radiation.

Total background radiation varies from 0.01 to 0.1 mr/hr, varying with location. This constitutes a yearly dose of from 0.09 o 0.9 r for everyone.

Concentrations of uranium and radium in drinking water may vary from 10^{-10} to 10^{-7} microcuries per cc, according to the source of the water. Cow's milk contains 6×10^{-8} microcuries per cc of K^{40}. An average human body contains 0.12 microcuries of K^{40}). Comparison of these quantities with the maximum permissible concentrations listed in Table 1.10 should serve to emphasize how conservative ICRP has been.

Considerable data on natural background radiation levels have been accumulated and surveys on radiation levels are being continued at many places throughout the world. It will thus be possible, as the use of nuclear energy increases, to evaluate the effect of this program on the radiation background. These survey points are also very useful in evaluating the local effect, on both radiation and contamination levels, of specific nuclear energy facilities.

1.26 Comparison with nonoccupational exposures

The maximum permissible exposure levels discussed in the previous sections were established to apply only to persons aware that they are working in the field of radiation. Permissible levels of radiation and the quantities of radioactive materials released in areas accessible to the general public should be much lower. In addition to the occupational exposures accumulated by persons working with radiation and continuous exposures to background radiation experienced by everyone, important radiation exposures are occasionally sustained by laymen from other sources.

Radiation levels as high as 10 mr/hr have been observed at the face of a radium-dial watch. At such a dosage rate, the weekly permissible dose of 100 mr could be accumulated in a mere 10 hours. The fact that this dose is very localized when received, and is received only intermittently, substantially reduces the net hazard. There is no record of any serious external radiation injury from radium watches.

X-ray and fluoroscopic examination result in occasional radiation exposures considerably in excess of permissible levels, both to individuals employed with radiation and to the general public. Figure 1.7 illustrates some common X-ray exposures. Notice the dosage received during fluoroscopic examination. An inexperienced or over-enthusiastic fluoroscope operator could easily deliver a damaging dose of radiation during a prolonged exposure (89).

Permanent total sterility of the human male or female requires dosages of from 400 to 1000 rep. to the gonads. As such exposures would usually be

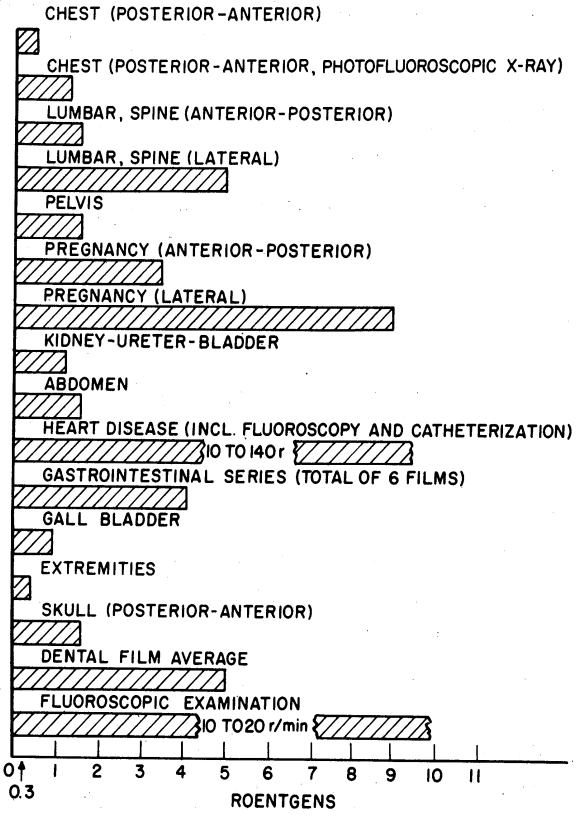

Figure 1.7 Exposures from common X-ray examinations (17)

Figure 1.8 Engine crew moving car loaded with highly radioactive waste to Hanford burial site. Note spacing of several cars to provide protection through distance (Courtesy General Electric Co.)

lethal if received by the whole body, the common fear of being made sterile by radiation exposure is largely academic. However, reduced fertility has been reported at lower levels of exposure (8).

As more and more people become aware of the problems of radiation exposure control, better records will be kept of cumulative individual radiation exposures, and greater care will be taken to minimize total exposure during necessary medical procedures.

1.27 Three safety rules for protection from external radiation

Minimization of personal injury from external radiation can be accomplished by judicious use of three simple rules involving: distance, time, and mass.

Distance A radioactive material emits radiation in all directions. As the distance between the worker and the radioactive material is increased, the exposure rate decreases. For a point source of gamma radiation this rate of decrease is inversely proportional to the square of the distance.

Thus, the first and simplest rule for protection of personnel exposed to external radiation hazard is: "Stay as far away from the radiation source as possible while working with the source or in a radiation area." In laboratory work the use of tongs and long-handled tools is preferable to hand manipulation. Remote control is preferable to the use of tongs.

When large amounts of radioactive material must be handled without shielding, special techniques are used. Figures 1.8, and 1.9 show techniques used in the burial of highly radioactive equipment at the Hanford burial site. The equipment is first prepared for removal and burial behind heavily shielded walls called "canyons" with the use of remote manipulators. The material is removed from the canyon and taken to the burial site by railroad using a train of several cars to provide sufficient distance between the engine crew and the source of radiation (see Figure 1.8).

The car is lifted from the track by a long-boom crane shown in the upper left of Figure 1.9 and dragged by a long cable to a pit previously excavated. Figure 1.9 also shows the radiation field being monitored with a "Cutie-Pie" type survey meter by the health physicist employee shown at the right. Earth will be pushed into the pit by use of bulldosers with metal shields for protection of the operators.

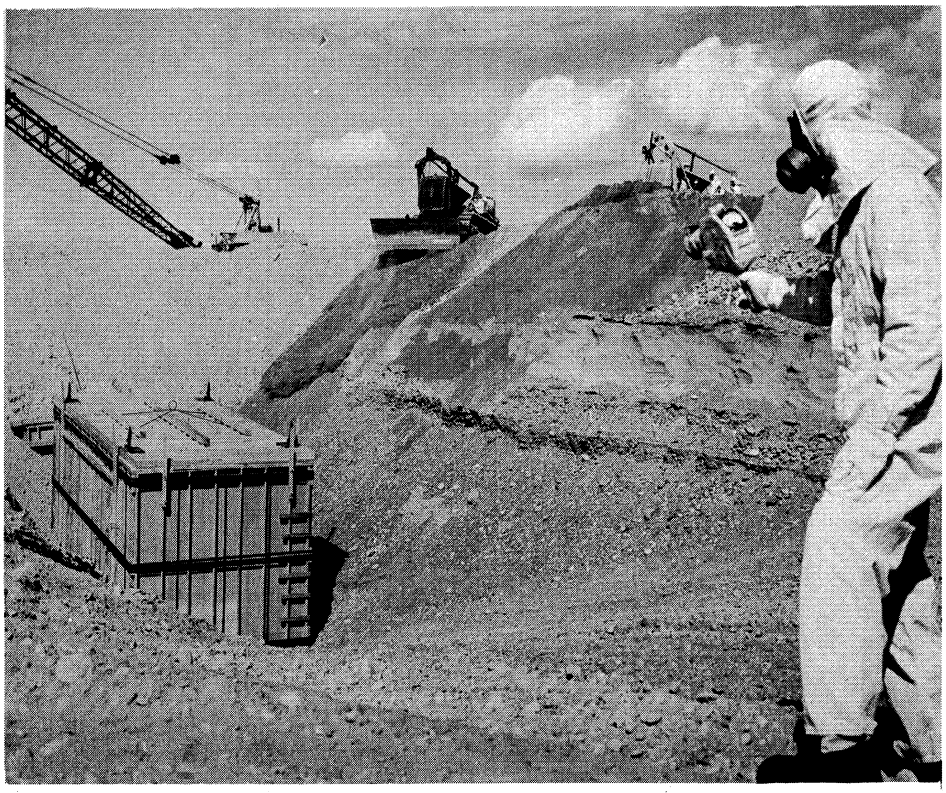

Figure 1.9 Burial of highly radioactive waste at Hanford (Courtesy of General Electric Co.)

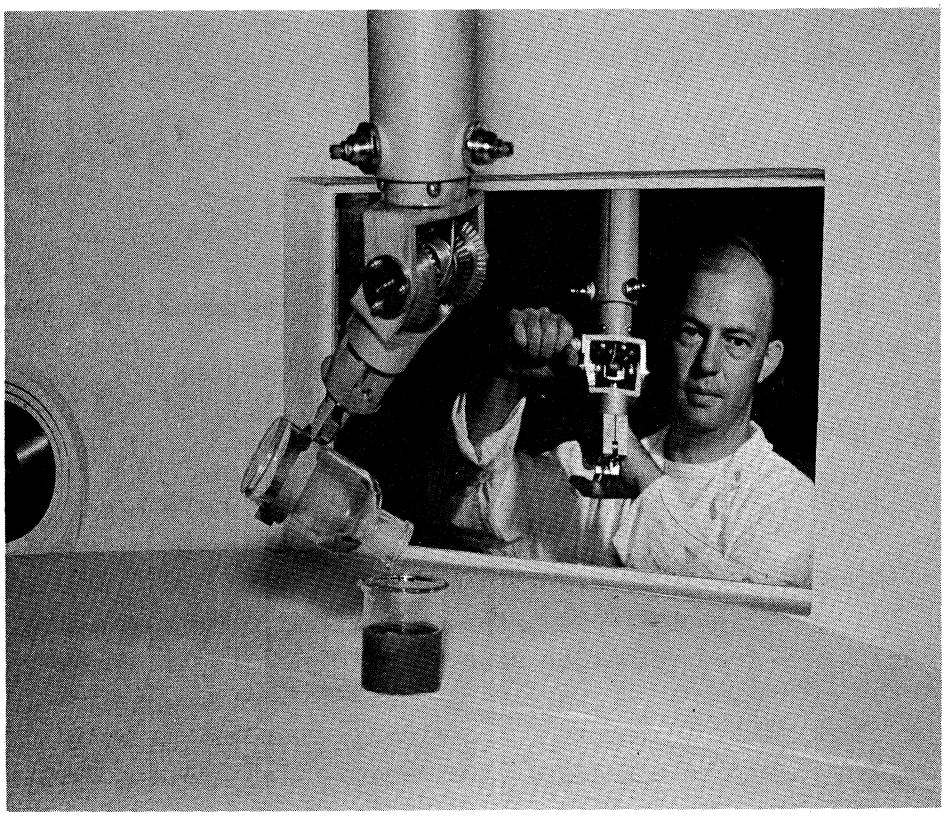

Figure 1.10 Operator working behind heavy shield and using remote manipulator (Courtesy General Electric Co.)

Time When the task to be performed with radioactive materials is such that high dosage rates are found where the workers must be during the operation, personal exposure may be minimized by reducing the time spent in the radiation field to a minimum. A second rule might be stated: "Leave the radiation area as soon as possible."

Repeated "cold runs" prior to an experiment with radioactivity provide the best assurance that the experiment can proceed safely and quickly when the radioactivity arrives and the "hot run" proceeds. In this way, mechanical and manual operations which may cause unexpected delay are discovered and corrected with no radiation hazard to personnel and the "hot run" can proceed with minimal delays. Of prime importance, also, in minimizing delays during operations with radioactive materials is the elimination or simplification of complex or intricate assembly steps. Close mechanical tolerances and squeeze fits of mechanical equipment and parts should be eliminated wherever possible to prevent binding or jamming during a transfer.

Mass When the use of distance and time are not sufficient to reduce exposures to a tolerable level, the use of shielding materials becomes necessary. As has been previously discussed, radiation interacts with matter and thus intensities may be reduced. The placing of mass (water, concrete, lead) between the radioactive material and the worker results in reduced radiation levels. The third rule might state: "When it is necessary to remain near a source of radiation for an extended period, be certain that there is sufficient shielding material."

For a point source, these qualitative rules may be stated mathematically for a particular physical configuration,

$$R = K\int_0^t \frac{e}{r^2}^{-\mu x}\, dt$$

where R = dose received

K = a constant determined by the nature of the source and the absorber, including build-up factors.

t = exposure time

μ = linear absorption coefficient of shielding material

x = thickness of absorber

r = distance from radiation source

It is clear that, in order to minimize R, r should be maximized (the first rule), t should be minimized (the second rule) and x should be maximized (the third rule).

The concept of a permissible dose was introduced previously. If, however, one accepts a certain dose as being "acceptable" or "safe" when taken for a certain (limited) time then the further reduction of R, once this level has been reached, is unnecessary. The use of shielding in addition to distance to protect personnel is illustrated in Figure 1.10 which shows an operator at Hanford working behind a heavy shield, using a remote-manipulation tool. The observation opening is of the lead-glass shielded-window type. The operator is using the mechanical hand to pour a liquid from one container to another and controls the procedure from behind the protective wall.

Additional information on shielding is given in Chapters 2 and 4 and on health physics in References 108-118.

References - Chapter 1

1. Morgan, K. Z., "Health Physics and Radiation Protection," in Medical Physics, Vol. II, Chicago Yearbook Publishers, Inc., Chicago, Ill., 1950

2. Braasch, N. K. and Nielson, M. J., "A Study of the Hands of Radiologists," Radiology, 51, 719, 1948

3. Robinson, J. N. and Engle, E. T., "The Effect of Neutron Radiation on the Human Testes: A Case Report," J. Urol., 61, 1949

4. Frieben, J., "Cancroid des rechten Handmekens," Dtsch. med. Wschr., 28, 335, 1902

5. Becquerel, H. and Curie, P., "Action Physiologique des rayons radium," C. R. Acad. Sci., Paris, 132, 1289, 1901

6. Curie, E., "Madame Curie," Translated by V. Sheean. Wm. Heinemann Ltd., London and Toronto, 1938

7. "Control of Radiation Hazards in the Atomic Energy Program," U.S. Atomic Energy Commission, Wash., D.C.,1950

8. "Concepts of Radiological Health," U. S.Dept. of Health, Educ. and Welfare, U.S. Govt. Print. Office, Wash., D.C., 1954

9. Martland, H.S., "The Occurrence of Malignancy in Radioactive Persons: A General Review of Data Gathered in the Study of Radium Dial Painters with Special Reference to Occurrence of Osteogenic Sarcoma and Interrelationship of Certain Blood Diseases," Amer. J. Cancer, 15, 2435, 1931

10. Code, S., "Malignant Disease and its Treatment by Radium, Williams and Wil-

11. Hempelmaun, L. H., Sisco, H. and Hoffman, J. G., "The Acute Radiation Syndrome: A Study of Nine Cases and a Review of the Problem," Ann. intern. Med., 36, 1952

12. "Radiation Safety and Major Activities in the Atomic Energy Programs, July-December 1956," U.S. Atomic Energy Commission, Wash., D.C., January 1957, ibid, Jan.-Dec. 1959, USAEC, Wash., D.C., Jan. 1960

13. Morgan, K. Z., "Historical Sketch of Radiation Protection Experience and Increasing Scope of Radiation Protection Problems," in Lectures at In-service Training Course in Radiological Health," The University of Michigan, Ann Arobr, Mich., 1951

References Chapter 1 (Contd.)

14. "Report of the International Commission on Radiological Units and Measurements (ICRU), 1956," National Bureau of Standards Handbook 62, April 10, 1957

15. Tischer, R. G. and Kurtz, G. W., "Mechanism of Action of Ionizing Radiations on Living Matter," U.S. Army Quartermaster Corps., U.S. Dept. Comm., Off. of Tech. Services, Wash. D.C., 178, 1957

16. Title 10 - Atomic Energy, Chapter 1 - Atomic Energy Commission, Part 20 - Standards for Protection against Radiation. Federal Register, January 29, 1957

17. Plough, H. H., "Radiation Tolerances and Genetic Effects," Nucleonics, 10, No. 8, 16, 1952

18. Hine, G. J. and Brownell, G. L., Radiation Dosimetry, Academic Press, New York, New York, 1956

19. Warren, S. and Bowers, J. Z., "The Acute Radiation Syndrome in Man," Ann. intern. Med., 32, 1950

20. Wolf, B. S., "Medical Aspects of Radiation Safety," Nucleonics, 3, 25, 1948

21. Lawrence, J. and Hamilton, J., "Advances in Biological and Medical Physics," Academic Press, Inc., N. Y., 1951

22. Henshaw, P. and Hawkins, J., "Incidence of Leukemia in Physicians," J. Nat. Cancer Inst., 4, 339, 1944

23. March, H., "Leukemia in Radiologists in a 20-year period," Amer. J. med. Sci.,220, 1950

24. Auerbach, O., Friedman, M., Weiss, L., and Amory, H. I., "Extraskeletal Osteogenic Sarcoma Arising in Irradiated Tissue," Cancer, N. Y., 4, 1095, 1951

25. De Young, R., "The Development of Sarcoma in Bone Subjected to Irradiation," Amer. Surgeon, 18, 816, 1952

26. Evans, R. D., "Quantitative Aspects of Radiation Carcinogenesis in Humans," Acta Un. int. Cancr., 6, 1229, 1952

References Chapter 1 (Contd.)

27. Furth, J. and Upton, A. C., "Vertebrate Radiobiology: Histopathology and Carcinogenesis," Annu. Rev. Nuc. Sci. 3, 303, 1953

28. Goldberg, R. C. and Chaikoff, I. L., "Induction of Thyroid Cancer in the Rat by Radioactive Iodine," Arch. Path. (Lab. Med.) 53, 22, 1952

29. Spitz, S. and Higginbotham, N. L., "Osteogenic Sarcoma Following Prophylactic Roentgen-ray Therapy," Cancer, N. Y., 4, 1107, 1951

30. Evans, T. C., "Biological and Medical Effect of R diation at Low Levels," in Lectures at Inservice Training Course in Radiological Health, the University of Michigan, Ann Arbor, Mich., 1951

31. Yockey, H. P., "Radiation Aging and its Relation to the Principles of Health Physics," Health Physics, Vol. I, No. 4, 417, 1959

32. Chital, C. M., "Studies on the Dynamics of Morphogenesis and Inheritance in Experimental Reproduction," J. exp. Zool., 14, 1913

33. Jacobson, L. O. and Marks, E. K., "The Hematological Effects of Ionizing Radiations in the Tolerance Range," Radiology, 49, 286, 1947

34. Burstone, M. S., "Radiobiology of the Oral Tissues," J. Amer. Dent. Ass. 47, No. 6, 630, 1953

35. Burstone, M. S., "Studies on Effect of Radioactive Colloidal Gold on the Development of the Oral Structures of the Mouse," Arch. Path. (Lab. Med.), 50, 419, 1950

36. Ferguson, J. H., Andrews, G. A. and Brucer, M., "Blood-clotting Studies on Dogs Internally Irradiated with Radiogold,"Proc. Soc. exp. Biol., N.Y., 80, 541, 1952

37. Furth, J., Andrews, G. A., Storey, R. H. and Wish, L., "The Effect of X-irradiation on Erythrogenesis, Plasma and Cell Volumes," Sth. med. J. Nashville, 44, 85, 1951

38. Goldie, H., Tarleton, G. J., Jr., Jeffries, B. R. and Hahn, P. F., "Effect of Repeated Doses of External and Internal Irradiation on Structure of the Spleen," Proc. Soc. exp. Biol., N.Y., 82, 395, 1953

References Chapter 1 (Contd.)

39. Odeblad, E., "A Study of the Short-time Effects on the Mouse Ovary of Internal Irradiation with P-32," Acta radiol., Stockh., 38, 33, 1952

40. Taymor, M. L., Gold, N., Sturgis, S. H., Meigs, J. V. and MacMillan, J., "Effects of Irradiation Upon the Uptake of Labeled Phosphorus in Human Carcinoma of the Cervix," Cancer, N.Y., 5, 469, 1952

41. Wachowski, T. J. and Chenault, H., "Degenerative Effects of Large Doses of Roentgen Rays on the Human Brain," Radiology, 45, 227, 1945

42. Warren, S., Holt, M. W. and Sommers, S. C., "Some Early Nuclear Effects of Ionizing Radiation," Proc. Soc. exp. Biol., N.Y., 77, 288, 1951

43. Watts, W. E. and Mathieson, D. R., "Studies on Lymphocytes from Persons Treated with Radioactive Iodine," J. Lab. Clin. Med., 35, 885, 1950

44. Edelmann, A., "AAAS Symposium on Radiobiology," Nucleonics, 8, No. 4, 1951

45. Lampe, I. and Hodges, F. J., "Differential Tissue Response to Neutron and Roentgen R diation," Radiology, 41, 1943

46. Storer, J. and Harris, P., "Incidence of Lens Opacities in Mice Exposed to X-rays and Thermal Neutrons," LA-1455, Los Alamos Scientific Lab., U.S. Atomic Energy Commission, Wash., D.C., 1952

47. Brennan, J. T. et al., "The Biological Effectiveness of Thermal Neutrons on Mice," LA-1408, Los Alamos Scientific Lab., U.S. Atomic Energy Commission, Wash., D.C., 1952

48. Beck, J. S. and Meissner, W. A., "Radiation Effects of the Atomic Bomb Among the Natives of Nagasaki, Kyushu," Amer. J. clin. Path., 16, 586, 1948

49. Bennett, L. R., Chastain, S. M., Flint, J. S., Hansen, R. A. and Lewis, A. E., "The Late Effects of Roentgen Irradiation, I. Studies on Rats Irradiated Under Anoxic Anoxia," Radiology, 61, 441, 1953

References Chapter 1 (Contd.)

50. Bowers, J. Z. and Scott, K. G., "Distribution and Excretion of Electrolytes After Acute Whole-body Irradiation Injury, I. Studies and Radiopotassium," Proc. Soc. exp. Biol., N.Y., 78, 645, 1951

51. Brues, A. M., Stroud, A. N. and Rietz, L., "Toxicity of Tritium Oxide to Mice," Proc. Soc. exp. Biol., N.Y., 79, 174, 1952

52. Conger, A. D. and Giles, N. H., Jr., "The Cytogenetic Effect of Slow Neutrons," Genetics, 35, 397, 1950

53. DeCoursey, E., "Human Pathological Anatomy of Ionizing Radiation Effects of the Atomic Bomb Explosions," Military Surgeon, 102, 427, 1948

54. Evans, R. D., "Quantitative Inferences Concerning the Genetic Effects of Radiation on Human Beings," Science, 109, 299, 1949

55. Graff, W. S., Scott, K. G. and Lawrence, J. H., "Histological Effects of Radiophosphorus on Normal and Lymphomatous Mice," Amer. J. Roentenol., 55, 1946

56. Hale, W. M. and Stoner, R. D., "The Effect of Cobalt 60 Gamma Radiation on Antibody Formation and Immunity," International Record of Medicine, 165, 358, 1952

57. Hemplemann, L. H. et al., "The Acute Radiation Syndrome: A Study of Nine Cases and a Review of the Problem," Ann. intern. Med., 36, 279, 1952

58. Hennessey, T. G. and Huff, R. L., "Depression of Tracer Ion Uptake Curve in Rat Erythrocytes Following Total Body X-Irradiation," Proc. Soc. exp. Biol., N.Y., 73, 436, 1950

59. Holt, M. W., Sommers, S.C. and Warren, S., "Intra-nuclear Changes Resulting from Exposure to Ionizing Radiation as Detected in Frozen-dried Preparations," Lab. Investigation, 2, 408, 1953

60. Huff, R. L. et al., "Tracer Iron Distribution Studies in Irradiated Rats with Lead-shielded Spleens," J. Lab. clin. Med., 36, 40, 1950

References Chapter 1 (Contd.)

61. Hursh, J. B., Van Valkenburg, P. A. and Mohney, J. B., "Effect of Roentgen Radiation on Thyroid Function in Rats." Radiology, 57, 411, 1951

62. Koletsky, S. and Christie, J. H., "Effect of Antibiotic on Mortality from Internal Radiation," Proc. Soc. exp. Biol., N.Y., 75, 363, 1950

63. Lavik, P. S., Leonards, J. R., Buckaloo, G. W., Heisler, C. and Friedell, H. L., "Ineffectiveness of In Vivo Dialysis in Prolonging Life in X-irradiated Dogs," Proc. Soc. exp. Biol., N.Y., 83, 618, 1953

64. MacIntyre, W. J., Friedell, H. L. and Berg, M., "The Influence of X-Irradiation on the Disappearance of Radioactive Tracers from Circulating Blood," NYO-4014, Western Reserve University Report No. 110, U.X. Atomic Energy Commission, Wash., D.C., 1952

65. Martland, H. S., "The Occurrence of Malignancy in Radioactive Persons: A General Review of Data Gathered in the Study of Radium Dial Painters with Special Reference to Occurrence of Osteogenic Sarcoma and Interrelationship of Certain Blood Diseases," Amer. J. Cancer, 15, 2435, 1931

66. Mole, R. H., "Whole Body Irradiation -- Radiobiology or Medicine?" Brit. J. Radiol., N. S., 26, 234, 1953

67. Noonan, T. R. and Noonan, A. M., "Effect of Roentgen Irradiation Upon Growth and Peripheral Blood Cell Levels of the Albino Rat," Fed. Proc., 11, 114, 1952

68. Patt, H. M., "Protective Mechanisms in Ionizing Radiation Injury," Physiol. Rev., 33, 35, 1953

69. Rugh, R., "Radiobiology Irradiation Lethality and Protection," Military Surgeon, 112, 395, 1953

70. Soberman, R. J., Keating, R. P. and Maxwell, R. D., "Effect of Acute Whole-body X-irradiation Upon Water and Electrolyte Balance," Amer. J. Physiol., 164, 450, 1951

References Chapter 1 (Contd.)

71. Supplee, H., Hauschildt, J. D. and Entenman, C., "Plasma Proteins and Plasma Volume in Rats Following Total-body-X-irradiation," Amer. J. Physiol., 169, 483, 1952

72. Thomson, J. F. Tourtellotte, W. W., Carttar, M. S., Cox, R. S., Jr. and Wilson, J. E., "Studies on the Effects of Continuous Exposure of Animals to Gamma Radiation from Cobalt 60 Plane Sources," Amer. J. Roentgenol., 69, 830, 1953

73. Trum, B. F., Haley, T. J., Bassin, M., Heglin, J. and Rust, J. H., "Effect of 400 Fractional Whole Body-irradiation in the Burro (Equus asinus asinus)," Amer. J. Physiol., 174, 57, 1953

74. Walso, C. E., "Toxicity of Inhaled or Ingested Radioactive Products," Nucleonics, 3, 1948

75. Copp, D. H. et al., "The Deposition of Radioactive Metals in Bone as a Potential Health Hazard," Amer. J. Roentgenol., 58, 1947

76. Code, S., "Malignant Disease and its Treatment by Radium," Williams & Wilkins Co., 270, 1941

77. Skow, R. et al., "Hazard Evaluation and Control After a Spill of 40 mg. of Radium," Nucleonics, 11, No. 8, 45, 1953

78. Messler, R. and Widdoes, L., "Evaluating Reactor Hazards From Airborne Fission Products," Nucleonics, 12, No. 9, 39, 1954

79. Faarman, A. and Shamos, M., "Effect of Fall-Out from Atomic Blast on Background Counting R te," Nucleonics, 11, No. 6, 80, 1953

80. Lewis, W. B., "The Accident to the NRX Reactor on December 12, 1952," Report DR-32, Chalk River, Canada, 1953

81. Hurst, D. G., "The Accident to the NRX Reactor, Part II, Report 6PI-14 Chalk River, Canada, October 23, 1953

82. Gilbert, F. W., "Decontamination of the Canadian Reactor," Chem. Eng. Progress 50, 267-71, May, 1954

83. Russell, W. L., Russell, L. B. and Kelly, E. M., "Radiation Dose Rate and Mutation Frequency," Science 138, 19 December 1958

References Chapter 1 (Contd.)

84. National Acad. of Science "Digest of Findings and Recommendations," U.S. Govt. Print. Office, Wash., D.C., 1956

85. Cantril, S. T. and Parker, H. M., "The Tolerance Dose," MDDC-110 US Atomic Energy Commission, Wash., D.C., 1945

86. Carling, E. R. et al., "Radiological Protection - International Commission Recommendations," Nucleonics, 8, No. 1, 31, 1951

87. National Committee on Radiation Protection "Maximum Permissible Body Burdens and Maximum Permissible Concentrations of Radionuclides in Air and in Water for Occupational Exposure," National Bureau of Standards Handbook 69, June 5, 1959

88. Cowan, F. P., "Inantitative Summary of Natural Radiation and Naturally Occurring Isotopes," in Lectures at Inservice "Training Course in Radiological Health" The University of Michigan, Ann Arbor, Mich., 1951

89. Lewis, L. and Coplan, P. E., "The Shoe-Fitting Fluoroscope as a Radiation Hazard," Calif. Med., 72, 1950

90. "Control of Radiation Hazards in the Atomic Energy Program," U.S. Atomic Energy Commission, Wash., D.C., 1950

91. Lane, W. et al., "Contamination and Decontamination of Laboratory Bench Top Materials," Nucleonics, 11, No. 8, 49, 1953

92. Ross, D. H., "Cleaning Contaminated Surfaces," Soap Sanit. Chemicals, 27, 1951

93. Brown, R. E. et al., "Disposal of Liquid Wastes to the Ground," A/Conf./p 565, United Nations, N.Y., 1956

94. Mawson, C. A., "Waste Disposal Into the Ground," AECL-211, A/Conf./p 12; Atomic Energy of Canada Ltd., Chalk River, Ont. Canada, United Nations, N.Y. 9, 676, 1956

95. Ginell, W. S. et al., "Ultimate Disposal of Radioactive Wastes," Nucleonics, 12, No. 12, 14, 1954

96. Jensen, J. H., "Radioactive Waste Disposal in the Ocean," Nat. Bur. Standards, Handbook 58, U.S. Govt. Print. Office, Wash. D.C.

References Chapter 1 (Contd.)

97. Seligman, H., "The Discharge of Radioactive Waste Products in the Irish Sea," A/Conf./p 418, United Nations, N.Y., 9, 401, 1956

98. Renn, C. E., "Disposal of Radioactive Wastes at Sea," A/Conf./p 569; United Nations, N.Y., 9, 718, 1956

99. Taylor, L. S., Paper Presented Before Amer. Nuc. Soc., Wash., D.C., Dec., 1956

100. "The Biological Effects of Atomic Radiation," National Academy of Sciences, U.S. Govt. Print. Office, Wash. D.C., 1956

101. Anonymous, "Nuclear Industry Takes Report on Radiation Effects in Stride," Nucleonics, 14, 1956

102. Braestrup, C. B. and Wyckoff, H. O., "Radiation Protection," Charles C. Thomas, Springfield, 1958

103. Recommendations of the ICRP, Main Commission Report Sept. 9, 1958 Pergamon Press, London, England

104. Recommendations of the ICRP, Report of the Committee on Permissible Dose for Internal Radiation 1958 revision, Pergamon Press, London 1958

105. Maximum Permissible Body Burdens and Maximum Permissible Concentrations of Radionuclides in Air and Water for Occupational Exposure Recommendations of the NCRP National Bureau of Standards Handbook 69

106. Addendum to National Bureau of Standards Handbook 59, Permissible Dose from External Sources of Ionizing Radiations, NBS, April 1958

107. "Rules and Regulations, Title 10-Atomic Energy, Part 20-Standards for Protection Against Radiation," Federal Register, Nov. 17, 1960

108. Davidson, H. O., "Biological Effects of Whole-Body Gamma Radiation on Human Beings," The John Hopkins Press, Baltimore, Md., 1957

109. Price, W. J., "Radiation Detection," McGraw-Hill Book Co., New York, 1958

110. "Protection against Neutron Radiation up to 30 Million Electron Volts," National Bureau of Standards Handbook 63, November 22, 1957

References Chapter 1 (Contd.)

111. Claus, W. D., "Radiation Biology and Medicine," Addison-Wesley Publ. Co., Reading Mass., 1958

112. "Medical Research Council, "The Hazards to Man of Nuclear and Allied Radiations," Her Majesty's Stationery Office, London, June 1956

113. "Effect of Radiation on Human Heredity," World Health Organization, Geneva, 1957

114. Blatz, H., "Radiation Hygiene Handbook," McGraw Hill Book Co., New York, 1959

115. Neel, J. V. and Schull, W. J., "The Effect of Exposure to the Atomic Bombs on Pregnancy Termination in Hiroshima and Nagasaki," National Academy of Sciences-National Research Council, Wash., D.C., 1956

116. Novak, J. R., "Radiation Safety Guide, ANL-5574," June 1956

117. National Committee on Radiation Protection, "Permissible Dose from External Sources of Ionizing Radiation," National Bureau of Standards Handbook, 59, September 24, 1954. Addendum, January 8, 1957

118. Glasstone, S., "The Effects of Nuclear Weapons," U.S. Atomic Energy Commission, June 1957

Chapter 2

The Design and Use of Radiation Laboratories

The major problem in the design of a radioisotope or radiation laboratory is the attainment of safety, economy, and convenience. These three features, while always interrelated, often seem incompatible. Consideration of public safety requires that no hazardous materials be released to the environs by way of the water effluent, the discharged air, or the homeward-bound employee.

Economy is a consideration of major importance to the industry or institution entering this relatively new field. It is, of course, a relative problem which is quite dependent upon the circumstances. A laboratory that might be relatively expensive as compared to other laboratories on a university campus could at the same time be austere by the standards of large radiation laboratories.

The burden of defining economy, in light of a particular laboratory design, can best be borne by a qualified architect in consultation with a competent radiation expert. Expenditures are justified only if they enhance personnel safety or adequately increase laboratory versatility. The architect should consider critically suggestions relating to such things as (1) strippable coatings on walls and ceiling; (2) stainless steel on all bench tops; (3) thick concrete shield walls around tracer-level laboratories; (4) "special" pipe and valves for low-level waste lines; and a myriad other expenses usually unnecessary. Convenience, with respect to laboratory design, might be defined as "that design which places nearest to the laboratory worker (a) those things which he uses most frequently and (b) those places to which he ventures most often." Consideration of convenience is important in all instances,

including the single-room laboratory as well as the complex multiroom arrangement. Again the problems of a specific design are best referred to the architect-consultant team capable, on the one hand, of defining architectural practice as it has evolved to date and, on the other hand, of modifying these practices to conform to the needs and restrictions of an isotope or radiation facility.

Morgan (1) has defined five design variables: the type and level of radioactivity, the type of investigation; the variety of isotopes and uses, the work volume, and the number of people involved. The applicability of each of these design variables to a specific laboratory is apparent. For instance, the design of a microcurie-level laboratory for tracer investigations has only one thing in common with the design of a hot-cell metallurgical laboratory for the investigation of the effects of neutron irradiation upon metal samples. The common bond between these two situations is the presence of nuclear radiations. In all other respects the two laboratories vary tremendously.

The term "hot lab" or "high-level" laboratory is used to describe a laboratory and manipulation facility designed to accommodate multicurie levels of radioactivity. In its most broad use this term would describe a building with its enclosed shielding facilities together with the required remotely operated tools and handling devices. The function of such a laboratory is to permit the investigator to carry on research, development, testing, or experimental work, as is normally required, but in a new and different fashion. The investigator works with highly hazardous material in facilities specifically designed to protect him from the damaging effects of the radiation.

Safety in hot-laboratory design is most easily attained by adopting a philosophy of containment of all radioactive materials from the time they enter the building as samples until the time they leave the building as concentrated, confined wastes. This criterion is most satisfactorily approached by providing

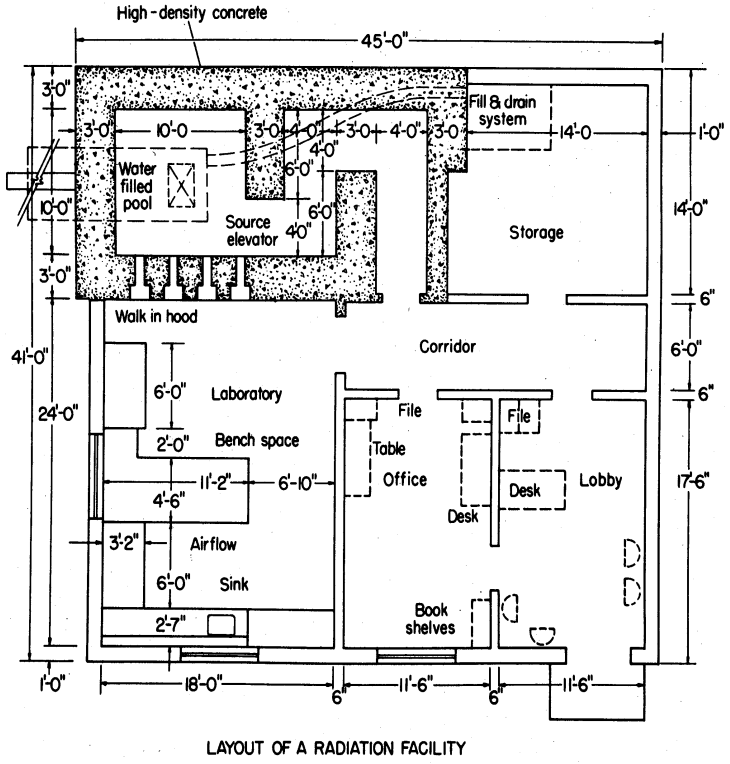

Figure 2.1 Floor plan of a proposed concrete-shielded gamma-irradiation hot cell

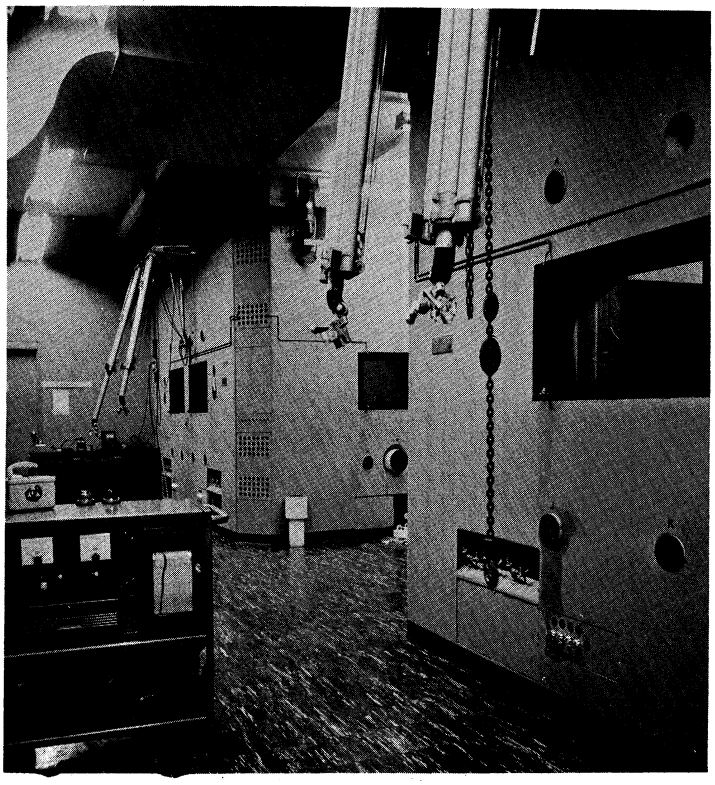

Figure 2.2 Hot cells in the Michigan Memorial-Phoenix Laboratory constructed of barytes concrete in a steel-plate shell and equipped with Argonne Model 8 Manipulators

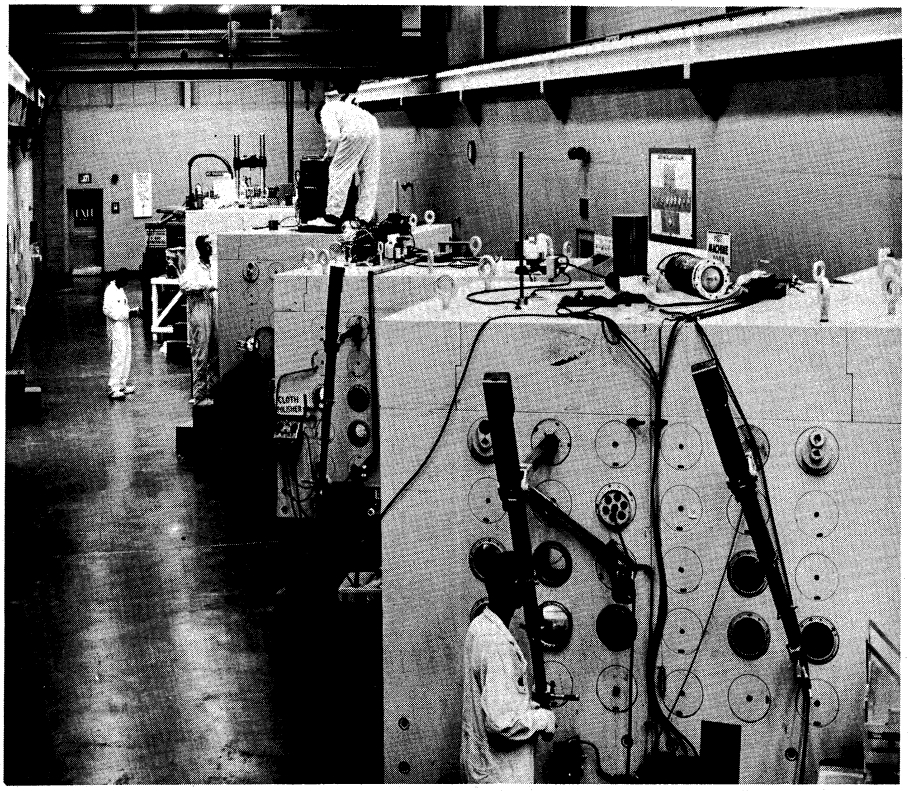

Figure 2.3 Canyon view in radiometallurgy building at Hanford showing battery of hot cells constructed of cast iron (Courtesy General Electric Co.)

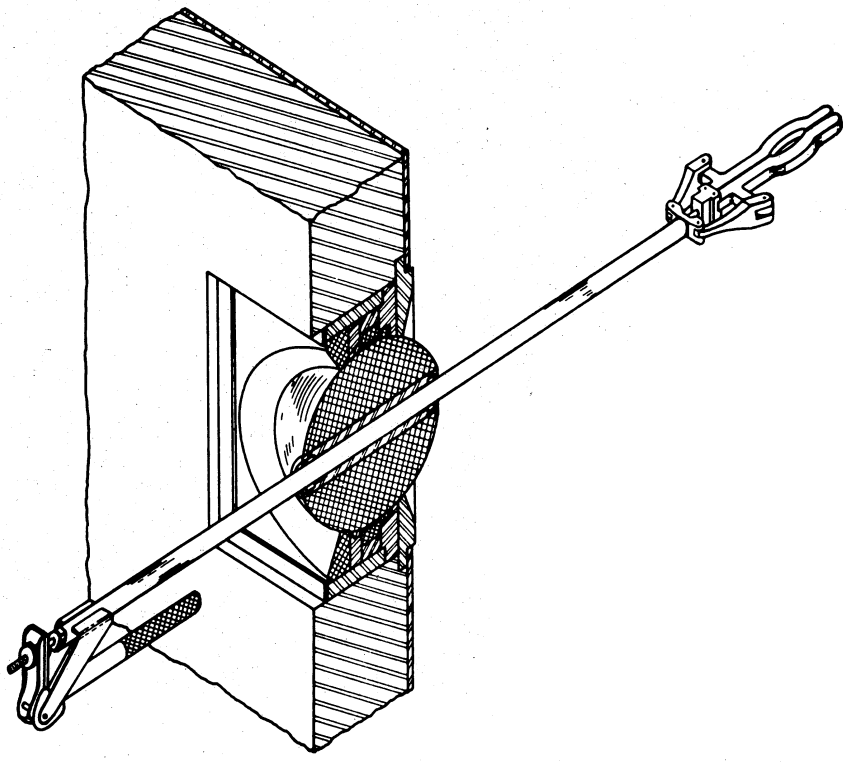

Figure 2.4 Ball-socket manipulator in radiation-shield wall (6)

a pyramid of varying application units. To illustrate: at the top of the pyramid one finds the high-level "hot cell" capable of handling thousands of curies of activity. Since the occasional very high-level sample gives rise to numerous intermediate-level samples as cut-off pieces or solutions of a portion of the hot sample, there exists a necessity for a number of the intermediate-level facilities. The next step down the pyramid finds one faced with confinement requirements for lower-level millicurie quantities of radioactive materials since the samples from the junior caves or shielded gloved-box facilities will yield low-level samples for further analysis. In this third step on the pyramid, one would find gloved boxes or hoods with temporary shielding built up to meet the immediate need. The broad base of the pyramid includes facilities for waste handling, decontamination, and sample storage.

2.1 Hotcells

The hot cell is a small laboratory space completely isolated from the laboratory worker by heavy shielding walls. Operations are performed within the laboratory space by the operator positioned outside the shielding wall and using a remote-type manipulator which operates over or through the wall. The hot cells in existence may be divided into high-level or intermediate-level facilities, depending on their designed capacity for radioactive materials. They may further be subdivided into open-top or completely closed units. The open-top units have an upper-limit capacity defined by the "sky shine" from sources located within the shield enclosure. This upper limit is in the neighborhood of 25 to 50 curies of a gamma-emitting source. The completely closed hot cell facility may be designed with shielding adequate to handle any contemplated radiation-intensity source.

Laboratory space should be provided immediately adjacent to the hot cell source. It is recommended that these supporting laboratories be located on eigher or both unrestricted walls as illustrated in Figure 2.1. This permits

the installation of plugged holes through the walls for passage of process lines, heating elements, control instrumentation, etc., with the shortest possible runs from the laboratory into the irradiation space.

The design as pictured in Figure 2.1 incorporates the advantages of an outside loading facility with an under-the-wall water canal. Further, it also includes a laboratory area immediately adjacent to the gamma-irradiation room with controlled plugged holes leading through the wall. The walls of the gamma-irradiation area may be constructed of ordinary or high-density barytes concrete. If the water pool is designed to permit draining and repainting, the inner surface may be finished with Amercoat paint. The remainder of the building could be constructed of cement-block wall finished in masonry paint. The floors could be asphalt tile covered, except in the cave area where they are vinyl or rubber-base cement enamel painted (asphalt tile will not withstand continued irradiation).

The ports leading through the wall from the laboratory to the irradiation room are standard steel pipe collared to eliminate the radiation leakage from a straight-through crack. To use any one of the access holes, the steel pipe filled with concrete would be removed and in its place may be inserted a steel pipe with a helix of copper tubing leading through the pipe. The area surrounding the helix would be filled with lead. An alternative arrangement for short-term irradiation studies would be to place the process lines through the tubes and pack lead-shot-filled bean bags into the tubes around the process lines. Still a third alternative would be to place the copper tubing within the pipe then fill the pipe with a cement-lead mixture (2).

Figure 2.2 pictures two hot cells installed at the University of Michigan hot laboratory. These hot cells are patterned after the Argonne National Laboratory Metallurgy Cell (3). The cell has walls of high-density concrete

thirty-six inches thick contained with a 3/8" steel-plate shell. Window openings and ports for the passage of air, gas, water, and service lines were made in the shell before the concrete was poured. Tests on the 30-day aged concrete samples indicate that wall densities of about 220 pounds per cubic foot were attained in this shield. The cells are fitted with lead-glass windows of density comparable to the concrete wall. A set of two Argonne Model 8 Master_Slave Manipulators and a thousand-pound pot-lid crane are provided in each of the cells. Inside cell dimensions are 6 by 10 by 12-1/2 feet with a back opening of 6 by 7 feet closed by two fourteen-inch-thick steel doors.

The cell interior (walls, ceiling, and floor) is finished in Amercoat 33. Lighting is provided by overhead fluorescent tubes or sodium-vapor lamps mounted around the windows. Roughing filters for exhaust air are located inside the cave followed by two fiberglas prefilters and a Model A-1000 Cambridge absolute filter located outside and to the back of the cell. The cost (as of 1955) for a single 10,000-curie hot cell as pictured in Figure 2.2 is listed in Table 2.1.

The designer of the hot cell must consider such things as (a) shield structure, (b) ventilation and filtration, (c) manipulator choice, (d) viewing methods, (e) cell lighting, and (f) services to be provided in the cell. The first of these two, that is shield structure and ventilation-filtration techniques, have to do with the safety of the laboratory occupants.

The shield may be lead, iron, concrete, dense concrete, or any high-density material which will provide adequate shielding from the radiation sources contemplated within the cell structure. Thicknesses of these materials required will range in the neighborhood of from 2 to 12 inches of lead, 6 to 15 inches of iron, 20 to 70 inches of ordinary concrete, and 10 to 40 inches of high-density concrete. It is of first importance that the shield wall be of

uniform thickness and homogeneous construction to minimize the possibility of radiation leakage through a void area within the shield. With this in mind, concrete shields are constructed with care (4). It is important that the interior surfaces of the cell be smooth and fissure free to permit easy decontamination.

Table 2.1

Costs* For A 10,000-Curie Hot Cell (5)

Steelwork, including follow blocks, doors, shell, port plugs, etc.	$ 54,200
Barytes concrete (44 yd^3 at $120/$yd^3$)	5,280
Windows (3)	30,000
Pot-lid crane	3,400
Manipulators (1 pair Argonne Model 8)	8,000
Manipulator mounting blocks	1,000
Sodium-vapor lamps	1,750
Electrical and sheetmetal	3,500
Door drives and installation	4,100
Painting	800
Contract costs	15,000
	$ 127,030

* Based on 1955 prices

Multicurie hot-cells constructed of cast iron are used in the radiometallurgy building at Hanford for research with radioactive metals (see Figure 2.3). The cells afford safe working conditions with highly radioactive alpha-beta-and gamma-emitting materials, while allowing a high degree of flexibility in operation. The cells are put together in sections and can be dismantled with the aid of an overhead crane. Numerous plugs in the sides can be removed

to permit installation of special plugs containing lead-glass windows or the insertion of remote-manipulation equipment. Electrical and gaseous services are available inside the cells.

The completely closed cell must always be ventilated or exhausted to the point that it is the low-pressure area of the whole building. This insures that all air leakage will be from outside into the cell and provides protection to personnel from the possible hazard of airborne contamination. In the open-top or canyon type of shield enclosure, air ventilation must be away from the operator and into the enclosure. All ventilation air from the hot cells should be filtered before it is exhausted to the atmosphere.

2.2 Manipulators

The manipulator is a tool or device which translates the operator's movements from his hands to a mechanical contrivance remotely located. The simplest manipulator would be a pair of tongs which provide the operator with distance protection. The manipulators of greatest interest in hot-cell design are those which provide the operator with maximum dexterity for minimum mental effort.

The manipulator type available may be divided into essentially three categories, the ball-socket units, the electrically actuated units, and the pantagraph or mechanical models.

Figure 2.4 illustrates a ball-socket manipulator. It consists of a rod which pushes through a shield ball which in turn rides in a socket mounted in the shielding wall. These manipulators are applicable to wall thicknesses of about 6 inches or less. Up and down and right to left motion is attained by moving the ball in its socket. Front to back motion is attained by sliding the tube through the ball. The tube may be turned to tip the end of the manipulator and items are grasped by actuating the handle which opens and closes the tong slave end. (6,7)

Electrically or hydraulic driven manipulators are available with slave motions in x, y, and z coordinates. The manipulator rides on tracks mounted on the front and rear walls of the hot cell. A control console is provided which mounts external to the hot cell and provides control for the x, y, z motions as well as tong gripping, wrist rotation, elbow swing, and shoulder rotation. The main attribute lies in their capacity to lift or move large weights. Electric manipulators may be procured which will handle a 5,000-lb vertical lift. The main disadvantage lies in the lack of force indication of tong squeeze. The pressure applied by the tong may be indicated to the operator by sounds, lights, or a dial-pointer position, none of which are comparable to the actual hand resistance which one experiences in the mechanical or pantagraph-type manipulator.

Several models of the mechanical pantagraph manipulator have evolved over the past years. The most common unit presently being utilized is the Model 8 Argonne Master-Slave Manipulator pictured in Figure 2.2. Figure 2.5 is a sketch of a Model 8 Master-Slave installation showing the mounting conditions as well as the rotary and linear degrees of freedom. (8)

2.3 Viewing techniques

There are essentially four viewing techniques available to the hot-cell designer. The simplest of these is a combination of mirrors. A mirror system has the advantage of initial low cost and the disadvantage of reversed images at seemingly greater distances. A mirror system of viewing is particularly applicable in open-top cells.

A second system of viewing which combines mirrors with an optical-lens system is the periscope. They may be used in open-top cells for viewing over the walls with an assembly in the shape of a large U or they may be used in closed cells by putting a tube through the wall. A movable mirror can be

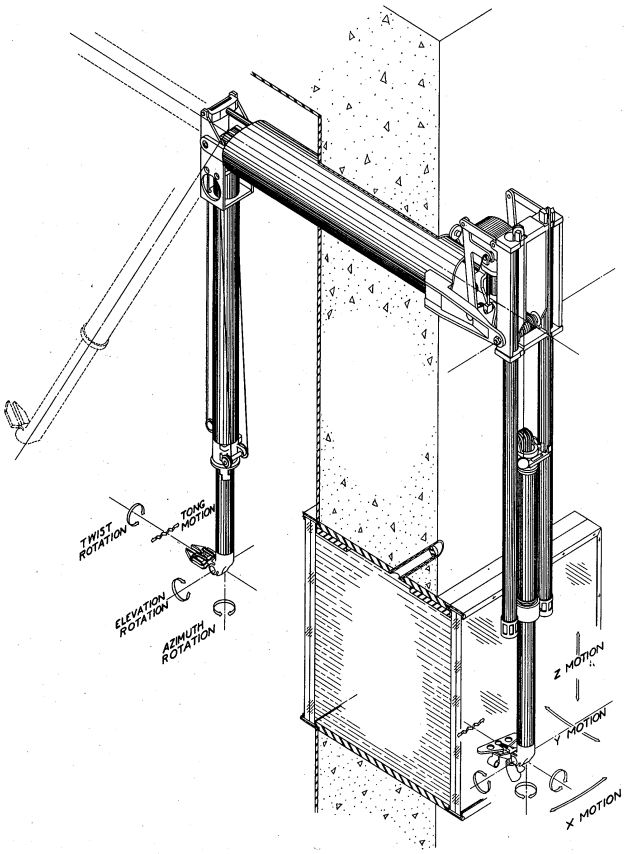

Figure 2.5 Argonne Model-8 Manipulator, illustrating the degrees of freedom (connecting linkages pass through the 8-inch-diameter tube. Rollers mounted around the tube permit rotation about the horizontal tube axis). (8)

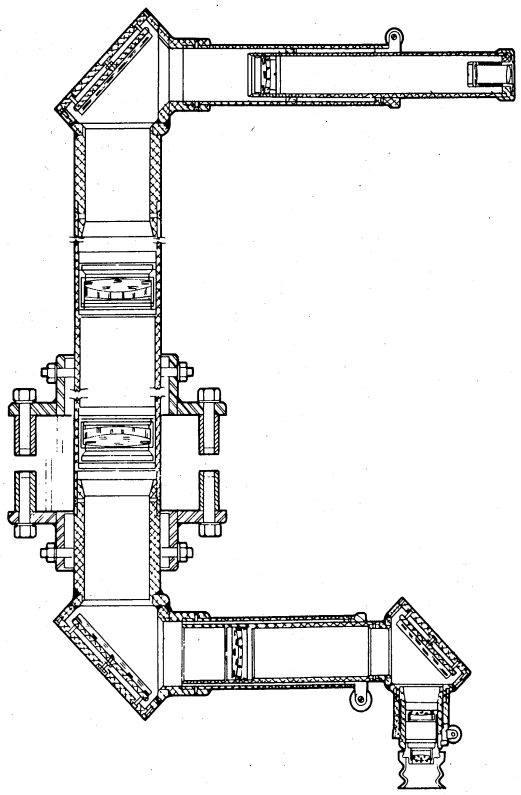

Figure 2.6 Sectional diagram of a periscope for viewing through the shield wall (7)

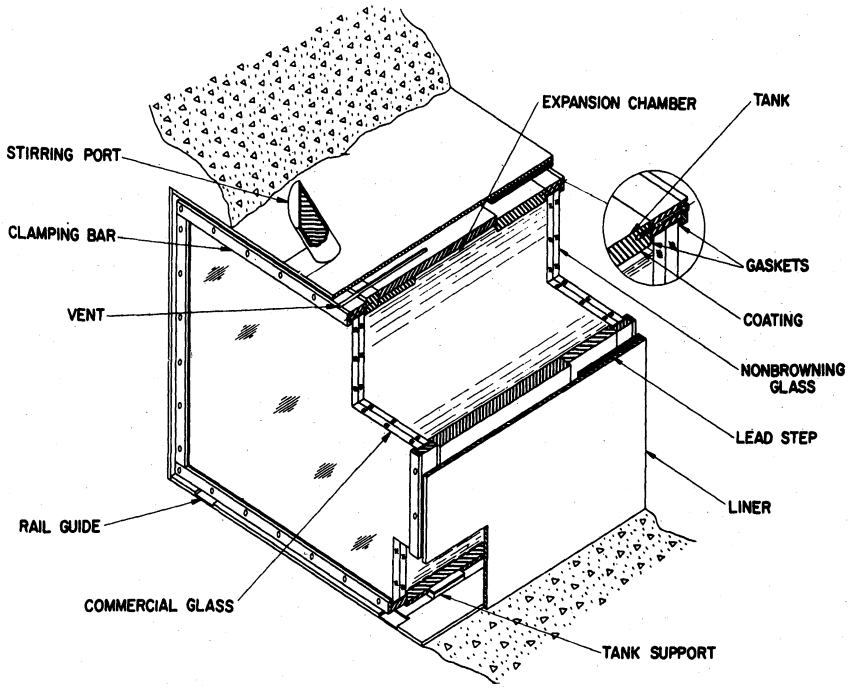

Figure 2.7 Isometric sketch showing construction details of a zinc-bromide window (7)

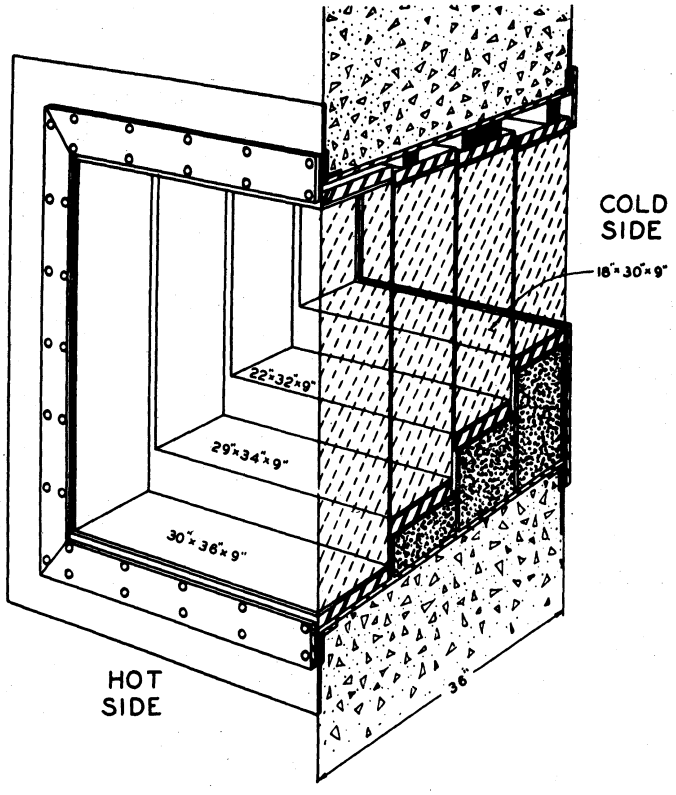

Figure 2.8 Isometric sketch showing construction details of a lead-glass shield window (8)

attached on the radiation side, with which the operator may scan the cell horizontally. Figure 2.6 is a sketch of a periscope for viewing through a shield wall. (7)

The most satisfactory viewing of the cell interior is attained by the use of windows through the cell wall. There are any number of window configurations available, varying from a small, cylindrical port to a large, square window. There are liquid windows made up of a zinc-bromide solution contained on the viewer's side by a laminated glass plate and on the radiation side by a cerium-stablized, nonbrowning, laminated glass plate. These windows have a specific gravity of 2.4, which is comparable to ordinary concrete. Figure 2.7 illustrates construction details of a zinc-bromide-solution window.(7)

Figure 2.8 shows details of a lead-glass window. This window may be constructed of lead glass of 3.5 specific gravity, in which case it would provide shielding equivalent to barytes concrete, or it may be made up of plates of glass of specific gravity 6.5, which would approach shielding equivalent to steel. An alternate technique is the construction of a combination lead-glass--zinc-bromide window. The failure of such a window would not leave one completely without shielding. (8)

These windows are normally fabricated as a unit contained within a closed tank which is installed in the shield wall. The inside and outside faces are of relatively inexpensive plate glass to protect the lead glass from abrasion and corrosive fumes. The inside plate-glass cover is made up of nonbrowning cerium-stabilized glass. The lead-glass windows are constructed of 4 to 6-inch-thick sheets with a mineral-oil filling between sheets to reduce interfacial reflections and increase light transmittance.

Closed-circuit television has been used to a very limited extent in hot-cell viewing to date. The lack of application appears to arise from two

causes. There has been little experience in the application of closed-circuit TV in radiation work and, second, there is the problem of attaining binocular vision, with its decided attribute of depth perception, by available TV systems.

Figure 1.11 shown in Chapter 1 is a view from the interior of a hot cell. The operator is pouring a radioactive solution into a beaker by use of a manipulator and is observing the operation through a lead-glass window.

2.4 Hot-cell operational problems

If one uses lead-glass windows or remote TV installations, the cell lighting requirements are quite stringent. Precise viewing of delicate operations requires from four to five hundred foot candles of light delivered in the closed cell. In addition to flourescent or incadescent lights, the cell designer normally provides sodium-vapor lamps capable of providing a single-spectrum light emission which minimizes the refraction problems inherent in multilayer glass windows.

One of the more complex operations to perform in a hot cell is the rotating of a crank or faucet. Therefore, all services are arranged on the cell face with controls within easy reach of the cell operator. Services such as air, gas, steam, hot-water, cold-water, vacuum, and drain lines should be installed on the face of the cell. These services are in turn taken into the hot-cell enclosure through pass-through ports in the shield wall. An alternative arrangement is to put the valve controls external to the cell and the delivery spigots within the cell.

In addition to the six major variables discussed, consideration must be given to the introduction, removal, and storage of radioactive samples. There are a number of techniques presently utilized, the simples being the introduction of the sample cask through doors located behind the hot cell. The cask is brought in and the cover removed by means of a crane located

either between the master-slave manipulators or on tracks at the ceiling of the hot cell. An alternative would be to locate a sample entry beneath the floor of the hot cell and hydraulically bring the sample into the hot-cell interior. Then it may be removed from its shield container and placed in position for testing, machining, or other studies. Still a third technique is sample entry into the hot cell from an underwater canal located adjacent to the hot-cell structure. This is a relatively simple entry technique which provides one with standby storage facilities beneath the water shield. If portions of the radioactive sample are to be removed from the hot cell, it is possible to design sample-removal trays which travel through the ports located in the walls of the hot cell.

Radiation contamination is a constant problem in hot-cell operations. Facilities must be provided for in-cell cleanup at the completion of any particular experiment. These facilities may consist of permanently mounted in-cell washdown hoses and in-cell vacuum cleaners with attached cyclone-type separators and absolute filters. Initial decontamination is done with the cell completely closed. When the radiation level is low enough, the cell is entered by the cell operators, attired in protective clothing, shoe covers, respirators, or supply air masks. These people remove the cell equipment piece by piece to a buffer or a secondary decontamination zone located external to the hot cell, where equipment is given a final decontamination or wrapped in protective tape to minimize the possibility of airborne contamination, and then relegated to storage.

Operation of a hot cell requires continuous mechanical maintenance together with intricate design and fabrication of mechanical devices capable of being remotely operated within the cell. This design, fabrication, and maintenance work is best performed by shop facilities located in the immediate

vicinity of the hot cell. The operating personnel of the hot lab must be provided with lockers, clothing-change rooms, and office space.

2.5 Junior caves and shielded glove boxes

The intermediate-level radiation sources of 1 to 100 curies are handled remotely in junior cave assemblies or lead-shielded gloved boxes. Figure 2.9 is a photograph of one of the junior caves at Hanford. It consists essentially of a chemical laboratory bench, complete with water, gas, and other services surrounded by a thick steel shield to protect the operator from radiation while working with radioactive materials. The operator can see what takes place through a thick window consisting of laminated plate glass or lead glass. The window is thick enough to provide the same protection from radiation as several inches of steel. The work is performed by means of remote handling devices that consist of rods placed in ball-and-socket joints in the front of the cave. These rods are equipped with pinchers that can be opened and closed to pick up glassware and other equipment and can be moved laterally and vertically in the ball joints or back and forth through sleeves in the joints.

Figure 2.10 is a photograph of two gloved-box units. The unit on the left is a 2-1/2 inch lead-shielded assembly for remote chemistry work. There are two ball-socket manipulators through the shield wall. The shield assembly is mounted on casters and rolls into position around a standard box such as the unit on the right in the photograph. Services for the gloved boxes are provided from the enclosed pipe chase pictured behind the boxes. Services provided are gas, water, air, vacuum, waste-water drain, and filtered exhaust-air outlet.

The shielded box is a small (about 9 cubic feet) self-contained laboratory which can be used for remote chemical, metallurgical, or biological

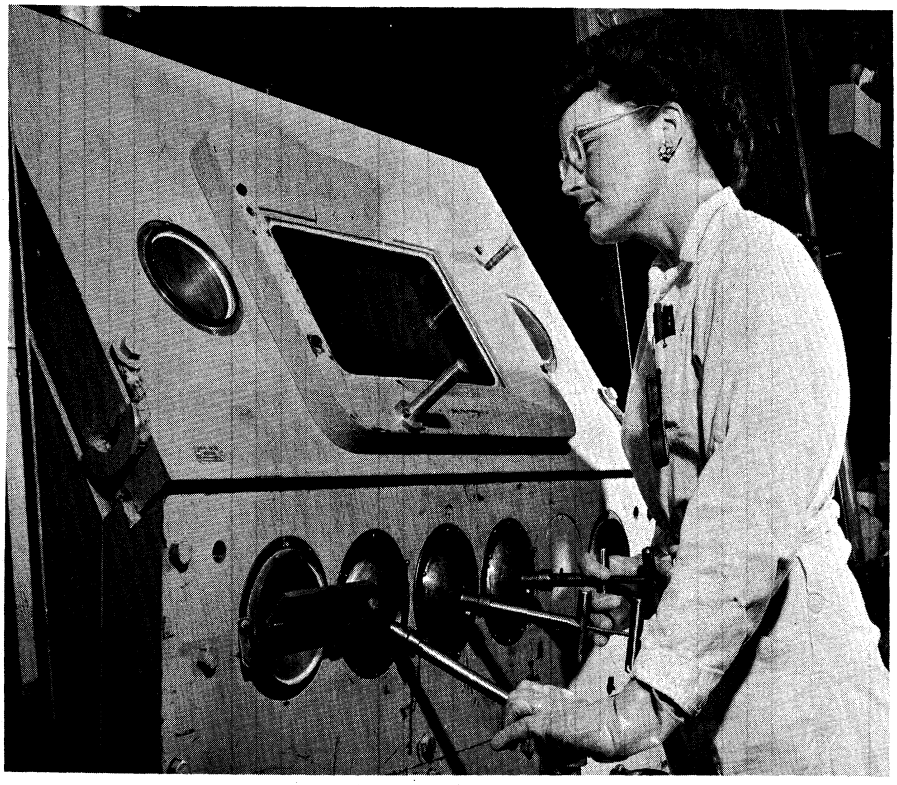

Figure 2.9 Junior cave used at Hanford (Courtesy of General Electric Co.)

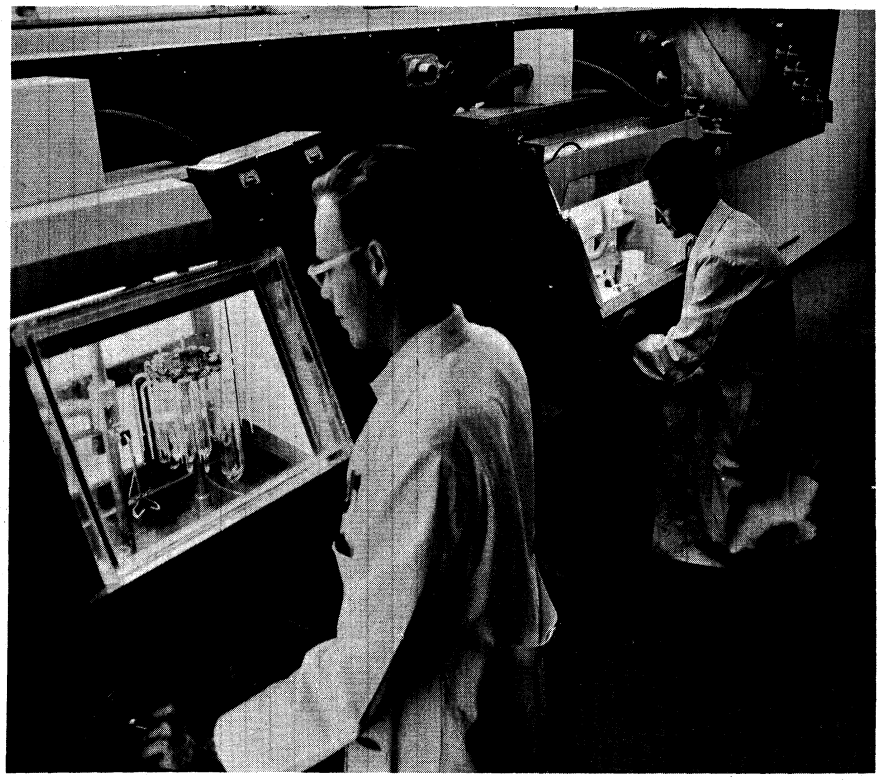

Figure 2.10 On the left, shielded-box assembly with ball-socket manipulators. On the right, standard gloved-box unit

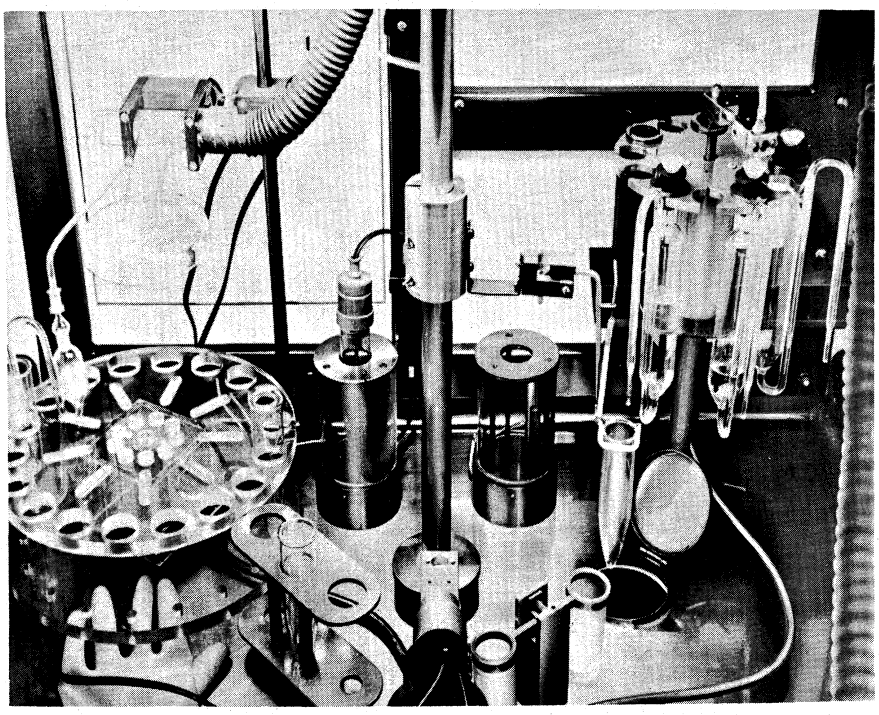

Figure 2.11 Interior view of a shielded-box unit equipped for remote radiochemistry work (Courtesy Kewaunee Mfg. Co., Adrian, Michigan)

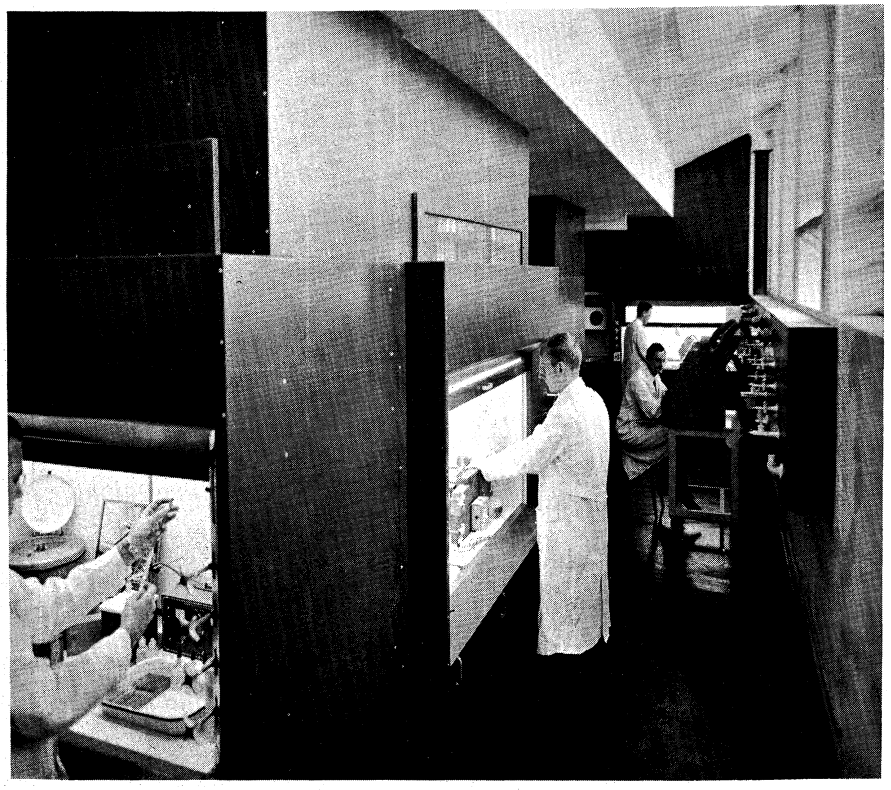

Figure 2.12 Photograph of a radiochemistry laboratory, showing the hood installations and gloved-box manifold assembly on the right (5)

investigations. Figure 2.11 is a photograph of the interior of a shielded box with remote-operated equipment for radiochemical separations. Table 2.2 is a cost summary for a basic shielded-box unit.

Table 2.2

Approximate Cost For A 1 to 10-Curie Shielded Box*

Item	Approximate Cost
Basic glove box	$ 595.00
Mobile stand for box	50.00
Lead-shield assembly, 2-1/2 inches	2,000.00
Two ball-socket tong manipulators	714.00
Fluorescent box light	75.00
Power panel assembly	52.00
High-efficiency exhaust filter	46.00
Lead-glass window	1,400.00
Miscellaneous small parts (trays, flexible duct, etc.)	200.00
	$ 5,132.00

*Courtesy Kewaunee Mfg. Co., Adrian, Mich.

One of the attributes of gloved boxes is the small-volume exhaust-air requirement. Most box installations are operated at 5 to 15 cubic feet per minute of exhaust. The box units should be used as open-front hoods for low-level work only since the airflow velocity into the box with the glove panel removed will be from 2 to 10 linear feet per minute. This is not sufficient airflow to guarantee transport of fumes or particulate.

Figure 2.12 is a photograph of a chemistry laboratory installation. The

hoods pictured are equipped with a bypass airflow arrangement which provides a constant airflow face velocity of 50 linear feet per minute independent of the area of the face opening. These hoods have rounded corners to eliminate turbulent airflow. Air filtration is provided by filter boxes mounted above each hood. The filter boxes contain fiberglas prefilters followed by Model A-1000 Cambridge absolute filters.

Figure 2.13 is a photograph of a walk-in hood installation. This hood is used to house large organic-syntheses assemblies for the preparation of carbon-14 labeled compounds. The exhaust-air filter boxes are mounted above the hood. The two manometers visible at each corner of the hood indicate pressure drop through the filter box and provide a constant check on the extent of filter dirt load.

2.6 The low-level or radioisotope laboratory

The simplest design for a radioisotope laboratory uses one room and contains a hood (or glove box), a sink, bench space, and storage room. A plan for a typical design for such a laboratory is given in Figure 2.14 and 2.15. The 300 square feet of floor space indicated provides areas for experimentation, sample assaying, and paper work. The desk section is lower than the bench section so the investigator may work comfortably when seated. A source storage location may be provided by building a temporary lead-brick shield assembly either under the glove box or in the storage closet. This one-room laboratory contains essential working facilities and is suitable for low-level tracer research work.

The restricted quarters in the one-room laboratory do, however, present some operational difficulties. First, there is the possibility of contaminating the counting equipment and desk section on one side of the room with radioactive materials from the experimental side of the room. The experimenter

Figure 2.13 Photograph of a "walk-in" hood capable of housing assemblies 6-1/2 feet high. A standard chemistry hood-bench assembly is visible in the background (5)

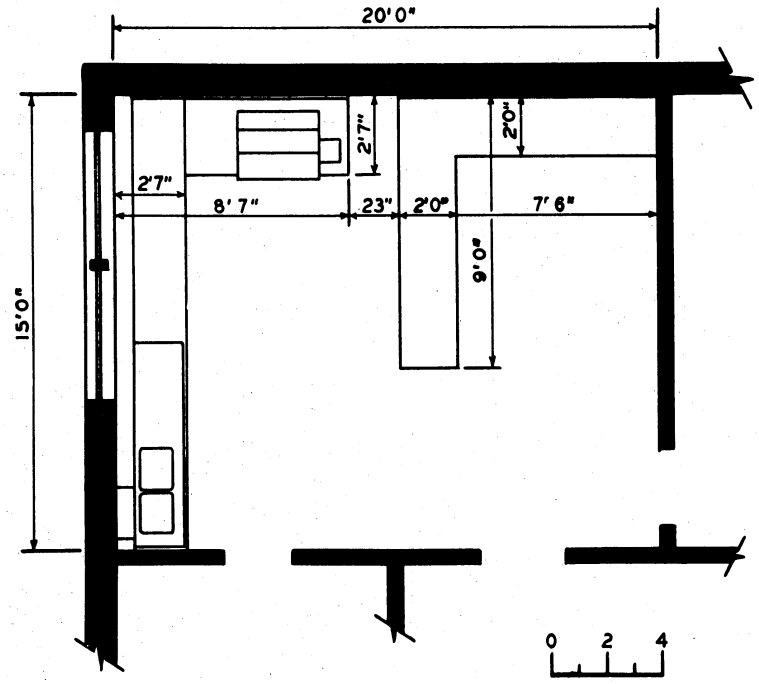

Figure 2.14 Plan view of typical one-room radioisotope tracer laboratory (Courtesy of Kewaunee Mfg. Co., Adrian, Mich.)

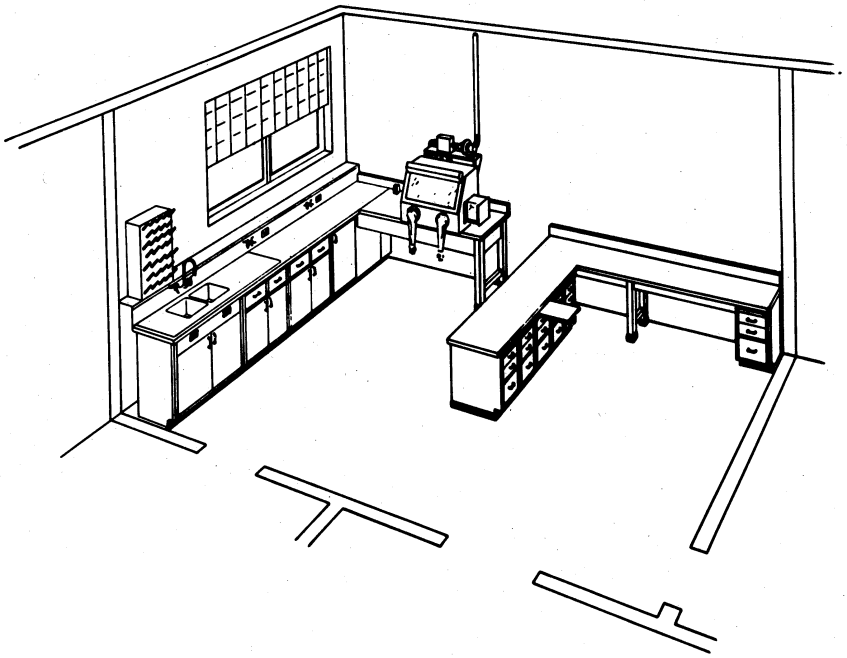

Figure 2.15 Isometric view of typical one-room radioisotope tracer laboratory (Courtesy of Kewaunee Mfg. Co., Adrian, Mich.)

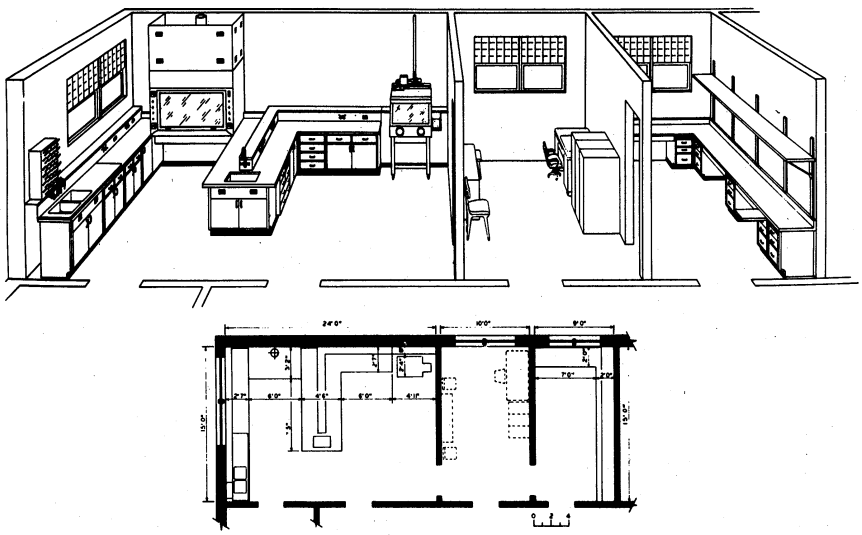

Figure 2.16 Isometric and plan view for a typical three-room radioisotope tracer laboratory (Courtesy of Kewaunee Mfg. Co., Adrian, Michigan)

must exercise extreme care in order to prevent the spread of traces of contamination. Another difficulty is the presence within the room of the radioactive source material which may interfere with the counting of low-level radioactive samples. If relatively large quantities of radioactive source materials are ordered and stored in the lab, the unused portions must be shielded to keep the background radiation at a minimum.

A question is sometimes raised regarding the difference between this radioisotope-laboratory design and other typical chemical-laboratory designs. Actually, there is no significant difference and existing laboratory facilities are entirely adequate for most low-level tracer experiments that can be performed with radioactive materials. Only the techniques of the investigator must be changed.

The need for strippable coatings, stainless steel, and special finishes has frequently been overemphasized. Since the problem of wall and ceiling contamination in the low-level tracer laboratory is practically nonexistent, a standard wall finish such as paint on plaster or cement block gives a durable, easy-to-maintain finish. The floors may be asphalt tile, mastopave, linoleum, or any other comparable sealant covering that is comfortable to stand on.

If two rooms are available for the laboratory, the logical arrangement would place the office operations and counting equipment in the second room and leave the first room exclusively for the experimental work. If three rooms can be made available, the counting equipment could be further isolated from the laboratory by placing the office between the laboratory and counting room. An alternative arrangement would be to establish a low-level laboratory, a higher-level laboratory, and a combination counting room and office. The decision as to which layout would be most satisfactory is to a large degree dependent on the type and level of radioactive material which will be needed

to carry out the desired investigations.

An isometric view and floor plan for a typical three-room radioisotope laboratory are shown in Figure 2.16. One room is used for all experimental manipulations. The middle room is an office and the third is a counting room. Such a laboratory provides ample work space for two research people and two technicians.

The estimated cost for furnishing each of the three laboratories is $6,000 for the one-room tracer laboratory, $8,000 for the two-room combination, and $10,000 to $12,000 for the three-room combination. These estimates include the furniture indicated in the figures but do not include the cost for plumbing, lighting, wall finishing, or an air-exhaust system.

Table 2.3 summarizes costs for the initial establishment of a laboratory. Table 2.4 gives an estimated budget for equipment for a one-room laboratory using a single radioisotope. Table 2.5 lists appropriate instrumentation (and approximate prices) for a versatile three-room radioisotope laboratory. Estimated annual operating expenses for the small laboratory are given in Table 2.6.

Additional information on the use and design of radioisotope and radiation laboratories is given in references 37 to 117.

Table 2.3

Radioisotope Laboratory Equipment

and Alterations Cost (9) *

	One-Room Lab	Two-Room Lab	Three-Room Lab
Minimum	$ 3,700	$ 4,300	$ 6,900
Typical	6,400	7,500	12,900
Maximum	9,100	11,800	21,300

Table 2.4

Small Radioisotope-Laboratory

Equipment Costs (10) **

Safety Instruments	$ 715
Counting Instruments	1,800
Shield Equipment	2,020
General Laboratory Equipment	1,500
	$ 6,035

* Based on 1952 prices
** Based on 1956 prices

Table 2.5

Equipment For The Versatile

Three-Room Radioisotope Laboratory

Item	Number	Total Cost
Scalers	2	$ 1,600.00
Vertical lead shield	1	285.00
Geiger tubes	2	100.00
Q-gas tank and regulator	1	93.00
Flow-gas counter	1	395.00
Scintillation-well counter	1	970.00
Geiger-type survey instrument	1	300.00
Ion-chamber-type survey instrument	1	300.00
Count-rate meter	1	500.00
Recorder	1	400.00
Pocket ion chambers	12	120.00
Charger-reader for pocket chambers	1	225.00
Film-badge holders	12	12.00
Counting calibration standards (set)	1	80.00
Laboratory cart	1	50.00
Lead shield bricks	20	200.00
General laboratory equipment (centrifuge, refrigerator, glassware, hot plates, balance, pH meter, etc.)		3,000.00
		$ 8,630.00

Table 2.6

Estimated Annual Laboratory Operating Expenses

Of The Small Radioisotope Laboratory (10)*

Salaries, Administration, and Service	$ 13,000.00
Laboratory Supplies	1,000.00
Consulting Services and Travel	1,500.00
Building Space and Services	1,500.00
Depreciation and Maintenance	1,000.00
Analysis and Testing	200.00
Miscellaneous	250.00
	$ 18,450.00

* Based on 1956 prices

2.7 Common hazard parameters

All radiation and tracer laboratory design concepts must include consideration of the two hazard parameters. That is, the external radiation hazard and the internal radiation hazard. The former is dealt with by the erection of proper shield walls, whether they be temporary or fixed as in the case of the gamma-irradiation facility. The latter, the internal radiation hazard, is dealt with by providing glove-box facilities, hood facilities, radioactive-waste drain systems, exhaust-air filter systems, and general control of contamination. A first step toward general control of contamination is taken when one lays out the laboratory, grouping the higher-level radiation laboratories or high-risk facilities away from those areas of long-term occupancy or favored intake such as office space and lunch rooms.

2.8 Exhaust-air control

In general, one tries to lay out the laboratory facility in such a

manner that minimum traffic is directed into the high-level areas of the lab. In turn, the airflow throughout the total facility is directed from areas of occupancy to areas of high-level operations as illustrated in Figure 2.17.

There are two alternative techniques for air filtration from radioactive facilities. One is to place filters immediately adjacent to the point of contamination. For example, some facilities have filter boxes located directly above the hoods, as illustrated in Figure 2.18. Located in this manner, a high contamination incident within the hood contaminates only a single filter unit. The second alternative method is to place a single large filter bank to service all the hood facilities. This latter technique results in total filter-bank contamination in the event of a single hood facility contamination incident. The problems inherent in the design of an exhaust system for handling radioactive off gases or dusts are dealt with quite extensively in a publication by the Building Research Advisory Board (11).

2.9 Monitoring with instruments

Electronic radiation-monitoring devices carried or strategically placed in the vicinity of an experiment involving radioisotopes can be kept in continuous operation throughout the experiment. These devices can indicate the instant a predetermined "safe" level of radioactivity is exceeded.

Typical instruments used are: (1) meters for recording fast neutrons, known as "Neuts"; (2) Geiger counters for low-level monitoring; (3) portable ionizing chambers called "Cutie-Pies"; (4) beta-gamma meters with probes; (5) meters to detect the presence of alpha-emitter substances, termed "Poppies"; and (6) "Juno" meters, widely-used general-purpose meters that can detect alpha-particle radiation as well as beta and gamma.

Figure 2.19 shows a fixed ionization chamber which constantly records the radiation level behind a massive concrete wall. It indicates precautions

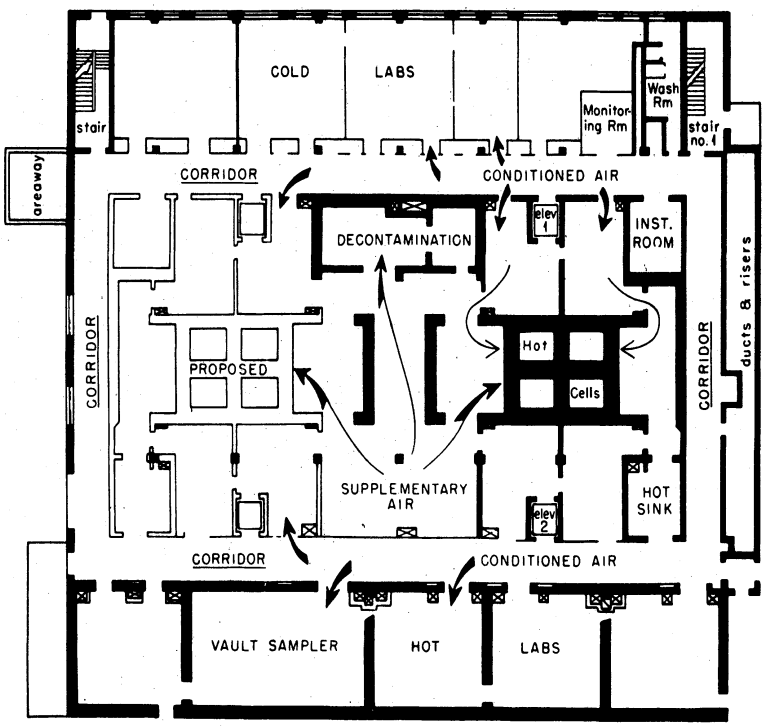

Figure 2.17 Floor plan of a radiochemical laboratory building with radiation zoning and airflow planning (6)

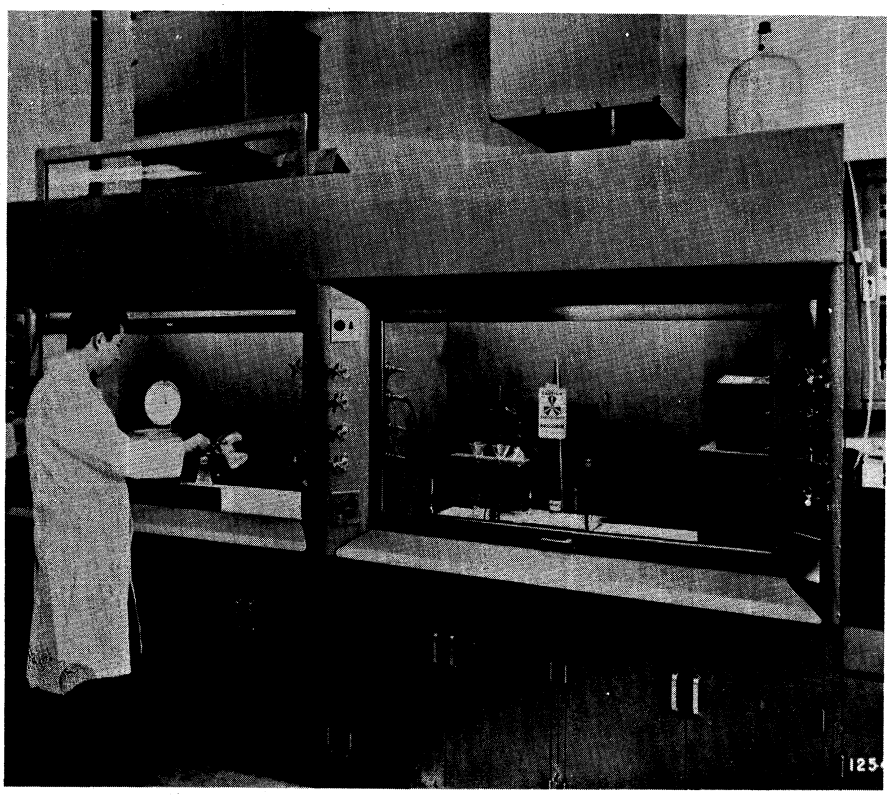

Figure 2.18 Double hood installation with exhaust-air filtration boxes above. (Courtesy Kewaunee Mfg. Co., Adrian, Michigan)

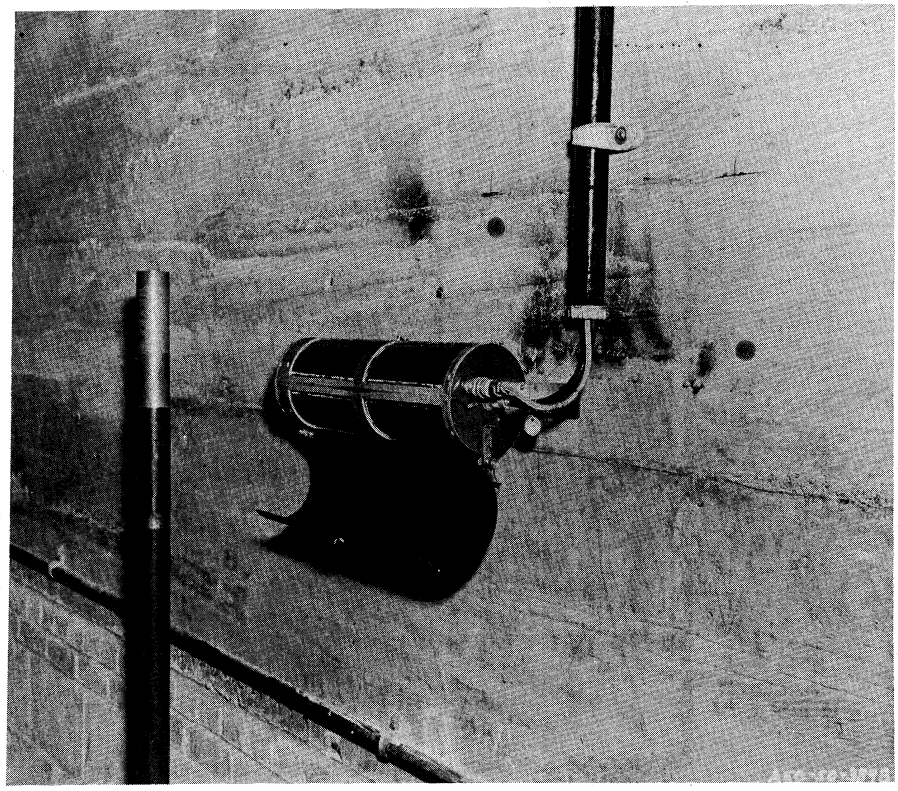

Figure 2.19 A fixed ionization chamber which measures radiation level at point inside shielding wall (Courtesy General Electric Co.)

Figure 2.20 Routine check of hands and feet of workers for possible contamination before leaving building at Hanford Plant (Courtesy General Electric Co.)

required for personnel entering such a zone.

Permanent instruments can provide a continuous record of radioactivity levels at a remote location, or a warning signal to enable disaster procedures to be set into instant operation to minimize exposures (12). Figure 2.20 shows a final radiological check of workers' hands, feet, and clothing as they leave the laboratory. This procedure is good protection for the worker as well as a positive prevention of the spread of radioactive material from the laboratory.

Hand-and-foot counters are located adjacent to areas of possible contamination. These enable employees, leaving a building after removing protective clothing (or after walking down a hallway also used by people who have just removed protective clothing) to stand on one pair of instruments and place their hands next to another set of instruments that measure and record the amount of radiation being given off by material on the skin or shoes.

This is a final check to determine if the protective equipment and procedures have performed their functions properly and to assure that the employees are free of contamination. That such measures can be very successful is shown by the record at Hanford where no employee has ever been seriously or permanently injured by radiation or by radioactive material.

2.10 Personnel film badges

In the routine operation of any radiation laboratory or area of significant radiation level, records must be kept of the radiation dosages received by all personnel having access to the radiation areas. This is usually accomplished by the use of film badges such as that shown in Figure 2.9. For the personnel this is essential to prevent excessive and harmful exposure to radiation as a result of continual working about an area of high radiation level. Also, such records provide protection from legal action by eigher employees or visitors

who unjustly claim over-exposure to radiation.

The same badge is worn daily by laboratory employees and the film packet is changed periodically, usually once per week or twice per month or immediately after a radiation incident of suspected over-dosage. The exposed film packets are returned to the supplier where they are developed and returned with a report of the accumulative dosage given each badge.

Nuclear radiations and x-radiation darken the x-ray type films that are used in the badges in a manner similar to the darkening of photographic film as a result of the exposure of the film to light. Both the x-ray and ordinary photographic films consist of a light-sensitive emulsion layer deposited on a cellulose acetate or glass base. The light-sensitive emulsion layer consists of a colloidal dispersion of crystals of a silver halide (or a mixture of silver halides) in gelatin.

All emulsions show a great variation in sensitivity to the energy of the activating x- or gamma-radiation. In practice this is taken into account by covering the film with filters that reduce the sensitivity of the film, and flatten its response to radiation of various energies. For a given film the degree of darkening is dependent upon the properties of the film and the type, duration and intensity of the radiation that reaches the film. To cover a wide radiation dosage range, two or more films are usually used. If two films are used in the packet, one of the films is usually highly sensitive and may cover the range of radiation dosages from 0 to 2 roentgens. The other film usually is less sensitive and may cover the dosage range up to 30 roentgens (300 times the maximum tolerance for one week).

The two films are wrapped together in thin opaque paper to keep out light which would expose the films. In one type of badge a portion of the film is located at a "window" and a portion behind a thin cadmium shield. In the case

of exposure to mixed radiation (beta and gamma) the beta particles are stopped by the cadmium shield but the penetrating gamma photons pass on through and expose the film. Beta particles readily penetrate the film packet at the window and expose the film but do not penetrate cadmium shield.

In another type of badge a stepped copper wedge is used in place of the cadmium. This type of badge is particularly useful in determining dosages resulting from exposure to x-radiation. In case of x-radiation the film density varies greatly with the kilovoltage used in the machine. The use of copper steps permits the comparison of the film density under each step with standards exposed to known dosages of x-radiation produced by machines operated at known kilovoltages.

If there is a possibility of neutron exposure a third film which is sensitive to proton radiation is placed behind the "beta-gamma" films. With such a film badge fast neutrons pass through both the window and the cadmium barrier, but slow neutrons are readily captured by the cadmium and, therefore, pass only through the window. The fast neutrons interact with hydrogen atoms in the film to produce recoil protons that expose the film. The slow neutrons also produce protons from the N^{14} (n,p) C^{14} reaction giving an additional proton exposure. The protons produced by both processes leave "tracks" on the third film. The dosage for fast and slow neutrons can be estimated by counting the tracks after development of the film. This involves microscopic analysis and use of the phase microscopy principle. One commercial laboratory uses Eastman Type NTA film with an emulsion thickness of 25 to 30 microns, calibrates the film with polonium-beryllium neutron sources, and analyses the film at 860X.

The beta-gamma dosages are obtained by comparison of the film density at the window and behind the cadmium with that of calibrated control films

exposed to known dosages of radiation. To avoid errors from variables in developing, control films are developed and fixed with the test films.

2.11 Use of special clothing

Radioactive material may enter the body by three main routes: inhalation, ingestion, injection. Air-borne particles or radioactive gases, such as $C^{14}O_2$, may be inhaled and incorporated into the tissues. Radioactive materials unconsciously or absent-mindedly transferred to food, cigarettes, or pencils may find its way into the body through the mouth. The accidental puncturing of protective clothing and the skin during work may inject radioactivity directly into the blood stream.

Accidents, or "spills," in the laboratory occasionally release radioactive materials into the air and on to laboratory surfaces(13). Ventilating systems must not exhaust radioactive gases or dust into the atmosphere and sewage effluents must not release radioactive materials into lakes and rivers. Laboratory workers must not carry the radioactivity from the laboratory on their bodies or clothes to "clean" areas. Figure 2.21 shows a worker returning from an operation in a highly contaminated area at the Hanford Atomic Products Operation. The special suit provides adequate protection from contamination of the skin surface as well as inhalation exposure.

Before removing the outer layer of protective clothing, a radiation monitoring unit worker (health physicist) checks the clothing with an instrument. This worker is wearing full protective clothing including two pairs of gloves. The space between the inner gloves and the sleeve of the coveralls is sealed with masking tape to prevent air-borne contamination from getting inside. The hood-type head cover is tucked inside the outer coverall but outside the inner coverall. Mask is fresh-air type that furnishes air from outside the contaminated work area.

Figure 2.21 Worker with special suit for protection in radiocontaminated areas being checked for contamination. (Courtesy General Electric Co.)

Figure 2.22 Routine check of floor for possible contamination (Courtesy Atomic Energy Research Establishment, Harwell, England)

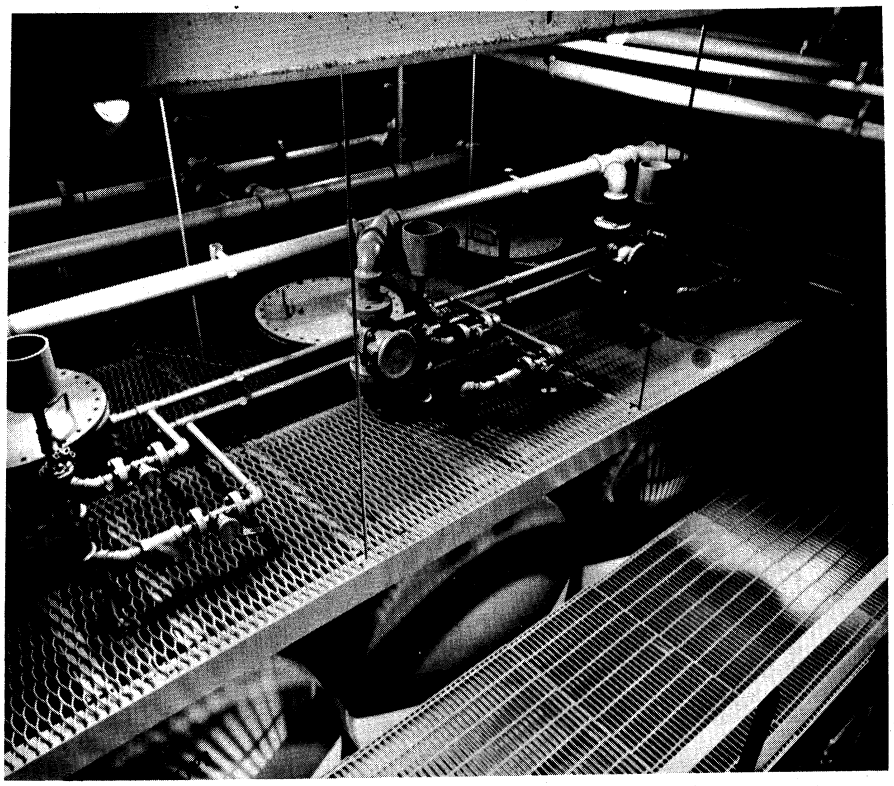

Figure 2.23 Radioactive liquid-waste tank farm of 10,000-gallon storage capacity. Michigan Memorial-Phoenix Laboratory, Ann Arbor, Michigan

The special clothing worn by the worker shown in Figure 2.21 (and also by workers shown previously in Figures 1.2, 1.3, and 1.9) is of primary importance when working in areas in which the atmosphere is possibly contaminated by alpha-particle emitters such as plutonium. If these same workers were using encapsulated alpha-particle sources or working with gamma radiation in uncontaminated areas, conventional laboratory clothing with suitable radiation shields and survey instruments would be sufficient protection. (See Figures 2.3, 2.9, and 2.10)

Alpha-particle radiation is completely absorbed in a small volume of tissue leading to severe localized tissue damage, sarcoma, and related injuries. If an equal amount of energy in the form of beta radiation is absorbed in the body, it is distributed throughout a much larger tissue volume. Tissue damage in this case is more diffuse but still localized. Internal gamma radiation would penetrate still further and, in fact, be expected to produce no local injury, only gross, total body radiation damage. Thus, while gamma radiation is more damaging than alpha radiation when the exposure is from an external source, the reverse is true if the source is internal.

2.12 Decontamination procedures

Decontamination may be required for protection against excessive radiation levels or radioactive material entering the body. The risk of radiation injury due to ingested, inhaled or injected radioactive materials can be minimized by careful planning, continuous radiological monitoring and good housekeeping procedures.

The initial design of an experiment or process must take into account the degree of contamination hazard involved. For instance, in general, all work with alpha-particle emitters must be performed in closed systems, such as gloved fume-hoods or glove boxes. Good experimental design can minimize the

possibility of an incident which might spread contamination, as well as include safe procedures in the event of such an incident.

The procedures involved in keeping a laboratory radiologically "clean" are no different in principle from those used in good housekeeping procedures. No dust or dirt is allowed to collect. Waste is disposed of before large amounts accumulate. Smooth-finish surfaces, such as stainless steel, are used when possible. Otherwise, cheap, easily removable surfacing material is used. Porous surfaces such as unglazed ceramic tile, wood, mortar or concrete are avoided or are coated or covered with nonporous materials. This type of laboratory operation coupled with suitable monitoring procedures can minimize the risk of workers carrying radioactivity away from the laboratory.

However, in spite of all precautions, human error, mechanical failure, and accidents could be responsible for serious instances of radio-contamination. In such cases, protection consists primarily of detailed surveys to delineate the dangerously contaminated areas and of keeping away from these areas until decontamination is complete. Decontamination, the removal of radioactive material from an area, is much the same in principle as the removal of any other contaminant (14). Soap and water, and abrasives when necessary, are satisfactory decontaminating agents (15).

This process differs from other types of cleaning, however, in two respects. The contaminant is not normally detectable to the sight, smell or touch. Frequent surveys with a Geiger tube or ionization-chamber instrument during the decontamination procedure are necessary to evaluate the efficiency of the procedure. Figure 2.22 shows a routine check for possible contamination being carried out at Harwell, England.

The material removed, including detergents and wash liquids remaining in mops and clothes, is itself a radiation hazard and cannot be disposed of by

ordinary means. These materials, depending on the degree of hazard involved and other factors, must be diluted before disposal, stored for decay, or shipped to a site of permanent radioactive storage, as must any radioactive waste material.

Table 2.7 outlines factors to be considered in area decontamination. Additional information on this subject is given in references 16 to 21.

Table 2.7

Outline of Factors to be Considered

in Area Decontamination (*)

I. PRE-INCIDENT PLANNING:

- A. Proper Facilities
  - 1. Laboratory design
  - 2. Experiment design
- B. Isotope Choice
  - 1. Properties required
  - 2. Example: Sr^{89} vs Sr^{90}
- C. Experience available
- D. Assistance needed
- E. Equipment required to handle contamination incident
  - 1. Low-level liquid
    - (a) Absorbent paper
    - (b) Trays
    - (c) Mop and bucket
    - (d) Shoe covers
  - 2. High-level liquid
    - (a) Isolation equipment (signs, barriers, etc.)

* Private communication from A. H. Emmons

(b) Flush hose (in cell)

(c) Mop and bucket and detergents

(d) Waste storage container

(e) Shoe covers

(f) Protective clothing

(g) Shower facility

3. Low-level dusts

(a) Respirators

(b) Vacuum cleaner

(c) Shoe covers

(d) Caps

4. High-level dusts

(a) Supply air mask

(b) Vacuum cleaner

(c) Shoe covers

(d) Protective clothing (caps, coveralls, etc.)

(e) Shower facility

(f) Waste storage facility

(g) Isolation equipment (signs, barriers, etc.)

II. ACUTE PHASE: (Incident has Occurred)

A. Evacuate (but don't go home!)

1. Not necessary with low level liquid

2. Call for Health Physicist assistance

3. Think!

B. Assemble equipment to begin clean-up

C. Assign specific duties

D. Be prepared to rotate personnel (if necessary)

E. Obtain an air-sample (if possible)

III. RECOVERY PHASE:

A. Instrumentation-Take correct instrumentation capable of detecting the contamination into the contaminated area

B. Plan and execute decontamination procedures

C. Evaluate the efficiency of each procedure

D. Rotate personnel

E. Keep calm and use good sense!

IV. TECHNIQUES:

A. General

1. Leave the area (or object) vacant and allow natural decay to reduce the levels.

2. Decontaminate

B. Types of Decontamination

1. Rough decontamination (limited use, or occupation of area)

2. Detailed decontamination (restore to original condition)

C. Processes of Decontamination

1. Wet contamination on smooth surfaces - Flush with water and detergents followed by scrubbing and flushing. Steam under pressure is very helpful. Treatment is more difficult if the contamination has been allowed to dry.

2. Contamination in form of dust - Use vacuum cleaning. If further treatment is necessary, brush and vacuum again.

3. Contamination of greasy surfaces - Remove greasy material with dry-cleaning solvents. If necessary, follow by scouring with water, soaps, and detergents.

4. Deeply absorbed contamination - Removal of surface, at the same

time preventing further penetration of contaminant (e.g. removal of top few inches of earth, caustic paint removers, abrasion, acids, or special chemical compounds).

5. Firmly-held contamination - Covering with suitable thickness of sealing material, or disposal of contaminated objects or clothing by deep burial in the earth or at sea in weighted, sealed container. Decontamination may have to be carried out in several stages, and a combination of methods may be necessary.

D. Facts about Contamination

1. It <u>will not</u> be uniform
2. Smooth surfaces less susceptible than rough
3. Cracks or crevices collect it
4. Movement of men and equipment will spread it
5. The more porous the material, the tougher the job.
6. <u>No</u> process will neutralize it

E. Details regarding rough decontamination

1. Speed is main consideration
2. Simplicity is usually forced
3. Most practical technique is water <u>washing</u>. Add soap or detergent if available. Use hot water if available.
4. Land areas
   (a) Bulldozer
   (b) Graders
   (c) Wet it down first
5. Best protection - - distance!
6. Points to consider:
   (a) Method must work quickly

(b) Method must be suitable for material

(c) Should not require large quantities of special or dangerous chemicals

(d) Should make use of available equipment, services, and material

F. Procedures for detailed decontamination

1. Summary of methods applicable to surface decontamination:

(a) Vacuum cleaning

(b) Water

(c) Steam

(d) Detergents

(e) Complexing agents

(f) Inorganic acids

(g) Organic solvents

(h) Caustics

(i) Abrasion

(j) Flame cleaning

(k) Remove outer layer of material with contamination

2. Disposal techniques

(a) Burial on land

(b) Entombment

(c) Burial at sea

G. Personnel decontamination

1. Soap and water scrub (no water, then wipe)

2. Remove contaminated clothes

3. Scrub

4. Check

5. Scrub

6. Stay out of clean areas unless you are clean!

2.13 Radioactive wastes

For the small tracer or isotope laboratory, the problems of radioactive-waste handling are relatively minor. Short-lived liquid wastes of low-level concentrations may be dumped directly into the sewage lines, provided concentrations and quantities are kept below the limits established by the National Committee on Radiation Protection and local codes. Higher concentrations of short-lived wastes may be retained for decay and then disposed of with adequate dilution. The short-lived solid wastes may be stored. Those things of value may be recovered by decontamination procedures. Those things of no value, such as paper towels, rubber gloves, used or broken laboratory equipment, may be stored for decay and eventually disposed of in a moral fashion. A suitable solid-waste handling technique for a tracer laboratory, using a short-lived tracer, might be illustrated by consideration of an average problem.

Consider a laboratory which receives 55 millicuries of P32 every 14 days. If all this P32 is disposed of into a radioactive-waste can, 55 millicuries, less that lost by decay, will be added to this can every two weeks. Eventually an equilibrium concentration will be reached of 109 millicuries of P32 in the can. This concentration of activity would be attained after approximately 70 days. If this filled can is now replaced with an empty one and the filled can is placed in storage for 120 days, there would be 0.27 millicurie of P32 activity remaining in the can. At that time, the filled can could be removed from storage and the contents burned in an incinerator, with no problem. These numbers, of course, are quite unrealistic in that it is highly improbable that one would discard the total P32 shipment every fourteen days. A more realistic value would be three to six per cent of the shipment going into the

active solid-waste containers. Then after 128 days decay, one could expect a concentration of eight to 16 microcuries in the filled waste can.

For the small tracer laboratory, the easiest approach to the liquid-waste problem is to confine all suspected liquid wastes to one-gallon waste jugs placed conveniently in the corners of the hoods. After a number of jugs of liquid wastes are accumulated, a sample is taken from each and assayed to determine the activity levels. If the jugs display long-lived radioactive contamination, the user is faced with two alternatives. He may process the waste into concrete by using the liquid waste as the water component of a concrete mix, then designate a controlled area as storage for the final blocks. A second alternative is to procure the services of a company handling radioactive waste*, or make arrangements to ship the wastes to a suitable government-operated burial facility.

For the larger laboratory specifically designed for work with radioactive materials, it is often most convenient to connect the drain located in the floor of the hood directly into a five-gallon polyethylene carboy. The radioactive liquid wastes are collected in this five-gallon carboy. In the event of a spill within the hood, the spill as well as the contaminated wash water drains directly into the carboy. If this approach is taken, it is important that one locate any drains connected with the sanitary sewer system above the floor of the hood in such a manner that nonactive run-off water must be actually placed in the sewer line.

* Radioactive-waste disposal service

Several companies providing are:

Crossroads Marine Disposal Corp.
26T Warf
Boston, Mass.

Radiological Service Co.
92-15 172nd St.
Jamaica 33, N. Y.

Reed-Curtis Nuclear Industries, Inc.
307 Culver Blvd.
Plaza del Rey, Calif.

In the large, integrated, multilaboratory facility it is advantageous to lead all the drains into a retention tank with a liquid-level indicator mounted within the laboratory facility. In this arrangement the normal laboratory wastes are allowed to accumulate within the retention tank. As the tank fills the wastes are monitored to determine the activity level. If the activity level is below maximum permissible dump level, the tank is drained or pumped into the sanitary sewer system. If the wastes in the tank are above permissible dump levels, they are pumped into storage drums for concentration or long-term storage. Figure 2.23 pictures a retention-tank "farm" for radioactive wastes. Often this latter system of retention tanks is operated together with a normal sanitary sewer system, where the sanitary sewer drains (or the hot drains) are painted a distinctive color to identify one from the other. This approach minimizes the total volume of possible contaminated wastes.

For a very large laboratory facility, particularly one operated in conjunction with a reactor, it is essential that space be reserved for the installation of some type of concentrating equipment capable of handling low- to medium-level radioactive wastes. Various approaches have been made to this problem. In general, if the wastes are low in total salt content, one may use ion-exchange equipment. If the wastes are of high salt content, one is forced to use flocculation, evaporation, filtration, or some similiar concentrating technique (22).

Plans and procedures for such "ultimate" disposal from the smaller laboratories usually involve either burial in the ground or dumping into the sea. The release of radioactive wastes directly into the ground relies on the filtration, absorption, and ion-exchange properties of the soil (23, 24) to fix the radioactivity within a limited, controlled volume and thus prevent

contamination of local bodies of water or water supplies. When geological, meteorological or ecological considerations do not justify the assumption that the activity will be retained, artificial absorption on clay (25) or "permanent" storage in steel and concrete tanks may be undertaken.

Because so little is known about the diffusion and mixing properties of the oceans, and the biological processes by which isotopes may be concentrated by marine organisms (26), the disposal of large quantities of waste into the sea for dilution may not be feasible. No maximum permissible concentrations of radioactive material in sea water have been set because of these uncertainties. Permanent packaging and storage in areas remote from fishing areas and having geological characteristics favorable to long-term undisturbed storage seems desirable at this time (27). Ocean deeps and deep-sea ooze may not be as promising storage areas as many believe, however, owing to oceanographic disturbances (29).

Additional information on the problem of disposal of radioactive wastes is given in references 116 to 124.

2.14 Example design of a multipurpose hot-lab

Figure 2.24 is the first floor plan of the Michigan Memorial-Phoenix Laboratory located at the University of Michigan. This floor plan will be used to illustrate some safety features and design concepts which have been incorporated into this building. This laboratory is designed for use in a wide range of research studies and for work with radioisotopes having activities ranging from microcuries to kilocuries of gamma activity. Figures 2.10, 2.11, 2.12, 2.13, 2.18 and 2.22 show views of some of the installations in this laboratory.

Entrance to the hot-laboratory section is by way of a short side-corridor opening into the restricted-access corridor. This short corridor passes by the locker-change room and the health-physics office. The short corridor is used as a pick-up point for film badges and pocket chambers and houses a hand-

and-foot counter for personnel monitoring. As one enters the restricted-access corridor and progresses toward the far end the installations become ever-increasingly "hot." Behind the two hot cells is a large isolation and decontamination area for the cleanup and storage of contaminated equipment arising from hot-cell operations. Beneath the floor of the isolation-decontamination area there are three large storage tanks, as pictured in Figure 2.24. These tanks hold the radioactive waste water from the chemistry laboratory, hot cells, and all hood installations throughout the building.

The laboratory is equipped with a double drainage system. All floor drains, hood floor drains, sinks in the decontamination area, and certain sinks in the low-level area drain into the active waste-storage tanks. The waste-storage tanks are designed to handle up to millicurie levels of radioactive liquid wastes. Wastes of levels higher than this are placed in collection bottles within the hot cells and chemistry hoods. These bottles are in turn collected and placed in storage. The radioactive liquid wastes are decontaminated by sand-bed filtration and mixed-bed ion-exchange resin columns. A second sanitary drain system in the hot-lab area is arranged in such a manner that accidental entry of active wastes can be made with difficulty. This installation of the sanitary system minimizes the amojnt of water that must be treated in the decontamination facilities.

The rear wall of the decontamination area is below grade-level with a storage facility for radioactive materials. There are 31 sample storage holes and five lead-shielded sample storage drawers built into this below-grade wall.

There is a fifteen-ton hydraulic lift, capable of rising above grade to truck-bed height, provided in the decontamination-area rear. It is possible to place a fork lift on the elevator, rise up to truck-bed height, lift off a large shipping container, and move it down to the hot cells. (5)

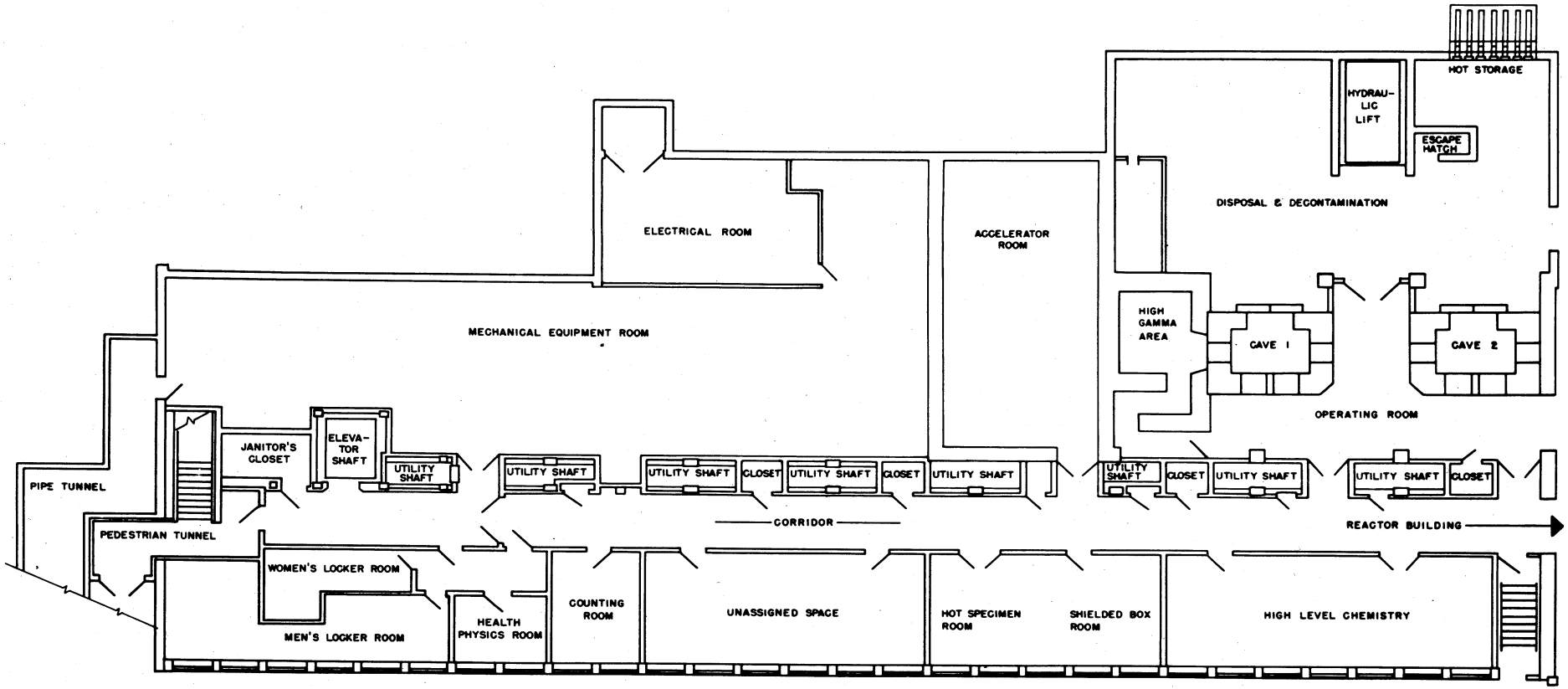

PHOENIX MEMORIAL LABORATORY — FIRST FLOOR PLAN

Figure 2.24 Michigan Memorial-Phoenix Laboratory hot-lab floor plan

The second floor of the Michigan Memorial-Phoenix Laboratory is at grade level and houses the administrative and nonradioactive functions of the laboratory. Office space, conference room, library, machine shop, and an electronic shop are located on the second-floor area.

Accidents will happen in the best designed and staffed laboratories. Preparation in advance will reduce personnel injury, property damage, and assist in the maintenance of operational continuity. Laboratory design should include careful consideration of disaster or emergency situations. Detailed planning should include such things as emergency warning alarm systems, exhaust-stack monitoring system, interlaboratory communications, monitoring equipment and protective clothing located at a site remote from high-risk area, emergency fire-fighting equipment, evacuation procedures, consequences of power failure, and medical-treatment facilities.

Chapter 2

References

1. Morgan, G. W., "Basic Safety Requirements in Radioisotope Work," Paper 20 of a Conference on the Use of Isotopes in Plant and Animal Research. USAEC, TID-5098, 1953

2. Editorial
"Cold Setting Lead Cement in Mobile Radiation Shield"
Lead, 20, No. 1, 4, 1950

3. Goertz, R. C.
"Fundamentals of General-Purpose Remote Manipulators"
Nucleonics, 10, No. 11, 36, 1952

4. Davis, Harold S.
"How to Choose and Place Mixes for High-Density Concrete Reactor Shields"
Nucleonics, 13, No. 6, 60, 1955

5. Meinke, W. W., Emmons, A. H. and Gomberg, H. J.,
"A Versatile Hot Lab for University Research"
Nucleonics, 13, No. 11, 1955

6. Dismuke, S. E., Feldman, M. J., Parker, G. W., Ring, F., Jr.
"Hot Laboratory Facilities and Techniques for Handling Radioactive Material"
International Conference on the Peaceful Uses of Atomic Energy. A/Conf. 8/P/723, 1955

7. Atomic Energy Commission, United States
"Volume Three, Reactor Handbook: Engineering"
"Volume Six, Chemical Processing and Equipment"
U. S. Government Printing Office, Washington 25, D. C.

8. Goertz, R. C.,
"Mechanical Master-Slave Manipulator"
Nucleonics, 12, No. 11, 1954

9. Ward, D. R.
"Design of Laboratories for Safe Use of Radioisotopes"
AECU-2226, November 1952

10. Meyer, A. W.
"Installing a Small Hot Atomic Laboratory"
Industrial Laboratories, p. 62 May 1956

11. Building Research Advisory Board
"Laboratory Design for Handling Radioactive Materials"
Conference Report No. 3 1951

12. "Control of Radiation Hazards in the Atomic Energy Program,"

U.S. Atomic Energy Commission, Wash., D.C., 1950

13. Skow, R. et al., "Hazard Evaluation and Control after a Spill of 40 mg. of Radium," Nucleonics, 11, No. 8, 45, 1953

14. Lane, W. et al., "Contamination and Decontamination of Laboratory Bench Top Materials," Nucleonics, 11, No. 8, 49, 1953

15. Ross, D.H., "Cleaning Contaminated Surfaces," Soap Sanit. Chemicals, 27, 1951

16. Lane, J. A. "Contamination and Decontamination of Laboratory Bench Top Materials", Nucleonics, 11, No. 8, 49, 1953

17. Skow, "Hazard Evaluation and Control after a Spill of 40 mg. of Radium," Nucleonics, 11, No. 8, 45, 1953

18. Barry, et. al., "Radioactive Contamination Sampling by Smears and Adhesive Disks," Nucleonics, 11 No. 10, 60, 1953

19. Anon. "Decontamination Chart," Nucleonics, 9, No. 11, C-12, 1951

20. Breslin, A. J. and Solon, L. R., "Fallout Countermeasures for AEC Facilities," NYO-4682-A, Dec. 1955

21. "Radiation and Monitoring Fundamentals for the Fire Service," Published by International Association of Fire Chiefs, Hotel Martinique, Broadway at 32nd. Street, N. Y. 1, N. Y., 1955

22. Curtis, R. L., "Decontamination - A Literature Search," Y-964, May 19, 1953, Bibliography of material on decontamination; 70 titles are included, May 19, 1953

23. Rodger, Walton A. and Fineman, Phillip "A Complete Waste Disposal System for a Radiochemical Laboratory" Nucleonics, 9, No. 6, 50, 1951

24. Brown, R. E. et al., "Disposal of Liquid Wastes to the Ground", A/Conf./p 565, United Nations, N.Y., 9, 120, 1956

25. Mawson, C. A., "Waste Disposal Into the Ground," AECL-211 A/Conf./ p12; Atomic Energy of Canada Ltd., Chalk River, Ont. Canada. United Nations, N.Y. 9, 676, 1956

26. Ginell, W. S. et al., "Ultimate Disposal of Radioactive Wastes," Nucleonics, 12, No. 12, 14, 1954

27. Jensen, J. H., "Radioactive Waste Disposal in the Ocean," Nat. Bur. Standards, Handbook 58, U.S. Govt. Print. Office, Wash. D.C.

28. Seligman, H., "The Discharge of Radioactive Waste Products in the Irish Sea," A/Conf./p 418, United Nations, N. Y., 9, 701, 1956

29. Renn, C.E.,"Disposal of Radioactive Wastes at Sea," A/Conf./p 569; United Nations, N. Y., 9, 718, 1956

30. Angel, C. W. and Ring, F., Jr., "Wall Transfer Unit and Transfer Carrier for Hot Cells," Nucleonics, 11, No. 9, 69, 1953

31. Argonne National Laboratory "The Argonne High Level Gamma Irradiation Facility," Argonne National Laboratory, Lemont, Illinois

32. Atkins, M. C. and Lorentz, W. N., "Space-Saving Hot Cell," Nucleonics, 13, No. 10, 79, 1953

33. Atomic Energy Commission, United States "Fourth Annual Symposium on Hot Laboratories and Equipment," held in Washington, D.C., September 29, and 30, 1955. TID-5280, Technical Information Service, Wash., D.C., 1955; TID-5280 (Suppl. 1), Jan. 1956

34. Bagnall, K. W. and Spragg, W. T., "The Handling of Radioactive Materials - I",Atomics and Atomic Technology, 6, No. 3, 71, 1955

35. Braestrup, C. B. and Quimby, E. H., "Design and Recommendations for the Radioisotope Laboratory" in Chapter 20, "Planning Guide for Radiologic Installations", Scott Year Book Publishers, Inc., 220 East Illinois Street, Chicago, Ill., 1953

36. Bralove, A. L., "Radioactive Dust Separation Equipment, I, II, and III," Nucleonics, 8, No. 4, 37, No. 5, 60, No. 6, 15, 1951

37. Editorial, "Adapting Glove Boxes to Gamma Work," Nucleonics, 7, No. 6, 83, 1950

38. Editorial, "Conoco Gets 'Hot'," Chem. Engng. News, 4753 Oct.1, 1956

39. Editorial, "Equipment Guide for Radioactivity Laboratories," Nucleonics, 7, No.11, 90, 1952

40. Farmakes, J. R., "Snare-Type Remote Handling Device," Nucleonics, 10, No.11, 90, 1952

41. Ferguson, K. R., "Design and Construction of Shielding Windows," Nucleonics, 10, No. 11, 46, 1952

42. Fields, P. R. and Youngquist, C. H., "Hot Laboratory Facilities for a Wide Variety of Radiochemical Problems," A/Conf./p 725; United Nations, N. Y., 7, 44, 1956

43. Garden, N. B., "Semihot Laboratories," Industr. Engng. Chem., (Industr.) 41, No. 2, 237, 1949

44. Garden, N. B., "Laboratory Handling of Radioactive Material," A/Conf./p 722; United Nations, N. Y., 7, 62, 1956

45. Glen, H. M., "An Engineering Approach to Hot Cell Design,"

Proc. Amer. Soc. Civ. Eng., 80, No. 446, 1954

46. Goertz, R. C., "Fundamentals of General-Purpose Remote Manipulators," Nucleonics, 10, No.11, 36, 1952

47. Gore, T. W., "The New Radiometallurgy Laboratory at the Hanford Atomic Operation," Metal. Progr., 65, No. 6, 81, 1954

48. Grune, W. N. and Klevin, P. B., "Redesign of a Sanitary Engineering Laboratory to Permit the Use of Radioisotopes," Nucleonics, 9, No. 2, 59, 1951

49. Hawkins, M. B., "The Design of Laboratories for the Safe Handling of Radioisotopes," Isotopes Division Circular B-5 U.S. Atomic Energy Commission Isotopes Division Oak Ridge, Tenn., 1949

50. Kohl, J. and Newacheck, R. L., "Mobile Radiochemical Laboratory," Nucleonics, 10, No. 5, 44, 1952

51. Lane, J. A., "How to Design Reactor Shields for Lowest Cost," Nucleonics, 13, No. 6, 56, 1955

52. Levy, H. A., "Remodeling a Laboratory for Radiochemical Instruction or Research," Industr. Engng. Chem., (Industr.) 41, No. 2, 248, 1949

53. McIntosh, W. W., "Ventilation for Radioactive Work, Balancing, Operation, Maintenance," Heat. Pip. Air Condit., 25, No. 7, 98, 1953

54. Manov, G. G., "Radioisotope Laboratories for Animal and Agricultural Research," in: "The Role of Atomic Energy in Agricultural Research" TID-5115, U.S. Atomic Energy Commission, Wash., D.C., 81 Jan. 1953

55. Manov, G. G. and Bizzell, O. M., "Design of Radioisotope Laboratories for Low and Intermediate Levels of Activity," in: "Symposium on Radioactivity -- An Introduction." ASTM Special Technical Publication No. 159

56. Miller, H. S., Fahnoe, F. and Peterson, W.R., "Survey of Radioactive Waste Disposal Practice," Nucleonics, 12, No. 1, 68, 1954

57. Monk, G. S., "Coloration of Optical Glass by High-Energy Radiation," Nucleonics, 10, No. 11, 52, 1952

58. Morris, G., "An Approach to Hot Laboratory Design," Proc. Amer. Soc. Civ. Engrs., 80, No. 448, 1954

59. Norris, W. P., "Radiobiochemical Laboratories," Industr. Engng. Chem., (Industr.) 41, No. 2, 231, 1949

60. Obrycki, R. F., Ball, R. M. and Davidson, W. C., "Economical Shielding for Multicurie Sources," Nucleonics, 11, No. 7, 52, 1953

61. Olson, O. L. and Gifford, J. F., "Facilities for Decontamination of

Laboratory Equipment," HW-26502, Hanford Atomic Products Operation, U.S. Atomic Energy Commission, Wash., D.C., 1953

62. Pravdjuk, N. V., "Metal-Research Hot Laboratory," A/Conf./p 673; United Nations, N. Y., 7, 49, 1956

63. Preuss, L. E. and Watson, J.H.L., "Design and Construction of a Small Radioactivity Laboratory," Nucleonics, 6, No. 5, 11, 1950

64. Quimby, E. H. and Braestrup, C. B., "Planning the Radioisotope Program in the Hospital," Amer. J. Roentgenol., 63, No.1, 1950

65. Remote Control Engineering Division "A Manual of Remote Viewing," ANL-4903, Argonne National Laboratory, Chicago, Illinois, 1953

66. Rice, C. N., "Laboratory for Preparation and Use of Radioactive Organic Compounds," Industr. Engng. Chem., (Industr.) 41, No. 2, 244, 1949

67. Ring, F., Jr., "Shielding Structure Facilities for Atomic Energy Research," Proc. Amer. Soc. Civ. Engrs., 80, No. 447, 1954

68. Ryberg, J., "Shielded Box for Chemical Work," Nucleonics, 13, No. 10, 65, 1955

69. Rylander, E. W. and Blomgren, R. A., "Operating Procedures of a Hot Laboratory for Solid State Tests," Nucleonics, 12, No. 11, 98, 1954

70. Selected Authors, "Hot Labs -- A Special Report," Nucleonics, 12, No. 11, 35, 1954

71. Somerville, A., "General Motors Builds Radioisotope Laboratory," Nucleonics, 13, No. 10, 68, 1955

72. Spence, R., "An Atomic Energy Radiochemical Laboratory Design and Operating Experience," A/Conf./p 438; United Nations, N.Y., 1956

73. Steele, R. V., "Remote Radioactive Materials Testing Laboratory at Livermore Research Laboratory," LRL-150, U.S. Atomic Energy Commission, Wash., D.C., June, 1954

74. Swallow, A. J., "The Hot Laboratory at the University of Birmingham," Atomic Scientists News, 1, No. 4, 130, 1952

75. Swartout, J. A., "Research with Low Levels of Radioactivity," Industr. Engng. Chem., (Industr.) 41, No. 2, 233, 1949

76. Tompkins, P. C., "A Radioisotope Building," Industr. Engng. Chem., (Industr.) 41, No. 2, 239, 1949

77. Tompkins, P. C. and Levi, H., "Impact of Radioactivity on Chemical Laboratory Techniques and Design," Industr. Engng. Chem., (Industr.) 41, No. 2, 228, 1949

78. Ulm, R. W. et all, "Portsmouth Technical Services Building," K-1148, U.S. Atomic Energy Commission, Wash., D.C., Nov. 29, 1954

79. Wadey, W. G., "Simple Radiation Shielding Doors," Nucleonics, 12, No. 5, 54, 1954

80. Ward, D. R., "Design of Laboratories for Safe Use of Radioisotopes," Chapter 8 in "Radioisotopes in Industry," Reinhold Publishing Co., N. Y., 1953

81. Whittlesay, E. and Givens, E., "Radiation Protection of Personnel and Radiochemical Laboratories, Their Design and Operation," AECU-1020, U.S. Atomic Energy Commission, Wash., D.C., July 1950

82. Yakovlev, G. N. et al., "A Hot Analytical Laboratory," A/Conf./p 672; United Nations, N. Y., 7, 57, 1956

83. Arnott, D. G. and Wells-Cole, J., "A Rapid Method for the Extraction of Radioiodide from Urine," Nature, Lond., 171, 269, 1953

84. Browder, F. N., "Liquid Waste Disposal at Oak Ridge Natl. Lab.," Industr. Engng. Chem., (Industr.) 43, 1509, 1951

85. Carter, M. W., "Removal of Radioactive Iodine by Laboratory Trickling Filters," Sewage Industr. Wastes, 25, 560, 1953

86. Cowan, F. P. and Nehemias, J. V., "Sensitivity of the Evaporation Method of Liquid-Waste Monitoring," Nucleonics, 7, No. 5, 39, 1950

87. Eden, G. E., Elkins, G.H.J. and Truesdale, G.A., "Removal of Radioactive Substances from Water by Biochemical Treatment Processes," Atomics, 5, 133, 1954

88. Eliassen, R., Kaufman, W.J., Nesbitt, J. B. and Goldman, M. I., "Studies on Radioisotope Removal by Water Treatment Processes," J. Amer. Wat. Wks. Ass., 43, 615, 1951

89. Foster, R. and Rostenbach, R., "Distribution of Radioisotopes in Columbia River," J. Amer. Wat. Wks. Ass., 46, 633, 1954

90. Ginell, W. S., Martin, J. J. and Hatch L. P., "Ultimate Disposal of Radioactive Wastes," Nucleonics, 12, No. 12, 14, 1954

91. Goldin, A. S., Nader, J. S. and Setter, L. R., "The Detectability of Low-level Radioactivity in Water," J. Amer. Wat. Wks. Ass., 45, No. 1, 73, 1953

92. Gorman, A. E., "Mutual Interests of the Water Works and Atomic Energy Industries," J. Amer. Wat. Wks. Ass., 43, 865, 1951

93. Grune, W. N. and Eliassen, R., "Studies on the Effect of Radioactive Phosphorus on the Biochemical Oxidation of Sewage," Sewage Industr. Wastes 23, 141, 1951

94. Hayner, J. H., "Atomic Energy Industry," Industr. Engng. Chem., 44, 472, 1952

95. Herrington, A. C. et at., "Economic Evaluation of Permanent Disposal of Radioactive Wastes," Nucleonics, 11, No. 9, 34, 1953

96. Higgins, E., "Atomic Radiation Hazards for Fish," J. Wildlife Management, 15, 1, 1951

97. Kochtitzky, O. W. and Placak, O. R., "How to Survey a Stream for Radioactive Substances," Publ. Wks., 83, 76, 114, 1952

98. Loosemore, W. R., "Monitoring of Water for Fission-Product Contamination," Nucleonics, 11, No. 10, 1953

99. Monowitz, B. and Hatch, L. P., "Processes for High-Level Waste Disposal," Chem. Engng. Progr., Sump. Ser. No. 12, Nuclear Engng., Part 2, Amer. Inst. Chem. Engrs., N. Y., 144, 1954

100. McCullough, G. E., "Concentration of Radioactive Liquid Wastes by Evaporation," Industr. Engng. Chem., (Industr.) 43, 1505, 1951

101. McKay, H. A. C. and Walton, G. N., "Safety Criteria in Radioactive Water Monitoring," Nucleonics, 5, 12, Aug. 1949

102. Newell, J. F. and Christenson, C. W., "Radioactive Waste Disposal," Sewage Industr. Wastes, 23, 861, 1951

103. Newell, J. F. and Christenson, C. W., "What Treatment for Radioactive Wastes," Engng. News-Record, 147, 37, 1951

104. Powell, C. C. and Andrews, H. L., "Radioactive Waste Disposal," Publ. Hlth. Rep. Wash., 67, No. 12, 1214, Dec. 1952

105. Rodger, W. A., Fineman, P., "A Complete Waste-Disposal System for a Radio-Chemical Laboratory," Nucleonics 9 , 51, 1951

106. Rodgers, W. A. and Fineman, P., "Radioactive Waste Disposal," Chem. Engng., 58, 146, 1951

107. Ruchhoft, C. C. and Feitelberg, S., "Estimates on the Concentration of Radioiodine in Sewage and Sludge from Hospital Wastes," Nucleonics, 9, No. 6, 29, 1951

108. Ruchhoft, C. C., Gorman, A. E. and Christenson, C. W., "Wastes Containing Radioactive Isotopes," Industr. Engng. Chem. (Industr.) 381, 545, 1952

109. Ruchhoft, C. C. and Setter, L. R., "Application of Biological Methods in the Treatment of Radioactive Wastes," Sewage Industr. Wastes, 25, 48, 1953

110. Rudolfs, W., Ed. "Industrial Wastes: Their Disposal and Treatment" Reinhold Co., N. Y. 1953

111. Setter, L. R., Goldin, A. S. and Nader, J. S., (Robert A. Taft Sanitary Engineering Center, Cincinnati, Ohio) "Radioactivity Assay of Water and Industrial Wastes with Internal Proportional Counter," Analyt. Chem., 26, 1304, 1954

112. Straub C. P., "Observations on the Removal of Radioactive Materials from the Waste Solutions," Sewage Industr. Wastes 23, 188, 1951

113. Straub, C. P., "Effect of Radioactive Materials on Environmental Health," Publ. Hlth. Rep., Wash., 67, No. 3, 1952

114. Straub, C. P., Morton, R. J. and Placak, O. R., "Studies on the Removal of Radioactive Contaminants from Water," J. Amer. Wat. Wks. Ass., 43, 773, 1951

115. Western, F., "Health Safety Considerations in the Disposal of Radioactive Wastes," Ind. Hyg. Quarterly, 14, No. 3, Sept. 1953

116. Lieberman, J. A., "Engineering Aspects of the Disposal of Radioactive Wastes from the Peacetime Applications of Nuclear Technology," J. Am. Public Health Assoc., March 1957

117. Silverman, L., "Air and Gas Cleaning For Nuclear Energy Processes," Proceedings of the International Conference on the Peaceful Uses of Atomic Energy, Geneva, p. 571, 1955; United Nations, New York: 9, 1956

118. Craig, H., "Disposal of Radioactive Wastes in the Ocean: The Fission Product Spectrum in the Sea as a Function of Time and Mixing Characteristics," Scripps Institute of Oceanography, 1958

119. "The Disposal of Radioactive Waste on Land," Report of the Committee on Waste Disposal of the Division of Earth Sciences, Natl. Acad. Sci.-Natl. Res. Council, 1957

120. Rhodes, D. W., "Waste Characteristics Governing Fixation in Soils," USAECReport TID-7550, Hanford Atomic Products Operation, 1958

121. Grimmett, E. S., "Calcination of Aquenous Reactor Fuel Wastes in a Fluidized Bed," USAEC Report TID-7550, Phillips Petroleum Co., 1958

122. Thomas, R. G. and Christenson, C. W. "Leaching Studies on Fired Clays Containing Radionuclides," USAEC Report TID-7550, Los Alamos Scientific Laboratory, 1958

123. Goldman, M. I., Servizi, J. A., Lauderdale, R. A. and Eliassen, R., "Fixation of Fission Products in Ceramic Glazes," USAEC Report TID-7505 Massachusetts Institute of Technology, 1958

124. Gloyna, E. F., Schecter, R. and Serato, S., "Storage of Reactor Fuel Wastes in Salt Formations," USAEC Report TID-7550, University of Texas, 1958

CHAPTER 3

FILM, GLASS, CHEMICAL AND CALORIMETRIC DOSIMETRY

The term "dosimetry" originated in the medical profession and involves the methods of the determination of the "dose" of radiation absorbed by a body or material placed in a radiation field for a given period of time. In general, dosimetry is concerned with the measurement of radiation dosage by the chemical or physical change the radiation produces in a measuring system. Examples of such a system are a photographic plate which is "exposed" by the radiation, or a chemical solution in which a cation is oxidized or reduced in the presence of radiation.

The early use of X-rays and radium in cancer therapy introduced the need to measure the radiation dose given to patients. Electronic instruments of advanced design such as described in Chapter 11* were not available at that time although simple forms of the ion chamber were used extensively. Numerous chemical and biological systems were explored for use in dosimetry. Crude photographic films were available and were used in the early 1900's to measure radiation dosage. For convenience in treatment the dosimeters will be discussed under the following categories:

A. Film and Plastic Dosimeters
B. Glass Dosimeters
C. Chemical Dosimeters
D. Calorimetric Dosimeters
E. Miscellaneous Types of Dosimeters

The first three of these systems depend on chemical changes to detect radiation whereas the fourth measures the heat effect of the absorbed radiation in a substance of known heat capacity, and hence depends on a physical change.

3.1 Film Dosimeters

In addition to the silver halide photographic-type film, plastic films containing dyes have been used in various dosimetry studies, but much less extensively than the silver halide films.

3.2 Film Badges

Silver halide films are used in every radiation laboratory in the film packets of personnel film badges. In the routine operation of any radiation laboratory or area of significant radiation level, records must be kept of the radiation dosages received by all personnel having access to

*Radiation Uses in Industry and Science.(B7)

the radiation areas and this is usually accomplished by the use of film badges. This is essential to prevent excessive and harmful exposure of the personnel to radiation as a result of continual working in an area of high radiation level. Also, such records provide protection from legal action by either employees or visitors who unjustly claim over-exposure to radiation. Tolerance levels and the general problem of health physics are discussed in Chapter 1.

Figure 3.1 shows an employee in a radiation laboratory inserting a film packet in a badge. Note that he is also wearing a film badge on the lapel of his laboratory coat.

The same badge is worn daily by laboratory employees and the film packet is changed periodically, usually once or twice per month or immediately after a radiation incident of suspected over-dosage. The exposed film packets are returned to the supplier where they are developed and returned with a report of the accumulative dosage received by each badge.

Nuclear radiations and X-radiation darken the X-ray type films that are used in the badges in a manner similar to the darkening of photographic film as a result of the exposure of the film to light. Both the X-ray and ordinary photographic films consist of a light-sensitive emulsion layer deposited on a cellulose acetate or glass base. The light-sensitive emulsion layer consists of a colloidal dispersion of crystals of a silver halide (or a mixture of silver halides) in gelatin. According to the Gurney and Mott theory,[1] light or ionizing radiation incident upon a halide crystal will transfer some energy to the crystal, causing one or more of its electrons to reach conduction energy levels. These mobile electrons then move about in the lattice until they are trapped by centers of a deformity or impurity. The coulomb forces set up by the trapped electrons cause silver ions in the crystal to migrate to those electrons where the ions are neutralized to form silver atoms. The silver atoms form the so-called photographic "latent image" and catalyze the reduction of the entire crystal to metallic silver when the film is developed. If overdevelopment is avoided only those crystals that have been activated will be reduced to metallic silver. The unreduced halide is then removed by forming a water-soluble complex with thiosulfate ion in the fixing bath. After fixing, the film is washed and dried and is ready for use.

Figure 3.2 shows the range and sensitivity of some typical emulsions to gamma radiation from a radium source.[2]

All emulsions show a great variation in sensitivity to the energy of the activating X- or gamma-radiation. In practice this is taken into

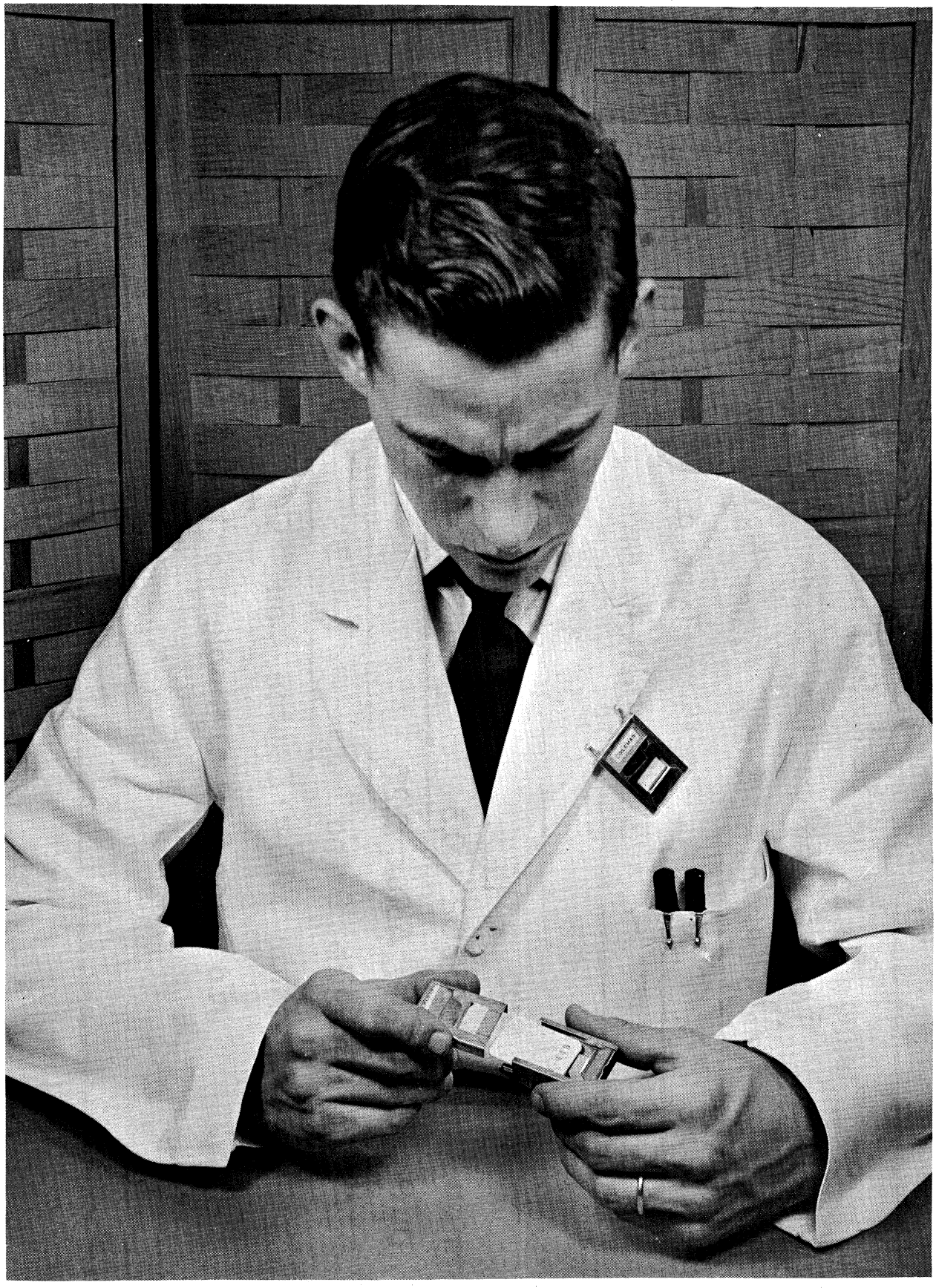

Figure 3.1. Insertion of Film in Film Badge.

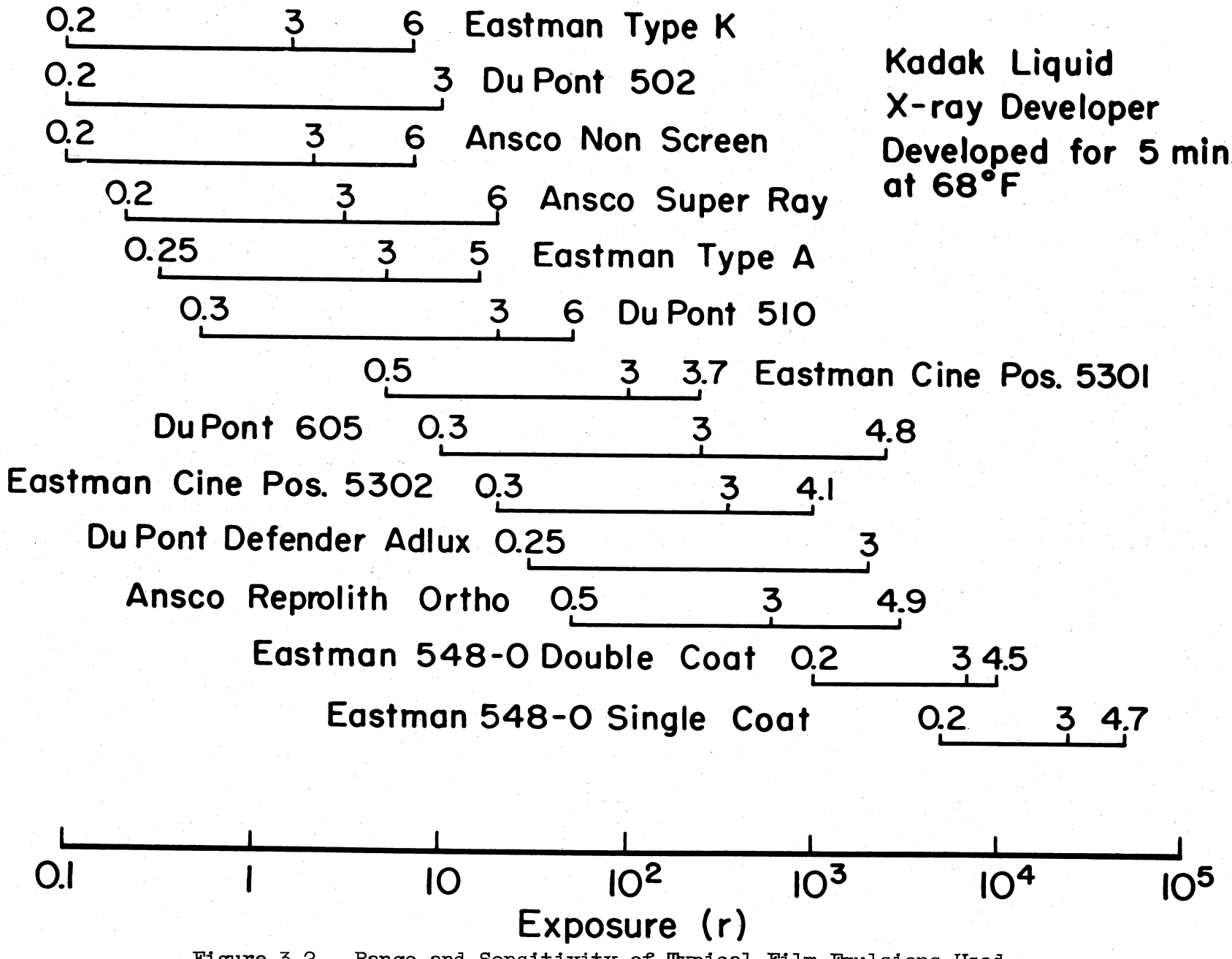

Figure 3.2. Range and Sensitivity of Typical Film Emulsions Used in Film Badges. (2)

account by covering the film with filters that reduce the sensitivity of the film and flatten its response to radiation of various energies. This effect is illustrated in Figure 3.3 for which the "sensitivity" is defined (2) as "the ratio of radium gamma ray exposure to the exposure at a given energy, in roentgens, which is necessary to produce the same film density."

For a given film the degree of darkening is dependent upon the properties of the film and the type, duration and intensity of the radiation that reaches the film. To cover a wide radiation dosage range, two or more films are usually used as indicated for one type of film packet shown in Figure 3.4.

If two films are used in the packet one of the films is usually highly sensitive and may cover the range of radiation dosages from 0 to 2 roentgens. The other film usually is less sensitive and may cover the dosage range up to 30 roentgens (100 times the maximum tolerance for one week).

The two films are wrapped together in thin opaque paper to keep out light which would expose the films. In one type of badge shown at the right in Figure 3.3, a portion of the film is located at a "window" and a portion behind a thin cadmium shield. In the case of exposure to mixed radiation (beta and gamma) the beta particles are stopped by the cadmium shield but the penetrating gamma photons pass on through and expose the film. Beta particles readily penetrate the film packet at the window and expose the film but do not penetrate the cadmium shield.

In another type of badge shown at the left in Figure 3.4 a stepped copper wedge is used in place of the cadmium. This type of badge is particularly useful in determining dosages resulting from exposure to X-radiation. The film density varies greatly with the kilovoltage used in the X-ray machine. The use of copper steps permits the comparison of the film density under each step with standards exposed to known dosages of X-radiation produced by machines operated at known kilovoltages.

If there is a possibility of neutron exposure, a third film which is sensitive to proton radiation is placed behind the "beta-gamma" films as indicated in Figure 3.5.

With a film badge such as shown in Figure 3.5 fast neutrons pass through both the window and the cadmium barrier but slow neutrons are readily captured by the cadmium and, therefore, pass only through the window. The fast neutrons interact with hydrogen atoms in the film to produce recoil

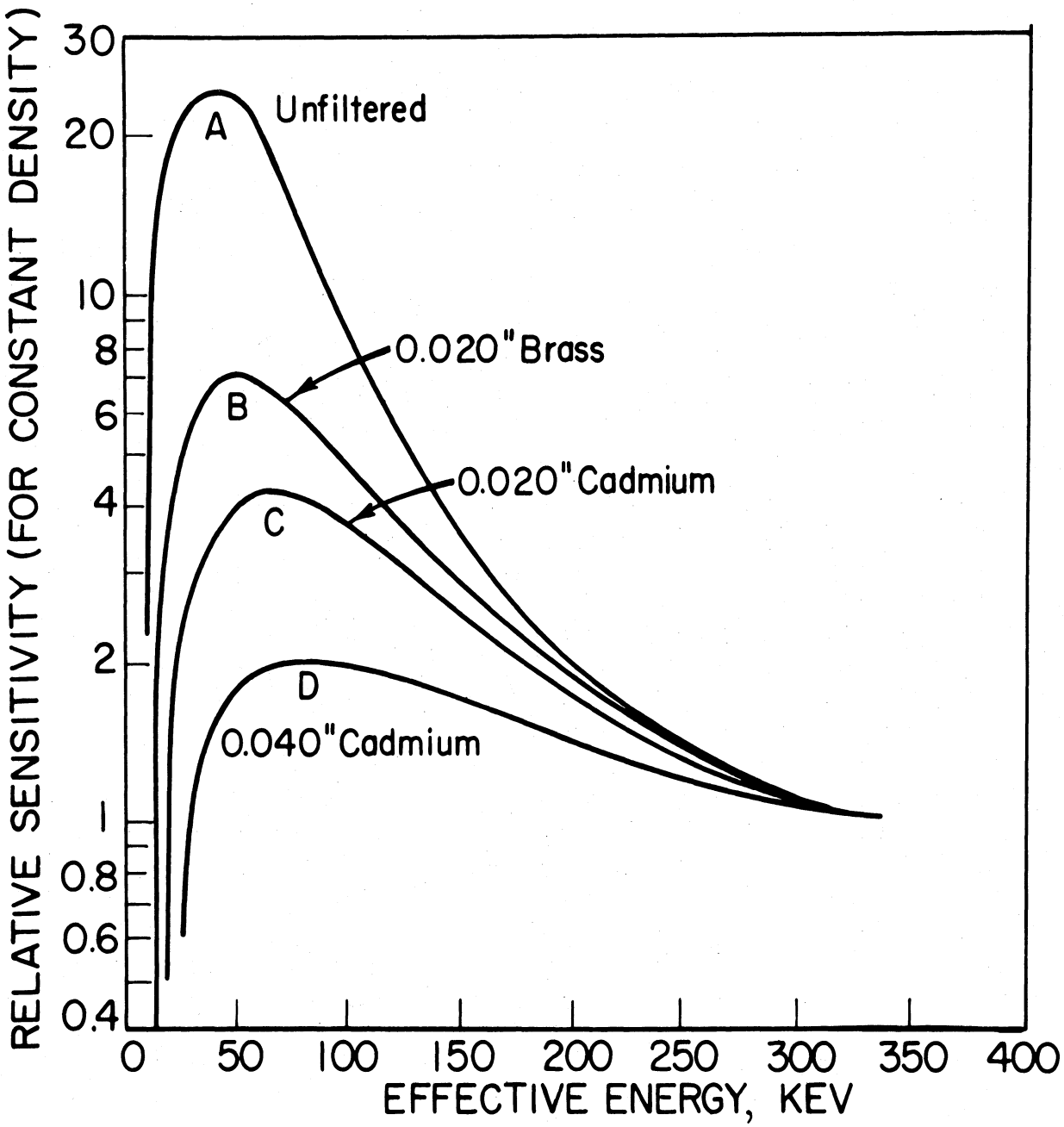

Figure 3.3. Relative Sensitivity vs. Effective Energy for duPont 502 Emulsion and Filtered X-Radiation. (2)

Figure 3.4. Cross-Section of X-Ray and Beta-Gamma Film Badges (Courtesy of Tracerlab, Inc.).

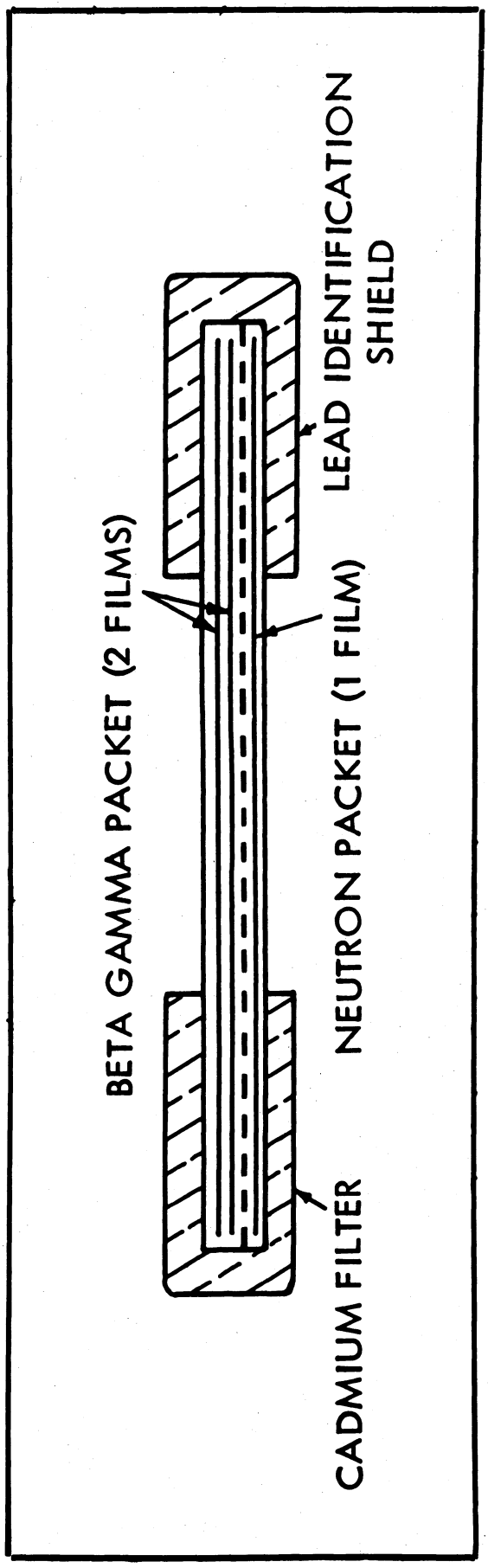

Figure 3.5. Cross Section of Neutron Film Badge (Courtesy of Tracerlab, Inc.).

protons that expose the film. The slow neutrons also produce protons from the N^{14} (n,p) C^{14} reaction, giving an additional proton exposure. The protons produced by both processes leave "tracks" on the third film. The dosage for fast and slow neutrons can be estimated by counting the tracks after development of the film. This involves microscopic analysis and use of the phase microscopy principle. One commercial laboratory[4] uses Eastman Type NTA film with an emulsion thickness of 25 to 30 microns, calibrates the film with polonium-beryllium neutron sources, and analyses the film at 860X.

The beta-gamma dosages are obtained by comparison of the film density at the window and behind the cadmium with that of calibrated control films exposed to known dosages of radiation. To avoid errors from variables in developing, control films are developed and fixed with the test films.

Table 3.1 summarizes commercial film-badge services that were available in 1955. The table does not include the AEC operated film-badge service available only to contractors of AEC, nor a listing of neutron-badge services. Additional information on dosimetry with silver halide films is given in References 6-32.

3.3 Polyvinyl Chloride Films

The application of polyvinyl chloride films to gamma-radiation dosimetry measurements was suggested by Steigman[33] and investigated in greater detail by Henley and Miller.[34] The reaction is thought to take place by the action of gamma radiation on the plastic to liberate HCl within the film. If an acid-alkali indicator has been incorporated into the film, a color change will occur under the influence of the HCl.

Henley and Miller give the following four requirements that a system must meet for acceptance as a dosimeter method:

1. The system must vary in an exact manner and be independent of radiation intensity, wavelength, temperature, pH, etc.
2. The reaction must be irreversible.
3. The results must be reproducible within a few percent.
4. The chemical system must be stable under ordinary storage conditions.

Polyvinyl chloride films were studied also by Welshans in the Fission Products Laboratory, The University of Michigan, to check their use as a gamma-radiation dosimeter.[35] Briefly their procedure involved the

TABLE 3.1

SUMMARY OF COMMERCIAL FILM-BADGE SERVICE
(Courtesy of Nucleonics, Feb., 1955)(5)

Firm Name and Address	Cost of Service (per badge)	Minimum		How Often Are Badges Supplied	Control Badge Provided	Time To Report Exposures	Interval Badge is Kept on File
		No. of Badges	Subscript. Period				
Atomic Research Lab., 2633 Santa Monica Blvd., Santa Monica, Calif.	$1-1, 80¢ -2, 65¢ -3-10, 60¢ - 11-25	None	None	Weekly, bi-	Yes	7 days	Permanently
Isotopes Specialties Co., 3816 San Fernando Rd., Glendale, Calif.	50¢ apiece (quantity discounts allowed)	13	None	Weekly	Yes	Within 7 days	6 years
R. S. Landauer, Jr. and Co., P.O. Box 102, Park Forest, Ill.	$1.20-1, 50¢ each add. Over 50-quantity prices	None	13 weeks (shorter at higher price)	Weekly, bi-weekly, or special ar-	Yes	About 2 days*	Permanently
Nuclear Consultants, Inc., 33-61 Crescent St., Long Island City 6, N. Y.	$1-1, 60¢ - 2-9, 50¢ - 10 and over	1	3 months	Twice a month	No	7 days	2 years
Nuclear Inst. and Chemical Corp., 223 W. Erie St., Chicago 10, Ill.	65¢ -3-24, 60¢ -25-49, 55¢ -50-99, 50¢ - >100†	None	None	Weekly, bi-weekly, or monthly	Yes (3 or more badges)	4 days*	Permanently
Radiation Detection Co., 576 College Ave., Palo Alto, Calif.	50¢ (weekly) 60¢ (bi-wk.) $10 per yr. (monthly)	None	26 wk. if 1-2, 13 wk if 3	Weekly, bi-weekly, or monthly	Yes	Within 2 days*	Permanently
R-C Scientific Inst. Co., 307 Culver Blvd., Playa del Rey, Cal.	60¢ apiece $2.50 min. quantity discounts	None	13 periods	Weekly or longer scheduled period	Yes	Within 7 days	Indefinite
St. John X-Ray Lab., Califon, New Jersey	50¢ per badge $75/yr min.	None	1 year	As desired user holds supply	Yes	Within a few days	Badge is returned to user
Technical Associates, 140 W. Providencia Ave., Burbank, Calif.	60¢ ; less on quant. or yr contracts	3	13	Weekly, bi-weekly, or special arrangement	Yes	Within 7 days	Indefinite
Technical Operations, Inc., 6 Schouler Ct., Arlington, Mass.	75¢ each (discounts on contracts)	None	None	As ordered (3 mo. max.)	Yes (sold)	3 days	Indefinite
Tracerlab, Inc.,‡ 130 High St., Boston 110, Mass.	60¢ apiece, over 25-quantity discounts	3	13 weeks	Weekly or any regular schedule	Yes	Within 5 days*	Permanently

* Will notify of any overexposures by collect telegram, if requested.

† Deduct 5% for yearly contract on weekly basis.

‡ For the 17 western states; Tracerlab, Inc., Western Division Film Badge Service, 759 23rd St., Richmond 2, Calif.

addition of powdered resin to a filtered solution of dye in chlorobenzene and heating the mixture for 1 hour at 110°C. The solution is then poured on level glass plates and set aside until dry.

Welshans reported[35] that films cast from cyclohexanone were clear and free from surface imperfections found with chlorobenzene as the only solvent, with the additional advantage that stock solutions of uniform-quality plastic can be prepared and cast at room temperature. However, the drying time was increased to 9-19 days instead of the 1-3 days for chlorobenzene. Hence, in practice about 40 percent chlorobenzene was added to the solvent to decrease the drying period without affecting the appearance of the film.

A typical stock solution has the composition:

200 c.c. chlorobenzene (tech)
300 c.c. cyclohexanone (Eastman)
0.11 g methyl violet 6B (General Aniline)
23.7 g polyvinyl chloride resin (Geon 101)

The dye is dissolved in the mixed solvents and resin added slowly to avoid lumps. The mixture is heated to 115°C for 1 hour, cooled, and filtered through cotton into a dark-brown bottle. If 76.5 cc of the solution are poured on a 19 x 29 cm glass plate, the dried film is from 0.0016 to 0.0018 inch thick.

These films were cast on an 8 x 12 inch glass plate which had a wall of sauereisen cement around the edges to act as a dam for the solution. The plate was floated in a pool of mercury contained in a large pyrex dish, to keep the surface of the plate perfectly level.

The plate containing the dried film is placed under water and a edge of the film lifted with a sharp knife. Then the film can be peeled off in one piece without tearing. It is finally dried with blotting paper and cut into the proper shape with a razor blade.

The stability of the film was demonstrated by boiling it with water for several minutes. The appearance and shape of the film remained the same after the test and the water remained colorless, although the dye is normally water-soluble.

It is necessary to provide some type of support to hold the films during exposure or reading in the spectrometer. One method is the insertion of the film in a 35-mm Kodak ready-mount.

In Welshans' studies, the films were placed in a holder and transmission readings taken before and after exposure to gamma radiation with a Beckman Model DU spectrophotometer kept at a wavelength of 600μ and a slit width of 0.80 mm. The tungsten lamp was used in all measurements with the Beckman filter in the "in" position and the phototube in the "out" position. The sensitivity of the instrument was adjusted to give 100 percent transmission in air without the film in the holder. Using this technique it was possible to make readings on the same film that agreed within 1 percent.

If the reciprocal of the exposure time is plotted versus the percent transmission, a value of the transmission, T_{inf}, is obtained when the curve is extrapolated to infinite time as shown in Figure 3.6.

Welshans reported that unfiltered (250-kv) X-radiation is about 2-1/2 times as effective in bleaching as the cobalt-60 radiation for equal dosages. This is in agreement with previous findings and indicates that it is not possible to use the films to compare various sources of gamma radiation and that each wavelength must have its own calibration curve.

As a result of these observations Welshans[35] made the following conclusions regarding the use of PVC films as dosimeters for gamma radiation:

1. The system does not vary in an exact manner. It has been shown to be a function of wavelength, pH, and possibly intensity at high levels of radiation. The effect of temperature was not studied.

2. The reaction is irreversible as carried out in dosimetry methods.

3. The results indicate that they are reproducible, over a limited range, within 5 percent.

4. The system is stable if stored out of sunlight or bright artificial light. Sunlight will almost completely bleach the film in two days. A No. 2 photoflood, 2 feet from the film, will cause a 10 percent increase in transmission in 20 minutes. However, it appears that limited exposure to normal levels of artificial light has no effect.

If the PVC films are used in a gamma radiation field of constant energy, such as cobalt-60, and the total exposure is kept below 10 million roentgens, they provide a convenient and reproducible method of measuring dosages.

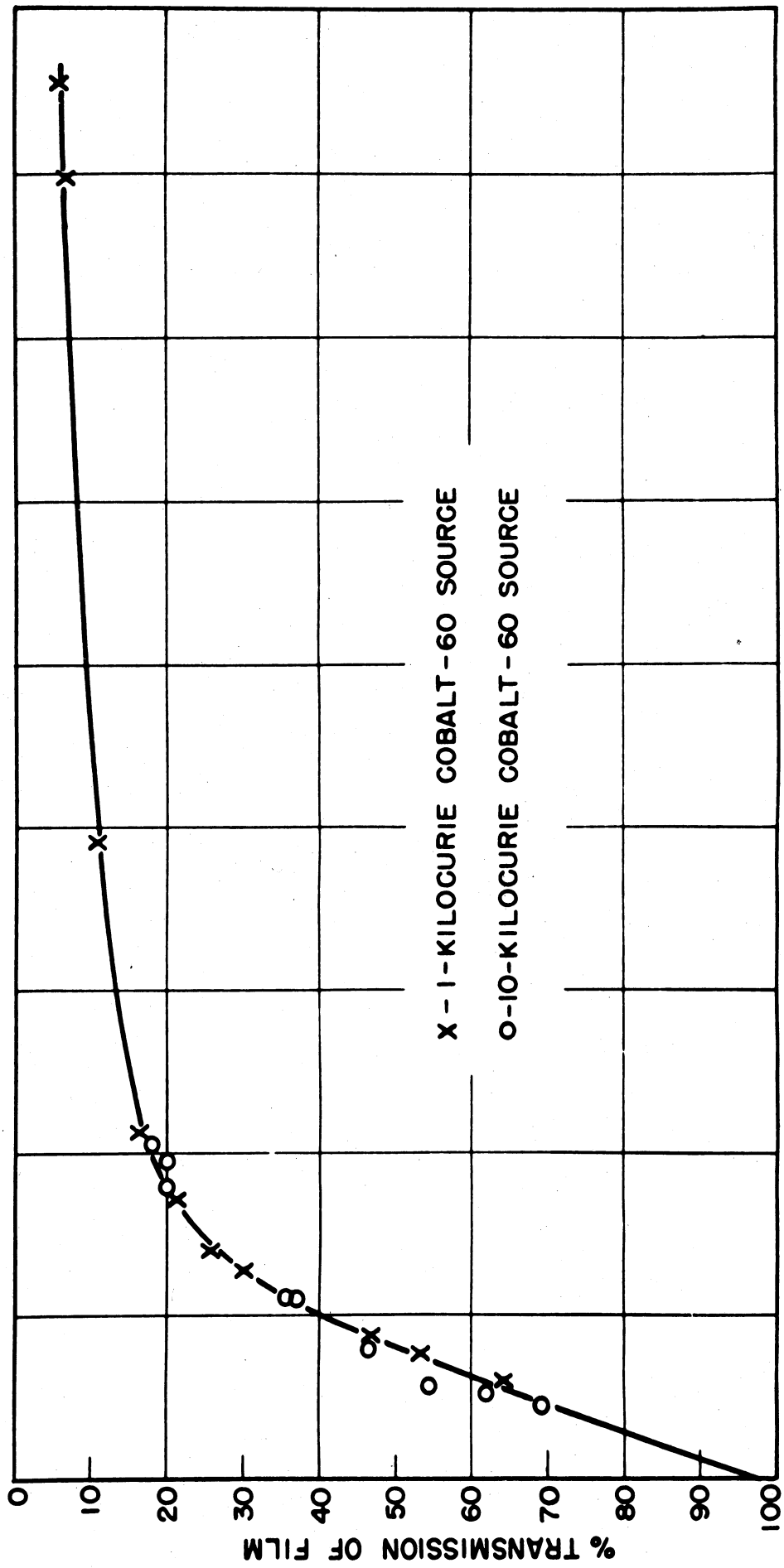

Figure 3.6. Percentage Transmission of PVC Film vs. Reciprocal of Relative Dosage from Cobalt-60 Gammas.

3.4 Cellophane Films

The principal disadvantages of the PVC films were the long exposure time required, the difficulty of preparing uniform, good quality film in the laboratory, and the necessity of calibrating each sheet of film. Also, the hand made film is quite expensive because of the man-hours involved in its preparation. Henley[36,37] recently reported the use of a moisture-proof, heat-sealable cellophane containing a dimethoxy-diphenyl-disazobis-8 amino-1-naphthol-5, 7-disulphonic acid dye.[38] The film is quite inexpensive, being priced at only 0.042 cent per 1000 sq in. The physical and optical characteristics are quite uniform. The commercial film identified as duPont No. 300 MSC[39] has a controlled thickness of 1 mil and an initial transmission that is fairly constant.[36]

In using Henley's technique, sheets of cellophane are cut into strips about 1-3/4 inches long and 1/2 inch wide. The sheets are then placed in an aluminum holder especially constructed to fit the standard Beckman cell holder.

Henley reports that the most satisfactory absorption peak was found at 6550 Angstroms. This wavelength was used with a DU Model Beckman spectrophotometer with a slit width of 0.15. Henley exposed cellophane films of the type described to varying dosages of gamma radiation from cobalt-60. In all radiation exposures the film was sandwiched between 1/8-inch-thick sheets of polyethylene. The changes observed in percent transmission as a function of radiation dosage are shown in Figure 3.7 and difference in percent transmission as a function of radiation dosage is shown in Figure 3.8. Figure 3.8 shows calibrations at dose rates of about 100,000 roentgens per hour from cobalt-60 sources and includes data from the large gamma source (40-42) in the Fission Products Laboratory, The University of Michigan.

According to Henley, the dye in the film is decolorized as a result of reduction by radiation in a statistically random manner. A given fraction of the dye is reduced to the leuco form following a first-order chemical reaction. Color is not regained and there is no subsequent darkening of strips stored over 1 month. Also neither the addition of acid or base nor contact with oxygen will produce a return of the color.[37]

An equation for the curves of percent transmission vs. dosage may be written as:

$$r = (0.68 \pm .01)(10^6)(T - T_0) \qquad (3.1)$$

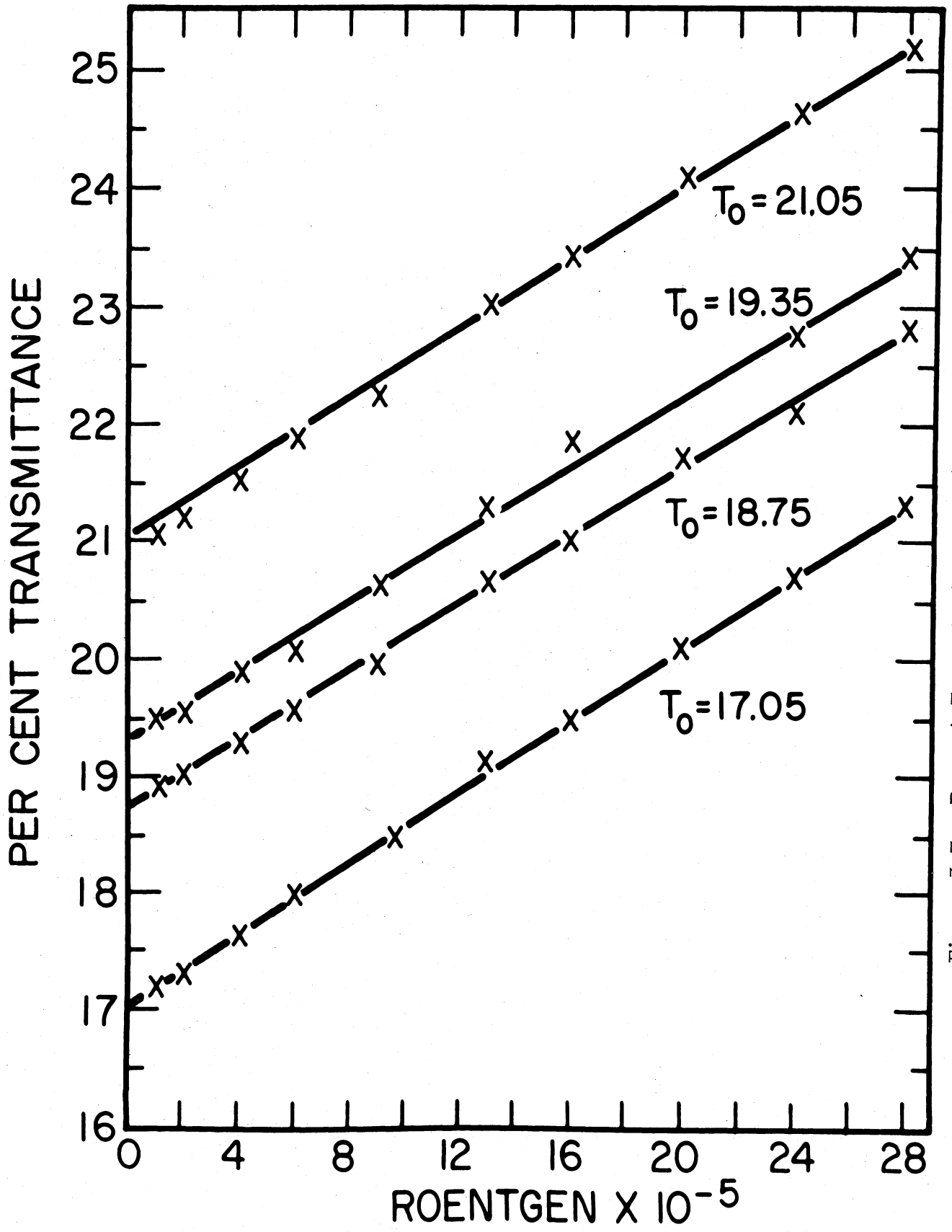

Figure 3.7. Percent Transmission vs. Gamma-Radiation Dosage for Cellophane Film. (36)

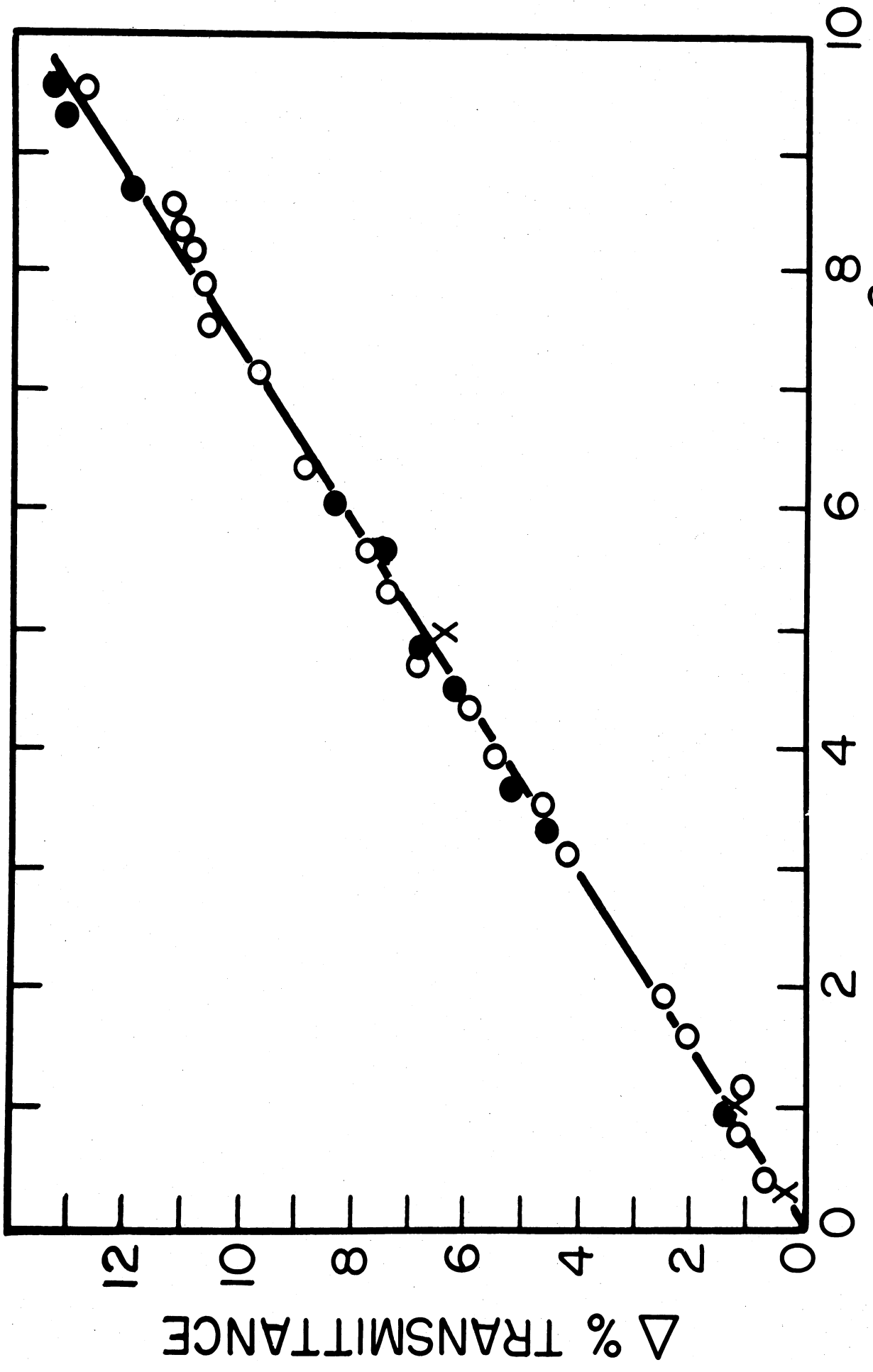

Figure 3.8. Change in Percent Transmission vs. Gamma-Radiation Dosage for Cellophane Film. (37)

where:

r = dosage in roentgens
T = percent transmission at dosage r
T_o = percent transmission at zero dosage

According to Henley, the probable error of the calculated dosage over the range shown in Figure 3.7 varies from about 7 percent at 3×10^6r up to 60 percent for dosages as low as 200,000 r. However, at higher dosages for which the transmittance change is more than about 20 percent the decomposed dye molecules begin to compete with the dye for radiation and the kinetics of the reaction are changed. In this range Henley recommends plotting the log of absorbance vs. dose. Such a plot gives a straight line indicating that destruction follows the "direct hit" or "target" theory.

A comparison of the results obtained from cobalt-60 gamma radiation with those obtained from high-speed electron bombardment using accelerators is shown in Figure 3.9. Note that the change in transmittance for a dose of 10^6 roentgens is independent of dose rate but that those for electron radiation are 2.2 times greater than for cobalt-60 gamma radiation. Henley suggests that this difference is explained on the basis of the difference in linear energy transfer (LET) between cobalt-60 gamma photons and 2-Mev electrons.[37] Figure 3.9 shows Henley's calibration curve for electron radiation.[37]

3.5 Coloration in Plastics

The polyvinylchloride (PVC) film dosimeter described previously incorporates an acid-base indicator. However, the color changes in PVC itself and in other plastics such as polymethyl methacrylate and polystyrene could possibly be used for dosimetry. The coloration of PVC by radiation is proportional to absorbed dose and Artandi[43] has suggested its use as a dosimeter in the range of 10^5 to 10^7 rads. In polymethyl methacrylate radiation causes changes in both color and ultraviolet absorption. Fowler and Day[44] have investigated these changes in both polystyrene and polymethyl methacrylate. However, Artandi[45] concludes that according to their findings neither effect in polymethyl methacrylate is usable for dosimetry as nonlinearity was observed in the range $1 - 6 \times 10^6$ rads.

3.6 Chemical Changes in Plastics

In addition to color changes as described above use of certain chemical changes produced by irradiation of plastics have been investigated for dosimetry. These changes include polymerization, degradation, and gas evolution.

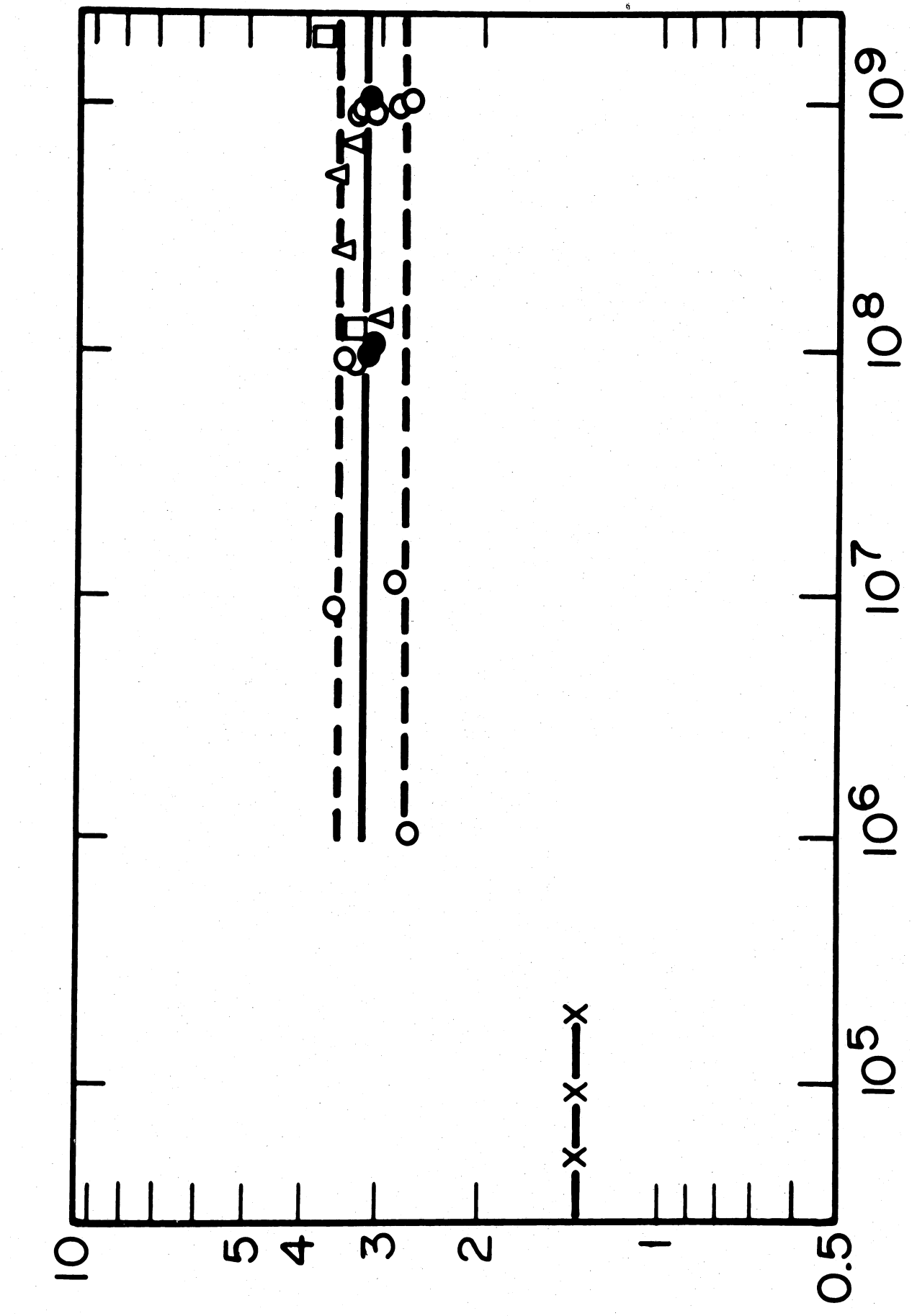

Figure 3.9. Comparison of Gamma Photon and Electron Radiation and Different Dose Rates for Cellphane Films (Semi-Log Scale). (37)

(a) Polymerization

The effect of radiation on various polymerization reactions have been studied. Such systems are dependent on radiation intensity and on impurities and the techniques of measurement are rather complicated, and hence are not very practical, for dosimetry.

(b) Degradation

Alexander has studied the degradation of solid polymethyl methacrylate by ionizing radiation.(46) He suggested use of intrinsic viscosity measurements of the degraded polymer as a method of dosimetry. The reciprocal of viscosity molecular weight varies linearly with the dose over a hundredfold change in molecular weight or over a dose from a fraction of a megarad to 100 megarads.

Feng has proposed a dosimetry method based on degradation of polystyrene in carbon tetrachloride solution.(47)

(c) Gas Evolution

Certain gases, particularly hydrogen, are evolved upon irradiation of polymers. The evolution of hydrogen is associated with free radical or double-bond formation and cross linking. The dehydrochlorination of polyvinylchloride and its use as a method of dosimetry is already described.

The amount of gas evolved can be used as a measure of the dose received by a polymer. However, difficulties are encountered because of slow diffusion and dependence of the rate of evolution on sample size and shape.

3.7 Glass Dosimeters

Irradiation of glass causes changes in the absorption characteristics for both ultra violet and visible light. These changes have been used as a basis for several types of glass dosimeters.

3.8 Phosphate Glass Personnel Dosimeter

A phosphate glass dosimeter based on the principle of radiophotoluminescence was developed as a personnel dosimeter for the U.S. Navy.(48-51) The dosimeter is known as the DT - 60/PD and is used to measure radiation

exposure levels received by military personnel in the same way that film badges are used for laboratory personnel. The waterproof glass dosimeter is much more rugged than the film badge and is useful over a range of 10 r to 600 r. In the energy range from 5 Mev down to 80 kev the radiation dosage can be measured within an accuracy of ± 20 percent (except for the range of 120 to 150 kev).

The glass used is a silver-activated phosphate glass of relatively low cost and adapted to large-scale manufacture. The phosphate glass base has[49] a composition by weight of: 50 percent $Al(PO_3)_3$, 25 percent $Ba(PO_3)_2$ and 25 percent KPO_3. To this base glass, 8 percent $AgPO_3$ is added to produce the optimum properties for dosimetry. This silver-activated phosphate glass emits a fluorescence when it is exposed to light in the violet and near-ultraviolet region. The intensity of the fluorescence peaks sharply at about 2400 Å as shown in Figure 3.11.

When the glass is irradiated the peak at the shortest wavelength is shifted so that the glass no longer fluoresces appreciably at 2400 Å but requires a longer wavelength as is indicated in Figure 3.11 by the dashed line peaking at about 3300 Å. The increase in intensity of the fluorescence at the longer wavelength is directly proportional to the radiation dosage received as shown in Figure 3.12.

It is believed that electrons produced by the interaction of radiation and glass are trapped by Ag^+ ions in the glass, reducing the ions to "atomic" silver centers, Ag^0, which are responsible for the new absorption band.[49] The fluorescence is also a function of the radiation intensity.

The dependence upon the energy of the radiation is reduced by placing two lead shields on either side of the glass with a small hole (0.107 in. diameter) to improve the response to the lower energy radiation.[50] This corresponds more or less to the window in the film badge.

The increase in fluorescence at the longer wavelength is permanent. This is an advantage as it permits keeping glass dosimeters on file over a long period of time. Storage for months at room temperature does not affect the sensitivity of the dosimeter.

The dosimeter itself is a locket type which is designed to be worn around the neck. A block of the glass 3/4 x 3/4 x 3/16 inch is enclosed in a circular black plastic case 1/2 inch thick and 1-1/2 inches in diameter. The case is made in two threaded mating halves which are firmly screwed together to hold the glass as shown in Figure 3.13.

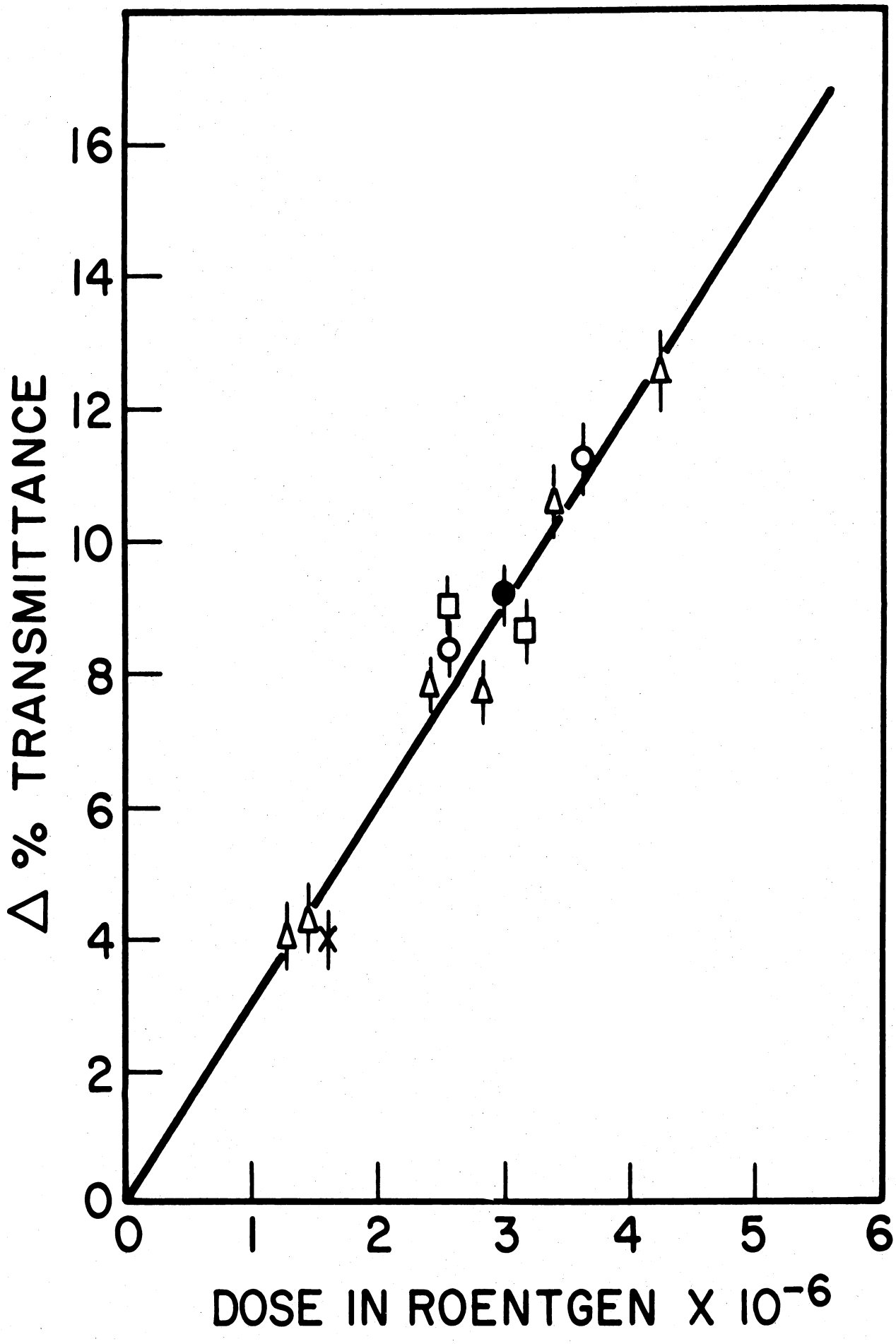

Figure 3.10. Calibration Curve for Electron Radiation of Cellophane Films. (37)

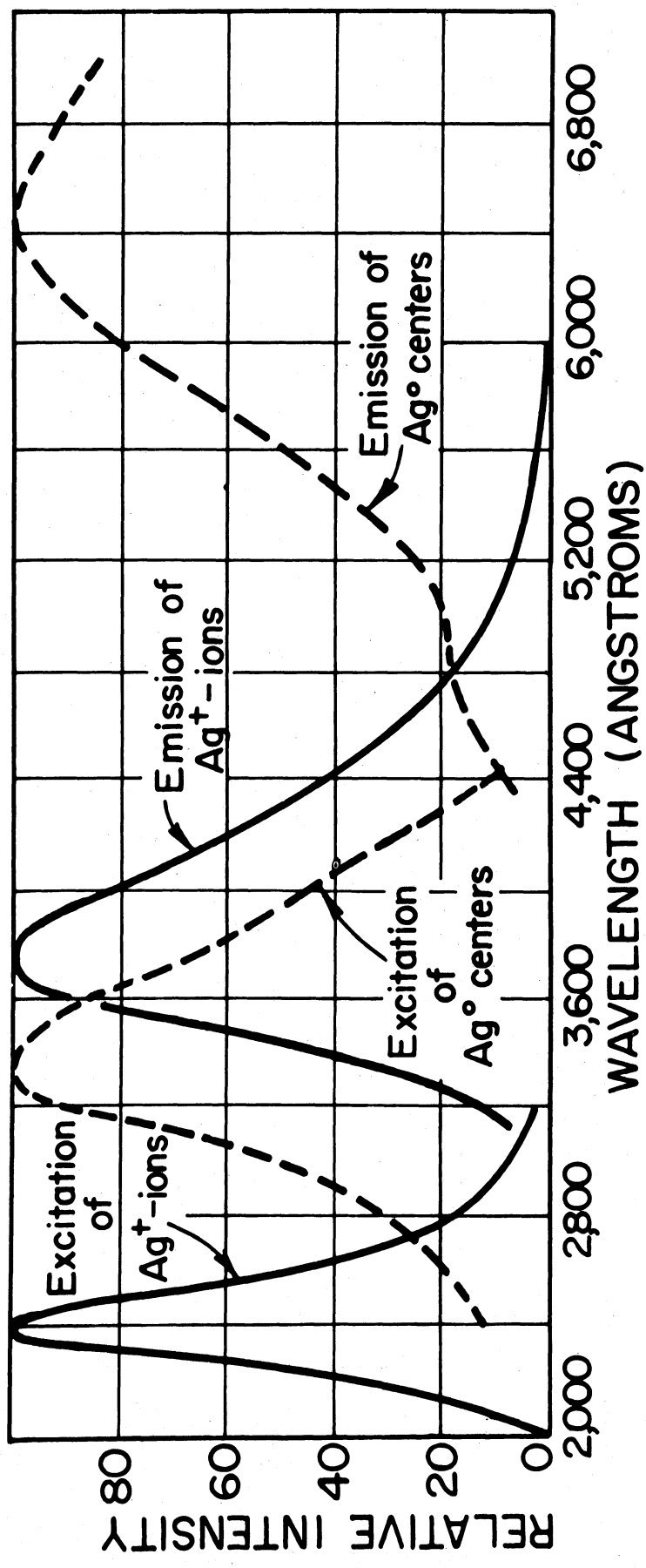

Figure 3.11. Spectra of Nonirradiated (Ag^+ Centers) and Irradiated (Ag^0) Phosphate Glass. (49)

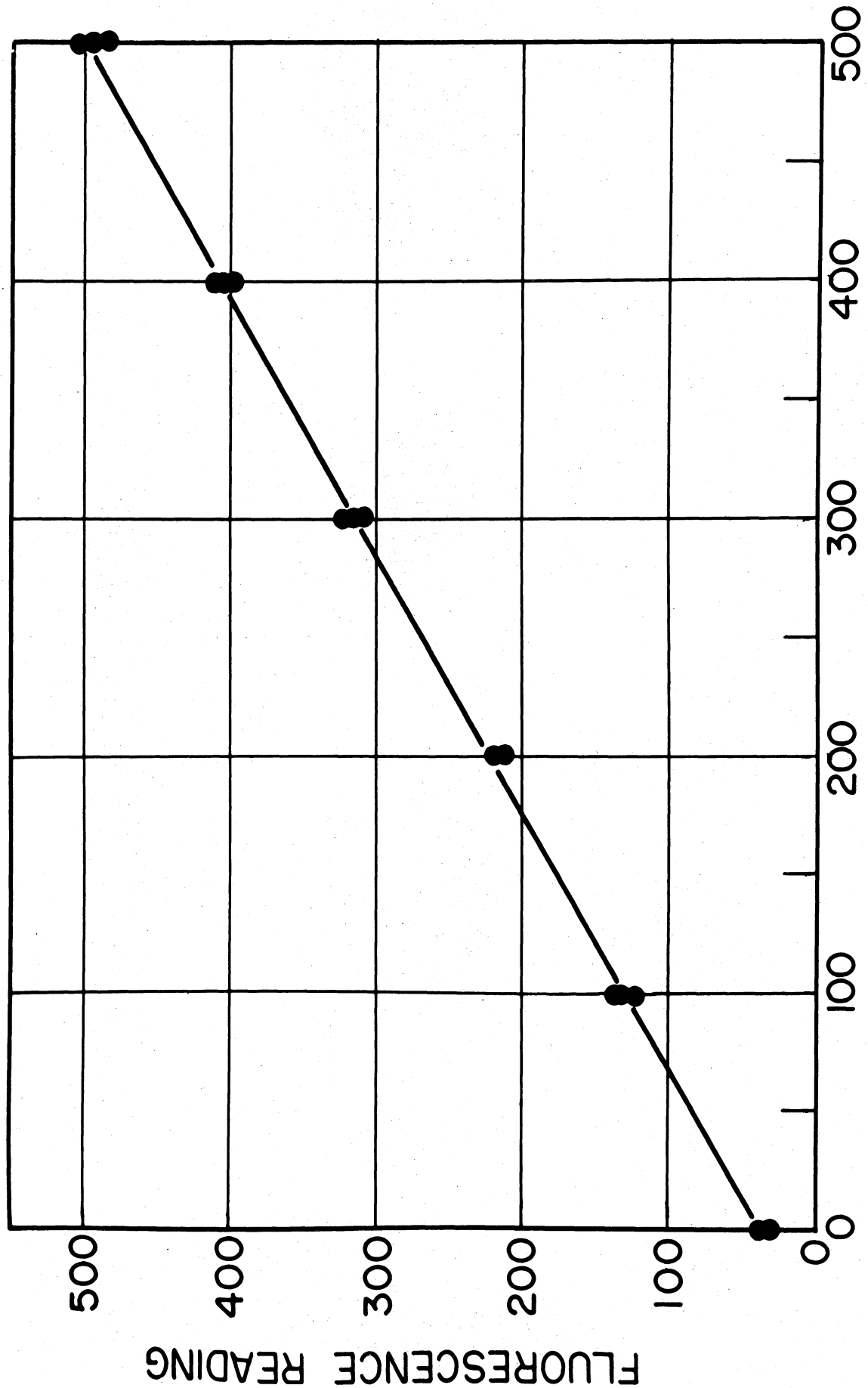

Figure 3.12. DT-60/PD Dosimeter Response. (49)

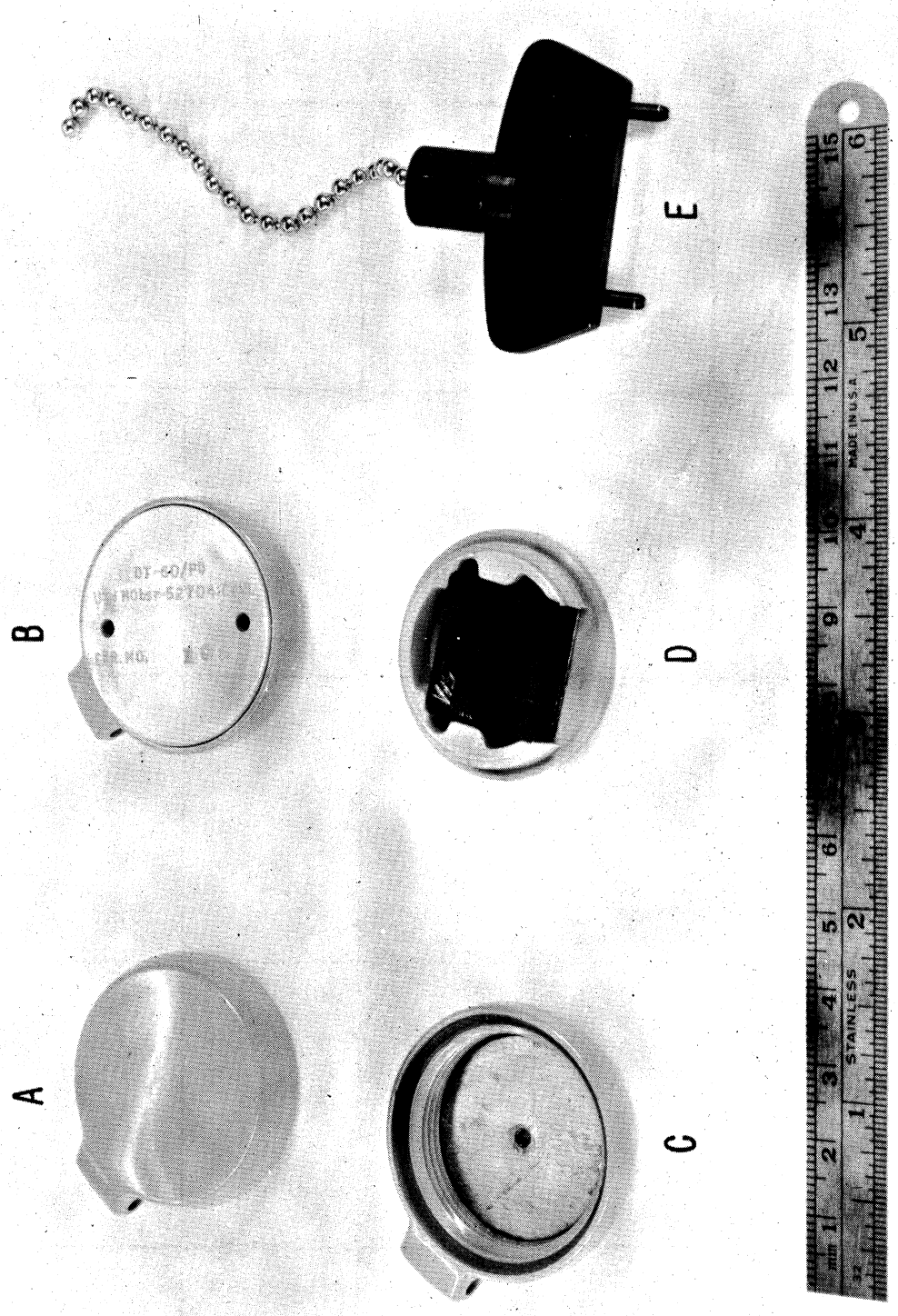

Figure 3.13. Phosphate Glass Dosimeter, (A) Assembled Topside, (B) Assembled Underside, (C) Cover Portion Showing Lead Shield, (D) Base Portion Showing Glass Block, and (E) Wrench for Assembly and Disassembly. (49)

To read the dosimeter the locket is opened with a small spanner wrench type tool (see E of Figure 3.13) and the glass block is removed and placed in a special instrument called a "fluorimeter" or "dosimeter reader". Here the glass is exposed to 3650 Å light and the fluorescence read directly from the calibrated scale of the meter. The longer wavelength is used to isolate the Ag^0 emission band from the Ag^+ emission band. A photograph of one model of dosimeter reader is shown in Figure 3.14.

3.9 High-Dosage Phosphate Glass

Schulman[52,53] has reported that the phosphate glass used in radiophotoluminescence dosimetry by the U.S. Navy also can be used for measuring much higher dosages than the 600 r limit for personnel dosimeters.

For multimillion rep exposures, another property of the same glass has been found useful as a dosimeter. Changes of optical density, under standard time and temperature treatment, have yielded simple, inexpensive, and reproducible means of measurement of radiation exposure. Figure 3.15 shows a photograph of the glass blocks before and after irradiation. After irradiation the glass develops a broad absorption band which peaks at 3200 Å and then spreads out into the visible region and which gives a yellow-brown coloration to the irradiated glass. The optical density as a function of wavelength is shown in Figure 3.16 for phosphate glasses with and without silver before and after irradiation.

Figure 3.17 shows the dose dependence of the absorption of phosphate glass measured at different wavelengths. At low dosages, adequate optical-density measurements are made at 3500 Å using 3 mm thick glass. However, at higher doses and 3500 Å the optical density is too great and a longer wavelength should be used.

The optical density resulting from a given dose to glass or film, as determined by a primary method, such as ferrous sulfate dosimetry, is found to vary sharply with radiation energy. Thus, although this method provides, after calibration, a useful tool for a particular source and geometry, care must be taken in applying data from one laboratory to the work of another. Figure 3.18 shows the variation in phosphate glass sensitivity to X-radiation of different energies relative to its sensitivity to cobalt-60 gamma radiation.

Figure 3.18 shows that the sensitivity between 200 kev and 1 Mev is quite constant. This is the range of energies of gamma photons for most

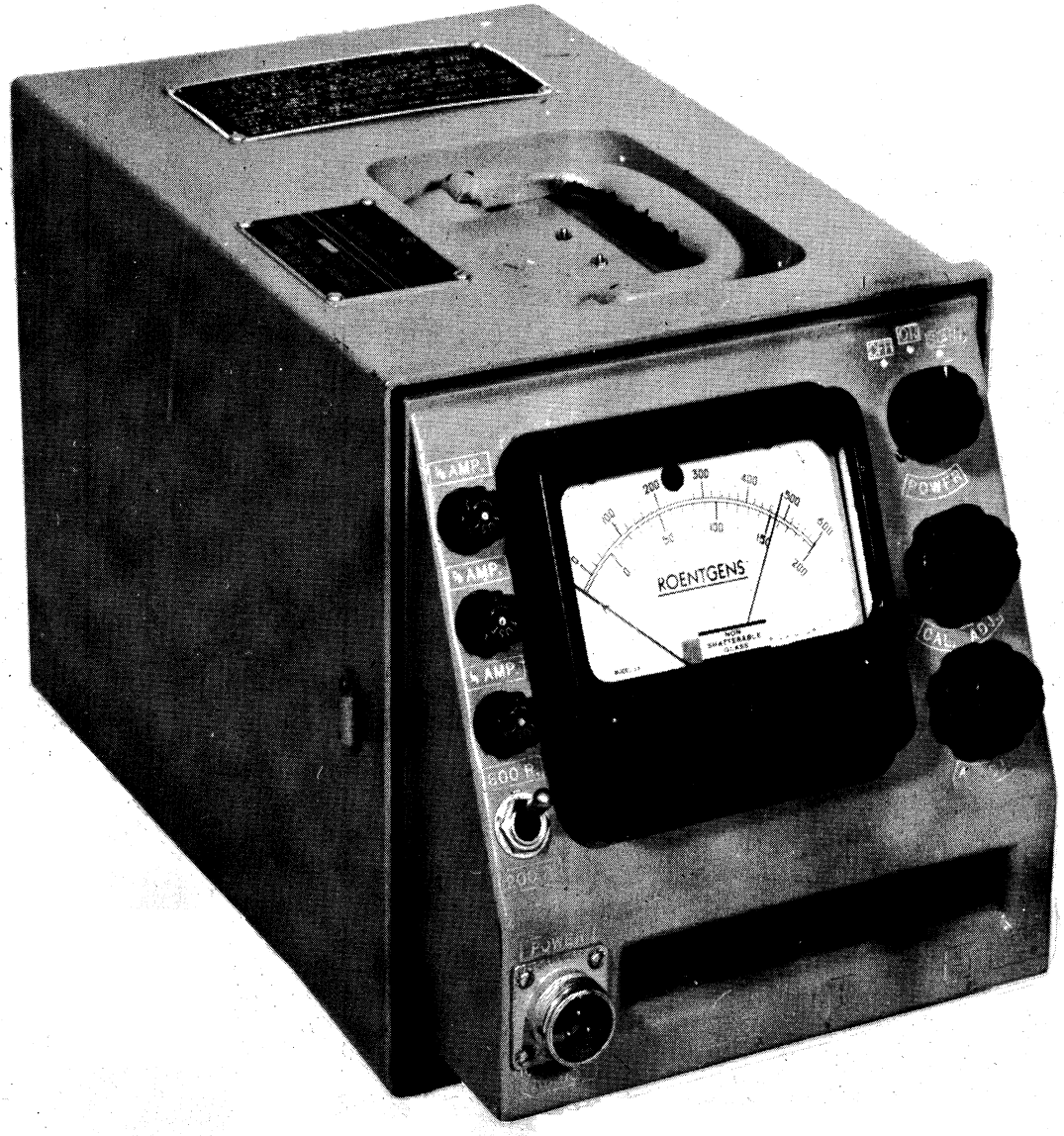

Figure 3.14. One Type of Reader for Phosphate Glass Dosimeter. (49,50)

Figure 3.15. Photograph of Phosphate Glass Blocks Before and After Irradiation.

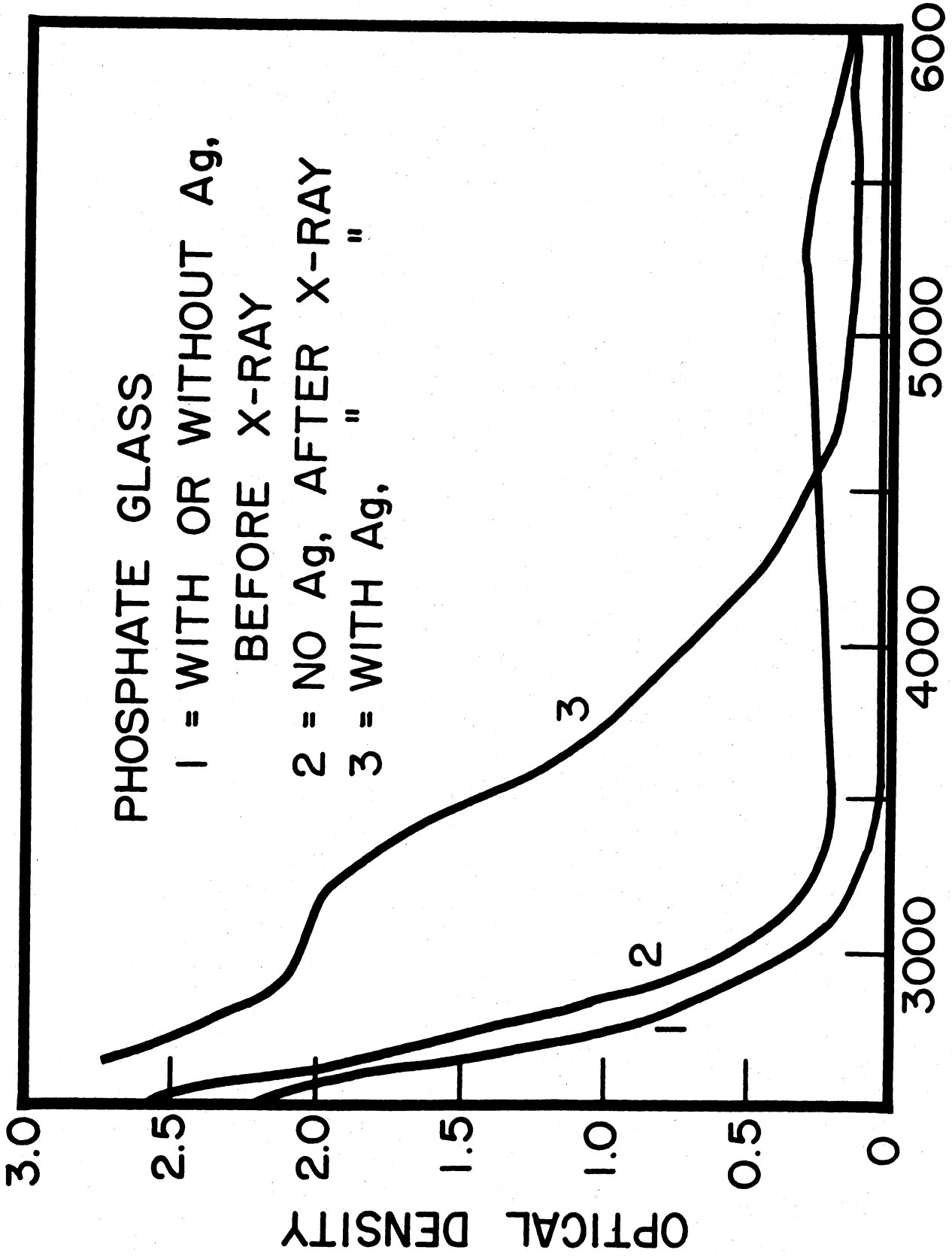

Figure 3.16. Absorption Spectra of Phosphate Glasses. (53)

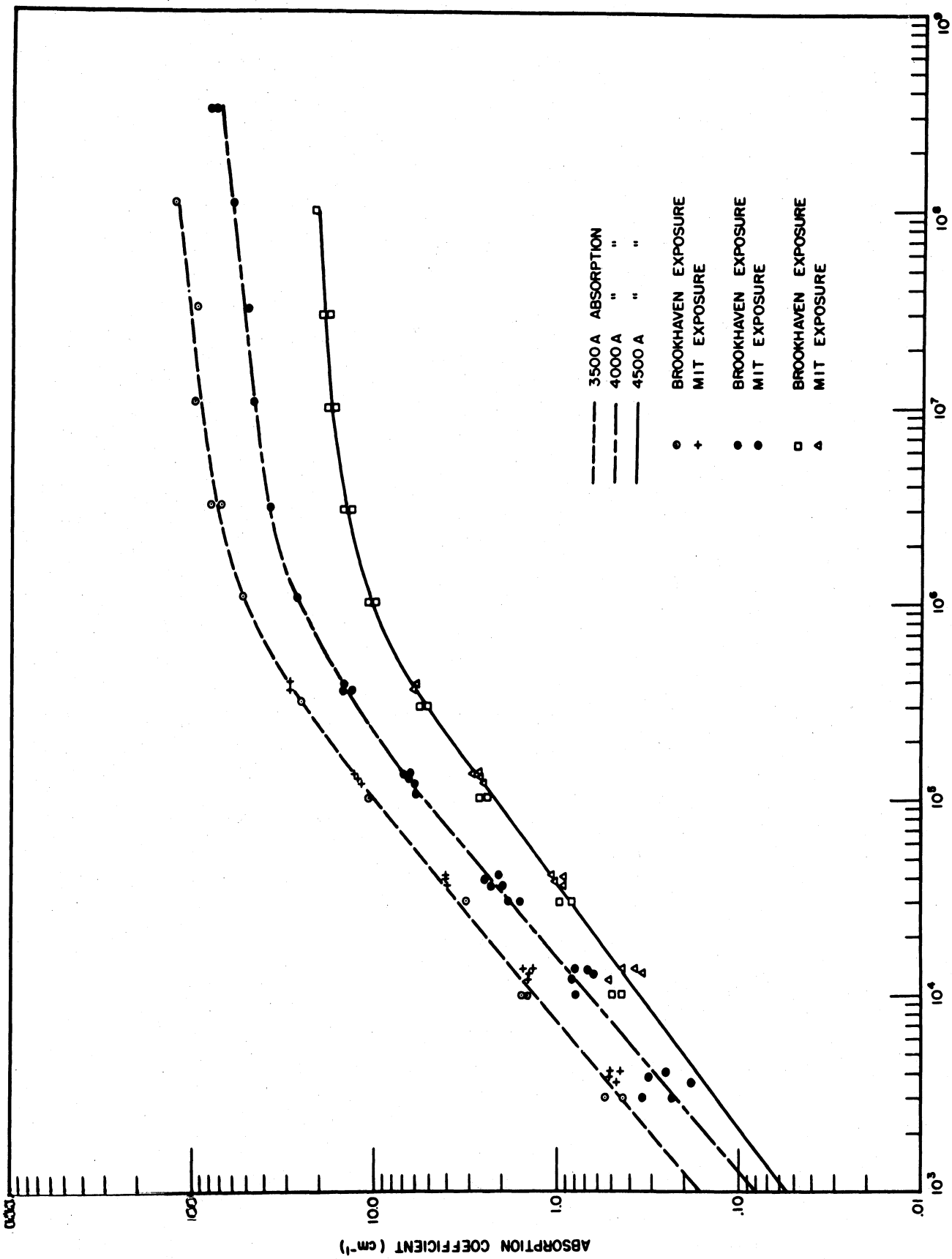

Figure 3.17. Dose Dependence of Absorption of Phosphate Glass Measured at Different Wavelengths. (53) (log-log scale)

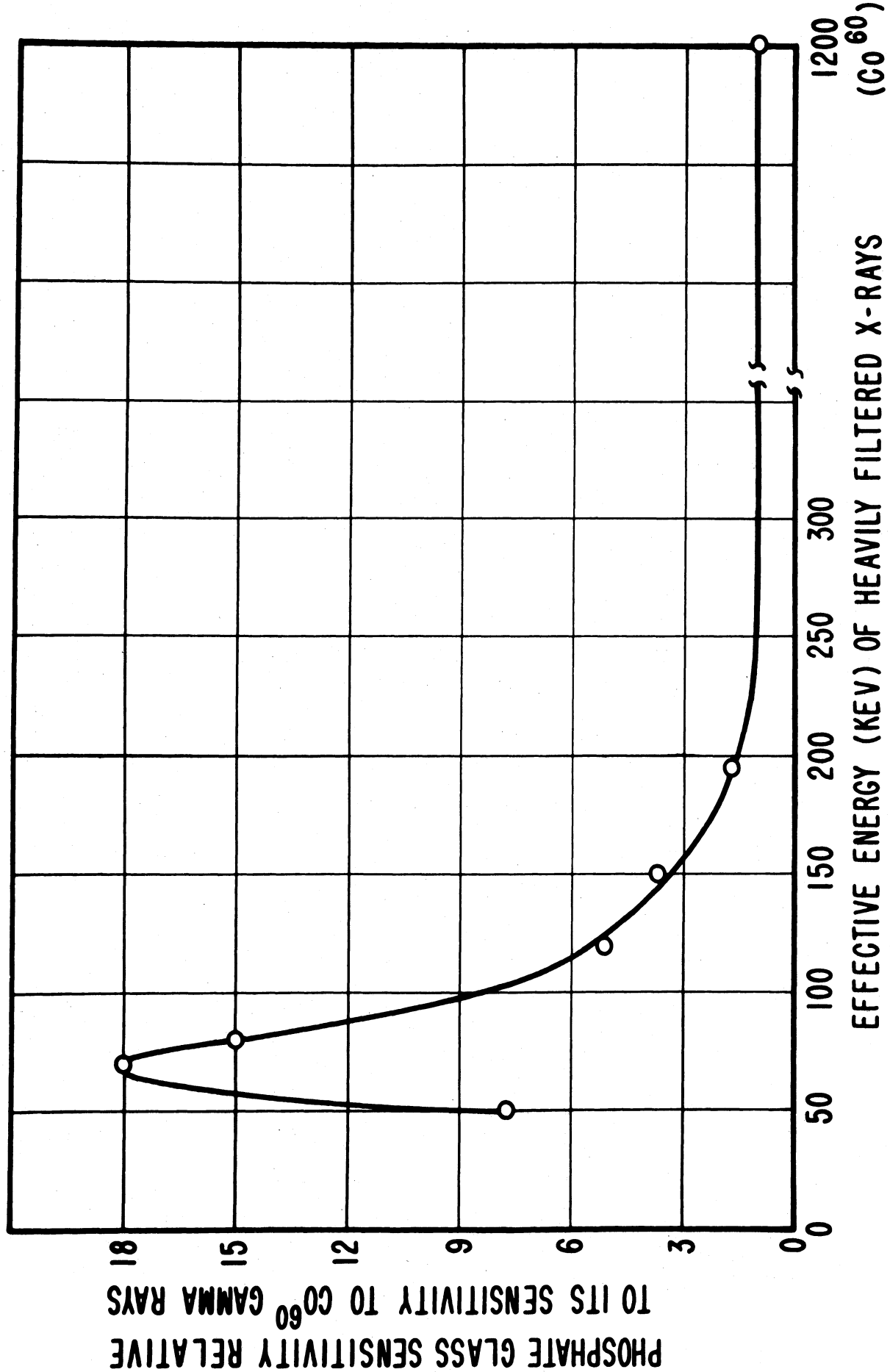

Figure 3.18. Dependence of Phosphate Glass Sensitivity Upon Energy of Radiation. (53)

radioisotopes of commercial interest; such glass dosimeters should therefore be useful for radiation spectra in this range.

Another problem is the tendency of the glass to fade with time. This effect may be reduced by heating the glass to 130°C for 13 minutes after exposure. This accelerates the removal of early fading without destroying the more stable color centers. A comparison of the fading in heat treated and non-heat treated glass is shown in Figure 3.19.

Using optimum procedures, dosages up to 2×10^6 rep can be determined within an accuracy of 5 percent. At higher dosages the curve of density vs. dose becomes so flat (see Figure 3.16) that the accuracy is decreased. A special development is the small volume dosimeter shown in Figure 3.20 which may be inserted in the body to measure doses used in radiation therapy.(55)

3.10 High Dosage Cobalt Glass

A "cobalt" glass has recently been developed(56,57) that shows considerable promise for use in high level dosimetry. The glass has the approximate composition of:

62%	SiO_2
11%	Na_2O
21%	B_2O_3
6%	Al_2O_3
0.1%	Co_3O_4

This glass exhibits absorption vs. dosage characteristics similar to those of phosphate glass described previously. Good linearity is obtained up to about 10^6 **rad** with less sensitive response at higher dosages. The primary advantage of this glass over the phosphate glass is its greater stability against fading as shown in Table 3.2.

3.11 Chemical Dosimeters

Radiation dosage was measured almost exclusively by means of gas ionization chambers until the advent of nuclear reactors, and the large-scale production of radioisoptopes. These developments led to a renewed interest in chemical techniques for measuring high-level dosage and also for measuring dosage in media other than air. The use of ionization chambers to measure radiation dosage is a very satisfactory procedure if the sample to be irradiated is air or some other gas. However, in a great many

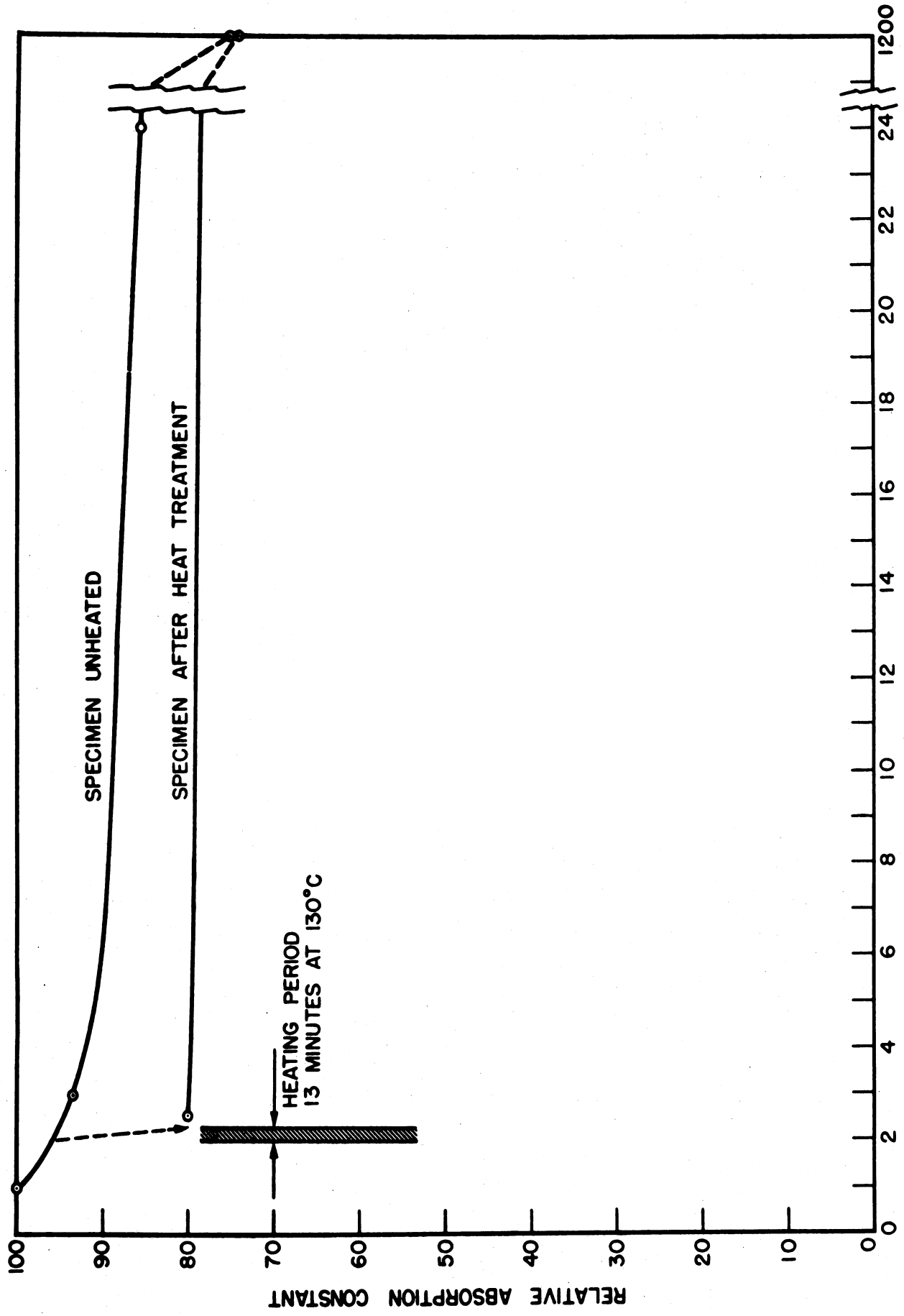

Figure 3.19. Stabilization of Coloration of Silver-Activated Phosphate Glass by Thermal Acceleration of Fading. (48)

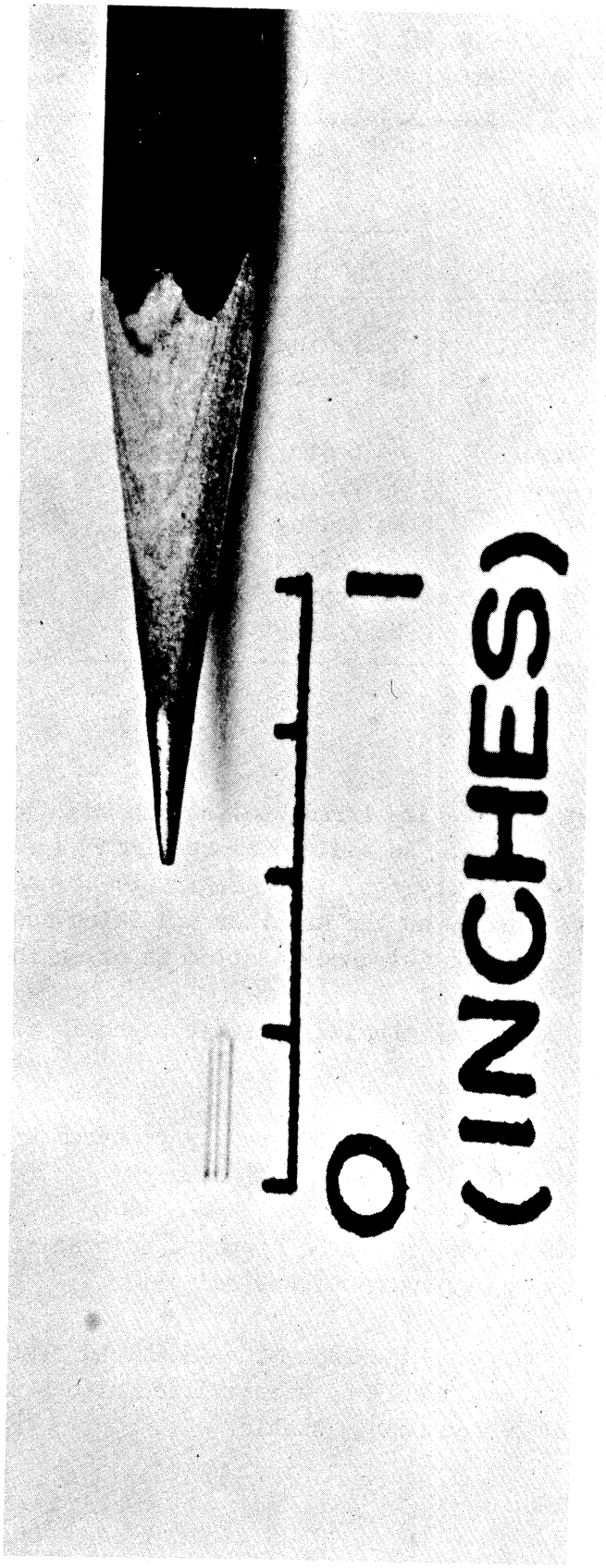

Figure 3.20. Photograph of the Small-Volume Phosphate Dosimeter. (55)

TABLE 3.2

FADING OF IRRADIATED COBALT GLASS AFTER STORAGE IN DARK AT ROOM TEMPERATURE(57)

Measuring Wavelength	Storage Time	Fading (%) Normalized at 1 hr. After Various Irradiation Doses			
		10^4 r	10^5 r	10^6 r	10^7 r
350	1 day	No fading	No fading	No fading	Too dense
	1 week	No fading	No fading	7	to read
	2 months	3	5	9	
400	1 day	No fading	No fading	4	Too dense
	1 week	No fading	2	10	to read
	2 months	No fading	4	12	
500	1 day	No fading	2	7	8
	1 week	No fading	6	18	14
	2 months	No fading	12	23	23

studies, liquids and solids are irradiated and these have stopping powers quite different from gases. An additional requirement for accurate dosimetry is similarity in geometry, so, it is desirable to use a dosimeter which has the same stopping power as the absorber and which has a sufficiently flexible geometry to permit its incorporation in or on the absorber.

The most practical chemical dosimeter should meet the following requirements:

1. The dosimeter should be readily prepared and stable in storage for long periods of time.

2. It should give a linear response to dose, independent of the energy spectrum of the radiation.

3. The product of the radiation-catalyzed reaction should be readily measurable by standard techniques of analysis and should be reasonably stable.

At the present no chemical system is known that rigorously meets all of the above specifications, although many systems have been developed that show promise and are being steadily improved.

Two reactions for use in dosimetry which have received considerable interest are: 1) the oxidation of ferrous sulfate to ferric sulfate; 2) the reduction of ceric sulfate to cerous sulfate.[58,59] Figures 3.21 and 3.22 give respectively the curves for the oxidation of ferrous ion and the reduction of ceric ion as a function of radiation dosage. The oxidation of the ferrous ion has received more interest and use than the reduction of the ceric ion and therefore will be described in detail.

3.12 Ferrous-Ferric

The ferrous-ferric reaction was originally studied by Fricke[60-63] and as a result the ferrous sulfate dosimeter is sometimes referred to as the "Fricke" dosimeter.[59] The American Society for Testing Materials adopted this method in 1959 as a tentative standard for measuring the absorption of gamma radiation by chemical dosimetry.[64]

The ferrous-ferric reaction determines the combined free-radical and molecular-product yields in an aqueous solution. In particular, this system is most reactive with hydrogen, hydroxyl, or hyperoxy radicals formed in the solution. The ferrous ion is oxidized to ferric ion by hydroxyl and hydroperoxyl radicals, as well as by molecular hydrogen peroxide:

$$Fe^{++} + OH \rightarrow Fe^{+++} + OH^- \qquad (3.1)$$

$$H + O_2 \rightarrow HO_2 \qquad (3.2)$$

$$Fe^{++} + HO_2 \rightarrow Fe^{+++} + HO_2^- \qquad (3.3)$$

$$Fe^{++} + H_2O_2 \rightarrow Fe^{+++} + OH^- + OH \qquad (3.4)$$

The yield of the oxidation reaction, ferrous to ferric sulfate, has been found to be independent of the energy and of the dosage rate of the incident radiation over a wide range of the original ferrous ion concentration. However, it has been found that yields may be lowered by as much as 25 percent when dose rates exceeding 1,000 r/min are being measured.[65,66] This method is sensitive to pH and oxygen concentration. The former is overcome by the use of a standard acidity, 0.8N sulfuric acid; the latter by thorough aeration of the solution before use.[58]

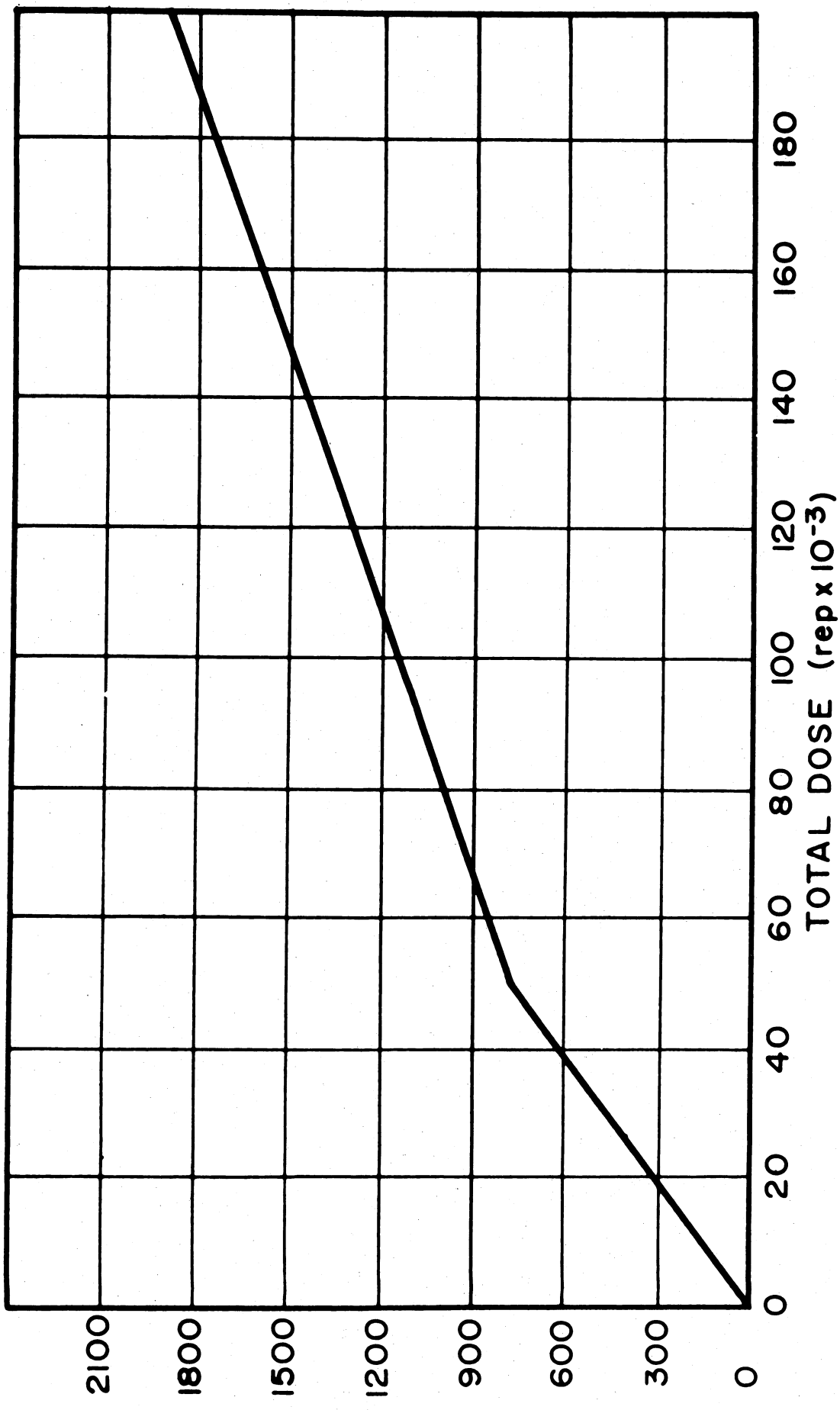

Figure 3.21. Micromoles of Ferrous Ion Oxidized as a Function of the Total Irradiation. (58)

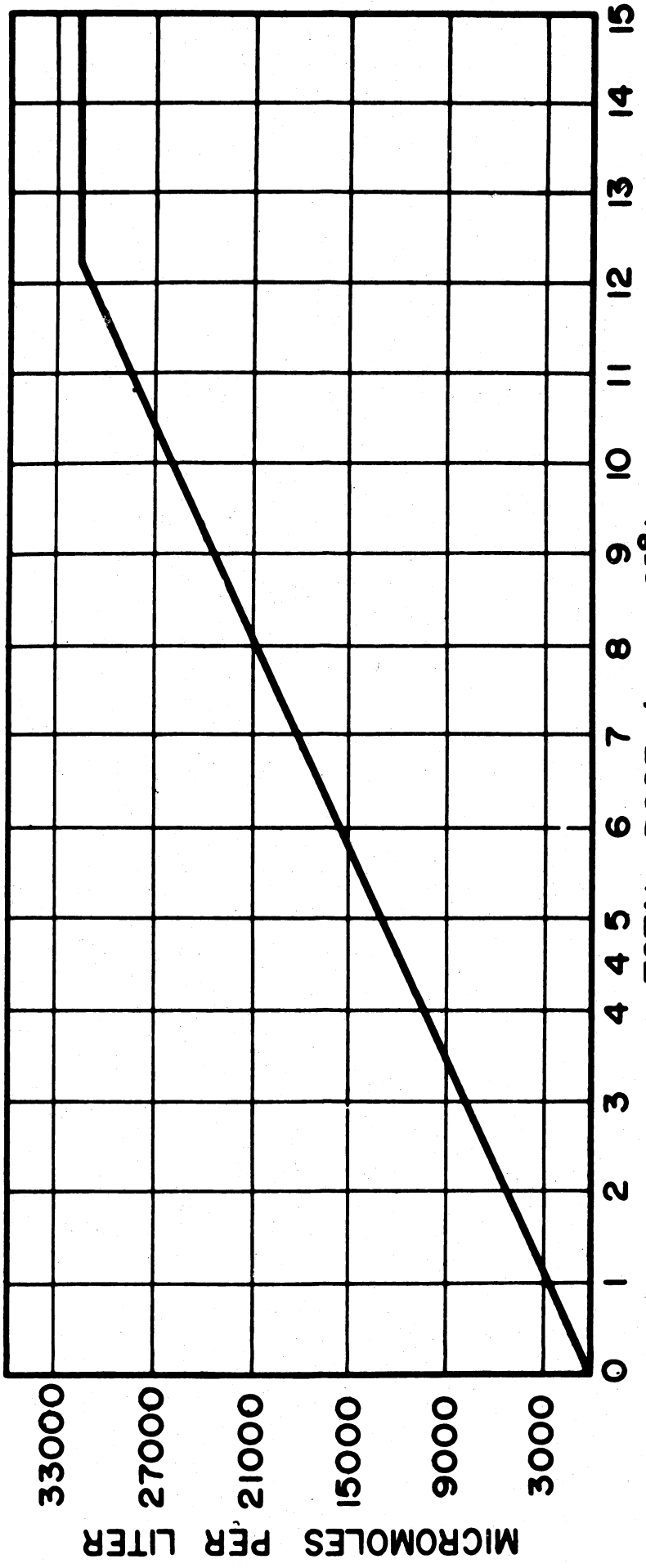

Figure 3.22. Micromoles of Ceric Ion Reduced as a Function of the Total Irradiation. (58)

Ferric ion concentration varies linearly with dose up to about 50,000 rep. A linear relationship is observed at high doses as well, but with different slope as shown in Figure 3.21. Because of this discontinuity, presumably the result of the consumption of all the original oxygen, it is best to maintain a total exposure of less than 50,000 rep.

Originally Weiss[58] recommended that the reagent solution used be prepared with considerable care. The best reagent-grade ferrous ammonium sulfate is diluted in triple-distilled water acidified with sufficient reagent-grade sulfuric acid to prevent hydrolysis. Later, Weiss stated[59] that small quantities of sodium chloride (0.15 gm NaCl/gm $FeSO_4 \cdot 7 H_2O$) inhibits organic impurity effects so that solutions may be made from ordinary material. The ferrous salt is added to the 0.8N H_2SO_4 but the exact concentration of ferrous ion need not be determined as the analysis depends upon the determination of the concentration of ferric ion.

To analyze for ferric ion concentration it is necessary to prepare a standard reference ferric ion solution. Weiss recommends commencing with a solution in which the ferric ion concentration is about 0.001 - 0.005 M.

This solution may be completely reduced by means of a Jones reductor and titrated with standard permanganate. A known amount of this reduced solution may then be quantitatively oxidized with peroxide and diluted to a known volume to prepare various concentrations of standard reference ferric ion solutions. These standard ferric ion solutions are then used to prepare a curve of optical density vs. concentration.

The optical density is conveniently determined by means of a Beckman spectrophotometer. The maximum absorption for ferric ion occurs at about 304 mμ. However, this absorption peak is rather broad and the results are not very sensitive to the wavelength. Weiss used a setting of 305 mμ with a slit width of 0.5 mm, quartz cells and a hydrogen lamp. In the analysis, a nonirradiated sample of the ferrous sulfate solution is used as a blank and the difference between the optical density of the irradiated solution and the blank is determined. This difference in optical density permits the calculation of the oxidation of ferrous ions by means of the calibration curve of optical density vs. micromoles of ferric ion. This determination permits the total dose to be estimated by means of Figure 3.21. By means of a conversion constant, the calibration curve may be combined with Figure 3.21 to give a curve which reads directly in kilorep dosage as shown in Figure 3.23.

Any laboratory using this method should prepare its own optical density calibration survey as different instruments will give slightly different curves. The curve in Figure 3.23 was prepared for the instrument in

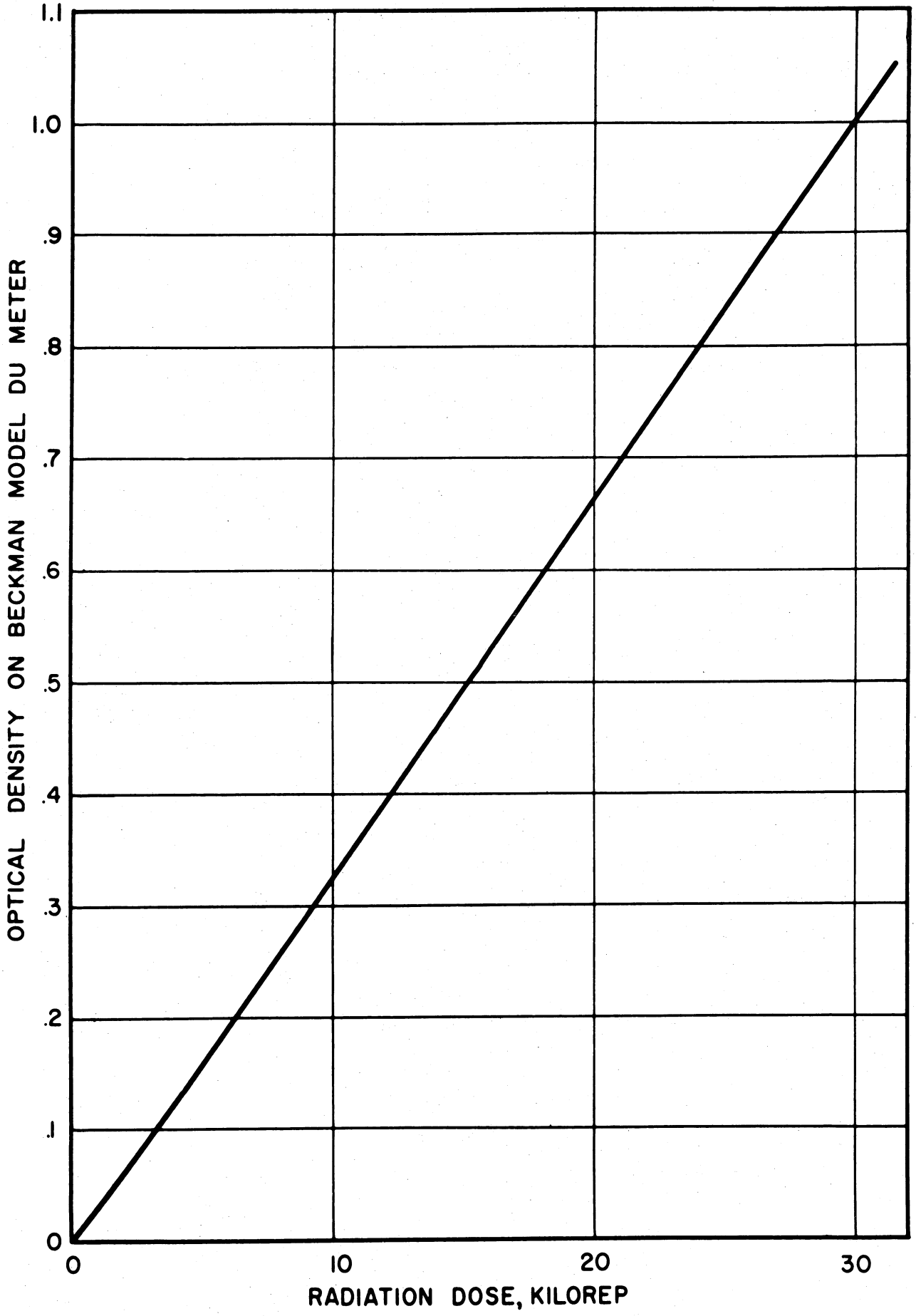

Figure 3.23. Calibration and Conversion Curve for Beckman Model DU Meter in the Fission Products Laboratory, The University of Michigan.

the Fission Products Laboratory and using a conversion constant of 15.6 micromoles per liter per kilorep.[67] A further precaution is that for best results dosage to dosimeters should be limited to less than 50,000 rep. The usual procedure in the Fission Products Laboratory is to limit the exposure time of the dosimeter so that the estimated dose is about 30,000 rep so as to stay below the break in the curve. Although this reaction is extensively used, it is not especially good for high-intensity sources because of the high G value and the fact that the iron oxidation is dependent upon the oxygen concentration.

The G value stated above for oxidation of ferrous sulfate holds for Co^{60} gamma radiation and electrons. However, the G value for this dosimeter varies for radiation of different quality and energy[68] and hence, a different conversion factor should be used.

For a given radiation exposure, ferric ion yield has been found to depend upon the diameter of the container used. This effect is presumably due to the increased production of secondary electrons in the vessel walls as compared to the production in the solution. Valid absorption measurements can best be obtained if the dosimeter vessel approximates the vessel to be used for irradiation. If this is not possible, the diameter of the dosimeter should not be less than 8 mm.[58,59] Additional information on the ferrous-ferric reaction and its use in dosimetry is given in References 69-76.

3.13 Ferrous Sulfate-Cupric Sulfate

The ferrous sulfate-cupric sulfate dosimeter is fairly new in the field.[77,78] It eliminates some of the difficulties experienced with the Fricke dosimeter. The reaction consists of the oxidation of the ferrous ion by hydrogen peroxide formed in the gamma-ray "hotspot" and is not due to oxidation by free radicals.

The addition of cupric ion to the ferrous-ferric system reduces the G value from 15.6 to 0.66.[77] The reason proposed for the decrease in ferric ion yield is that the cupric ion reacts with the hydrogen atoms and hydroperoxy radicals as follows:

$$Cu^{++} + H \rightarrow Cu^{+} + H^{+} \qquad (3.5)$$

$$Cu^{++} + HO_2 \rightarrow Cu^{+} + H^{+} + O_2 \qquad (3.6)$$

Reactions (3.5) and (3.6), competing with reactions (3.2) and (3.3) (see section on ferrous-ferric dosimetry) reduce the ferric ion yield. A further

reduction in the ferric ion yield is effected by the reaction:

$$Fe^{+++} + Cu^{+} \rightarrow Fe^{++} + Cu^{++} \qquad (3.7)$$

Thus, in the presence of cupric ion, the ferrous ion is oxidized only by molecular hydrogen peroxide, two ferrous ions being oxidized per molecule of hydrogen peroxide [cf. Equations (3.1) and (3.4)]. This system has been proposed as a chemical dosimeter(77,78) offering the advantages of oxygen independence and applicability over a wide range of dosage, as indicated in Figure 3.24.

The ferrous-cupric dosimeter has been employed in measuring gamma dosage from a cobalt-60 source and alpha-particle dosage from the boron-10 (n,α) lithium-7 nuclear reaction. It has been found that the hydrogen peroxide yields are higher for the heavy alpha-particles than for the gamma photons.

3.14 Ceric Sulfate

Ceric ions are reduced to cerous ions by the ionization products in the aqueous solution. The yield is linear with dose, independent of concentration over a wide range, energy independent from 100 kv to 2 Mev, and independent of dose rate. No difficulty is encountered with the consumption of oxygen in a closed system, as in the ferrous-sulfate reaction. The G value is about 2.4 molecules reacting per 100 ev energy absorbed.(58,70) The discontinuity in the cerous ion dose curve occurs above 10 million rep (see Figure 3.22), indicating that up to this total dosage the reaction is independent of the oxygen concentration. This makes much higher total dose measurements possible than with the ferrous-ferric ion system. Another advantage that the ceric-cerous system offers is that the yield is not diminished at high dose rates, as is observed with the ferrous-ferric system. However, trace amounts of organic compounds lead to erratic results, and also at low ionization energies the system shows a dependence on the ionization-energy spectrum. Although ferrous sulfate titration may be used, the most convenient method of analyzing the irradiated ceric-cerous solution is by means of a spectrophotometer. In this technique the absorption by ceric ion at 310 - 320 mμ is measured.(65) This technique gives an accuracy of 5 percent in determining dosage.

Although this reaction appears quite suitable for high intensity sources it has not been investigated as thoroughly as the more common ferrous sulfate reaction. It has been reported that considerable care must be used to obtain reproducible results. Inherently, however, the accuracy of

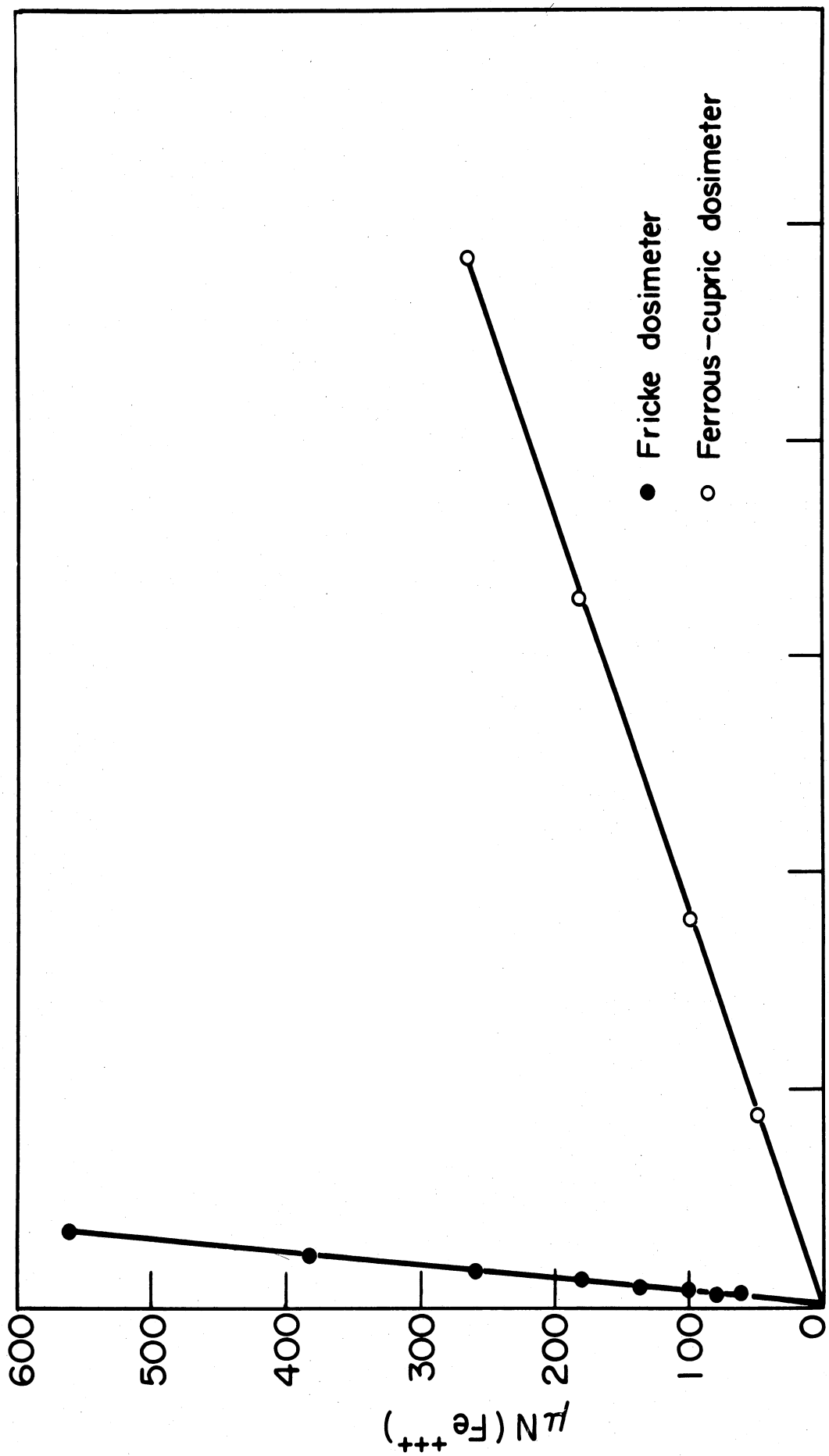

Figure 3.24. Comparison of Response Curves for Fricke and Ferrous-Cupric Dosimeters. (77,78)

the determination of the cerous content should be much better than the similar ion determination with the ferrous sulfate dosimeter since the change in optical density per unit change in ion concentration is greater.[79]

3.15 Chlorinated Hydrocarbons

Ionizing radiation may decompose halogenated hydrocarbons to form acid products which can be detected in aqueous solution by pH indicators. This principle has been used in the preparation of chemical dosimeters.[2,30,31,80] In the absence of inhibiting agents these reactions procede by a chain-reaction mechanism which is very sensitive to temperature and impurities. By introducing resorcinol or certain other alcohols (e.g., ethyl, hexyl and decyl) to the system, the long chain reaction is inhibited and the attendant disadvantages are eliminated.[81,82] Thus, the alcohol acts as a stabilizing agent.

This type of dosimeter may be either single-phase or two-phase.[83] In the single-phase system a small quantity of the halogenated hydrocarbon and a dye are dissolved in water to form the dosimeter directly. In the two-phase system[84] the halogenated hydrocarbon forms a separate phase. Both chloroform and tetrachloroethylene are used as reactants, although the latter is preferred because of its greater sensitivity to radiation and its greater temperature stability. The indicator employed most commonly is Bromcresol purple. The techniques of preparation, analysis, calibration, and use of this type of dosimeter are described in detail in the literature.[2]

Taplin described[85] three types of chemical systems, prepared from chlorinated hydrocarbons stabilized with resorcinol and using aqueous pH indicator dyes. One system consists of a chlorinated hydrocarbon overlayered with a pH indicator dye. The second system is prepared by saturating an aqueous pH indicator dye with relatively small amounts of a chlorinated hydrocarbon. Both of these systems can be adjusted to respond equally to gamma radiation. However, they differ by about a factor of 5 in their response to fast-neutron irradiation. By using both systems simultaneously in a mixed neutron-gamma field it is possible to estimate the separate dosage from each type of radiation. The third type of system described by Taplin[85] uses tetrachloroethylene, which is gamma-ray sensitive and devoid of hydrogen. Dosimeters using tetrachloroethylene are not affected by fast neutrons and therefore can be used to measure gamma radiation in a mixed field of gamma radiation and fast neutrons.

Hilsenrod[86] and Andrews *et al.*[87] have studied irradiation of chloral hydrate with x and gamma radiation and described a dosimeter which can be used with dose of 10^4 rads or more. Unpublished studies at the

University of Michigan indicate that the pH of a 0.2 M chloral hydrate solution varies in a linear manner with dose and the change in pH can be used to measure doses from 100 to 1000 rad.

3.16 Gaseous Nitrous Oxide

Dondes[88] and more recently Harteck and Dondes[89] describe a simple high-level dosimeter using nitrous oxide gas for the detection of beta, gamma, or thermal neutron radiations. The advantages of the use of nitrous oxide are its ease of purification, indefinite shelf life, and usefulness in temperature ranges of -80°C to 200°C. Also, the decomposition products produced by radiation consist of oxygen, nitrogen and nitrogen dioxide, which do not react with each other and which may be easily measured by vacuum techniques at any convenient time after irradiation.

The procedure used for ionizing-radiation dosimetry consists of filling a 20 cc quartze vessel with purified nitrous oxide at 500 mm Hg pressure at 0°C, sealing and exposing the filled vessel to radiation and then analysing the contents. The filling conditions of 500 mm at 0°C correspond to one atmosphere of air in defining the roentgen.[89] For dosages up to 3×10^7 r the dosage is determined from the analysis for N_2 and O_2. For dosages between 3×10^7 and 3×10^9 r, the dosage may be determined in the same manner or more easily by colorimetric analysis for nitrogen dioxide without opening the dosimeter. The dosimeter approaches saturation above 3×10^9 r and loses accuracy at higher doses. The reactions involved are given[89] as follows:

$$N_2O \longrightarrow N_2O^* \qquad N_2 + O_2 \qquad 80\% \qquad (3.8)$$

$$N_2O \longrightarrow N_2O^+ + e^- \qquad N + NO \qquad 20\% \qquad (3.9)$$

$$2NO + O_2 \rightarrow 2NO_2 \qquad (3.10)$$

$$NO_2 + N \longrightarrow 2NO \qquad (3.11)$$

$$NO_2 + N \longrightarrow N_2O + O \qquad (3.12)$$

$$NO_2 + N \longrightarrow N_2 + O_2 \qquad (3.13)$$

$$N_2O^+ + NO \longrightarrow N_2O + NO^+ \qquad (3.14)$$

$$NO^+ + e^- \longrightarrow N + O \quad \text{or} \quad NO + h\nu \qquad (3.15)$$

The primary yield (80 percent) from the irradiation of N_2O is $N_2 + O_2$ as indicated by Equation (3.8). This may result either from the formation of an excited molecule N_2O^* or an ion pair $N_2O^+ + e^-$ as a

result of interaction of the radiation and N_2O. A smaller yield of N + NO (20 percent) is produced by such interactions. These intermediate products enter into additional reactions indicated by Equation (3.10) through (3.15) to product NO_2 (Equation 3.10) and more $N_2 + O_2$ (Equation 3.13). Harteck and Dondes state the decomposition of nitrous oxide is linear with dosage up to 10^7 r and almost linear up to 10^8 r as shown by the calibration curve in Figure 3.25.

If the dosimeter is to be used to measure thermal neutrons in a reactor, 5 mg of U-235 oxide is inserted in the dosimeter as a powder before the addition of the gas. With reactor irradiation the neutron-induced fission results in about a 60 fold increase in the decomposition products over that obtained by reactor irradiation without U-235 oxide powder in the dosimeter.

Experiments were conducted using pressures in the dosimeter from less than one atmosphere to the critical pressure of N_2O. Temperatures were varied from room temperature to 150°C. Irradiations were conducted with cobalt-60, fission products, and in a reactor. The intensity of irradiation varied over a range of 4 decades. All results indicated[89] that in the linear region up to 10^7 r and almost up to 10^8 r, the nitrous oxide decomposes independently of pressure, temperature, radiation intensity, dose rate, and decomposition products present, in the ratio given by Equation (3.16)

$$N_2 : O_2 : NO_2 = 1:0.14:0.48 \qquad (3.16)$$

3.17 Other Chemical Systems

Chemical dosimetry with various other systems have been studied and some are indicated below. A review of chemical dosimetry methods was made by Harmer[90] in 1959.

1) Various dye solutions are suggested[91-93] of which aqueous methylene blue could be used up to a dose of 6×10^6.

2) Stein and Day have described a system of benzene and sodium benzoate in water.[94,95] Armstrong has described use of calcium benzoate[96] in water solution for use in low dose measurements.[96]

3) Draganic has described use of oxalic acid as a dosimeter over a large range of doses.[97]

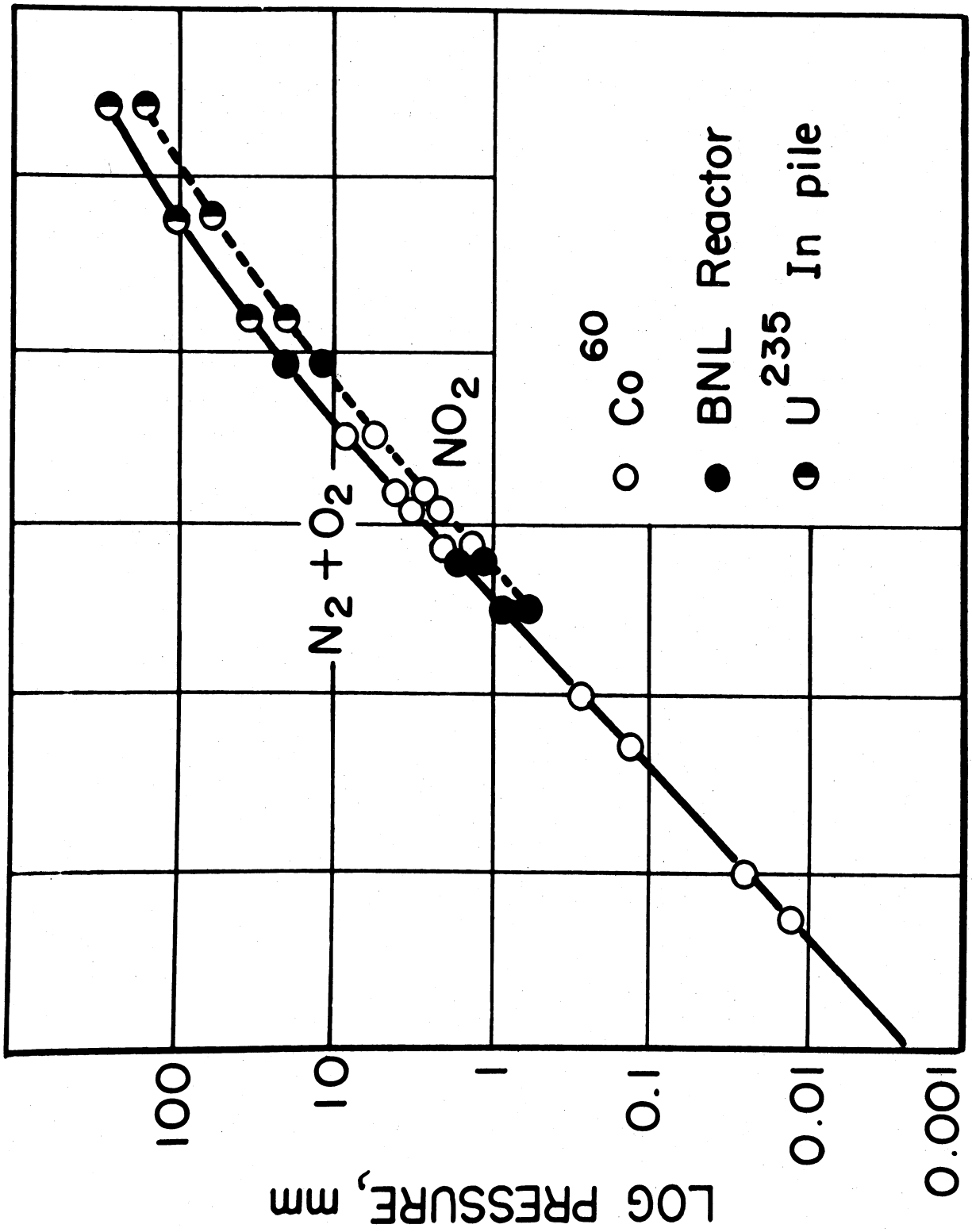

Figure 3.25. Calibration Curve for N_2O Dosimeter. (89) (log-log scale)

Other chemical methods include the production of iodine from iodides, and the decoloration of DPPH in organic solvents. Some investigations have been carried out with certain dye systems combined with gelatin or agar[98-101] to form a gel. This type of system is particularly useful to measure dose as a function of depth for electrons. Additional information on chemical dosimeters is given in References 102-123.

3.18 Calorimetric Dosimeters

Calorimetric dosimetry techniques are based on the fact that part or all of the energy of the ionizing radiation absorbed by matter is converted into heat energy. By measuring the rate of heat generation in the substance, the dose rate can be determined. If the substance is not chemically changed by the incident radiation, all the radiation that is absorbed is quantitatively converted to heat. If the substance is chemically altered by the radiation, part of the radiation goes to effect the change and the remainder is converted to heat.

The very small magnitude of the heat energy produced in matter by ionizing radiation requires extremely sensitive techniques and equipment for calorimetric dosimetry, although the basic principles involved are the same as those of conventional calorimetry. As an illustration consider the thermal value of one roentgen.[124]

$$1 \text{ roentgen} = 93 \text{ ergs/gram} \tag{3.17}$$

$$1 \text{ calorie} = 4.18 \times 10^{7} \text{ ergs/gram} \tag{3.18}$$

$$\therefore 1 \text{ r} = 2.22 \times 10^{-6} \text{ calories.} \tag{3.19}$$

Thus a dose of 1 million r corresponds to a temperature rise of only about 2.2°C in a water-equivalent material. Most experimental gamma sources currently in use produce dose rates that do not exceed 1 megarep per hour; therefore, a very sensitive calorimeter is necessary.

The calorimeter consists of a thermally insulated substance used to absorb part or all of the ionizing radiation and temperature-sensitive devices to measure the temperature of the material as a function of time. Knowing the heat content of the material as a function of temperature, the heat energy absorbed per unit time can then be determined. Two criteria are used in selecting the absorbing material for maximum sensitivity. First, it must have a high linear absorption coefficient, that is, a given mass should be able to absorb a large fraction of the incident radiation. Second, the material should have a low specific heat; that is, a small amount of heat should cause a large increase in temperature. Table 3.3[125]

gives the linear absorption coefficients for water, aluminum, iron and lead, together with their densities:

TABLE 3.3

LINEAR ABSORPTION COEFFICIENTS AND DENSITIES[125]

	LINEAR ABSORPTION COEFFICIENTS FOR			
Energy, (Mev)	Water	Aluminum	Iron	Lead
0.5	0.090	0.23	0.63	1.7
1.0	.067	.16	.44	.77
1.5	.057	.14	.40	.57
2.0	.048	.12	.33	.51
3.0	.038	.09	.30	.47
Density, gm/cc, 20°C	.998	2.699	7.86	11.35

Of the four materials listed in Table 3.3, lead is the best absorber for calorimetry.

The most accurate methods of measuring temperature changes in the absorber are resistance thermometry and thermoelectric thermometry. In applying the techniques of resistance thermometry, use is made of the fact that the resistances of electrical conductors change with temperature. Generally, metals have a positive temperature coefficient of resistance, that is, an increase in the resistor temperature causes an increase in resistance. Nonmetallic conductors may exhibit a negative temperature coefficient. Some transition metal (nickel, cobalt, manganese) oxides have high negative temperature coefficients (about 3.9 percent per degree C) and are often used in resistance thermometry. In thermoelectric thermometry the thermoelectric effect is employed. If two wires of dissimilar metals are laid side by side and connected at the ends, a temperature difference between the two ends will cause a difference of potential to be developed. The thermocouple so formed may be used to measure an unknown temperature with one junction by maintaining the other junction at a reference temperature, usually the ice-point.

A number of calorimeter designs have been developed for use as dosimeters. Laughlin et al. have described a calorimeter which uses lead as an absorber.[125,126] Lazo et al. has described a calorimeter which uses water as an absorber in a simple pyrex bulb containing a thermocouple.[127]

With this device the error was kept at ± 2%. The same group later described a calorimeter with an absorber made with polyethylene and free carbon. A graphite sphere calorimeter is under development at the US National Bureau of Standards and is described by Hart et al.(79) A graphite sphere suspended on polystyrene pegs inside a graphite shell which was heated to provide an adiabatic shield was used. This was exposed to a dose rate of approximately 5×10^5 r/hr from the NBS 2000 curie cobalt source. An error of less than 1% was claimed.

Taimuty has described a liquid calorimeter for calibration of ceric sulfate dosimeter.(128) He had also described a solid calorimeter for measurement of electron-beam intensity.(129) The latter could be used for energy-absorption in nonconducting solids by making measurements with and without the solid interposed in an electron beam in front of the calorimeter.

Figures 3.26 and 3.27 show one type of calorimetric absorber and measuring-chamber geometry.(126) The thermistor is used to measure the temperature of the lead cylinder. The calibration heater is used to determine the heat capacity of the absorber in the absence of radiation. The purpose of the radiation shield is to reduce the heat transfer by radiation from the absorber to the measuring-chamber wall. The absorber and radiation shield are suspended by nylon threads in the measuring chamber, which is under vacuum. The vacuum reduces heat transfer by convection from the absorber, and the nylon threads reduce the heat transfer by conduction. The nylon also has a relatively good resistance to radiation damage. The absorber assembly outer surface, radiation shield, and vacuum-chamber inner surface are all chromium plated to reduce further the heat transfer by radiation (gold is an even better surface for low emissivity). The measuring chamber is immersed in a water bath, whose temperature is controlled thermostatically.

3.19 Luminiscence Degradation

This method of measuring radiation dose is relatively in an early stage of development but offers a promise for measuring large doses.

The method is based on the decrease in luminiscence of many organic luminophosphors after exposure to high energy radiation. An "exciton" theory(131-132) suggests that radiation damage consists in introduction of impurities which cause luminiscence degradation. In a nonirradiated crystal the excited energy originally imparted by radiation is transferred between molecules by resonance until some molecules floresce. In an irradiated and thus damaged crystal the impurities can trap the excitons, and degrade it to heat or to a wave

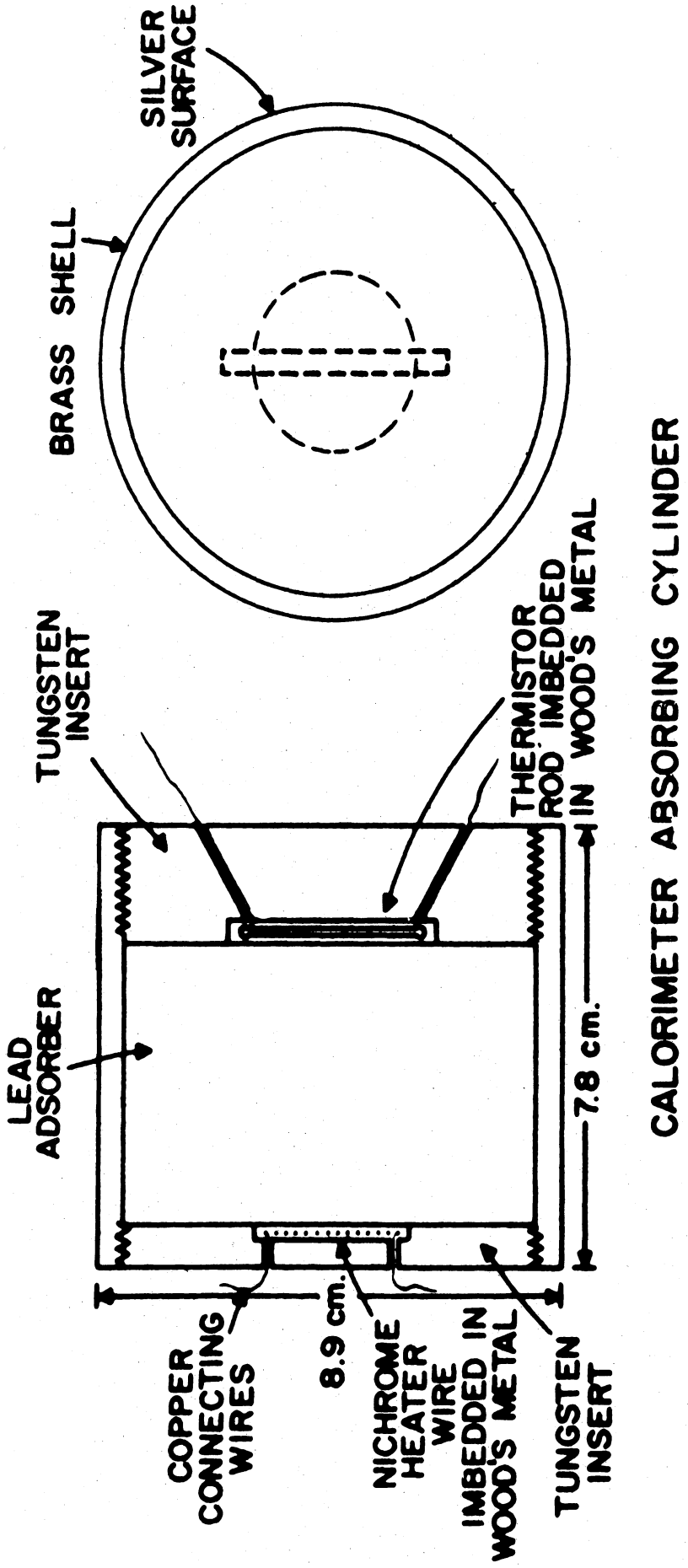

Figure 3.26. Construction of Calorimeter Cylinder. (126)

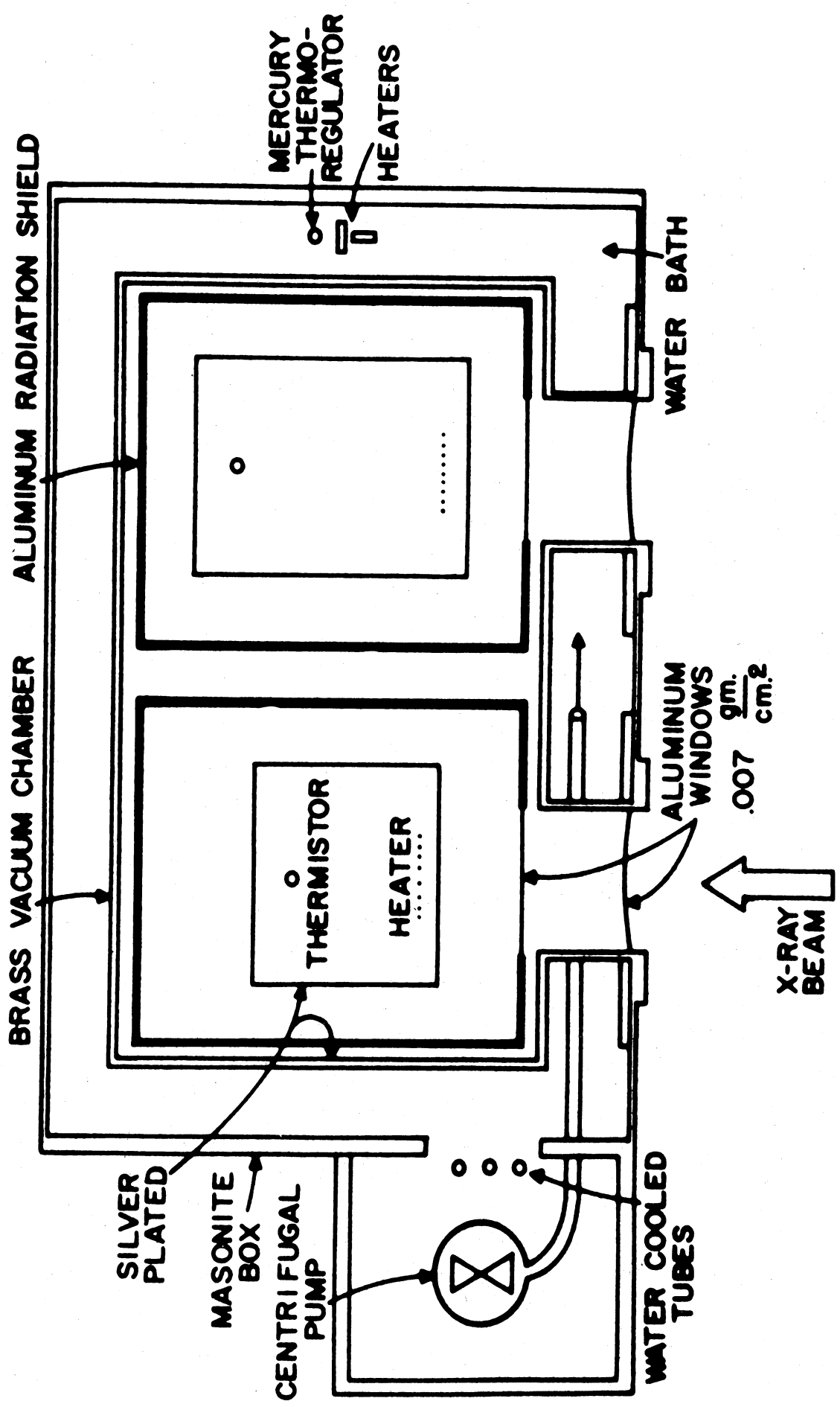

Figure 3.27. Horizontal Cross Section Showing Calorimeter Construction. (126)

length outside of the fluorescence band of the pure material. This effect can be used for dose measurements by observing the post-irradiation luminescence at a frequency in the visible or near-ultraviolet spectrum in response to a higher energy excitation.

Attix has described systems using wafers of anthracene and p-quarterphenyl which are excited at 3650 Å and read through a filter with a pass band centered at 4420 Å .(133,134) He described a certain amount of recovery of luminescence which is accelerated by heat treatment for 1 hr at 100°C and stabilized the readings.

Barr studied the destruction of the fluorescence of quinine in acid solution by 250 kvp x-rays.(135) Quinine concentrations of 10^{-5} to 10^{-8} moles/litre were used to measure doses from 5 to 2 x 10^{4} rads.

The decrease of scintillation efficiencies of crystal, plastic, and liquid scintillators could possibly be used for dose measurements. Rozman reported that damage to plastic scintillators is independent of dose rate but dependent upon the nature of radiation.(136)

3.20 Microbial Monitors

Microbial monitoring as a method of dosimetry could be applied to specialized applications like radiation sterilization. Various techniques have been described.(137,138) However, the choice of microorganism for monitoring should be made carefully since there are marked differences in radiation resistance among the various species.

3.21 Summary

The various dosimetry systems proposed have been described. The choice of any one depends upon various factors in a specific situation.

A wide number of dosimeters are now available for doses of 10^{5} - 10^{7} rads and dose rates of 10^{4} - 10^{6} rads/hr. Even though some of these methods such as the ferrous-sulfate dosimetry system show high accuracy, it demands a certain amount of care in laboratory procedures. On the other hand methods like the glass dosimetry system show fair accuracy with minimum of precautions.

Among the other factors that one may consider are such things as convenience in handling, stability of the acquired change and the complexity of the method of analysis with respect to time and cost. Glass or plastic

dosimeters do present problems of instability. However, they present the advantages of convenience in storage, extended life and rapid and easy measurement. Costs of equipment may be considerable in certain methods of dosimetry, but the added expense may be worthwhile because of convenience and precision of the measurement.

For doses larger than those mentioned above one has only a limited choice. Luminiscence degradation and nitrous oxide dosimetry may be used.

Schall has compiled a table from questionnaires sent to different experts on the evaluation of dosimetry methods. This is reproduced as Table 3.4,(140) with slight modifications. A table of characteristics of various secondary standard dosimeters has been compiled by Hart.(79)

Table 3.4

Chemical Dosimeter Systems

(Courtesy Nucleonics, McGraw-Hill Publishing Co.) (90)

No.	Dosimetry system	Total-dose range (rads)	Reproducibility %	Dose-rate range (rad/hr)	Equipment cost (dollars)	Materials cost (dollars per measurement)	Time for measurements (min) 1	20	100	Delay time (min) (must be)	(can be)	Fraction of change that is permanent (%)	Advantages	Disadvantages
1	Ferrous-ferric (Fricke) (Hart)	4×10^3 - 4×10^4	± 2	4×10^3 - 10^6	2,500*	0.01	2	20	100	0	10^5	100	high accuracy; direct analysis without further treatment; solution can occupy space and volume of sample	need of operator experience; need for care in irradiation
2	Ceric-cerous (Hart)	5×10^4 - 2×10^8	± 4	4×10^3 - 10^9	100* or 2,000†	0.05	30	200	1,000	0	10^3	100	simplicity; accuracy	need for titration at high doses and rates
3	Ferrous-cupric (Swope)	4×10^4 - 10^7	± 5 - 10	4×10^3 - 8×10^8	2,000	0.01	5	40	200	0	10^3	100	extends range of ferrous-ferric system	solutions less stable than ferrous-ferric ones; nonlinear at high doses
4	Halogenated-hydrocarbon-acidimetric dye (Sigoloff)	10^4 - 10^7	± 5	4×10^3 - 10^{10}	2,000	0.10	15	80	300*	30	∞	100	size; insensitivity to neutrons; range; ease of evaluation	need for production know-how; need for glass container (research is looking for a suitable plastic vial)
5	Nitrous oxide (Harteck & Dondes)	10^5 - 4×10^8	± 5	10^7 - 10^9	500-1,000	0.25* or 5†	30	500	2,500†	0	∞	100	temperature range - 80°-200°C; decomposition products don't interact; wide dose and rate ranges; unlimited shelf life	need for vacuum and liquid air; need to break seals in vacuum
6	Methylene blue (Goldblith)	10^4 - 10^7	± 2 - 5	10^4 - 2×10^8	250	0.01 - 0.02	15	60	180	0	10^5	100	ease and simplicity for routine work	need for standardization of each batch of dye
7	Gas evolution (Hart)	2×10^5 - 2×10^{10}	± 2 - 5	10^4 - 2×10^{10}	200	<0.01	*	*	*	0	$>10^3$	100	usefulness for continuous source monitoring; response to all radiations including neutrons	need for individual gas-collection system for each measurement
8	Starch-iodine (Gerantman)	4×10^3 - 10^5			300	0.25	1	15	60	60	10^3	100	simplicity of colorimetric measurement; little need for attention to purification; range adjustment by varying iodine concentration	energy dependence; starch fraction must be soluble; need of time lag for color growth; not tissue-equivalent (but it can be made so)
9	Photography (print-out paper) (Nitka) (visual evaluation)	4×10^4 - 10^7	± 20	4×10^3 - 2×10^5	0	0.10	0.3	5	20	0	>5,000	100	speed; cost; simplicity; lack of need for processing after exposure	lack of commercial availability
	(instrumental evaluation)	4×10^4 - 10^7	± 5	4×10^3 - 2×10^5	400									
10	Dyed plastics (Henley)	2×10^4 - 4×10^7	± 2 - 5	4×10^3 - 2×10^{10}	2,300	0.01	1	5	20*	0	∞	100	convenience; cost; simplicity	variation of accuracy with different batches of plastics
11	Darkening of plastics (Artandi)	10^5 - 2×10^7	± 5	10^5 - 2×10^{10}	600-1,200	0.004	10	20	60	10	1,440	>80	simplicity; cost; applicability of visual evaluation	need for standard color development
12	Depolymerization (Feng)	4×10^3 - 10^8	± 5	5×10^4 - 5×10^7	200	0.02	3	60	200	0	10^3	100	wide range (4 decades for one dosimeter; 6 decades for system)	limited accuracy; need for temperature control or correction and standard reading time
13	Polymerization (styrene polyesters) (Hoecker)	10^4 - 10^7	± 2 - 5	5×10^3 - 5×10^7	0*	0.05*	0.1	3	10	0	∞	100	go-no-go system; wide range; cost; lack of need for auxiliary equipment	decrease of sharpness of index at highest doses; requirement of cold storage for periods of a month or more
14	Glass fluorescence (Schulman)	4×10^3 - 4×10^4	± 5	5×10^3 - 5×10^8	250 - 350	0*	0.5	10	50	15	$>5 \times 10^5$	80-100	convenience; ruggedness; solid, indefinite storage, dosed or undosed	useful at intermediate dose range (10-10,000 r)
15	Luminescence degradation (Schulman)	10^5 - 10^{10}	± 5	5×10^3 - 5×10^8	200 - 300	0.05 - 0.10	0.5	10	50	0	$>4 \times 10^4$	>95†	smallness; solid; long-term storage, dosed or undosed; use of cheap, readily available chemicals; wide range; ability to reread; simplicity	need for heat treatment (if one is to avoid all recovery effects)
16	Scintillator damage (quinine in acid) (Barr)	5×10^3 - 10^4	± 2	5×10^3 - 5×10^4	1,000	0	1	20	100	0	10^3	100	speed; convenience; reproducibility; sensitivity	logarithmic response
17	Glass darkening (Kreidl & Blair)	5×10^3 - 10^6	± 2	5×10^3 - 5×10^{10}	250	0.30	1	15	60	0	10^5*	50-95†	simplicity; accuracy; cost; ruggedness	need for calibration; limits of dose range
		10^6 - 10^7	± 5											
18	Photovoltaic cells (Moody)	5×10^3 - 10^9	± 5	5×10^3 - 10^{10}	100*	0*	†	†	†	0	0	†	simplicity; speed	lack of total-dose response
19	Cerenkov-photovoltaic monitor (Thomas)	Gate device 6×10^6 - 2×10^7	± 2	10^5 - 6×10^7	50	0	‡	‡	‡	0	0	‡	simplicity; cost; lack of time delay; logarithmic response	need for radiation energy great enough to produce Cerenkov radiation (for electrons in water, 0.26 Mev)
		4×10^5 - 6×10^4	± 5											
20	Cadmium-sulfide (rate device) cells (Hollander) (dose device)	Dose device 4×10^3 - 6×10^5	± 2	5×10^3 - 10^7	600	0.50 - 2	0.2	3	15	~0.5*	4×10^4	(little)		need for more research to establish feasibility
					10									
21	Faraday cages, cups, plates* (Trageser)	10^5 - 2×10^8	± 2 - 5	10^{10} - 5×10^{10}	200	0	0	0	0	0	---	0	electrical nature; applicability to continuous monitoring; lack of need for recalibration	failure to tell absorbed dose directly; requirement of careful original design and calibration; not go-no-go
22	Ionization chambers (Siebentritt)	5×10^3 - 10^6	± 5	5×10^3 - 5×10^{10}	<500	0	*	*	*	---	---	---	direct reading; availability of recycling; unlimited shelf life	
23	Calorimetry (Taimuty)	5×10^4 - 5×10^7	± 2	2×10^4 - 2×10^9	2,500	---	---	---	---	0	---	0		suitability for standardization only; need for skilled personnel
24	Microbial monitors (Mayernik)	4×10^3 - 4×10^6	± 20	5×10^3 - 5×10^{10}	200* or 2,500†	1	15	120	600	10^4	∞	100	direct measurement of sterilization; applicability for establishing a sterilization process and for witnessing sterilization during irradiation	need for 7 days to obtain results; need for bacteriological training

Ferrous-ferric: *for spectrophotometer
Ceric-cerous: *titration method; †spectrophotometer method
Halogenated-hydrocarbon-acidimetric-dye: *all times include data reduction to final answer
Nitrous oxide: *Pyrex vessel; †quartz vessel; ‡special apparatus could cut the time by a factor of 10
Gas evolution: *times depend on intensity of source and composition of solution since liquids other than water can be used [see E. J. Hart, S. Gordon, NUCLEONICS 12, No. 4, 40 (1954)]

Starch-iodine: *actual accuracy is ± 10%
Photography: *total range for 1-3-Mev photons can be extended by factor of 50 with 3-in. lead filter
Dyed plastics: *times assume no use of automatic reading device
Polymerization (styrene polyesters): *no equipment is required for reading: chemical balance, beakers and flasks are required for preparation; measurement cost is for actual materials; preparation of 100 dosimeters requires ~1 hr
Glass fluorescence: *Glass can be reused after annealing for 5 hr at 400°C

Luminescence degradation: *Range can undoubtedly be extended upward (and probably downward) with other materials. †After heat treatment (1 hr 100°C)
Glass darkening: *delay between exposure and reading depends on particular glass dosimeter chosen and precision desired; F-0621 glass (Bausch and Lomb) is relatively stable when measured at 3,500 and 4,000 A for exposures in the 10^5-rad range; †fading is <5% 2 mo after irradiation; fading increases with dose and wavelength, but precision is still within 5% if measured a few hours after irradiation; in general, ~95% of change is permanent at low dose when measurement is with short wavelengths, and 75% of change is permanent with doses of 10^6 - 10^7 rads when measured at 5,000 A; this is true only for this specific system; for other glass dosimeters fading may result in loss of 50% or more of change with exposure
Photovoltaic cells: *$5-10 for a silicon solar cell; $100 for an adequate voltmeter; after 10^9 rads total dose silicon cell must be replaced; †device reads rates, essentially instantaneously
Cerenkov-photovoltaic monitor: *wide range of total dose has not been investigated: device was exposed to ~1.8×10^9 rads at 3.4×10^3 - 1.7×10^6 rads/sec with no apparent damage; †reproducibility is ±5%; absolute accuracy has not been determined; ‡device reads rates instantaneously
Cadmium-sulfide cells: *reading as a dose device is probably very critical for 0.5 hr after exposure

Faraday cages, plates, cups: *these systems are not dosimetry methods in themselves, but rather beam-measuring devices for electrons only; must be used with energy sensors to determine dose
Ionization chambers: *times vary with flux and total dose
Microbial monitors: *assuming normal bacteriological facilities available; †assuming laboratory facilities available but bacteriological facilities have to be provided

CHAPTER 3 REFERENCES

1. Gurney, R. W. and Mott, N. F. "The Theory of Photolysis of AgBr and the Photographic Latent Image." Proc. Roy. Soc., A, 164, (1938) 151.

2. Hine, G. J. and Brownell, G. L. Radiation Dosimetry. Academic Press, Inc., N. Y., 1956.

3. Ehrich, M. and Fitch, S. H. "Photographic X- and Gamma-Ray Dosimetry." Nucleonics, 9, No. 3, (1951) 5.

4. Tracerlog No. 62, "Neutron Film Badge Service." Tracerlab, Inc., Boston, Mass., Sept., 1954.

5. Anonymous, "Commercial Film-Badge Services." Nucleonics, 13, No. 2, 1955.

6. Beiser, A. "Nuclear Emulsion Technique." Rev. Mod. Phys., 24, (1952) 273.

7. Cheka, J. S. Neutron Monitoring by Means of Nuclear Track Film. ORNL-547, Oak Ridge National Laboratory, Oak Ridge, Tenn., 1950.

8. Cheka, J. S. "Fast Neutron Film Dosimeter." Phys. Rev., 90, (1953) 353.

9. Cheka, J. S. "Recent Developments in Film Monitoring of Fast Neutrons." Nucleonics, 12, No. 6, (1954) 40.

10. Cobb, J. and Solomon, A. K. "The Detection of Beta Radiation by Photographic Film." Rev. Sci. Instrum., 19, (1948) 441.

11. Deal, L. J., Robertson, J. H. and Day, F. H. "Roentgen-Ray Calibration of Photographic Film Exposure Meter." Amer. J. Roentgenol., 59, (1948) 731.

12. Demers, P., Lapalme, J. and Thovenin, J. "Fading of the Latent Image Formed by Charged Particles." Canad. J. Phys., 31, (1953) 295.

13. Dudley, R. A. The Measurement of Beta Radiation Dosage with Photographic Emulsions. Ph.D. Thesis, The Massachusetts Institute of Technology,

14. Dudley, R. A. "Photographic Detection and Dosimetry of Beta Rays." Nucleonics, 12, No. 5, (1954) 24.

15. Ehrlich, M. Photographic Dosimetry of X- and Gamma Rays. NBS Handbook 57, U.S. Gov. Printing Office, Wash., D.C., 1954.

16. Goldschmidt-Clermont, Y. "Photographic Emulsions." Ann. Rev. Nuclear Sci., 3, (1953) 141.

17. Greenberg, L. H. and Haslam, R. N. H. "On the Shrinkage Factor of Nuclear Emulsions." Canad. J. Phys., 31, (1953) 1115.

18. Greening, J. R. "The Photographic Action of X-Rays." Proc. Phys. Soc., Lond., B, 64, (1951) 977.

19. Hoerlin, H. Development of a Wavelength Independent Radiation Monitoring Film. ANL-5168, U.S. Atomic Energy Commission, Wash., D.C., 1953.

20. Jetter, E. S. and Blatz, H. "Film Measurement of Beta Radiation Dose." Nucleonics, 10, No. 10, (1952) 43.

21. McLaughlin, W. L. and Ehrlich, M. "Film Badge Dosimetry, How Much Fading Occurs?" Nucleonics, 12, No. 10, (1954) 34.

22. Mees, C. E. K. The Theory of the Photographic Process. Macmillan, Co., Inc., N. Y. , 1954.

23. Rosen, L. "Nuclear Emulsion Techniques for the Measurement of Neutron Energy Spectra." Nucleonics, 11, No. 7, (1953) 32.

24. Rosen, L. "Nuclear Emulsion Techniques for the Measurement of Neutron Energy Spectra." Nucleonics, 11, No. 8, (1953) 38.

25. Simons, H. A. B. "Use of Nuclear Emulsions for Fast Neutron Dosimetry." Nature, Lond., 168, (1951) 835.

26. Titterton, E. W. "Slow Neutron Monitoring with Boron and Lithium Load-Nuclear Emulsions." Nature, Lond., 163, (1949) 990.

27. Titterton, E. W. and Hall, M. E. "Neutron Dose Determination by the Photographic Plate Method." Brit. J. Radiol., 23, (1950) 465.

28. Tochilin, E. and Golden, R. "Film Measurement of Beta-Ray Depth Dose." Nucleonics, 11, No. 8, (1953) 26.

29. Yagoda, H. Radioactive Measurements with Nuclear Emulsions. John Wiley and Sons, Inc., N. Y., 1949.

30. Army Chemical Corps, Technical Command, Symposium No. IV: Chemistry and Physics of Radiation Dosimetry, Part I, Army Chemical Center, Maryland, Sept., 1950.

31. Army Chemical Corps, Technical Command, Symposium No. IV: Chemistry and Physics of Radiation Dosimetry, Part II, Army Chemical Center, Maryland, Sept., 1950.

32. "The Effect of Atomic Weapons." Chapter 7, U.S. Atomic Energy Commission Wash., D.C., (1950) 238.

33. Miller, A. Gamma-Ray Dosimetry with Polyvinyl-Chloride Films. B.S. Thesis, Department of Chemistry, Brooklyn Polytechnic Inst., Brooklyn, N.Y., 1951.

34. Henley, E. J. and Miller, A. "Gamma-Ray Dosimetry with Polyvinyl-Chloride Films." Nucleonics, 9, No. 6, (1951) 62.

35. Brownell, L. E., et al. Utilization of the Gross Fission Products. Progress Report 5 (COO-196), Engng Res. Inst., Proj. M943, The University of Michigan, Ann Arbor, Mich., 175, Sept., 1953.

36. Henley, E. J. "Gamma Ray Dosimetry with Cellophane-Dye Systems." Nucleonics, 12, No. 9, (1954) 62.

37. Henley, E. J. and Richman, D. "Cellophane-Dye Dosimeter for 10^5 to 10^7 Roentgen Range." Analyt. Chem., 28, (1956) 1580.

38. Row, F. M. "Color Index." Society of Dyers and Colourists, Index, (1924) 518.

39. Personal Communication to L. E. Brownell from Mr. C. L. Blair, Sales Development and Technical Services, I. E. DuPont De Nemours and Company, Inc., 1956.

40. Brownell, L. E., Meinke, W. W., Nehemias, J. V. and Coleman, E. W. "Design and Use of Ten-Kilocurie Source of Gamma Radiation." Chem. Engng. Progr., 49, No. 11, 1953.

41. Nehemias, J. V., Brownell, L. E., Meinke, W. W. and Coleman, E. W. "Installation and Operation of Ten-Kilocurie Cobalt-60 Gamma-Radiation Source." Amer. J. Physics, 22, No. 2, 1954.

42. Brownell, L. E. and Nehemias, J. V. "Techniques Used in Studies with High-Intensity Gamma Radiation." Sci. Mon., N.Y., 82, No. 2, 1956.

43. Artandi, C., Stonehill, A. A. "Polyvinyl Chloride -- New High-Level Dosimeter." Nucleonics, 16, No. 5, (1958) 118.

44. Fowler, J. F. and Day, M. J. "High Dose Measurements by Optical Absorption." Nucleonics, 13, (1955) 52.

45. Artandi, C. "Plastics Dosimetry." Nucleonics, 17, (1959) 62.

46. Alexander, P., et al. "The Degradation of Solid Polymethylmethacrylate by Ionising Radiation," Proc. Royal Soc., London, 223, (1954) 392.

47. Feng, P. Y. "Polymer Degradation -- Wide-Range Dosimeter." Nucleonics, 16, No. 10, (1958) 114.

48. Kreidl, N. J. and Blair, G. E. "Glass Dosimetry." Nucleonics, 17, (1959) 58.

49. Schulman, J. H., Shuriliff, W., Ginther, R. J. and Attix, F. H. "Radiophotoluminescence Dosimetry System of the U.S. Navy." Nucleonics, 11, No. 10, (1953) 52.

50. Anonymous, Phosphate Glass Dosimetry. Civil Defense Tech. Bull., TB-11-15, U.S. Govt. Print. Office, Wash., D.C., July, 1954.

51. Schulman, J. H., Ginther, R. J., Klick, C. C., Alger, R. S. and Levy, R. A. "Dosimetry of X-Rays and Gamma-Rays by Radiophotoluminescence." J. Appl. Phys., 22, (1951) 1479.

52. Schulman, J. H. Measurement of High Doses of Co-60 Gamma Rays by Absorption Changes in Phosphate Glass. NRL Memorandum Report 266, Naval Research Laboratories, Wash., D. C., Feb., 1954.

53. Schulman, J. H. "Measuring High Doses by Absorption Changes in Glass." Nucleonics, 13, No. 2, (1955) 30.

54. Schulman, J. H., Klick, C. C., Etzel, H. W. and Ginther, R. J. Dosimetry of Ionizing Radiations. Report of NRL Progress, Naval Research Laboratory, Wash., D.C., Oct., 1954.

55. Schulman, J. H. and Etzel, H. W. "Small-Volume Dosimeter for X-Rays and Gamma-Rays." Science, 118, (Aug. 14, 1953) 184.

56. Kreidl, N. J. and Blair, G. E. "A System of Megaroentgen Glass Dosimetry." Nucleonics, 14, No. 1, (1956) 56.

57. Kreidl, N. J. and Blair, G. E. "Recent Developments in Glass Dosimetry." Nucleonics, 14, No. 3, (1956) 82.

58. Weiss, J. "Chemical Dosimetry Using Ferrous and Ceric Sulfate." Nucleonics, 10, No. 7, (1952) 28.

59. Weiss, J., Allen, A. O. and Schwarz, H. A. Use of the Fricke Ferrous-Sulfate Dosimeter for Gamma-Ray Doses in the Range 4 to 40 kr. Paper 155, Int. Conf. on Peaceful Uses of Atomic Energy, Geneva, 1955; Proc. ibid, United Nations, N. Y., 14, (1956) 179.

60. Fricke, H. and Morse, S. "Action of X-Rays on Ferrous Sulfate." Amer. J. Roentgenol., 18, (1927) 426.

61. Fricke, H. "The Oxidation of Ferrous-Sulfate in Aqueous Solutions by X-Rays of Different Wave-Lengths." Phys. Rev., 31, (1928)1117.

62. Fricke, H. and Morse, S. "The Action of X-Rays on $FeSO_4$ Solutions." Phil. Mag., Series VII, 7, (1929) 129.

63. Fricke, H. and Hart, E. J. "The Oxidation of Fe^{++} to Fe^{+++} by the Irradiation with X-Rays of Solutions of Ferrous Sulfate in Sulphuric Acid." J. Chem. Phys., 3, (1935) 60.

64. "American Society for Testing Materials. Tentative Method of Test for Absorbed Gamma Radiation Dose by Chemical Dosimetry, ASTM Method D1671-59T." ASTM Bull. No. 239, 30 and 52, July, 1959.

65. Hochanadel, C. "Effects of Cobalt Gamma-Radiation on Water and Aqueous Solutions." J. Phys. Chem., 56, (1952) 587.

66. Mooney, R. W. and Szasz, G. J. Discussion on Radiation Chemistry. ONRL, 48-52, Office of Naval Research, Lond., May, 1952.

67. Schuler, R. H. and Allen, A. O. "Yield of the Ferrous Sulfate Dosimeter: An Improved Cathode-Ray Determination." J. Chem. Phys., 24, (1956) 56.

68. Charlesby, A. Atomic Radiation and Polymers. Pergamon Press, London, 1960.

69. Lea, D. E. Actions of Radiation on Living Cells. The Macmillan Co., Inc., N.Y., 1947.

70. Hardwick, T. J. "The Reduction of Ceric Sulfate Solutions by Ionizing Radiation." Canad. J. Chem., 30, (1952) 23.

71. Dewhurst, H. A. "Effect of Organic Substances on the Gamma Ray Oxidation of $FeSO_4$." J. Chem. Phys., 19, (1951) 1329.

72. Bastian, R., Weberling, R. and Palilla, F. "Spectrophotometric Determination of Iron as Ferric Sulfate Complex." Analyt. Chem., 25, (1953) 284.

73. Dainton, F. S. and Sutton, H. C. "Hydrogen Peroxide Formation in the Oxidation of Dilute Aqueous Solutions of $FeSO_4$ by Ionizing Radiations." Trans. Faraday Soc., 49, (1953) 1011.

74. Hochanadel, C. J. and Ghormley, J. A. "A Calorimetric Calibration of Gamma Ray Actinometers." J. Chem. Phys., 21, (1953) 880.

75. Lazo, R. M., Dewhurst, H. A. and Burton, M. "The $FeSO_4$ Radiation Dosimeter: A Calorimetric Calibration with Gamma Rays." J. Chem. Phys., 22, (1954) 1370.

76. Farmer, F. T., Rigg, T. and Weiss, J. "The Absolute Yield of the Ferrous Sulfate Dosimeter." J. Chem. Soc., (1954) 3248.

77. Hart, E. J. and Walsh, P. D. "A Molecular Product Dosimeter for Ionizing Radiations." Rad. Res., 1, (1954) 342.

78. Hart, E. J. "Radiation Chemistry of Aqueous Ferrous Sulfate-Cupric Sulfate Solutions, Effect of Gamma-Rays." Rad. Res., 2, (1955) 33.

79. Hart, E. J., et al., Measurement Systems for High Level Dosimetry. Proceedings of the Second U.N. Conference on the Peaceful Uses of Atomic Energy, United Nations, Geneva, 21 (1958) 188.

80. Johnson, M. E., Swartz, J. C. and Hamilton, A. B. Monthly Progress Reports Nos. 1-8, to the Army Chemical Corps., Physics Research Department, Vacuum Distillation Products Industries, Eastman Kodak, Rochester, N. Y., 1952.

81. Taplin, G. V., Douglas, C. H. and Sigoloff, S. C. "The Chloroform-Alcohol-Dye System." UCLA-192, U.S. Atomic Energy Commission, Wash., D.C., 1952.

82. Taplin, G. V., Douglas, C. H. and Sigoloff, S. C. Quart. Progress Report 1-2, to the Army Chemical Corps., University of California, L. A., 1952, 1953.

83. Taplin, G. V., Douglas, C. H. and Sigoloff, S. C. Gamma and X-Ray Dosimetric Method. Quart. Progress Report 7, to the Army Chemical Corps., University of California, L. A., 1954.

84. Taplin, G. V., Douglas, C. H. and Sigoloff, S. C. Quart. Progress Report 5, to the Army Chemical Corps., University of California, L. A., 1952.

85. Taplin, G. V. Development of Direct-Reading Chemical Dosimeters for Measurement of X, Gamma, and Fast Neutron Radiation. Paper 153, Int. Conf. on Peaceful Uses of Atomic Energy, Geneva, 1955; Proc. ibid, United Nations, N. Y., 14, (1956) 227.

86. Hilsenrod, A. "Irradiation of Chloral Hydrate Solutions." J. Chem. Phys., 24, (1956) 917.

87. Andrews, H. L., Murphy, R. E., and LeBrun, E. J. "Gel Dosimeter for Depth-Dose Measurements." Rev. Sci. Instr., 28, (1957) 329.

88. Dondes, S. A High Level Dosimeter for the Detection of Beta and Gamma Radiation and Thermal Neutrons. Paper 151, Int. Conf. on Peaceful Uses of Atomic Energy, Geneva, 1955; Proc. ibid, United Nations, N.Y., 14, (1956) 176.

89. Harteck, P. and Dondes, S. "Nitrous Oxide Dosimeter for High Levels of Betas, Gammas, and Thermal Neutrons." Nucleonics, 14, No. 3, (1956) 66.

90. Harmer, D. E. "Chemical Dosimetry." Nucleonics, 17, (1959) 72.

91. Latuente, B., Goldblith, S. A. and Proctor, B. E. "Some Further Studies on the Application of Methylene Blue in Aqueous Solution as a Dosimeter for Intense Beams of High-Energy Radiation." Intern. J. Appl. Radiation Isotopes, 3, (1958) 119.

92. Goldblith, S. A., Proctor, B. E. and Hammenle, A. O. "Evaluation of Food Irradiation Procedures." Industr. Engng. Chem., 44, (1952) 310.

93. Shekhtaman, Ya. L., et al. Doklady Akad. Nauk., USSR, 74, (1950) 767.

94. Day, M. J. and Stein, G. "Chemical Dosimetry of Ionizing Radiations." Nucleonics, 6, No. 2, (1951) 35.

95. Armstrong, W. A. and Grant, G. A. "A Highly Sensitive Chemical Dosimeter for Ionizing Radiation." Nature, 182, (1958) 747.

96. Draganic, I. "Action des Rayonnements Ionisants sur les Solutions Aquenses d'acide Oxalique: Acide Oxalique Aqueux Utilise Comme Dosimetre Chimique Pour les Doses entre 1.6 ct 160 M rads." J. Chim. Phys., 56, (1959) 9.

97. Day, M. J. "Chemical Effects of Ionizing Radiations in Some Gels." Nature, Lond., 166, (1950) 146.

98. Proctor, B. E. and Goldblith, S. M. "Oxidation-Reduction Dyes as Radiation Indicators." Nucleonics, 7, No. 2, (1950) 83.

99. Gevantman, E. H., Chandler, R. C., and Pestaner, J. F. "Tridimensional Examination of Chemical Systems Irradiated in Gel Media." Radiation Research, 7, (1957) 318.

100. Pestaner, J. F. and Gevantman, L. H. "Depth Dosimetry by Means of a Gel-Incorporated Chemical System." Radiation Research, 9, (1958) 166.

101. Miller, N. "Quantitative Studies of Radiation Induced Reactions in Aqueous Solutions. I. Oxidation of Ferrous Sulfate by X- and Gamma-Radiation." J. Chem. Phys., 18, (1950) 79.

102. Miller, N. and Wilkenson, J. "Actinometry of Ionizing Radiation." Disc. Faraday Soc., 12, (1952) 50.

103. Allen, A. O. "The Yields of Free H and OH in the Irradiation of Water." Rad. Res., 1, (1954) 85.

104. Hart, E. J., Gordon, S. and Hutchison, D. A. "Free Radical-Initiated $O^{16}\ O^{18}$ - H_2O^{16} Exchange Reaction in Aqueous Solution." J. Amer. Chem. Soc., 75, (1953) 6165.

105. McDonell, W. R. and Hart, E. J. "Oxidation of Aqueous Ferrous Sulfate Solutions by Charged Particle Radiations." J. Amer. Chem. Soc., 76, (1954) 2121.

106. Barb, W. G., Baxendale, J. H., George, P. and Bargrave, K. R. "Reactions of Ferrous and Ferric Ions with Hydrogen Peroxide." Trans. Faraday Soc., 57, (1951) 462, 591.

107. Hart, E. J. "Gamma-Ray Induced Oxidation of Aqueous Formic Acid." J. Amer. Chem. Soc., 73, (1951) 68.

108. Krenz, F. H. and Dewhurst, H. A. "The Mechanism of Oxidation of Ferrous Sulfate by Gamma-Rays in Aerated Water." J. Chem. Phys., 17, (1949) 1337.

109. Rigg, T., Stein, G. and Weiss, J. "The Action of X-Rays on Ferrous and Ferric Salts in Aqueous Solutions." Proc. Roy. Soc., A, 211, (1952) 375.

110. Dainton, F. S. and Sutton, H. C. "Hydrogen Peroxide Formation in The Oxidation of Dilute Aqueous Solutions of Ferrous Sulphate by Ionizing Radiations." Trans. Faraday Soc., 49, (1953) 1011.

111. Dewhurst, H. A. "The X- and Gamma-Ray Oxidation of Ferrous Sulphate in Aqueous Solution." Trans. Faraday Soc., 49, (1953) 1174.

112. Hart, E. J. "Radiation Chemistry of Ferrous Sulfate Solutions." J. Amer. Chem. Soc., 73, (1951) 1891.

113. Amphlett, C. B. "Reduction of Ferric Ion in Aqueous Solution by Gamma Radiation." Nature, Lond., 171, (1953) 690.

114. Hart, E. J. "Gamma-Ray Induced Oxidation of Aqueous Formic Acid-Oxygen Solutions. Effect of pH." J. Amer. Chem. Soc., 76, (1954) 4198.

115. Samuel, A. H. and Magee, J. L. "Theory of Radiation Chemistry. II. Track Effects in the Radiolysis of Water." J. Chem. Phys., 21, (1953) 1080.

116. Dewhurst, H. A., Samuel, A. H., and Magee, J. L. "A Theoretical Survey of the Radiation Chemistry of Water and Aqueous Solutions." Rad. Res., 1, (1954) 62.

117. Weiss, J. "The Role of Hydrogen Molecule Ions in Aqueous Solutions." Nature, Lond., 165, (1950) 728.

118. Taplin, G. V., Douglas, C. H. and Sanchez, B. "Colorimetric Methods for Dosimetry of 10 to 100 r." Nucleonics, 9, No. 2, (1951) 73.

119. Taplin, G. V. Applicability of Chemical Dosimetry in Civil Defense. UCLA-304, U.S. Atomic Energy Commission, Wash., D.C., Sept. 15, 1955.

120. Clark, G. L. and Bierstedt, D. E. "X-Ray Dosimetry by Radiolysis of Some Organic Solutions." Rad. Res., 2, No. 3, (1955) 199.

121. Fricke, H. Army Chemical Corps Symposium No. IV: Chemistry and Physics of Radiation Dosimetry, Part I, Army Chemical Center, Maryland, 24, Sept., 1950.

122. Gomberg, H. L., Gould, S. E., Nehemias, J. V. and Brownell, L. E. "Using Cobalt-60 and Fission Products in Pork Irradiation Experiments." Nucleonics, 12, No. 5, (1954) 38.

123. Young, D. E. "Dosimetry." Sources of Radiation for Industry, IP-175 The University of Michigan, Ann Arbor, Mich., Aug., 1956.

124. Genna, S. and Laughlin, J. S. "Absolute Calibration of a Cobalt-60 Gamma Ray Beam." Radiology, 65, (1955) 394.

125. Laughlin, J. S., Genna, S., Danzker, M. and Vacirca, S. J. Absolute Dosimetry of Cobalt-60 Gamma Rays. Paper 70, Int. Conf. on Peaceful Uses of Atomic Energy, Geneva, 1955; Proc. ibid, United Nations, N. Y., 14, (1956) 163.

126. Lazo, R. M., Dewhurst, H. A., and Burton, M. "The Ferrous Sulfate Radiation Dosimeter: A Calorimetric Calibration With Gamma Rays." J. Chem. Phys., 22, (1954) 1370.

127. Taimuty, S. I., Glass, R. A. and De La Rue, R. Calorimetric Determination of the Yield of the Ceric Sulfate Dosimeter. Paper presented at third annual meeting, American Nuclear Society, Pittsburgh, June 24-28, 1957.

128. Taimuty, S. I. Electron Beam Dosimetry and Experimental Techniques. Paper presented at Symposium on Electron Beam Radiation, General Electric Co., Milwaukee, 1957; see also Nucleonic, 15, No. 11, (1957) 182.

129. Schall, P. "A Comparison of Dosimetry Methods." Nucleonics, 17, (1959) 68.

130. Birks, J. B. "Scintillations from Napthalene-Anthracene Crystals." Proc. Phys. Soc., Lond., 63A, (1950) 1044.

131. Bowen, E. J., Mikiewicz, E., and Smith, F. W. "Resonance Transfer of Electronic Energy in Organic Crystals." Proc. Phys. Soc., Lond., 62A, (1949) 26.

132. Schulman, J. H., Etzel, H. W. and Allard, J. C. "Application of Luminescence Changes in Organic Solids to Dosimetry." J. Appl. Phys., 28, (1957) 792.

133. Attix, F. H. "High Level Dosimetry by Luminescence Degradation. Nucleonics, 17, No. 4, (1959) 142.

134. Barr, N. F. and Stark, M. B. "The Destruction of the Fluorescence of Quinine in Acid Solution by 250 kvp X-Rays." Radiation Research, 9, (1958) 89.

135. Rozman, I. M. and Zimmer, K. G. "The Damage to Plastic Scintillators by Ionizing Radiations." Atomnaya Energiya, 2, (1957) 54.; English translation, Intern. J. Appl. Radiation Isotopes, 3, (1958) 36.

136. Mayernik, J. J. and Daniels, T. "The Sterilization of Polyethylene Bags by Electron Irradiation and a Bacterial Monitor as a Measure of Sterility." J. Am. Pharm. Assoc. Sci. Ed., 48, (1959) 16.

137. Brownell, L. E., "Radiation Uses in Industry and Science," U.S. Government Print Office, Washington, D.C., June 1961.

CHAPTER 4

GAMMA SHIELDING

The operation of a large number of nuclear reactors, the construction of particle accelerators in the Bev range, and the use of megacurie quantities of gamma radiation in facilities using spent reactor fuel elements, cobalt and cesium sources, have made the shielding of these facilities an important branch of study. The interaction of nuclear radiations with matter has been the subject of extensive theoretical and experimental investigation, and neutron- and gamma-radiation attenuation processes have been studied in detail for the purposes of shielding. The study of shielding for a given facility involves, basically, analysis of the following factors:

1. The type of radiation source.
2. The nature of nuclear radiations involved.
3. Source strength and energy spectrum of the nuclear radiations.
4. Type of shields to be used, considering cost, weight, and type of facility.
5. The basic attenuation and spatial-distribution processes involved.
6. Evaluation of the nuclear constants of the materials involved for different energy groups.
7. Source geometry and the radiation field surrounding the source and the shield.
8. Over-all minimum shield thickness required so as not to exceed the maximum permissible dose permitted by AEC regulations.

This chapter considers the calculations involved in the shielding of nuclear radiation facilities and deals primarily with gamma-radiation shielding and the concept of the "build-up factor." As an illustration, the analysis of the heterogeneous gamma-radiation spectrum from the MTR fuel element from the point of view of shielding is given. The report contains graphs for determining the standard integrals involved in calculating the radiation flux for standard geometries and also an extensive bibliography.

4.1 ATTENUATION OF GAMMA-RADIATION FROM POINT SOURCES

There are no less than twelve different processes by which gamma rays can interact with matter. However, three of them, photoelectric absorption, Compton scattering, and pair production are the most important. See Chapter 2 of "Radiation Uses in Industry and Science" for greater discussion.(1) The photoelectric effect is predominant for low photon energy and materials with high atomic numbers ($E \lesssim 0.15$ Mev for $Z = 29$; $E \lesssim 0.5$ Mev for $Z = 82$). At energies greater than 1.02 Mev, pair production predominates ($E > 80$, 15, or 5 Mev for $Z = 1$, 13, or 82, respectively). For intermediate energies, Compton scat-

tering is predominant. The cross sections per atom for the photoelectric and Compton effectsand pair-production process vary approximately as Z^5, Z, and Z(Z+1), respectively. Materials of high atomic numbers are more suitable as absorbers in the low-energy region, while they are not quite as efficient in the high-energy region. Lead, zinc bromide, concrete, and water are the materials commonly used for shielding, the actual choice depending on space, weight, and cost considerations. In fixed-source facilities, special types of concrete and water solutions are frequently used.

The stream of photons emitted from the source in all directions decreases in intensity inversely as the square of the distance for a point source. This relationship can be expressed simply as

$$\phi = \frac{\phi_o}{r^2} . \qquad (4.1)$$

Here ϕ is flux, r is distance, and ϕ_o is a measure of the strength of the source (see Fig. 4.1). Equation 4.1 is referred to as the "inverse-square law." Thus, if space is available, the problem of gamma shielding can be reduced by increasing the distance of closest approach permitted.

The above equation applies to trasmission through a vacuum or a thin gas. The penetration of photons in material media of greater densities is now considered. Assume a point monoenergetic source of gamma rays in vacuum is shielded from a point detector located at a distance R by a rod of some material, of length X, and oriented as shown in Fig. 4.2. The other dimensions will be assumed infinitesimally small relative to X, R, and (R-X). In such a configuration every collision which a photon from the source experiences in the rod will then serve to remove it from the beam which ultimately reaches the detector. Such an arrangement of source, shield, and detector is termed a "good geometry." In such a case, the rate of reduction of flux is proportional to the flux level, i.e.,

$$d\phi/dx = -\mu\phi \qquad (4.2)$$

or

$$\phi = \phi_o e^{-\mu x} . \qquad (4.3)$$

Here ϕ_o is the flux level entering the rod, ϕ is the flux level existing at a point in the rod at a distance x from the "inside" end, and μ is a constant (the "attenuation coefficient") the value of which depends on the photon energy and the particular material constituting the rod. The dimension of μ is cm^{-1}, so that μ times the thickness of the absorber in cm is a dimensionless constant which termed the thickness in "relaxation lengths." Equations 4.2 and 4.3 are valid only if the gamma rays are monoenergetic and the beam is collimated.

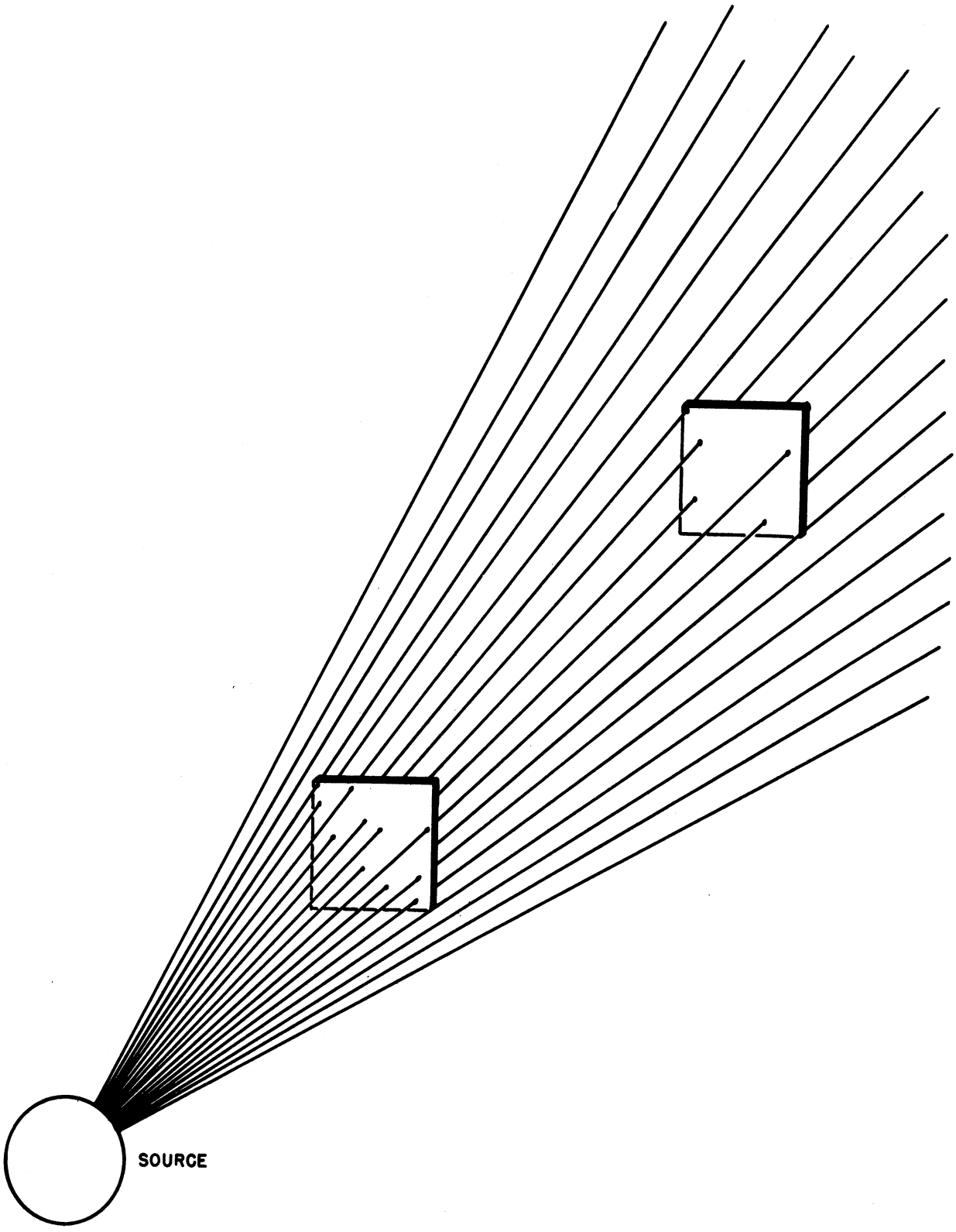

Fig. 4.1. Flux reduction with distance.

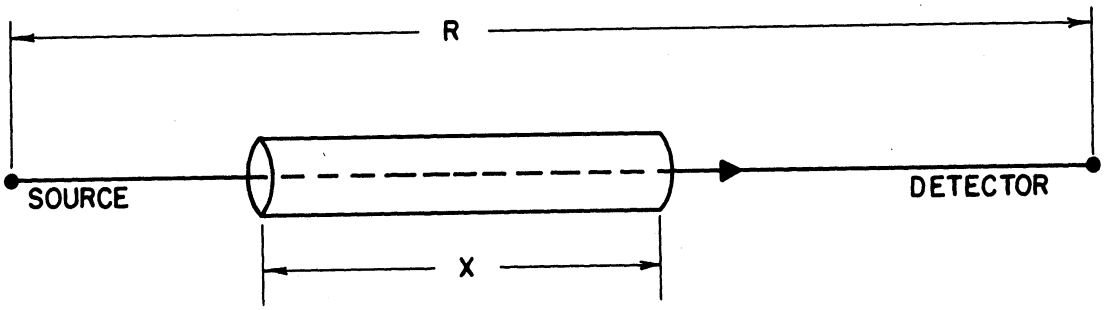

Fig. 4.2. Good-geometry configuration.

If the source emits isotropically, then for a narrow rod absorber and a point detector, a combination of Equations 4.1 and 4.3 may be used to express ϕ as

$$\phi = \frac{\phi_o \, e^{-\mu x}}{r^2} . \qquad (4.4)$$

Now if the diameter of the rod is not small, the arrangement is termed "bad geometry." Here photons can be scattered into the detector as well as away from it (see Fig. 4.3). Equation 4.4 does not properly describe gamma attentuation in "bad geometries," but must be corrected for the effect of the scattered photons.

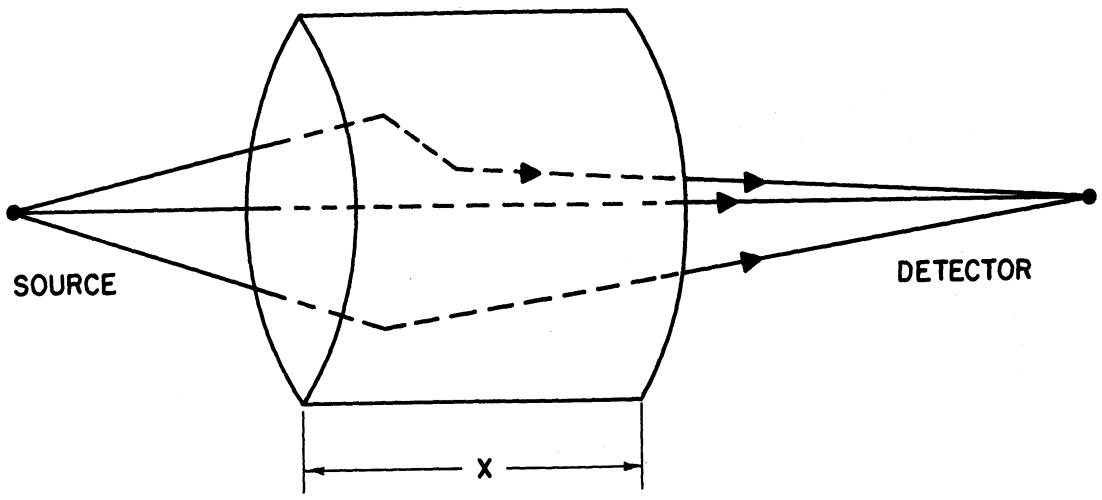

Fig. 4.3. Bad-geometry configuration.

The total attenuation coefficient (a function both of energy and absorber material) is

$$\mu(E_o) = \tau(E_o) + \sigma(E_o) + \kappa(E_o) , \qquad (4.5)$$

where τ, σ, and κ denote the photoelectric, Compton, and pair-production coefficients, respectively. Of these three interaction processes, the photoelectric effect and pair-production may be treated as purely absorptive. The third, Compton scattering, is the only scattering process of the three and gives rise to a spectrum of photons degraded in energy.

4.2 NARROW BEAM ATTENUATION

Figure 4.4 shows a plot of the linear attenuation coefficient for "narrow beam" (collimated) gamma radiation in lead.(2) The three components τ, σ, and κ corresponding to the three processes of interaction are also shown in Fig. 4.4 and the dependence of each upon the energy of the radiation is apparent. As previously pointed out, attenuation by photoelectric effect, τ, is most important in the low energy region, particularly for the heavy elements. Figure 4.4 shows that below 0.5 Mev the primary contribution to μ is from τ. However the curve of τ versus Mev drops very rapidly in this range with the result that above 1.0 Mev there is very little attenuation of gamma radiation by photoelectric effect. At medium energies of from 0.5 to 5 Mev Compton scattering σ is the most important attenuation process. For the heavy elements Compton scattering is less important below 0.5 Mev than the photoelectric effect but for the lighter elements the relative importance of scattering continues to lower energies.

In using Equation 4.3 it is not necessary to express the absorber thickness in units of length. Sometimes it is more convenient to use mass, especially in considering a non-homogeneous absorber. In such a case x may be expressed in gms per sq cm or in lb per sq ft. The attenuation coefficient is then termed the mass attenuation coefficient μ_m and has the units of sq cm per gm or sq ft per lb respectively. The simple relationship $\mu_m = \mu/\rho$ where ρ is the density of the absorber is conveneint in relating these coefficients. Figures 4.5, 4.6, and 4.7 give mass attenuation coefficients for the photoelectric range, the Compton scatter range and the pair-production range respectively for some of the common elements as a function of energy.(3,4) Table 4.1 gives values for some common elements, air and water as a function of photon energy.(3)

4.3 HALF-VALUE AND TENTH-VALUE THICKNESSES

Instead of using attenuation coefficients it is often more convenient to express the attenuation in terms of half-value layers or tenth-value layers.

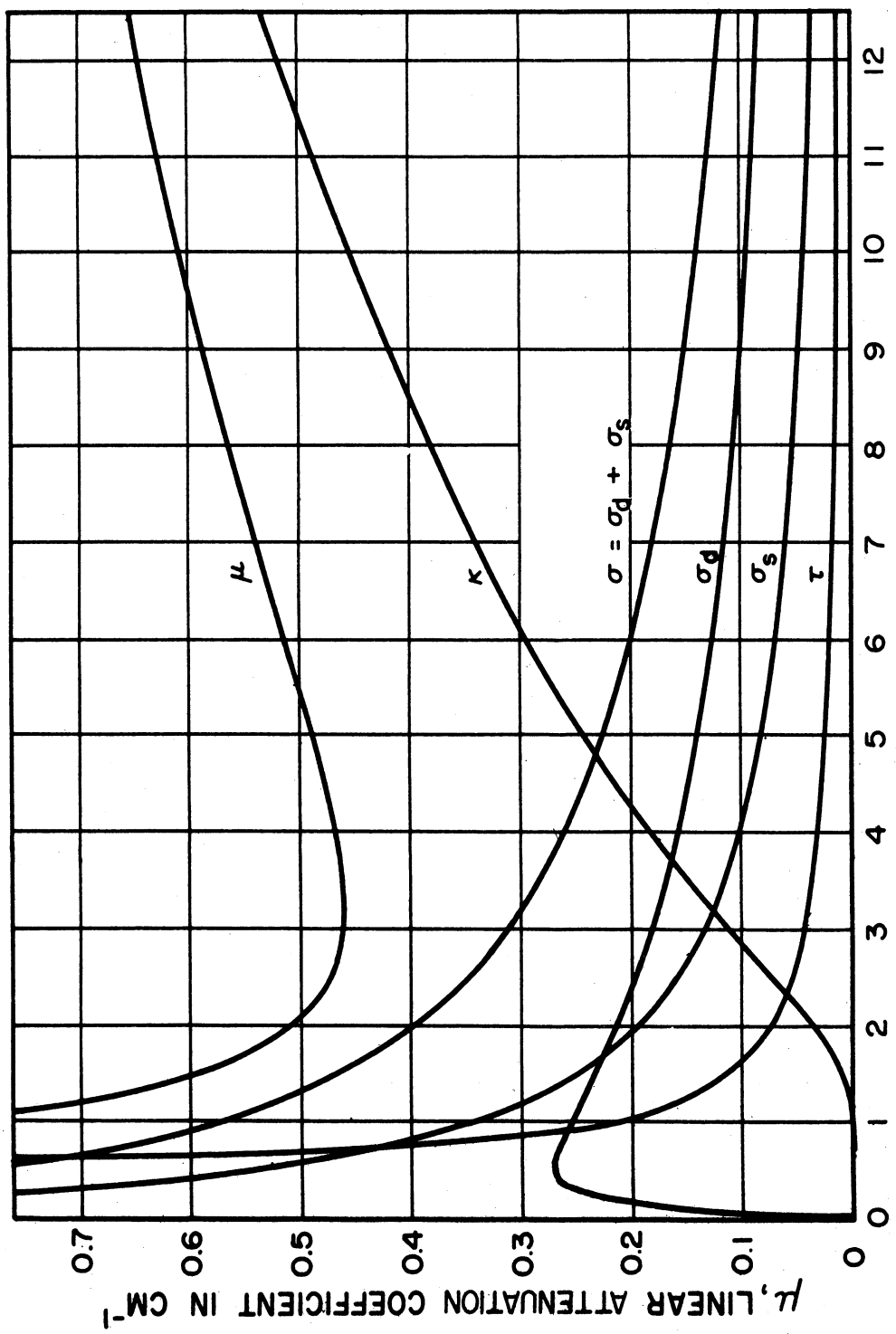

Fig. 4.4. Linear attenuation coefficient of gamma rays in lead.(2)

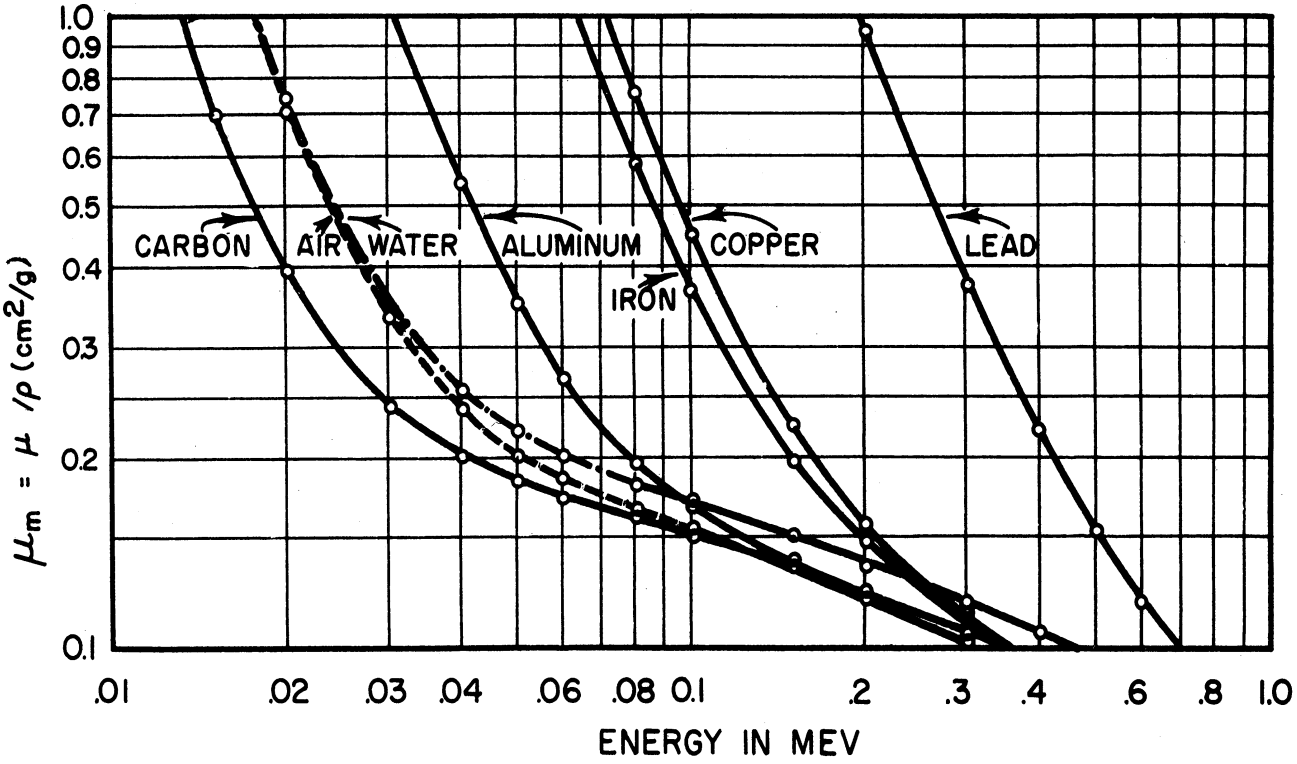

Fig. 4.5. Total mass attenuation coefficients, μm, for x- and gamma radiation in the range of photoelectric effect.(3)

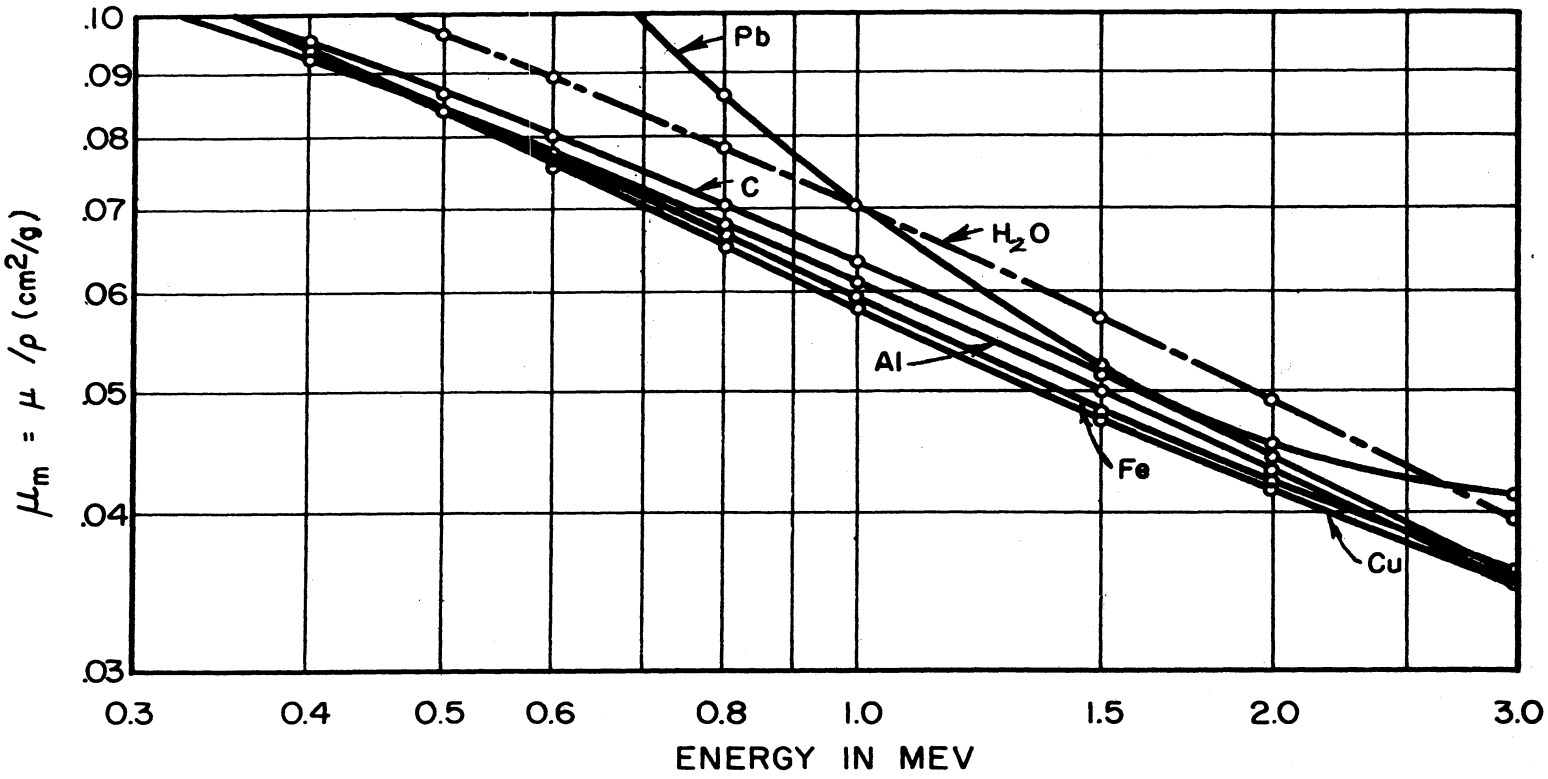

Fig. 4.6 Total mass attenuation coefficients, μ_m, for x- and gamma radiation in the range of Compton scatter. (3)

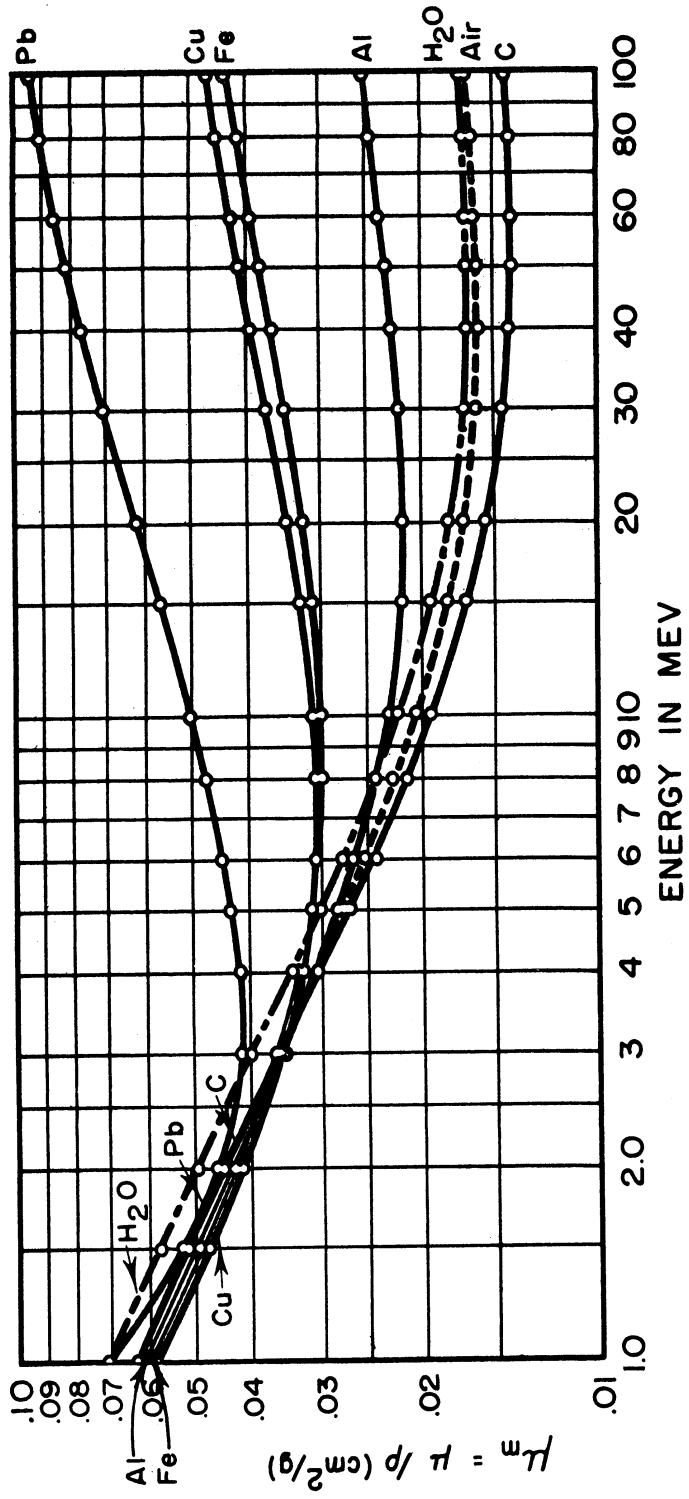

Fig. 4.7 Total mass attenuation coefficients, μ_m, for x- and gamma radiation in the range of pair formation. (3)

TABLE 4.1

GAMMA RAY MASS ATTENUATION COEFFICIENTS, μ_m, WITHOUT COHERENT SCATTERING, IN cm^2/g [3]

	Material									
E, Mev	H	Be	C	O	Na	Al	Si	Fe	Air	H_2O
0.01	0.385	0.533	2.13	5.69	15.6	26.3	34.1	178	4.88	5.09
0.015	0.376	0.261	0.701	1.68	4.61	7.84	10.3	58.2	1.48	1.53
0.02	0.369	0.200	0.382	0.766	1.95	3.33	4.35	25.8	0.695	0.720
0.03	0.357	0.168	0.229	0.334	0.646	1.04	1.35	8.03	0.317	0.336
0.04	0.345	0.158	0.193	0.232	0.351	0.507	0.633	3.48	0.226	0.245
0.05	0.335	0.151	0.178	0.196	0.249	0.325	0.389	1.83	0.194	0.212
0.06	0.326	0.146	0.169	0.179	0.206	0.249	0.288	1.13	0.178	0.196
0.08	0.309	0.138	0.157	0.161	0.168	0.186	0.204	0.555	0.161	0.178
0.10	0.294	0.132	0.149	0.151	0.151	0.161	0.172	0.344	0.151	0.167
0.15	0.265	0.118	0.134	0.134	0.130	0.133	0.139	0.183	0.134	0.149
0.20	0.243	0.109	0.122	0.123	0.118	0.120	0.125	0.138	0.122	0.136
0.30	0.211	0.0944	0.106	0.106	0.102	0.103	0.107	0.106	0.106	0.118
0.40	0.189	0.0846	0.0953	0.0954	0.0912	0.0922	0.0956	0.0919	0.0952	0.106
0.50	0.173	0.0772	0.0870	0.0871	0.0833	0.0840	0.0869	0.0828	0.0869	0.0967
0.60	0.160	0.0714	0.0805	0.0805	0.0770	0.0777	0.0804	0.0761	0.0804	0.0894
0.80	0.140	0.0628	0.0707	0.0708	0.0677	0.0682	0.0706	0.0664	0.0706	0.0786
1.0	0.126	0.0564	0.0635	0.0636	0.0608	0.0613	0.0635	0.0595	0.0635	0.0706
1.5	0.103	0.0459	0.0518	0.0518	0.0496	0.0500	0.0517	0.0484	0.0516	0.0576
2.0	0.0876	0.0393	0.0443	0.0445	0.0427	0.0432	0.0447	0.0424	0.0443	0.0493
3.0	0.0691	0.0313	0.0356	0.0359	0.0348	0.0353	0.0367	0.0360	0.0357	0.0396
4.0	0.0579	0.0265	0.0304	0.0309	0.0303	0.0310	0.0323	0.0330	0.0307	0.0339
5.0	0.0502	0.0233	0.0270	0.0276	0.0274	0.0282	0.0296	0.0313	0.0274	0.0301
6.0	0.0446	0.0211	0.0245	0.0254	0.0254	0.0264	0.0277	0.0304	0.0250	0.0275
8.0	0.0371	0.0180	0.0213	0.0224	0.0229	0.0241	0.0255	0.0295	0.0220	0.0240
10.0	0.0321	0.0161	0.0194	0.0206	0.0215	0.0229	0.0243	0.0295	0.0202	0.0219

A half-value layer is the thickness of an absorber that will absorb 1/2 of a beam and similarly a tenth-value layer is the thickness of absorber that will transmit 1/10 of a beam. The following relationships exist:

$$t_{\frac{1}{2}} = \text{half-value thickness} = 0.693/\mu \qquad (4.6)$$

$$\phi = \frac{\phi_o}{2^n}, \text{ where } n = \text{number of half-value thicknesses} \qquad (4.7)$$

Figure 4.8 shows some 1/10 value thicknesses (narrow beam)[5] for some common materials as a function of energy.

4.4 MIXED ENERGIES

In the case of mixture of gamma emitting radioisotopes such as the fission products, gamma radiation of a mixture of different energies is obtained. However, the attenuation coefficients and half- and tenth-value thicknesses given are constant only for a given absorber and energy. When a mixture of energies is involved the decrease in the flux of a collimated beam is given by:[6]

$$\phi = \phi_1 e^{-\mu_1 x} + \phi_2 e^{-\mu_2 x} + \ldots\ldots\ldots \phi_n e^{-\mu_n x} \qquad (4.8)$$

where: $\phi_1, \phi_2, \ldots \phi_n$ = the flux at the surface of the absorber from each of n-radiation energies

$\mu_1, \mu_2, \ldots \mu_n$ = attenuation coefficients for the corresponding radiation energies.

If a large number of different energies are involved or if the energy is continuous in distribution approximate methods or laboratory measurements are required.

4.5 ATTENUATION "BUILD-UP" FACTORS FOR POINT SOURCES

In the ideal case of absorption of a perfectly collimated beam the degradation of energy, scattering, and the production of secondary radiation can be eliminated from consideration. But in most real applications the "build-up" of secondary radiation is an important consideration. The radiation intensity at any point in an absorber consists of the primary gamma photons, the photons resulting from Compton scatter, and the secondary radiation of (photoelectrons, and electrons from Compton scatter and pair production) plus the x radiation produced by the absorption of these electrons. The secondary electrons are absorbed much more readily than the primary gamma radiation.

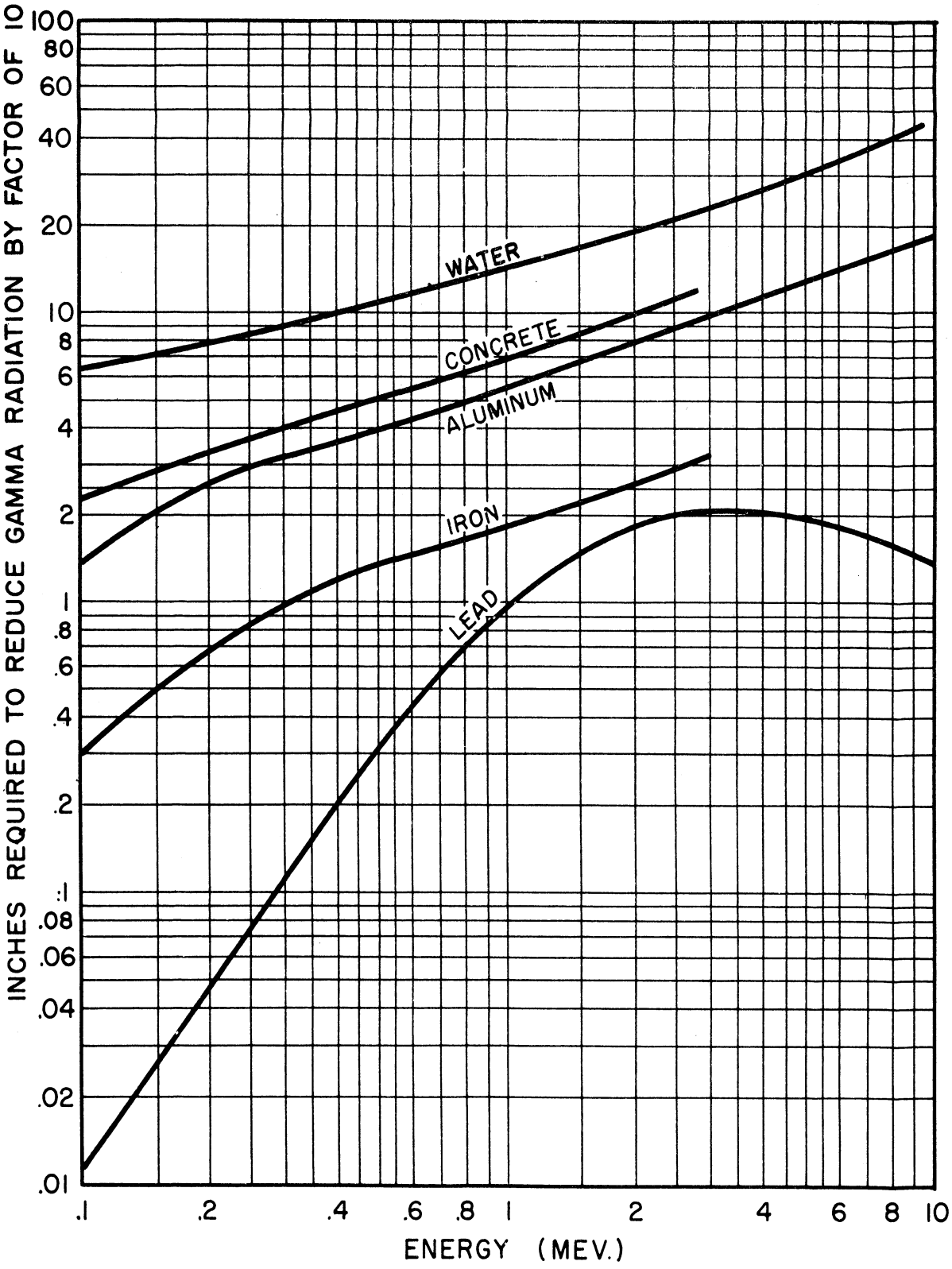

Fig. 4.8. Narrow beam tenth value thicknesses of various materials for gamma radiation.(5)

For primary gamma radiation of a given energy passing through a given absorber an equilibrium level is reached in the production of secondary radiation which is characteristic of the energy and the absorber. If the primary radiation passes from a poor absorber such as air to a denser medium the increase in absorption of the primary radiation will result in a corresponding increase in the formation of secondary radiation. This produces a "build-up" of secondary electrons and x radiation from the absorption of these electrons. Figure 4.9 is a diagram (not to scale) showing such a "build-up" of secondaries as a primary photon passes through a denser medium.(6)

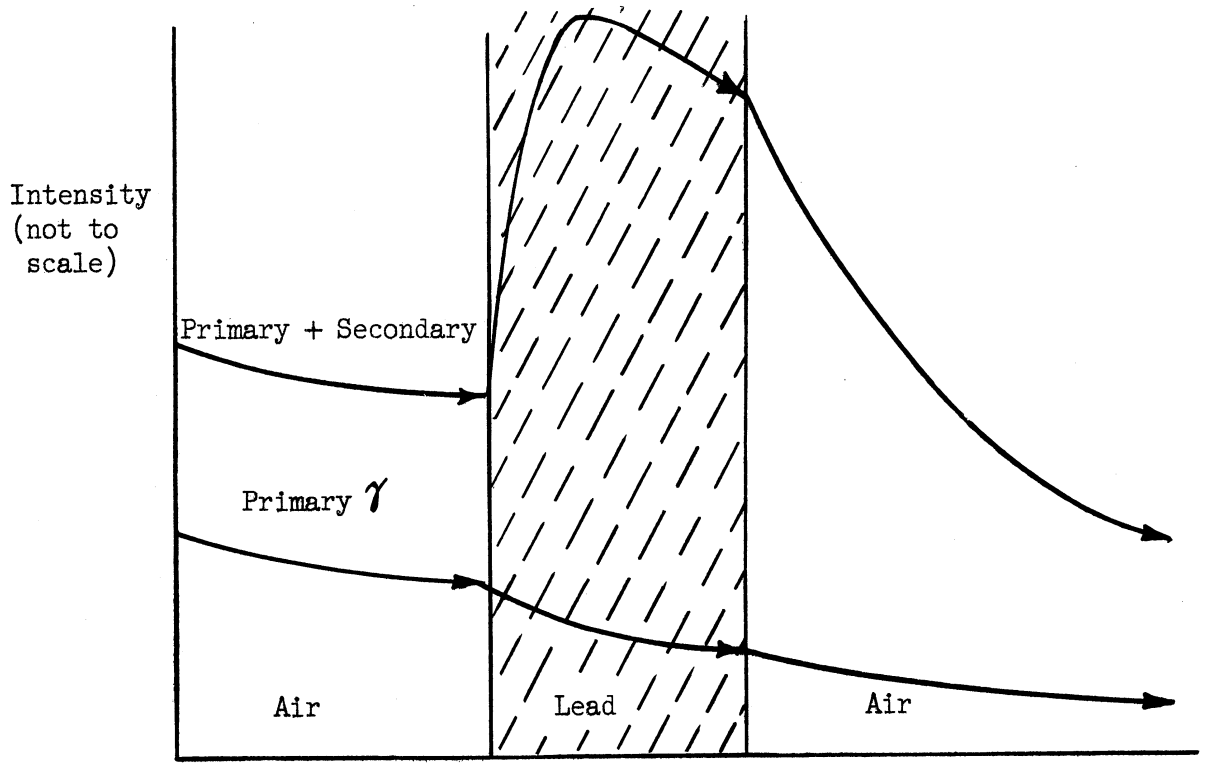

Fig. 4.9. Diagram of "build-up" in lead. (6)

Tables 4.2, 4.3, 4.4, and 4.5 give the experimentally determined dose build-up factors B from a point source for H_2O, Al, Fe and Pb respectively.(7) In using these factors the calculated flux intensity ϕ based upon absorption of a collimated beam is multiplied by factor B or:

$$\phi = B \phi_0 e^{-\mu x} \qquad (4.9)$$

TABLE 4.2

DOSE BUILD-UP FACTOR B IN WATER FOR AN ISOTROPIC POINT SOURCE(7)
(Relaxation lengths, μx)

E_o(Mev)	1	2	4	7	10	15	20
.256	3.09	7.14	23.0	72.9	166	456	932
.5	2.52	5.14	14.3	38.8	77.6	178	334
1.0	2.13	3.71	7.68	16.2	27.1	50.4	82.2
2.0	1.83	2.77	4.88	8.46	12.4	19.5	27.7
3.0	1.69	2.42	3.91	6.23	8.63	12.8	17.0
4.0	1.58	2.17	3.34	5.13	6.94	9.97	12.9
6.0	1.46	1.91	2.76	3.99	5.18	7.09	8.85
8.0	1.38	1.74	2.40	3.34	4.25	5.66	6.95
10.0	1.33	1.63	2.19	2.97	3.72	4.90	5.98

TABLE 4.3

DOSE BUILD-UP FACTOR B IN ALUMINIUM FOR AN ISOTROPIC POINT SOURCE(7)
(Relaxation lengths, μx)

E_o(Mev)	1	2	4	7	10	15	20
.5	2.37	4.24	9.47	21.5	38.9	80.8	141
1.0	2.02	3.41	6.57	13.1	21.2	37.9	58.5
2.0	1.75	2.61	4.62	8.05	11.9	18.7	26.3
3.0	1.64	2.32	3.78	6.14	8.65	13.0	17.7
4.0	1.53	2.08	3.22	5.01	6.88	10.1	13.4
6.0	1.42	1.85	2.70	4.06	5.49	7.97	10.4
8.0	1.34	1.68	2.37	3.45	4.58	6.56	8.52
10.0	1.28	1.55	2.12	3.01	3.96	5.63	7.32

TABLE 4.4

DOSE BUILD-UP FACTOR B IN IRON FOR AN ISOTROPIC POINT SOURCE(7)
(Relaxation lengths, μx)

E_o(Mev)	1	2	4	7	10	15	20
.5	1.98	3.09	5.98	11.7	19.2	35.4	55.6
1.0	1.87	2.89	5.39	10.2	16.2	28.3	42.7
2.0	1.76	2.43	4.13	7.25	10.9	17.6	25.1
3.0	1.55	2.15	3.51	5.85	8.51	13.5	19.1
4.0	1.45	1.94	3.03	4.91	7.11	11.2	16.0
6.0	1.34	1.72	2.58	4.14	6.02	9.89	14.7
8.0	1.27	1.56	2.23	3.49	5.07	8.50	13.0
10.0	1.20	1.42	1.95	2.99	4.35	7.54	12.4

TABLE 4.5

DOSE BUILD-UP FACTOR B IN LEAD FOR AN ISOTROPIC POINT SOURCE[7]
(Relaxation lengths, μx)

E_o(Mev)	1	2	4	7	10	15	20
.5	1.24	1.42	1.69	2.00	2.27	2.65	2.73
1.0	1.37	1.69	2.26	3.02	3.74	4.81	5.86
2.0	1.39	1.76	2.51	3.66	4.84	6.87	9.00
3.0	1.34	1.68	2.43	3.75	5.30	8.44	12.3
4.0	1.27	1.56	2.25	3.61	5.44	9.80	16.3
5.1097	1.21	1.46	2.08	3.44	5.55	11.7	23.6
6.0	1.18	1.40	1.97	3.34	5.69	13.8	32.7
8.0	1.14	1.30	1.74	2.89	5.07	14.1	44.6
10.0	1.11	1.23	1.58	2.52	4.34	12.5	39.2

4.6 "BROAD-BEAM" COEFFICIENTS

Another method of calculation is to use coefficients experimentally determined for a "broad" beam rather than a narrow (collimated) beam. Figures 4.10, 4.11, and 4.12 give transmission in concrete, Fe and Pb respectively of primary radiation from Ra, Co-60, and Cs-137 with corrections for secondary radiation. These Figures are based on "broad" beam coefficients.[8]

A necessary quantity for shielding calculations is the specific radiation flux ϕ_o given as a function of the energy of the emitted gamma radiation. This quantity is plotted in Fig. 4.13 as roentgens per sq cm at one centimeter distance per photon emitted per disintegration per millicurie of radioisotope.[9]

4.7 ENERGY ABSORPTION COEFFICIENTS, μ_a

The previous sections discuss the attenuation of primary radiation flux from point sources and the build-up of secondary radiation. The decrease in the number of primary photons may be determined by use of narrow beam attenuation coefficients and corrections may be made for the attenuation of secondary radiation by use of broad beam coefficients or build-up factors. However these procedures do not give the amount of energy absorption in the medium under consideration.

Customary units of dose (roentgen, rep and rad) are units of energy absorp-

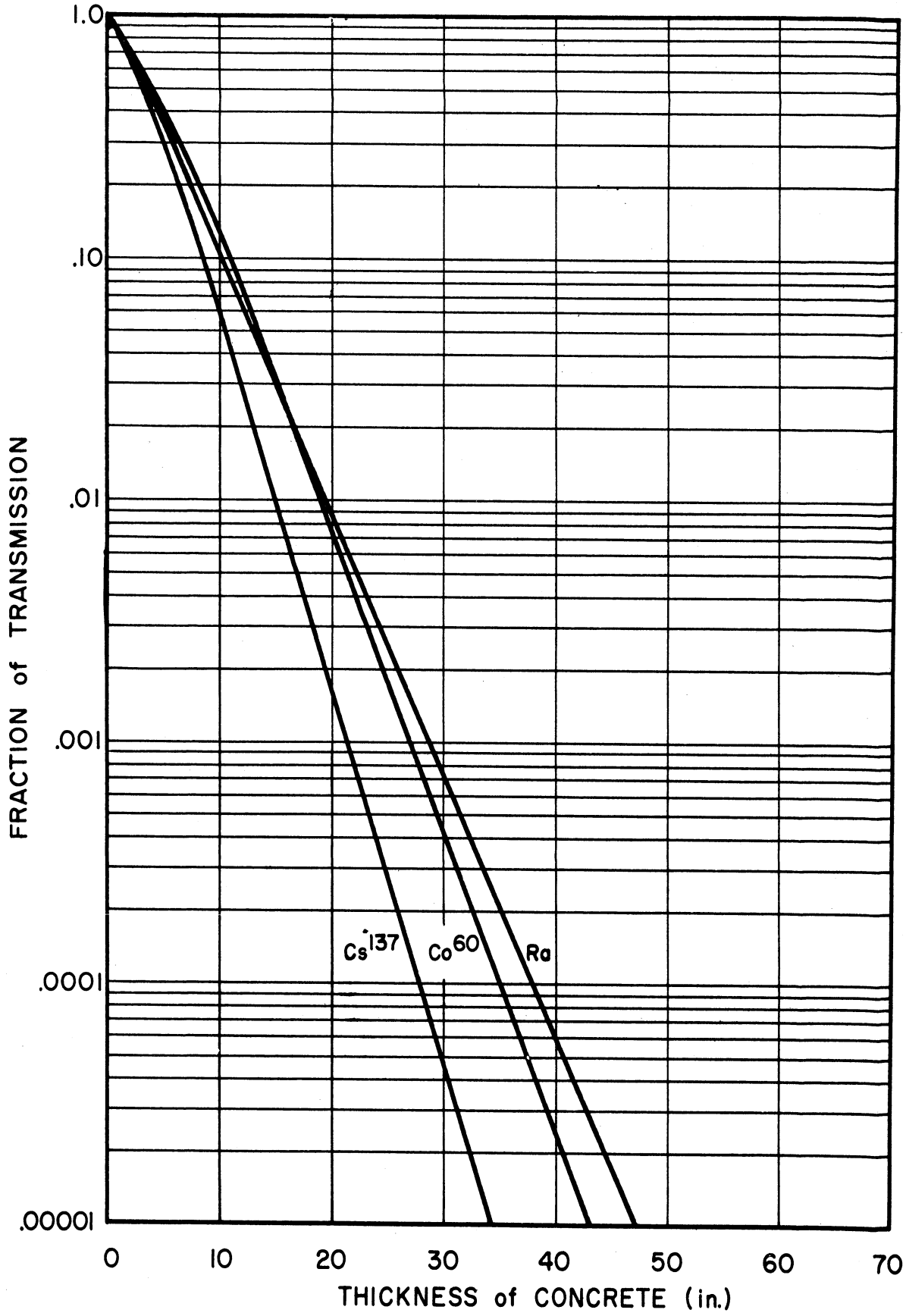

Fig. 4.10. "Broad-beam" transmission of radium, cobalt-60 and cesium-137 gamma rays in concrete.(8)

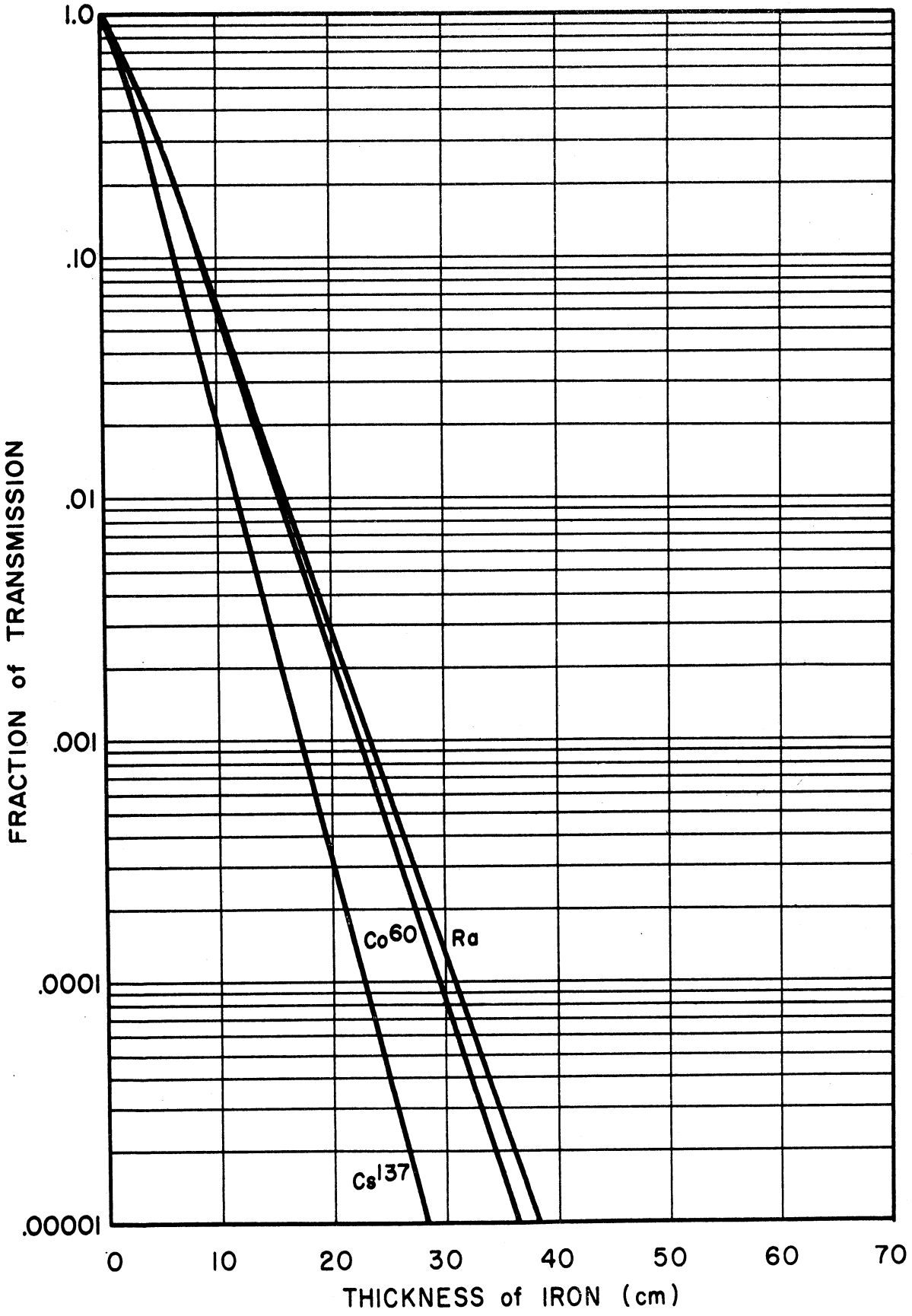

Fig. 4.11. "Broad-beam" transmission of radium, cobalt-60 and cesium-137 gamma rays in iron.(8)

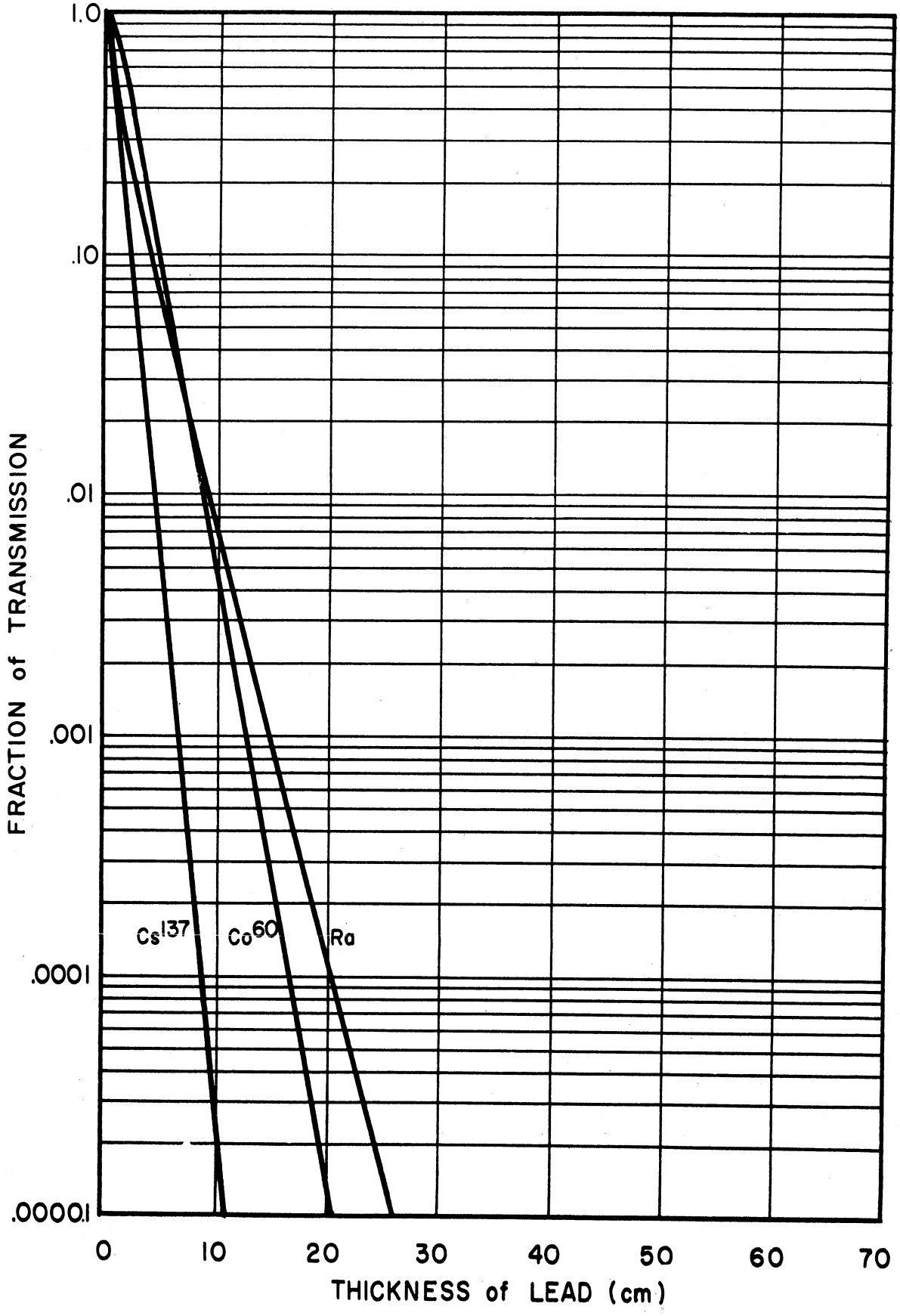

Fig. 4.12. "Broad beam" transmission of radium, cobalt-60 and cesium-137 gamma rays in lead.(8)

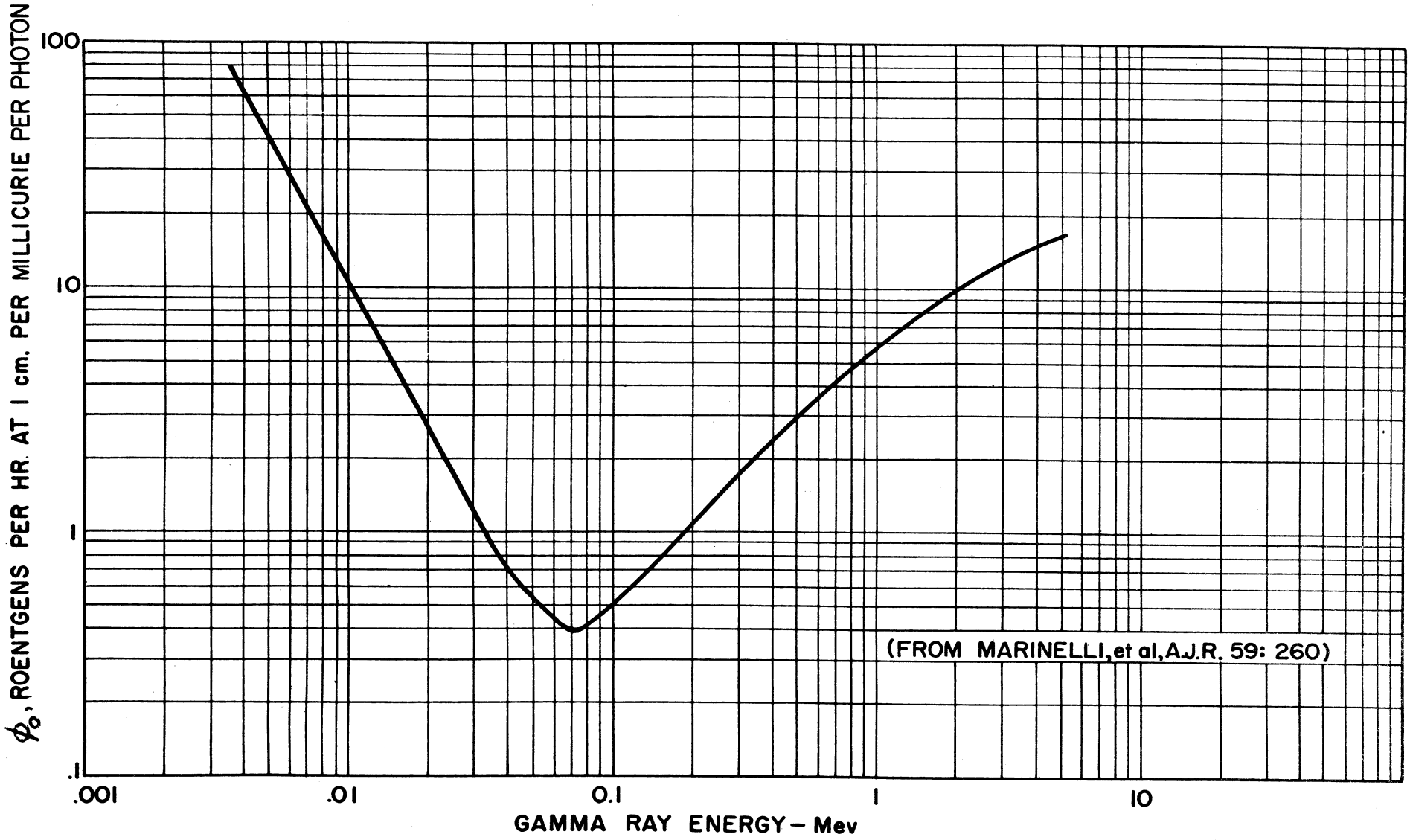

Fig. 4.13. Specific radiation flux, ϕ_o, as a function of energy in Mev of gamma radiation.(9)

tion (as defined in Chapter 1) rather than units of photon flux. Table 4.6 gives values of energy absorption coefficients, μ_a, for some common elements, air and water as a function of the energy of the primary radiation. A comparison of corresponding values for energy absorption and flux attenuation can be made from Tables 4.1 and 4.6.

For radiation in the range from 100 kev to several Mev the energy absorption is approximately proportional to Z/A for the absorber. For the case of air this ratio is about 0.50 whereas for water and tissue this ratio is about 0.55. Thus if unit masses of air and water are exposed to the same radiation flux for the same length of time the water will absorb 0.55/0.50 times as much energy as the air. That is if the air is given a dose of one roentgen (83.8 ergs per gram of air) the water will receive 83.8 (0.55/0.50) or about 93 ergs per gram of water. This unit of dose to water or tissue has been called the rep. Since materials other than water and tissue have different energy absorption coefficients the use of the rep as a unit has caused considerable confusion and has been discontinued in favor of the more general unit, the rad which is equal to 100 ergs per gram of absorber.

The rad at present is the preferred unit of radiation dosage and is equal to same amount of energy absorbed per unit mass (100 ergs/gm) for all materials. If the radiation flux (photons per sec), the exposure time, and the energy of the radiation are known the dose in rads may be calculated by use of Table 4.6.

4.8 EXAMPLE PROBLEM1, POINT SOURCE

An example, Problem 1 will demonstrate the use of the experimentally determined total mass attenuation coefficient, build-up factor, per cent transmission and tenth value thickness, in determining the change in flux due to an isotropic point source when a material shield is interposed.

Example 1:

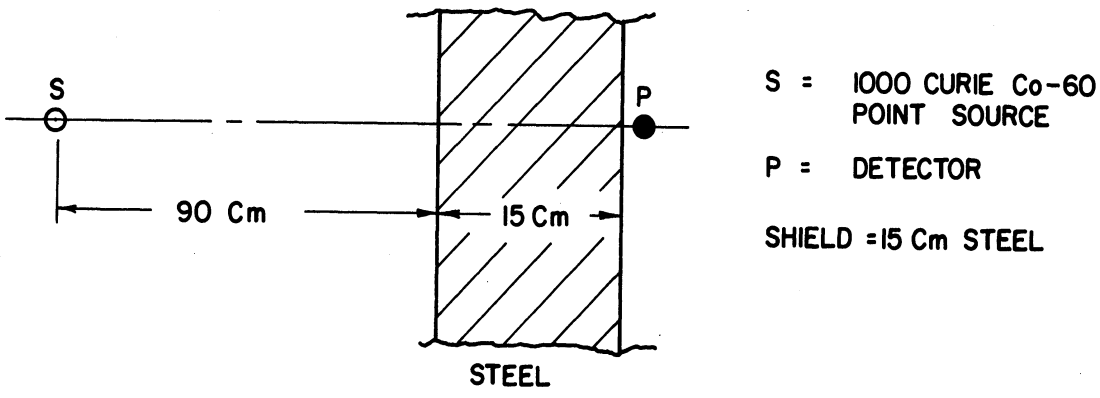

Fig. 4.14. Configuration for example Problem 1.

TABLE 4.6

ENERGY ABSORPTION COEFFICIENT, μ_a, FOR GAMMA RAYS,(1) IN cm^2/gm;(2) IN THOMPSON UNITS/ELECTRON(10)

	H_2O		Air		Al		Fe		Sn		W		Pb		U	
E, Mev	(1)	(2)	(1)	(2)	(1)	(2)	(1)	(2)	(1)	(2)	(1)	(2)	(1)	(2)	(1)	(2)
0.01	4.89	22.0	4.70	23.5	26.1	135	178	953								
0.015	1.33	5.96	1.30	6.48	7.67	39.7	58.0	311								
0.020	0.520	2.34	0.516	2.58	3.15	16.3	25.6	137								
0.030	0.15	0.66	0.15	0.74	0.877	4.54	7.87	42.2	41.3	245						
0.040	0.064	0.29	0.064	0.32	0.351	1.82	3.34	17.9	18.7	111						
0.050	0.0396	0.178	0.0388	0.194	0.17	0.90	1.68	9.03	10.1	59.7						
0.060	0.0282	0.127	0.0270	0.135	0.10	0.54	0.990	5.31	6.14	36.4						
0.080	0.0256	0.115	0.0238	0.119	0.0535	0.277	0.427	2.29	2.75	16.3	7.38	45.8				
0.10	0.0251	0.113	0.0234	0.117	0.0378	0.196	0.224	1.20	1.47	8.73	4.11	25.5	5.20	32.8	0.961	6.21
0.15	0.0278	0.125	0.0250	0.125	0.0278	0.144	0.0813	0.436	0.472	2.80	1.35	8.39	1.76	11.1	2.34	15.1
0.20	0.0298	0.134	0.0264	0.132	0.0276	0.143	0.0489	0.262	0.223	1.32	0.630	3.91	0.819	5.17	1.10	7.08
0.30	0.0318	0.143	0.0284	0.142	0.0280	0.145	0.0336	0.180	0.0876	0.519	0.229	1.42	0.295	1.86	0.392	2.53
0.40	0.0331	0.149	0.0296	0.148	0.0290	0.150	0.0308	0.165	0.0536	0.318	0.12	0.75	0.16	0.98	0.207	1.34
0.50	0.0329	0.148	0.0296	0.148	0.0286	0.148	0.0293	0.157	0.0401	0.238	0.0787	0.488	0.0995	0.628	0.13	0.85
0.60	0.0329	0.148	0.0296	0.148	0.0286	0.148	0.0287	0.154	0.0346	0.205	0.0601	0.373	0.0737	0.465	0.097	0.625
0.80	0.0322	0.145	0.0288	0.144	0.0278	0.144	0.0274	0.147	0.0295	0.175	0.0426	0.264	0.0504	0.318	0.0628	0.406
1.0	0.0311	0.140	0.0280	0.140	0.0268	0.139	0.0263	0.141	0.0268	0.159	0.0353	0.219	0.0403	0.254	0.0481	0.311
1.5	0.0287	0.129	0.0256	0.128	0.0249	0.129	0.0242	0.130	0.0240	0.142	0.0282	0.175	0.0306	0.193	0.0347	0.224
2.0	0.0265	0.119	0.0238	0.119	0.0234	0.121	0.0231	0.124	0.0233	0.138	0.0271	0.168	0.0293	0.185	0.0325	0.210
3.0	0.0233	0.105	0.0212	0.106	0.0212	0.110	0.0224	0.120	0.0245	0.145	0.0287	0.178	0.0306	0.193	0.0331	0.214
4.0	0.021	0.095	0.019	0.097	0.0201	0.104	0.0224	0.120	0.0258	0.153	0.0310	0.192	0.0328	0.207	0.0351	0.227
5.0	0.020	0.089	0.018	0.091	0.0193	0.100	0.0228	0.122	0.0277	0.164	0.0335	0.208	0.0353	0.223	0.0375	0.242
6.0	0.019	0.085	0.017	0.086	0.0189	0.098	0.0231	0.124	0.0292	0.173	0.0355	0.220	0.0372	0.235	0.0395	0.255
8.0	0.017	0.078	0.016	0.080	0.0183	0.095	0.0239	0.128	0.0317	0.188	0.0390	0.242	0.0412	0.260	0.0432	0.279
10.0	0.0165	0.0743	0.015	0.077	0.0183	0.095	0.0250	0.134	0.0342	0.203	0.0426	0.264	0.0452	0.285	0.0474	0.306

A. What is flux at point P if no shield is used?

1. Base calculations on ϕ_o (spec. rad. flux) (see Fig. 4.13).

2. Base calculations on photons emitted. And $\mu_a = 0.027$ cm^2/gm (see Table 4.6) give answers in r/hr.

B. What is flux at point P with shield?

1. Base calculations on % transmission.

2. Base calculations on 1/10 value thickness.

3. Base calculations on narrow beam coef. $\mu_m = 0.054$ cm^2/gm (see Table 4.1).

4. Base calculations on build-up factor B + μ_m, ρ steel = 7.78gm/cc.

Solution:

A.

1. From Fig. 4.13 using avg Mev Co-60 = $\frac{1.17+1.38}{2}$ = 1.25 Mev:

$$\phi_o = 7 \text{ r/hr per mc at 1 cm (per photon)}$$

$$\phi = \frac{7 \text{ r/hr (2 photons) } 10^3 \text{ curies}}{\text{photon } (10^{-3} \text{ curies}) \left(\frac{105 \text{ cm}}{1 \text{ cm}}\right)^2}$$

$$= \underline{1.27 \times 10^3 \text{ r/hr}} \quad \text{(without shield).}$$

2.

$$\phi = \frac{10^3 \text{ curies } (3.7 \times 10^{10} \text{ dis/sec - curie})(2 \text{ phots/dis})}{4\pi(105 \text{ cm})^2}$$

$$= 5.34 \times 10^8 \text{ photons/sec - cm}^2$$

$$= \frac{5.34(10)^8 \gamma/\text{sec}}{\text{cm}^2} \frac{(1.25 \text{ Mev})}{\gamma} \frac{(1.6 \times 10^{-6} \text{ ergs})}{\text{Mev}} \frac{(3600 \text{ sec})}{\text{hr}}$$

$$= 3.83 \times 10^6 \text{ ergs/hr - cm}^2$$

$$\frac{d\phi}{dx} = -\mu_m \phi = \frac{0.027 \text{ cm}^2}{\text{gm(air)}} \frac{(3.83 \times 10^6 \text{ ergs/hr - cm}^2}{\frac{83.8 \text{ ergs/gm (air)}}{\text{r}}}$$

$$= \boxed{1.24 \times 10^3 \text{ r/hr}}$$

B.

1. From Fig. 4.11 fraction transmission = 0.012:

$$\phi = 0.012 \ (1.24 \times 10^3 \text{ r/hr})$$

$$= \boxed{14.9 \text{ r/hr}} \qquad \text{(From broad beam calculations.)}$$

2. From Fig. 4.8:

$$t_{10} = 2 \text{ in}, \quad n = \frac{15 \text{ cm}}{2.54 \text{ cm/in } (2 \text{ in}/t_{10})} = 2.95 \ t_{10}$$

$$\phi = \phi_o / t_{10}^n = \frac{1.24 \times 10^3 \text{ r/hr}}{10^{2.95}} = \frac{1.24}{890} \times 10^3 \text{ r/hr}$$

$$= \boxed{1.39 \text{ r/hr}} \quad \text{(Obviously narrow beam calculations.)}$$

3.

$$\phi = \phi_o \, e^{-\mu x}$$

$$\mu = 0.054 \text{ cm}^2/\text{gm} \ (7.78 \text{ gm/cc}) = 0.420 \text{ cm}^{-1}$$

$$\mu x = 0.42 \text{ cm}^{-1} \ (15 \text{ cm}) = 6.3$$

$$\phi = (1.24 \times 10^3 \text{ r/hr}) e^{-6.3} = 1.24 \times 10^3 \ (0.00183)$$

$$= \boxed{2.27 \text{ r/ hr}}$$

4. From Table 4.3

For $\mu x = 7$

at 1 Mev B = 10.2

2 Mev B = $\frac{7.25}{2.95}$ x 0.25 = 0.739

$B_{1.25\ Mev} = 10.2 - 0.74 = 9.46$

For $\mu x = 4$

at 1 Mev B = 5.39

2 Mev B = $\frac{4.13}{1.26}$ x 0.25 = 0.315

$B_{1.25\ Mev} = 5.39 - 0.32 = 5.07$

For $\mu x = 6.3$

at $\mu x = 7$, $B_{1.25} = 9.46$

$\mu x = 4$, $B_{1.25} = \frac{5.07}{4.39} \times \frac{2.3}{3} = 3.37$

$\mu x = 6.3$, $B_{1.25} = 5.07 + 3.37 = 8.44$

$$\phi = B \phi_0 e^{-\mu x} = 8.44\ (1.24 \times 10^3\ r/hr) e^{-6.3}$$

$$= 8.44\ (2.27)\ r/hr$$

$$= \underline{19.2\ r/hr}$$

4.9 CALCULATION PROCEDURES FOR VARIOUS GEOMETRIES AND MULTIPLE SHIELDS

Various methods of calculation have been devised to solve the problem of penetration of gamma rays in "bad geometry" situations. One such method employs the "build-up factor," B, which, used as a multiplier in Equation 4.4, corrects for the scattering effect listed above:

$$\phi = B \phi_0 \frac{e^{-\mu x}}{r^2} \qquad (4.10)$$

For an isotropic point source of strength s_o, the inverse square law may be expressed as $\phi = s_o/4\pi r^2$, since all the flux is emitted isotopically in a solid angle of 4π radians. Then Equation 4.6 can be expressed as

$$\phi = \frac{B\, S_o}{4\pi r^2} e^{-\mu x} \tag{4.11}$$

The build-up factor introduced in Equation 4.10 has been defined as the ratio of total intensity from scattered plus unscattered photons to the intensity from unscattered photons only. Several build-up factors based on number of photons, energy transmission, dose rate, and energy-absorption factors have been defined. Assume that one photon per second is being emitted from an isotropic point source. Let the scattered flux density measured by an isotropic detector insensitive to the unscattered photons be equal to ϕ_s. At a distance r from the source in an absorber of absorption coefficient μ corresponding to source energy E_o. Various build-up factors can then be defined as follows.

Types of Build-Up Factors

1. Number Build-Up Factor, B_N

$$B_N(r,E_o) = 1 + \frac{\text{scattered photon flux}}{\text{unscattered photon flux}}$$

$$B_N(r,E_o) = 1 + \phi_s \cdot 4\pi r^2\, e^{\mu r} . \tag{4.12}$$

2. Energy Build-Up Factor, $B_E(r,E_o)$

$$B_E(r,E_o) = 1 + \frac{\text{scattered energy flux}}{\text{unscattered energy flux}}$$

The energy flux, I, is a function of r and E, and

$$I(r,E) = E\phi_s(r,E) \tag{4.13a}$$

$$B_E = 1 + \frac{1}{E_o}\int 4\pi r^2\, e^{\mu r}\, I(r,E)dE \tag{4.13b}$$

where E_o is source photon energy and E is scattered photon energy. Similarly, dose rate and energy-absorption factors are defined.

3. Dose Build-Up Factor, B_r (in air)

Dose intensity = (photon flux) x (energy) x (absorption coefficient).

$$B_r = 1 + \frac{1}{E_o \mu_a^{air}(E_o)} \int 4\pi r^2 e^{\mu r} \mu_a^{air}(E) I(r,E)dE , \qquad (4.14)$$

where $\mu_a^{air}(E_o)$ is the absorption coefficient of dry air at energy E_o and $\mu_a^{air}(E)$ is the absorption coefficient of dry air at energy E. Since μ_a^{air} is practically constant with energy, energy and dose build-up factors are practically the same, i.e., $B_E \simeq B_r$.

4. Energy-Absorption Build-Up Factor, B_A (in absorbing medium)

$$B_A = 1 + \frac{1}{E_o \mu_a(E_o)} \int 4\pi r^2 e^{\mu r} \mu_a(E) I(r,E)dE \qquad (4.15)$$

where $\mu_a(E)$ is the absorption coefficient for material at energy E and $\mu_a(E_o)$ is the absorption coefficient for material at energy E_o. This build-up factor is important for heat-absorption calculations.

4.10 ONE-MATERIAL SHIELD

From the safety point of view, the dose build-up factor B_r is most important. Extensive numerical calculations using isotropic point sources and monodirectional plane sources in infinite media have been carried out by Goldstein and Wilkins[7] for lead, iron, aluminum, and water in the energy range of 0.5-10 Mev using the "Standard Moments Method" developed by Spencer and Fano.[11] The build-up factors obtained by Goldstein and Wilkins are given in Tables 4.1 - 4.4. An empirical formula consisting of two exponentials in three parameters has been obtained by Taylor[12] to fit the data on build-up factor for point isotropic sources in infinite media obtained by the NBS-NDA group.[7] In a simple form, the build-up factor for a point source in an infinite homogeneous medium can be expressed as the sum of two exponentials:

$$B(\mu x, E_o) = A_1(E_o) \exp [- \alpha_1(E_o) \mu x] + A_2(E_o) \exp [- \alpha_2(E_o) \mu x] \qquad (4.16)$$

A_1, A_2, α_1, and α_2 depend on energy, material of absorption, and type of build-up factor and are given in Figs. 4.15 - 4.18 for lead, iron, concrete, and water, respectively. From the definition of build-up factor, $A_1 + A_2 = 1$, and $\mu(E_o)$ is the narrow-beam absorption coefficient of the absorber for an

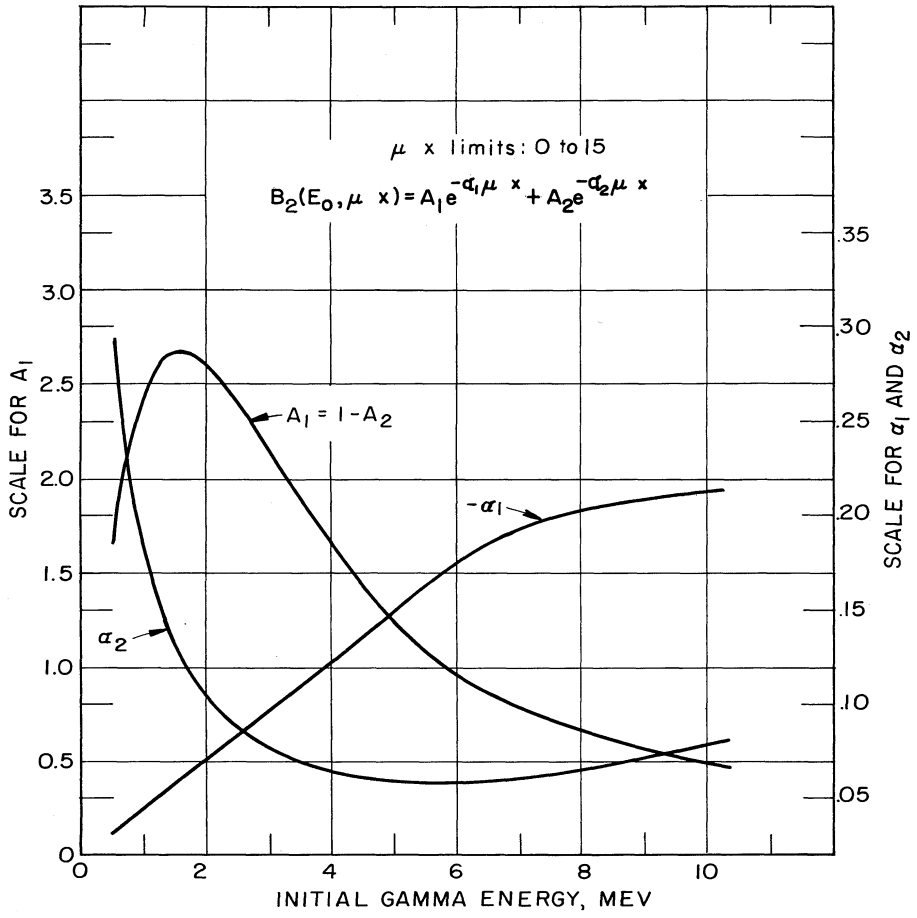

Fig. 4.15a. Dose build-up factor in lead for isotropic point source.(13)

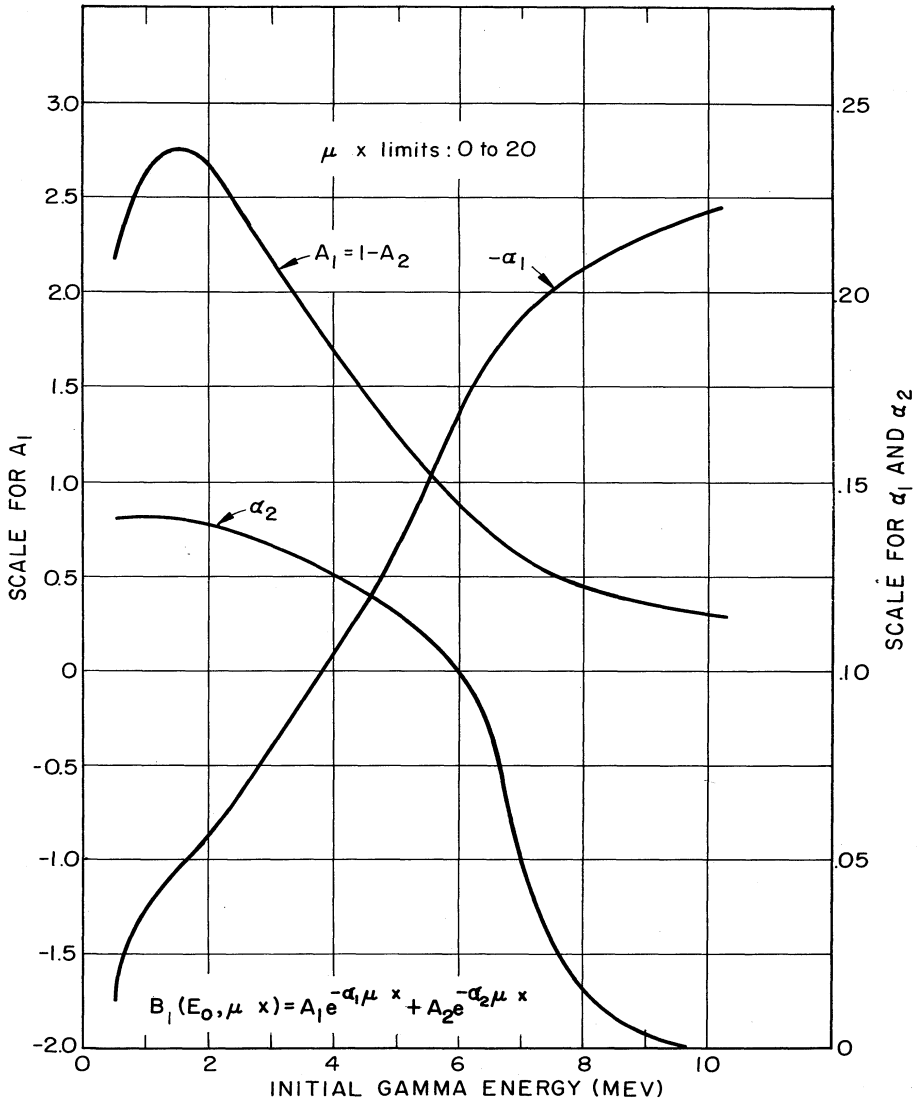

Fig. 4.15b. Energy-absorption build-up factor in lead for isotropic point source.(13)

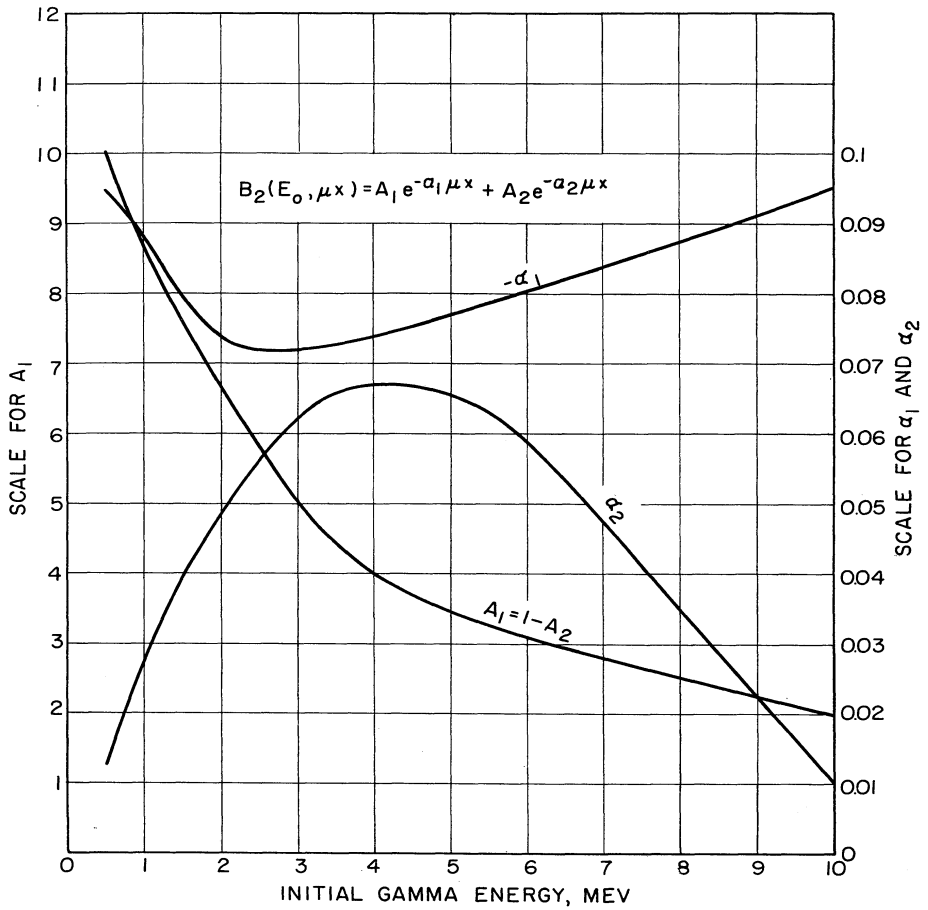

Fig. 4.16a. Dose build-up factor in iron for isotropic point source.(13)

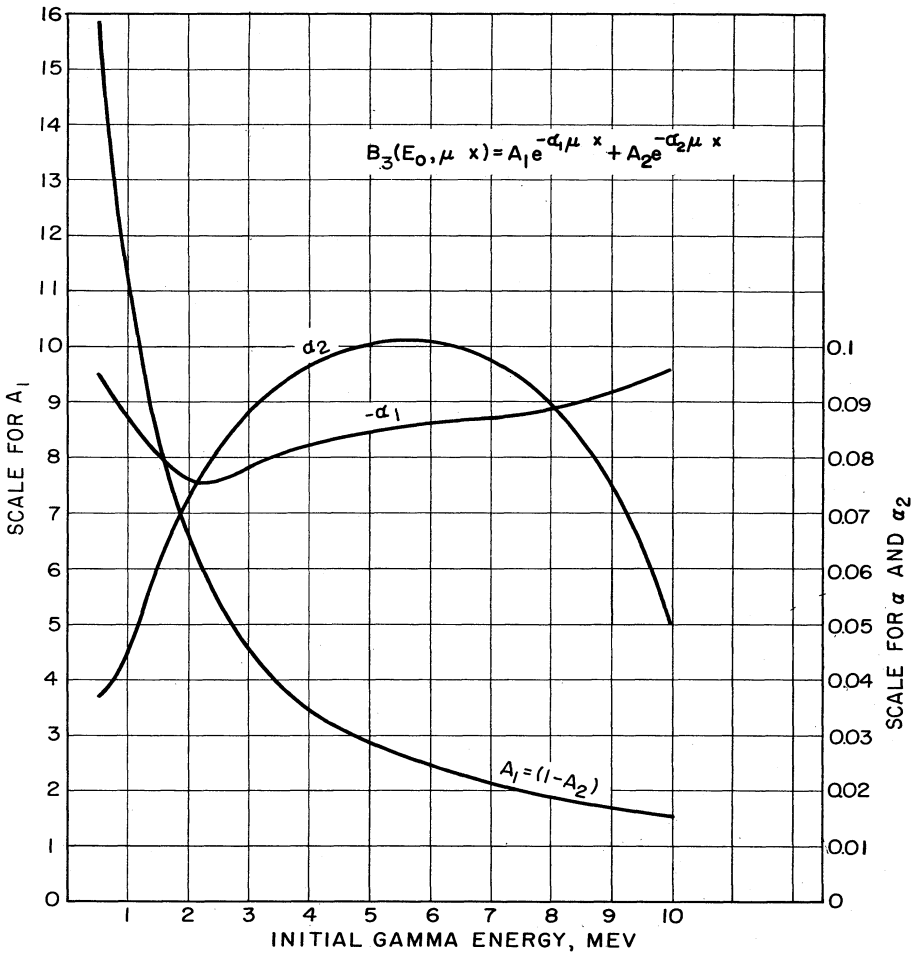

Fig. 4.16b. Energy-absorption build-up factor in iron for isotropic point source.(13)

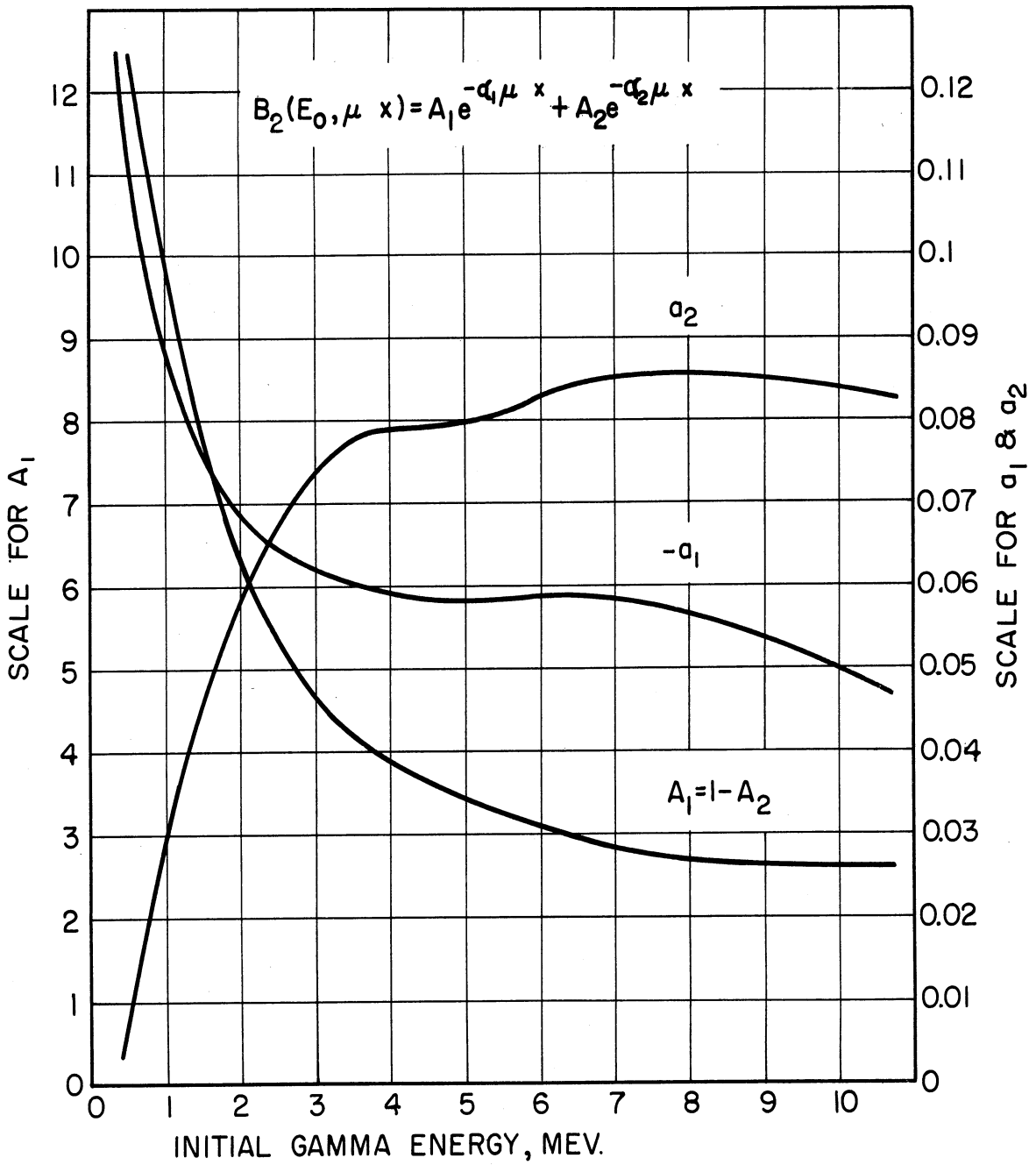

Fig. 4.17. Dose build-up factor in concrete (sp. gr. = 2.3) for isotropic point source.(13)

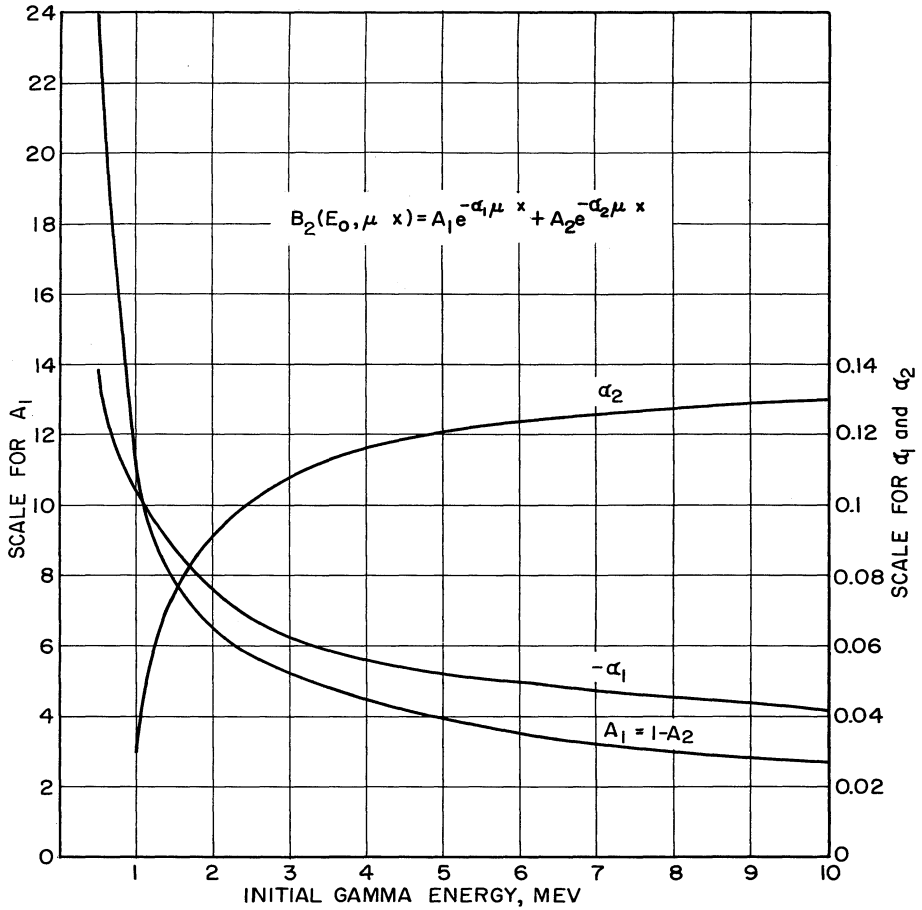

Fig. 4.18a. Dose build-up factor in water for isotropic point source.(13)

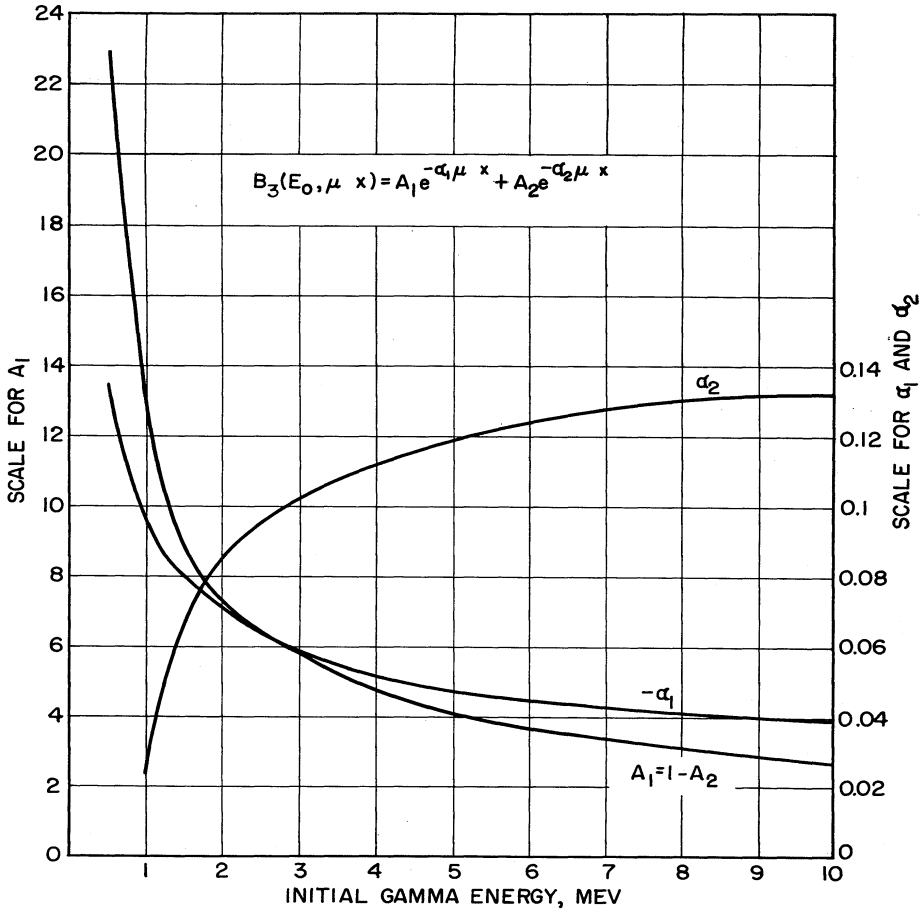

Fig. 4.18b. Energy-absorption build-up factor in water for isotropic point source.(13)

unscattered photon energy E_0. An advantage of using this analytical expression is the simplicity of integrating the attenuation kernel, which stays exponential, though modified by the build-up factor.

4.11 SEVERAL SLABS OF DIFFERENT MATERIALS

In the case of composite shields, several different methods for using the build-up factors have been proposed.

1. For a light material, followed by a heavy material, the build-up factor of the heavy material only is used. For example, water followed by the concrete, the build-up factor of the concrete must be employed.

2. For a heavy material followed by a light material, the product of the individual build-up factors is taken. For more than two materials, this leads to conservative, high results.

3. The build-up factor may be weighted according to the number of relaxation lengths of each material.

4. The shield may be converted to an equivalent shield of known material and the build-up factor for that material may be used. This conversion may be obtained by assuming that the radiation flux, ϕ_0, on the source side of the shield are the same in both cases.

$$\phi_0 B_1 \, e^{-\mu_1 t_1} = \phi_0 B_2 \, e^{-\mu_2 t_2} \qquad (4.17)$$

where

ϕ_0 = the radiation flux on the source side of the shield (assumed to be plane monodirectional),

μ_1 and μ_2 = attenuation coefficients for the materials represented by suffixes, and

t_1 and t_2 = thicknesses of the shields.

$\therefore$ Taking logarithms of both sides,

$$\mu_1 t_1 - \mu_2 t_2 = \ell n \frac{B_1}{B_2}$$

$$t_1 = \frac{\mu_2}{\mu_1} t_2 + \frac{1}{\mu_1} \left(\ell n \frac{B_1}{B_2} \right) . \qquad (4.18)$$

Equation 4.18 can be solved for $\mu_1 t_1$ by an iterative process. As a first approximation, assume $\mu_1 t_1 = \mu_2 t_2$, and use the build-up factor B_1[1] for that value of $\mu_1 t_1$ and solve for t_1. The process is repeated to obtain the second approximation, using the build-up factor B_1 for the calculated value of $\mu_1 t_1$. Generally two approximations are sufficient to obtain the equivalent thickness t_1 in terms of the known material thickness t_2.

4.12 EFFECT OF GEOMETRY (FROM ROCKWELL)[13]

Equations for the gamma-radiation flux from sources of standard geometry such as point, line, disc, cylinder, and sphere are given in the following pages. Curves for evaluating the standard integrals and the functions appearing in the equations of the flux are reproduced from "The Reactor Shielding Design Manual", edited by Rockwell.[13] For a more complete discussion Ref. 13 should be consulted. The nomenclature used in these equations is as follows:

ϕ	Scalar flux ($cm^{-2}sec^{-1}$)
S_o	Source strength of point source (sec^{-1})
S_L	Source strength of line source ($cm^{-1}sec^{-1}$)
S_A	Source strength of plane source ($cm^{-2}sec^{-1}$)
S_V	Source strength of volume source ($cm^{-3}sec^{-1}$)
μ_s	Macroscopic cross section of source material (cm^{-1})
$\mu_1, \mu_2, \ldots \mu_n$	Macroscopic cross sections of shields 1, 2,...n(cm^{-1})
t_i	Thickness of ith shield (cm)
b_1	$\sum_i^n \mu_i t_i$
b_2	$b_1 + \mu_s Z$
b_3	$b_1 + \mu_s h$
h	Thickness of slab source (cm)
Z	Effective self-attenuation distance (cm)
R_o	Radius of disk, cylinder, or sphere (cm)
B	Symbolic build-up factor
$E_n(b)$	$b^{n-1} \int_b^\infty \frac{e^{-t}}{t^n} dt$ for $n \geq 0$. When $n = 0$, this becomes $E_o(b) = \frac{e^{-b}}{b}$
$F(\theta,b)$	$\int_o^\theta e^{-b \sec \theta'} d\theta'$
$G(a,b)$	$\int_o^b F\left(\tan^{-1} \frac{a}{b'}, b'\right) db'$ where F is the function defined above
$F_n(t,a)$	$\int_o^t e^{ab} E_n(b)\, db$

A number of relationships for sources of various shapes may be derived from Equation 4.11.

A. Point Source

From Equation 4.11, the flux at P_1 in Fig. 4.19 from an istropic point source is

$$\phi = B \frac{S_o}{4\pi a^2} e^{-\sum_i \mu_i t_i}$$

where $\sum_i \mu_i t_i = \mu_1 t_1 + \mu_2 t_2 + \mu_3 t_3 + \ldots$, is the sum of the individual products of macroscopic cross section and thickness for the various shields.

In the notation given on page 32, this equation may be written

$$\phi = B \frac{S_o}{4\pi a^2} e^{-b_1} \qquad (4.19)$$

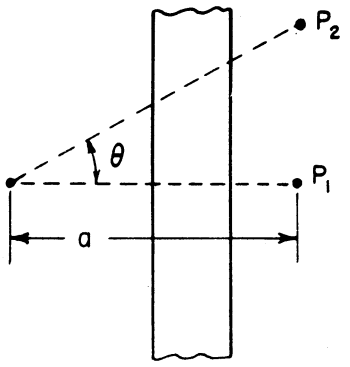

Fig. 4.19. Geometry of point source.(13)

At point P_2 in Fig. 4.19, trigonometrical factor must be included in the calculation, and

$$\phi = B \frac{S_o}{4\pi (a \sec \theta)^2} \cdot e^{-b_1 \sec \theta} \qquad (4.20)$$

B. Line Source

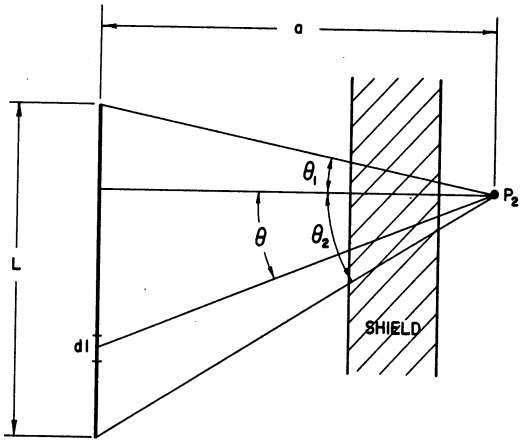

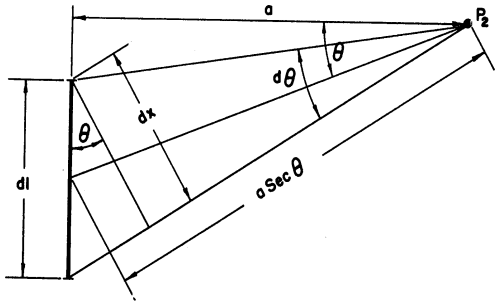

Fig. 4.20a
eometry for element
of line source

See Fig. 4.20a

S_L = Activity/Unit Length

For element $d\ell$

At point P_2

$$d\phi = \frac{S_L(d\ell)e^{-b_1 \sec \theta}}{4\pi(a \sec \theta)^2} \qquad (4.21)$$

For small angles:

$dx = (a \sec \theta)\, d\theta$

and $d\ell = dx \sec \theta$

$d\ell = a(\sec \theta)^2\, d\theta$

Substituting

$$d\phi = \frac{S_L(a \sec \theta\, d\theta)e^{-b_1 \sec \theta}}{4\pi(a \sec \theta)^2}$$

$$= \frac{S_L\, e^{-b_1 \sec \theta}\, d\theta}{4\pi a} \qquad (4.22)$$

Integrating between limits θ_1 and θ_2

$$= \frac{S_L}{4\pi a}\left(\int_0^{\theta_1} e^{-b_1 \sec \theta}\, d\theta + \int_0^{\theta_2} e^{-b_1 \sec \theta}\, d\theta \right) \qquad (4.23)$$

Or in terms of the function $F(\theta,b)$ (Figs. 4.35-4.41)

$$\phi = B \frac{S_L}{4\pi a}[F(\theta_2,b_1) + F(\theta_1,b_1)] \qquad (4.24)$$

At P_1 (see Fig. 4.20b) this equation used with the limits of integration $-\theta_1$, θ_2, gives the flux

$$\phi = B \frac{S_L}{4\pi a}[F(\theta_2,b_1) - F(\theta_1,b_1)] \qquad (4.25)$$

If P_2 is such that θ_1, $= \theta_2$, then the integral becomes

$$2 \int_0^{\theta_1} e^{-b_1 \sec \theta}\, d\theta ,$$

and

$$\phi = B \frac{S_L}{2\pi a} F(\theta_1,b_1) \qquad (4.26)$$

For no absorber, $b_1 = 0$ and Equation (4.23) becomes

$$\phi = \frac{S_L}{4\pi a}\left(\int_0^{\theta_1} d\theta - \int_0^{\theta_2} d\theta\right)$$

$$= \frac{S_L}{4\pi a}(\theta_1 - \theta_2) \qquad (4.27)$$

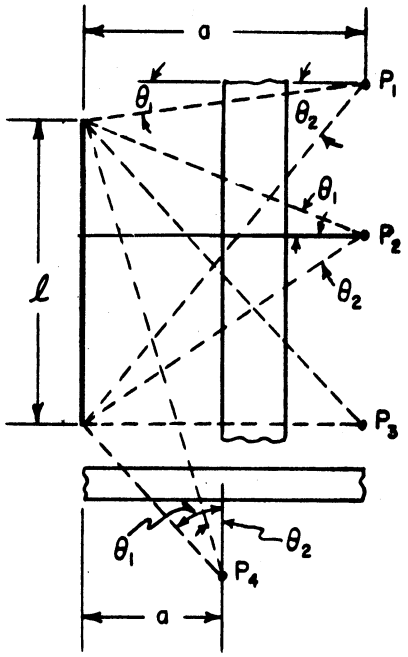

Fig. 4.20b Geometry for line source.(13)

For an infinite line source, $\ell = \infty$, and hence

$$\theta_1 = \frac{\pi}{2} = \theta_2 ,$$

so the flux is then given by

$$\phi = B\frac{S_L}{2\pi a}\int_0^{\frac{\pi}{2}} e^{-b_1 \sec\theta}\, d\theta \qquad (4.28)$$

$$= B\frac{S_L}{2\pi a} F\left(\frac{\pi}{2}, b_1\right)$$

At P_3, for a non-infinite line source, $\theta_2 = 0$ and

$$\phi = B \frac{S_L}{4\pi a} \int_{-\theta_1}^{0} e^{-b_1 \sec \theta} \, d\theta$$

$$= B \frac{S_L}{4\pi a} F(\theta_1, b_1) \qquad (4.29)$$

For a semi infinite line source, the flux at P_3 is given by putting $\theta_2 = 0$ and $\theta_1 = \pi/2$, and

$$\phi = B \frac{S_L}{4\pi a} F(\tfrac{\pi}{2}, b_1) \qquad (4.30)$$

At the point P_4, for a non-infinite line source, the flux is

$$\phi = B \frac{S_L}{4\pi a} \int_{\theta_2}^{\theta_1} e^{-b_1 \sec \theta} \, d\theta$$

$$= B \frac{S_L}{4\pi a} [F(\theta_1, b_1) - F(\theta_2, b_1)] \qquad (4.31)$$

C. Disk Source (K curves)

At P_1 on the center line of the disk, the contribution to the flux from an elemental of radius r and width dr is

$$d\phi = B. \frac{S_A \, (2\pi r dr)}{4\pi \rho^2} e^{-b_1 \sec \theta'} \qquad (4.32)$$

But $\rho^2 = a^2 + r^2$, $S_o \quad \rho d\rho = r dr$

and $\sec \theta' = \rho/a$, so

$$d\phi = B. \frac{S_A}{2} \frac{d\rho}{\rho} e^{-\frac{b_1 \rho}{a}} \qquad (4.33)$$

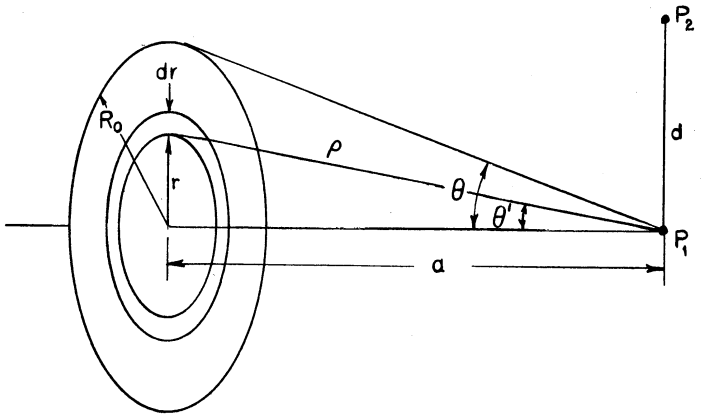

Fig. 4.21. Geometry for disk source.(13)

Integrating, making the substitution $\frac{b_1\rho}{a} = t$

$$\phi = B.\frac{S_A}{2}\int_{b_1}^{b_1 \sec\theta}\frac{e^{-t}}{t}\,dt$$

$$= \frac{BS_A}{2}\left[E_1(b_1) - E_1(b_1 \sec\theta)\right] \qquad (4.34)$$

At an off-axis point, a similar though considerably more complex derivation gives

$$\phi = B.\frac{S_A}{2}\left[\int_{b_1}^{b_1 \sec\theta}\frac{e^{-t}}{t}\,dt\right] . \quad K\left(\frac{d}{R_o}, \frac{a}{R_o}, \bar{\mu}R_o\right)$$

$$= \frac{BS_A}{2}\left[E_1(b_1) - E_1(b_1 \sec\theta)\right] . \quad K\left(\frac{d}{R_o}, \frac{a}{R_o}, \bar{\mu}R_o\right) \qquad (4.35)$$

where $\bar{\mu}$ is a mean absorption coefficient defined by $\bar{\mu} = \frac{\sum_i \mu_i t_i}{\sum_i t_i}$, K is to be evaluated from the curves given in Figs. 4.23 - 4.26.

4.13 EXAMPLE PROBLEM 2, POINT SOURCE USING METHOD FROM ROCKWELL[13]

Example 2: Revaluate Example 1, Part B-4 for a point source using the method from Rockwell, Equation 4.16.

Solution:

Build-up factor for point source from Fig. 4.16a.

$$A_1 = 8.1, \quad A_2 = 1 - A_1 = -7.1$$

$$-\alpha_1 = 0.083, \quad \alpha_2 = 0.034$$

by Equation 4.16

$$B = A_1 e^{-(\alpha_1 \mu x)} + A_2 e^{-(\alpha_2 \mu x)}$$

$$= 8.1\, e^{+(.083)(6.3)} - 7.1\, e^{-(0.034)(6.3)}$$

$$= 8.1\, e^{+0.522} - 7.1\, e^{-0.214}$$

$$= 8.1\,(1.686) - 7.1\left(\frac{1}{1.239}\right) = 13.65 - 5.73 = 7.92$$

$$\phi = B\left(\frac{S_o}{4\pi a^2}\right) e^{-b_1}$$

$$S_o = 1000(2)(1.25)(3.7 \times 10^{10})(1.6 \times 10^{-6})(3600) = 5.33 \times 10^{11} \text{ ergs/hr}$$

$$\frac{5.33(10^{11})(0.027)}{83.8} = 1.72 \times 10^{8} \text{ r/hr}$$

$$\phi = 7.92\left(\frac{1.72 \times 10^{8}}{t(\pi)(105)^2}\right) e^{-6.3}$$

$$7.92(1.24 \times 10^{3})(.00183) = \boxed{18.0 \text{ r/hr}}$$

or:

$$\phi = \frac{S_o}{4\pi a^2}\left[A_1 e^{-(1+\alpha_1)\mu t} + A_2 e^{-(1+\alpha_2)\mu t}\right]$$

$$= \frac{1.72 \times 10^{8}}{4\pi(105)^2}\left[8.1\, e^{-0.917(6.3)} - 7.1\, e^{-1.034(6.3)}\right]$$

$$= 1.24 \times 10^{3}\ (8.1/340 - 7.1/680)$$

$$= \boxed{16.7\ \text{r/hr}}$$

4.14 EXAMPLE PROBLEM 3, LINE SOURCE USING METHOD FROM ROCKWELL[13]

A. Using the Rockwell method for a line source calculate the flux at point P in Fig. 4.22 for:

1. A 1000 curie Cobalt-60 line source without 15 in. steel shield.
2. The same line source with the 15 in. steel shield.

B. Add 10,000 curies of Gold-198 (which emits a gamma photon of .411 Mev) to the 1000 curies of Cobalt-60 and calculate the flux at "P" for a line source by making an individual calculation for each energy and build-up factor.

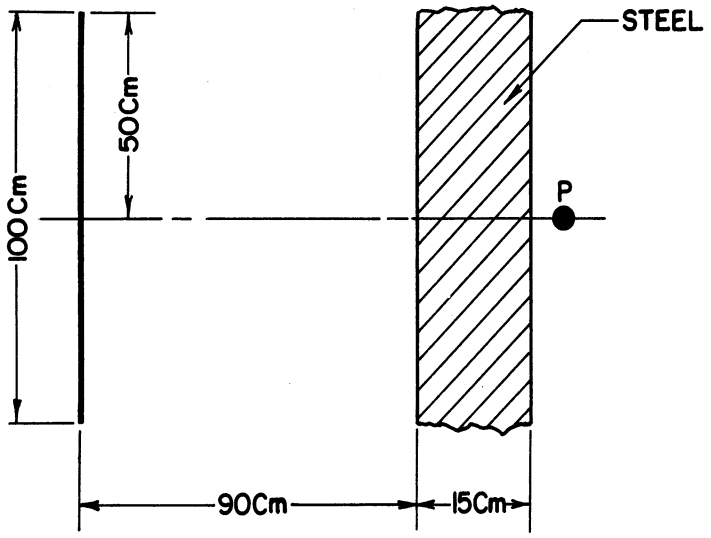

Fig. 4.22. Configuration for example 4.3.

Solution:

A.1. Line source without shield

$$S_L = \frac{1000(3.7 \times 10^{10})2}{100} = 7.4 \times 10^{11}\ \frac{\text{photons/sec}}{\text{cm}}$$

$$\tan \theta_1 = 50/105 = 0.476$$

$$\theta_1 = 25.5^\circ = 0.444 \text{ radians}$$

$$\phi = \frac{S}{2\pi a} F(\theta_1, b_1)$$

From Fig. 4.35, for

$$b = 0, \quad \theta = 25.5^\circ \quad F = 0.40$$

$$\phi = \frac{7.4(10^{11})(0.4)}{6.28(\pi)(105)} = 0.448\ (10^9)\ \frac{\text{photons/sec}}{\text{cm}^2}$$

$$= \frac{0.448(10^9)(1.25)(1.6 \times 10^{-6})(3600)(0.027)}{83.8} = \boxed{1.035(10^3) \text{r/hr}}$$

A.2. Line source with shield

$$\phi = \frac{S_L}{2\pi a}\left[A_1 \int_o^{\theta_1} e^{-(1+\alpha_1)\mu t \sec \theta} d\theta + A_2 \int_o^{\theta_2} e^{-(1+\alpha_2)\mu t \sec \theta} d\theta\right]$$

$$= 1.035(10^3)\left[8.1 \int_o^{\theta_1} e^{-(1-.083)(6.3)\sec \theta} d\theta - 7.1 \int_o^{\theta_2} e^{-(1+.034)(6.3)\sec \theta} d\theta\right]$$

$$= 1.035(10^3)\left[8.1 \int_o^{25.5} e^{5.77 \sec \theta} d\theta - 7.1 \int_o^{25.5} e^{-6.51 \sec \theta} d\theta\right]$$

From Fig. 4.35, for

$$b = 5.77, \quad \theta = 25.5^\circ, \quad F = 1.02(10^{-2})$$

$$b = 6.51, \quad \theta = 25.5^\circ, \quad F = 5.0\ (10^{-3})$$

$$\phi = 1.035(10^3)\left[8.1(1.02)(10^{-2}) - 7.1(5.0)(10^{-3})\right]$$

$$= \boxed{8.17 \text{ r/hr}}$$

B. Multiple group calculation.

$$\phi \text{ cobalt-60} = 8.17 \text{ r/hr}$$

$$\phi \text{ gold-193}$$

$$A_1 = 10.2, \quad A_2 = -9.2$$

$$\alpha_1 = -0.096, \quad \alpha_2 = -0.011$$

$$S_L = \frac{10{,}000(3.7)(10^{10})(.41)(1.6)(10^{-6})(3600)(0.027)}{100 \times 83.8} = 2.81(10^6)\frac{r/hr}{cm}$$

From Fig. 4.6

$$\mu = 0.09, \quad \mu x = .09(7.78)(15) = 10.48$$

$$\phi = \frac{2.81(10^6)}{2\pi(105)}\left[10.2\int_0^{\theta_1} e^{-(1-.096)(10.48)\sec\theta}d\theta - 9.2\int_0^{\theta_2} e^{-(1+.011)(10.98)\sec\theta}d\theta\right]$$

$$= 4.27(10^3)\left[10.2\int_0^{25.5} e^{-9.48\sec\theta}d\theta - 9.2\int_0^{25.5} e^{-Lo.60\sec\theta}d\theta\right]$$

From Fig. 4.36, for

$$b = 9.48, \quad \theta = 25.5, \quad F = 2.2(10^{-5})$$

$$b = 10.60, \quad \theta = 25.5, \quad F = 0.80(10^{-5})$$

$$\phi = 4.27(10^3)\left[10.2(2.2)(10^{-5}) - 9.2(0.80)(10^{-5})\right]$$

$$= 4.27(10^3)(15.08)(10^{-5}) = 0.642 \text{ r/hr}$$

$$\phi_{total} = 8.17 + 0.64 = 8.81 \text{ r/hr}$$

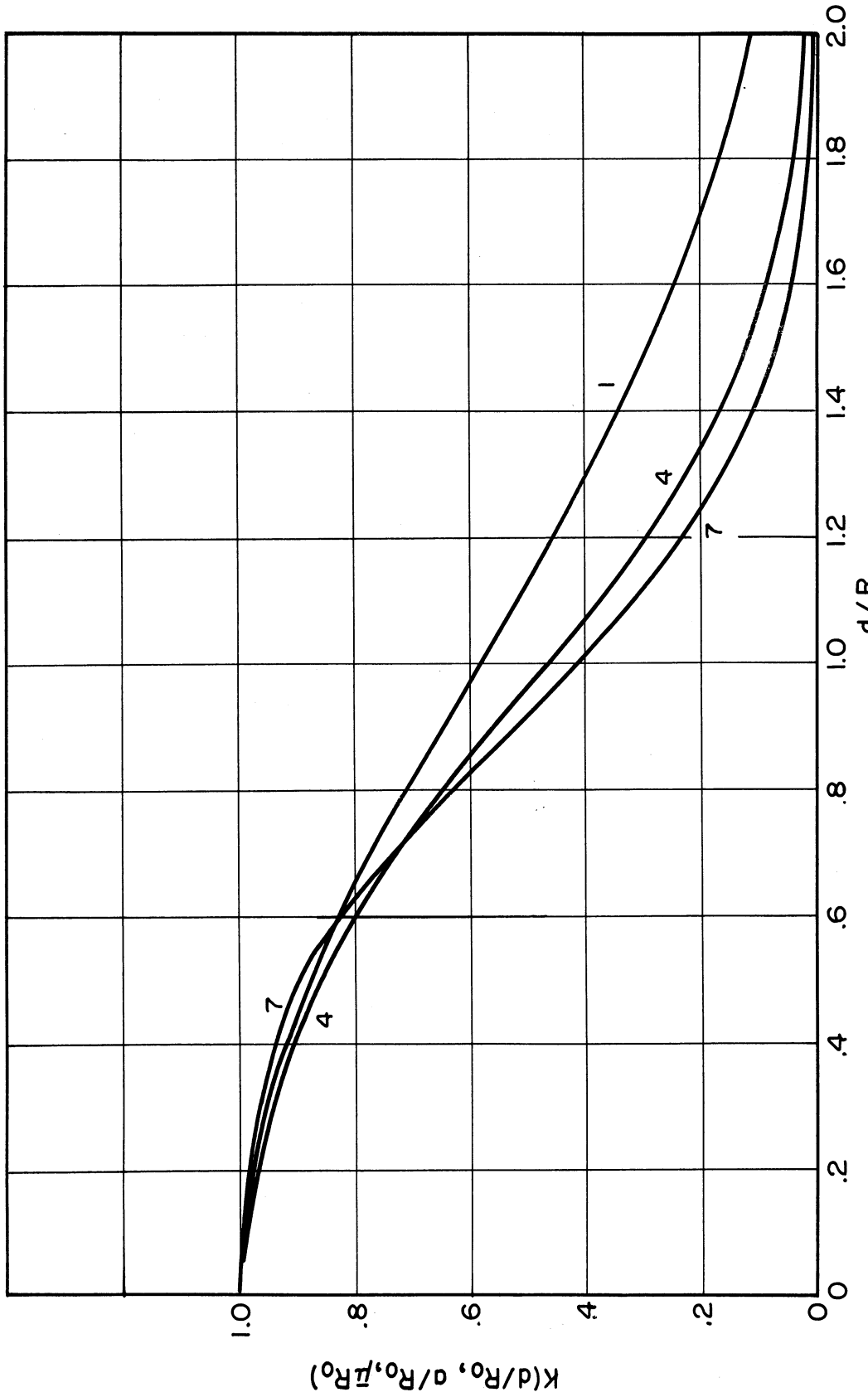

Fig. 4.23 K curves for disk source off center line with $a/R_o = 1.0$ for u R_o parameters of 1, 4, and 7. (13)

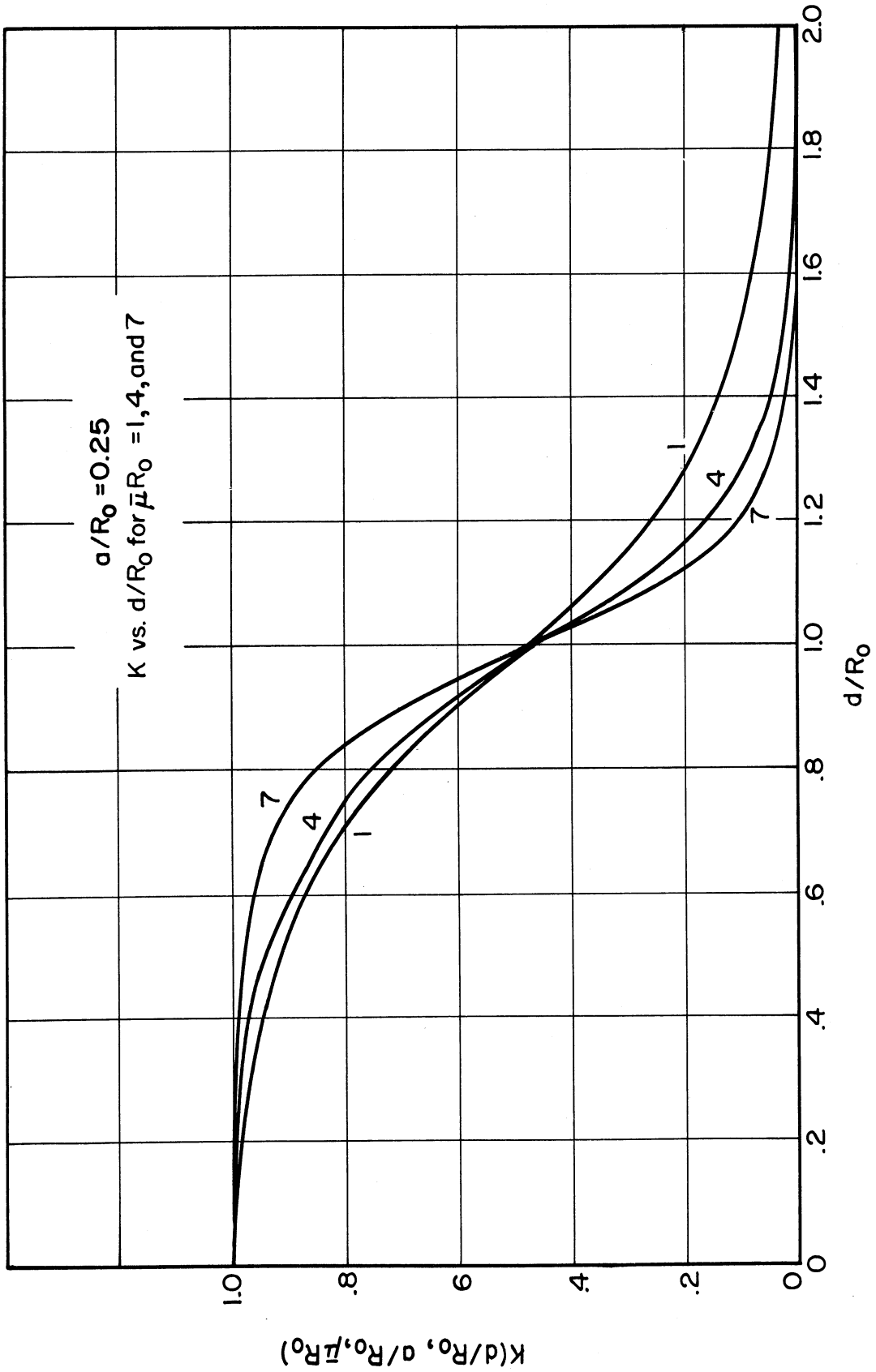

Fig. 4.24. Disk source off center line.(13)

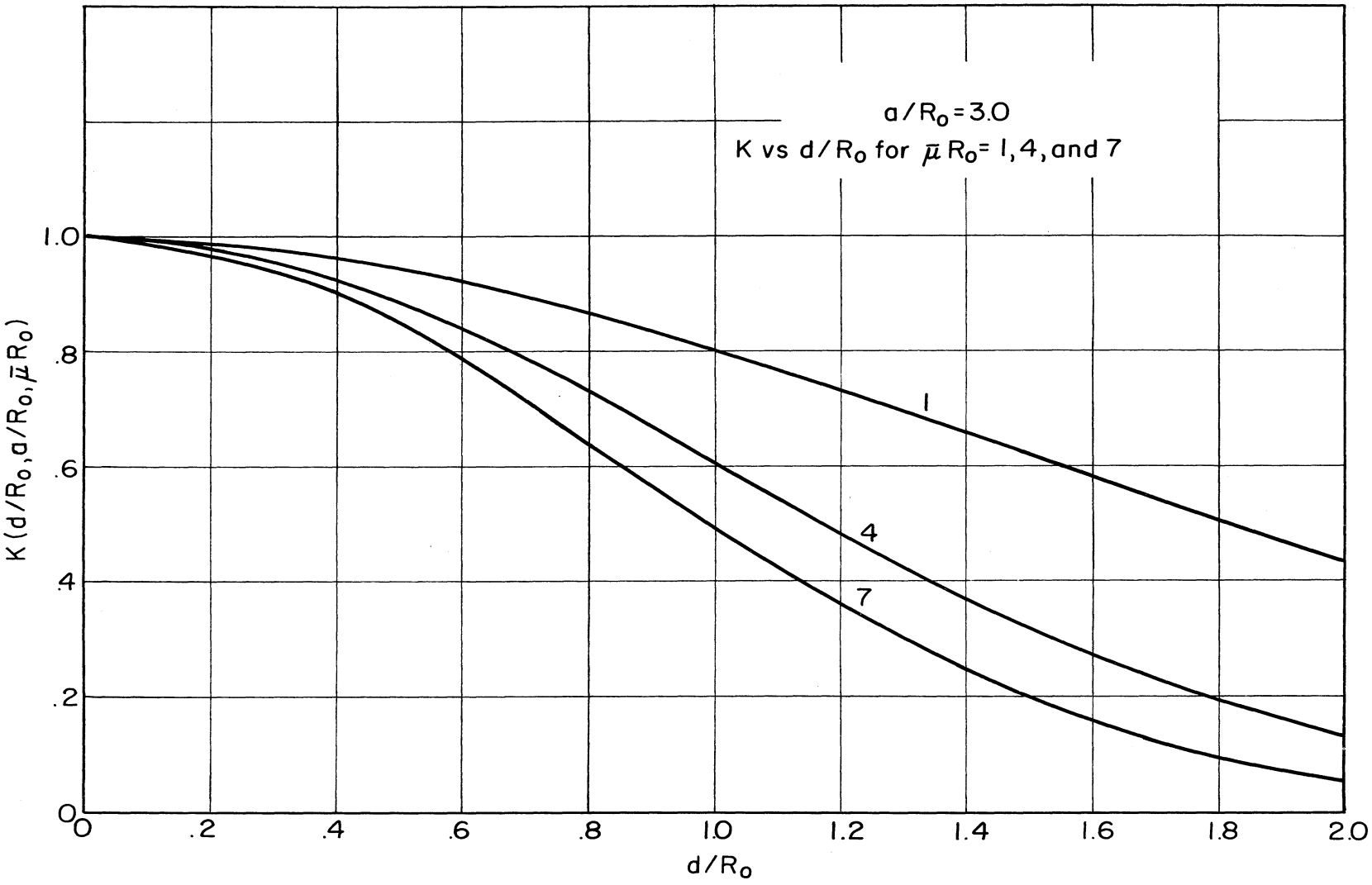

Fig. 4.25. Disk source off center line.(13)

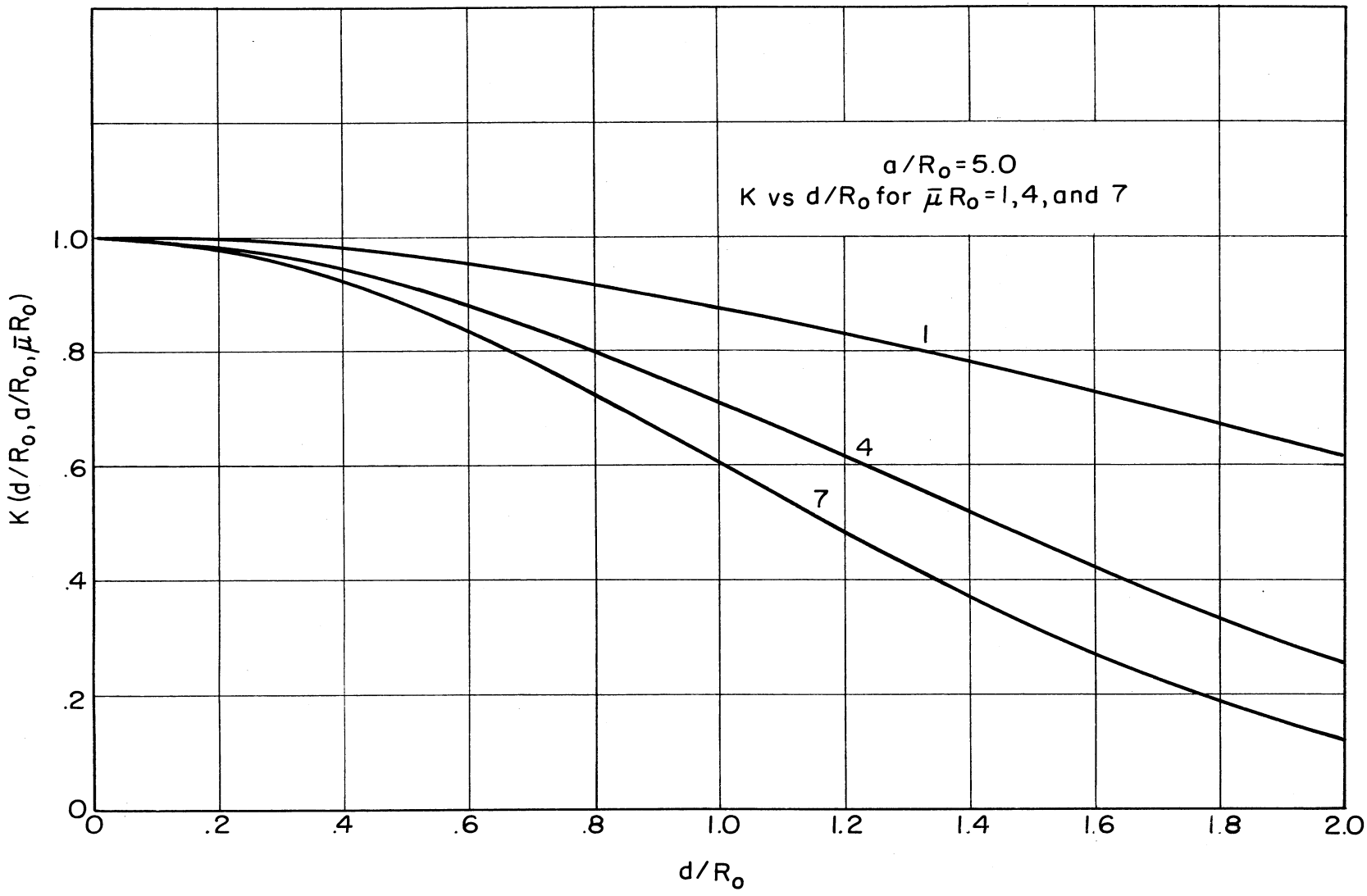

Fig. 4.26. Disk source off center line.(13)

4.15 INFINITE SLAB SOURCE [13]

(a) For exterior points.

This case may be considered by putting $\theta = \pi/2$ in the case of the disk source with $R_o = \infty$. This process gives in the notation given on page 32, when S_V is considered as a function of x and

$$S_V(x) = \sum_i S_i e^{k_i x},$$

$$\phi = \frac{B}{2\mu_s} \sum_i S_i e^{k_i b_3/\mu_s} \left[F_1(b_3, \frac{-k_i}{\mu_3}) - F_1(b_1, \frac{-k_i}{\mu_s}) \right] \qquad (4.36)$$

If the slab is infinitely thin, h = o and

$$\phi = B \cdot \frac{S_A}{2} \int_{b_1} \frac{e^{-t}}{t} dt \qquad (4.37)$$

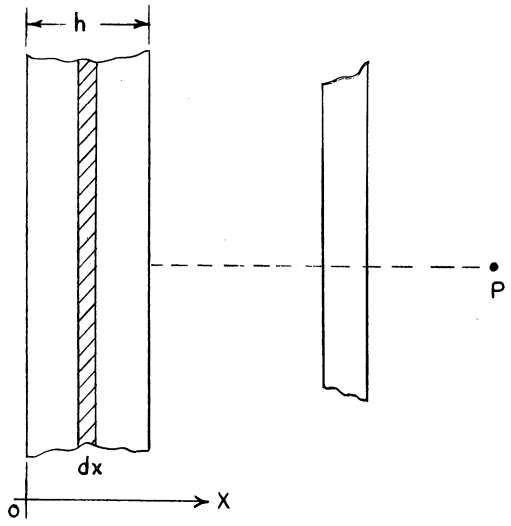

Fig. 4.27. Geometry of an infinite slab source and exterior point. [13]

(b) Interior points.

If, as before S_V is a function of x and is $S_V(x) = \sum_i S_i e^{k_i x}$ the flux is given by

$$\phi = \frac{B}{2\mu_s} \sum_i S_i e^{k_i d} \left\{ F_1(\mu_s d, \frac{-k_i}{\mu_s}) + F_1 \left[\mu_s (h-d), \frac{k_i}{\mu_s} \right] \right\} \qquad (4.38)$$

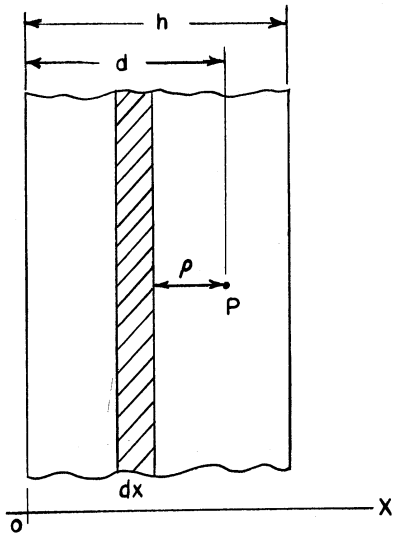

Fig. 4.28. Geometry of infinite slab source and interior point.(13)

$F_1(t,a)$ which appears in Equations 4.36 and 4.38 may be evaluated from the curves given in Figures 4.29 - 4.33.

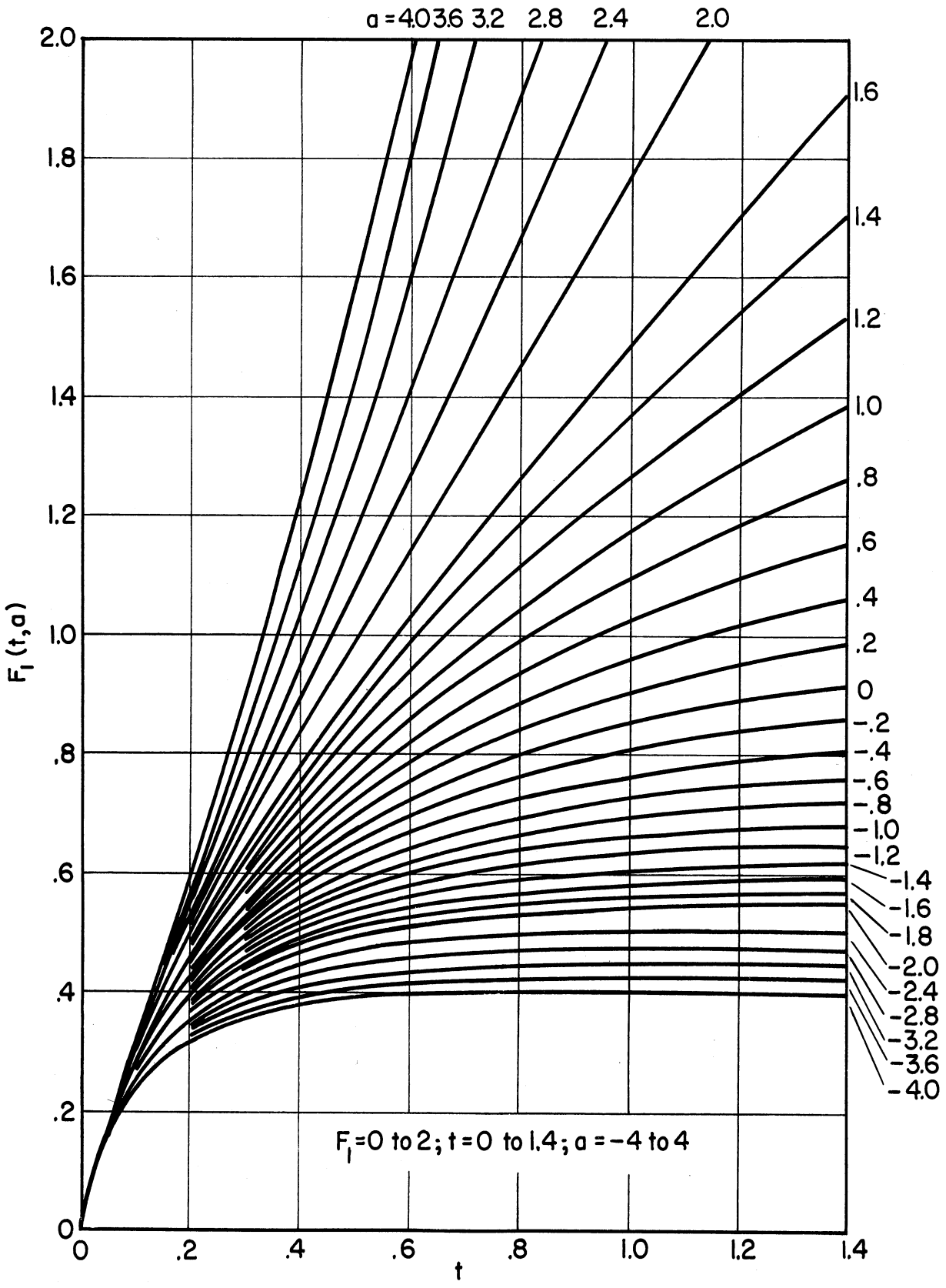

Fig. 4.29. The function $F_1(t,a)$.[13]

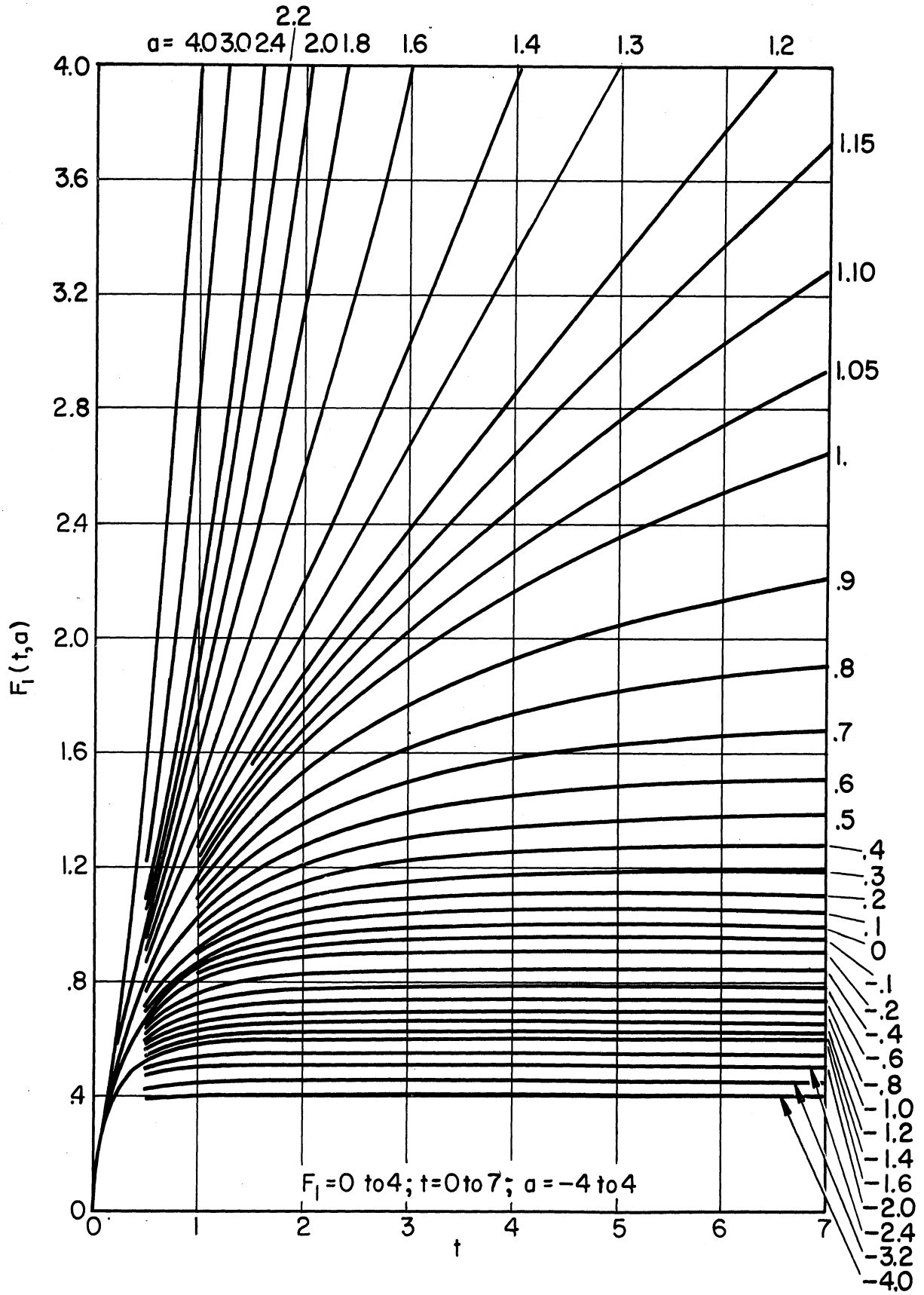

Fig. 4.30. The function $F_1(t,a)$.[13]

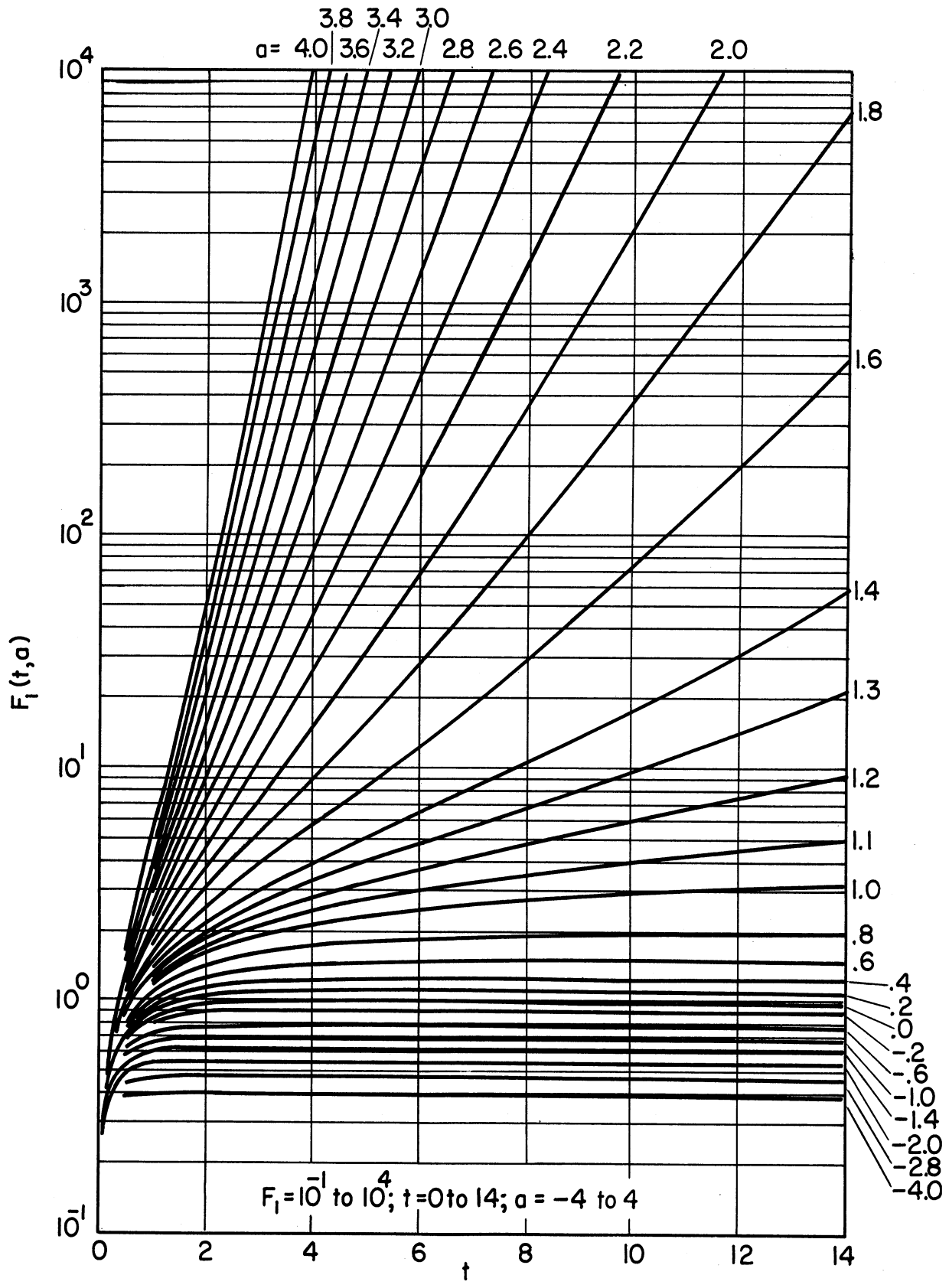

Fig. 4.31. The function $F_1(t,a)$.[13]

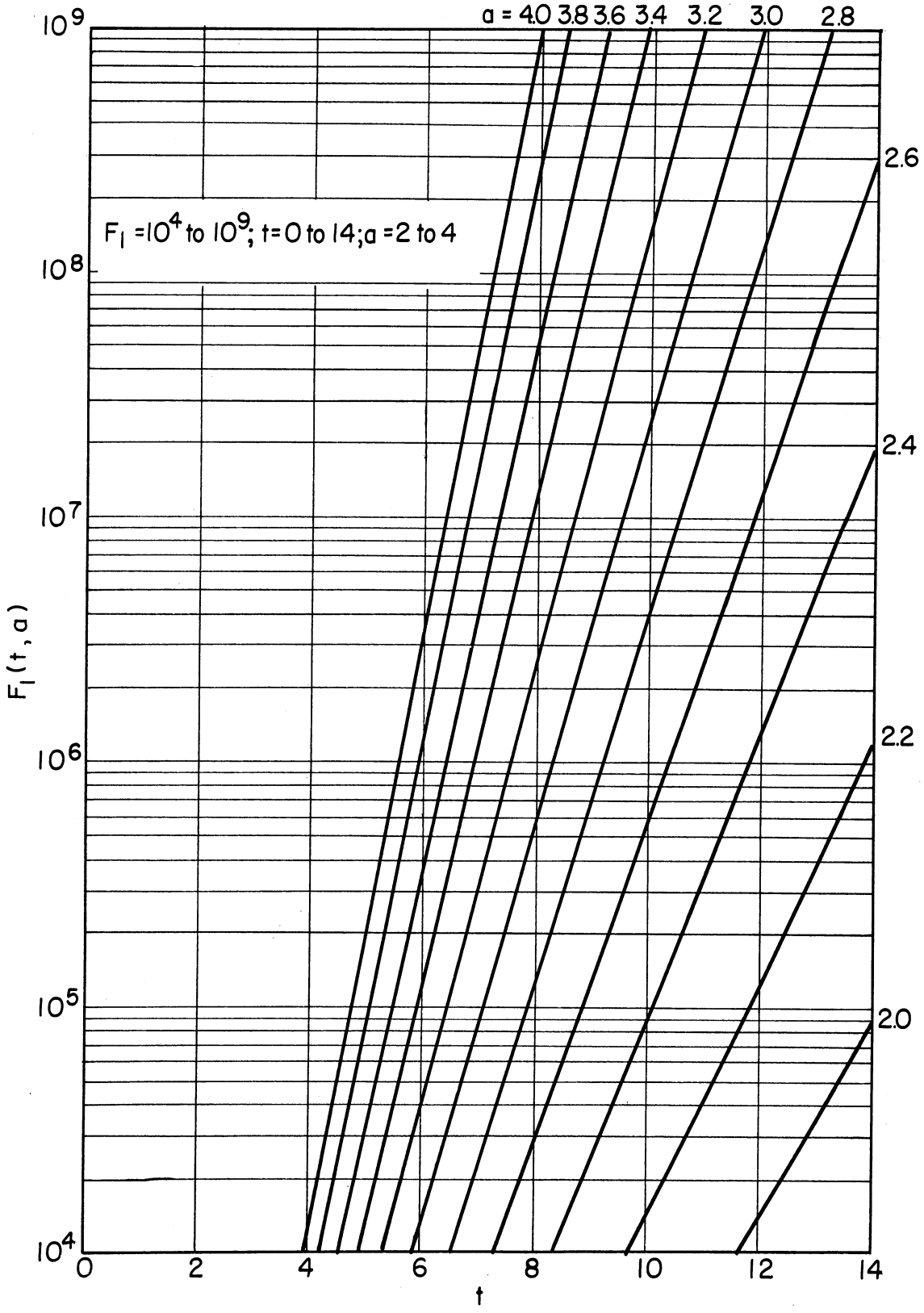

Fig. 4.32. The function $F_1(t,a)$.[13]

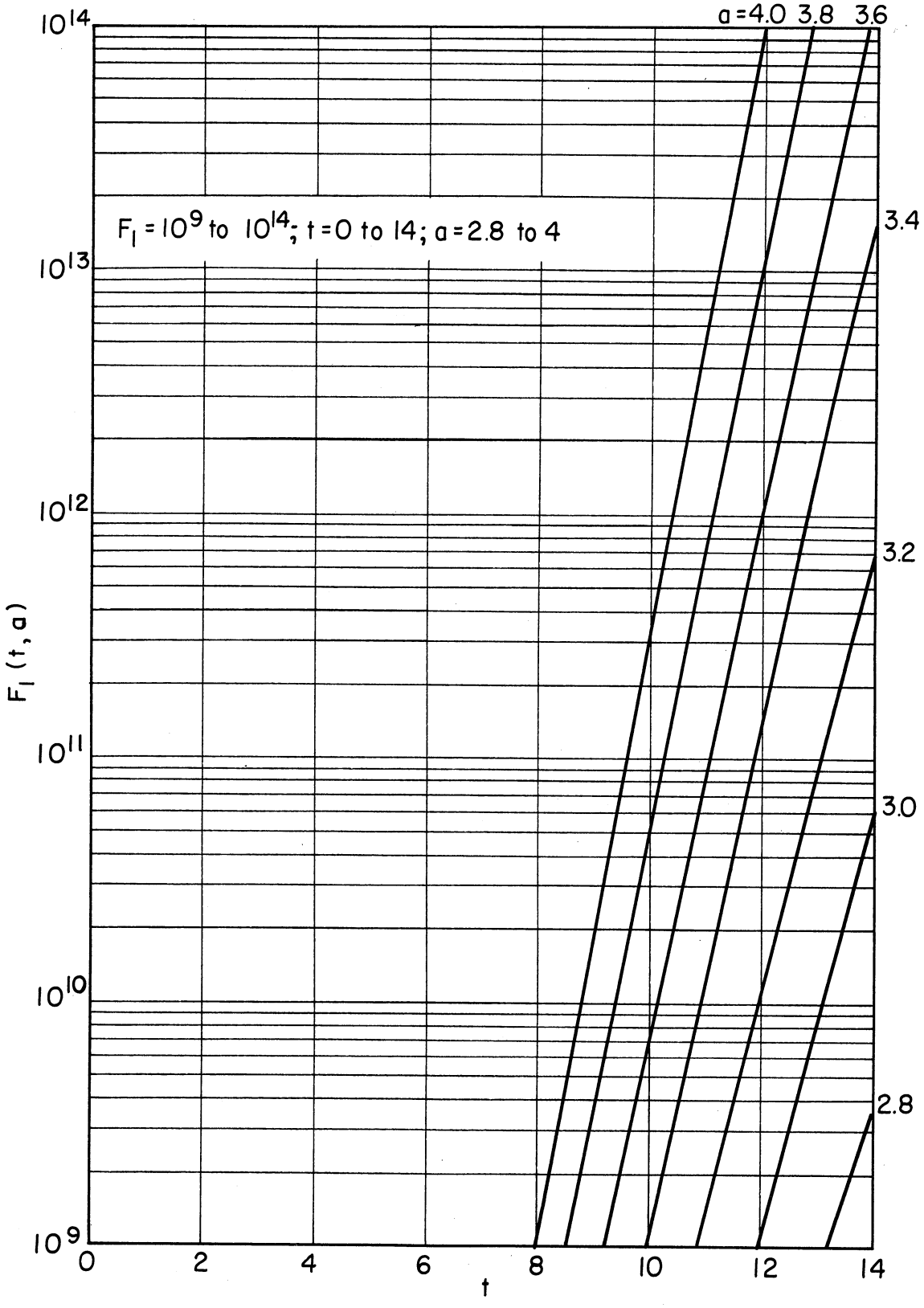

Fig. 4.33. The function $F_1(t,a)$.[13]

4.16 CYLINDRICAL SOURCE[13]

Exterior on Side ($\mu_S Z$ Curves)

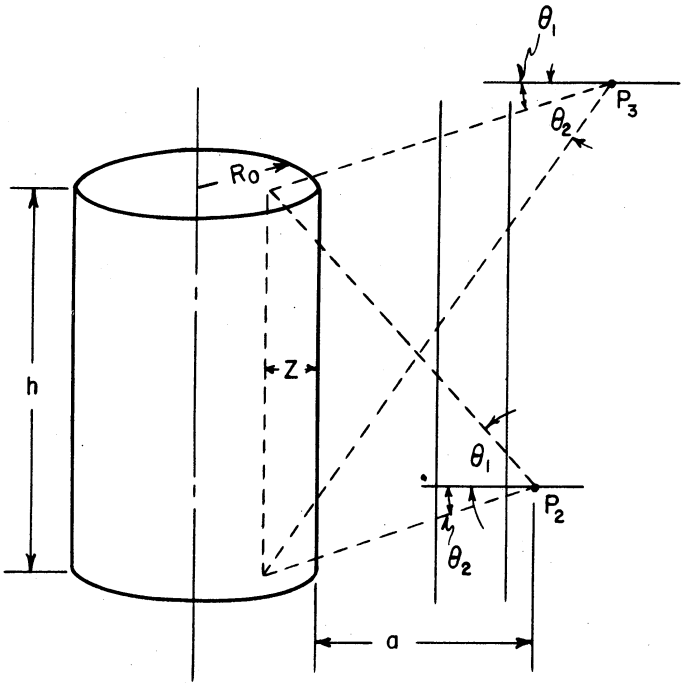

Fig. 4.34. Geometry for cylindrical source.[13]

The cylindrical source may be approximated by a line source corrected for self-absorption. At P_2, to the side of the cylinder, as shown in Fig. 4.34, the flux is given by

$$\phi = \frac{BS_V R_o^2}{4(a+z)} [F(\theta_1 b_2) + F(\theta_2, b_2)] \tag{4.39}$$

where θ_1 is different from θ_2.

At P_2, if $\theta_1 = \theta_2 = \theta$,

$$\phi = \frac{BS_V R_o^2}{2(a+z)} F(\theta, b_2) \tag{4.40}$$

If $h = \infty$, i.e., it is an infinite cylinder, then $\theta = \pi/2$.

At P_3

$$\phi = \frac{BS_V R_o^2}{4(a+z)} [F(\theta_2, b_2) - F(\theta_1, b_2)] \tag{4.41}$$

Function $F(\theta,b)$, plotted for different arguments of θ and b, is given in Figs. 4.35 - 4.40.

Figure 4.41 gives the curve for self-absorption distance Z for a cylinder with $a/R_o \geqslant 10$. Curves for the case of $a/R_o \leqslant 10$ are given in Figs. 4.42 and 4.43.

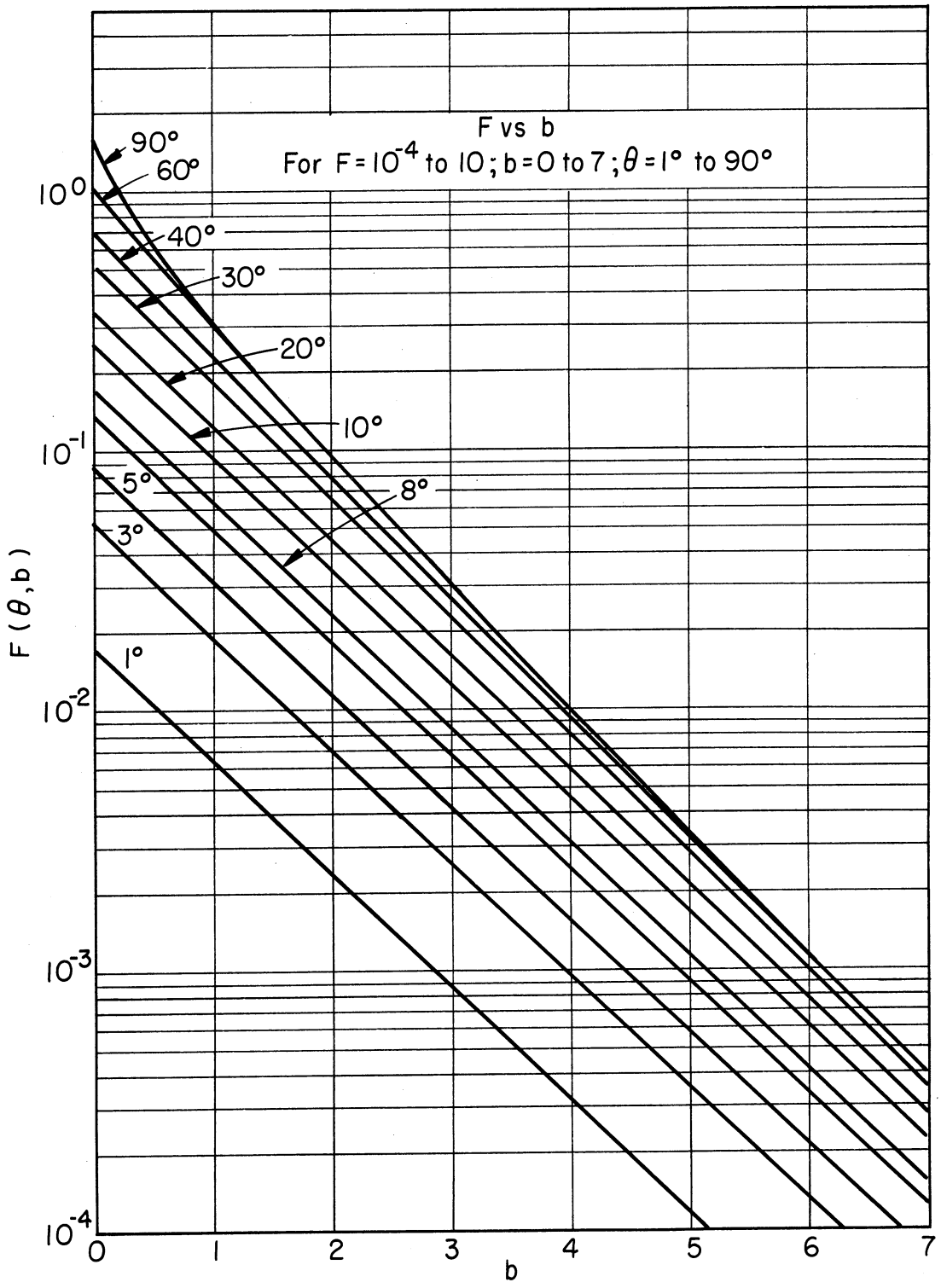

Fig. 4.35. The function F(θ,b).[13]

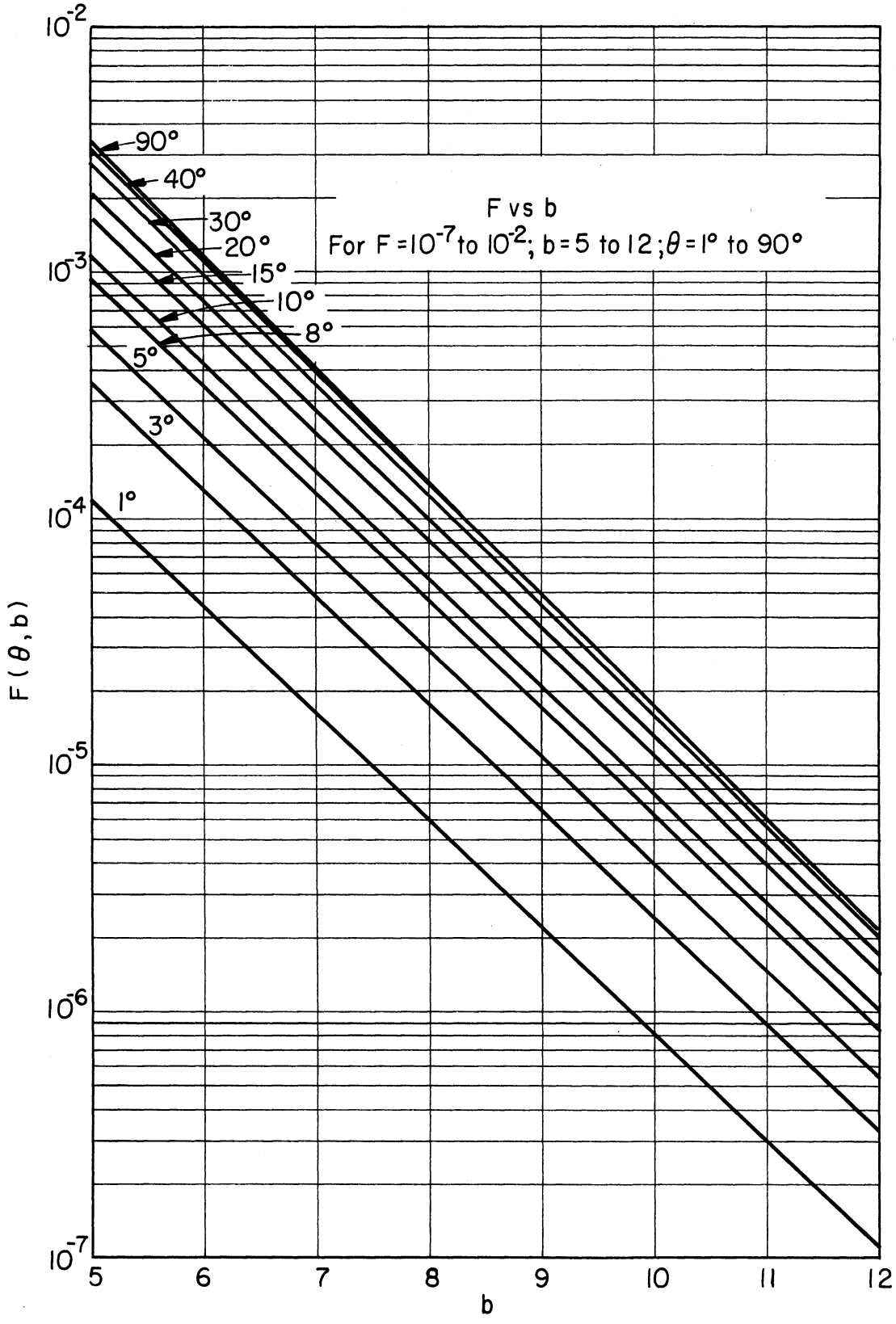

Fig. 4.36. The function F(θ,b).[13]

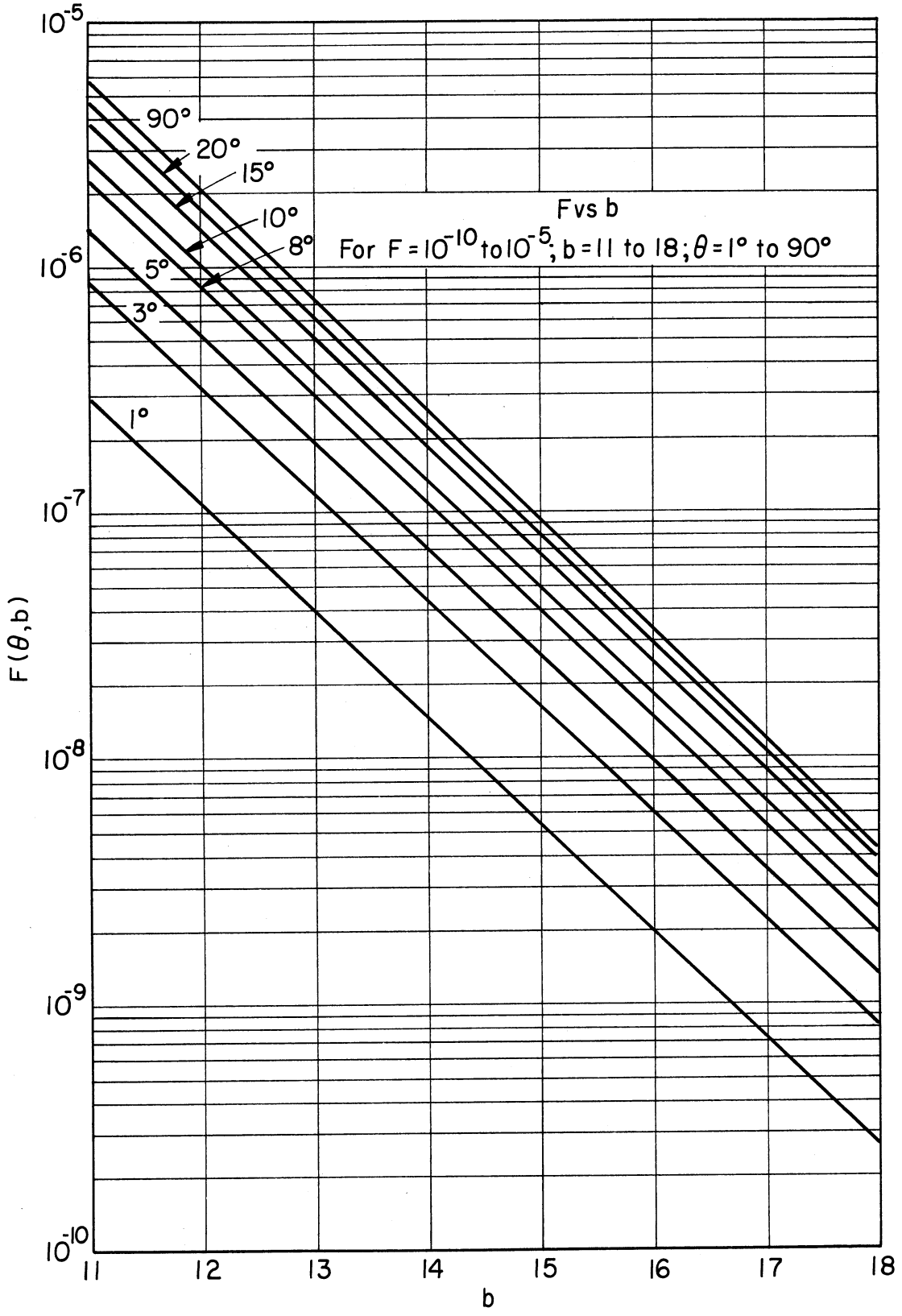

Fig. 4.37. The function F(θ,b).[13]

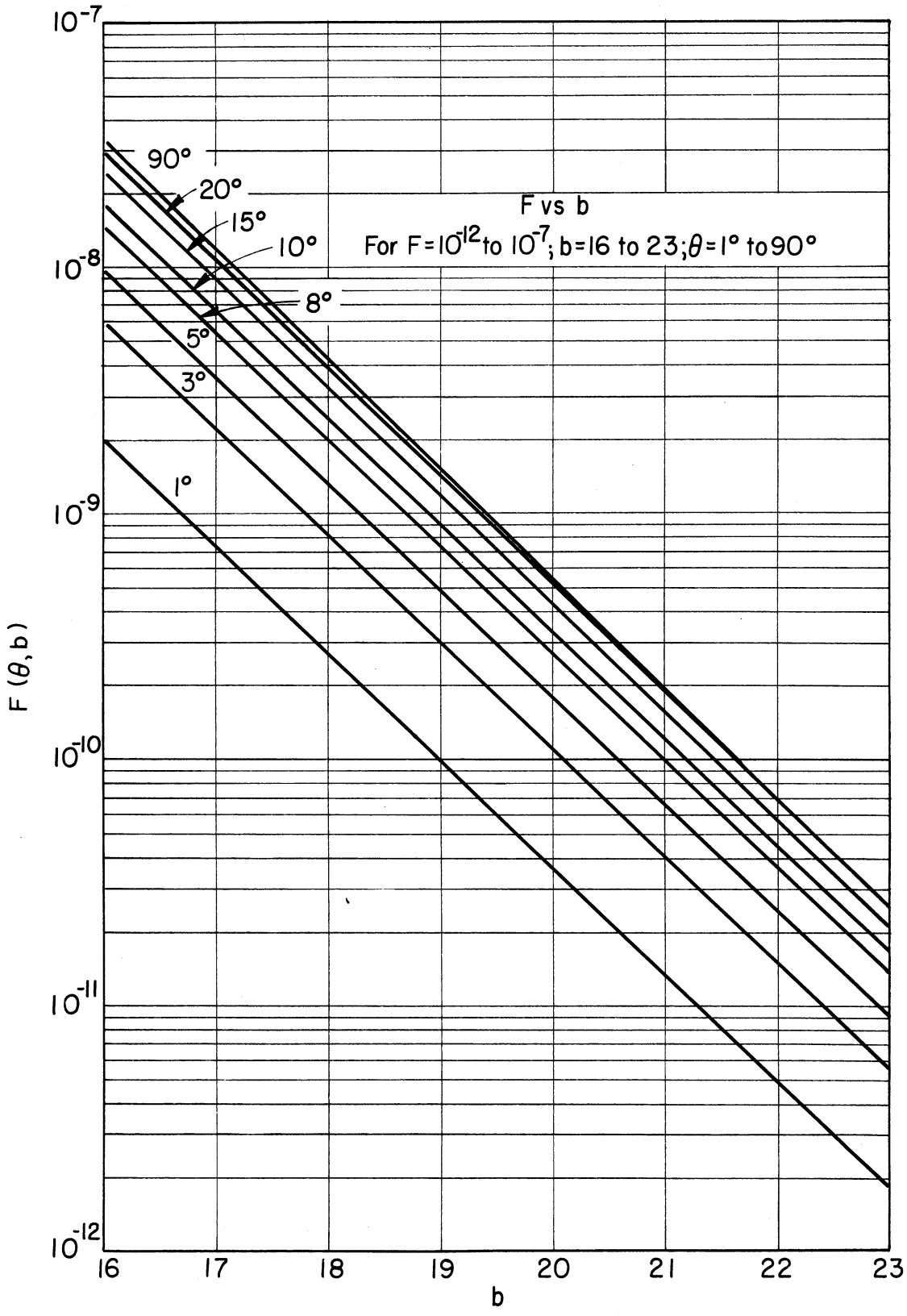

Fig. 4.38. The function F(θ,b).[13]

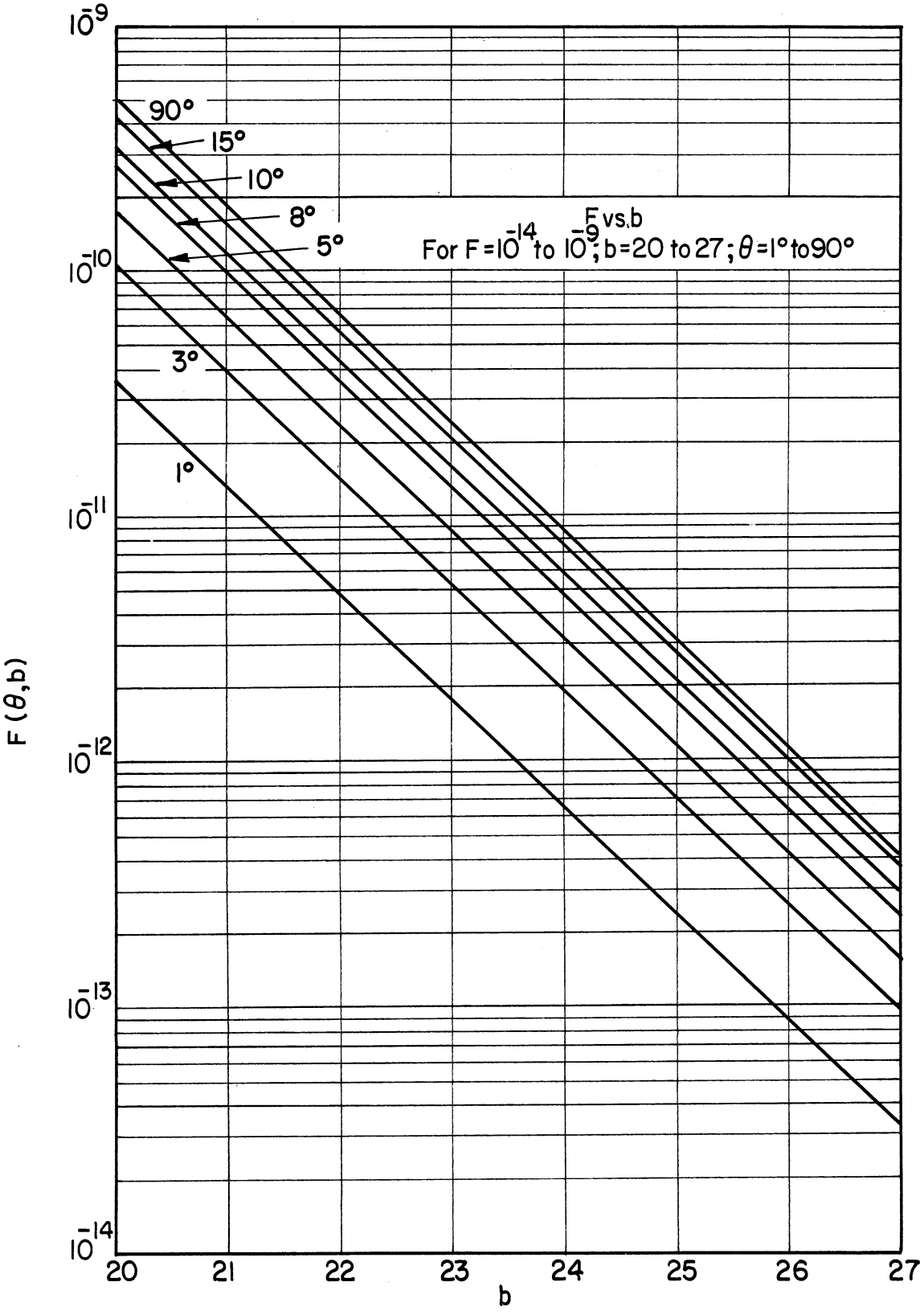

Fig. 4.39. The function F(θ,b).[13]

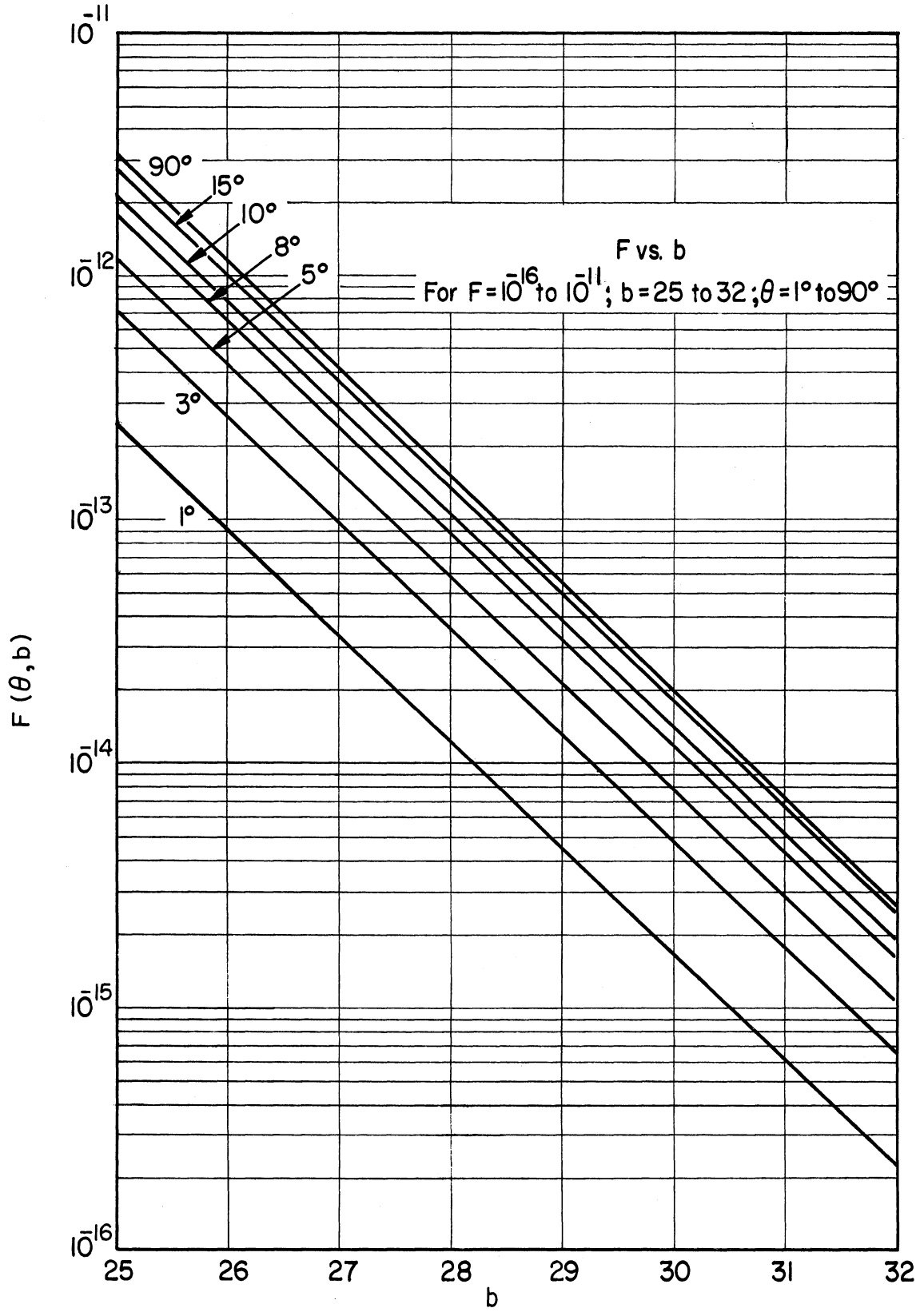

Fig. 4.40. The function F(θ,b).[13]

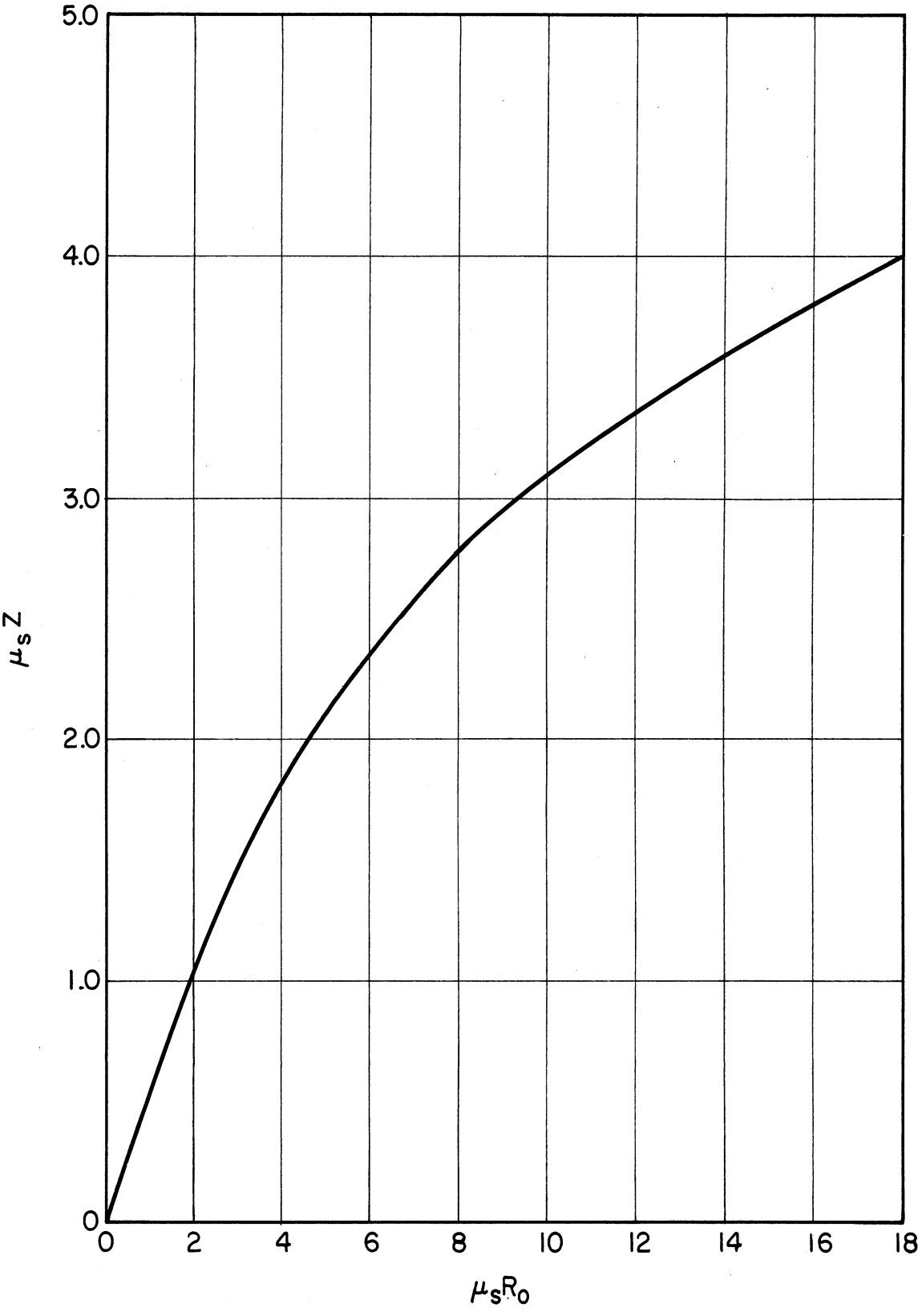

Fig. 4.41. Self-absorption distance, Z, for cylinder with $a/R_0 \geq 10$.[13]

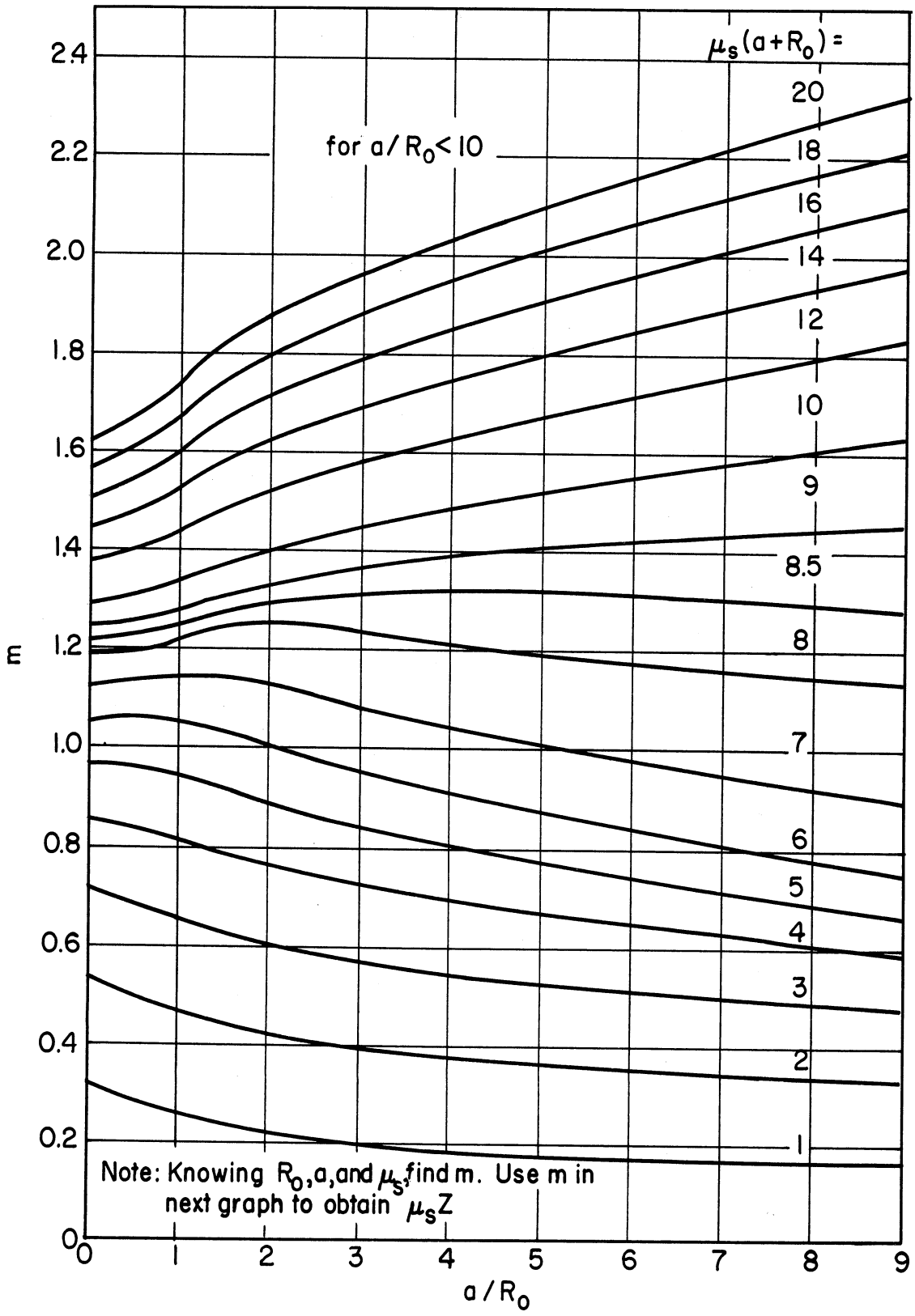

Fig. 4.42. Self-absorption distance, Z, of a cylinder as a function of cylinder diameter, R_0, for $a/R_0 \leq 10$.(13)

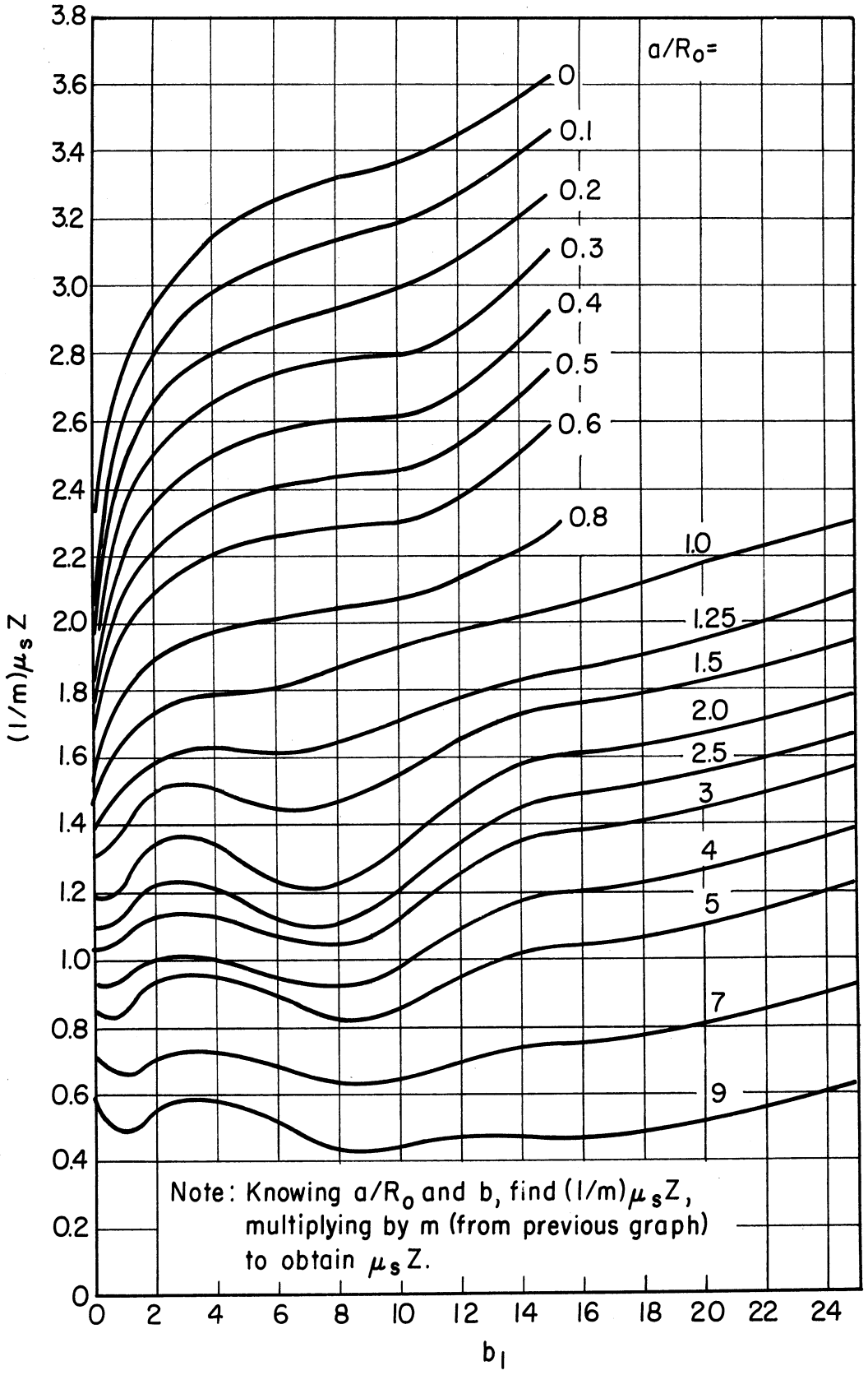

Fig 4.43. Self-absorption distance, Z, of a cylinder as a function of cylinder diameter, R_o, for $a/R_o \leq 10$.(13)

Exterior on End ($h < 3/\mu_s$): The problem can be dealt with by considering two truncated cones with half angle θ_1 and θ_2. This gives the upper and lower limits for the flux.

1. Upper limit

At P_1 in Fig. 4.44

$$\phi = \frac{BS_V}{2\mu_s}\left[E_2(b_1) - E_2(b_3) + \frac{E_2(b_3 \sec \theta_1)}{\sec \theta_1} - \frac{E_2(b_1 \sec \theta_1)}{\sec \theta_1}\right] \quad (4.42)$$

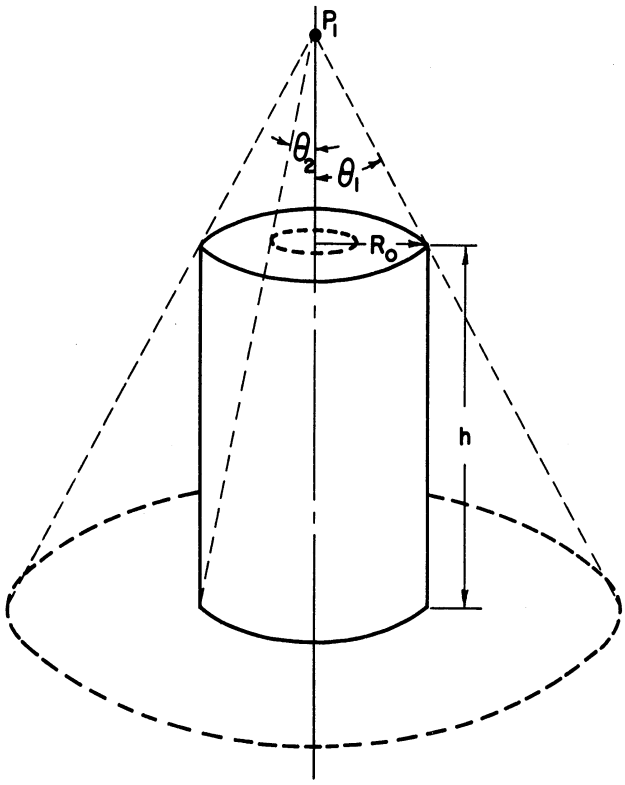

Fig. 4.44. Cylinder.

2. Lower limit

At P_1

$$\phi = \frac{BS_V}{2\mu_s}\left[E_2(b_1) - E_2(b_3) + \frac{E_2(b_3 \sec \theta_2)}{\sec \theta_2} - \frac{E_2(b_1 \sec \theta_2)}{\sec \theta_2}\right] \quad (4.43)$$

These are rather wide limits which can be reduced if $h \geqslant 3/\mu_s$. In this case the flux may be given the following limits:

1. Upper limit

At P_1

$$\phi = \frac{BS_V}{2\mu_s}\left[E_2(b_1) - \frac{E_2(b_1 \sec \theta_1)}{\sec \theta_1}\right] \tag{4.44}$$

2. Lower limit

At P_1

$$\phi = \frac{BS_V}{2\mu_s}\left[E_2(b_1) - \frac{E_2(b_1 \sec \theta_3)}{\sec \theta_3}\right] \tag{4.45}$$

where θ_3 is given by

and

$$\left.\begin{aligned} \theta_3 &= \tan^{-1}\frac{R_o}{(a+h')} \\ h' &\equiv \frac{3}{\mu_s} \end{aligned}\right\} \tag{4.46}$$

Interior (G Curves)

For this case, the results will be given briefly to avoid lengthy mathematics. If P_1 and P_2 are on axial center line, the flux at P_1 is given as

$$\phi = \frac{BS_V}{2\mu_s}\left[G(\mu_s h_1, b) + G(\mu_s h_2, b)\right] \tag{4.47}$$

where $b \equiv \mu_s R_o$.

And at P_2

$$\phi = \frac{BS_V}{2\mu_s} G(\mu_s h, b) \tag{4.48}$$

where $b \equiv \mu_s R_o$.

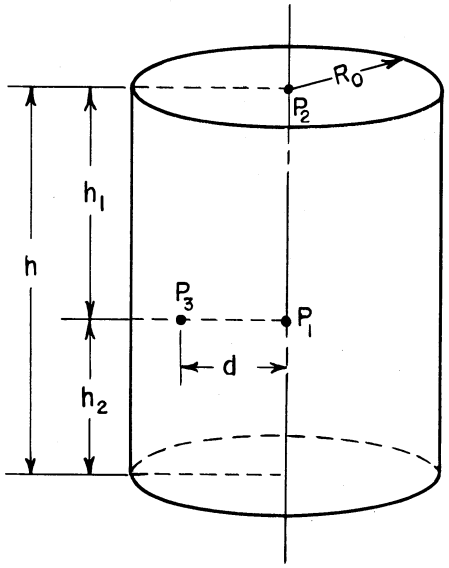

Fig. 4.45. Cylinder.(13)

At P_3, only the limits can again be stated, and the upper limit of the flux is:

$$\phi = \frac{BS_V}{4\mu_s} [G(\mu_s h_1, b_5) + G(\mu_s h_2, b_5) + G(\mu_s h_1, b_6) + G(\mu_s h_2, b_6)] \quad (4.49)$$

At P_3, the lower limit is

$$\phi = \frac{BS_V}{4\mu_s} [G(\mu_s h_1, b_6) + G(\mu_s h_2, b_6) + G(\mu_s h_1, b_4) + G(\mu_s h_2, b_4)] \quad (4.50)$$

where $b_4 \equiv \mu_s(R_o - d)$, $b_5 \equiv \mu_s(R_o + d)$, and $b_6 \equiv \mu_s \sqrt{R_o^2 - d^2}$

Function $G(\mu_s h, b)$ for different values of the argument $\mu_s h$ may be obtained by referring to Figs. 4.46 and 4.47.

4.17 SPHERICAL SOURCE(13)

(a) Interior points.

The mathematics is again complicated for this case and only the results are quoted. The flux at P_1 is given by

$$\phi = \frac{BS_V}{\mu_s} (1 - e^{-\mu_s R_o}) \quad (4.51)$$

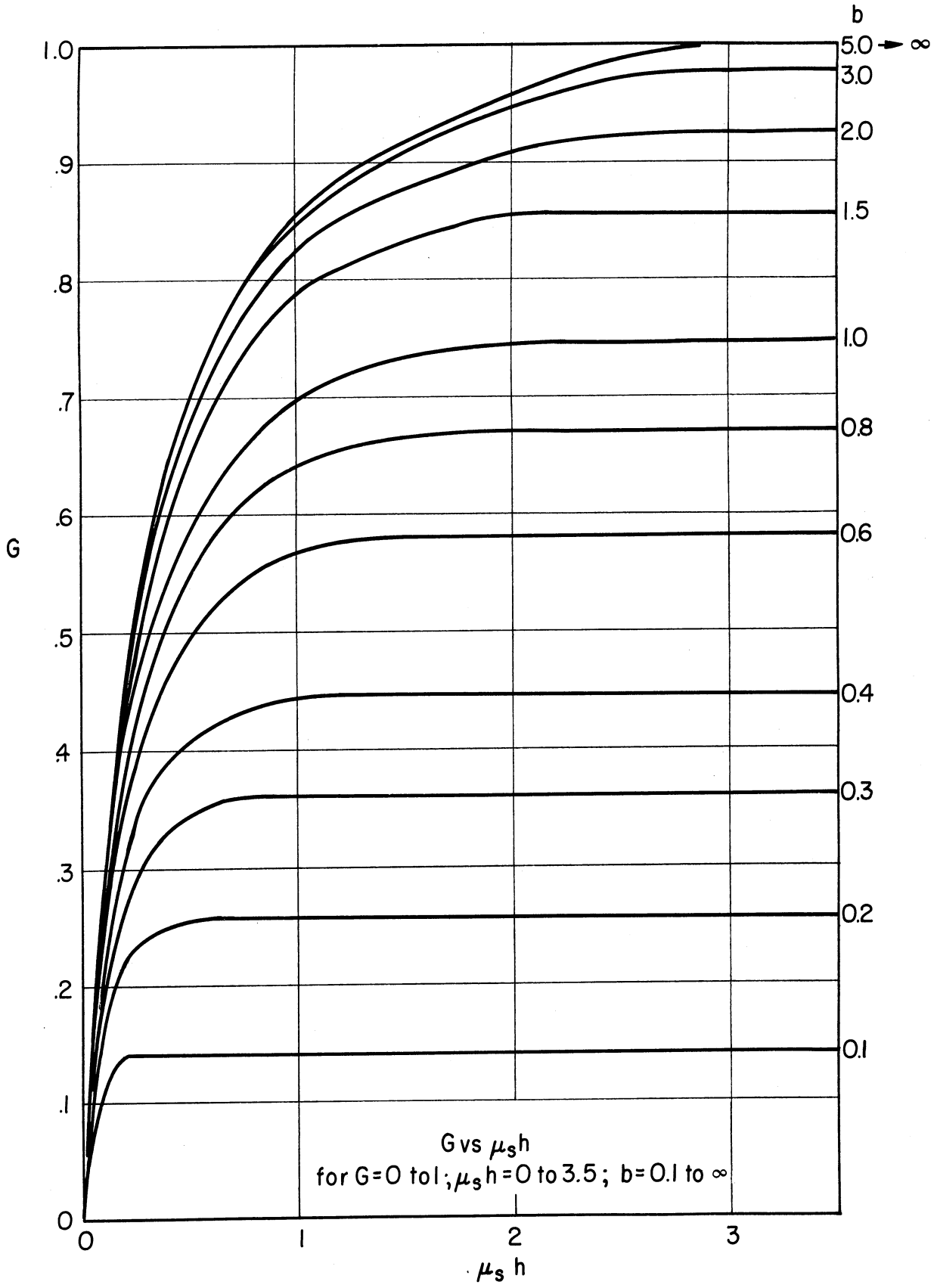

Fig. 4.46. The function $G(\mu_s hb)$.[13]

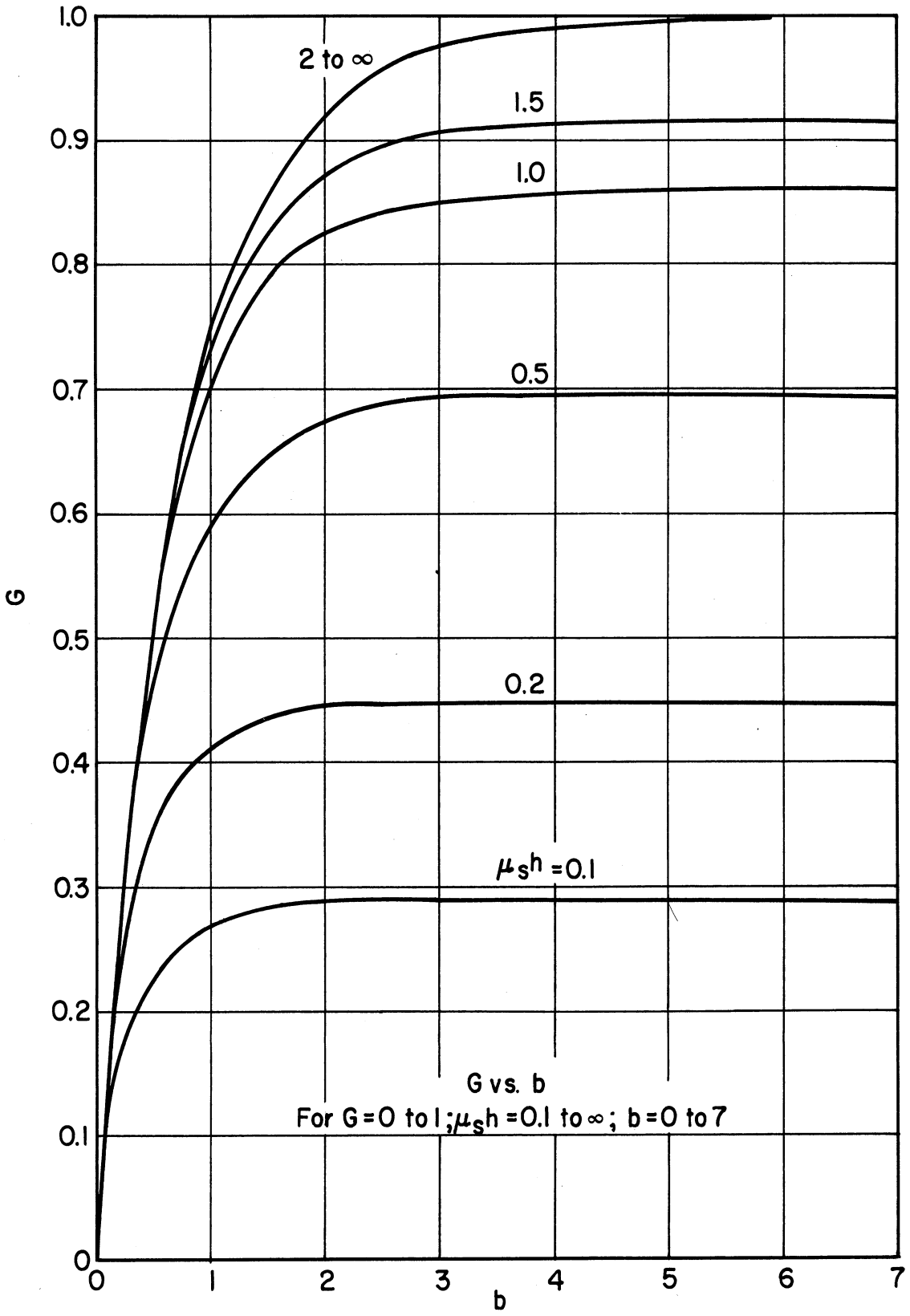

Fig. 4.47. The function $G(\mu_s hb)$.[13]

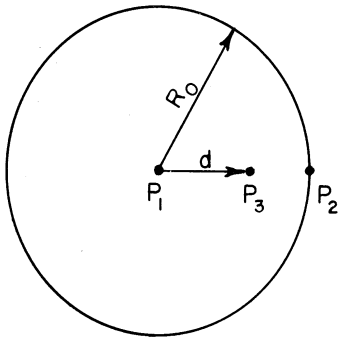

Fig. 4.48. Sphere. (13)

And at P_2,

$$\phi = \frac{BS_V}{2\mu_s}\left(1 - \frac{1}{2\mu_s R_o} + \frac{e^{-2\mu_s R_o}}{2\mu_s R_o}\right) \qquad (4.52)$$

At P_3

$$\phi = \frac{BS_V}{\mu_s}\left\langle 1 - \frac{e^{-b_4}}{2} - \frac{e^{-b_5}}{2} - \frac{1}{4\mu_s d}\left[e^{-b_4}(1+b_4) - e^{-b_5}(1+b_5)\right] + \frac{b_4 b_5}{4\mu_s d}\left[E_1(b_4) - E_1(b_5)\right]\right. \qquad (4.53)$$

where $b_4 \equiv \mu_s(R_o - d)$ and $b_5 \equiv \mu_s(R_o + d)$.

(b) Exterior points (Z curves).

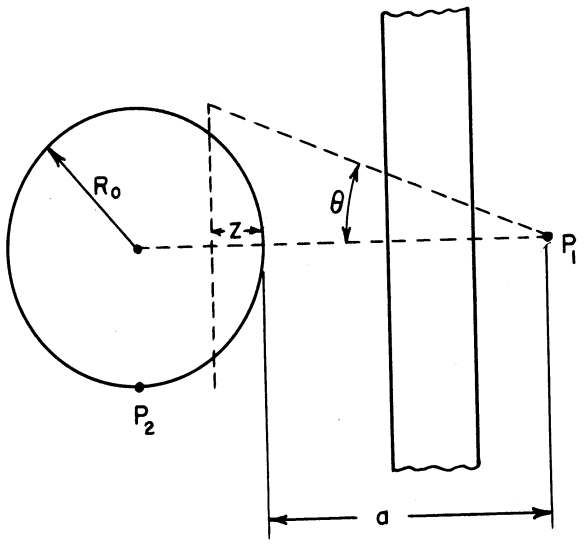

Fig. 4.49. Geometry of spherical source.(13)

At P_1

$$\phi = 2/3\ BS_V R_o [E_1(b_2) - E_1(b_2 \sec \theta)] \tag{4.54}$$

At P_2, if $b_1 = 0$,

$$\phi = \frac{BS_V}{2\mu_s}\left(1 - \frac{1}{2\mu_s R_o} + \frac{e^{-2\mu_s R_o}}{2\mu_s R_o}\right) \tag{4.55}$$

Figures 4.50 and 4.51 show curves for the self-absorption distance Z for sphere with $a/R_o \geqslant 1$ and for $a/R_o \leqslant 1$, respectively.(13)

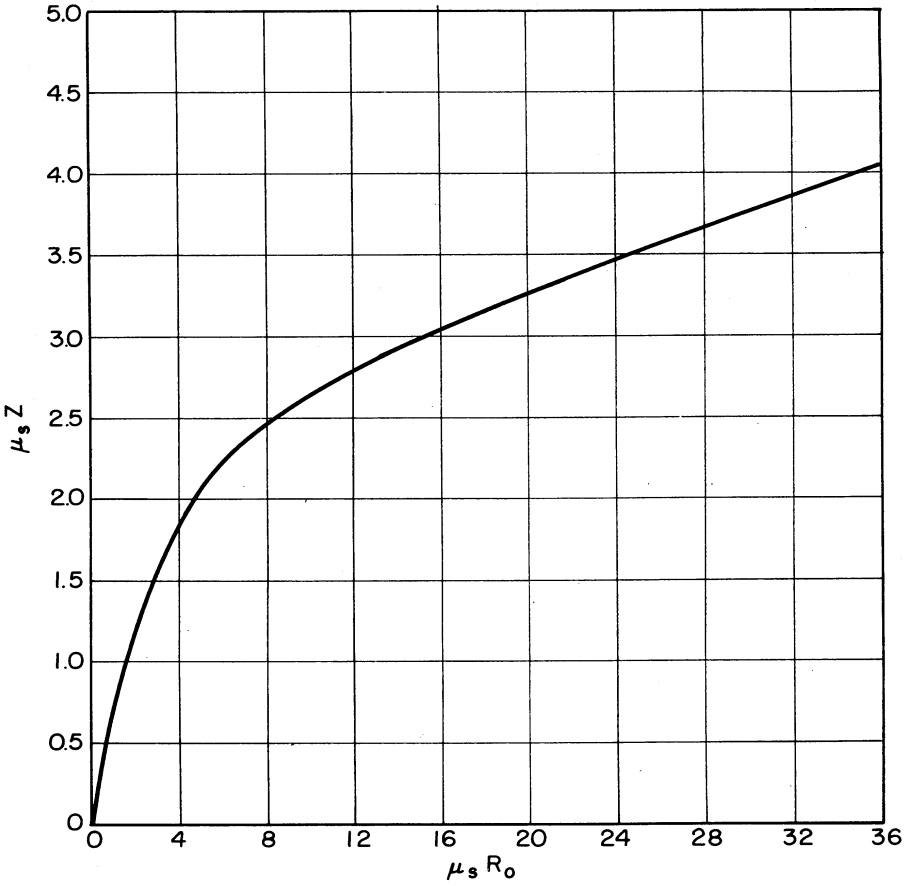

Fig. 4.50. Self-absorption distance Z for sphere with $a/R_o = 1$. (13)

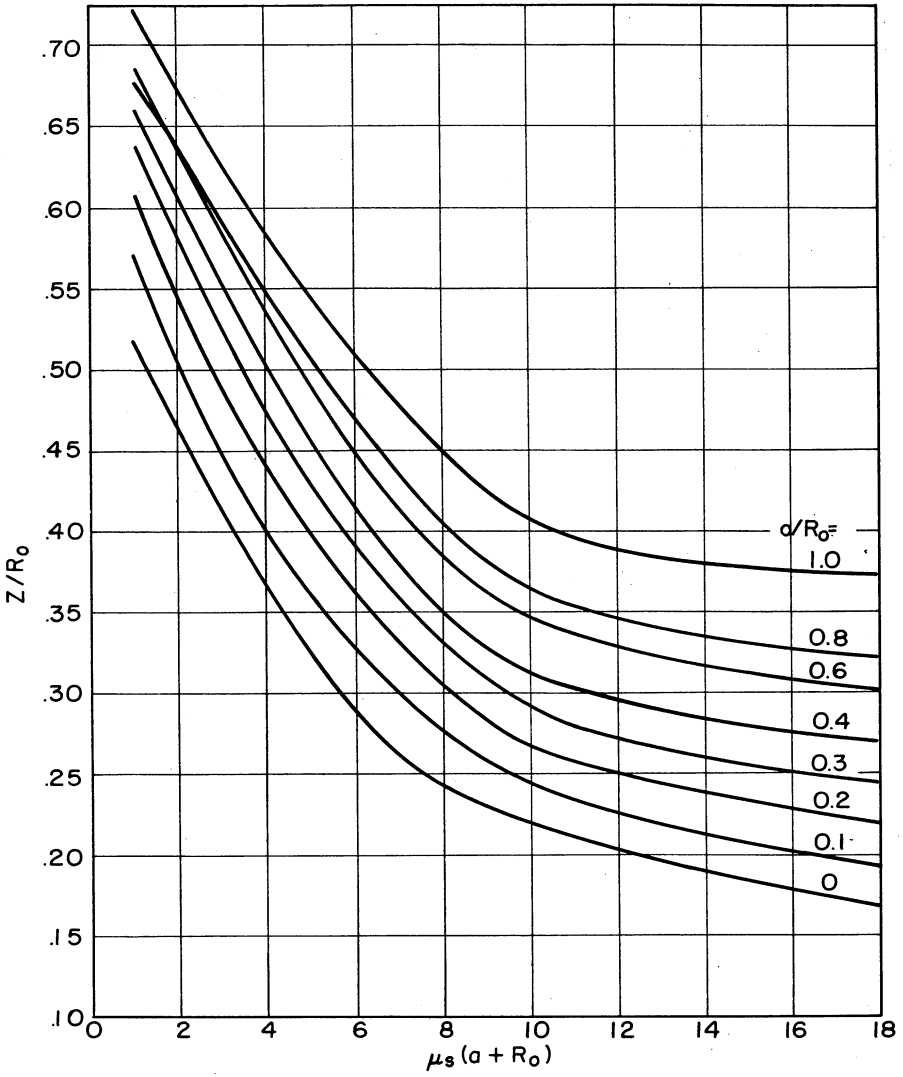

Fig. 4.51. Ratio of self-absorption distance to radius of sphere, Z/R_o, for $a/R_o = 1$. (13)

4.18 TYPES OF GAMMA RADIATION SOURCES

Large-scale operation of research and power reactors will make available gamma-radiation sources of strengths varying from millicuries to megacuries. The majority of these isotopes emit one, two, or three gamma rays with well-defined energies and the calculation of shielding for such sources is consequently easier than for complex-spectrum sources. However, the gross fission-product waste produced by an operating reactor has an extremely complex spectrum and yield. In the class of well defined gamma energies, cobalt-60 and caesium-37 sources merit consideration while the fission gases and spent fuel elements are examples of complex-spectrum sources. The whole spectrum may be divided into a set of discrete energy groups whose source strengths have been estimated. The problem is, therefore, reduced to the determination of the total intensity due to the discrete set. Typical of these complex spectrum sources is a spent MTR fuel element.

4.19 MTR FUEL ELEMENTS

Spent MTR-type fuel elements may be made available in large quantity as sources of gamma radiation for industry. Transportation and installation of these sources require detail shielding considerations. The MTR fuel element may be considered to emit seven groups of gamma rays of energies 0.35, 0.5, 0.7, 0.9, 1.25, 1.75, and 2.5 Mev. Extensive theoretical and experimental studies of the gamma-decay dose rate and heating from the spent MTR fuel elements of different histories had been reported by Francis and Marsden.(14) Figure 4.52 shows a sketch of an MTR fuel element as described in the above report.

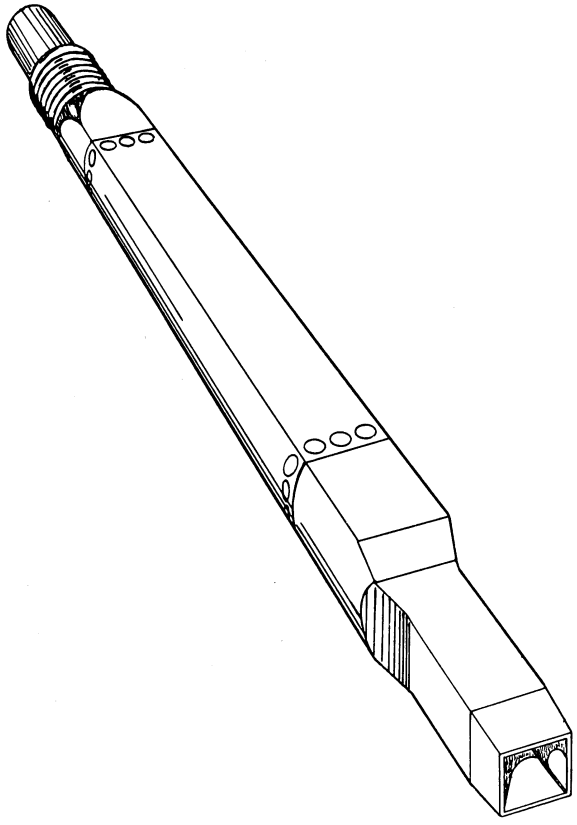

Fig. 4.52. Sketch of MTR type fuel element.(15)

4.20 EXAMPLE OF GAMMA SHIELDING CALCULATION FOR MTR FUEL ELEMENT[16]

The calculation of the radiation field and the minimum shield thickness required to reduce the dose rate to the desired tolerance level can be carried out in the following steps.

1. Type of Radiation Source.—An MTR fuel element is used in a 30-megawatt reactor for 17 days and the spent element is then cooled for 30 days. The source is surrounded by 2 inches of water.

2. Nature of Nuclear Radiations.—Gamma radiation.

3. Sources and Energy Spectrum.—Q_V is the source strength in photons/sec at equilibrium and E is the energy of the different energy groups of gamma radiation, tabulated for one fission/sec (see Table 4.7).

To obtain the total energy per sec (Mev/sec), S should be multiplied by the total number of fissions/sec, obtained from the irradiation history.

4. Type of Shield.—For transporting a fuel element, the shield used should be as light and compact and preferably as economical as possible. From

TABLE 4.7

ENERGY SPECTRUM FOR MTR FUEL ELEMENT[14]

No.	Energy-$\bar{E}$ (Mev)	Source Strength-Q_V (photons/sec)	$Q_V E = S$ (Mev/sec)
1	2.5	2.6×10^{-4}	6.5×10^{-4}
2	1.75	5.99×10^{-3}	1.05×10^{-2}
3	1.25	2.6×10^{-5}	3.25×10^{-5}
4	0.9	2.72×10^{-3}	2.45×10^{-3}
5	0.7	7.9×10^{-3}	5.53×10^{-3}
6	0.5	5.98×10^{-3}	2.99×10^{-3}
7	0.35	8.5×10^{-3}	2.98×10^{-3}

the point of view of compactness, lead is to be preferred. In addition to the lead, the two inches of cooling water and two inches of structural steel may also be considered to be attenuating the gamma radiation. In addition to these external attenuation media, self-absorption due to the source itself may be considered.

5. Attenuation Processes.—Gamma-radiation intensity is affected by spatial attenuation, exponential attenuation, and the build-up factor due to scattering. Since the heavier material (lead) follows the lighter materials (water and steel), the build-up factor for lead is used. For steel and water then, only exponential attenuation is considered.

6. Nuclear Constants.—The linear absorption coefficients (μ cm^{-1}) for energy groups for water, source material, steel, and lead and the energy-absorption coefficient (μ-σ_s/ρ)(cm^2/gm) for tissue are given in Table 4.8)

TABLE 4.8

ABSORPTION COEFFICIENTS FOR VARIOUS ENERGY GROUPS OF MTR ELEMENT[14]

No.		$\bar{E}$ = (2.5 Mev)	(1.75)	(1.25)	(0.9)	(0.7)	(0.5)	(0.35)
1	μ_{H_2O}	0.044	0.054	0.064	0.075	0.085	0.098	0.113
2	μ_{source}	0.067	0.083	0.097	0.112	0.125	0.146	0.169
3	μ_{steel}	0.290	0.328	0.399	0.485	0.540	0.635	0.767
4	μ_{lead}	0.485	0.54	0.66	0.86	1.1	1.65	3.08
5	$(\mu-\sigma_s/\rho)_{tissue}$	0.0225	0.0255	0.028	0.0305	0.0315	0.032	0.032
6	Z, self-absorption distance, cm	2.69	2.69	2.68	2.59	2.56	2.47	2.43

Besides these nuclear constants, the dose build-up factor coefficients for lead are given in Table 4.9 for these energies for a point source in an infinite homogeneous medium.

TABLE 4.9

DOSE BUILD-UP FACTOR COEFFICIENTS[12,13]

No.		$\bar{E}$ = (2.5 Mev)	(1.75)	(1.25)	(0.9)	(0.7)	(0.5)	(0.35)
1	A_1	2.3	2.75	2.6	2.5	2.3	2.2	2.1
2	A_2	-1.3	-1.75	-1.6	-1.5	-1.3	-1.2	-1.2
3	α_1	-0.65	-0.05	-0.04	-0.03	-0.02	-0.015	-0.01
4	α_2	0.125	0.135	0.14	0.14	0.14	0.14	0.14

7. Source Geometry.—For the purpose of calculation, the MTR fuel element may be considered as a cylinder of 2 ft effective length and 3 inch diameter. Intensity at any point can be determined by referring to Equation 4.39. However, for the purpose of illustration, the intensity at an exterior point P on the midplane perpendicular to the source as indicated in Fig. 4.53, is discussed, where

h = height of cylinder = 61 cm,
R_o = radius of cylinder = 3.81 cm,
r = distance between the surface of source and the field point P,
= (5.08 cm of water + 5.08 cm of steel + t cm of lead + t' cm of air),
Z = effective self-absorption distance (it depends on geometry of the source and the energy of the radiation), and

$$\theta = \tan^{-1} \frac{h}{2(r+Z)} .$$

8. Total Intensity, (I).—The total intensity is the sum of the intensities contributed by the seven energy groups at the point P.

$$I = \sum_{k=1}^{7} I_k \text{ (r/hr} \tag{4.56}$$

where I_k = intensity for k-th group.

9. Intensity for k-th Group, I_k.—Intensity I_k for k-th gamma-ray group is the product of I_{ok} = intensity at P due to spatial attenuation, B_k = build-up factor, and $F_k(\theta,b)$ = exponential attenuation.

$$I_k = I_{ok} \cdot B_k \cdot F_k(\theta,b) \text{ r/hr} \tag{4.57}$$

As stated earlier, the build-up factor B_k, if expressed as the sum of two exponentials, as shown in Equation 4.58 can be incorporated in the exponential attenuation factor

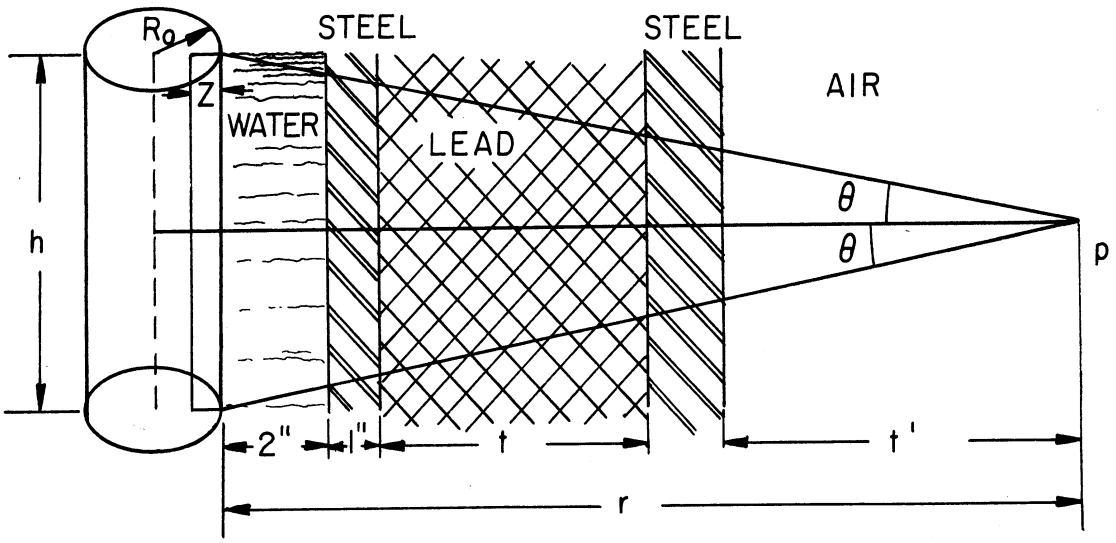

Fig. 4.53. Geometry for example calculation.

$F_k(\theta,b)$, i.e.,

$$B_k = A_1 e^{-\alpha_1 \mu t} + A_2 e^{-\alpha_2 \mu t} \tag{4.58}$$

The product of B_k and $F_k(\theta,b)$ can then be replaced by $G_k(\theta,b)$ i.e.,

$$G_k(\theta,b) = B_k, F_k(\theta,b) \tag{4.59a}$$

$$\therefore \quad I_k = I_{ok} \cdot G_k(\theta,b) \text{ r/hr} \tag{4.59b}$$

a. Determination of G_k.

$$G_k = \sum_{n=1}^{n} A_n \int_o^{\theta} e^{-b_n \sec \theta'} \, d\theta'$$

As pointed out by Taylor,[12] the use of only two exponential terms in the build-up factor is sufficient for most calculations. This simplifies the above expression (if build-up is considered significant only in the lead) to:

$$G_k = \left\{ A_1 \int_o^{\theta} e^{[\mu_s Z + 5.08\, \mu_{H_2O} + 5.08\, \mu_{Fe} + (1+\alpha_1)\, \mu_{Pb}\, t] \sec \theta'} \cdot d\theta' + A_2 \int_o^{\theta} e^{-[\mu_s Z + 5.08\, \mu_{H_2O} + 5.08\, \mu_{Fe} + (1+\alpha_2)\, \mu_{Pb}\, t] \cdot \sec \theta} d\theta' \right\} \tag{4.60}$$

All the quantities in Equation 4.60 for G_k are known. Therefore, G_k can be calculated by referring to Figs. 4.54, 4.55, and 4.56 for the evaluation of the above integral $F(\theta,b_2)$.

b. Determination of I_{ok}.

$$I_{ok} = (\phi_{ok})(\lambda_k)\, P \text{ r/hr} . \tag{4.61}$$

To determine I_{ok}, the factors ϕ_{ok}, λ_k, and P must be evaluated individually.

(1) ϕ_{ok} (Energy Flux)

$$\phi_{ok} = \text{energy flux (Mev/cm}^2 \cdot \text{sec)}$$

According to Equation 4.40

$$\phi_{ok} = \left\{\frac{S_v R_o^2}{2(r+Z)}\right\}_k \left\{\frac{\text{Mev}}{\text{cm}^2 \cdot \text{sec}}\right\}$$

where S_v = source strength (Mev/cm^3·sec)

or S_v = S/volume = $Q_v E/\pi R_o^2 h$

Converting the units of time from seconds to hours,

$$\phi_{ok} = \left\{\frac{S}{2\pi h(r+Z)}\right\}_k (3.6 \times 10^3) \left(\frac{\text{Mev}}{\text{cm}^2 \cdot \text{hr}}\right) . \qquad (4.62)$$

ϕ_{ok} can be evaluated since for the different energy groups S and Z are known.

(2) λ_k (Conversion Factor)

λ_k = conversion factor to obtain dose rate in r/hr.

$$\lambda_k = \left\{\frac{\text{gm of air}}{83 \text{ ergs}}\right\} \left\{\frac{1.6 \times 10^{-6} \text{ ergs}}{\text{Mev}}\right\} (r) \left\{\frac{\mu-\sigma_s}{\rho}\right\}_{k(\text{tissue})} \left\{\frac{\text{cm}^2}{\text{gm}}\right\} .$$

$$\lambda_k = \left\{\frac{\mu-\sigma_s}{\rho}\right\}_{k(\text{tissue})} (1.93 \times 10^{-4}) (r) (\text{cm}^2/\text{Mev}). \qquad (4.63)$$

This is based on the fact that one roentgen is equivalent to the absorption of 83 ergs of gamma radiation by one gram of standard air.

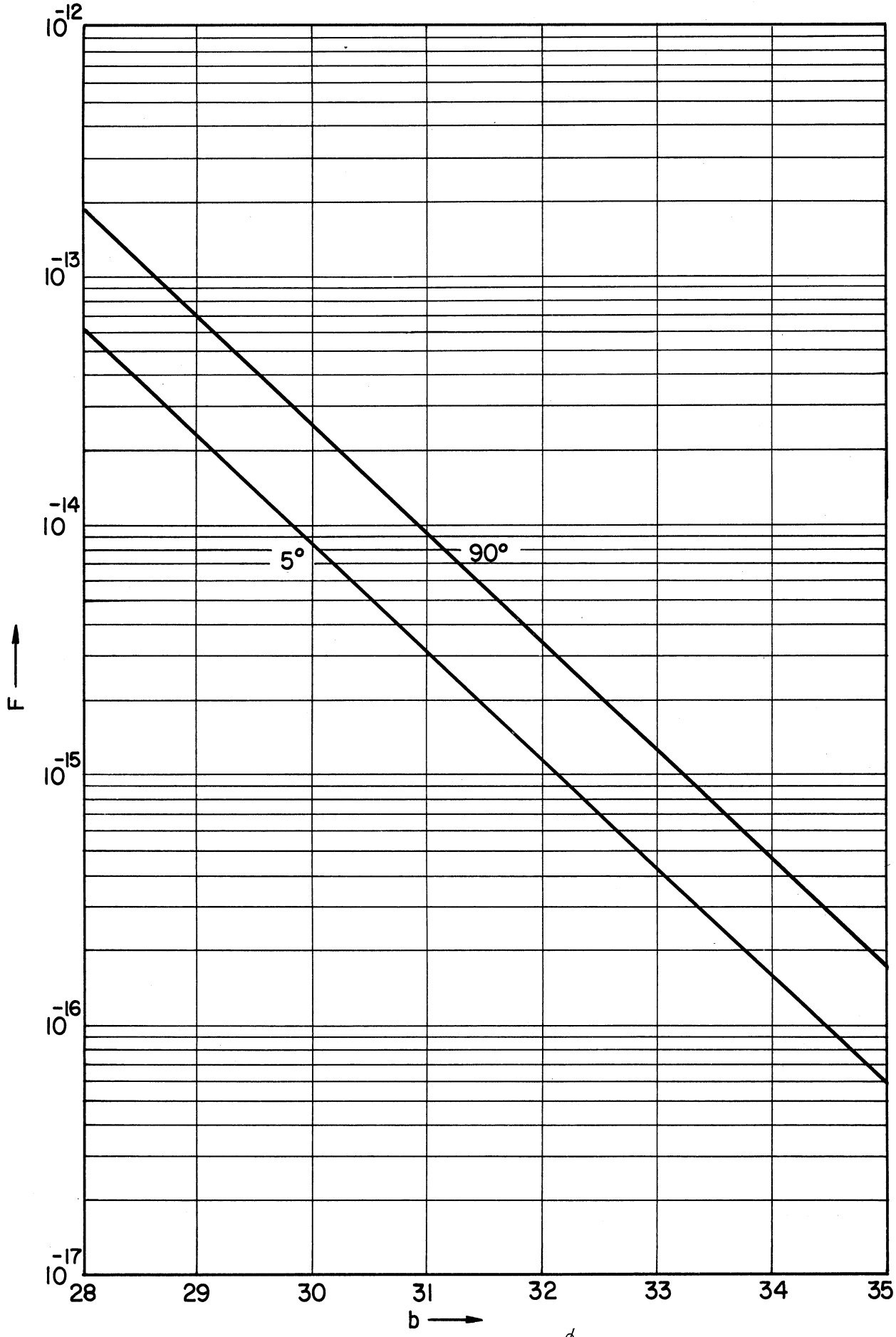

Fig. 4.54. Evaluation of $F(\phi,b) = \int_0^{\phi} e^{-b\sec\phi} d\phi$. (16)

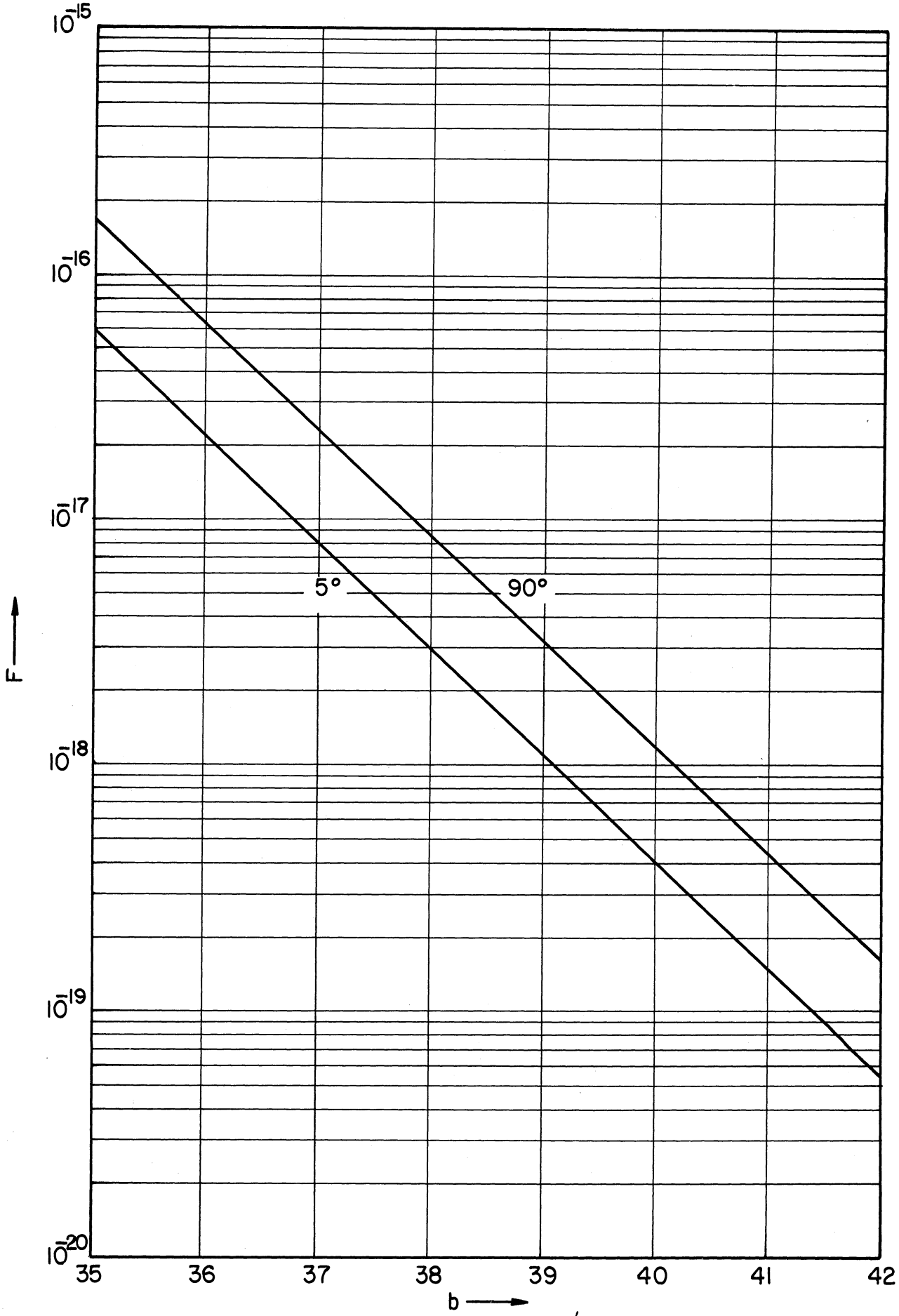

Fig. 4.55. Evaluation of $F(\phi,b) = \int_0^{\phi} e^{-b\sec\phi} d\phi$. (16)

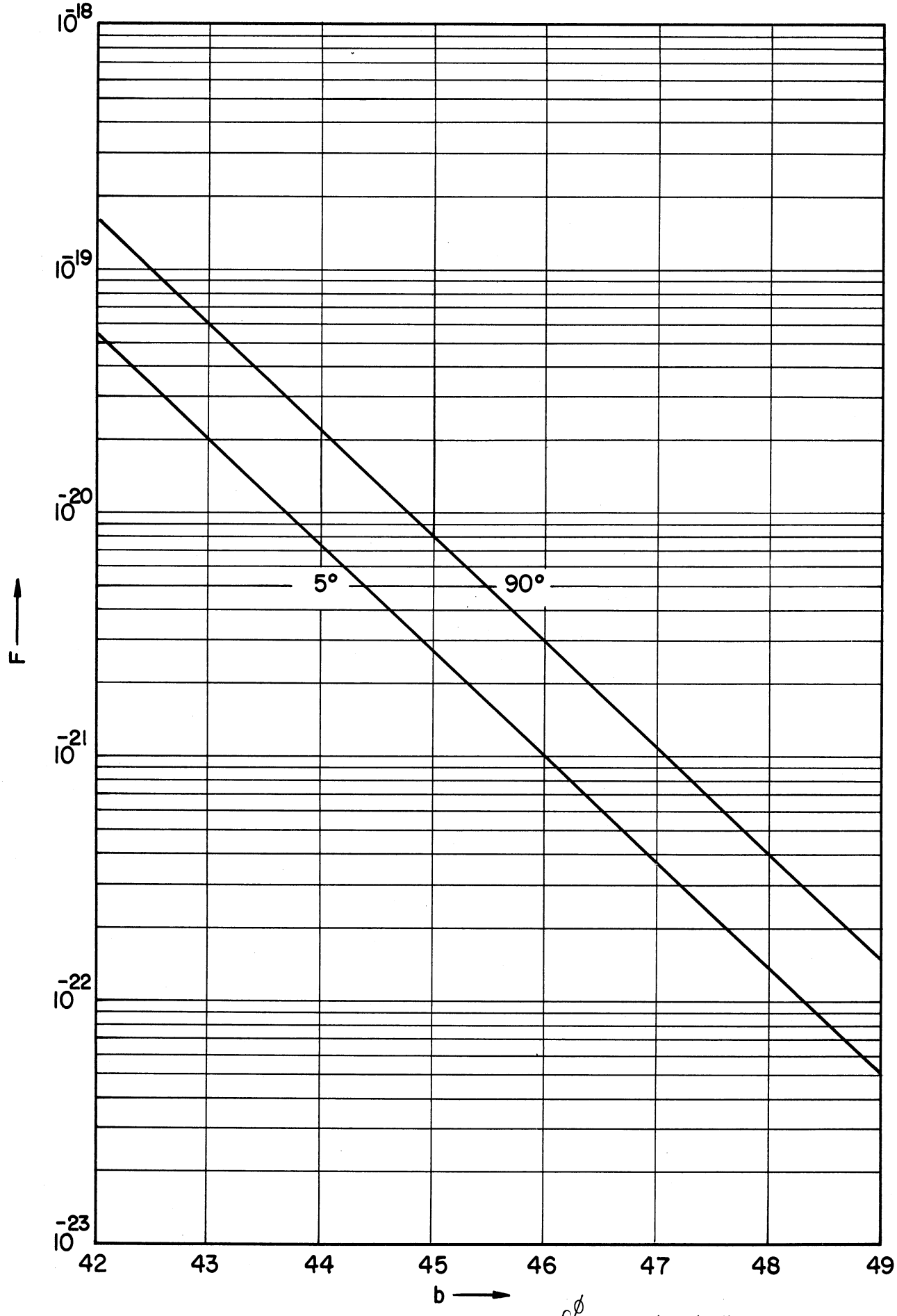

Fig. 4.56. Evaluation of $F(\phi,b) = \int_0^{\phi} e^{-b\sec\phi} d\phi$. (16)

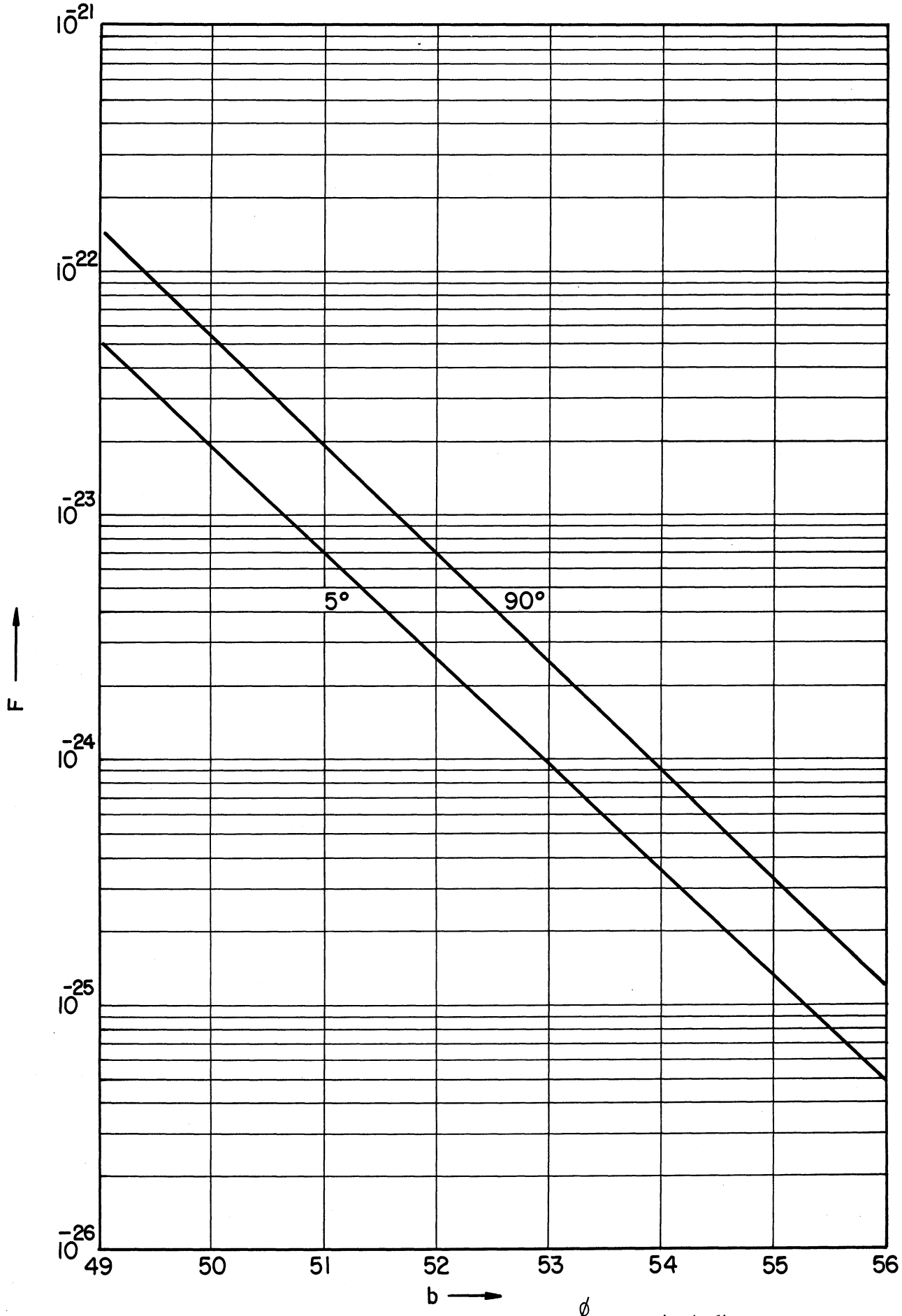

Fig. 4.57. Evaluation of $F(\phi,b) = \int_0^{\phi} e^{-b\sec\phi} d\phi$ (16)

(3) P (Total Fissions/Sec)

P is the total number of fissions in 1 sec and is given by

$$P = \frac{\Delta M}{235} \times \frac{6.02 \times 10^{23}}{T} \text{ (fissions/sec)} \qquad (4.64)$$

where

ΔM = burnup of the fuel element (gm/sec)

and

T = irradiation time in sec (MWD/MW x 86400)

where

1 day = 86400 sec

MWD = megawatt days

MW = power rating of the nuclear reactor in megawatts.

$$\therefore I_{ok} = \left\langle \frac{S}{2\pi h(r+Z)} \right\rangle_k (3.6 \times 10^3) \left\langle \frac{\text{Mev}}{\text{cm}^2 \cdot \text{hr}} \right\rangle \left\langle \frac{\mu - \sigma_s}{\rho} \right\rangle_{k(\text{tissue})} (1.93 \times 10^{-4})$$

$$\cdot \left\langle (r) \frac{\text{cm}^2}{\text{Mev}} \right\rangle [2.97 \times 10^{16}] \frac{\Delta M(\text{gm})}{T(\text{days})}$$

or

$$I_{ok} = \left\langle \frac{S}{2\pi h(r+Z)} \right\rangle_k \left\langle \frac{\mu - \sigma_s}{\rho} \right\rangle_{k(\text{tissue})} \left\langle \frac{\Delta M}{T} \frac{(\text{gm})}{(\text{days})} \right\rangle (2.06 \times 10^{16}) \text{ r/hr} . \qquad (4.65)$$

When I_{ok} and G_k for the k-th energy group have been determined the total intensity due to the whole spectrum can be obtained by summing up the contributions due to the individual groups. For shielding purposes, only two groups (2.5 Mev and 1.75 Mev) need be considered. Thus summation of intensity for k = 1 and k = 2 is sufficient.

For additional information on gamma shielding calculations the reader is referred to References 17-72.

REFERENCES — CHAPTER 4

1. Brownell, L. E., "Radiation Uses in Industry and Science," USAEC, OTI, June, 1961.

2. Goodman, C., "The Science and Engineering of Nuclear Power," Addison-Wesley, 1952.

3. White, G. R., "Gamma Ray Attenuation Coefficients from 10 Kev to 100 Mev," NBS-1003, May 13, 1952, Revised version published as NBS Circular 583, April 30, 1957.

4. Kinsman, S., "Radiological Health Handbook," Sanitary Engineering Center, Cincinnati, Ohio, 1954.

5. Lovewell, P., "Industrial Uses of Radioactive Fission Products," Stanford Research Institute Report, 1951.

6. Siri, W., "Isotopic Tracers and Nuclear Radiations," McGraw Hill, 1949.

7. Goldstein, H., and Wilkins, J. E., Jr., "Interim Report on the NDA-NBS Calculations of Gamma Ray Penetration," Memo 15C-20, Nuclear Development Associates, Inc., White Plains, N. Y., Sept., 1953.

8. Braestrup, C., et al., "Protection Against Radiations from Radium, Cobalt-60 and Cesium-137," Nat. Bur. of Standards Handbook 54, 1954.

9. Marinelli, L. D., Quimby, E. H., and Hines, G. J., "Dosage Determination with Radioactive Isotopes, II--Practical considerations in therapy and protection." Amer. J. Roent., 59, 260, 1948.

10. Goldstein, H., "The Attenuation of Gamma Rays and Neutrons in Reactor Shields," USAEC Contract AT(30-1)-862, U. S. Govmt. Print. Office, Wash. 25, D. C., May 1, 1957.

11. Spencer, L. V., and Fano, U., "Penetration and Diffusion of X-Rays; Calculation of Spatial Distributions by Polynomial Expansion," J. Research Natl. Bur. Stds., 46, 446, 1951; Phys. Rev., 81, 464L, 1951.

12. Taylor, J. J., "Application of Gamma Ray Build-Up Data to Shield Design," AEC publication, WAPD-RM-217, Jan., 1954.

13. Rockwell, Theodore, III, "Reactor Shielding Design Manual," Rept. TID-7004, Office of Technical Services, Washington 25, D. C., March, 1956.

14. Francis, W. C., and Marsden, L. L., "Experimental and Theoretical Values of the Gamma Decay Dose Rate and Heating from Spent MTR Fuel Elements," AEC Research and Development, Rept. IDO-16247, Jan., 1956.

15. Fahnoe, F., et al., "MTR Rods as Fission Product Sources for Industrial Sterilization," KLX-1395, Vitro Corp., Jan. 2, 1954.

16. Dennis, R., Purohit, S. N., and Brownell, L. E., "Procedures for Shielding Calculations," Rept. 1943:8-86T, Eng. Res. Inst., The University of Michigan, Ann Arbor, Mich., Jan., 1957.

17. Gamble, R. L., "Fission Gamma-Ray Spectrum," Rept. 1620, Oak Ridge National Laboratory, 1953, p. 15.

18. Francis, J. E., and Gamble, R. L., "Prompt Fission Gamma Rays," Rept. 1879, Oak Ridge National Laboratory, 1955.

19. Moteff, J., "Fission Product Decay Gamma Energy Spectrum," APEX 134, General Electric Company, 1953.

20. Clark, F. H., "Decay of Fission Product Gammas," Rept. 27-39, Nuclear Development Associates, Inc., 1954.

21. Mittleman, P. S., and Liedtke, R. A., "Gamma Rays from Thermal-Neutron Capture," Nucleonics, 13(5), 50, 1955.

22. Stephenson, R., "Introduction to Nuclear Engineering," McGraw-Hill Book Co., N. Y., 1954.

23. Preiser, S., Mittelman, P. S. and Berndtson, C. R., Plane Isotropic Gamma Ray Buildup Factors in Lead and Water with Applications to Shielding Calculations, NDA 10-144 (Dec. 21, 1954).

24. Blizard, E. P., Paper presented at the Nuclear Engineering Congress at Cleveland, Ohio, Dec., 1955.

25. Moteff, J., "Miscellaneous Data for Shielding Calculations," APEX 176, General Electric Company, Dec. 1, 1954.

26. Blizard, E. P., "Nuclear Radiation Shielding," Annual Review of Nuclear Science, 1955.

27. Way, K., and Wigner, E. P., "The Rate of Decay of Fission Products," Phys. Rev., 73, 1318, 1948.

28. Ajzenberg, F., and Lauritsen, T., "Energy Levels of Light Nuclei," Revs. Mod. Phys., 24, 321, 1952.

29. Fano, U., "Gamma-Ray Attenuation," Reactor Handbook, Technical Information Service; U. S. Atomic Energy Commission Document, AECD-3645, Aug., 1955.

30. Fano, U., "Gamma Ray Attenuation I," Nucleonics, 11(8),8, 1953.

31. Fano, U., "Gamma Ray Attenuation II," Nucleonics, 11(9), 55, 1953.

32. Heitler, W., "Quantum Theory of Radiation," 3d ed., Oxford University Press, New York, 1954.

33. Bethe, H. A. and Ashkin, J., in E. Segrè (Ed.), "Experimental Nuclear Physics," Vol. 1, pp. 305, 349, John Wiley and Sons, Inc., New York 1953.

34. Spring, K. H., "Photons and Electrons," John Wiley and Sons, Inc., New York, 1950.

35. Hughes, A. L. and Dubridge, L. A., "Photoelectric Phenomena," p. 193, McGraw-Hill Book Company, Inc., New York, 1932.

36. Nelms, Anna T., Graphs of the Compton Energy Angle Relationship and the Klein Nishina Formula from 10 kev to 500 Mev, NBS-542 (Aug. 1953).

37. Latter R. and Kahn, H., Gamma Ray Absorption Coefficients, R-170 (Sept. 19, 1949).

38. Goldstein, H., Estimates of the Effect of Fluorescence and Annibhilation Radiation on Gamma Ray Penetration, NDA 15C-31 (Feb. 26, 1954).

39. White, W. E., High Energy Gamma Ray Penetration in Lead, NEPA-1324 (Mar. 6, 1950).

40. Snyder, W. S. and Powell, J. L., Absorption of Gamma Rays, ORNL-421 (Mar. 14, 1950).

41. Goldstein, H. and Wilkins, Jr., J. E., Calculations of the Penetration of Gamma Rays, NYO-3075 (June 30, 1954).

42. Placzek, G., The Functions of $E_n(x) = \int_1^\infty e^{-xu} u^{-n} du$, Chalk River Report MT1 (NRC 1547), Nat. Research Council Can. (Nov. 1946); reprinted in Tables of Functions and of Zeros of Functions, Applied Mathematics Series, No. 37, p. 57 f., Nat. Bur. of Standards (1954).

43. Goldstein, H. and Aronson, R., Status Report on Calculations of Gamma Ray Penetration, NYO-3079, NDA 15C-1 (Aug. 20, 1953).

44. Rossi, B., "High Energy Particles," p. 228 f., Prentice-Hall, New York 1952.

45. Welton, T. A., A Review of Analytical Methods for the Calculation of Neutron and Gamma Ray Attenuations, TID-256 (Nov. 15, 1955).

46. Young, G., Piece-wise Grueling Solutions for Hydrogen, ORNL-415 (Sept. 28, 1949); also, On Straight Ahead Gamma Transmission with A Minimum in the Cross Section, ORNL-416 (Sept. 26, 1949).

47. Bethe, H. A., Fano, U. and Karr, P. R., Penetration and Diffusion of Hard X-rays through Thick Barriers. I. The Approach to Spectral Equilibrium, Phys. Rev., 76:538 (Aug. 15, 1949).

48. Wilkins, Jr., J. E., Openheim, A. and Solon, L., The Transport Equation in the Straight Ahead Case, NYO-633 (Sept. 1, 1950).

49. Solon, L. R. and Wilkins, Jr., J E., Straight Ahead and Root Mean Square Angle Calculations for 20 mc^2 Gamma Rays in Lead, NYO-635 (Dec. 15, 1950).

50. Solon, L. R., Wilkins, Jr., J. E., Oppenheim, A. and Goldstein, H., Gamma Transmission in Iron, Tungsten, Lead, Uranium and a Pure Compton Scatterer by Root Mean Square Angle Calculation, NYO-637 (Apr. 5, 1951).

51. Cave, L., Corner, J. and Liston, R.H.A., The Scattering of Gamma Rays in Extended Media, I: Perpendicular Incidence on a Plane Slab, Proc. Roy. Soc. A, 204: 223 (Dec. 7, 1950).

52. Corner, J., and Liston, R.H.A., The Scattering of Gamma Rays in Extended Media,II: Back-Scattering of Gamma Rays from a Thick Slab, Proc. Roy. Soc. A, 204:323 (Dec. 22, 1950).

53. Peebles, G. H. and Plesset, M. S., Transmission of Gamma Rays Through Large Thicknesses of Heavy Materials, P-155 (June 9, 1950).

54. Peebles, G H., Gamma Ray Transmission Through Finite Slabs, Part I, AECD-3239, RM-653 Pt. I (July 23, 1951); and Part II, RM-653 Pt. II (May 2, 1952).

55. Peebles, G. H., Gamma Ray Transmission Through Finite Slabs, R-240 (Dec. 1, 1952).

56. Whittaker, E. T. and Watson, G. N., "A Course of Modern Analysis," Chap. 15, Cambridge University Press, New York, 1946.

57. Erdelyi, A., et al., "Higher Transcendental Functions," Vol. 2, Chap. 10, McGraw-Hill Book Company, Inc., New York, 1953.

58. Berger, M. J. and Doggett, J. A., Gamma Radiation in Air Due to Cloud or Ground Contamination, NBS-2224 (June 1, 1953).

59. Berger, M. J., Penetration of Obliquely Incident Gamma Rays, unpublished NBS Report (1955). See also J. Research Nat. Bur. Standards, 56:111 (1956).

60. Wilkins, Jr., J. E., Singly Scattered Angular Flux of Gam a Rays at the Source Energy and at the Single Scattering Cutoff, NYO-6273, NDA-15C-46 (Feb. 10, 1955).

61. Certaine, J., Angular Distribution of Photons from Plane Monoenergetic Sources, NYO, 3074, NDA 15C-10 (June 1, 1953)

62. Householder, A S., "Principles of Numerical Analysis," pp. 242-246, McGraw-Hill Book Company, Inc., New York, 1953.

63. Meyer, H. A. (ed.), "Symposium on Monte Carlo Methods," John Wiley and Sons, Inc., New York, 1956. In succeeding references to this volume it will be labelled SMCM.

64. Goertzel, G., Quota Sampling and Importance Functions in Stochastic Solution of Particle Problems, ORNL 434 (June 21, 1949). See also H. Kahn, Modification of the Monte Carlo Method, P-123 (Rand) (Nov. 14, 1949), and article by M. Kalos and G. Goertzel to appear in Vol 2, Series I, "Progress in Nuclear Energy."

65. Kahn, H., Stochastic (Monte Carlo) Attenuation Analysis, Rand P-88 (rev.) (July 14, 1949); and quoted in T. A. Welton, A Review of Analytical Methods for the Calculation of Neutron and Gamma Ray Attenuations, TID-256 (Oct. 5, 1949).

66. Shor, S. W., V. Computation of Radiation Shield Thickness by the Monte Carlo Method, MIT Tech. Report No. 32 (Jan. 1950).

67. Hayward, E. and Hubbell, J. H., The Albedo of Various Materials for 1 Mev Photons, NBS-2768 (Sept. 11, 1953); also Phys. Rev., 93:955 (1954).

68. Preliminary Report in M. H. Kalos, A Monte Carlo Calculation of the Transport of Gamma Rays, NDA 56-7 (July 31, 1956).

69. Carlson, B., The Monte Carlo Method Applied to a Problem in Gamma Ray Diffusion, LADC 1633, AECU-2857, 1953.

70. Ogievetskii, I., The Theory of Propagation of Gamma Rays through Matter, Soviet Physics JETP (New York), 2(2):312 (Mar. 1956); and Angular Distribution of Gamma Rays at Great Depths of Penetration in Matter, ibid., 319 (Mar. 1956).

71. Aronson, R., Some Remarks on Source Geometry and Single Scattering of Gamma Rays, NDA Memo 15C-37 (May 1, 1954).

72. Taylor, J. J., Applications of Gamma Ray Buildup Data to Shield Design, WAPD Memo RM-217 (Jan 25, 1954). See also Chap. 9, Part V of Reactor Shielding Design Manual, TID-7004 (Mar. 1956).

Chapter 5

Counting Nuclear Radiations

A number of problems of radioanalysis depend on the accurate determination of the disintegration rate of a radioactive sample. This is true for "tracer" techniques, determination of half-life for radioisotope identification, and various other assay methods. For a given radioisotope the rate of disintegration is directly proportional to the rate of emission of nuclear radiations. The "counting" of the nuclear radiations over a given period of time permits determination of the rate of emission. Today, electronic instruments known as "counters" are used for this procedure. However, early workers counted alpha particles by the tedious process of observing with a microscope individual scintillations on a plate coated with a phosphor and counting the events by eye. The equipment required for rapid and accurate counting consists of a detector such as a G-M tube, scintillation counter, etc., and auxiliary equipment for shielding the sample and timing and recording the counts.

This chapter describes first the auxiliary equipment of shielding and electronic counting devices. The theory of counting randomly occurring events is discussed in detail: consideration is given to standard errors and systematic corrections for dead-time, geometry, tube efficiency, scattering, absorption etc. The chapter ends with paragraphs on the major problems associated with counting alpha, beta and gamma radiations.

5.1. Auxiliary and counting equipment

A certain radiation level is always present because of the "background" produced by cosmic radiation, the radon in the air and the

presence of minute amounts of radioactivity in structural materials and in the earth. This background level of radiation establishes a lower limit for accurate counting if the counting rate of the sample is small. The background level changes from day to day, depending on weather conditions (for example fresh rain dissolves and removes the radon in the atmosphere and thereby lowers the background). To provide a low, more uniform background level for accurate counting a lead or iron shield is used around the sample and detection tube. Figure 5.1 shows a typical vertical lead shield.

Manual counting of pulses is very tedious and can only be used for low count rates. Most counting is performed by instruments known as "counters" or "scalers." The counter contains a vacuum-tube amplification circuit similar to those described previously for the various types of detectors (ion chambers, G-M tubes, scintillation wells, etc.). The pulse is amplified to provide sufficient output to operate a mechanical register. However, the maximum rate a mechanical register will accept is about 30 to 50 counts per second. To permit counting at a higher rate, an electronic instrument called a "scaler" is included in the measuring system. The "binary" scaler permits only one count in every 2, 4, 8, 16, 32, or 64 to be recorded by the mechanical register. The use of a scale in which the register records once for every 64 counts is common. Scalers called "decade" scalers are also much used and are based on factors of 10 rather than factors of 2. In using a scaler the number indicated on the register is multiplied by the scaling factor to give the total number of counts for the period that the scaler is operated. Figure 5.2 shows a typical scaler.

Figures 5.1

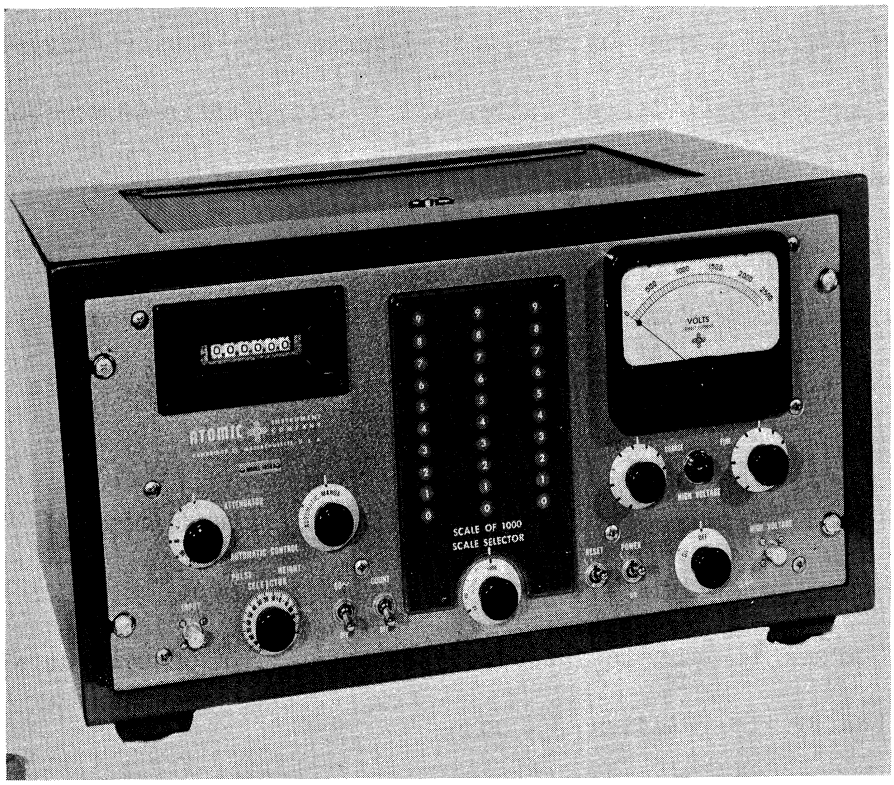

Figure 5.2: Scaler (Courtesy of Atomic Instrument Co.)

The scaler shown in Figure 5.2 may be operated on any decade scale of 10, 100, or 1000, or on any binary scale of 16, 64, 256, 1,024, and 4,096, by setting the selector on the face of the scaler. The scaler contains a built-in register shown at the upper left of the instrument. Controls for the voltage regulation, pulse height, attenuation, and automatic or manual operation are also shown on the face of the instrument. An external timer is used with this scaler.

More elaborate scalers containing both a built-in timer and register are available for use in counting with G-M and scintillation counters as well as with proportional counters.

A great variety of other types of auxiliary and counting equipment is available and is described in the catalogs of the various manufacturers.

5.2. The counting of randomly occurring events (1)

The decay of radioactive nuclei occurs spontaneously and seems to be influenced in no way by its external environment. It is impossible to predict the decay of any individual nucleus. It is possible, however, to measure the average number of decays that occur over a given time interval from a large population of nuclei and to use these measurements in determining useful information concerning the population. The situation is analogous to the use of mortality tables by life insurance companies. No valid prediction concerning the lifetime of an individual can be made from such a table. However, predictions concerning the average lifetime of a population are quite good and extremely useful.

In order that the results of measurements made on the decay of radioactive nuclei be used intelligently, something must be known of the statistics which can be used to interpret the data. Radioactive decay can be described by the relation

$$N = N_o \epsilon^{-\lambda t} \qquad 5.1$$

where $1/\lambda$ is the mean life of a nucleus, N_o is the number of radioactive nuclei in the source at zero time, and N is the number present at time t. It follows that the average number of decays per second is equal to λN. Consider the case where a certain number of disintegrations from a source of known N are measured over a known period. The question then arises as to how λ should be computed from such a measurement. Experience indicates that the number of events measured over a fixed time interval fluctuates if the process is a random one; thus, some method is needed for estimating how far a particular measured value of disintegrations departs from the average or expected value.

5.3. The Poisson distribution

Consider a time interval of arbitrary length divided into k equal parts as shown in Figure 5.3. Let the probability of the occurrence of an event in any one interval be the same as its occurrence in any other interval. Call this probability p and make (1/k) small enough so that the probability of finding two events in the same interval is vanishingly small.

Now the probability of finding an event in the first interval is just p. The probability of finding an event in the first interval and also an event in the second interval is p^2. Similarly, for the first, second, and third intervals one gets p^3.

The probability of not finding an event in the first interval must therefore be (1 - p). Similarly, for not finding one in the first and the second interval one gets $(1 - p)^2$.

Thus, the probability of finding an event in the first n intervals and at the same time not finding one in the next k - n is:

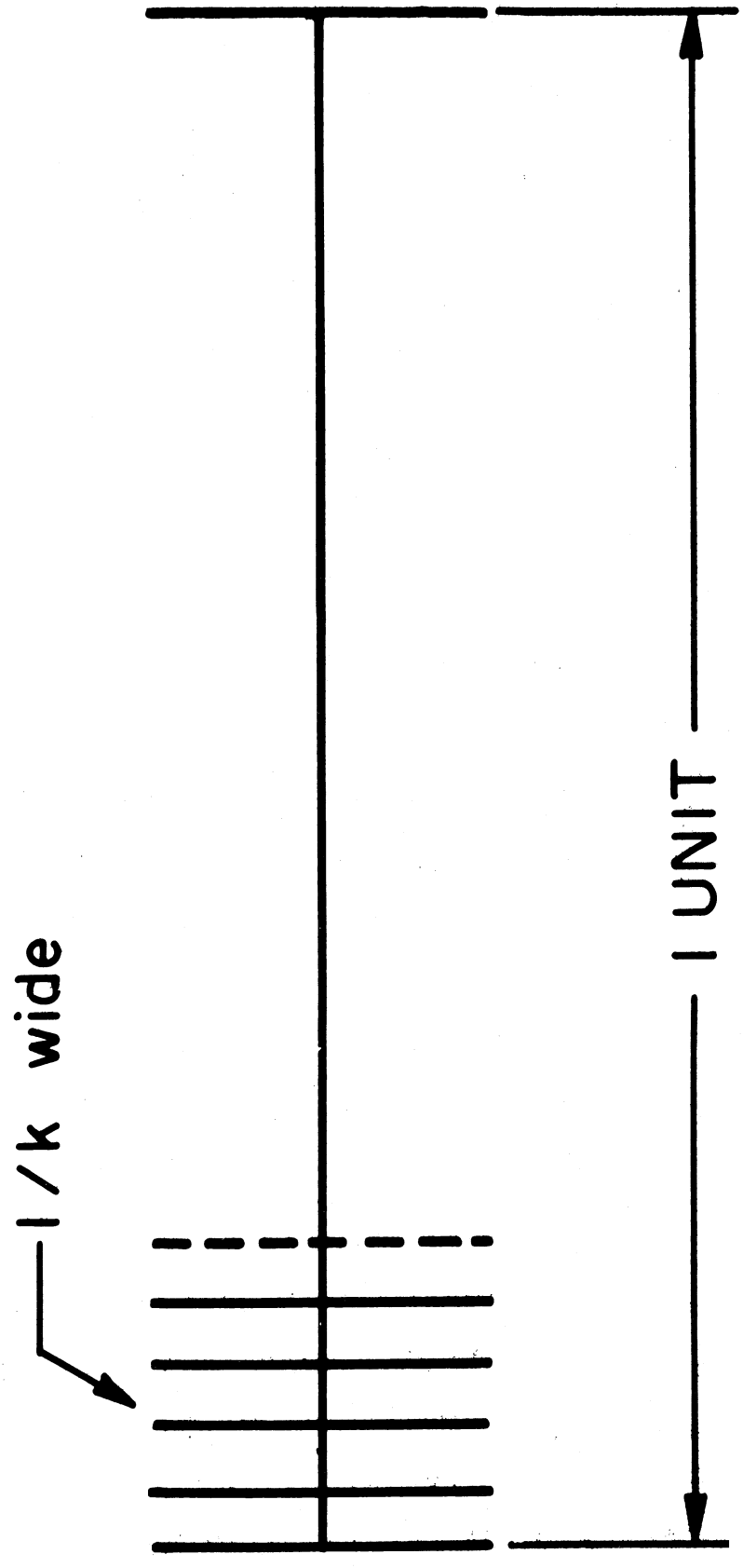

Figure 5.3: Time Interval Divided into k Units
Each 1/k Wide

$$P' = p^n (1 - p)^{k-n} \qquad 5.2$$

One sees that this is one possible arrangement leading to the finding of exactly n events in the total time interval. There are many other arrangements which also give exactly n events. The number of ways of arranging k objects in groups of n each is:

$$C_n^k = \frac{k!}{(k - n)!\, n!} \quad . \qquad 5.3$$

It follows that the probability of finding exactly n events in the arbitrary interval is the product of Eqs. 5.2 and 5.3. Call this probability $P_{(n)}$. Then

$$P_{(n)} = \frac{k!}{(k - n)!\, n!} (p)^n (1 - p)^{k-n} \qquad 5.4$$

Assume that k is very much larger than n. This is legitimate since k can be as large as is necessary, the only requirement being that the product kp is constant. In this case

$$\frac{k!}{(k - n)!} \cong \frac{k^n (k - n)!}{(k - n)!} = k^n \quad . \qquad 5.5a$$

Hence,

$$P_{(n)} \cong \frac{(kp)^n (1 - p)^{k-n}}{n!} \qquad 5.5b$$

Consider the term $(1 - p)^{k-n}$. Note that this can be written as

$$(1 - p)^{k-n} = \left[(1 - p)^{k-n/-kp}\right]^{-kp} \qquad 5.6$$

As k becomes very large and p becomes correspondingly small (since kp is constant), it is seen that the expression on the right-hand side of Eq. 5.6 approaches ϵ^{-kp}. Hence, for k very large and p very small, but the product kp still finite, the probability of finding n events, $P_{(n)}$, becomes

$$P_{(n)} = \frac{\nu^n \epsilon^{-\nu}}{n!} \quad . \qquad 5.7$$

Here ν has been substituted for the constant kp. The expression on the right of Eq. 5.7 is called Poisson's distribution and is the probability of finding exactly n events in the interval concerned.

This distribution is suitable for use in describing radioactive decay where, for example, the number of intervals k of the above might correspond to the number of radioactive nuclei in a source, and p might correspond to the probability that any one of them decays in, say, one second. For a gram of U-238, for example, k is around 10^{21}, but p is very small, about 10^{-18}. However, the restrictions of the above derivation, that is that kp be finite, are still readily met. Note that the product kp corresponds to the λN of Eq. 5.1.

It should be pointed out that for large values of both n and ν, and for values of n not very different from ν, the Poisson distribution is closely approximated by the Gaussian distribution. This may be written as

$$G_{(n)} = 1/(2\pi\sigma)^{1/2} \qquad \epsilon \ \frac{-(n - \nu)^2}{2\sigma} \quad . \qquad 5.8$$

In contrast to the Poisson distribution, which describes integral numbers of events, the Gaussian distribution describes a continuous variable. It is, however, a good approximation for the Poisson distribution for large n and is frequently so used.

5.4. Mean value

Suppose one asks for the mean value of n in the interval discussed. This is found by taking each value of n from 0 to ∞, multiplying by the probability of that value's occurring, and summing. Formally this is expressed as

$$\bar{n} = \sum_{n=0}^{\infty} nP_{(n)} \cdot \qquad 5.9$$

For a Poisson distribution this is

$$\bar{n} = \sum_{n=0}^{\infty} \frac{n\nu^n \epsilon^{-\nu}}{n!} .$$

Since the first term of the above series is zero,

$$\bar{n} = \epsilon^{-\nu} \nu \sum_{n-1=0}^{\infty} \frac{\nu^{n-1}}{(n-1)!} = \epsilon^{-\nu} \nu \sum_{n=0}^{\infty} \frac{\nu^n}{n!} .$$

Or,

$$\bar{n} = \nu, \qquad 5.10$$

since

$$\sum_{n=0}^{\infty} \frac{\nu^n}{n!} = \epsilon^{\nu}.$$

Hence, ν or kp has the significance of a mean value. $P_{(n)}$ is thus the probability that n events will be found in an interval if the mean value of events in the interval is ν. Experimentally ν is the limit of the number found by looking a large number of times in the interval, summing the numbers of events found, and dividing by the number of trials.

In the case of the counting of nuclear radiations, ν might be set equal to $N\tau$ where τ is some time interval and N is the average number of counts per unit time. (Note that N here is equivalent to the term λN in Eq. 5.1.) Hence, the probability of counting n events in an interval τ when the average number to be expected in the interval is $N\tau$ is

$$P_{(n)} = \frac{(N\tau)^n \epsilon^{-N\tau}}{n!} . \qquad 5.11$$

An interesting case is the probability of zero.

$$P_{(o)} = \frac{(N\tau)^o \epsilon^{-N\tau}}{0!} = \epsilon^{-N\tau} . \qquad 5.12$$

This is the probability of zero counts occurring in an interval, if the average count rate is N counts per unit time. It follows that the probability that counts will occur in the interval is $1 - P_{(o)}$, i.e.,

$$P_{(\text{not zero})} = 1 - P_{(o)} = 1 - \epsilon^{-N\tau} . \qquad 5.13$$

If a series expansion is used, this gives

$$1 - \epsilon^{-N\tau} = N\tau + \frac{(N\tau)^2}{2!} + \frac{(N\tau)^3}{3!} + \cdots$$

Hence, if $N\tau \gg (N\tau)^2$, which means that $N\tau$ must be much less than unity,

$$P_{(\text{not zero})} \cong N\tau .$$

5.5. Coincidence losses and corrections

This result has a practical application in radiation counters which have finite resolving times, since it gives the average number of counts to be expected in the dead interval of a counter with resolving time τ if the counting rate of a counter with zero resolving time is given by N. Note that the approximation is what one would intuitively expect, but the additional series terms are not given by intuition.

As an example, consider a Geiger counter with a resolving time of 200 microseconds and an expected counting rate of 10,000 counts per minute or (10,000/60) per second. The average number of counts occurring in each dead interval is approximately $200 \times 10^{-6} \times (10^4/60)$ or 1/30 count. In one minute approximately $(1/30) \times 10^4$ or 333 counts are missed, on the average. Of course, if this is known, this number is simply added to the total counted to get the number that would have been counted had the counter had zero resolving time.

Let N be the number actually counted per unit time, and η be the number per unit time that should have been counted with zero resolving time. The relationship between the two is given by

$$\eta = N + N(\eta\tau) \ . \qquad 5.14$$

This gives

$$\eta = \frac{N}{1 - N\tau} = N(1 + N\tau + \frac{(N\tau)^2}{2} + \cdots) \ .$$

And since $N\tau$ is usually much less than unity,

$$\eta \cong N\ (1 + N\tau) \ . \qquad 5.15$$

It should be remarked that this analysis assumes a constant τ or counter resolving time. This assumption is not strictly true for Geiger counters, but is a reasonable approximation as long as $N\tau$ is considerably smaller than unity.

5.6. Deviations from the mean value

The voltage output pulses from a counter represent both the nuclear radiations that are being measured or that one wants to measure, together with any other event which may cause a pulse to be produced by the counter. Among the sources of spurious pulses are the naturally radioactive elements that may be incorporated, perhaps as a contaminant, in the counter walls. Others are cosmic rays. In addition, around a laboratory in which radioactive materials are used, additional unwanted sources may be present as accidental contamination or as laboratory sources.

The counts which occur as a result of the events in which one is not interested are referred to as "background." They correspond to "noise" in a communication system. If the source that is being measured can be removed from the neighborhood of the counter, measurements

of the background alone can be made. If the background were constant, and equal to the measured count rate, it could then be subtracted from the count observed, which is due to both source and background to give source alone. However, the background pulses themselves will usually occur at random. If they do not, they are due to some systematic source, say electrical line noise, which can be eliminated by suitable precautions. Since they occur at random, several measurements of background over the same length of time interval may be expected to produce different numbers of counts, but usually of the same order of magnitude.

By definition the mean value of a background count is the limit of the average of the counts per interval as the number of intervals considered approaches an infinite number. However, since it is impracticable to measure an infinite number of intervals, it is useful to ask for the expected accuracy of a single measurement or the deviation expected. Such information is useful not only as far as background is concerned, but also with reference to measured count rate of a source. Again, since a limited amount of time is available, one is interested in the expected deviation of a single measurement from the mean value.

Experience has shown that a useful quantity for describing this expected deviation is the "variance" of a variable, or the square root of the variance, the "standard deviation." For a variable, x, the variance σ^2 is defined as

$$\sigma^2 = \overline{(x - \bar{x})^2} \qquad 5.16$$

Here the bar over a quantity indicates a mean value. In words, σ^2 is the mean value of the square of the difference between x and the mean value of x. Hence, on the average, one might expect a deviation equal to the square root of σ^2.

Consideration will show that

$$\overline{(x - \bar{x})^2} = \overline{x^2} - \overline{2x\bar{x}} + \bar{x}^2 = \overline{x^2} - \bar{x}^2 \quad . \tag{5.17}$$

If the variable of interest can be described by a Poisson distribution, we need only to know the value of $\overline{x^2}$ in order to compute σ or σ^2 since $\bar{x}$ is known from Eq. 5.10.. If x is the variable n, then

$$\overline{n^2} = \sum_{n=0}^{\infty} n^2 P_{(n)} = \sum_{n=0}^{\infty} n^2 \frac{\nu^n \epsilon^{-\nu}}{n!} \quad .$$

Since the first term of the series is zero, it may be written as

$$\overline{n^2} = \epsilon^{-\nu} \nu \sum_{n-1=0}^{\infty} \frac{n\nu^{n-1}}{(n-1)!}$$

or

$$\overline{n^2} = \epsilon^{-\nu} \nu \left\{ \sum_{n-1=0}^{\infty} \frac{(n-1)\nu^{n-1}}{(n-1)!} + \sum_{n-1=0}^{\infty} \frac{\nu^{n-1}}{(n-1)!} \right\}$$

But this is equivalent to

$$\overline{n^2} = \epsilon^{-\nu} \nu \left\{ \sum_{n=0}^{\infty} \frac{n\nu^n}{n!} + \sum_{n=0}^{\infty} \frac{\nu^n}{n!} \right\} \quad .$$

However, the first term in the bracket is just $\nu/\epsilon^{-\nu}$ and the second term is ϵ^{ν}. Thus,

$$\overline{n^2} = \nu^2 + \nu \, . \tag{5.18}$$

It follows from Eq. 5.18 that:

$$\sigma^2 = \nu,$$

or

$$\sigma = \sqrt{\nu} \quad . \tag{5.19}$$

This equation says that for a Poisson distribution the standard deviation is equal to the square root of the mean value. Hence, the larger the mean value, the greater the expected deviation.

It is useful, however, to define a percent standard deviation as

$$\Delta n = \frac{\sigma(n)}{\bar{n}} \times 100 \ . \qquad 5.20$$

For a Poisson distribution this is

$$\Delta n = \frac{\sqrt{\nu}}{\nu} \times 100 = \frac{100}{\sqrt{\nu}} \ .$$

Hence, as ν gets larger the percent standard deviation gets smaller and, in fact, can be made as small as desired by making ν large enough.

Since deviations are to be expected in any set of data, the question now arises as to how an average value is determined experimentally. One answer is that as an approximation one may take a set of data and determine an arithmetic average from it, calling this the mean value. Using this experimentally determined mean value as the actual mean value for, say, a Poisson distribution, one can then predict the standard deviation and the percent standard deviation. These are of course dependent on the experimental choice of ν.

Another method that can be used is to choose an approximate value of ν and for this value plot a Poisson distribution. This is then compared with the experimental distribution. Other values of ν can be tried until a best fit has been obtained for the data. The value of ν that gives the best fit is then the mean value. For other standard methods of determining ν and σ from a set of experimental data see References 2 and 3.

5.7. The effect of background on the interpretation of counting data

In the counting of nuclear radiations from radioactive nuclei one usually counts the number of background counts and also for the same time interval the number of counts of source plus background. Suppose n_s represents source plus background, background is n_b, and n represents source alone. Experimentally, one determines n as

$$n = n_s - n_b \ . \qquad 5.21$$

The question then arises as to the error to be expected or the standard deviation of an n determined as above. This may be expressed in terms of variances as

$$\sigma_n^2 = \sigma^2 (n_s - n_b) \ .$$

But this is

$$\sigma_n^2 = \overline{[(n_s - n_b) - \overline{(n_s - n_b)}]^2} \qquad 5.21$$

or

$$\sigma_n^2 = \overline{(n_s - n_b)^2} - \overline{2(n_s - n_b)\,(\overline{n_s - n_b})} + \overline{(n_s - n_b)^2} \ .$$

Expanded, the right-hand side gives

$$\overline{n_s^2} - \overline{2\,n_s n_b} + \overline{n_b^2} - \overline{2\,n_s^2} - \overline{2\,n_b^2} + \overline{4\,n_s n_b} + \overline{n_s^2} - \overline{2\,n_s n_b} + \overline{n_b^2} \ .$$

This gives, when consolidated,

$$\sigma_n^2 = (\overline{n_s^2} - \overline{n_s}^2) + (\overline{n_b^2} - \overline{n_b}^2) \ ,$$

which is equivalent to

$$\sigma_n^2 = \sigma_s^2 + \sigma_b^2 \ ;$$

and thus,

$$\sigma_n = \sqrt{\sigma_s^2 + \sigma_b^2} \ . \qquad 5.22$$

Note that <u>if source and background conform to Poisson distributions</u>,

$$\sigma_n = \sqrt{\overline{n_s} + \overline{n_b}} \ .$$

An assumption frequently made for computing standard deviations approximately is that

$$\overline{n_s} \cong n_s$$

and

$$\overline{n_b} \cong n_b \ .$$

That is, the measured number of counts is almost equal to the mean value for source and background. Hence, n_s is expressed as $n_s \pm \sqrt{n_s}$ and n_b as $n_b \pm \sqrt{n_b}$. It follows, according to Eq. 5.22, that if one uses this system, the count is expressed as

$$n = n_s - n_b \pm \sqrt{n_s + n_b} \ . \qquad 5.22$$

The percent deviation to be expected is thus,

$$\Delta_n = \sqrt{n_s + n_b} \times 100/(n_s - n_b) \ . \qquad 5.23$$

The count rate may frequently be of more interest than total counts. Let rate be denoted by caps. Then

$$N = \frac{n}{t} \pm \frac{\sqrt{n_s + n_b}}{t} = \frac{n}{t} \pm \sqrt{\frac{N_s}{t} + \frac{N_t}{t}}$$

The percent deviation expected in the rate determination is

$$\Delta_N = (\sqrt{N_s/t + N_b/t}) \times 100/(N_s - N_b) \ . \qquad 5.24$$

Implicit in the above discussion is the assumption that the background is counted for the same period of time as is the source. This may not be true. Consideration will be given to the case in which the counting times are different.

Note that

$$\sigma_n^2 = \overline{(n - Nt_n)^2} \quad . \qquad 5.25$$

is an alternative definition of the variance of n, where t_n is the time interval over which N is computed. However,

$$n = n_s(t_n/t_s) - n_b(t_n/t_b) \quad .$$

Substituting into Eq. 5.25 gives

$$\sigma_n^2 = \overline{[n_s(t_n/t_s) - n_b(t_n/t_b) - Nt_n]^2}$$

Substitution of $(N_s - N_b)$ for N and appropriate rearrangement give

$$\sigma_n^2 = (t_n/t_s)^2 [\overline{n_s^2} - \overline{N_s^2}\, t_s^2] + (t_n/t_b)^2 [\overline{n_b^2} - \overline{N_b^2}\, t_b^2],$$

which is equivalent to

$$\sigma_n^2 = (t_n/t_s)^2 \sigma_s^2 + (t_n/t_b)^2 \sigma_b^2 \quad . \qquad 5.26$$

Note that when $t_n = t_s = t_b$ this is the same as Eq. 5.22. Assuming that the variables follow a Poisson distribution and further that $\sigma_s^2 = N_s t_s$ and $\sigma_b^2 = N_b t_b$, Eq. 5.26 becomes:

$$\sigma_n^2 = t_n^2 \quad (N_s/t_s + N_b/t_b) \quad . \qquad 5.27$$

This expression shows the effect of counting times on the expected error of the result. Note that large counting times produce small values of standard deviation per unit time. Several investigators have studied the

most efficient use of counting time for the achievement of minimum error. For detailed results the literature on the subject should be consulted (4).

5.8. The standard deviation

The "standard" deviation for a Poisson distribution of events is equal to the square root of the mean value. The probable error is defined as 0.67σ. In the case of different sets of events, the resultant standard deviation is represented as σ_N and is given by:

$$\sigma_N^2 = \sum \left(\frac{\delta N}{\partial n}\right)^2 \sigma_n^2 \qquad 5.28$$

where:

σ_N = Resultant standard deviation.

σ_n = Standard deviation for the set of events having n mean value in a certain time interval.

N = Resultant of the mean values of different sets in different time interval.

Assume n_1 and n_2 to be the numbers of the counts taken in time intervals t_1 and t_2 for a disintegration event represented by a Poisson distribution.

Resultant of mean values $N = n_1 + n_2$

The square of the resultant or the standard deviation $$\sigma_n^2 = \left\{ \frac{\partial(n_1 + n_2)}{\partial n_1} \sigma_{n_1}^2 + \frac{\partial(n_1 + n_2)}{\partial n_2} \sigma_{n_2}^2 \right\}$$

Assuming independence of n_1 and n_2

$$\sigma_N^2 = \sigma n_1^2 + \sigma n_2^2 \qquad 5.29$$

$$\sigma_N^2 = \sqrt{n_1^2} + \sqrt{n_2^2}$$

Magee (10,12) has developed a method of using the reciprocals of the counts so as to limit the effects of geometry on an uranium ore assay. Consider the case in which a counter is located on both sides of a conveyor belt carrying a source. Pulses are recorded from each counter alternately. Let the pulses in a fixed time of integration be equal to n_1 and n_2.

$$\text{Resultant} \quad N = \frac{1}{\frac{1}{n_1} + \frac{1}{n_2}} = \frac{n_1 n_2}{n_1 + n_2}$$

$$\sigma_N^2 = \left\{ \frac{\partial}{\partial n_1} \left(\frac{n_1 n_2}{n_1 + n_2} \right) \right\}^2 \sigma_{n_1}^2 + \left\{ \frac{\partial}{\partial n_2} \left(\frac{n_1 n_2}{n_1 + n_2} \right) \right\}^2 \sigma_{n_2}^2$$

$$\sigma_N^2 = \frac{n_1 n_2^4 + n_1^4 n_2}{(n_1 + n_2)^4} \qquad 5.30$$

Case 1. $n_1 = n_2 = n$

$$\sigma_N^2 = \frac{h}{8} \; ; \quad N = \frac{n}{2}$$

$$\frac{\sigma_N}{N} = \frac{1}{\sqrt{2n}} \qquad 5.31$$

Case 2. If $n_1 \gg n_2$

$N = n_2$ as $\frac{1}{n_1}$ is small .

$$\therefore \quad \sigma_N^2 = n_2$$

$$\frac{\sigma_N}{N} = \frac{1}{\sqrt{n_2}} \qquad 5.32$$

Thus, the statistical fluctuations are dependent upon the lower count.

In many cases, the output of the pulses is recorded by a rate meter through a resistance-capacitance (R-C) network. For such a case let N be the mean count rate and q be the charge per pulse fed to condenser in the time interval between t and t + dt.

$$\text{Charge fed to condenser} = qN\,dt$$

$$\text{The standard deviation of this charge} = q\sqrt{N\,dt}$$

The electric charge decays exponentially in a R-C network with a time constant equal to RC.

$$\text{The standard deviation at time } t_1 = q\sqrt{N\,dt}\;\; e^{-(t_1-t)/RC} \qquad 5.33$$

The total standard deviation on the output at time t_1 is:

$$\sigma_q^2 = \int_{-\infty}^{t_1} q^2 N e^{-2(t_1-t)}$$

$$\sigma_q^2 = q^2\,\frac{NRC}{2}$$

$$\therefore\;\; \sigma_q = q\sqrt{\frac{NRC}{2}} \qquad 5.34$$

The relative standard deviation

$$\frac{\sigma_q}{Q} = \frac{q\sqrt{\frac{NRC}{2}}}{\text{total charge}}$$

$$\text{Total charge} = q^{NRC}$$

$$\therefore \quad \frac{\sigma_q}{Q} = \frac{1}{\sqrt{2NRC}} \qquad 5.35$$

Thus, in the case of the use of a rate meter for recording the output, the standard deviation depends on the time constant of the electric network feeding the meter in addition to the mean count rate.

Figure 5.4 shows the standard deviation curve and Figure 5.5 shows schematically the effect of the number of counts on the probability of error.

5.9. Percentage probable error

The percentage of probable error is given in the case of N-total individual counts as:

$$\% \text{ Probable Error} = (67.45) \times (\text{Relative Standard Deviation})$$

$$\% \text{ P.E.} = 67.45 \frac{\sigma N}{N}$$

$$\% \text{ P.E.} = \frac{67.45}{\sqrt{N}} \qquad 5.36$$

In Figure 5.6 the percent probable error (% P.E.) is plotted versus the total number of counts.

In the case of the use of a rate-meter counting device, the percentage probable error is given as:

$$\% \text{ P.E.} = \frac{67.45}{\sqrt{2\ NRC}} \qquad 5.37$$

5.10. Corrections in beta counting

The ultimate purpose of counting is to measure disintegration rates. In the counting process, for various reasons, counting rate is generally not equal to the disintegration rate. That is:

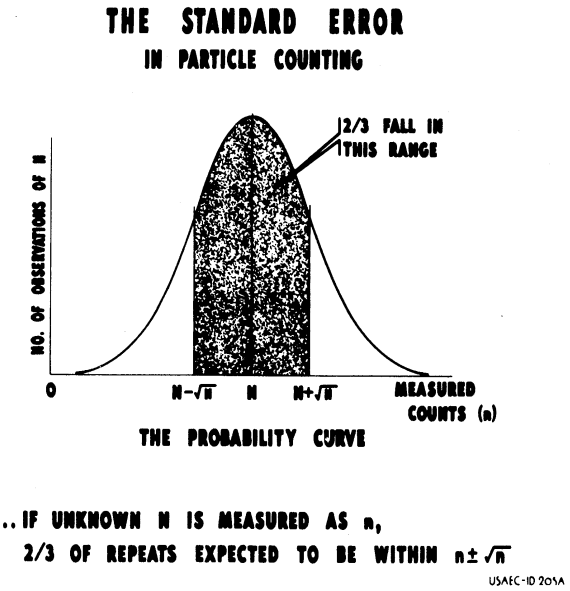

Figure 5.4: The Standard Error in Particle Counting

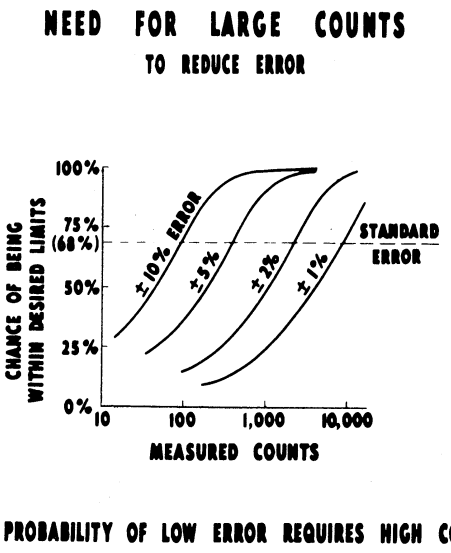

Figure 5.5: Dependence of Error on Counts

Counts per min = E (disintegrations per min)

where: $E \neq$ unity .

The factor E is sometimes referred to as "geometry" but in this text will be referred to as "overall efficiency." Several physical factors listed in Table 5.1 affect the inequality of counting rate and disintegration rate. Some of the factors listed in Table 5.1 are shown schematically in Figure 5.7.

Table 5.1

Factors Influencing Counting

dead time
geometry
tube efficiency
process efficiency
scattering
absorption
sample thickness
particle energy

5.11. Dead time

After a counting system receives and records a count, there is a finite time during which the system is insensitive to further counts. This is called dead time and is shown schematically in Figure 5.8. When a count is lost owing to the arrival of a particle at the sensitive volume of the counter during dead time, this is called a coincidence loss. Sensitive volume is defined as that volume in which a passing particle may cause a count.

There are two experimental means in common use for measuring coincidence losses. In one method, a sample whose half-life is known with great precision is counted as a function of time. The theoretical curve (dotted in Figure 5.9) is extrapolated from the lower counting rate portion of the experimental curve as shown (5).

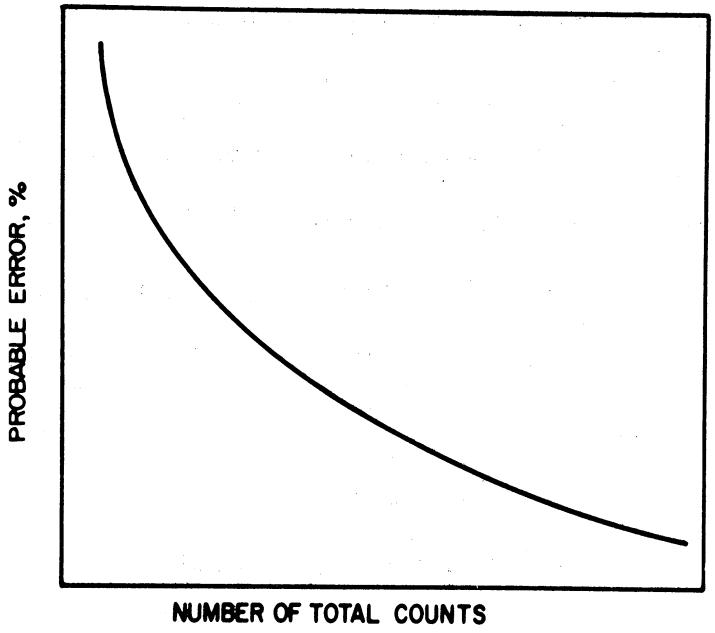

Figure 5.6: Percent Probable Error vs. Total Number of Counts

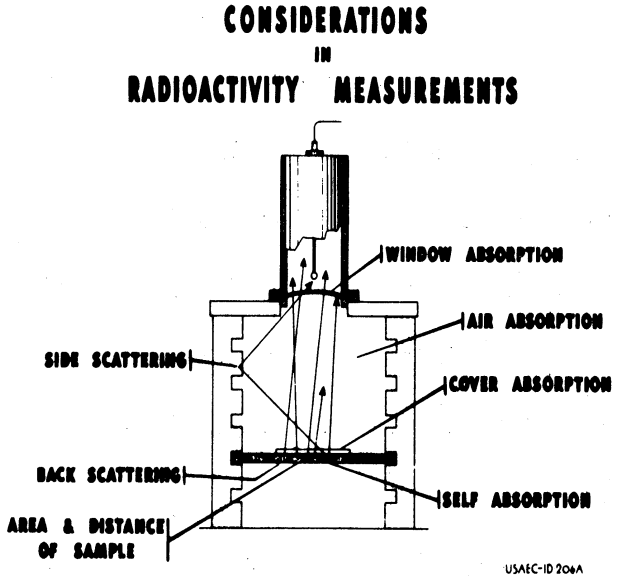

Figure 5.7: Considerations in Radioactivity Measurements

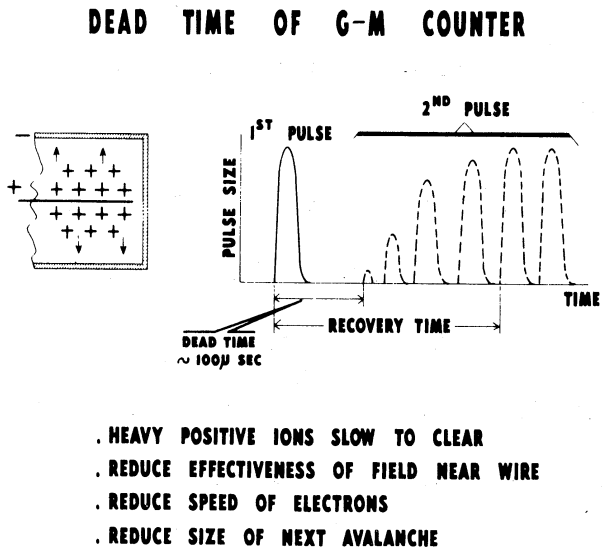

Figure 5.8: Deat Time in a G-M Counter

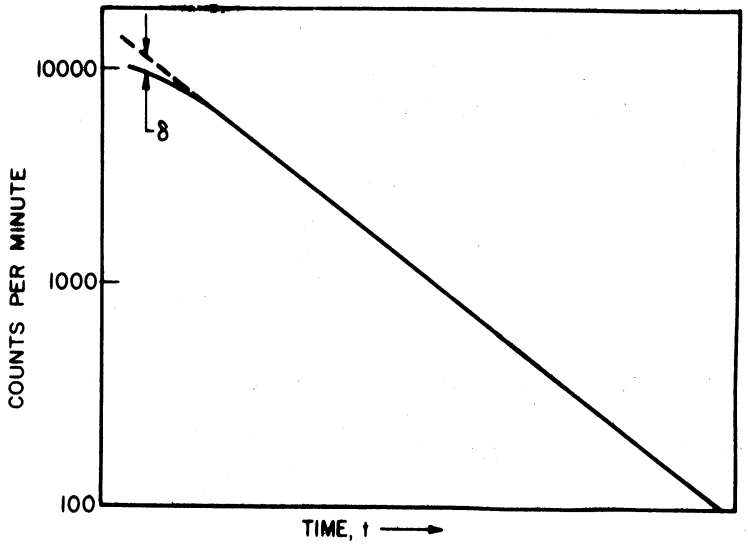

Figure 5.9: Schematic Diagram of Coincidence Losses Due to Dead Time

Referring to Figure 5.9, the difference between the two curves (δ) is the coincidence loss. For usual dead times, of the order of 200 microseconds per count, the coincidence correction is negligible below 4000 counts per minute.

The second method proceeds as follows. If N particles per second pass through the sensitive volume with the production of enough ionization to cause a count, and n particles per second do cause counts, then N-n counts per second are lost. If T (dead time) is time lost per count, then nT is time lost per second and NnT is counts lost per second (5,6).

Therefore,

$$N-n = NnT ,$$

from which

$$N = \frac{n}{1 - nT}$$

Using two sources, each alone and together, and substituting,

$$N_1 = \frac{n_1}{1 - n_1 T} ; \quad N_2 = \frac{n_2}{1 - n_2 T} ; \quad N_1 + N_2 = \frac{n_{12}}{1 - n_{12} T} .$$

Eliminating N_1 and N_2 and solving for T,

$$T = \frac{n_1 + n_2 - n_{12}}{2 n_1 n_2} . \qquad 5.38$$

T is a function of applied voltage, age of tube, operating temperature and electronic circuit elements.

5.12. Geometry

Geometry is defined as that fraction of the particles from a source which start out in the direction of the sensitive volume of the counter (7).

Referring to Figure 5.10, consider a point source (S) being counted through a circular opening (W). The computation is simple, the geometry factor is merely the ratio of the area of the cap intercepted by the opening to the area of the sphere.

$$\text{Area of cap } k = \int_0^A 2\pi \; r \, R d\theta \quad \text{but} \quad r = R \sin\theta$$

$$\therefore \; k = \int_0^A 2\pi \; R^2 \sin\theta d\theta = 2\pi \; R^2 \; (1 - \cos A)$$

$$\text{Area of sphere } K = 4\pi R^2$$

$$\therefore \; g = k/K = \frac{1 - \cos A}{2} \qquad 5.39$$

where g = "geometry"

When the size of the source is not negligible compared with the other dimensions as indicated in Figure 5.11, the function just derived is subjected to an area integration over the area of the source (7,8).

This integration involves an infinite series and yields (7):

$$G = \frac{1}{2}\left[1 - \frac{1}{(1+\beta)^{1/2}} - \frac{3}{8}\cdot\frac{\beta\gamma}{(1+\beta)^{5/2}}\right.$$

$$\left. - \gamma^2\left(-\frac{5}{16}\cdot\frac{\beta}{(1+\beta)^{7/2}} + \frac{35}{64}\cdot\frac{\beta^2}{(1+\beta)^{9/2}}\right)\right.$$

$$\left. - \gamma^3\left(- - -\right)\right] \quad - - - - - \qquad 5.40$$

where G = "geometry" with area integration

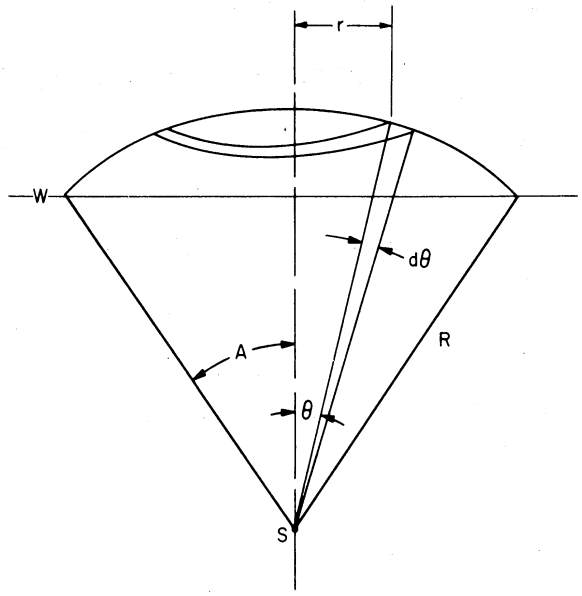

Figure 5.10

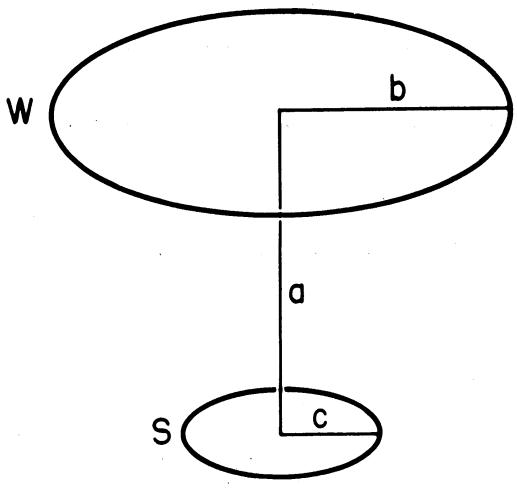

Figure 5.11: Geometry for Source of Radius "c"

where: $\beta = \frac{b^2}{a^2}$ and $\gamma = \frac{c^2}{a^2}$

The series converges if γ is not too large.

If γ is allowed to approach zero, G reduces (7) to:

$$G_o = \frac{1}{2}\left(1 - \frac{1}{(1+\beta)^{1/2}}\right) = \frac{1}{2}(1 - \cos A) = g \qquad 5.41$$

Accurate experimental determination of the influence of geometry depends on the previous determination of several of the other factors listed, which will be discussed.

5.13. Tube efficiency

There exists a finite probability that a particle of the type being measured will pass through the sensitive volume of the counter without causing a count. The probability that a count will be caused by such a particle is defined as tube efficiency (5,6). In accord with present knowledge regarding the discharge mechanism of Geiger tubes, it may be assumed that the formation of one ion pair within the sensitive volume of the tube will produce a discharge. If x is the average number of electrons produced by a particle as it passes through the sensitive volume, the probability that such a particle can pass through producing no electrons is e^{-x}. The probability that a count will be caused by such a particle (tube efficiency) is, therefore, $1 - e^{-x}$.

If specific ionization is known for the particle to be detected, x can be easily evaluated. The specific ionization s is defined as the number of ion pairs per centimeter of path per atmosphere pressure formed by the passing particle. The total average number of electrons so formed then is sLp, where L is the average path length through the counter and p is pressure of the gas in atmospheres. From which (5):

$$E_o = 1 - e^{-sLp} \qquad 5.42$$

Consider the case of an argon-filled counter at 0.1 atmosphere pressure. Then s = 30, and if L = 2 cm,

$$E_o = 1 - e^{-30(2)(0.1)} = 1 - e^{-6} = 99.8\%$$

In general, for accurate work, an E_o of less than 98 percent is not tolerable.

For a given energy particle, s varies linearly with number of electrons per atom of the gas. Thus, to increase efficiency, gases which yield a higher specific ionization are used, and pressure, or the average path length is increased. The simplest way to do the latter is to move the source farther away from the tube.

A straightforward means of measuring E_o involves a triple coincidence circuit. Since efficiency is defined as the ratio of number of observed counts per unit time to the number of ionizing particles passing through the sensitive volume of the tube in that time (e.g., $E = N_o/n$), one can state that, for a triple coincidence circuit,

$$E_o = E_1 E_2 E_3 = N_t/n \qquad 5.43$$

E_1, E_2, E_3 are the respective efficiencies of the individual tubes and N_t is the observed counting rate. If the center tube is then disconnected and left in place,

$$E = E_1 E_3 = N_d/n \ , \qquad 5.44$$

where N_d is the observed counting rate.

From Eqs. 5.43 and 5.44:

$$E_2 = N/N_d \qquad 5.45$$

5.14. Process efficiency

Inefficiencies in sample preparation and in the counting process must be known and reproducible for accurate absolute counting. Some typical inefficiencies are: (i) adsorption on glassware during sample preparation, (ii) loss of volatile components during evaporation, (iii) spattering during evaporation, (iv) and lateral shifting of the source during a series of counts. In the case of counting in which the aim is to measure relative counting rates, these inefficiencies need not be considered if both the unknown and the standard are prepared and counted in the same manner.

Losses due to adsorption may often be kept to a negligible amount by techniques such as acidification of the solution, by repeating rinsings of glassware after each operation, and by the addition of carrier (nonradioactive isotope of the same element). The loss of volatile components is inevitable in evaporation processes, but it may be estimated by chemical or radiological survey of the escaping gas and often may be minimized by the addition of suitable chemicals. Spattering is best kept at a minimum by very slow evaporation and may be estimated by a radiological survey of the area surrounding the evaporating specimen.

Lateral shifting from the center has the effect of reducing the angle subtended at each point of the source by the window. The magnitude of the effect is best determined experimentally for a particular counting arrangement. Figure 5.12 shows some typical results of displacement from the center (7).

When an absorption curve is taken with the absorbers near the source, a maximum will appear at the early portion of the curve. The effect increases with the atomic number of the absorber, and also increases as the absorber is brought nearer the source. This is called forescatter (8).

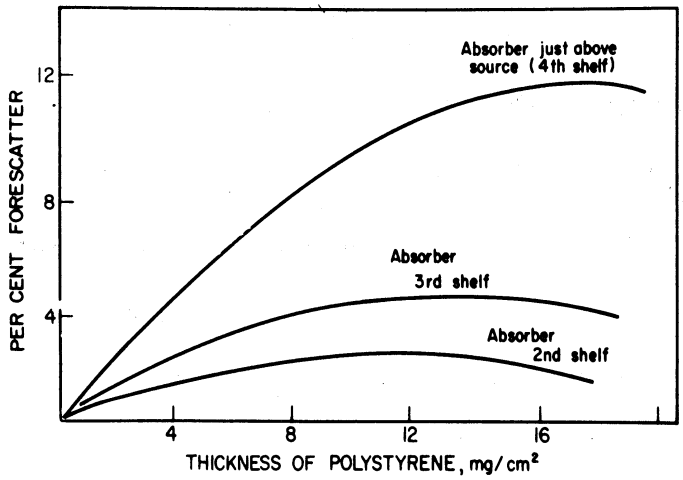

Figure 5.13: Percent Forescattering As Determined with Polystyrene

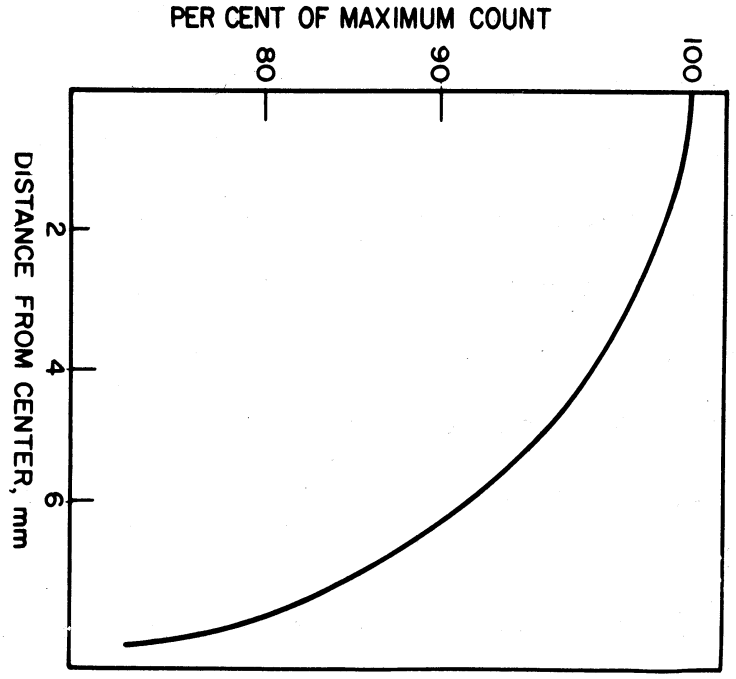

Figure 5.12: Effect of Asymmetry on Efficiency of Counting

Polystyrene, which has about the same atomic number as air, can be used to make an estimate of forescattering due to the air between source and window. In this procedure successive thicknesses of polystyrene film are inserted at various positions between source and window. The percent of counting increase over the count with no polystyrene is plotted against film thickness in Figure 5.13.

The initial slope of these curves is a measure of percentage increase per unit thickness and gives the differential scattering effect for each position. An integration of this differential scattering effect between source and window gives an estimate of the forescatter factor due to the air thickness. This factor increases with source-to-window distance and decreases with energy, and varies for usual counting conditions from 1.001 to 1.060. Obviously the effect is best minimized by having absorbers as close as possible to the tube.

5.16. Backscatter

The counting rate has been found to depend on the backing upon which a source rests. A measure of the effect may be obtained by comparison with the counting rate of a source backed by a film of the order of 50 micrograms/cm^2, for which the backscatter factor is effectively unity. As polystyrene film was added, the factor was found to go up to 1.01 -1.05. The factor increases with increasing energy and with increasing atomic number of backing material. Figure 5.14 shows the variation of backscattered radiation as a function of atomic number and energy (8).

Figure 5.15 illustrates how the backscatter coefficient approaches its maximum value with the addition of backing material (8).

The maximum value of backscatter coefficient, as approached asymptotically in Figure 5.15, is referred to as saturation backscatter. It

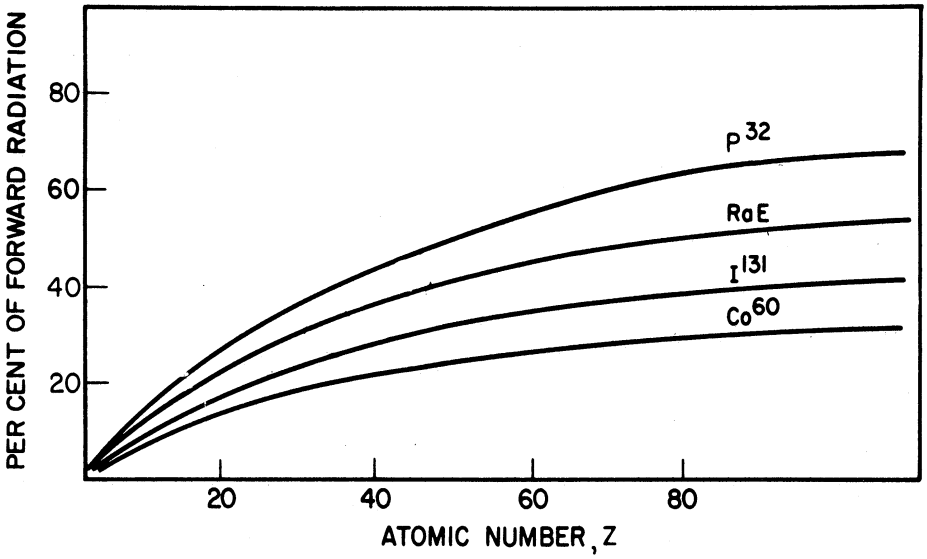

Figure 5.14: Backscatter as a Function of Atomic Number and Energy of Radiation

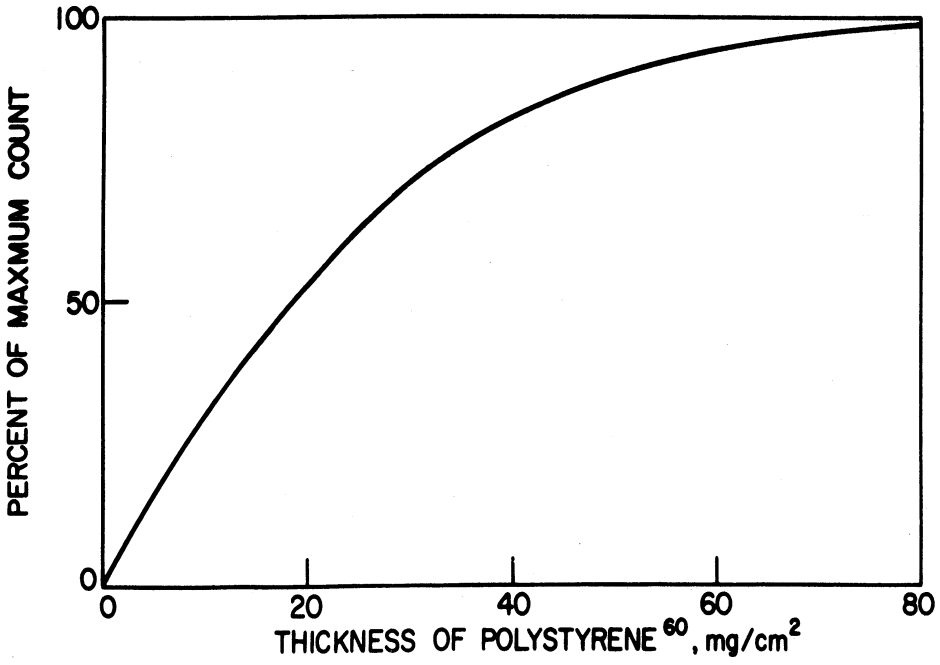

Figure 5.15: Saturation Backscatter

is characteristic for a specific energy and backing material. The value of the coefficient varies from 1.1 for paper to 1.8 for platinum.

An additional contribution to backscatter is presented by the source support structure and the inner walls and floor of the lead shield. To measure this effect, a tube and a source support structure of negligible mass were arranged and the various components of a typical counting mechanism brought to their normal positions. The integrated effect upon counting rate was taken to be the contribution to backscatter due to housing alone. It was determined experimentally that this factor differs appreciably from unity only on shelves near the floor of the housing. In this case, the factor had values as high as 1.10.

5.17. Self-scatter

When the source is thick and the radiation from a point within is considered, it is obvious that both fore- and backscatter by the source, itself are involved. The magnitudes of the two effects can be estimated, if the average atomic number is known, from the work of the two previous sections. In actual experimental practice, however, these are extremely difficult to measure separately. Their effects are often lumped into measurements of self-absorption.

5.18. Self-absorption

As the source thickness is increased, absorption within the source material itself assumes importance. In general, the self-absorption factor would merely be the ratio of counting rate for the thick sample to counting rate for a source of zero thickness. There are two experimental approaches to this measurement. In one case, one prepares sources of varying thicknesses containing the same amount of radioactive material. The resulting curves are similar to the usual absorption curve, as

indicated in Figure 5.16. The slight downward concavity at low sample thickness is the same phenomenon exhibited at low absorbers of forescatter. The self-absorption coefficient, of course, can be read directly from the ordinate for the particular element being studied at the sample thickness involved.

In the other case, samples of equal specific activity but varying sample weights are prepared and counted. For samples of zero thickness, the self-absorption coefficient, of course, is unity. This is a very desirable state of affairs, but is unattainable in general practice. Another simple situation occurs when the source is thick compared with the range of the beta particles involved. Such a sample is called "infinitely thick." In this case, specific activity is proportional to the radiation emitted per square centimeter of surface. An advantage of using samples of infinite thickness is that, for a particular particle energy and absorber, specific activity is directly measurable. Also, the larger mass of sample material is more precisely measurable to exacting degrees of precision. It is advisable for such measurements to have a large quantity of radioactive material, since only a small fraction of the beta-particles originating in the source can be detected. The quantities are, however, not always available.

In the region of absorber thickness between zero and infinite thickness (approximately):

$$dA_m \cong e^{-x/\mu}\, dA_t \quad \text{where} \quad dA_t = \alpha \cap dx$$

(The contribution of each additional increment of thickness).

$$A_m = \int_c^x \alpha \cap e^{-x/\mu}\, dx = \alpha \cap \mu\, (1 - e^{-x/\mu})$$

$$\frac{A_m}{A_t} = \frac{1 - e^{-x/\mu}}{x/\mu} \qquad 5.46$$

where A_m = measured disintegration rate

A_t = actual disintegration rate

σ = specific activity

x = thickness of sample

μ = absorption coefficient (mg/cm^2)

Ω = surface area of sample.

This relation, of course, must be consistent both as x approaches zero and as x exceeds particle range. In the former case:

$$\text{at} \quad x = 0 , \qquad A_m = 0 , \qquad A_t = 0 \tag{5.47}$$

Since the specific activity is constant, the count must go to zero with decreasing thickness. In the latter case:

$$\lim_{x \to \infty} \frac{A_m}{A_t} = \frac{}{x_\infty} = \bar{R} \tag{5.48}$$

where R = range.

Making x greater than R obviously will have no further effect upon A_m/A_t. Increasing the energy will tend both to increase particle range and decrease the absorption coefficient, which gives the expected reduction in the self-absorption coefficient. Increasing atomic number of the absorber, on the other hand, will tend to increase the absorption coefficient and thus increase the self-absorption.

5.14. Window and air absorption

The magnitude of the factor for absorption in the air and in the tube window is evaluated by extrapolation of an aluminum absorption curve to zero absorber, as shown in Figure 5.17.

The ratio of counts under experimental conditions to counts for zero absorber is the factor for air and window absorption. It is essential

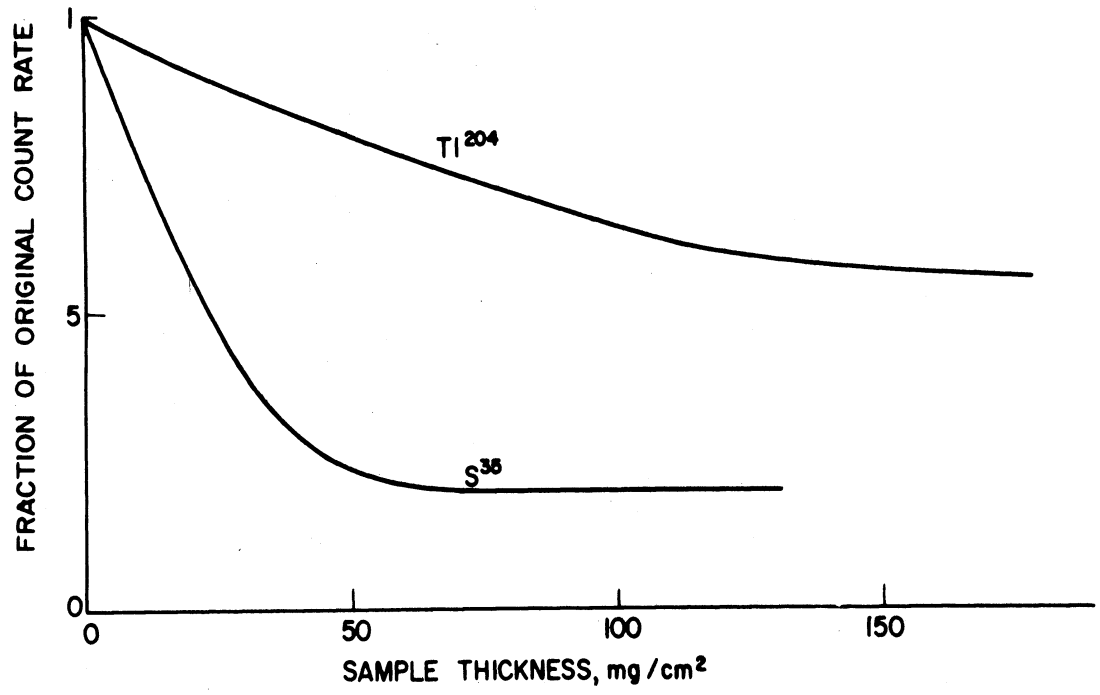

Figure 5.16: Self-Absorption

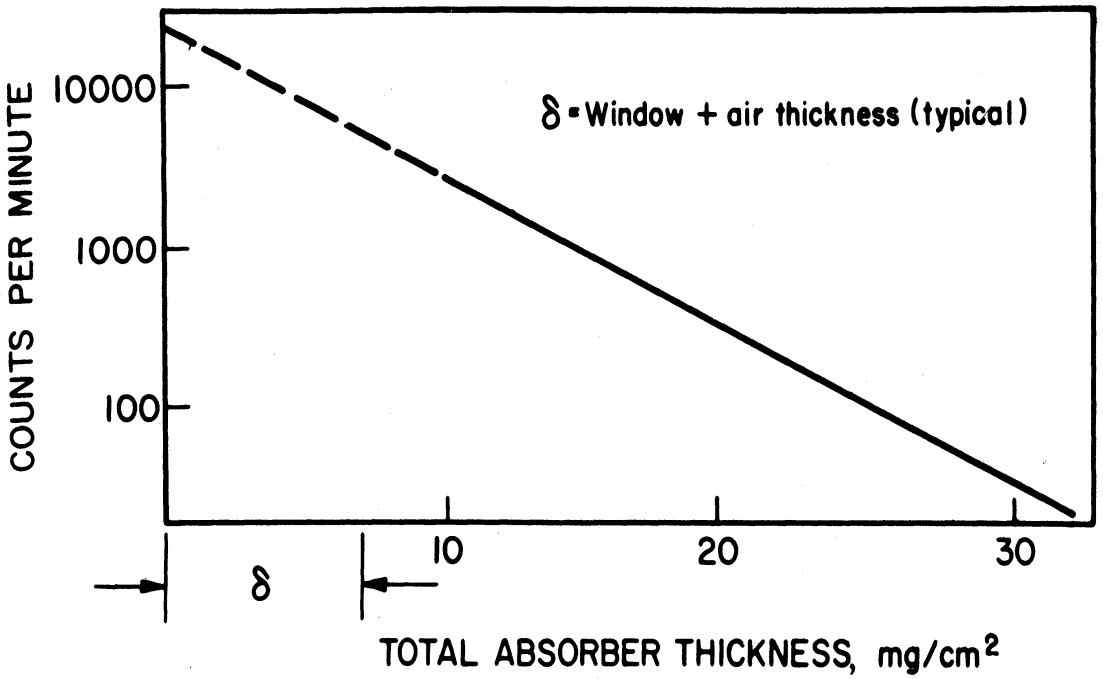

Figure 5.17: Absorption in Air and Window

that very high total counts be used in the low absorption region of the curve in order to avoid extrapolation errors.

This linear extrapolation is sound since, for most beta particles, absorber thicknesses of the order of 6 to 10 mg/cm^2 are on the linear portion of the curve. This, of course assumes that forescatter has been minimized. For a rigorous measurement of low-energy particles, such as from carbon-14, air and window absorption must be considerably reduced.

5.20. Energy

The dependence of overall efficiency on energy is not direct, but shows itself rather in the energy dependence of the various factors previously discussed. Experimentally, however, overall efficiency is known to vary with energy. At energies greater than 1 Mev this variation is slight, but at lower energies the overall efficiency falls sharply. This is primarily due to the increasing effect of window and air absorption. As low energies are approached, there will finally appear a critical energy, below which no counts can be recorded. This "threshold" energy will vary with window and air thicknesses.

Of the foregoing, the following are demonstrably energy-dependent:

tube efficiency -- increasing energy means greater velocities and therefore less specific ionization and reduced efficiency.

forescattering -- increasing energy increases the forward momentum of the particles and thereby reduces the effect.

backscattering -- increasing energy enables more of the backscattered particles to enter the counter and increases the apparent effect.

self-scattering -- combination of two previous effects.

absorption -- increasing energy reduces the probability of interaction and reduces absorption effects.

In the case of assaying techniques, it is generally possible to make a precise determination without a detailed knowledge of the foregoing factors. In most such techniques, energy and sample weight must be independent variables.

In order to determine overall efficiency as a function of energy and sample weight, however, it is possible to hold other factors constant. If standards of the same energy as the unknown are prepared in the same way on the same backing and counted in the same counter for roughly equal total counts, then the only corrections which need be made are those due to energy and sample thickness or weight variation as shown in Figures 5.18 and 5.19, respectively (9).

5.21. Relative importance of correction factors in beta counting

The geometry factor is always important since it describes the maximum percentage of the total number of particles which can be counted. It varies from approximately 50 percent for a windowless flow counter to values ranging from about 30 percent to 1 percent or less for end window counters.

The absorption factor may vary for a thin window (1.8 mg/cm^2) tube from approximately 1.05 for energetic betas, as from phosphorus-32, to as high as 1.2 or 1.3 for weak betas, such as from carbon-14. With thicker windows or longer air paths, the absorption factor may be much higher for weak beta emitters. Similarly, the effects of self-absorption become appreciable with the weak beta emitters.

The information derived from most experiments is the relative disintegration rates or activities between samples. The efficiency can be made quite high, approaching 100 percent for gamma rays with a scintillation detector and suitable arrangements of phosphor and source. The

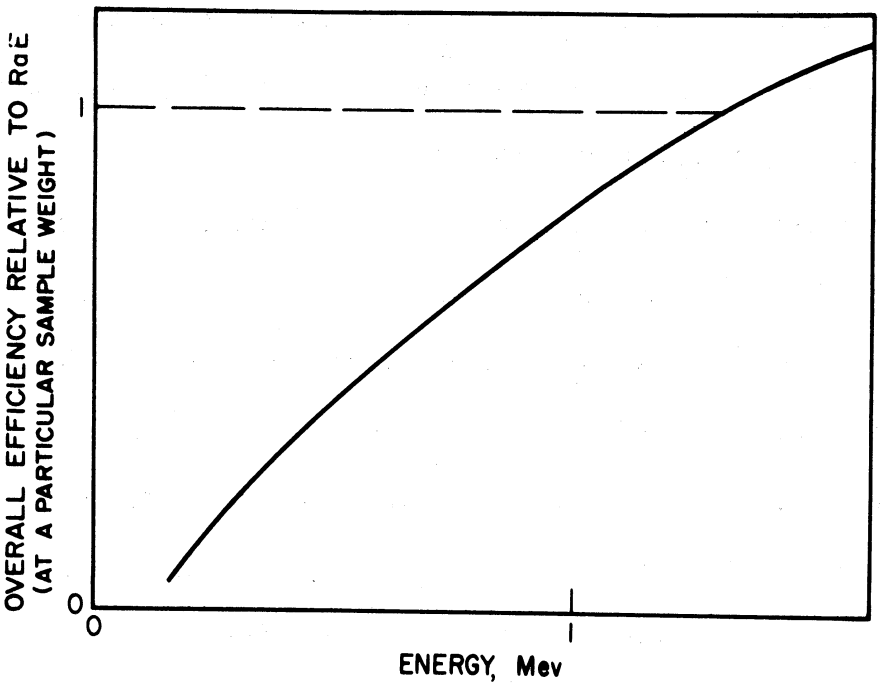

Figure 5.18: Effect of Energy on Beta Counting

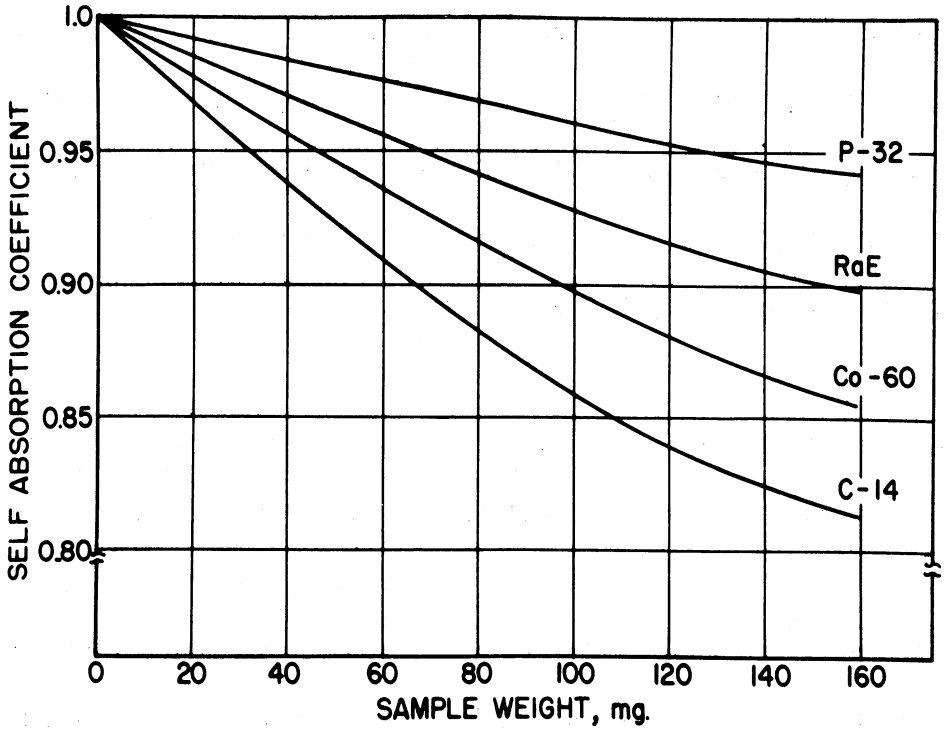

Figure 5.19: Effect of Sample Weight on Self-Absorption Coefficient in Beta Counting

scintillation detector can usually be made much more efficient for the detection of gammas than can the Geiger counter. In each case the geometry will depend on the physical arrangement used.

For relative measurements, all the correction factors need not be known if they can be kept constant. This means in all cases using a fixed geometry and mounting all the samples in the same way. In the case of the weak beta emitters, one must be sure that all the samples are of the same thickness (preferably of infinite thickness) and in the same chemical form since the self-absorption factor will depend on the density of the material also. For example, in carbon-14 tracer experiments it is quite common to convert all samples to barium carbonate before counting.

5.22. The counting of gamma emitters

G-M counters can be used for gamma emitters, but their efficiency is very low (around 1 percent) compared to their high efficiency for betas. Nevertheless, when the activity levels are high enough, G-M tubes are used. Special tubes have been designed incorporating high density plates made of bismuth metal within the counting volume in order to increase the gamma interaction probability. Such tubes have efficiencies as high as 4 or 5 percent.

If it is necessary, or expeditious, to use an ordinary Geiger counting tube as a gamma detector, then the following information may be helpful.

If it is assumed that no photons enter the counting volume except through the thin window and that the effect of scattering on counting rate may be neglected (57):

$$c/m = E\ (d/m) = g\ (\alpha)\ (\beta)\ (3.7 \times 10^7 \times 60)\ E_o \qquad 5.49$$

where E = overall efficiency (p. 5.21)

g = geometrical factor (eq. 5.39)

α = number of millicuries

β = number of photons per disintegration

E_o = tube efficiency (Eq. 5.42).

If it is assumed that tube efficiency for gamma counting is linearly related to photon energy, ξ (58):

$$E_o = 0.0069\xi \qquad 5.50$$

and that

$$\beta = 1 ,$$

the calculated counting rate is conveniently plotted in Figure 5.20 as a function of the ratio of source to counter distance to counter radius (cot A from Figure 5.10).

If a counting sample is so thick that self-absorption must be considered, but not thick enough to introduce a significant variation in the geometrical factor "g" throughout the sample thickness, the following simple correction can be made (57):

$$\frac{N}{N_1} = \frac{1 - e^{-\mu X_o}}{\mu X_o} \qquad 5.51$$

where N_o = counting rate with no absorption

N = counting rate with absorption correction

μ = linear absorption coefficient for the sample medium and photo energy

and X_o = sample thickness.

For greater efficiency a gamma scintillation counter is often used. These counters usually have gamma efficiencies of 20 - 50 percent. The high efficiency results both from the high densities of some phosphors that are available and from the large possible detecting volumes that can

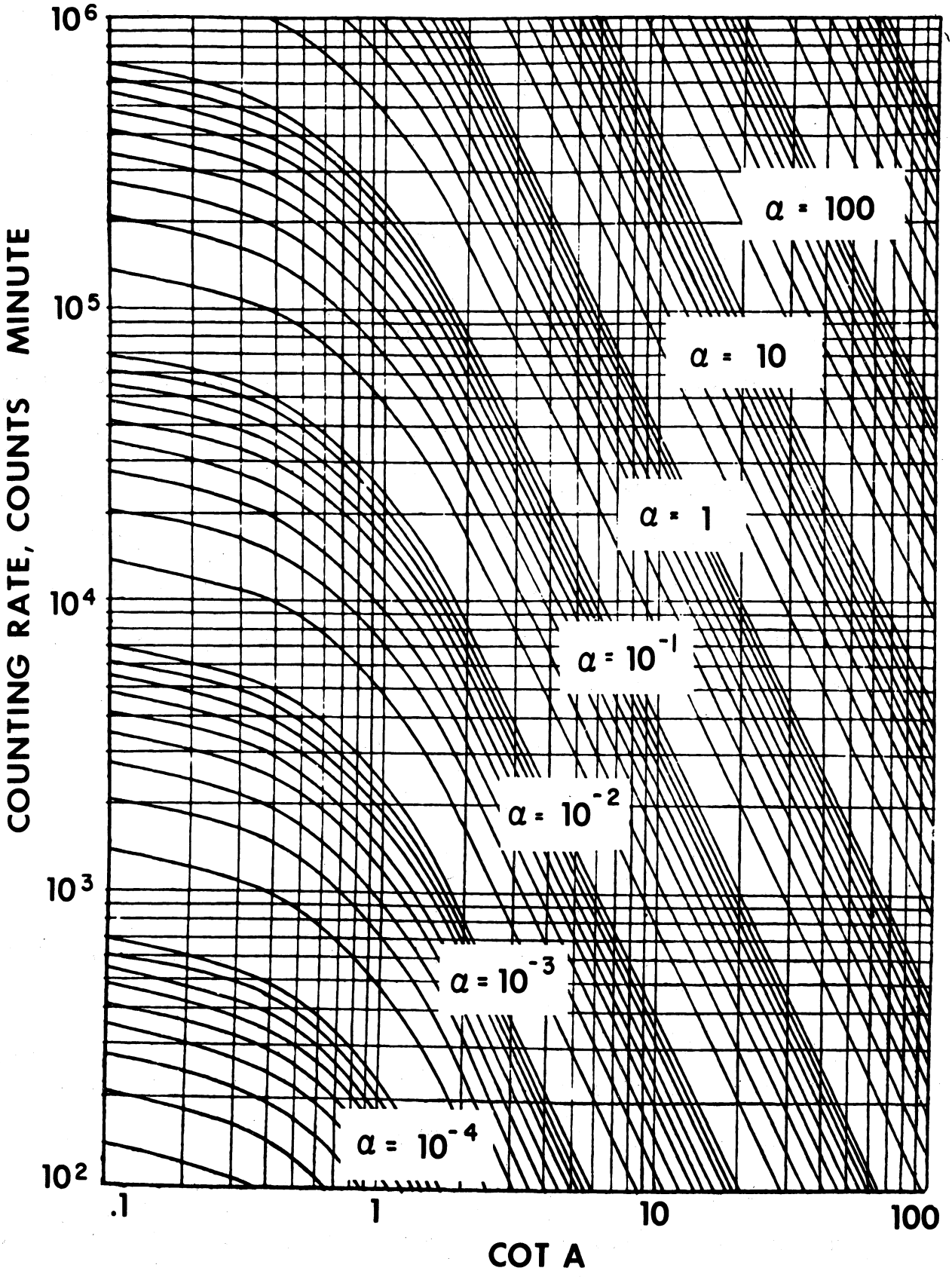
COUNTING RATE, COUNTS MINUTE
10^6
10^5
10^4
10^3
10^2
$\alpha = 100$
$\alpha = 10$
$\alpha = 1$
$\alpha = 10^{-1}$
$\alpha = 10^{-2}$
$\alpha = 10^{-3}$
$\alpha = 10^{-4}$
.1
1
10
100
COT A

Figure 5.20

be used. The latter point is particularly well illustrated by the plastic and liquid scintillators that have been devised for use in well-type counters in which the source is nearly surrounded by the phosphor. High counting rates with minimum dead time losses are achieved by using phosphors with very short light pulses such as stilbene which has a light pulse decay constant of about 10^{-8} seconds. The resolving time of the counter can thus be made quite low.

The most commonly used gamma counter is the well-type scintillation counter. It has the advantage of good gamma efficiency and excellent geometry. The gamma scintillation counter has the additional advantage in that it is capable of energy discrimination, i.e., it can be used in a gamma spectrometer system to distinguish one isotope from another.

The sample preparation is much simpler for gamma emitters than for beta emitters since in most cases absorption and self-absorption are negligible. This means that usually there is no problem in regard to sample thickness, chemical form, or density.

Absolute gamma counting is usually done by comparison with a known standard of the same isotope or some standard with a long half-life which has a similar gamma spectrum.

5.23. Counting alpha particles

The efficiency of scintillation detectors may be made very nearly 100 percent for alphas and for betas with energies of about 100 kev or more. However, owing to their very low penetrating power, alpha particles are generally counted in a windowless flow counter, operated either in the G-M or proportional region, or with some form of ionization chamber.

Alpha emitters are rarely used in tracer experiments. The only elements having alpha-emitting isotopes are polonium, thorium, uranium, radium, and elements of atomic number 206 and higher.

Additional information on counting statistics is given in References 10 and 11 and on counting in general in References 13-56.

Chapter 5

References

1. Kerr, W., "Nuclear Engineering Measurement" in Nuclear Reactors and Radiations in Industry, 1, The University of Michigan, Ann Arbor, Mich., 1956.

2. Nichols, H. and Rauch, L. L. "Engineering Measurements and Instrumentation," Automatic Control Course Notes, The University of Michigan, Ann Arbor, Mich., June, 1955.

3. Feller, W., "An Introduction to Probability Theory and Its Applications," John Wiley and Sons, Inc., N.Y., 1951.

4. Loevinger, R., and Berman, M., "The Efficiency Criteria in Radioactivity Counters," Nucleonics, 9, No. 1, 26, 1951.

5. Korff, S., "Electron and Nuclear Counters," D. Van Nostrand, Co., Inc., N.Y., 1946.

6. Hoag, J. B., and Korff, S., "Electron and Nuclear Physics," D. Van Nostrand, Co., Inc., N.Y., 1928.

7. Burtt, B., "Absolute Beta Counting," Nucleonics, 5, No. 2, 28, 1949.

8. Zumwalt, L. R., "Absolute Beta Counting Using End Window Geiger-Müller Counters and Experimental Data on Beta-particle Scattering Effects," AECU-567, Oak Ridge National Laboratory, Oak Ridge, Tenn. Sept. 14, 1949.

9. Cowan, F. and Nehemias, J., "Sensitivity of the Evaporation Method of Liquid Waste Monitoring," Nucleonics, 7, No. 5, 39, 1950.

10. Shaw, E. N., "Statistics of Radiation Measurements," Nuclear Engng., 1, No. 4, 152, 1956.

11. Fry, T. C., "Probability and Its Engineering Uses," D. Van Nostrand Co., Inc., N.Y., 1928.

12. Magee, K. W., Austronic Engineering Laboratories, Melbourne, Australia, unpublished.

13. Lorenz, E., Weikel, J. and Norten, S. G., "A Counting-Plate and Frequency Meter," Rev. of Sci. Instrum., 17, 276, 1946.

14. Kip, A., Bousquet, A., Evans, R. and Tuttle, W., "The Design and Operation of an Improved Counting-Rate Meter," ibid., 17, 323, 1946.

15. Schultz, H. L., "A Frequency Meter for Random and Uniformly Spaced Pulses," ibid., 18, 223, 1947.

16. Elmore, W. C., "Electronics for the Nuclear Physicist - Part III - A Counting-Rate Meter," Nucleonics, 2, No. 4, 43, 1945.

17. Kleopper, R. M. and Hoecker, F. E., "A Double-Channel Direct-Reading Low-Frequency Counting-Rate Meter and Counting-Rate Comparitor," Rev. sci. Instrum., 20, 17, 1949.

18. Cooke-Yarborough, E. H., "A New Pulse-Amplitude Discriminator Circuit," J. sci. Instrum., 26, 96, 1949.

19. Rose, M. E., and Korff, S. A., "An Investigation of the Properties of Proportional Counters," Phys. Rev., 59, 850, 1941.

20. Simpson, J. A., Jr., "A Precision Alpha-Proportional Counter," Rev. of sci. Instrum., 18, 884, 1947.

21. Corson, D. R. and Wilson, R. R., "Particle and Quantum Counters," Rev. of sci. Instrum., 19, 222, 1948.

22. Putman, J. L., "Analysis of Spurious Counts in Geiger Counters," Proc. phys. Soc., Lond., 61, 312, 1948.

23. Curran, S. C. and Rae, E. R., "Analysis of the Impulses from Geiger-Müller Tubes," Rev. of sci. Instrum., 18, 871, 1947.

24. Jurney, E. T. and Maierschein, F., "The Gamma-Ray Counting Efficiency of a Lead-Cathode G-M Counter," Rev. sci. Instrum., 20, 932, 1949.

25. Miller, W. W., "High Efficiency Counting of C^{14} as CO_2," Science, 105, 123, 1947.

26. Cooke-Yarborough, E. H. and Pulsford, E. W., "A Counting-Rate Meter of High Accuracy," Proc. Instr. elect. Engrs., 98, 191, 1951.

27. Cooke-Yarborough, E. H. and Pulsford, E. W., "An Accurate Logarithmic Counting-Rate Meter covering a Wide Range," ibid., 98, 196, 1951.

28. Rotblat, J., Thomas, D. G. A. and Sayle, E. A., "Scale-of-Hundred Counting Unit," J. sci. Instrum., 25, 33, 1948.

29. Taylor, D., "Count and Time Control in Radiometric Assay," ibid., 81, 1950.

30. Taylor, D., "Radioactivity Surveying and Monitoring Instruments," ibid., 81, 1950.

31. Taylor, D., "Electronic Instrumentation in Atomic Research," Engineering, Lond., 169, 631 and 644, 1950.

32. Greinacher, H., "Spark Counter for Counting Corpuscles and Photons," Helv. phys. acta., 9, 590, 1936.

33. Chang, W. Y., and Rosenblum, S., "A Simple Counting System for Alpha-Ray Spectra and the Energy Distribution of Po Alpha-Particles," Phys. Rev., 67, 222, 1945.

34. Keuffel, J. W., "Parallel-Plate Counters," Rev. sci. Instrum., 20, 202, 1949.

35. Neddermayer, S. H., Althus, E. J., Allison, W. and Schatz, E. R., "The Measurement of Ultra-Short Time Intervals," ibid., 18, 488, 1947.

36. Kallman, H. and Broser, I., "Die Erregung von Phophoren durch schnelle Teilchen," Z. Natur., 2a, 439, and 642, 1947.

37. Jurney, E. T. and Maienschein, F., "The Gamma-ray Counting Efficiency for a Lead Cathode Counter," Rev. sci. Instrum., 20, 942, 1949.

38. Novey, T. B., "Ra DEF Standards of Absolute Activity Measurements," UAC-104, AECU-947, U.S. Atomic Energy Commission, Wash., D.C., May 31, 1949.

39. Pannell, J. H., "Radioactivity Measurement Techniques," Massachusetts Institute of Technology Document, AECD-2270, U.S. Atomic Energy Commission, Wash., D.C., Nov., 1947.

40. Reiss, M., Badrick, F. E., Halkerston, J. M. and White, J. H., "A Method for Continuous Graphic Recording of Radioactive Tracer Concentrations from Various Body Regions Simultaneously," Biochem. J., 44, 255, 1949.

41. Sinclair, W. K. and Newberry, S. P., "A Direct Reading Meter for the Measurement of Highly Active Samples of Gamma-emitting Radioisotope," J. sci, Instrum., 28, 234, 1951.

42. Taylor, D., "The Measurement of Radioisotopes," Methuen and Co., Ltd., Lond., 1951.

43. Brownell, G. L. and Lockhart, H. S., "CO_2 Counter Techniques for C-14 Measurement," Tech. Report No. 30, Lab. for Nucl. Sci. and Engng., Mass. Inst. of Tech., Cambridge, Mass., 1949.

44. Bruceb, M., King, E. R., and Bruner, H. D., "A Method for Standardization of Gallium 72," ORO-44, U.S. Atomic Energy Commission, Wash., D.C., 1951.

45. Burch, G., Reaser, P., Ray, T. and Threefoot, S., "A Method of Preparing Biologic Fluids for Counting Radioelements," J. Lab. clin. Med., 35, 626, 1950.

46. Burch, G., Reaser, P., Threefoot, S. and Ray, T., "A Micropipette for Preparation of Samples for Counting in Radiobiology," J. Lab. clin. Med., 35, 631, 1950.

47. Cannon, C. V., "Conference on Absolute Beta Counting, Preliminary Report No. 8," Nuclear Science Series, National Research Council, U.S. Gov. Print. Office, Wash., D.C., 1950.

48. Feiterlberg, S., "Standardization of Radioactive Iodine," Science, 109, 456, 1949.

49. Freedman, A. J. and Hume, D. N., "A Precision Method of Counting Radioactive Liquid Samples," Science, 112, 461, 1950.

50. Goodwin, W. E. and Harris, W. D., "A Method for the Determination of Small Doses of I-131 in the Urine," J. Lab. clin. Med., 38, 470, 1951.

51. Hill, R. F., Hine, G. J. and Marinelli, L. D., "Quantitative Determination of Gamma Radiation in Biological Research," Amer. J. Roentgenol., 63, 160, 1950.

52. Jordan, W. H., "Detection of Nuclear Particles," Ann. Rev. Nuclear Sci., 1, 207-244, 1952.

53. Keene, J. P., "An Absolute Method for Measuring the Activity of Radioactive Isotopes," Nature, Lond., 166, 601, 1950.

54. Kirby, H. W., "Determination of Tracers in the Presence of their Radioactive Daughters," Analyt. Chem. 24, 1678, 1952.

55. Loevinger, R. and Berman, M., "Efficiency Criteria in Radioactivity Counting," Nucleonics, 9, No. 1, 26, 1951.

56. Mayncord, W. V. and Roberts, J. E., "An Attempt at Precision Measurements of Gamma Rays," Brit, J. Radiol., 10, 365, 1937.

57. Aiba, S., "Effects of Various Geometrical Factors on Gamma-Ray Counting," J. sci. Res. Inst., Tokyo, 49, 144, 1955.

58. Sinclair, W. K., "Comparison of Geiger-Counter and Ion-Chamber Methods of Measuring Gamma Radiation," Nucleonics, 7, No. 6, 21, 1950.

Experimental Techniques in Nuclear Tracer Studies

By A. Gordus

6.1 Introduction (By L. E. Brownell)

In the field of research no other tool since the invention of the microscope has been as useful as radioactive "tracers" in extending knowledge. Many important results have been obtained during the few years that radioactive tracers have been used and many more will be obtained in the years to come. During the past twenty years, and particularly since the last great war, thousands of reports have been published on the use of tracer amounts of radioisotopes for diagnosis in medicine, for control of variables in industrial processes, and for research studies in science. Most of these reports are technical and describe particular applications in specific and widely different fields. It is difficult, therefore, to comprehend the great importance of the new tool of radioactive tracers.

Tracer methods of analysis and research would appear to be "made to order" for studies in the biological fields. The use of tracer techniques has resulted in remarkable progress in the fields of medicine and agriculture. Photosynthesis is one of the most important but has been one of the most baffling processes in the latter field. A better understanding of this process has been possible as a result of the use of tracer methods.

The role of mineral nutrients in the soil has been extensively studied by tracer techniques. It has long been known that plants require appreciable quantities of phosphorus, nitrogen and potassium, together with trace amounts of other elements for normal growth.

In the past the requirements for soil fertilization have been judged largely from crop yields. However, other variables such as rainfall, temperature and disease complicate such procedures. By tracer methods the capacity of the soil to supply a plant nutrient can be determined by adding a labeled fertilizer to the soil as a partial source of the nutrient.

Tracer analysis has been employed in a wide range of fields for solving research problems. In all the branches of pure and applied science, tagged atoms are being used to obtain quantitative and qualitative information. Studies of chemical reactions, rates of diffusion of metals, vulcanization of rubber, and water analysis are some selected examples of fields in which the radioactive isotopes have been used to advantage. Some of the most useful radioisotopes in such research are carbon-14, sulphur-35, and tritium, an isotope of hydrogen.

Tracer analysis has been used for wear studies in the tool and the machinery industries, for the study of mass transfer in the transistor field, for the detection of minute amounts of impurities or residues, for oil prospecting in the petroleum industry, for the determination of the optimum time of mixing in the chemical industry, and for a multitude of other industrial applications.

The principle of analysis using radioactive tracers has received much publicity but the story of G. Hevesy, the originator of the method, may not be as familiar to the average scientific investigator, even though Hevesy received the Nobel award in 1943 for this important contribution to science.

In 1911 Hevesy was working with Rutherford in England where he attempted to separate RaD from lead by chemical means. At that time, it was not known that these two materials were isotopes and therefore could not be separated by chemical means but only by physical means. As a result of these studies Hevesy correctly concluded that RaD participated in every chemical reaction in which lead was involved. In 1913 at the Vienna Institute of Radium, Hevesy used this information to measure the solubility of nearly insoluble lead salts, such as the chromate and sulfide, using lead having some natural radioactivity.

As a result of his studies in the use of radioisotopes in chemical analysis, Hevesy in 1932 proposed the technique of analysis by isotope dilution. Two years later the Joliots reported artificial radioactivity in elements exposed to alpha-particle radiation from natural radioisotopes. This was followed by the development of particle accelerators such as the cyclotron and then the nuclear reactor, which made available new radioisotopes covering the entire range of atomic numbers. This opened the door to the use of the tracer method which became a new tool in the study and analysis of many different systems.

With the availability of a means of producing artificial radioactivity, Hevesy in 1936 also pioneered the development of another tracer technique known as activation analysis. Seaborg and Livingood in 1938 reported studies on the technique of activation analysis. The method of isotope dilution is still the widely used tracer technique, however. Other methods such as reverse isotope dilution, derivative dilution, activation analysis, and autoradiography have greatly increased the range of application of radioactive tracers. Most of these methods are discussed by Hevesy in his book.

6.2 Outline for first three weeks of study (A.A. Gordus)

The first three weeks of the course will be devoted to the discussion and measurement of radiations of various types, i.e., gamma, beta, and alpha.

The following experiments will be performed in the laboratory section during this time.

First Week:

Determination of Plateau
Coincidence Counting

References: (* - Optional)

Overman and Clark,
p. 25-31; 51-61; 84-86*, 259-262; 271-274*

Glasstone,
p. 136-140 (p's 6.25-6.39); 291 (P 11.24); 477
P's 17.9-17.10

Friedlander and Kennedy,

coincidence correction	265-266
determination of	273-274*
coincidence counting	244-245
for disintegration rate measurements	295-296*
in decay scheme studies	284*
coincidence resolving time	245
coincidence spectrometry	246*, 284*
in study of Au^{198} decay	286-287*
coincidence, delayed	141-142, 245
Geiger-Mueller counters,	231-235
computed efficiency of	264-265
dead time of	234
discharge mechanism of	233-234
filling mixtures for,	234
plateau of	233
portable	248
self-quenching	234

Second Week:

Absorption of Radiation

References:

Overman and Clark,
(see previous page)

Friedlander and Kennedy
(op.cit.)

overall combination of above pages
141-142; 197-203; 205-211; 231-235;
244-245; 246*; 248; 264-265; 265-266*;
273-274*; 276; 284*; 286-287*; 292;
294-295; 296*.

6.3 GENERAL LABORATORY RULES FOR NUCLEAR CHEMISTRY

The following rules must be observed in the group to insure efficient and contamination-free laboratories and equipment.

1. All work with radioisotopes is to be done in the hood and not on the bench top. Ratioisotopes are not to be removed from the hood except in the form of mounted samples, stoppered tubes or packaged sources.

2. All samples taken into the counting room must be "tied down" to prevent spread of contamination; solids must be covered with plastic, scotch tape, etc.; tubes of liquid must be stoppered. The outside of these samples must be absolutely free from contamination.

3. For all measurements with the well counter the sample tube must be placed inside a second plastic tube to protect the crystal from contamination. Similarly, extreme care must be used with the scintillation spectrometers. (Crystals cost a lot of money and take a long while to replace!)

4. Extreme care must be taken to guard against contamination of electronic equipment in the counting rooms. Check your hands for contamination before operating the equipment. Be sure prepared standards and samples are properly mounted and safely stored between runs.

5. Radioactive wastes should be accumulated in cartons and jugs inside the hood and then transferred to the waste storage can or cupboard in the laboratory. The Radiation Control Service (RCS) at extension 2592 will pick these wastes up. Radioactive wastes should include any wastes that are possibly contaminated.

6. Gloves are to be used in the hood whenever the hands would contact radioactive materials. Gloves or other possibly contaminated objects are not to be removed from the hot lab.

7. Procedure for cleaning contaminated equipment should include: rinses in the hood, soak in active cleaning solution, and finally wash in an active sink. Materials used to work with high (millicurie) levels of activity must be kept separate from other equipment and so labelled.

8. Glassware and other materials are not to be put back in the general stock drawers or cupboards unless the user is positive that they contain no contamination. When in doubt place with possibly contaminated items.

9. Stock solutions of carriers in plastic bottles are not to be used at the bench. They should serve merely as reservoirs to fill individual dropping bottles with a few ml for use in the hood.

SCALE OF 64

	0	1	2	3	4	5	6	7	8	9
0	00000	00064	00128	00192	00256	00320	00384	00448	00512	00576
1	00640	00704	00768	00832	00896	00960	01024	01088	01152	01216
2	01280	01344	01408	01472	01536	01600	01664	01728	01792	01856
3	01920	01984	02048	02112	02176	02240	02304	02368	02432	02496
4	02560	02624	02688	02752	02816	02880	02944	03008	03072	03136
5	03200	03264	03328	03392	03456	03520	03584	03648	03712	03776
6	03840	03904	03968	04032	04096	04160	04224	04288	04352	04416
7	04480	04544	04608	04672	04736	04800	04864	04928	04992	05056
8	05120	05184	05248	05312	05376	05440	05504	05568	05632	05696
9	05760	05824	05888	05952	06016	06080	06144	06208	06272	06336
10	06400	06464	06528	06592	06656	06720	06784	06848	06912	06976
11	07040	07104	07168	07232	07296	07360	07424	07488	07552	07616
12	07680	07744	07808	07872	07936	08000	08064	08128	08192	08256
13	08320	08384	08448	08512	08576	08640	08704	08768	08832	08896
14	08960	09024	09088	09152	09216	09280	09344	09408	09472	09536
15	09600	09664	09728	09792	09856	09920	09984	10048	10112	10176
16	10240	10304	10368	10432	10496	10560	10624	10688	10752	10816
17	10880	10944	11008	11072	11136	11200	11264	11328	11392	11456
18	11520	11584	11648	11712	11776	11840	11904	11968	12032	12096
19	12160	12224	12288	12352	12416	12480	12544	12608	12672	12736
20	12800	12864	12928	12992	13056	13120	13184	13248	13312	13376
21	13440	13504	13568	13632	13696	13760	13824	13888	13952	14016
22	14080	14144	14208	14272	14336	14400	14464	14528	14592	14656
23	14720	14784	14848	14912	14976	15040	15104	15168	15232	15296
24	15360	15424	15488	15552	15616	15680	15744	15808	15872	15936
25	16000	16064	16128	16192	16256	16320	16384	16448	16512	16576
26	16640	16704	16768	16832	16896	16960	17024	17088	17152	17216
27	17280	17344	17408	17472	17536	17600	17664	17728	17792	17856
28	17920	17984	18048	18112	18176	18240	18304	18368	18432	18496
29	18560	18624	18688	18752	18816	18880	18944	19008	19072	19136
30	19200	19264	19328	19392	19456	19520	19584	19648	19712	19776
31	19840	19904	19968	20032	20096	20160	20224	20288	20352	20416
32	20480	20544	20608	20672	20736	20800	20864	20928	20992	21056
33	21120	21184	21248	21312	21376	21440	21504	21568	21632	21696
34	21760	21824	21888	21952	22016	22080	22144	22208	22272	22336
35	22400	22464	22528	22592	22656	22720	22784	22848	22912	22976
36	23040	23104	23168	23232	23296	23360	23424	23488	23552	23616
37	23680	23744	23808	23872	23936	24000	24064	24128	24192	24256
38	24320	24384	24448	24512	24576	24640	24704	24768	24832	24896
39	24960	25024	25088	25152	25216	25280	25344	25408	25472	25536
40	25600	25664	25728	25792	25856	25920	25984	26048	26112	26176
41	26240	26304	26368	26432	26496	26560	26624	26688	26752	26816
42	26880	26944	27008	27072	27136	27200	27264	27328	27392	27456
43	27520	27584	27648	27712	27776	27840	27904	27968	28032	28096
44	28160	28224	28288	28352	28416	28480	28544	28608	28672	28736
45	28800	28864	28928	28992	29056	29120	29184	29248	29312	29376
46	29440	29504	29568	29632	29696	29760	29824	29888	29952	30016
47	30080	30144	30208	30272	30336	30400	30464	30528	30592	30656
48	30720	30784	30848	30912	30976	31040	31104	31168	31232	31296
49	31360	31424	31488	31552	31616	31680	31744	31808	31872	31936

	0	1	2	3	4	5	6	7	8	9
50	32000	32064	32128	32192	32256	32320	32384	32448	32512	32576
51	32640	32704	32768	32832	32896	32960	33024	33088	33152	33216
52	33280	33344	33408	33472	33536	33600	33664	33728	33792	33856
53	33920	33984	34048	34112	34176	34240	34304	34368	34432	34496
54	34560	34624	34688	34752	34816	34880	34944	35008	35072	35136
55	35200	35264	35328	35392	35456	35520	35584	35648	35712	35776
56	35840	35904	35968	56032	56096	56160	56224	56288	56352	56416
57	36480	36544	56608	56672	56736	56800	56864	56928	56992	57056
58	37120	57184	57248	57312	57376	57440	57504	57568	57632	57696
59	37760	57824	57888	57952	38016	78080	78144	78208	78272	78336
60	38400	38464	38528	38592	38656	38720	38784	38848	38912	38976
61	39040	39104	39168	39232	39296	39360	39424	39488	39332	39616
62	39680	39744	39808	39872	39936	40000	40064	40128	40192	40256
63	40320	40384	40448	40512	40576	40640	40704	40768	40832	40896
64	40960	41024	41088	41152	41216	41280	41344	41408	41472	41536
65	41600	41664	41728	41792	41856	41920	41984	42048	42112	42176
66	42240	42304	42368	42432	42496	42560	42624	42688	42752	42816
67	42880	42944	43008	43072	43136	43200	43264	43328	43392	43456
68	43520	43584	43648	43712	43776	43840	43904	43968	44032	44096
69	44160	44224	44288	44352	44416	44480	44544	44608	44672	44736
70	44800	44864	44928	44992	45056	45120	45184	45248	45312	45376
71	45440	45504	45568	45632	45696	45760	45824	45888	45952	46016
72	46080	46144	46208	46272	46336	46400	46464	46528	46592	46656
73	46720	46784	46848	46912	46976	47040	47104	47168	47832	47296
74	47360	47424	47488	47552	47616	47680	47744	47808	47872	47936
75	48000	48064	48128	48192	48256	48320	48384	48448	48512	48576
76	48640	48704	48768	48832	48896	48960	49024	49088	49152	49216
77	49280	49344	49408	49472	49536	49600	49664	49728	49792	49856
78	49920	49984	50048	50112	50176	50240	50304	50368	50432	50496
79	50560	50624	50688	50752	50816	50880	50944	51008	51072	51136
80	51200	51264	51328	51392	51456	51520	51584	51648	51712	51776
81	51840	51904	51968	52032	52096	52160	52224	52288	52352	52416
82	52480	52544	52608	52672	52736	52800	52864	52928	52992	53056
83	53120	53184	53248	53312	53378	53440	53504	53568	53632	53696
84	53760	53824	53888	53952	54016	54080	54144	54208	54272	54336
85	54400	54464	54528	54592	54656	54720	54784	54848	54912	54976
86	55040	55104	55168	55232	55296	55360	55424	55488	55552	55616
87	55680	55744	55808	55872	55936	56000	56064	56128	56192	56256
88	56320	56384	56448	56512	56576	56640	56704	56768	56832	56896
89	56960	57024	57088	57152	57216	57280	57344	57408	57472	57536
90	57600	57664	57728	57792	57856	57920	57984	58048	58112	58176
91	58240	58304	58368	58432	58496	58560	58624	58688	58752	58816
92	58880	58944	59008	59072	59136	59200	59264	59328	59392	59456
93	59520	59584	59648	59712	59776	59840	59904	59968	60032	60096
94	60160	60224	60288	60352	60416	60480	60544	60608	60672	60736
95	60800	60864	60928	60992	61056	61120	61184	61248	61312	61376
96	61440	61504	61568	61632	61696	61760	61824	61888	61952	62016
97	62080	62144	62208	62272	62336	62400	62464	62528	62592	62656
98	62720	62784	62848	62912	62976	63040	63104	63168	63232	63296
99	63360	63424	63488	63552	63616	63680	63744	63808	63872	63936

6.5 Experiment 1. Counter Operation (Adapted from G. Wilkinson)

A. Plateau and operating voltage: In turning on a scaling unit, the master switch is first turned on, with the high voltage knob turned to the "off" position. Scalers are usually left on for some time before use to obtain thermal equilibrium and stable operation. It is of utmost importance that the scaler be allowed to warm up at least one minute before the high voltage is turned on. If this procedure is not followed, the Geiger tube may be damaged by going into discharge. To start operating, the high voltage switch is turned on. The count switch should be on and a radioactive source in the counter. When the high voltage has warmed up, as evidenced by reading of the meter, the voltage is raised slowly until the counter begins to count. This voltage is the "starting voltage", or "threshold", which has a value of about 600-1200 volts. If the counter is counting at more than 15,000 counts per minute (240 scales of 64 or 120 of 128 per minute) the source should be lowered. Geiger tubes are likely to count erratically at rates that are too high.

In order to select a good "operating" voltage at which to count, it is necessary to obtain a "plateau". This is done by taking a series of counts at intervals of 25-50 volts from starting voltage up for 250 or 300 volts and back down again. If the counts are plotted vs. voltage, a curve is obtained which should have a relatively flat portion which extends down to within 50 or 100 volts of starting voltage. The operating voltage should be in the plateau region near its lower end. Usually this means between 75 to 150 volts above the starting voltage.

The operating voltage for a proportional counter is found in a similar way, but there is no sharp starting voltage.

NOTES:

(1) In the chlorine quenched "Amperex" tubes used in these experiments an excessive voltage does no appreciable damage. However, with more conventional counter tubes which are filled with argon plus an organic quenching substance such as alcohol, an excessive voltage will quickly ruin the counting tubes. For such tubes, if the scaler does not begin to register counts by the time the voltage on the tube

has been raised to, say, 1500 volts, check over the connections and ensure that the rest of the apparatus is working.

Plot a graph for the plateau determination as you proceed: you should find that a sharply rising portion is followed by a more or less level 'plateau'. After this, the counting rate will again rise fairly steeply. This region is to be avoided since here the counter tube is fairly rapidly damaged, due to the excessive rate of decomposition of the polyatomic component of the filling gas. In any case this region is useless for accurate work, because of the incipient instability which it represents. Counts in excess of 15,000 per minute should be avoided.

An alcohol quenched counter will not last indefinitely. It should operate satisfactorily for a total of about 10^8 counts. Various changes are likely to occur. The starting voltage usually increases, the background rate increases and the plateau becomes less flat. A plateau which has a slope of 5% or less per 100 volts is good. If the slope is more than 7%, it is bad. A tube that has deteriorated is likely also to display erratic counting as discussed below.

(2) Counter tubes. Some of those provided are of the end-window type, having a thin window of mica sealed to the lower end to permit the entry of reasonably weak beta particles. Please note:

1. The windows are extremely fragile, and should not be handled at all. The tubes cost $35.00 - $50.00 each and are very easily ruined.
2. As normally run, the outer case (cathode) is at ground potential, and the wire (anode) at about 1000-1500 v. positive with respect to ground. A piece of fine copper wire is used for the anode connection: make sure this does not touch any grounded metal. Turn off voltage before handling counter tube since the high voltage could give a very unpleasant shock.

3. At all costs avoid the possibility of radioactivity contaminating the inside of the lead housing, or, even worse, the sets of aluminum absorbing screens. Scrupulous care is called for in preparing and handling sources.
4. Counters should not be left unnecessarily with a source in place, or with the potential on the wire, since this shortens their useful life. It may be desirable at times, however, to leave the potential on the wire to prevent "warm-up" errors. At no time, though, should a sample be left in place when the counting is finished.
5. Remember that the stop-count switch merely connects the scaling stages to the tube so that the discharges can be counted. The tube still "counts" a sample when the count switch is off.
6. If a counter appears not to work at its normal voltage, be cautious in increasing the applied potential, and first check that the fault does not lie in some other part of the circuit of the tube.

B. Counting Techniques

The simple counting of radioactive samples requires a calibration of the counter consisting of (a) taking a plateau and selecting the operating voltage, (b) measuring the dead time. Each sample measurement involves the following steps:

(a) Measurement of the background rate.*
(b) Measurement of the sample-plus-background or "total rate".
(c) Correction of the total rate for dead time.
(d) Subtraction to find the rate due to the sample alone, the "net rate".
(e) Estimation of the probable error in the determination of the net rate.
(f) Correction for day to day change in counter efficiency.

The procedure for sample measurement is then as follows:

(a) Suppose that X_B background counts, say 605, are registered in a time t_B, say 30 minutes. The background rate N_B is

given by the fraction, $N_B = \frac{X_B}{t_B}$.

(b) Suppose also that X_s total counts, say 5261, are registered in a time t_s, say 2 minutes. The total rate is $N_s = X_s/t_s$, in this case 5261/2 = 2630.5 c/m.

(c) The correction for dead time is read from the table which has already been made up for the counter. For the rate of 2630 c/m, it may be 48.2 c/m. This is added to give the corrected total rate, $N'_s = 2630.5 + 48.2 = 2678.7$ c/m.

(d) The net rate M is $N'_s - N_B$ or 2678.7 - 20.2 = 2658.5 c/m.

(e) For rates of ten times background or more, the standard deviation in per cent is given to a sufficient degree of accuracy by the formula $100\sqrt{X_s}$. This formula can be plotted as per cent against total counts to facilitate the determination of the standard deviation.

Estimation of errors for slower counting rates is somewhat more complicated and is discussed later.

---

* It must not be overlooked that Geiger-Müller tubes count at an appreciable rate in the absence of radioactive sources. This rate due to cosmic radiation and natural contamination is called the background, and may be around 30-60 c/m in a clean laboratory. Heavy Pb shields cut the background to 15-25 c/m, and make the tubes nearly insensitive to activity being measured on nearby counters.

(f) The efficiency of counters often changes with time. Thus counts of samples must be normalized by counting a reference standard long-lived source regularly. After both sample and reference counts are corrected for background and resolving time giving M and R c/m, the ratio M/R gives the normalized count. Usually one reference count per 15 minutes is adequate- if variations outside the limits of error do not occur, the reference counts can be averaged over a period of say a day, before using the value for normalizing.

Make a complete measurement of several samples furnished you. Discuss the decay scheme and its relation to the counting rate of each isotope measured.

Experiment 1a. Determination of Counting Rate Losses by Extrapolation of a Decay Curve. (Adapted from G. Wilkinson)

The dead time: After a Geiger counter has counted a particle, there is a short period of time (of the order of 1/3 millisecond) during which no particle can be counted. For this reason, at high rates the count is less than the number of particles entering the sensitive region of the counter. The dead time of the counter may be measured and the total counting rates may be corrected for the loss. The correction varies as the square of the counting rate. The reason for this is that the number of counts lost is proportional to the product of the number of dead intervals and the number of particles which will arrive during a single interval. Each of these factors increases with the counting rate. As an example, if 8 c/m must be added to a rate of 1000 c/m, then 32 c/m must be added to 2000 c/m and 200 c/m must be added to 5000 c/m. A special graph or table is usually made up for correcting counts from each counter when its dead time has been measured . This is a plot of the measured counting rate (abscissa) counts per minute vs. the correction for dead time in counts per minute.

Background rates are low enough that they require no dead time correction. Proportional counters have practically no dead time and so counts made with them usually require no dead time correction.

The coincidence loss or dead time can be determined in several ways. One method outlined below involves the direct determination of counting rate losses by extrapolation of a known decay curve. The second main method is that known as the "split source" method.

Procedure

A source of radioactive material is prepared so that it has a counting rate of about 30,000 c/min.

Place in a suitable counter shelf or, if a solution, in a solution jacket, and start counting. Take a succession of counts at one minute intervals; the best procedure is probably to count for 50 seconds, from each minute , leaving ten seconds for noting the scaler reading. Leave the stopwatch running throughout this experiment, and then plot observed activity against time on a semi-log paper. Draw a straight line fitting it to the lower points on the graph. Plot also the discrepancies at the higher rates of counting,

i.e., extrapolated value minus the observed value, expressed as a percentage of the true (extrapolated) counting rate, as a function of the observed counting rate, and deduce the counter "dead time". Determine the half-life of the material.

If the observed counting rate is R, and the resolving time τ, then the true rate R' is given by $R' = \frac{R}{1 - R\tau}$ (R counts are observed in $1 - R\tau$ second, since $R\tau$ out of each second is 'dead time')

$$\text{so } \frac{R}{R'} = 1 - R\tau$$

$$\frac{R' - R}{R'} = R\tau$$

i.e. slope of % discrepancy vs. R curve $= \tau$

Half-life - determination of

The data obtained in the above section lends itself to the problem of half-life determination. The data for dead time correction was made using a hot sample of an unknown element. The data as collected and plotted above yield directly the half-life of the unknown radioisotope. What is the half-life? Can you determine the isotope involved? What is the equation of its formation and decay assuming bombardment with thermal neutrons from the nuclear reactor?

6.6 Experiment 2

Backscattering

See Special Dangers listed at end before beginning work!!

Nucleons are emitted from radioactive substances in a random manner and only a very small portion of these disintegrations are observed unless special tubes are used which completely surround the sample. The particular spatial arrangement used in measuring a sample with a tube will influence the efficiency of the counting. Also, the material used to hold the sample is very influencial since radiation is easily scattered by matter resulting in an increase in the number of particles actually passing into the counting tube and being observed. This scattering must be controlled if meaningful results are desired.

Scattering has been observed to be a function of spatial arrangement, atomic number of the backing (scattering) material, backing thickness and the energy of the radiation.

To measure these affects, begin by noting the background. Then place a radioactive beta emitter on a shelf such that the counting rate is about 4000 counts per minute. (This number is chosen so that effect of backscattering should be easily observed.) Make all countings for five minutes then take average. Place any absorbers used below the sample so that there is always a constant distance between the sample, backings, upper surface, and tube. One may have to tape additional plates under the first absorber when increasing backing thickness. See Figure 1.

Since scattering is also dependent on the backing's atomic number, try two or more different materials like plastic, copper, lead, aluminum, etc.

Plot a curve of net counts per minute minus background vs. (Z), the atomic number, of scatter for saturated condition (over 250 mg per cm^2 thick).

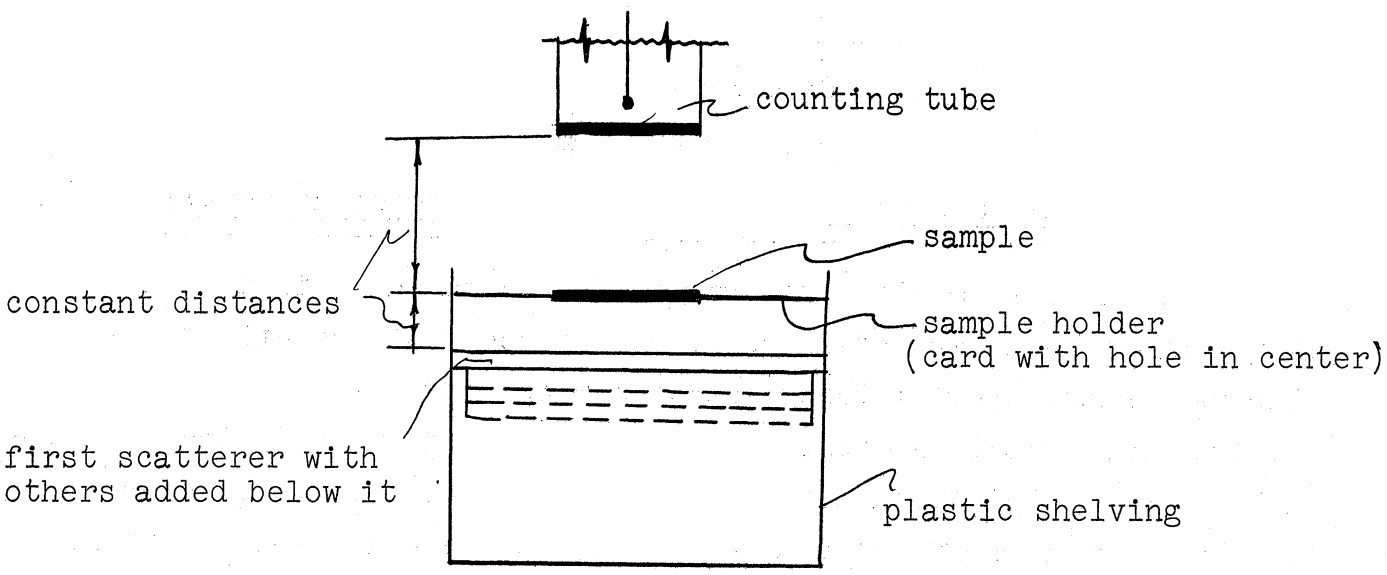

Figure 1

Determine the atomic number of an unknown material by utilizing backscattering. Can you suggest an analytical application for back-scattering?

Plot also the counting rate vs. the thickness of a backing material.

Discuss any ramifications of these facts as they would apply to designing equipment and experimental procedures in radio-tracer analysis.

As time permits. Determine what relationship exists between beta energy and backscatterer by using other beta sources if they are available and measuring the counting rate increase for any infinitely thick scatterer with various energy beta particles.

Table I

source	$t_{\frac{1}{2}}$	particals emitted	energy	
Tl^{204}	4.1y	β-	0.765	
Pm^{147}	2.52y	β-	0.223	
P^{32}	24.4d	β-	0.248	
I^{131}	8.05d	β- (γ's also)	0.608	87%
			0.335	9.3%
Cs^{137}	30.y	β-	0.523	92%
		β-	1.19	8%

Special Dangers

1. Be careful not to contaminate absorbers. (You should record the background before and after all experiments to determine if you have been careless and contaminated the equipment. You will be required to decontaminate your errors!)
2. Be careful not to break or scratch tube window. The windows are thin and puncture destroying the expensive tube very easily. Use extra special care when working on top shelf.

6.7

Experiment 3

(Adapted from G. Wilkinson)

A. Radiochemical Separation of Bi^{210} from Pb^{210}

Lead separated from uranium ores contains a very small amount of the radioactive isotope Pb^{210} ($T_{\frac{1}{2}}$ = 22.2y). This decays through the chain: $_{82}Pb^{210} \xrightarrow[22.2y]{\beta} {}_{83}Bi^{210} \xrightarrow[5.0d]{\beta} {}_{84}Po^{210} \xrightarrow[140d]{\alpha} {}_{82}Pb^{206}$ (stable)

The principle activity measured with a Geiger-Müller counter is that due to the β-rays from Bi^{210} (E_{max} = 1.17 Mev) since the very soft β-rays from Pb^{210} and the α-rays from Po^{210} are readily absorbed. Gamma Radiation from this chain is negligible. The specific activity of the lead is low, however, and it is desirable to isolate the Bi^{210} for counting.

The stock solution of lead contains 0.10 g. of $Pb(NO_3)_2$ and 0.0002 g. of Bi carrier (as the nitrate) per ml. of 0.15 N HNO_3 solution. Pipette 1.0 ml. of the stock solution into a 50 ml. centrifuge tube. Add dropwise a solution of Na_2CO_3 until the precipitate which forms dissolves with difficulty. This operation neutralizes the solution. Dilute the solution with 25 ml. of H_2O and add 0.5 g. $KBrO_3$. Boil the solution and add dropwise 1 M HNO_3 to clear the solution of any cloudy precipitate.

To the hot solution add 50% KBr dropwise until the solution is deep brown. Boil until the Br_2 is removed. A small precipitate of BiOBr should be present. Repeat the KBr addition and boiling until no more precipitate forms and the solution is a clear yellow. Three additions of KBr should be adequate. Centrifuge for about 2 minutes while still hot and decant the supernatant solution. Wash twice with 5-10 ml. H_2O centrifuging for about two minutes each time. Drain thoroughly by inverting the centrifuge tube on a paper towel for about 5 minutes.

Dissolve the precipitate in 0.1 ml. of 1 M HCl, and transfer to source mount with a capillary pipette (drawn from 6-8 mm tubing). Evaporate on special hot plate. Rinse the centrifuge tube with another 0.1 ml. of 1 M HCl and add to the source and evaporate to dryness.

Prepare a second source with 0.10 ml. of the Pb stock solution. Cover both sources with polystyrene films before counting.

Source mounts are prepared by fastening 1 mil polystyrene film over the hole in pre-cut counting cards. To do this put a thin layer of rubber cement over one face of the card and allow to dry throughly (2-3 minutes). Press a 2" square of the polystyrene film on to the card so that it is held taut over the 1" hole. The samples are than counted on the 2nd shelf of the counting unit.

Three sources will be used:
1. your separated Bi^{210} source
2. a stronger Bi^{210} source, which will be available in the counting room.
3. your Pb^{210} -Bi^{210} source

B. Determination of the Al Absorption Curve of Bi^{210} (RaE)

The radiations from a source may be qualitatively identified from the Al absorption curve, and the β energy of prominent constituents identified. It will be found that the absorption curves vary somewhat with the geometrical disposition of source and Al sheet absorbers with respect to the counter window. Accepted techniques involve placement of the source on the second or third shelf and the absorbers on the shelf immediately below the counter window.

Determine the counting rate with Al absorbers of roughly the following weights in mg. per cm_2: 0, 7, 20, 40, 70, 100, 150, 200, 300, 500, 700, 1000. The counting rate of the source will be reduced over 100-fold for the last few absorbers, and it is not feasible to count such a wide range of rates with one source. When the counting rate has fallen below 400 c/m replace your source No. 1 with source No. 2, after carefully determining the ratio of the counting rates of both sources through some convenient absorbers. The portion of the curve obtained with the second source can then be plotted on the same curve with your original source.

Plot your net activity (c/m) as ordinate against weight of absorber (mg/cm_2) as abscissa on 3 cycle semi-log paper. Be sure to

include in the absorber the weight of polystyrene cover film (3 mg.), the weight of the air between sample and counter and the weight of the counter window.

Extrapolate your curve to zero on the abscissa to obtain the counting rate of the sample with zero absorber. Extrapolate the curve to "zero" counting rate to obtain the visual range of Bi^{210} β rays (476 mg/cm_2). From your extrapolated range in Al calculate E_{max} for Bi^{210} β rays. Use this curve to construct a Feather Analyzer (see L. E. Glendenin, p. 17, Nucleonics, 2, January 1948).

Measure sources No. 1 and No. 3 under the same geometrical conditions through approximately 3.0 mg. of absorber and from these two measurements calculate the efficiency of your chemical separation. A slight error will be introduced by the thickness of the $Pb(NO_3)_2$ source. How will this error affect your yield calculated?

If one assumes that the overall counting efficiency for a sample on the second shelf is 4%, calculate specific activity (d/m/mg Pb) of the lead in the stock solution.

Repeat the measurement of aluminum absorption with another radioactive isotope which will be provided. Determine the visual range, and by the use of a Feather analysis the more accurate range. From range-energy relation curves determine the maximum energy of the β particle measured.

Notes on Aluminum Absorption Measurements

(1) Any penetrating radiation which is present (nuclear gamma rays, or secondary electromagnetic radiation -- 'Bremsstrahlung') must be allowed for by extrapolating back to the intensity axis any hard component, and subtracting the extrapolated values from the observed total intensity at each point. This procedure is exactly analogous to that for resolving a complex decay curve, by subtraction of the longer lived component, obtained by extrapolation, from the total activity at any time.

The curve should eventually turn downwards, and go more or less asymptotically to a value of the thickness of aluminum which represents the range of the beta particles. In the case of pure beta-emitters, this end-point will usually be fairly clear, but in the presence of appreciable gamma ray backgrounds, or with weak sources, the uncertainty in the measurements at lower intensities may mask this effect entirely, and a procedure due to Feather must be adopted, in which the more accurate, early part of the absorption curve is compared with that for a 'standard' substance (usually RaE).

(2) The relationship between energy of beta particles and their range is a fairly definite one, although frequently difficult to use on account of uncertainties in the estimation of the range. It is important to 'standardize' each individual counting set up with beta emitters of known energy, before reliance can be placed on any results obtained.

(3) The maximum energy of the β-particle spectrum of a radioactive substance is a valuable parameter for identifying the isotope responsible for the emission. It is only rarely that equipment (magnetic lens spectrograph, for example) for making an absolute measurement of this quantity is available in an ordinary laboratory, and one must therefore have recourse to indirect, comparative methods.

A good measure of the β-particle energy can be obtained by measuring the range of the particles, or, alternatively, their absorption coefficient (or equivalent half-thickness) in some suitable material. That normally chosen is aluminum, since this is about the lightest material readily obtainable in the form of thin foils. Heavier materials result in the production of greater amounts of continuous X-radiation ('Bremsstrahlung'), which remain as a penetrating background when all the β-particles have been absorbed.

To carry out the measurement, increasing thicknesses of aluminum foil are placed in front of the counter window and the counting rate for a constant source is determined. If the source decays significantly during the operation, correction must, of course, be applied. It is most desirable to use a thin source, mounted on a thin backing, and placed so as to minimize reflection of particles into the counter;

in this way one can preserve as far as possible the original energy spectrum. The logarithm of the net β-particle count (after deducting any background due to cosmic rays, γ-rays, or Bremsstrahlung) is plotted against the thickness of aluminum adding an allowance for the thickness of the counter window, and for the stopping power of the air gap between source and counter; 1 cm. of air at N.T.P. is equivalent to 1.29 mg./cm_2.).

From the initial, almost linear, part of this curve, the half-thickness or absorption coefficient may be deduced. For a pure β-emitter, with no γ-ray background present, the range of the β-particles, which is a more significant measure of their maximum energy than the absorption half-thickness, can be obtained by inspection. In the presence of a large γ-ray background, the statistical accuracy of this part of the curve is inevitably poor, and a method due to Feather (Proc. Camb. Phil. Soc., 34, 599. 1938) is frequently used. In this method a substance of known β-particle range is adopted as a reference substance (RaE, with range 0.476 g/cm_2 aluminum is frequently used). Logarithmic plots of the net β count for both RaE and the unknown are then made, and normalized so that both start from the same point on the log; plot (on semi-log paper this involves only the moving of the unknown curve bodily up or down until it coincides with the RaE curve for zero thickness of absorber.)

The known range of RaE βs is then divided into, say, 10 equal steps, and the ordinates which, for RaE, correspond to each of these abscissae are extended to cut the absorption curve for the unknown substance. The thickness of aluminum, X_nR_X, at which the ordinate corresponding to n/10 of the RaE range cuts the unknown curve, gives, when multiplied by 10/n, an estimate of the range of the unknown betas.

If the two absorption curves were identical in shape, this would be an exact relationship and R_X would be equal to $(10/n)x_nR_X$ for all values of (n). In practice this is not necessarily true, but this quantity will become a better approximation to the true range as (n) is increased towards 10. In the limit, for n = 10, the two are

identical, by definition, but this region is often experimentally inaccessible, and one has to rely upon extrapolation from smaller values of (n). One can, in fact, plot the apparent range as a function of (n), obtaining a curve which frequently has the appearance shown here; there is little difficulty in then obtaining quite a reliable value of the range of the betas, without having to carry the actual measurements down into the region where the gamma ray background is too large to permit accurate beta particle measurements.

With some modification, this method may also be used for thick sources, but for this the original paper should be consulted.

In general, the Feather method gives results which are more or less independent of the counting geometry; this will be true also for ranges obtained by visual inspection of absorption curves. In the case of absorption half-thicknesses, however, this is not necessarily true, and it should be borne in mind that the value which one obtains experimentally is, to some extent, dependent on the relative positions of source, absorbers, and detector; and on the nature of the detector (it is clearly somewhat dependent on the way in which the response of the detector varies with β-particle energy). For this reason, quoted values of half-thicknesses should be regarded in a slightly critical light, and not taken to apply, without further checking, to any other particular measuring system.

C. Analysis of γ ray absorption data

The purpose of this experiment is to make a preliminary study of the problem of identifying the gamma radiation from typical radioactive sources by absorption techniques and to make semiquantitative studies of the energy and yield of principal gamma constituents. There will be provided in the laboratory stock solution of the following radioactive systems at ~5μ c/ml:

5.3		
5.3y	Co^{60}	
8.0d	I^{131}	with 0.05 mg. carrier/ml. About 1 mg. of Ag^{+} carrier should be added to the I when it is taken to dryness to prevent volatilization.

12.8d Ba^{140} in equilibrium with 40 h La^{140}.

Each student will select one of these systems for study and will obtain the experimental absorption data on each of the others from a colleague. The report will consist of the β and γ absorption curves of each of the three radioactive systems, plus the graphical analysis, and discussion.

Reported values for the yields and energies of the main β and γ constituents of these radionuclides (Seaborg and Perlman, Table of Isotopes, Rev. Mod. Phys. 20, 585-667 (1948) are:

5.3y Co^{60} simple β-ray specturm of 0.31 Mev followed by two γ-rays in cascade of 1.16 and 1.32 Mev.

8.0d I^{131} 85% β of 0.600 Mev followed by γ of 0.367 Mev; 15% β of .315 Mev followed by α of 0.638 Mev.

12.8d Ba^{140} 75% β of 1.0 Mev and no α, 25% of β of 0.5 Mev. followed by γ of 0.53 Mev.; 40.0h La^{140} (disintegration rate in transient equilibrium is 1.15 times that of Ba^{140} parent) 70% of β = 1.4 Mev., 20% = 0.90 Mev., 10% = 2.12 Mev. and 77% of γ = 1.65 Mev., 12% 0.85 Mev., 6% 0.49 Mev., and 5% 2.3 Mev.

1. β Counting and the β:γ Ratio

A small known aliquot of solution (to give ~200 c/s on the second shelf) will be evaporated on a polystyrene film. The first portion of the absorption curve will be taken (0, 10, 20, 40 mg/cm^2 of added absorber), together with the activity through an Al absorber greater than the range of the hardest β component. This β absorption curve should be analyzed qualitatively to ascertain that it is in agreement with the data reported for the radioactive system. With the aid of this analysis, extrapolate the activity to zero total absorber. Compare this activity to that just beyond the range. This comparison is called the β γ ratio. It is a function of the number and energies of the rays.

Assuming the γ counting efficiency is approximately linear with γ-energy and has a value of 0.5% at 1.0 Mev. compute the β:γ ratio for each of the radioactive systems studied, using the decay schemes

reported above, and neglecting attenuation of γ-ray in the Al absorber used to reach the β range.

2. γ counting and lead absorption curve.

Mount an active sample of the stock activity so that when placed in the bottom shelf of the counter with an aluminum absorber of sufficient thickness to stop all β rays immediately above the sample, the sample counts about 5-8000 c/m.

Try the effect of placing a thin lead absorber (a) directly above the aluminum (b) on the middle shelf (c) as close to the counter as possible.

Explain the variation in counting rates observed.

Keep the sample in the bottom shelf with its aluminum cover; place a second aluminum absorber immediately below the counter window. This second absorber must be thick enough to stop any Compton or photoelectrons generated by the γ rays; calculate this thickness for the maximum γ energy involved. Now place lead absorbers between the aluminum sandwich, plot the activity vs g/cm^2 lead absorber, and estimate the energy of the γ rays from the half thickness-energy curves for γ radiation.

Note: In estimation of γ ray energies by absorption methods very serious errors can occur due to scattering phenomena; the best geometry is to have (1) an unshielded counter well away from scattering materials (2) the active source far away from the counter and its beam will collimated (3) the absorbers fairly close to the counter.

6.8 Experiment No. 4

Radiochemical Separations — Parent-Daughter Decay
Separation of Ce^{144} from Pr^{144} by Precipitation

References: Overman and Clark, Chapter 8 and Experiment 8-6, p. 333.
Writeup by A. S. Newton on "precipitates".

An inactive run should be made on this separation to check the problems involved in the chemical procedure before the active Ce-Pr is used.

The longest lived cerium isotope resulting from the fission of uranium is cerium-144. The decay is as follows:

$$Ce^{144} \xrightarrow[285\ \text{days}]{\beta\text{-}(0.35\ \text{Mev})} Pr^{144} \xrightarrow[17.3\ \text{minutes}]{\beta\text{-}(3.1\ \text{Mev})} Nd^{144}(\text{stable})$$

A small amount of gamma radiation of 0.15, 0.22, and 1.25 Mev is associated with the Pr^{144} decay

The purpose of this experiment is to chemically separate cerium from praseodymium activity, and, on the basis of the buildup and decay characteristics of this parent-daughter equilibrium, to calculate the degree of efficiency with which the separation was carried out. The separation is performed in the presence of carriers of Ce and La by the oxidation of the Ce to the plus four oxidation state followed by precipitation as cerium iodate. The precipitation is fairly complete but may carry with it some of the plus three rare earth ions. Pr can be precipitated later as the hydroxide using lanthanum carrier. Because of the fact that the Pr activity grows in very rapidly, it is necessary that as little time as possible pass between the precipitation of the cerium iodate (zero time, in terms of the separation) and the first counting of Ce-Pr "build-up" sample.

Procedure

Take sufficient of the Ce tracer solution to give between 5000 and 10,000 counts per minute of Pr^{144} (i.e. with aluminum absorber, 100 mg/cm^2, to shield out the Ce^{144} activity) on shelf three of the end-window counter. To this solution, in a 50 ml. centrifuge tube, add 10 mg of Ce carrier and 10 mg of La carrier. Also add 5 ml of conc. HNO_3 and 2 ml of 0.5 M $NaBrO_3$. Allow two minutes for reaction.

(Cerium is oxidized rapidly under these conditions, more rapidly and smoothly than with the use of $KClO_3$ in boiling HNO_3.) Add 20 ml of 0.35 M HIO_3 (note the precise time-to-the second) stir, and let stand for two minutes. Centrifuge. Transfer the supernatant solution to a spare tube. Wash the precipitate twice with 1 M HNO_3 plus a little HIO_3 and add the wash solutions to the supernatant solution. Slurry the precipitate in a small volume of water and mount on filter paper according to the instructions of Newton. Do not bother at this time to dry completely and weigh the sample. Instead, rinse with a few ml of alcohol and evacuate rapidly to dryness.

Mount the filter paper in the center of a mounting card and cover with cellophane or mylar film. Interpose an aluminum absorber to remove the Ce^{144} beta rays. Take as many one-half minute counts as possible until about 20 minutes since "zero time", (the time of separation). Equilibrium between the parent and daughter will occur about one to 1.5 hours after zero time. At this time, take a series of counts to determine the activity of daughter in equilibrium.

As soon as the initial "build-up" activity has been determined (i.e. about 20 minutes after zero time) carry out an isolation of the Pr activity removed in the precipitation process. Take a known fraction or all of the supernates plus washings containing the Pr activity. Neutralize this with NH_4OH, bring to a boil to coagulate $La(OH)_3$-$Pr(OH)_3$ precipitates, centrifuge in a 50 ml tube, and wash with two portions of slightly alkaline solution. Collect the precipitate, evacuate rapidly to dryness, mount, and count. Measure the decay curve of this Pr fraction using the absorber for the Ce^{144} activity.

Conclusions:

Calculate the percent Pr^{144} contamination in the separated Ce as well as the percent Ce^{144} contamination in the separated Pr. To obtain these data the following calculation should be performed.

1. Utilize the parent-daughter relation:

$$C_B = (C_B^\circ)_{extrap}(e^{-\lambda_A t} - e^{-\lambda_B t}) + C_B^\circ e^{-\lambda_B t}$$

Let us assume that build-up counts of one-half minute duration are recorded. The observed activity, corrected for background and coincidence counting corrections, is multiplied by two to yield a value of the activity in counts per minute. The time, t, relative to the zero time at which any of the one-half minute counts were taken is simply the mid-point of the count. These then are the observed values, C_B. $(C_B^\circ)_{extrapolated}$ is the average observed activity of the daughter at equilibrium, since the half-life of the parent is very long relative to the time at which the counts were taken with respect to zero-time. Refer to Figure 1. For each of these build-up counts, a value of C_B° may be calculated. Due to the fact that the calculation will involve the subtraction of two large values, and the numerical difference will become smaller as the time since separation becomes larger, thus, in general resulting in a greater accuracy associated with the earlier counts, it is probably worthwhile assigning weighting factors to the various calculated values of C_B° before the average value is computed.

The percent Pr^{144} contamination in the separated Ce is simply:

$$100 \times (C_B^\circ/(C_B^\circ)_{extrap})$$

2. Utilize the data obtained for the decay of the Pr^{144} activity. If no Ce^{144} was present, a straight-line semi-log plot should be obtained. The presence of any Ce^{144} will be evidenced through its daughter activity after the separated Pr activity has decayed away. Determine if any Ce was present in the Pr fraction. See Figure 2.

3. If the two samples are counted on the same shelf, if the samples are counted in an identical manner, and if none of the activity was lost in either sample preparation, then the value of the separated Pr^{144} activity, extrapolated back to zero time, plus the calculated value of C_B° should equal $(C_B^\circ)_{extrap}$.

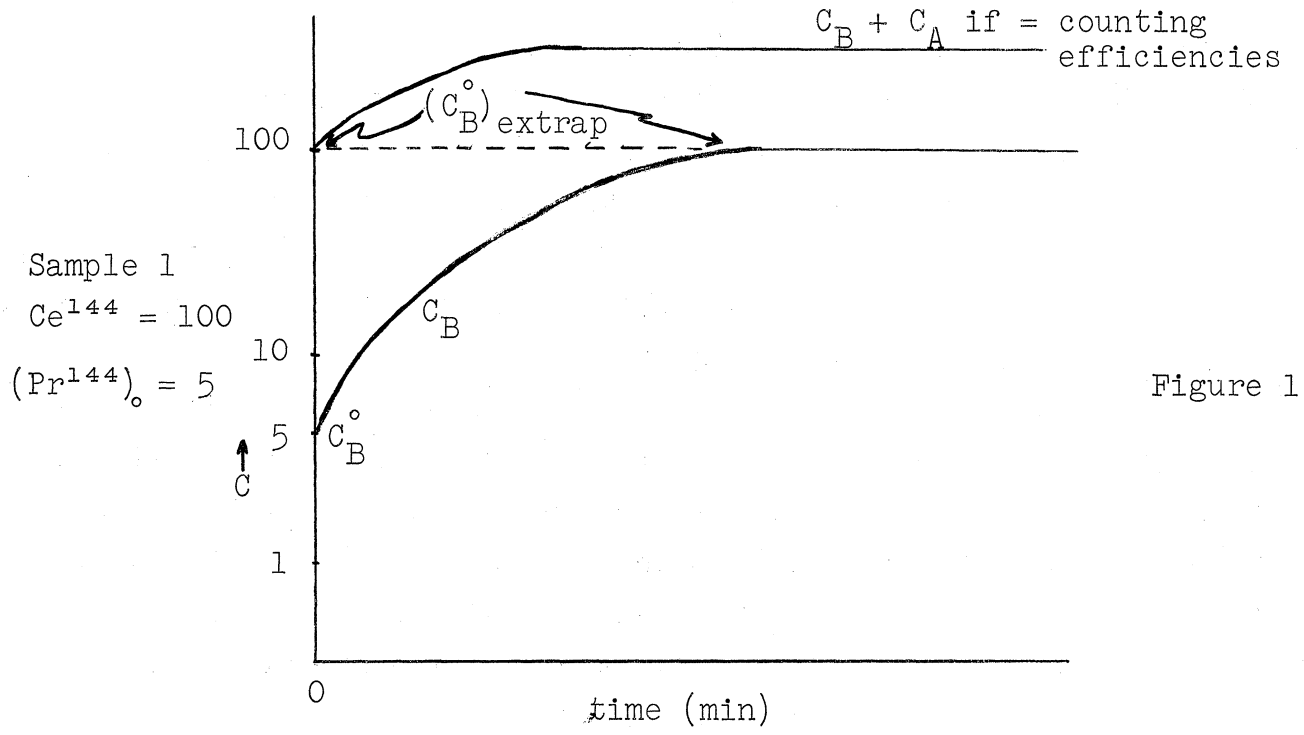

Figure 1

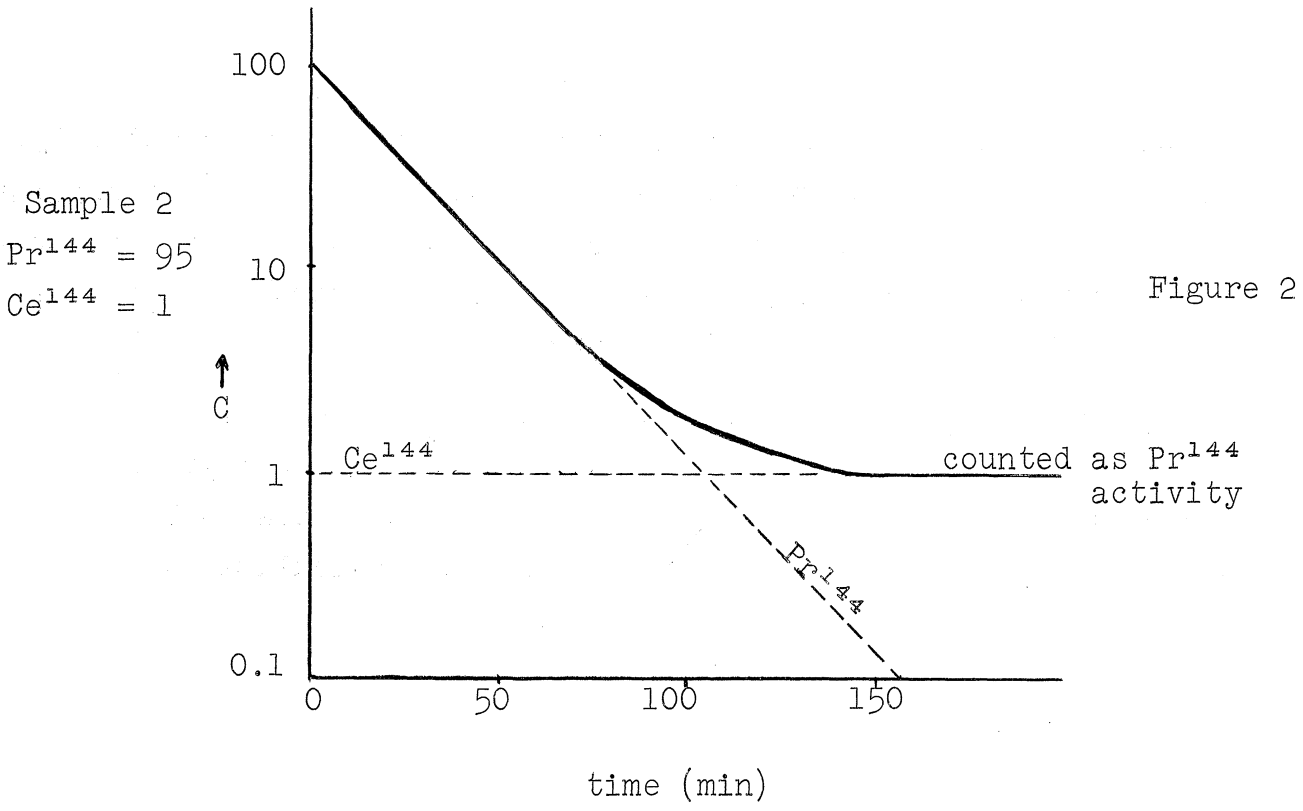

Figure 2

Experiment No. 5
Isotope Dilution

Principle: This technique utilizes the very simple principle of proprotional dilution. That is, in mixing two isotopes - (both in the same chemical state) - the relative amount of each in the final homogeneous mixture is proportional to the amount added. This principle is most useful since the relative amounts in the final mixture can be determined for a nonquantitatively separated sample. This method, therefore, is applicable to quantitative determination problems in which quantitative separations are impossibly difficult, very slow, etc.

The points needing special attention are: 1) the radioactive isotope used must be in The Same Chemical State as in the unknown, 2) the specific activity (counts per gm) of the known isotope mixture must be known, 3) the separations of the homogeneous mixture need not be quantitative and 4) the specific activity of a portion of the homogeneous mixture (see above, point 2) must be measured accurately.

Example: As an example of a quantitative problem to which isotope dilution is applicable consider the following case. A sample is known to contain a minute amount of sulfate and it is desired to know the specific quantity. Precipitation as the Barium or Strontium compound has proven unsatisfactory. Determine the amount of sulfate present by isotope dilution.

Method: Mix a given amount of labelled $H_2S^*O_4$ to the solution of the unknown mixture. The amount used must be adjusted so that the dilution affect is observable. It is suggested in Overman and Clark page 421, that duplicate samples be prepared and analyzed in the following manner:

1) use two 40 ml centrifuge tubes.
2) accurately pipet into each a "sample of the unknown in the range of 2 to 5 ml".
3) also, add to each tube an accurate aliquot of the labelled sulfuric acid of the size range 2 to 5 ml. (the sulfuric acid is assumed to be 0.110 M and have a counting rate of such a value that the rate is reduced one half on dilution with a reasonable aliquot as suggested above.

4) add 10 ml of "distilled" water and heat samples in water bath.
5) add slowly with stirring a slight excess of $BaCl_2$ (complete precipitation is not essential)
6) digest ppts for a few minutes then filter through similar weighed filter mounts and dry.
7) measure the specific activity of the ppts - adjusting counting rate for sample size (self absorption is a major problem with weak beta emitters like S^{35} and C^{14}) See experiment 6-3, page 240 Overman and Clark for methods for determining self absorption corrections.
8) Calculate the gms of sulfate in unknown.

6.10 DETERMINATION OF PERCENT HALOGEN BY ACTIVATION ANALYSIS

Activation analysis, a relatively new analytical technique, provides, in many instances, a very sensitive method for determining, qualitatively and quantitatively, the nature of unknown materials.

The procedure, briefly, is to irradiate the unknown material, normally by bombardment with neutrons. Usually,one or more of the various elements contained in the sample will become radioactive. The types of radioactive elements present may then be determined by ascertaining either the half-lifes of the decaying elements, the energies of the decay particles emitted by the elements, or a combination of the two. Using proper calibration procedures, the amount of radioactivity, and thus the amount of the element, may be determined.

Unknown samples have been prepared containing approximately 10^{-4} gm of an ammonium halide. To measure such a small quantity of a salt, the following procedure was used: 0.100 gm of a salt was weighed out and mixed thoroughly with 100.0 gm of sugar; a 0.100 gm sample of this mixture contains 10^{-4} gm of ammonium halide.

Referring to the table below, it is seen that carbon, nitrogen, and oxygen have very small neutron-absorption cross-sections compared with the halogens. (The cross-section for $^{14}N(n,p)^{14}C$ is 1.76 barns; however, the half-life of ^{14}C is so large, and the ^{14}C β^- energies so low that negligible ^{14}C counts are detectable.) As a result, only halogen activity is observed.

Before irradiating a sample, it is necessary to calculate the duration of the irradiation desired. To perform the calculation, it is necessary to know the nuclear properties of the isotopes (Table I) as well as the neutron flux and the counting efficiency of the scaler and associated Geiger tubes. The reactor will be operating at full power of one million watts, thus producing a thermal neutron flux of about 1.5×10^{12} neutrons per cm^2 per sec at the position where the sample will be placed in the reactor.

Although no accurate calibrations have been made, and the values vary from isotope to isotope, it can be assumed that between

5 and 10 per cent of the radioactive disintegrations will be recorded as counts by the scaler.

In general, using the counting setups available, and considering the statistics of radioactivity, it is desirable to have the level of activity such that between 5,000 and 10,000 counts per minute are recorded. In any case, because of coincidence counting corrections, it is undesirable to have the activity level greater than about 40,000 c/m. Thus, considering that some decay will occur during the counting period, it is probably worthwhile to irradiate the sample so that about 25,000 c/m are observed when counting is started. Using a 5% counting efficiency, this would require about 500,000 disintegrations per second.

Having decided upon the counting rate and having stipulated the reactor neutron flux, only two variables remain. These are the size of the sample (i.e. the number of halogen atoms to be bombarded) and the duration of the irradiation. Since we have designated the sample size as 10^{-4} gm ammonium halide, the duration of the irradiation is the remaining variable. For convenience this will generally be limited to 1 second to 10 minutes.

The average weight of an anion in a 10^{-4} gm ammonium halide sample will be approximately 8×10^{-5} gm. The isotopic abundance can be assumed to be 58%, the average of ^{37}Cl, ^{79}Br, and ^{127}I. Similarly, the average cross-section is 5.3×10^{-24} cm^2, the average half-life, 27.0 minutes, and the average atomic weight 81 amu.

Calculation of Irradiation Duration

$\sigma = 5.3 \times 10^{-24}$ cm^2

$\mathfrak{F} = 1.5 \times 10^{12}$ n/cm^2 - sec

$T_{\frac{1}{2}} = 27$ min

$\frac{dN^*}{dt} = 5 \times 10^5$

$N = (4.7 \times 10^{-5})(6.023 \times 10^{23})/81 = 3.5 \times 10^{17}$ atoms halogen

As a first approximation, we may utilize the expression valid for an irradiation of duration less than 1% of $T_{\frac{1}{2}}$.

$$\frac{dN^*}{dt} = n\sigma N\bar{\nu}(\ell n 2)$$

where $n = t/T_{\frac{1}{2}}$ and t is the irradiation time. Thus:

$5 \times 10^5 = n(5 \times 10^{-24})(6.5 \times 10^{17})(1.5 \times 10^{12})(60 \text{ sec/min})(0.693)$

$n = 4.6 \times 10^{-3}$

$t = 0.125 \text{ min} = 7.5 \text{ sec}$

Since $n<0.01$, the calculation is valid. Note: for $n>0.01$

$$\frac{dN^*}{dt} = \sigma N\bar{\nu}(1 - e^{-\lambda t}) = \alpha N\bar{\nu}(1 - \frac{1}{2^n})$$

PROCEDURE

I. Irradiate a sample of sugar-diluted ammonium halide for about 8 seconds in the reactor. Bring the sample, in lead carrying pig, to the laboratory hood and cut open the sample. Pour the solid contents in (approximately) 50 ml of H_2O; stir and dissolve. Fill a counting jacket and count the solution for a period sufficiently long so that it will be possible to ascertain the half-life and thus determine whether the activity is ^{38}Cl, ^{80}Br, or ^{128}I. This then serves to identify qualitatatively the unknown halogen.

II. Another sample of the unknown as well as a sample of diluted ammonium halide of known per cent and type of halogen are to be irradiated in the same capsule. Simultaneous irradiation of known and unknown results in the same t and $\bar{\nu}$ for both samples.* As a result:

$$\frac{(dN^*/dt)\text{ unk}}{(dN^*/dt)\text{ known}} = \frac{N\text{ unk}}{N\text{ known}}$$

---

*Note: depending on the relative positions of the two samples in the capsule, the neutron flux, $\bar{\nu}$, may differ by as much as 10 to 20%.

Thus, it is necessary to determine only the relative counting rates, corrected to the same moment of time since the irradiation.

Certain additional aspects must also be considered. Since the counting rates rather than the disintegration rates are being determined, it is necessary to count both the known and the unknown. on the same scaler using the same solution jacket, the same volume of H_2O solvent (50.0 ml), and the same Geiger tube. The per cent halogen in the unknown will be larger than that in the unknowns. Therefore, the known can be counted second. It is necessary to count each solution for more than about 10-15 minutes.

In the case of iodine, only one isotope, ^{128}I, is produced. Thus, the half-life is about 25.0 min. For chlorine, ^{36}Cl and ^{38}Cl are both produced. However, >1 count per minute ^{36}Cl activity showed to be observed; thus a 37.5 min half-life would be found.

For bromine, however, three isotopes: ^{80}Br (18 min), ^{80m}Br (4.5 hrs), and ^{82}Br (36 hrs) are formed. The ^{82}Br activity will be negligible. However, the ^{80m}Br activity will result in an overall half-life which is greater than 18 min. It is necessary to correct for the ^{80m}Br activity which will be a function of the time since the end of the irradiation. Therfore, if the halogen is bromine, it is necessary to know, for the mid-point of each count, the time since the end of the irradiation. Given in Table II is the per cent of the observed activity which is due to ^{80m}Br as a function of the time since the end of the irradiation. Before correcting (using $T_{\frac{1}{2}}$ = 18 min) the known and the unknown bromine activities to a common time, it is necessary to subtract the ^{80m}Br activity. Since the ^{80m}Br is counted only through its ^{80}Br daughter, no corrections for ^{80m}Br and ^{80}Br relative counting efficiencies are needed.

Coincidence correction data will be available.

6.11 Table I. Nuclear Properties of Selected Isotopes*

Natural Isotope	Percent Natural Abundance	Thermal Neutron Cross-section $Cm^2 \times 10^{24}$	Nuclear Reaction	Half Life of Product	Major Decay Particles; Energy in Mev
H^1	99.985	0.330	n,γ	Stable	
H^2	0.015	5.7×10^{-4}	n,γ	12.26 yrs	0.0180β⁻
C^{12}	98.89	0.0033	n,γ	Stable	
C^{13}	1.11	0.0007	n,γ	5600 yrs	0.156β⁻
N^{14}	99.635	0.10	n,γ	Stable	
		1.76	n,p	5600 yrs	0.156β⁻
N^{15}	0.365	2.4×10^{-5}	n,γ	7.36 sec	10β⁻, 6.1γ
O^{16}	99.759				
O^{17}	0.037				
O^{18}	0.204	2.1×10^{-4}	n,γ	29.4 sec	4.5β⁻, 1.4γ
Na^{23}	100.	0.53	n,γ	15.0 hrs	1.4β⁻, 2.7γ
P^{31}	100.	0.21	n,γ	14.3 days	1.7β⁻, No γ
S^{32}	95.018	0.00			
S^{33}	0.750	0.0023	n,p	24.4 days	0.25β⁻
S^{34}	4.215	0.26	n,γ	87.1 days	0.17β⁻
S^{36}	0.017	0.14	n,γ	5.04 min	1.6β⁻, 3.1γ
Cl^{35}	75.53	42	n,γ	3.2×10^5 yrs	0.71β⁻
		0.2	n,p	87.1 days	0.17β⁻
Cl^{37}	24.47	0.56	n,γ	37.5 min	4.8β⁻, 2.1γ
Br^{79}	50.54	2.9	n,γ	4.5 hrs	
		8.5	n,γ	18 min	2.0β⁻, 0.6γ
Br^{81}	49.46	3.1	n,γ	35.9 hrs	0.44β⁻, 0.8γ
I^{127}	100.	6.7	n,γ	24.98 min	2.1β⁻, 0.45γ

* Data from Trilinear Chart of Nuclides by William H. Sullivan, 1957+ revisions; U. S. Government Printing Office, Washington, 25, D. C.

6.12 Observed Activity vs. Time

Table II. Percent of the observed activity that is due to Br^{80m} as a function of time (min.) since the end of the irradiation. Data are valid for irradiation durations of zero to about 20-30 seconds.

time	%	time	%
5.00	3.6	24.00	7.0
6.00	3.7	25.00	7.3
7.00	3.9	26.00	7.5
8.00	4.0	27.00	7.7
9.00	4.2	28.00	8.0
10.00	4.4	29.00	8.2
11.00	4.5	30.00	8.5
12.00	4.7	31.00	8.7
13.00	4.8	32.00	9.0
14.00	5.0	33.00	9.3
15.00	5.2	34.00	9.5
16.00	5.4	35.00	9.8
17.00	5.6	36.00	10.1
18.00	5.8	37.00	10.4
19.00	6.0	38.00	10.6
20.00	6.2	39.00	11.0
21.00	6.4	40.00	11.3
22.00	6.6	41.00	11.6
23.00	6.8	42.00	11.9

RADIOACTIVE DECAY D. E. Hull - Activities of Radioactive Substances in Series Disintegration, J. Phys. Chem. 45, 1305 (1941)

t/T	$e^{-\lambda t}$	t/T	$e^{-\lambda t}$	t/T	$e^{-\lambda t}$	t/T	$e^{-\lambda t}$
0	1.000	0.52	0.6974	1.54	0.3439	3.80	0.0718
0.01	0.9931	0.54	0.6878	1.56	0.3391	3.85	0.0693
0.02	0.9862	0.56	0.6783	1.58	0.3345	3.90	0.0670
0.03	0.9794	0.58	0.6690	1.60	0.3299	3.95	0.0647
0.04	0.9726	0.60	0.6597	1.62	0.3253	4.00	0.0625
0.05	0.9659	0.62	0.6507	1.64	0.3209	4.10	0.0583
0.06	0.9592	0.64	0.6417	1.66	0.3164	4.20	0.0544
0.07	0.9526	0.66	0.6329	1.68	0.3121	4.30	0.0508
0.03	0.9461	0.68	0.6242	1.70	0.3078	4.40	0.0474
0.09	0.9395	0.70	0.6156	1.75	0.2973	4.50	0.0442
0.10	0.9330	0.72	0.6071	1.80	0.2872	4.60	0.0412
0.11	0.9266	0.74	0.5987	1.85	0.2774	4.70	0.0385
0.12	0.9202	0.76	0.5905	1.90	0.2679	4.80	0.0359
0.13	0.9136	0.78	0.5824	1.95	0.2588	4.90	0.0335
0.14	0.9075	0.80	0.5744	2.00	0.2500	5.00	0.0312
0.15	0.9013	0.82	0.5664	2.05	0.2415	5.10	0.0292
0.16	0.8950	0.84	0.5586	2.10	0.2333	5.20	0.0272
0.17	0.8888	0.86	0.5509	2.15	0.2253	5.30	0.0254
0.18	0.8827	0.88	0.5434	2.20	0.2176	5.40	0.0237
0.19	0.8766	0.90	0.5359	2.25	0.2102	5.50	0.0221
0.20	0.8705	0.92	0.5285	2.30	0.2031	5.60	0.0206
0.21	0.8645	0.94	0.5212	2.35	0.1961	5.70	0.0192
0.22	0.8586	0.96	0.5141	2.40	0.1895	5.80	0.0179
0.23	0.8526	0.98	0.5070	2.45	0.1830	5.90	0.0167
0.24	0.8467	1.00	0.5000	2.50	0.1768	6.00	0.0156
0.25	0.8409	1.02	0.4931	2.55	0.1708	6.20	0.0136
0.26	0.8351	1.04	0.4863	2.60	0.1649	6.40	0.0118
0.27	0.8293	1.06	0.4796	2.65	0.1593	6.60	0.0103
0.28	0.8236	1.08	0.4730	2.70	0.1539	6.80	0.0090
0.29	0.8179	1.10	0.4665	2.75	0.1487	7.00	0.0078
0.30	0.8122	1.12	0.4601	2.80	0.1436	7.20	0.0068
0.31	0.8066	1.14	0.4538	2.85	0.1387	7.40	0.0059
0.32	0.8011	1.16	0.4475	2.90	0.1340	7.60	0.0052
0.33	0.7955	1.18	0.4413	2.95	0.1294	7.80	0.0045
0.34	0.7900	1.20	0.4353	3.00	0.1250	8.00	0.0039
0.35	0.7846	1.22	0.4293	3.05	0.1207	8.20	0.0034
0.36	0.7792	1.24	0.4234	3.10	0.1166	8.40	0.0030
0.37	0.7738	1.26	0.4175	3.15	0.1127	8.60	0.0026
0.38	0.7684	1.28	0.4118	3.20	0.1088	8.80	0.0022
0.39	0.7631	1.30	0.4061	3.25	0.1051	9.00	0.0020
0.40	0.7579	1.32	0.4005	3.30	0.1015	9.20	0.0017
0.41	0.7526	1.34	0.3950	3.35	0.0981	9.40	0.0015
0.42	0.7474	1.36	0.3896	3.40	0.0948	9.60	0.0013
0.43	0.7423	1.38	0.3842	3.45	0.0915	9.80	0.0011
0.44	0.7371	1.40	0.3789	3.50	0.0884	10.00	0.0010
0.45	0.7320	1.42	0.3737	3.55	0.0854	10.50	0.0007
0.46	0.7270	1.44	0.3685	3.60	0.0825	11.00	0.0005
0.47	0.7220	1.46	0.3635	3.65	0.0797	11.50	0.0004
0.48	0.7170	1.48	0.3585	3.70	0.0770	12.00	0.0002
0.49	0.7120	1.50	0.3536	3.75	0.0743	13.00	0.0001
0.50	0.7071	1.52	0.3487				

t= time during which radioactive decay has been in progress. T= half life of the element. $e^{-\lambda t}$= fraction of the number of the atoms of the element which were present at time zero time which remain at time (t). $N= N_0 e^{-\lambda t}$.

6.14 Fractional Midpoint of Count vs. Duration of Count

Defining t as the duration of the count, T as the half-life of the isotope, and n as the ratio: t/T, x × t = moment during the count at which the instantaneous counting-rate equals the overall observed counting-rate.

$$x = \left(\frac{T}{0.30103\ t}\right) \log_{10}\left[\frac{0.69315\ t}{T\left(1 - e^{-\lambda t}\right)}\right] = \left(\frac{1}{0.30103\ n}\right) \log_{10}\left[\frac{0.69315\ n}{1-e^{-0.69315n}}\right]$$

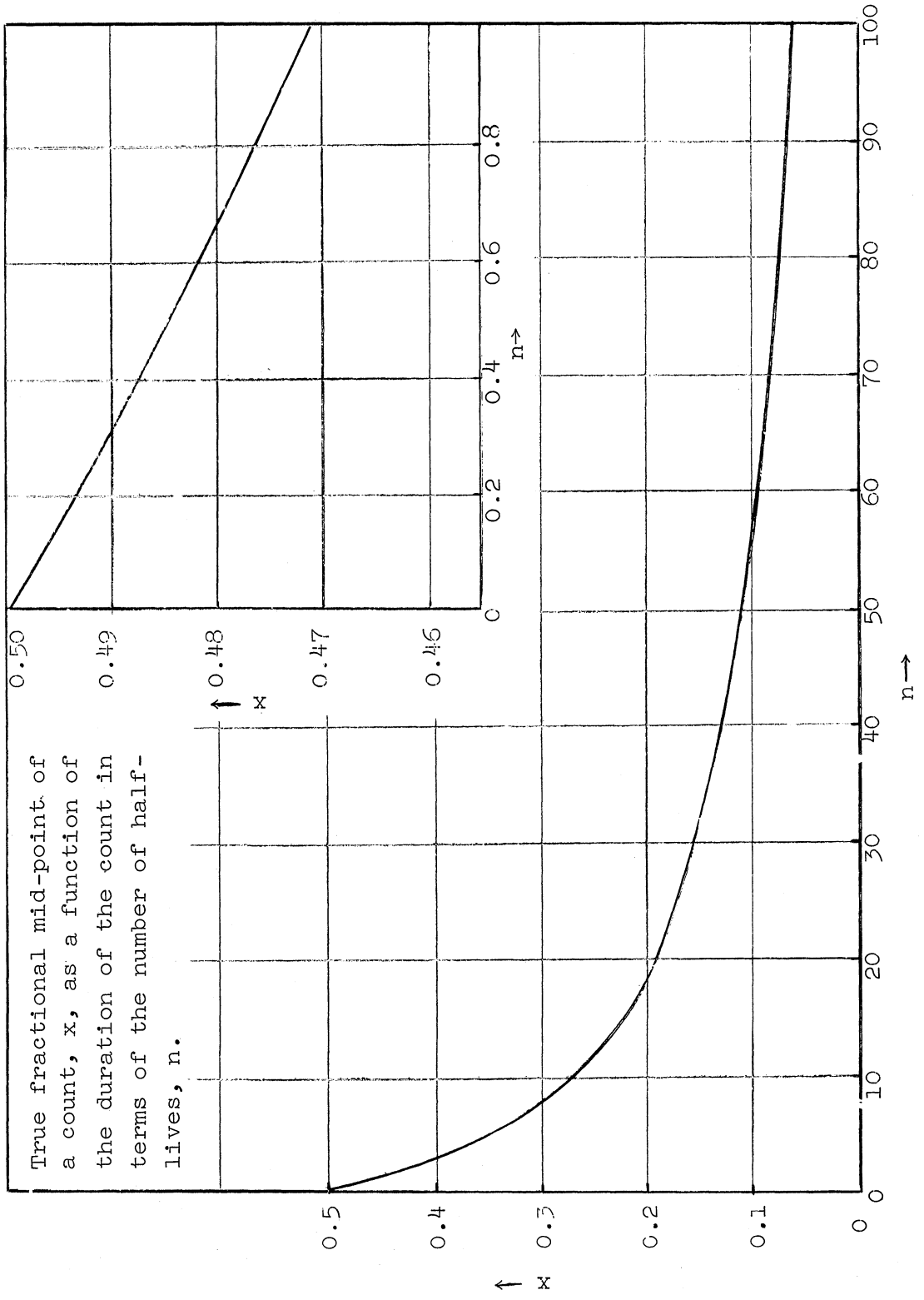

Figure 4

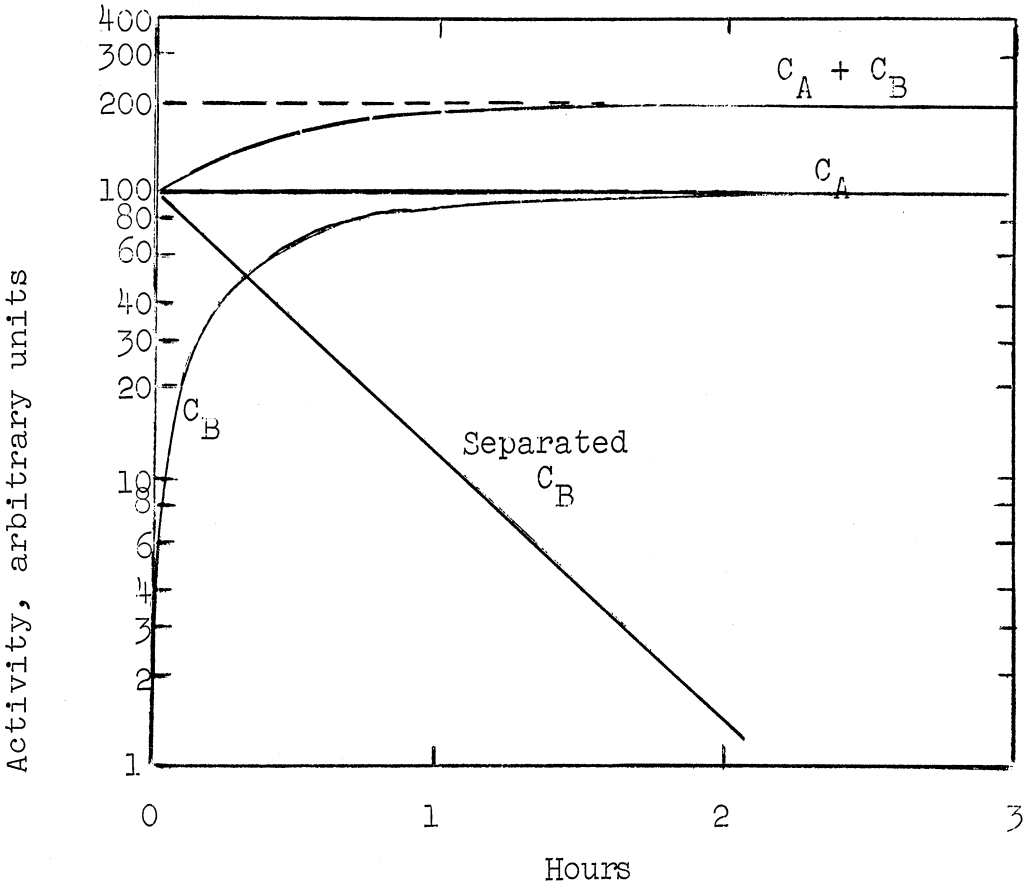

Above: C_A (200 days) → C_B (20 min) equilibrium.
$C_A^\circ = 100$, $C_B^\circ = 0$. At equilibrium, $C_B = C_A$.
Below: C_A (0.8 hours) → C_B (8 hours) equilibrium.
$C_A^\circ = 300$, $C_B^\circ = 0$. At equilibrium, $C_B = C_A$.

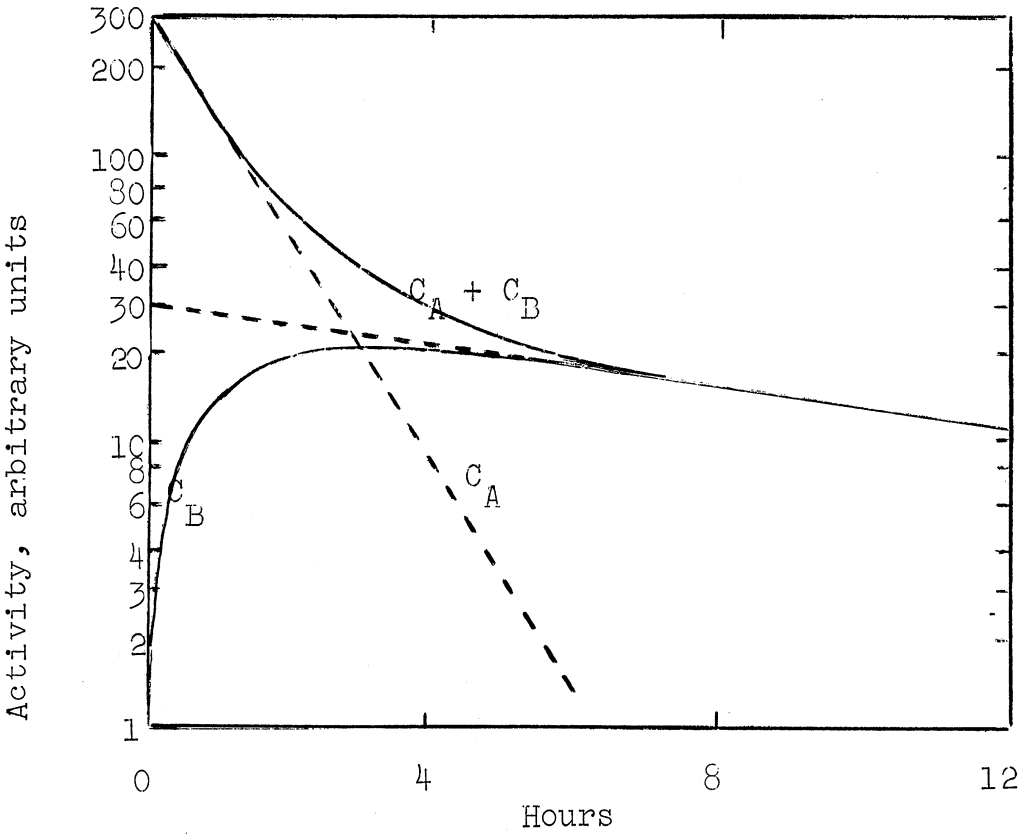

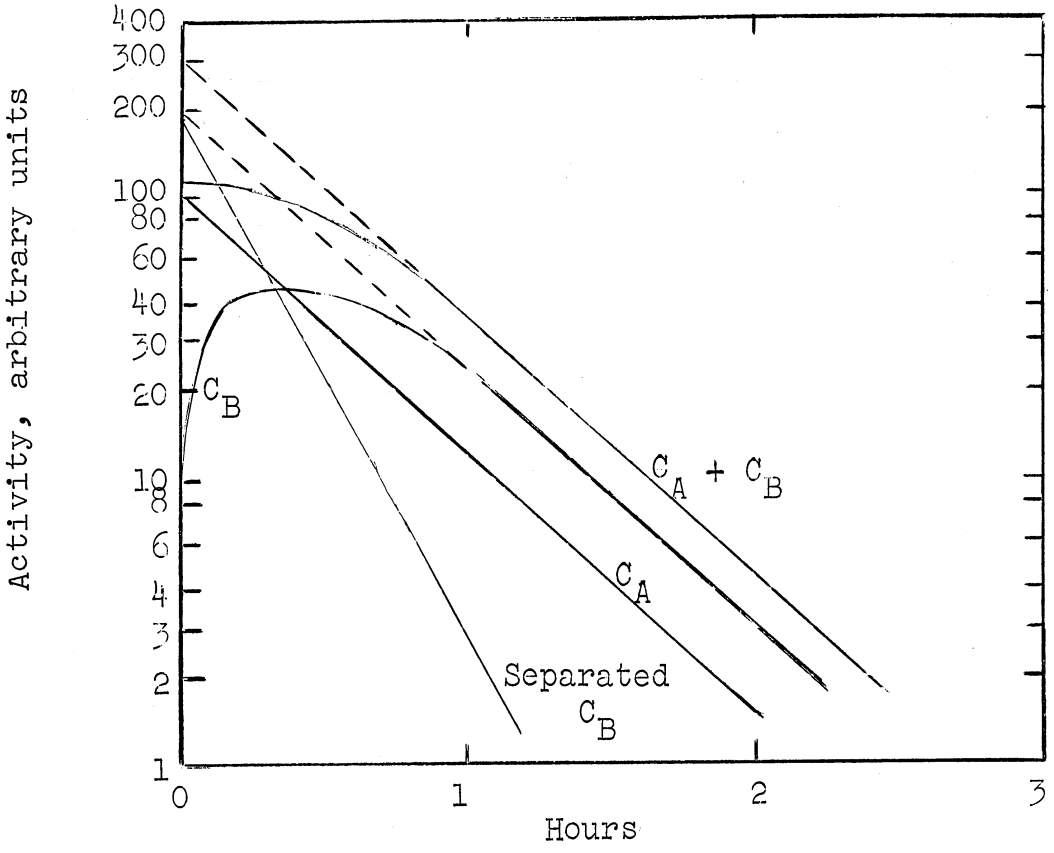

Above: A (20 min.) → B (10 min.) equilibrium.
$C_A^\circ = 100$, $C_B^\circ = 10$. At equilibrium, $C_B = 2.00\ C_A$.

Below: A (20 min.) → B (10 min.) equilibrium.
$C_A^\circ = 100$, $C_B^\circ = 140$. At equilibrium, $C_B = 2.00\ C_A$.

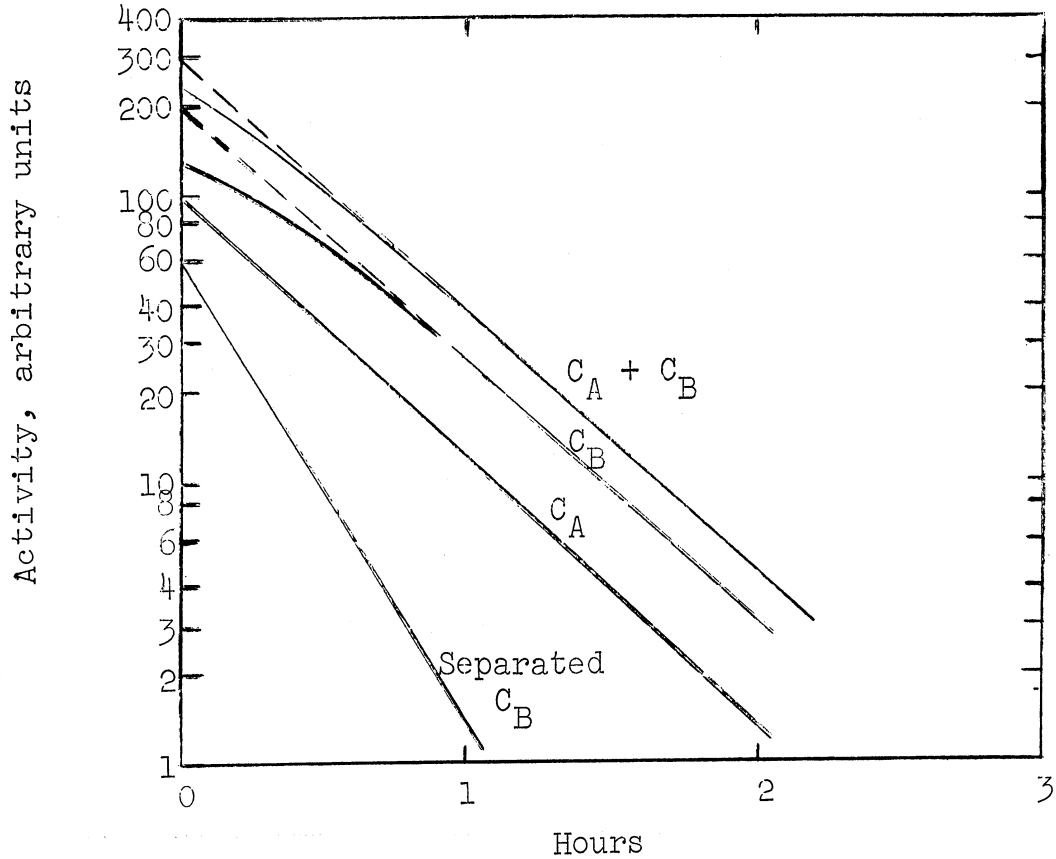

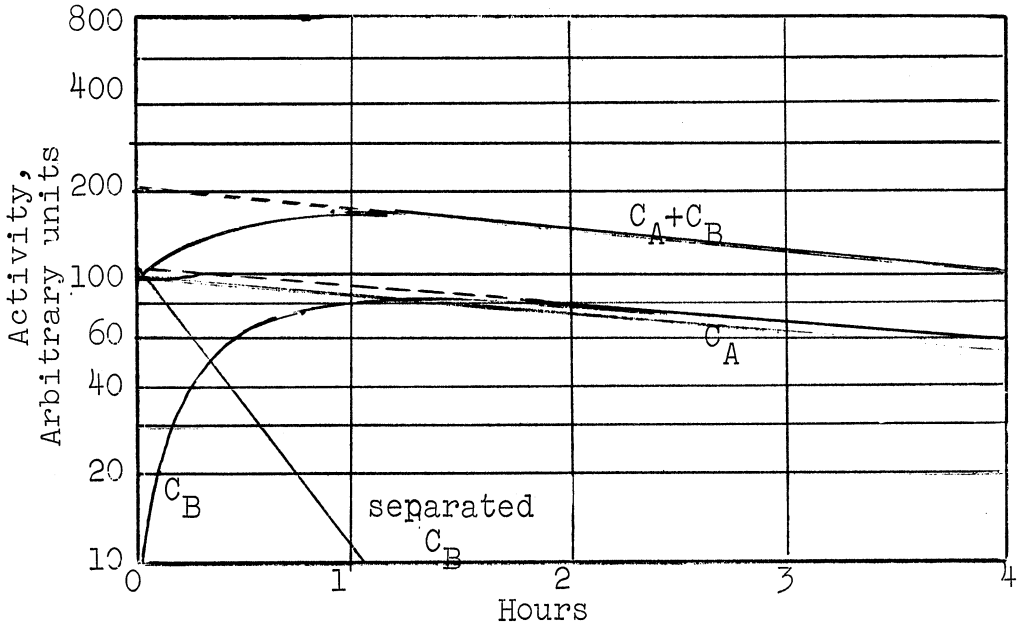

Above: Br^{80m} (4.5 hr) → Br^{80} (18 min.) equilibrium.
$C_A^\circ = 100$, $C_B^\circ = 0$. At equilibrium, $C_B = 1.07\ C_A$.

Below: A (20 min.) → B (10 min.) equilibrium.
$C_A^\circ = 100$, $C_B^\circ = 0$. At equilibrium, $C_B = 2.00\ C_A$.

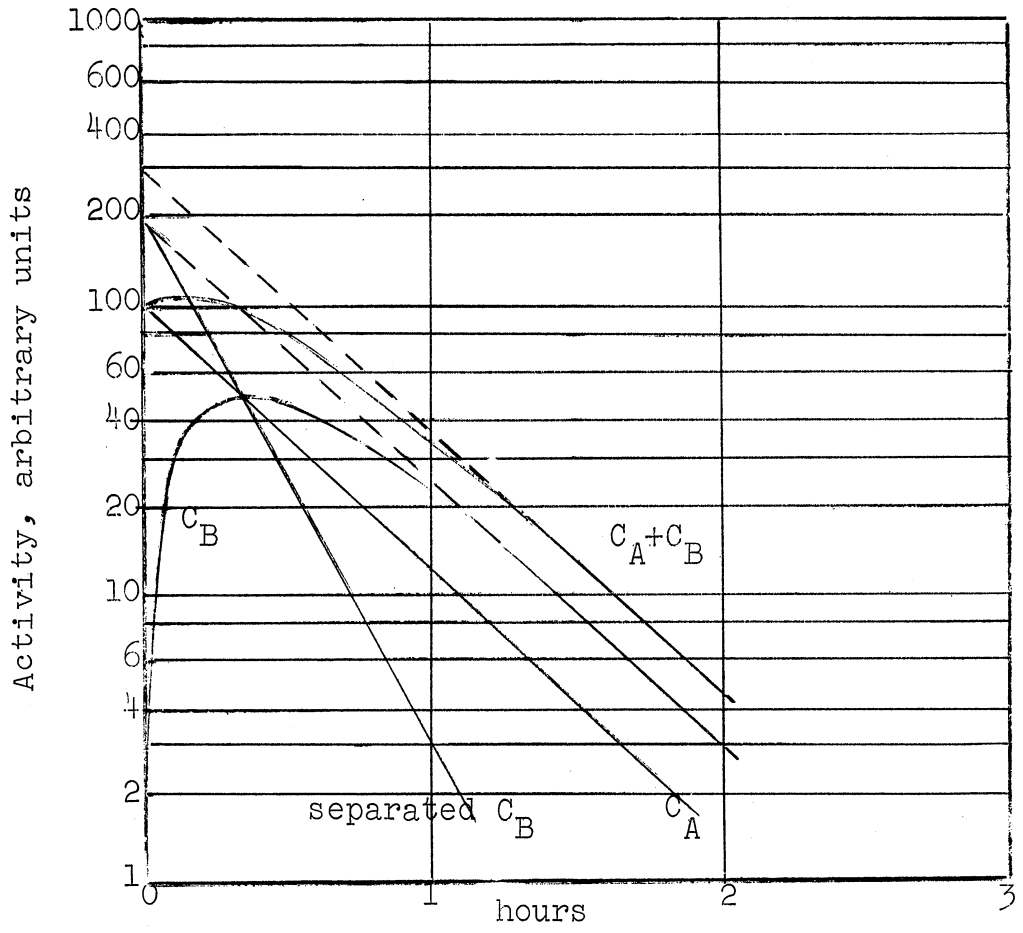

Chapter 7

Experiments in Radioisotope Technology

By R. Borcherts, J. Sickles, and L.E. Brownell

Background

The operation of nuclear reactors such as those used in the production of plutonium, has produced large quantities of radioactive fission-product waste materials. These materials cannot be used in the atomic-bomb program nor can they be disposed of, as is customary with ordinary industrial waste, that is, they cannot be discharged into streams or rivers, dumped on the ground, or released into the air by burning because of the hazard of contaminating air and water supplies and food materials with radioactive poisons.

As a result, the Atomic Energy Commission has been storing large quantities of these fission products in underground tanks designed to retain this material for many years. The problem of disposing of these fission products will become more important as the reactor program increases. If the fission products could be put to use in industry, what is at present an expensive waste material might be turned into an asset with the saving of taxpayer dollars.

The Atomic Energy Commission contracted with various universities to investigate some of these uses. In June, 1951, Michigan and later other universities (1) received cobalt-60 sources from the Brookhaven National Laboratory of the type described by Manowitz (9). The Michigan source (see Fig. 7.1) was installed in the Fission Products Laboratory of Engineering Research Institute, University of Michigan, and a variety of experiments were conducted and reported to the Commission (2-5). Additional experiments were supported by the Michigan Memorial Phoenix Project.

The small cobalt-60 source shown in Fig. 7.1 was a useful laboratory tool in the early experiments, but only a small percentage of radiation from the small source of cobalt-60 can be absorbed by the specimen placed in the radiation chamber. The small internal diameter of about 1 1/2 in. has greatly limited the size of the sample which might be irradiated and has made it difficult or impossible to conduct many experiments. Therefore, a decision was made to secure another gamma-ray source of greater flexibility.

In the second source the design was modified so that a greater percentage of the radiation would be usable (see Fig. 7.2).

In the experiments with irradiated food, it is desirable to place commercial-size cans in the irradiation chamber. It was found that preservation

of food by irradiation involves many problems other than sterilization as experienced in the canning industry and also that irradiated food must be protected from oxidation, dehydration, etc. as in the canning operation. Prior to use of the larger source, it was necessary to limit all food tests to food packaged in glass test tubes or plastic containers because the small source would not accommodate the smallest size of tin can. In the experiments on food sterilization the gamma flux must have sufficient strength so that the irradiation time will be short enough to assure non-spoilage of the irradiated sample before sterilization can be accomplished. With these considerations it was decided that a cylindrical radiation source of at least 3-kilocuries would be required and that this source should be designed to irradiate samples both outside and inside the cylinder. For added versatility it was decided that this source should be in the form of a number of rods which could be set into a cylindrical pattern or into a layer pattern, depending on what was desired.

A few comments regarding the efficiency of using gamma radiation sources might be mentioned. As the intensity of the gamma-ray source is increased, it can be used more efficiently, since a greater percentage of the radiation field can be used. For example, a 1-curie source is practically useless in promoting chemical reactions or sterilizing biological materials because the field is of such low intensity; whereas kilocurie sources can be used for these purposes.

Figure 7.2 shows a cutaway or phantom view and Fig. 7.3 shows a plan of the radiation cave. Essential features are the 4-ft. thick concrete walls necessary to shield both laboratory personnel and the surrounding area from gamma radiation and the 16-ft. well used for shutting off the source. The 4-ft. barrier wall provides a simple labyrinthine entrance and prevents the source from "seeing" the door. The barrier wall serves to diminish the radiation flux in the labyrinthine entrance so that a heavily shielded door is not required. The door is provided with a mechanical safety interlock, (see Fig. 7.4) making entrance to the radiation cave when the source is in the raised position, impossible. In addition to the safety provided by this interlock, a safety light immediately above the locking bar handle serves to indicate the position of the 10,000-curie source. This device is activated mechanically by the rods of the source itself. As the source is raised to its uppermost position, it contacts a vertical rod which is raised by the final travel of the source and which through a cable indicates the position of the source. Therefore, these two different mechanisms operate independently. These safety measures are supplemented by rigorous monitoring with instruments upon entry into the cave.

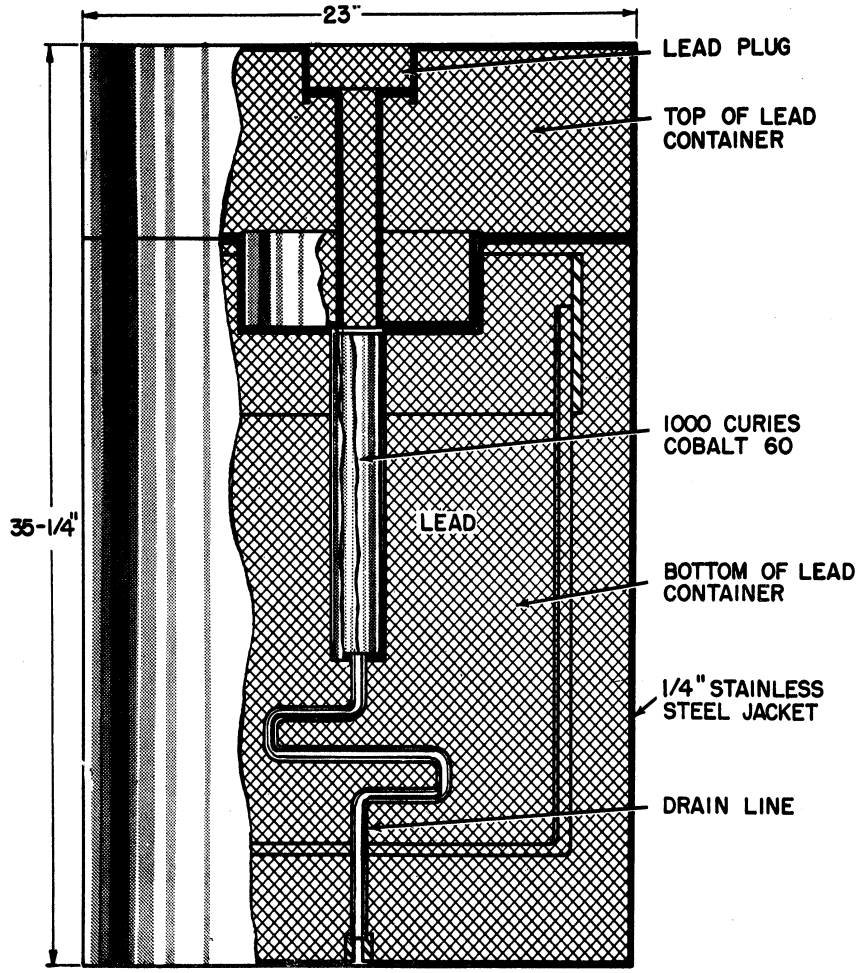

Figure 7.1 Small cobalt-60 source

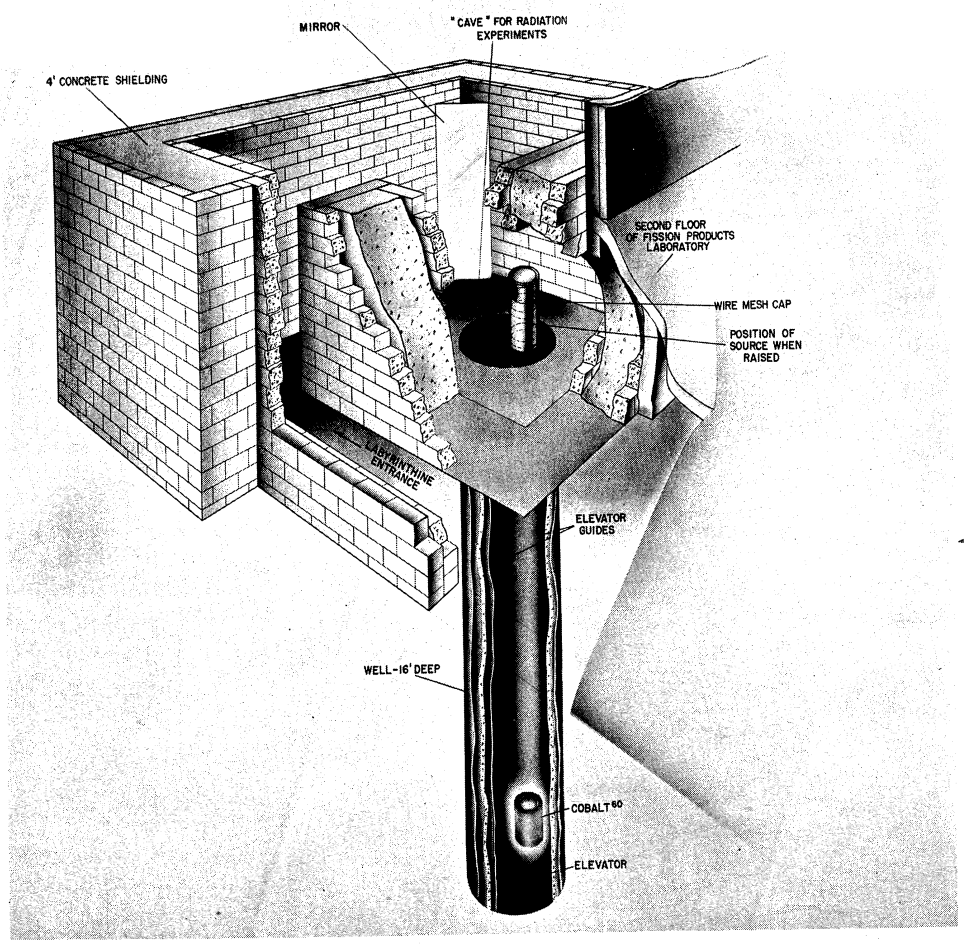

Figure 7.2 Cutaway perspective view of radiation cave

Figure 7.5 shows the loading of the cobalt rods into the aluminum rack by use of special tongs under 16 feet of water. The steel elevator rods, elevator platform supporting the rack, and the underwater light, are shown in the well. Part of the water circulation system required to maintain clarity and control the pH is shown at the left.

After several years of use the aluminum jackets on the rods corroded resulting in cobalt-60 leakage into the water of the well. This required enclosure of the rods and holder in a stainless steel annular container in 1960.

Safety Considerations

A number of the experiments described in this chapter involve the use of the large gamma radiation source, and the handling of radioactive materials with activities up to 1 curie. Because of the potential danger involved in working with radioactive material and large gamma radiation sources, a definite awareness and respect should be used when working with these materials. The following paragraphs attempt to define some of the precautions to be used with radioactive materials and radioactive sources (generally sealed radioactive materials). (See Chapter 1 and 2 of "Radioisotope Technology" entitled "Safety in Work with Radioisotopes," and "Design and Use of Radiation Laboratories" respectively.

Large Co^{60} Source (~1500 curies as of June 1961)

The large source in the Fission Products Laboratory in the form of a cylinder has a dose rate of 110,000 r/hr in the center well as of June 1961. The cave, holding the source, has a 4'-0" concrete (solid) wall surrounding it and a labrynth type entrance (see Fig. 7.8). From the entrance one can see whether the source is up or down. To enter the cave the source is slowly lowered by means of the hand crank into the well of water. (Note the interlock mechanism to prevent the door being opened unless all the cable is unwound). When entering the cave, always carry a monitoring instrument and check it with the Cs^{137} source inside the door to see if the instrument is working. As far as knwon, lethal doses of radiation in the low dose range cannot be felt, seen, or heard so that you must rely on your instrument. Another, though visible, check can be made by using the mirrors enabling the person entering the cave to see that the source is not in the up position. Upon leaving the cave be sure to remove the monitoring instrument and turn it off before raising the source.

Small Co^{60} Source (~70 curies)

Access to the radiation field of the small Co^{60} source is made by removing the plug at the top of the source. This act creates a rather intense

radiation field above the hole that is conical in shape and should be treated with caution. When using this source be sure to: (see Fig. 7.1 and 7.6)

1. Wear your film badge on the neck level

2. Wear finger tabs

3. Notify personnel upstairs that you are using the source

General Procedures

1. Always wear your film badge

2. When working with or around unsealed radioactive material, frequently check your hands and feet by means of a monitor capable of detecting the radiation

3. Know the properties of the radioisotope and know what you are doing

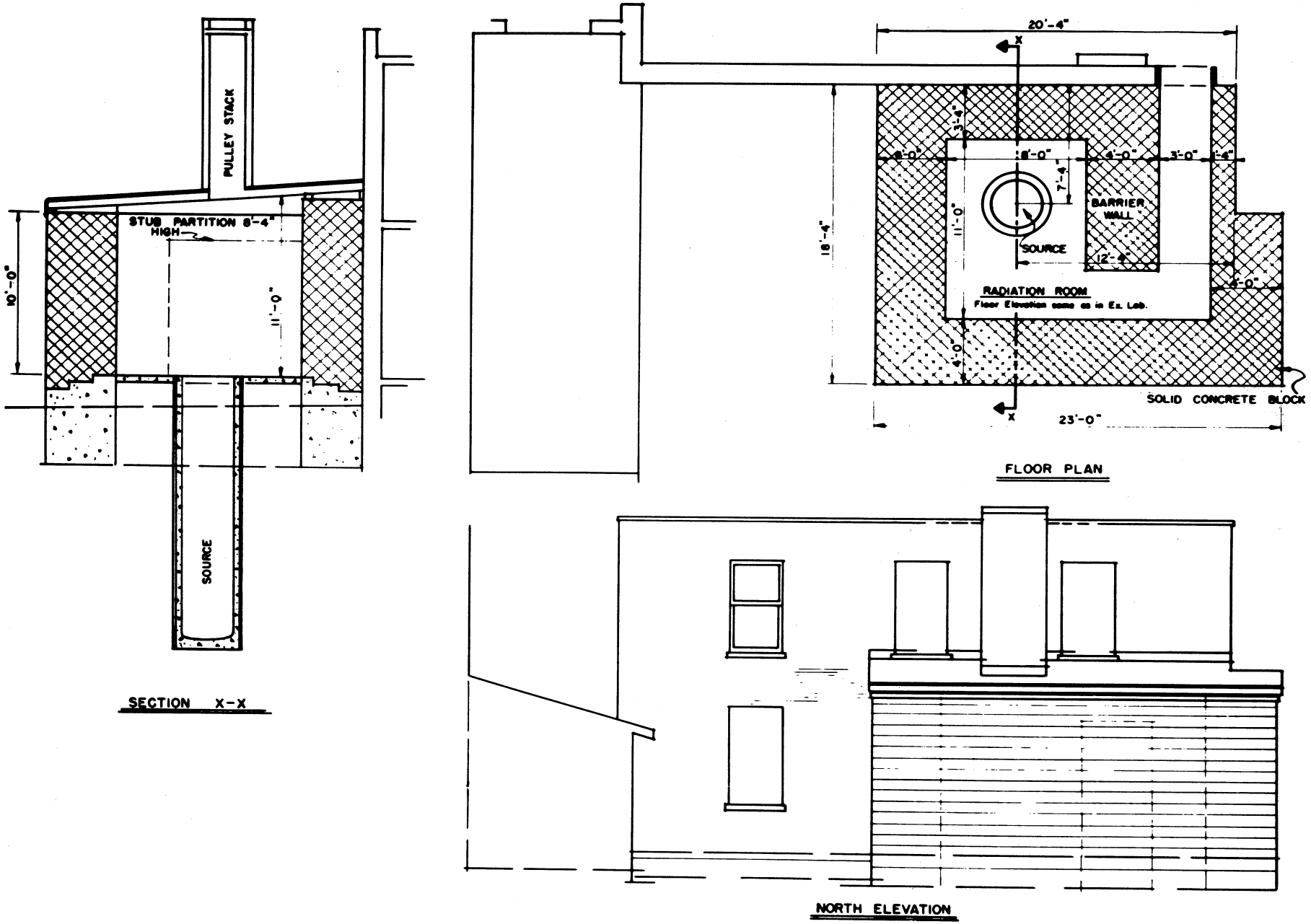

Figure 7.3 Plan and elevation sectional views of radiation cave

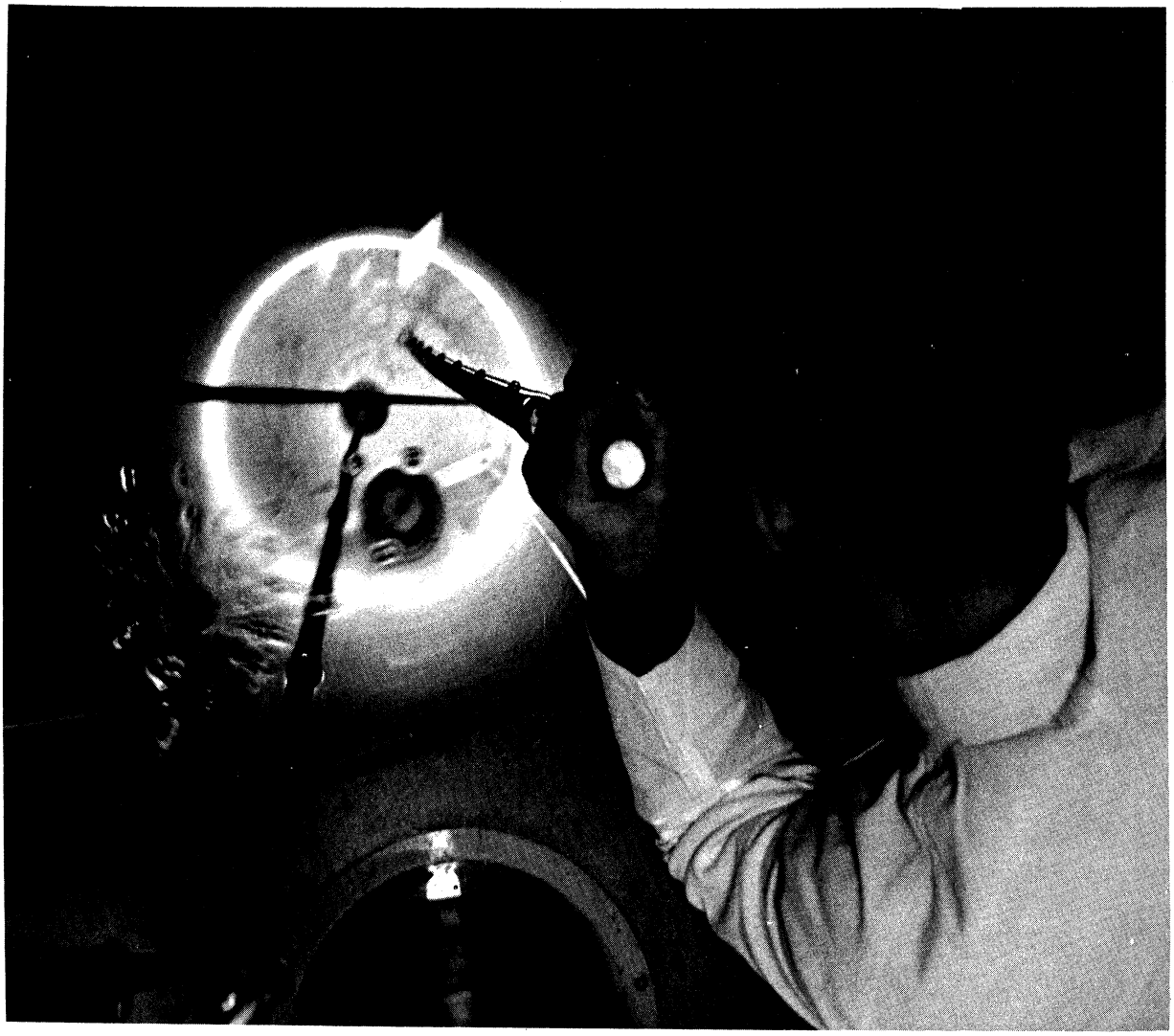

Figure 7.5 Loading cobalt-60 rods into holder under 16 feet of water used as shielding

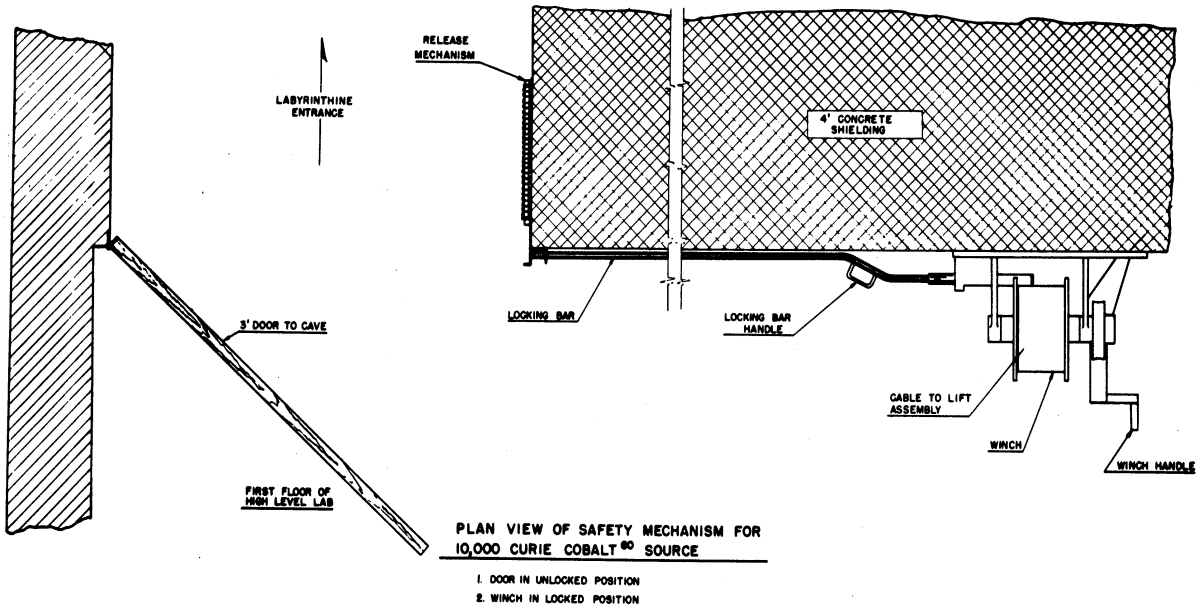

Figure 7.4 Door interlock to radiation cave

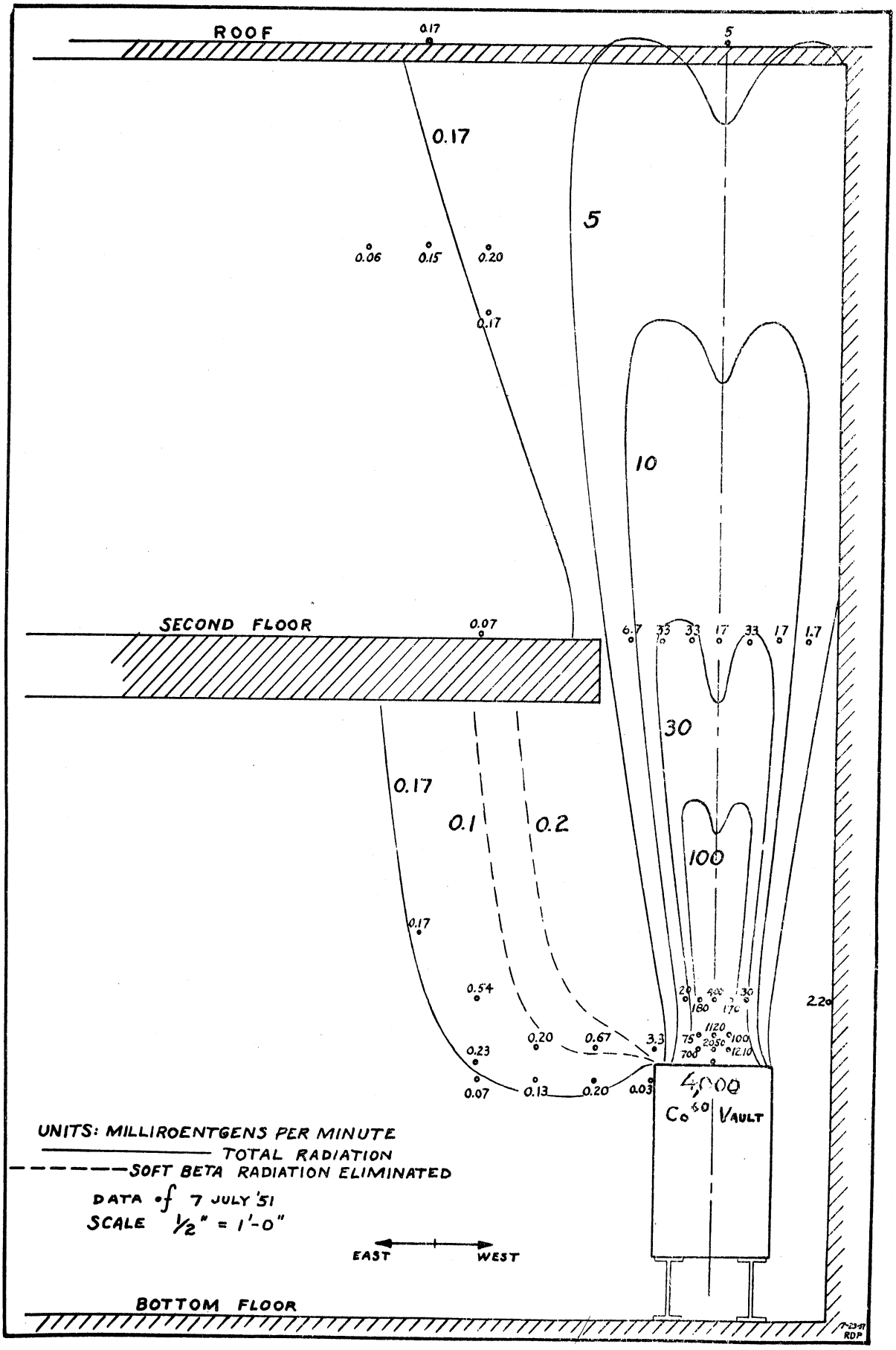

Figure 7.6 Original radiation flux measurements made on small cobalt-60 source

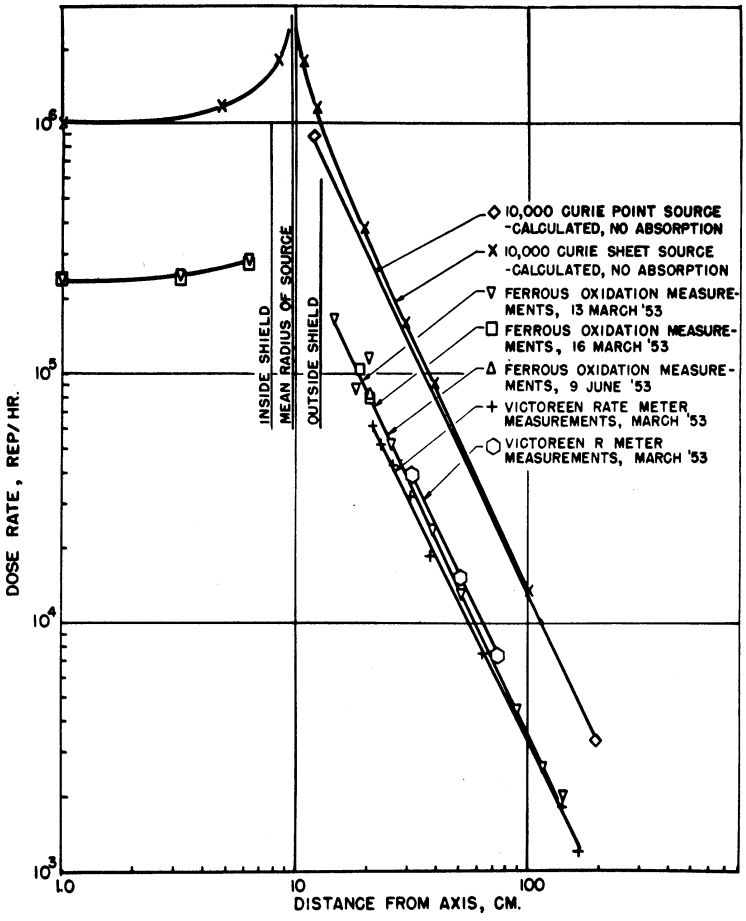

Figure 7.7 Dose rate on midplane of 10-kc Co^{60} source (4)

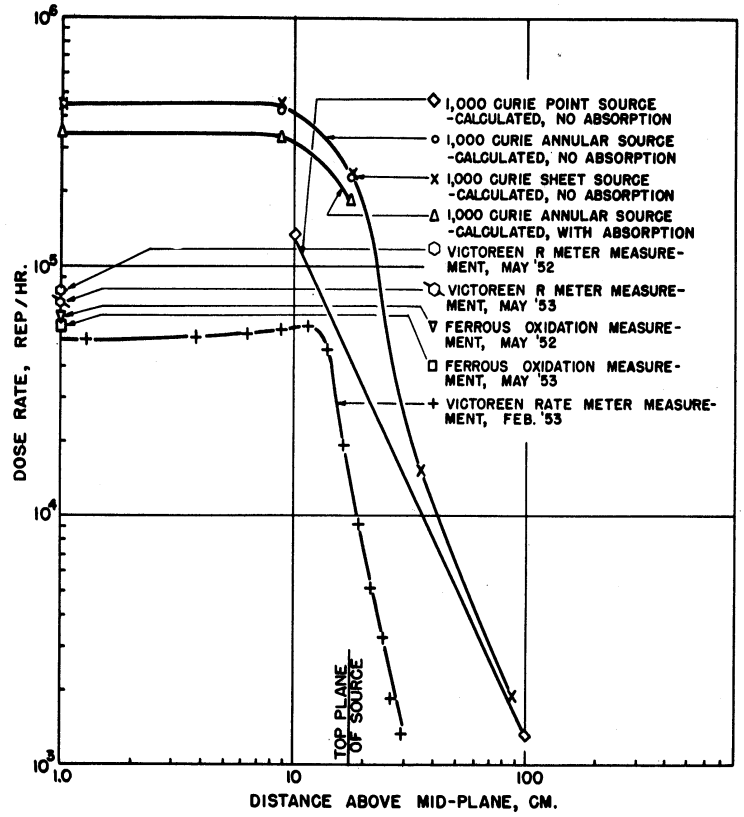

Figure 7.8 Dose rate on axis of 1-kc Co^{60} source (4)

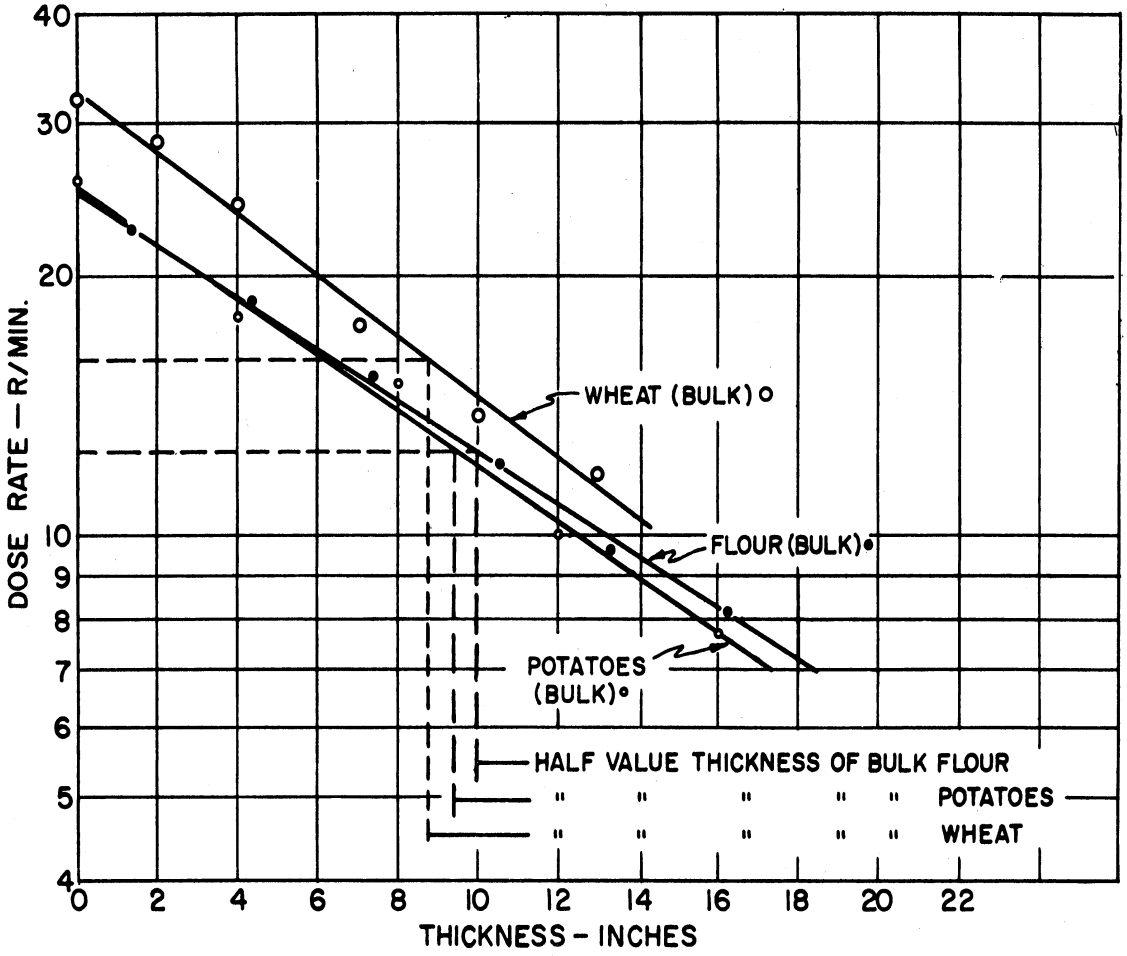

Fig. 7.9 "Broad-beam" absorption measurements showing "half-value thickness" of three foods (measured in the radiation cave, Fission Products Laboratory, University of Michigan).

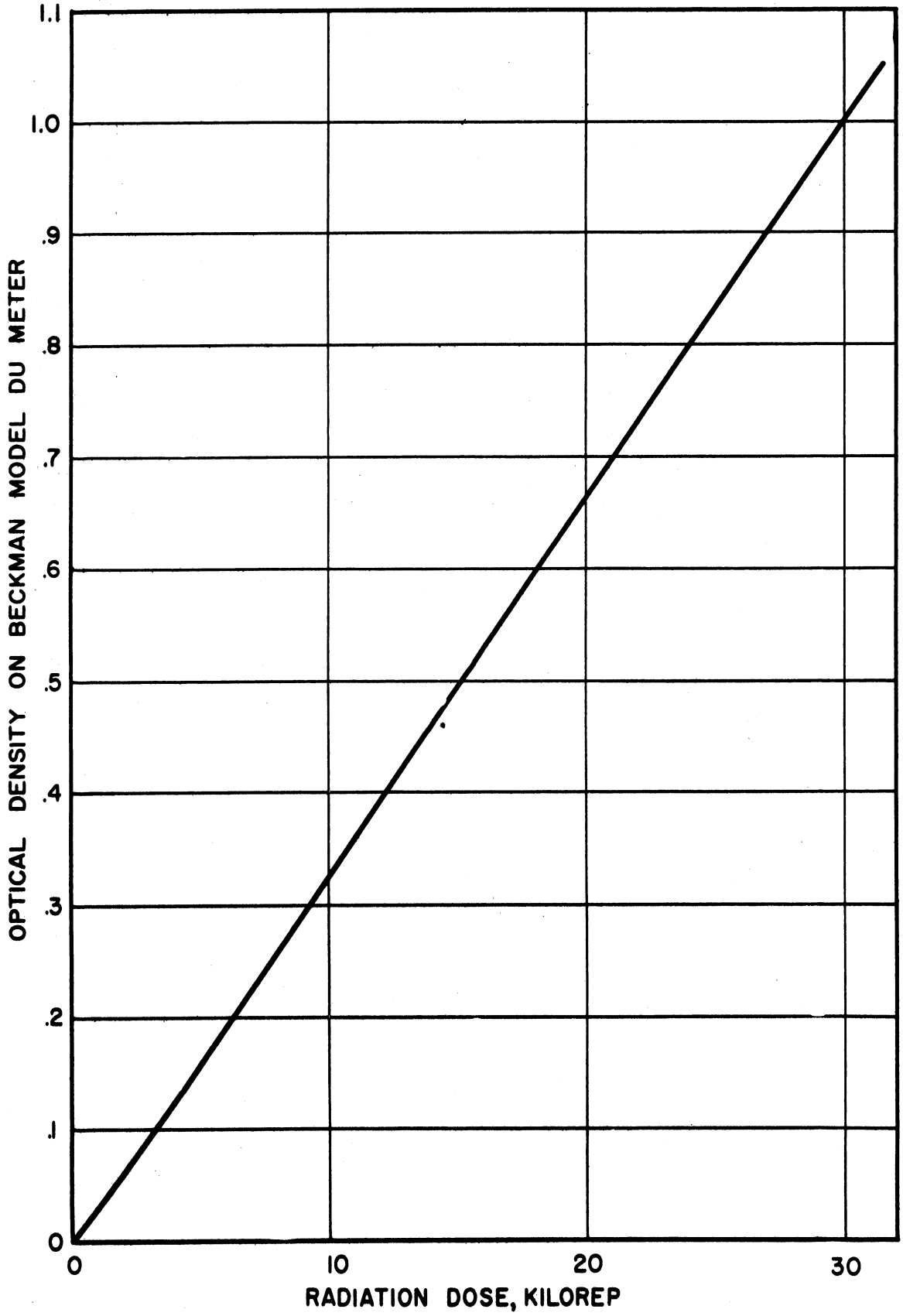

Fig. 7.10 Calibration and conversion curve for Beckman Model DU Meter in FPL.

7.1 Experiment No. 1

Measurement of Radiation Field of Small and Large Cobalt-60 Sources Using Various Instruments Operated by Ionization of Gases

Discussion

Before commencing work with cobalt-60 sources, a basic understanding of the danger of radiation exposure and the procedures for proper use of monitoring instruments are required. See Chapter 1 and 2 of "Radioisotope Technology" and Chapter 11 of "Radiation Uses in Industry and Science" or equivalent.

Large Source: Since the large Co^{60} source is finite in size it is expected that the dose rate will deviate from a $1/R^2$ curve close to the source. However, as the distance away from the source is increased the curve should approach a $1/R^2$ curve. Near walls and other objects the radiation field should deviate slightly from the expected due to scattering from these objects.

Small Source: With the plug removed from the access hole to the small source, the radiation field along the axis of the hole is expected to decrease as the distance along the axis is increased. Because of the effect of source-shielding geometry, this decrease will be greater than for a point source.

Procedure

Large Source: The probe of the Victoreen Rate Meter is set up inside the cave with the meter outside. For each probe position change, the source must be fully raised and lowered. At various distances from the source and on the mid plane of the source the radiation field should be measured.

Since the cylindrical geometry of the source is expected to give the most intense and most uniform field in the center, be sure to measure both across the midplane and along the vertical axis for the center well position. To check the several probes against each other, include an overlap region of measurements for each probe. Note: Allow five minutes for the Victoreen to completely warm up. Zero the instrument on the 3R scale every time a probe is changed. Do not exceed the maximum range of the instrument when raising the source.

Small Source: As the probe of the Victoreen is lowered into the small source, its position is remotely recorded with a meter stick relative to some position, say the top of the small source. When the radiation field fails to register on the Victoreen the Juno Ionization Chamber should be used. Take readings with the Juno meter across the cone of radiation at several distances above the top of the source. For the highest distances note the dip of the radiation field at the axis. When plotting the data, make iso-

dose curves, i.e. curves of constand radiation flux. Care should be taken to minimize the time spent in the field surrounding the small source. Wear film badges on the collars of your shirts and wear a finger tab when holding or adjusting the probe in the radiation field.

AEC Maximum Permissible Doses-----300 mr/wk--whole body
1500 mr/wk--hands and forearms

(See Chapter 1 of "Radioisotope Technology.")

Questions

1. Why does the radiation field along the center line of the small source fall off faster than a $1/R^2$ curve? (See Fig. 7.6 and 7.8)

2. Explain why the radiation field above the small source exhibits a cardioid shape. (See Fig. 7.6)

3. a. From the dose rate measurement at the geometrical center of the source, the dimensions of the source, and from the assumption that the source is a cylindrical shell of zero thickness and no self absorption, calculate the strength of both sources in curies.
   b. From the data of the $1/R^2$ region of the large source compute the "point source strength" of the source.
   c. How do your results compare with the given values of source activity?
      Large Source 2645 curies - Aug. 1955
      Small Source 300 curies - July 1951
   (See Figs. 7.7 and 7.8)

4. Explain the principles of operation of the Juno Ionization Chamber and the Victoreen Rate Meter

Additional References

1. Brownell, L.E. "Radiation Uses in Industry and Science" (Chap. 11) G.P.O., June 1961

2. NBS Handbook 59 and Addendum, "Permissible Dose From External Sources of Ionizing Radiation" and "Maximum Permissible Radiation Exposures to Man," September 24, 1954 and April 15, 1958, U.S. Government Printing Office.

3. NBS Handbook 62, "Report of the International Commission on Radiological Units and Measurements," April 10, 1957, U.S. G.P.O.

4. Lewis, J.G. et al., "Analysis of Radiation Fields of Two Gamma-Radiation Sources," Nucleonics 12, No. 1, 40, 1954

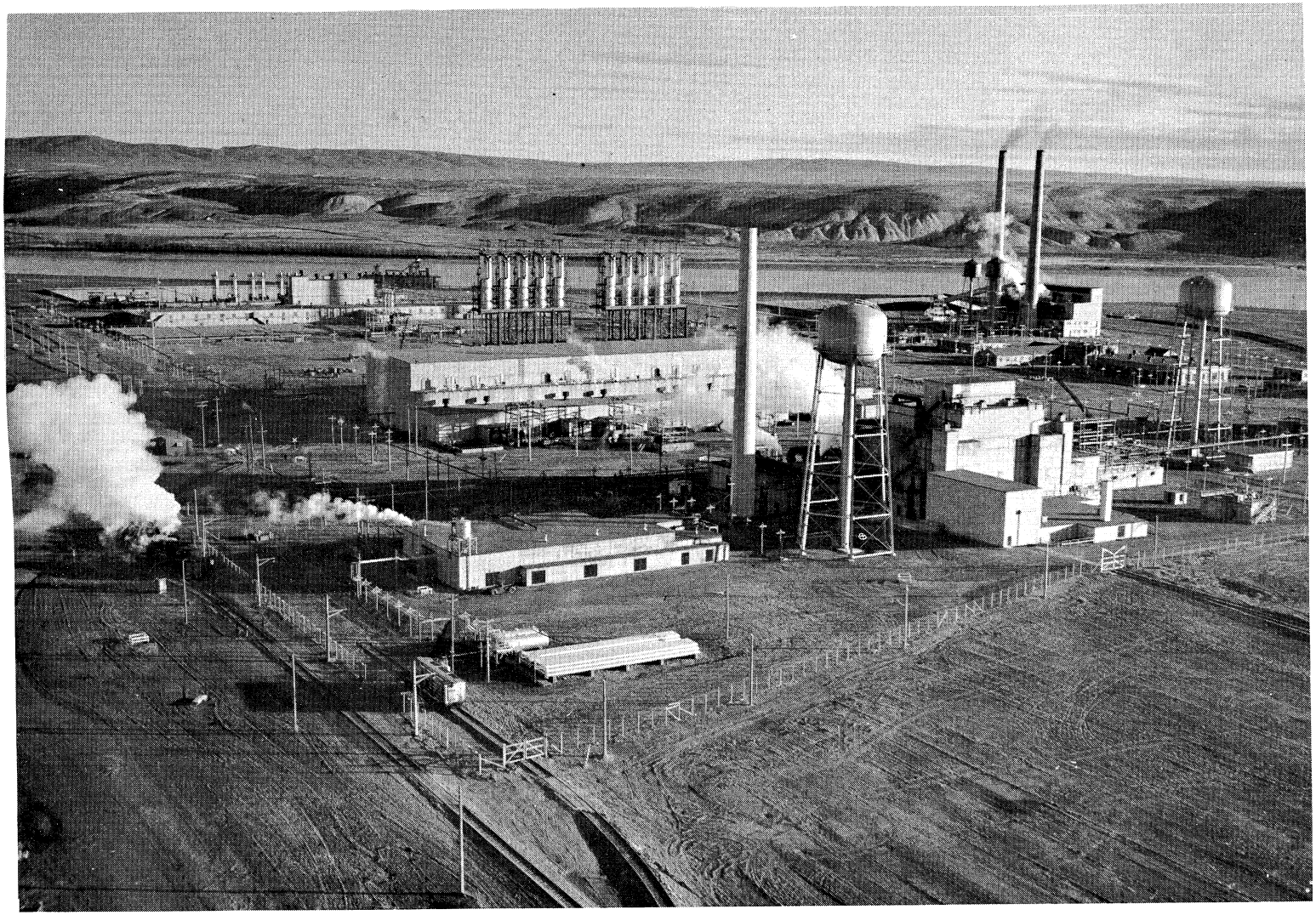

7.20 Typical reactor area at Hanford. (Courtesy General Electric Co.)

7.2 Experiment No. 2

A. Chemical Dosimetry and Dye (Film) Dosimetry

The subject of dosimetry is covered in Chapter 3 of "Radioisotope Technology." This chapter or its equivalent (4) should be read before conducting this experiment. For a background on radiation chemistry see Chapter 7 in "Radiation Uses in Industry and Science"(1).

Intermediate Field Dosimetry Ferrous Sulphate

Discussion

The operation of a gamma irradiation facility or laboratory requires the use of a standard method of measuring radiation. Generally the standard used is the ferrous sulphate dosimeter since it lends itself to wide ranges in dose rates, radiation times, and easily reproducible results even though it is a secondary standard itself. Upon absorbing radiation energy, the ferrous ions are converted to ferric ions which are easily detected by the rather broad resonance absorption of light having a wavelength of 3040 Angstroms. The mechanism of this conversion is discussed more fully in the article by Weiss (2).

Procedure

The intensity of the radiation fields measured in Experiment No. 1 will be checked by ferrous sulphate dosimetry. The dosimetric solution used in this experiment is: (see Ref. 3)

1. 2 gm Fe $SO_4 \cdot 7\ H_2O$, or Fe $(NH_4)_2\ (SO_4)_2\ 6\ H_2O$
2. 0.3 gm NaCl
3. 110 ml (95-98%) H_2SO_4 (analytical reagent grade) in sufficient distilled water to make 5 liters of solution.

A small quantity of the prepared solution is poured into small vials (about 3 ml per sample) and the vials are then placed in both the center well and the area adjacent to the center well of the large source. Each vial should be exposed to approximately 5-35 Kilorads. By using the data from Experiment No. 1, the approximate time for exposure can be determined. The optical densities of the irradiated samples are then read on the Beckman spectrophotometer and the relative change in optical density is converted to kilorads by using calibration curve of the spectrophotometer (see Fig. 7.10). For the Beckman use a setting of 304 mu and a slit width of 0.5 mm.

Questions

1. Why should the dose to the vials be kept below 40,000 rad?

2. Compare the data from the ferrous sulphate dosimetry to that obtained from the Victoreen in Experiment 1 and attempt to explain any discrepancies.

References

1. Brownell, L. E. "Radiation Uses in Industry and Science," US Government Printing Office, June, 1961

2. Weiss, "Chemical Dosimetry Using Ferrous & Ceric Sulphates," Nucleonics, July, 1952

3. Weiss, Allen & Schwarz, 1955, Geneva Conference, 14, p. 179

4. "Measuring Large Radiation Doses," Nucleonics, 17, 10, P. 58-78, 1959

B. High Field Dosimetry--Blue Cellophane and the Bragg Gray Effect

The small dose limitation of the ferrous sulphate technique has led to the search for an effective dosimeter at high doses. Henley (Ref. 1 and 2) discovered that commercial blue cellophane identified as duPont No. 300 MSC (4) containing a dimethoxy-diphenyl-disazo-bis 8 amino-1-napthol-5, 7-disulphonic acid dye gives satisfactory results for a dosimeter in the megarad region.

The dye in the film is decolorized as a result of reduction by radiation in a statistically random manner. A given fraction of the dye is reduced to the lenco form following a first order chemical reaction and the change in color is found by using the Beckman spectrophotometer. In Henley's technique, the strips of cellophane are sandwiched between polyethylene sheets and the resulting secondary electrons from the polyethylene cause the change in color of the blue cellophane. Having a fixed thickness of polyethylene provides a uniform production of secondary electrons. This production of ionization or ionization effects by secondary electrons is known as the Bragg-Gray Effect. (See Chapter 2 of "Radiation Uses in Industry and Science.") Since the lightening of the blue cellophane depends on the number of secondary electrons and the number of secondary electrons is dependent upon the thickness of polyethylene (up to a limit), it is possible to observe the effect of thickness on the cellophane by use of different thickness of polyethylene in the dosimetry measurements. An approximate theoretical analysis can be made in the following manner:

Let I_o be the number of gamma photons striking the face of the polyethylene of thickness t per unit area per unit time. Then the number of primary gamma photons at a distance x ($0 \leq x \leq t$) in the polyethylene is given by $\phi = \phi_o e^{-\mu x}$ where μ is the narrow beam attenuation coefficient of polyethylene. (See Chapter 4 of "Radioisotope Technology.") The number of secondary electrons produced between x and x + dx is

$$|d\phi| = \mu\phi_o e^{-\mu x}\, dx \qquad (7.2)$$

which is the number of gamma photons that have interacted between x and x + dx.

If, as an approximation, we assume that these secondary electrons are attentuated exponentially with an attenuation coefficient, σ, then the number of electrons produced between x and x dx that reach the blue cellophane is

$$dN = |d\phi| e^{-\sigma(t-x)} = \mu\phi_o (e^{-\mu x})(e^{-\sigma(t-x)})\, dx \qquad (7.3)$$

where t is the thickness of the polyethylene attached to the blue cellophane. The total number of electrons that reach the blue cellophane is then,

$$N = \int_o^t [\mu\phi_o (e^{-\mu x})(e^{-\sigma(t-x)})]\, dx \qquad (7.4)$$

and integrating,

$$N(t) = \frac{\mu\phi_o}{\sigma-\mu} [e^{-\mu t} - e^{-\sigma t}] \qquad (7.5)$$

The plot of Equation 7.5 will have the following shape:

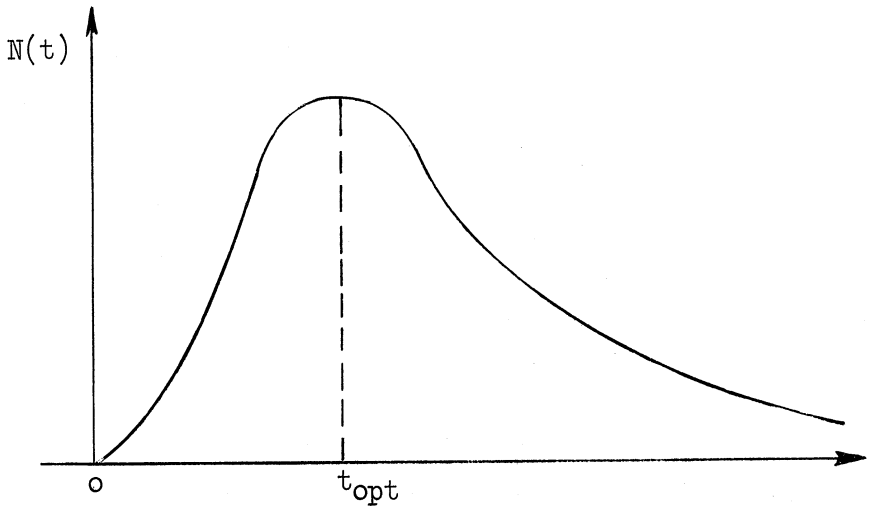

Figure. 7.11 Sketch Showing General Shape of Curve for Maximum Bragg-Gray Effect as Determined by Blue Cellophane Dosimetry.

The approximate value of the optimum thickness can be found by setting

$$\frac{dN}{dt} = 0 \qquad t_{opt} = \frac{1}{\sigma - \mu} \ln \frac{\sigma}{\mu} \qquad (7.6)$$

From the experimental data the optimum thickness can be obtained and from the literature, μ. The resulting transcendental equation (7.6) can be solved to determine the effective attenuation coefficient of the secondary electrons, σ.

Procedure

Sandwich the strips of blue cellophane between the 1/4" pieces of polytheylene and expose to a radiation field from 1 to 100 megarad. Have at least 4 samples in the 1 to 10 megarad region and 4 samples in the 10 to 100 megarad region. Measure the transmission of the blue cellophane at 6550 Angstroms with a slit width of .15 (Note that at this wavelength the tungsten bulb is used as the light source). To obtain optimum sensitivity set the Beckman so that the blue cellophane with largest dose corresponds to 100% transmission. For the samples with a small change use the expanded scale i.e., 0.1 scale. Plot the data as:

$$\frac{\%T \text{ sample} - \%T \text{ control}}{\%T \text{ control}} \quad \text{versus}$$

the dose on both linear and semilog paper.

Bragg Gray Effect

For the Bragg Gray data sandwich the blue cellophane between varying thicknesses of polyethylene and expose for the same dose (approximately 10 megarads). Since the changes in color for the different thicknesses are expected to be slight, use the expanded scale of the Beckman.

Questions

1. For low doses Henley gives the equation Dose (megarads) = .68 $(T-T_O)+C$ as representative of his data. What equation do you get for low doses? for high doses?

2. From the apparent relation $\%T = 100e^{-\rho\varphi}$ (φ is the optical density given and %T is the percent transmission given by the Beckman spectrophotometer) show that the number $\frac{\%T_S - \%T_C}{\%T_C}$ is independent of the initial setting.

Note that difference in optical density of two samples is independent of its initial or zero reading.

3. From the Bragg Gray data compute σ-----the effective attenuation coefficient for the secondary electrons.

References

1. Henley, E. J., "Gamma Ray Dosimetry with Cellophane Dye Systems," Nucleonics 12, 9, 62, 1954

2. Henley E. J., and Richman, D., "Cellophane-Dye Dosimeter for 10^5 to 10^7 Roentgen Range," Analytical Chemistry, 28, 1580, 1956

3. Evans, R. D., "The Atomic Nucleus," McGraw-Hill, New York, 1955

Low Field Dosimetry-Chloral Hydrate (0-1000 rad)

Certain chlorinated organics release HCl when subjected to gamma irradiation. Acid indicators in such a solution, or the testing of the conductivity of irradiated solutions can give a measure of the radiation absorbed.

Chloral hydrate, $CCl_3CH(OH)_2$ is an organic compound which is available commercially in crystalline form. It has a molecular weight of 165.42 and a solubility in water of 470 gms/100 ml. When irradiated while in a freshly prepared aqueous solution, the pH of the solution decreases in a linear manner with dosage over the range of 0 to 1000 rad.

Procedure

In this experiment the pH of the solution will be measured to determine its acidity. Prior to irradiation, prepare several chlorate solutions of different molarity (0.1M to 5M) of at least 100ml volume. Then irradiate small vials of the solutions in known fields for definite times. After checking the pH meter against the standard buffer solutions, measure the pH of each of the irradiated vials as well as a control.

Questions

1. What is pH factor?

2. Is there any change in the slope of the curve as a function of molarity? How do you explain this result?

3. From the data closest to the 1M solution compute the average energy absorbed to liberate one hydrogen ion.

References

1. Hilsenrod, J. Chem. Phys. 24, 917, 1956

2. Woods, R. J. and Spinks, J. W. T., "The Action of Co^{60} Gamma Rays and of Fenton's Reagent on Aqueous Bromal Hydrate Solution," Can. J. of Chem. 1475-86, 1957

7.3 Experiment No. 3

Experimental Determination of "Broad Beam" Attenuation of Gamma Radiation

Discussion

The practical calculation of gamma ray attenuation in shielding materials is simplified by the use of a "build-up" factor. The significance of "build-up" factors and the various types of build-up factors used are discussed in Chapter 4 "Shielding Calculations for Gamma Radiation" of "Radioisotope Technology" (1). There are at least twelve processes by which gamma radiation interacts with matter, but only three, the photoelectric effect, the Compton effect, and pair production are of primary importance (2). Of the three processes only the photoelectric process can be considered to represent complete absorption of gamma photons at or near the point of interaction. In this process all the energy of the gamma photon interacting is used to eject an electron from the electron cloud surrounding the absorber atom involved in the interaction. Pair production occurs only with high energy photons such as those produced in the core of a nuclear reactor. The interaction of these photons with absorber atoms results in the production of a pair, an electron, and a positron near the nucleus of the absorber atom involved in the interaction. The positron has a short life and is annhilated by interaction with an electron to produce two gamma photons at 180 degrees each having an energy of 0.51 Mev. Since the energy of these secondary photons is considerably less than the energy of the initial photon, they will be absorbed in a shorter distance thereby approximating true absorption.

The major problem in the calculation of attenuation of gamma radiation occurs with the Compton interaction. In this case the primary gamma photon interacts with an electron in the electron cloud around the absorber atom, ejecting the electron, but all the energy cannot be transfered to the electron. The surplus energy is expended in the production of a secondary photon of lesser energy than the primary photon and scattered at an angle from 0 to 180 degrees from the path of the initial photon. In some interactions in which only a small amount of energy is expended in ejecting the electron, the secondary photon may be almost as energetic as the primary incident photon resulting in subsequent interactions similar to the first. Thus, at the point of interaction the Compton effect results in a production of secondary photons without a decrease in the photon flux, but only a decrease in the average photon energy. The secondary electrons also produce x-ray photons by interaction with the absorber. Thus, there can be a "build-up' in the number of photons and in the number of interactions per unit distance. It is the purpose of this experiment to determine experimentally the "build-up" factor for some common materials.

The number of primary gamma photons which emerge from an absorber is given by the expotential equation

$$\phi = \phi_o e^{-\mu t}$$

where ϕ equals the initial gamma photon flux, μ equals the "narrow beam" attenuation coefficient for the absorber and t is the absorber thickness. In the case of Compton interaction, the above equation may be modified to include the build-up of secondary radiation as follows

$$f(N) = B_f f(N_o)$$

where $f(N_o)$ is the number of uncollided photons. B_f is the build-up factor that gives the correct answer $f(N)$ or for most cases

$$\phi = B_f \phi_o e^{-\mu t}$$

It is important to note that not only does the build-up factor (B_f) change for each $f(N_o)$, but it is also dependent on the geometry and atomic number of the absorber. If the radiation present at a point in an absorber is to be considered, the build-up of radiation due to Compton electrons, x-rays, electrons and annihilation quanta from pair production in addition to scattered photons are involved in B_f.

The build-up factor can also be incorporated in the exponential kernel of the equation giving

$$\phi = I_o e^{-(b_f \mu)t}$$

or

$$\phi = \phi_o e^{-\mu' t}$$

where μ' is now the broad beam absorption coefficient and is not a constant unless B_f varies exponentially.

Procedure

The Victoreen ratemeter is placed in a fixed position in the radiation field. The field is determined with no intervening test medium between the source and the thimble chamber. Subsequent measurements of radiation level are made with successively increasing thickness of the absorbing medium interposed between the source and the chamber. The build-up factors and the broad beam absorption coefficients should be shown as functions of absorber thickness.

To obtain data for calculating the effective density of the concrete shielding walls of the FPL cave, measurements of the radiation level at each of the outside faces of the cave are taken with the geiger tube instru-

ment. All measurements are made with the Cobalt-60 radiation source in the up position. The source is then lowered into the well and the same measurements repeated to determine background. Using the strength of the source computed in the first experiment, the known shielding configuration, and the build-up factors in concrete, apply the data to calculate the density of the concrete. Note any simplifying assumptions made. Figure 7.13 shows some half-value thickness for broad beam absorption in three food substances.

List in the results and compare your half-value thicknesses for each of the absorbers tested with those in Figure 7.13.

Questions

1. With increasing thickness of the denser materials such as lead and concrete you should observe a deviation in the slope of the curve with the larger thicknesses. What is the reason for this change?

2. With the less dense materials a plot of log of percent transmission versus thickness may show a slight increase before leveling off to essentially a straight line. Explain the reason for this phenomenon.

References

1. Brownell, L. E. "Manual for AEC-NSF Institute on Radioisotope Technology," June 1961.

2. Goldstein, H. "The Attenuation of Gamma Rays and Neutrons in Reactor Shields," USAEC, U.S. Government Printing Office 2, May 1, 1957.

3. Price, Horton, & Spinney, "Radiation Shielding."

4. Rockwell, T. "Reactor Shielding Design Manual."

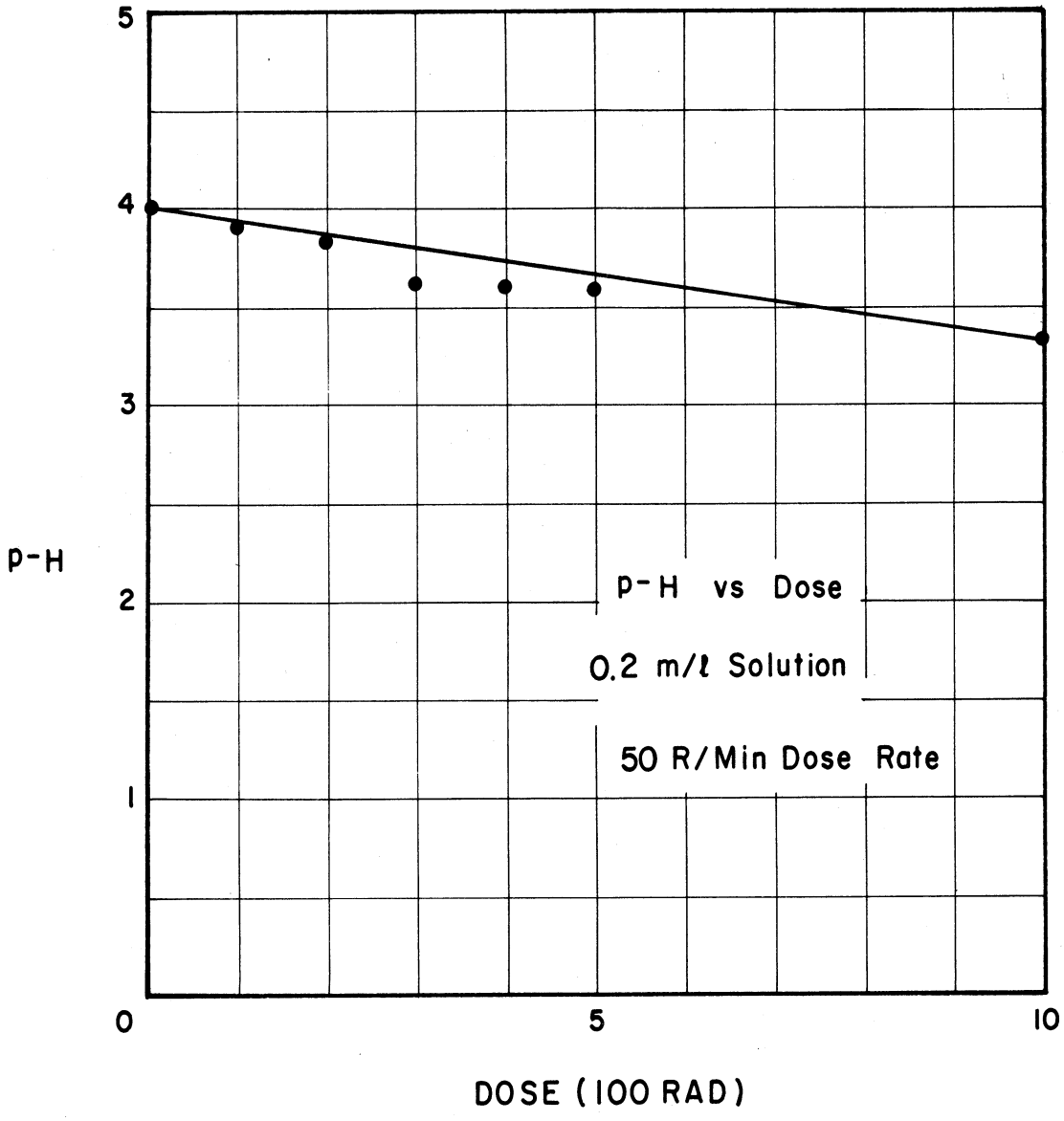

Figure 7.12. Experimental Observations of the Change of Ph of Freshly Prepared Chloral Hydrate Solution vs. Dosage of Gamma Radiation. (Unpublished work, J. F. Rice, University of Michigan.)

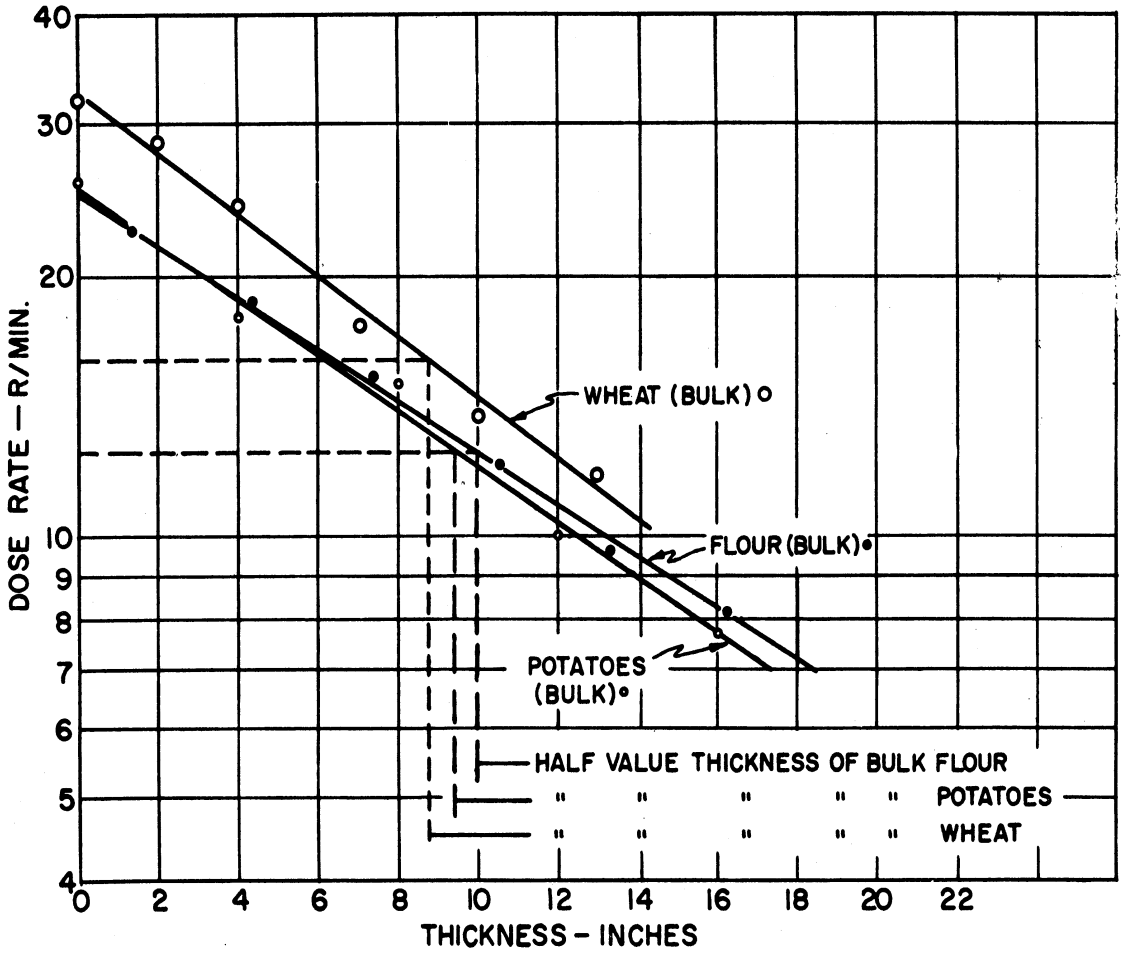

Fig. 7.13 Absorption measurements performed in the radiation "cave" at the Fission Products Laboratory.

7.4 Experiment No. 4

Radiography with a Source-Target Mixture

Discussion

There has been a real need for a rugged, portable X-ray facility for field radiography when it is not possible to transport the patient to a hospital where conventional X-ray equipment is available. Gamma radiation or the "bremsstrahlung" from various beta-particle sources offer a possible solution to this problem in the form of a portable radioisotopic sources. Studies of a promethium-147 tungstate source-target mixture for use as an X-ray source were reported by E. W. Coleman,* L. E. Brownell,** and C. J. Fox*** at the 1958 Geneva Conference on Peaceful Uses of Atomic Energy (1).

The successful application of radioisotopes in medical radiography requires an abundant supply of source material meeting the exacting requirements of the art. An isotope suitable for medical radiography must have a high specific activity so that sources of small diameter and high radiation intensity can be made. The radioisotope should emit radiation having essentially the same characteristics as the radiation from an X-ray tube used for diagnosis. To obtain a differential absorption between various body tissues, radiation is required with energies in the range of from 30 to 100 kev and preferably from 30 to 80 kev. The half-life of the radioisotope should be long enough to permit use of the source for a reasonable length of time before replacement is required.

Partable X-ray units utilizing radioactive sources of radiation have been reported by the Army Medical Research Laboratory. 2-6 While such units have certain advantages over conventional field radiographic equipment, the quality of radiographs produced is not considered acceptable. The presence of even a small amount of higher-energy radiation results in a loss of radiographic contrast between bone, muscle, and fat.

Thulium-170 was found to be a usable radiographic source, but because of high-energy bremsstrahlung originating within the source, the radiographic quality was poor. Radiographic sources using pure beta-emitting radioisotopes and external target foils have been proposed. The disadvantage is the limitation of source thickness to the depth of penetration of the beta particles in the source material, since all greater thicknesses will result in self-absorption

---

*Picker Research Center, Picker X-Ray Corporation, Cleveland, Ohio (formerly with Fission Products Laboratory, The University of Mich., Ann Arbor, Mich.

**Professor of Nuclear and Chemical Engineering and Supervisor, Fission Products Laboratory, The University of Michigan, Ann Arbor, Michigan.

***Research Assistant, Fission Products Laboratory, The University of Mich., Ann Arbor, Michigan

of beta particles in the source rather than in the target material. This is a severe restriction with sources of long half-life such as strontium-90, because the maximum specific activity of such sources is limited by their slow rate of decay. This means that if a small "point" source is used, the exposure times will be very long, and if a source of larger area is used, the X-rays will not be well collimated and a sharp radiograph will not be possible. Another disadvantage is that the electromagnetic radiation produced by self-absorption of beta particles in the source and from backscatter in the shield may not have the energy spectrum necessary for a good radiograph. Coleman and Brownell 7,8 proposed to avoid these difficulties by use of source-target mixtures. If the target is intimately mixed with the beta-particle source, the source thickness may be increased significantly because the electromagnetic radiation is more penetrating than the beta particles. Furthermore, if the atoms of the beta-particle source are chemically combined with the target atoms, each source atom will be surrounded by target atoms. This increases the probability of interaction between the beta particles and electrons surrounding the target atoms as compared to electrons surrounding other source atoms.

In view of logistic problems expected in storing, transporting, and replacing sources of short half-life, such as thulium-170 (127 days), only those isotopes with a half-life of one year of longer should be considered satisfactory. A "use-life" of three to four half-lives was considered reasonable, based on operating experience with thulium-170. Because of the low specific activity of strontium-90 and americium-241, these radioisotopes were not considered satisfactory, and the authors limited their sutdies to promethium-147 and thallium-204. Since the promethium-147 sources were found to be superior to the thallium-204 sources, only the promethium sources will be described.

A 1-curie promethium tungstate source was ordered from the Oak Ridge National Laboratory. The preparation of the tungstate and the encapsulation were performed by Mr. R. S. Pressley of the ORNL staff. This source was encapsulated in a modified Standard Oak Ridge capsule. The modification consisted of pressfitting a 4-mm-ID aluminum sleeve into the source cavity and machining the stainless-steel window to 0.005 in. Aluminum was chosen for the sleeve to minimize bremsstrahlung and characteristic X-ray production in the vertical walls of the source cavity, so that the effective focal spot size would be 4 mm. The capsule was silver-soldered after filling and placed in a larger lucite capsule with an air-path aperture to the window. The plastic capsule was used only to eliminate the possibility of accidental contact with the thin window during handling. The question of mechanical strength in a 0.005-in. stainless-steel window, and the relatively high absorption factor for low-energy radiation ($e^{-ux} = 0.25$ at 25 kev) suggests that a thicker beryllium metal window would be stronger and should improve the efficiency by attenuating a smaller part of the low-energy radiation.

Comparison of Spectra From Experimental Sources

In Fig. 7.14 the spectra of three possible radiographic sources (thulium-170, thallium-204 iodide, and promethium-147 tungstate) are shown and may be compared. Although all three sources have peaks in the characteristic X-ray region, the broad, flat, higher-energy bremsstrahlung spectra of the thulium-170 and thallium-204 sources indicate that shielding difficulties and poor radiographic contrast may be expected from these sources. The spectrum of the promethium sources is a definite improvement over thulium-170 with regard to higher-energy components. The major peak is at a higher energy than the thulium, but is still in the diagnostic region. A low-energy peak could be obtained by use of molybdate instead of tungstate as target material.

A radiograph of a human hand (Fig. 7.15) was made with the promethium tungstate. The original radiograph was well detailed considering the source diameter of 4 mm and the source subject distance. The quality of the radiograph was adequate for fracture or foreign-body localization. The wrist detail was good, and the fingernails are easily recognized in the original radiograph. Current technology indicates exposures of less than 1 hour are possible.

The major improvement over similar radiographs produced with thulium-170 is in radiographic contrast. Thulium radiographs exposed for maximum detail are grey and white, instead of the continuous gradation from black to white required for excellent contrast. The promethium radiograph shows improved contrast, probably due to the absence of high-energy bremsstrahlung in the spectrum.

Technical Radiographs Using Promethium-147 Tungstate Source

The use of promethium-147 sources for technical radiography is demonstrated in Fig. 7.16. A variety of small objects is shown in varying degrees of detail. The detail in the expandable metal watch band is sufficient to determine the integrity of the small spring in each link. The thin mica standoff insulators and the filaments in the electron tubes are easily visible. The lack of good detail in the stopwatch is perhaps the best example of the improved spectrum of promethium sources relative to thulium sources. Similar radiographs with thulium have shown complete detail of the watch, indicating the presence of a higher-energy spectrum.

As a result of these studies the conclusion was stated that radiographs made with promethium tungstate source-target mixtures show improved contrast compared to thulium-170 radiographs. Limited tests with radiographs of commercial objects of low mass indicate the possibility of use of promethium tungstate sources for industrial radiography of light-weight products. However, the efficiency of production of the radiographic image must be in-

creased to shorten the required length of exposure before medical application can be realized.

Procedure

The electromagnetic radiation spectrum of a source-target mixture of Promethium-147 tungstate is to be determined and a radiograph of several articles using this source-target mixture is to be produced. Promethium-147 is a pure beta emitter of 0.223 Mev with a half life of 2.7 years. Since it is a pure beta emitter, an intimate mixture of Pm^{147} with a heavy element should provide an electromagnetic radiation spectrum similar to that of an x-ray tube - i.e. a continuous spectrum due to bremsstrahlung superimposed on x-ray peaks that are characteristic of the elements in the mixture.

Such a source target mixture might have practical use as a portable x-ray machine. However, one of the major disadvantages of the source-target mixture idea is the long exposure times required to produce a radiograph. The time required to produce a radiograph could be reduced by making a larger volume of the source-target mixture. But this would result in poor definition of the radiograph and as the size of the source is increased, the increasing effect of self absorption gives somewhat of a "maximum effective volume" of the source.

The method used to determine the spectrum of the source-target mixture will use a NaI(Tl) crystal scintillation detector and a pulse height analyzer. The photo peak of a known monoenergetic gamma ray source will be analyzed to correlate the scale of the pulse height analyzer to Mev units. Then the spectrum of the source target mixture of Promethium tungstate will be observed.

A radiograph of several small objects will be made which will be observed a week later for the effect of source height distance on definition and contrast.

Questions

1. Why is the pulse height analyzer and associated components unable to resolve the characteristic x-ray peaks of the elements in the source-target mixture? What energy should these x-ray peaks be?

2. From the source-target spectrum obtained with the pulse height analyzer it is inferred that it is the actual spectrum of electromagnetic radiation from the source-target mixture. This is not true, for the spectrum is a measure of the energy deposited in the crystal. Why can we assume the spectrum of the source is the same or somewhat near the same as the spectrum we obtained?

3. From the source date (1 curie Pm^{147} - April, 1957, 2.6 year half life) compute the current required of an x-ray machine to produce a "radiograph" in 1 minute compared to an 8 hour exposure to the Pm^{147} source. Assume the spectrums of the x-ray machine and the source target mixtures to be the same.

4. An important parameter in the use of a radioisotope is its maximum specific activity (curies/gm or curies/cc). The source used in this experiment is cylindrical in shape having a diameter of 4 mm and a height of 3.5 mm. If the source-target material is pure $Pm_2(WO_4)_3$ and the promethium is pure Pm^{147}, what is the maximum activity that a source this size could have? (Assume the density of the source target mixture to be the density of tungsten).

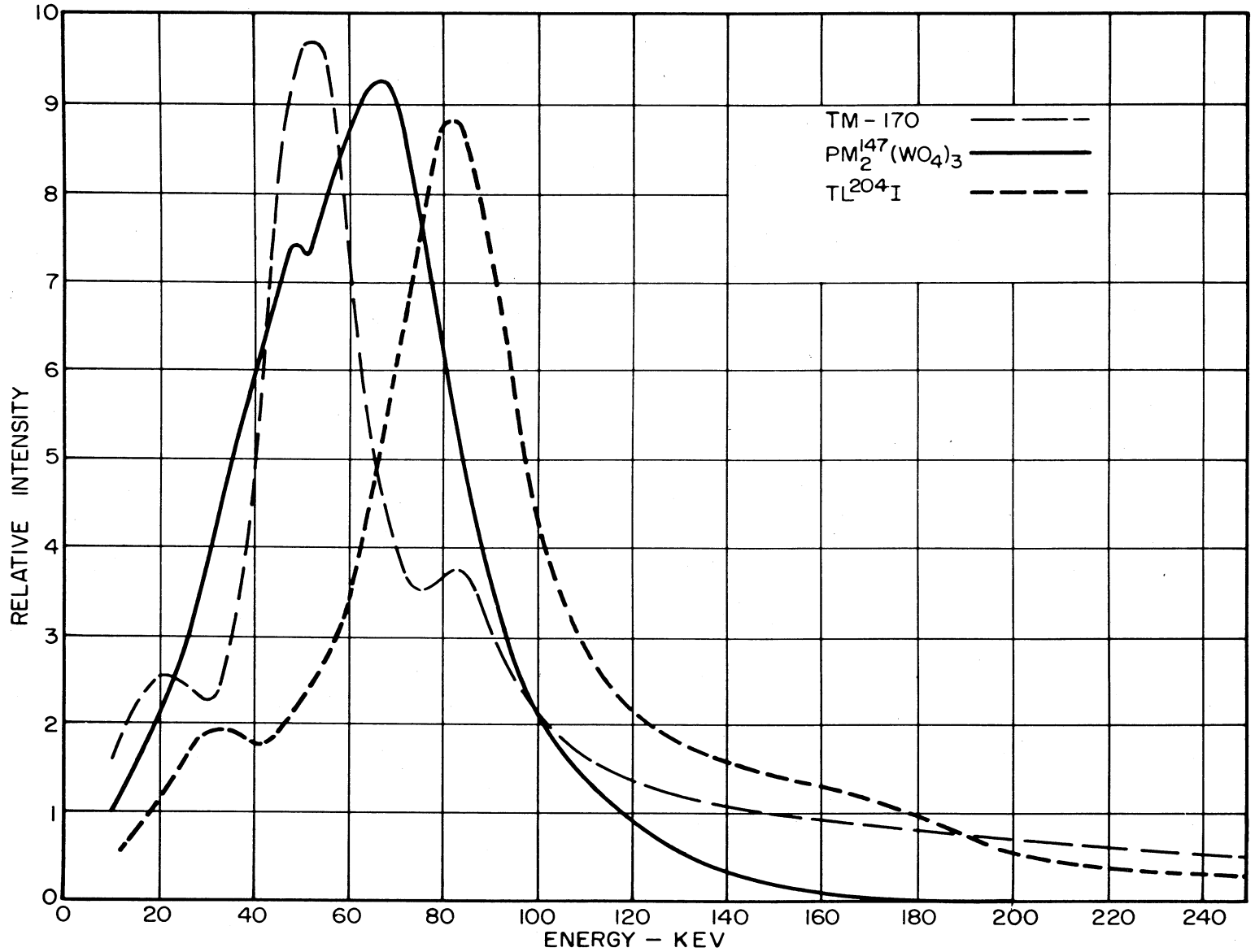

Fig. 7.14 Comparison of the spectra of three radiographic sources.

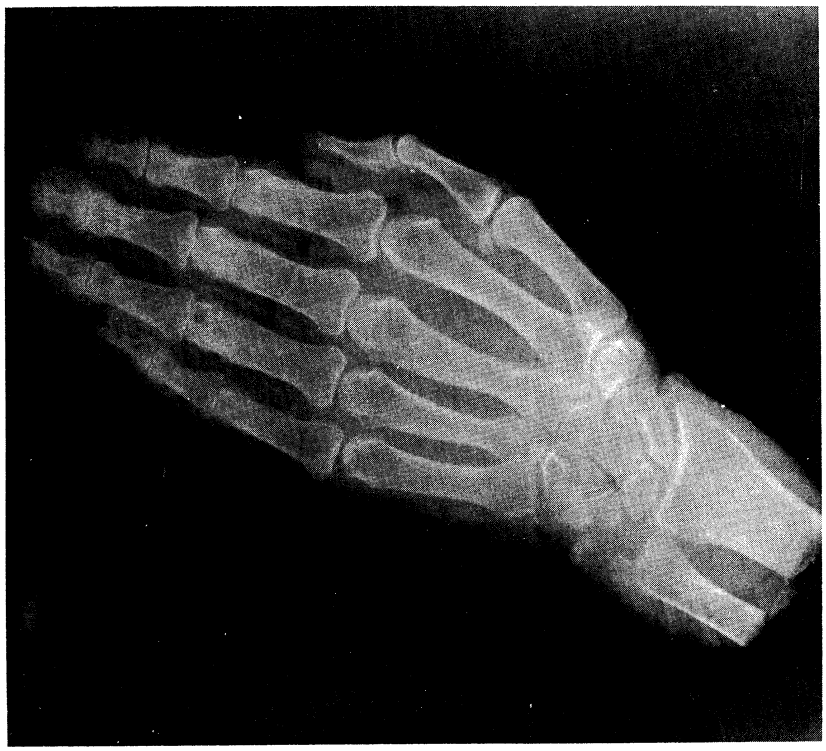

Fig. 7.15 Radiograph of human hand, 79-hr exposure at 20 in. from a promethium tungstate source.

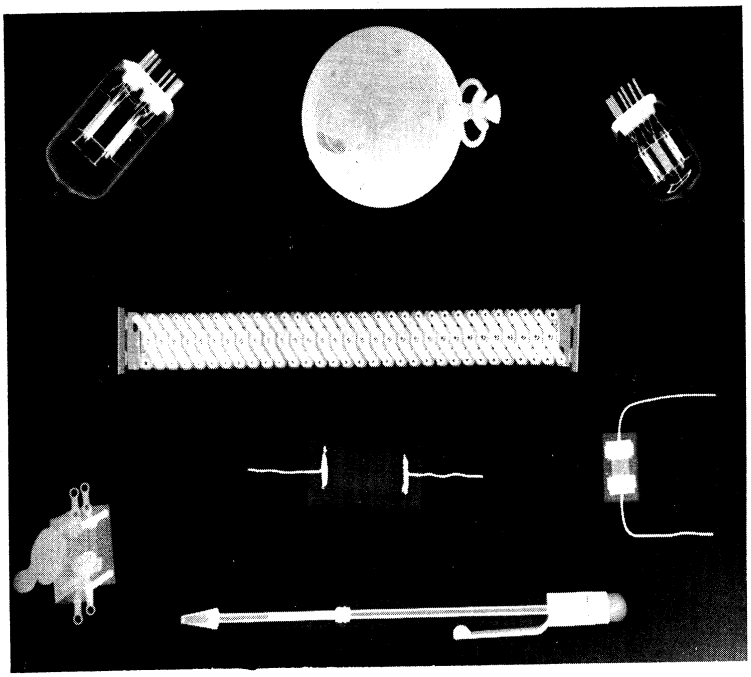

Fig. 7.16 Technical radiograph, 44-hr exposure at 10 in. from a promethium tungstate source.

7.5 Experiment No. 5

Area Decontamination

Discussion

Familiarity with the methods and techniques of low level area decontamination and with the effect of surface texture on the ease of surface decontamination is important to the Health Physicist. (See discussion and illustrations on decontamination in Chapter 2 of "Radioisotope Technology.")

Generally the subject of area decontamination can be divided into categories of pre-incident planning, the acute phase, recovery phase, and techniques. In pre-incident planning such items as proper facilities, and laboratory equipment and good experiment design are important as well as the choice of isotopes used. For example the use of 54 day Sr^{89} is much safer than the use of 28 year Sr^{90}. For a low-level contamination by liquid, absorbant paper, trays, a mop and bucket and shoe covers are essential. For high-level liquid contaminations isolation equipment such as signs and barriers, protective clothing, waste storage containers along with the previously mentioned equipment is needed for the incident. Dusts present additional problems. Respirators, vacuum cleaners, protective clothing, shower facility, isolation equipment and waste containers may be needed to handle the incident.

The acute phase occurs at the time of the incident. The first step may be to evacuate the area to a safe distance, but not to spread possible contamination nor to leave for clean areas until checked for personal contamination. Next, call a Health Physicist for assistance and begin to assemble equipment for decontamination. Rotation of personnel may be necessary if high radiation fields are involved. If radioactive dust is suspected to be present, an air sample should be taken.

In the recovery phase take instrumentation into the area that is capable of detecting the contamination. A Geiger tube type of instrument sensitive only to gamma rays is not suitable for detecting alpha or beta particle contamination. In planning and executing decontamination procedures, evaluate the efficiency of each procedure.

In general, decontamination techniques fall into two classes.

1. Isolate the area or object and allows natural decay to reduce levels.

2. Decontaminate

The types of decontamination can be classified as either "rough" to permit limited use or occupation of the area and a "detailed" decontamination which reduces radioactivity in so far as possible, to a satisfactory or low level.

The processes of decontamination depend on the type of contamination and the nature of the surface. The easiest surface to decontaminate is a wet contamination on a smooth non-absorbant surface. This can be cleaned by flushing with water and detergents followed by scrubbing and further flushing. Steam under pressure is sometimes helpful. For dust, use vacuum cleaning. If further treatment is necessary, brush and vacuum again. On greasy surfaces, remove the greasy material with dry cleaning solvents. If necessary, follow this with scouring with water soaps and detergents. Deeply absorbed contaminations present a problem that may only be disposed of by removal of the surface while at the same time preventing further penetration of the contaminant. For example, removal of the top few inches of earth, removal of floor covering or paints, abrasion, acids, or special chemical compounds. Firmly held contamination can only be "decontaminated" by covering the area with a suitable thickness of sealing material, or disposing of the contaminated object or clothing by burial in the earth or at sea in weighted sealed containers.

General facts about contamination are that it will not be uniform, smooth surfaces are less susceptible than rough surfaces, cracks or crevices collect it, movement of people and equipment will spread it, and no process will neutralize it.

In "rough" decontamination speed may be an essential consideration and as a result simplicity is usually required. The procedure selected should be rapid, suitable for the material, not require large quantities of special or dangerous chemicals, and make use of available equipment, services and material.

The decontaminating of personnel usually requires successive use of soap and water scrubbings, checking for reduction in activity more scrubbing. Remember to stay out of "clean" areas unless you are "clean."

Figure 7.17 shows the checking of shoe covers for possible contamination before stepping onto a "step-off" pad in the Hanford area. A "poppie" counter sensative to alpha particle radiation is being used. Health physics procedures require the employee to check his protecitve clothing before leaving a contaminated area. After checking his shoe covers, he can step onto a step-off pad. Here he removes his outer layer of protective clothing -- gloves, head-cover, coveralls, shoe covers. This procedure prevents spread of contamination (by particles) into clean areas.

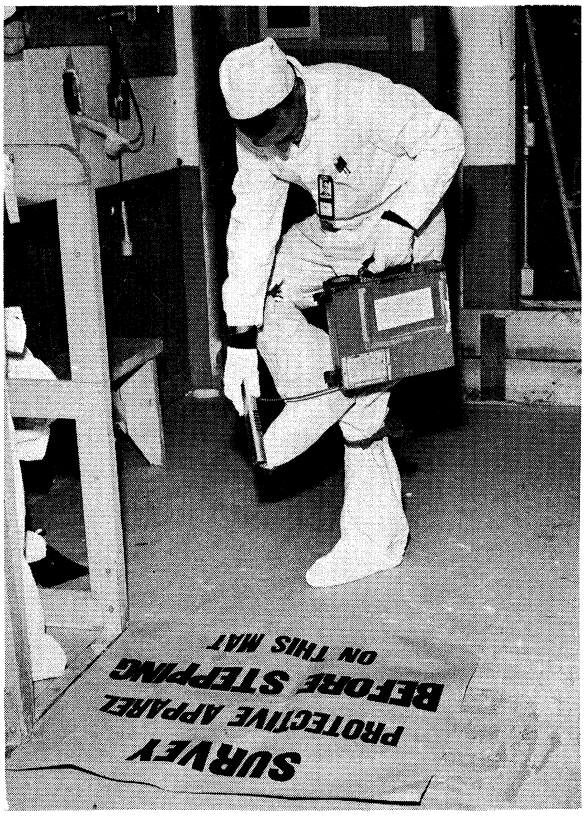

Fig. 7.17 Checking shoe covers at the Hanford Plant for contamination before stepping onto step-off pad (Courtesy General Electric Co.)

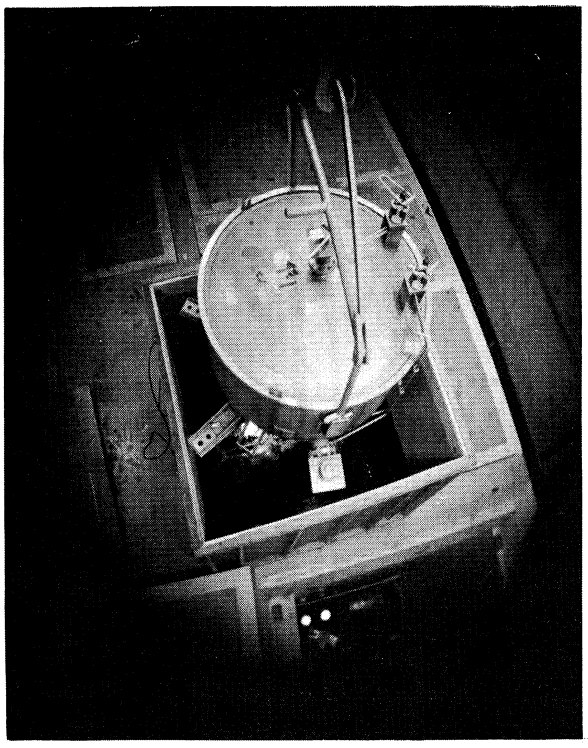

Fig. 7.18 Periscope picture of equipment in decontamination canyon at Hanford Plant (Courtesy General Electric Co.)

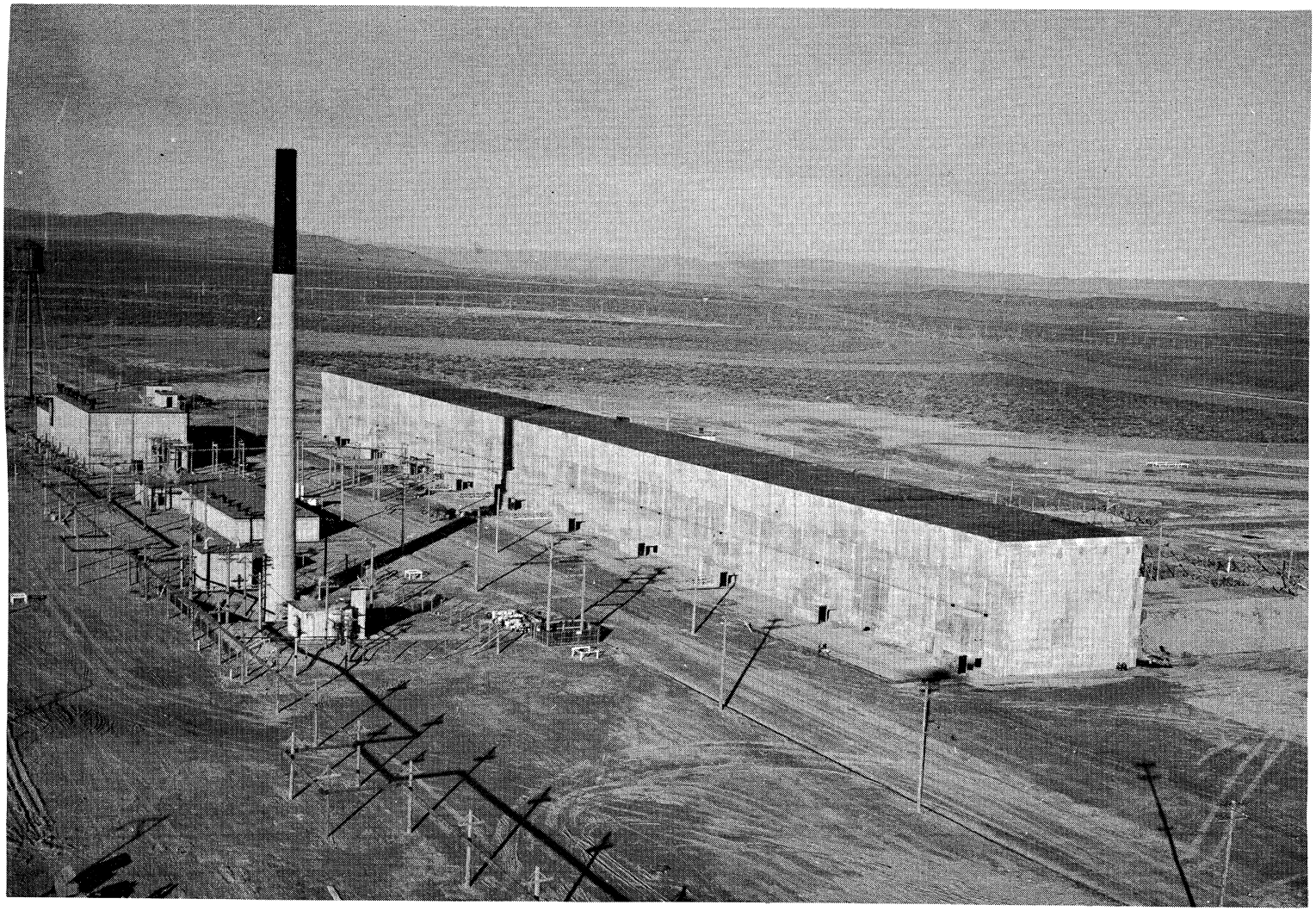

Fig. 7.19 A Hanford Works "canyon" building over 800 feet long
(Courtesy General Electric Co.)

Figure 7.18 is a copy of a photograph taken through a periscope from the over head crane in a canyon building at Hanford used specifically for decontamination. Expensive stainless steel equipment such as shown in the figure become highly contaminated with fission products during the processing of uranium fuel slugs. This equipment is decontaminated by handling remotely and transfered to canyon areas for disassembly by remote operations. The equipment is then washed by detergents, acids, and water to decrease the decontamination to a sufficient level to permit final decontamination and cleaning manually by operators dressed in SWP (Special Work Permit) protective clothing such as used by the worker shown in 7.17.

Figure 7.19 shows a typical canyon separations plant at Hanford. It is a long, windowless, concrete building, partly underground. The plant separates plutonium from irradiated uranium and recovers the uranium from the mixture of fission products for re-use in the atomic program. Many of the operations inside a canyon are controlled remotely by viewing and handling devices as a means of protecting the workers from radiation.

Procedure

From the above discussion, plan and conduct a decontamination test for Na^{-24} from painted and unpainted wood, concrete block, lead brick, linoleum, and or other surfaces.

References

1. Lane, "Contamination & Decontamination of Laboratory Bench-Top Materials," Nucleonics, August 1953, p. 49.

2. Breslin and Solon, "Fallout Countermeasures for AEC Facilities," NYO 4682-A, December 1955.

3. Curtis, R. L. "Decontamination - A Literature Search," Y-964, May 19, 1953-70 titles are included.

4. Handbook 48, "Control and Removal of Radioactive Contamination in Laboratories," U.S. GPO, December 15, 1951

5. Handbook 69, "Maximum Permissible Body Burdens and Concentrations of Radionuclides in Air and Water for Occupational Exposure," US GPO, June 5, 1959

7.6 Experiment No. 6

Treatment of Radioactive Wastes

Discussion

Familiarity with the methods for decontamination: simple distillation, cation exchange, anion exchange, and combinations of these processes is important.

Treating liquid radioactive wastes such as fission products, involves separating or concentrating the radioisotopes as much as possible and then disposing of the concentrate by approved techniques.

Figure 7.20 shows a typical reactor area at Hanford where plutonium is produced from natural uranium. Each reactor area contains its own water purification plant to provide cooling water for the reactor and its own steam plant for auxiliary power. The Columbia River is shown in the background. Fuel slugs from these plants are processed in canyon buildings such as shown in Figure 7.19 of Experiment 7.5. After recovery of plutonium and uranium, the fission product wastes are concentrated by evaporation for recovery of nitric acid. The acid solution is then neutralized which results in precipitation of some of the fission products. The slurry is sent to underground storage in large reinforced concrete tanks lined with plain carbon steel. Figure 7.21 shows a picture in the radioactive waste storage area located in the desert at the Hanford works. The four workmen in SWP clothing have emptied one of the storage tanks by pumping to another tank and are about to take photographs for inspection of the tank interior. Infrared film must be used because residual activity from the fission products will fog conventional photograph film.

In the ion exchange method of concentration, the radioactive ions are absorbed on the surface of a resin. The resin can be pictured as very large molecules linked and cross linked to form a chain. Protruding from the chain at regular intervals are groups (generally sulfonic groups for cation regions and amine groups for anion resins) like the spines on a porcupine. When the ions flow over the surface of the resin, the resin group absorbs it and in the case of the cation resin, releases hydrogen. The equilibrium between the hydrogen from cation resin and the cations can be represented by the equation

$$M^{+n} + n\ RH \leftrightharpoons n\ RM + nH^{+}$$

where R = the resin. As the equation shows the resin can be recharged and

M is the cation with an acid. Recharging with a complexing solution will selectively remove the ions. By this technique the ion exchange method can also be used to separate the fission products.

Procedure

In the distillation tests, samples of 1 to 5 cc of the distillate should be taken periodically to determine how the decontamination factor varies with the amount of standard solution left.

When setting up the ion exchange apparatus, the resin should be mixed in water and poured into the column. At no time during the filling of the column or filtering the fission product solution through the column, should the meniscus be allowed to drop below the surface of the resin, otherwise air entrainment will occur, lowering the amount of surface of the resin available to ion exchange. Samples should also be taken periodically from the ion exchange column since the first few samples will contain an excessive amount of water. In using the well type scintillation counter, make sure the plastic insert is in the well to avoid a contamination incident.

In cleaning glassware use the "hot" sink to wash out the major portion of radioactivity, then use the cold sink to finish the job.

Put spent resins and sand in the carton marked "solid waste" and place the liquid heel from the distillation flask in the bottle marked "wastes." Also check the rubber gloves. If they are "clean" replace in box, if not, toss them in the "hot" can.

In the hot lab everyone is to wear a lab coat and no one smokes, and no one is to leave the lab area without checking their hands and feet for contamination.

Questions

1. Is the difference in the counting rates of the standard solution between the beginning and end of the lab period enough to apply a correction to each of the readings?

2. Describe two procedures both of which would give a decontamination factor of 10^8. Each procedure may involve multiple steps.

References

1. Bleuler & Goldsmith, "Experimental Nucleonics," Experiment #12, Rinehart & Co., New York, 1957

2. Nachod, F. C., Ion Exchange, "Theory and Practice," New York, Academic Press Inc., 1949

3. Kunin, R., and R. J. Myers,"Ion Exchange Resins," New York, John Wiley & Sons, Inc., 1950

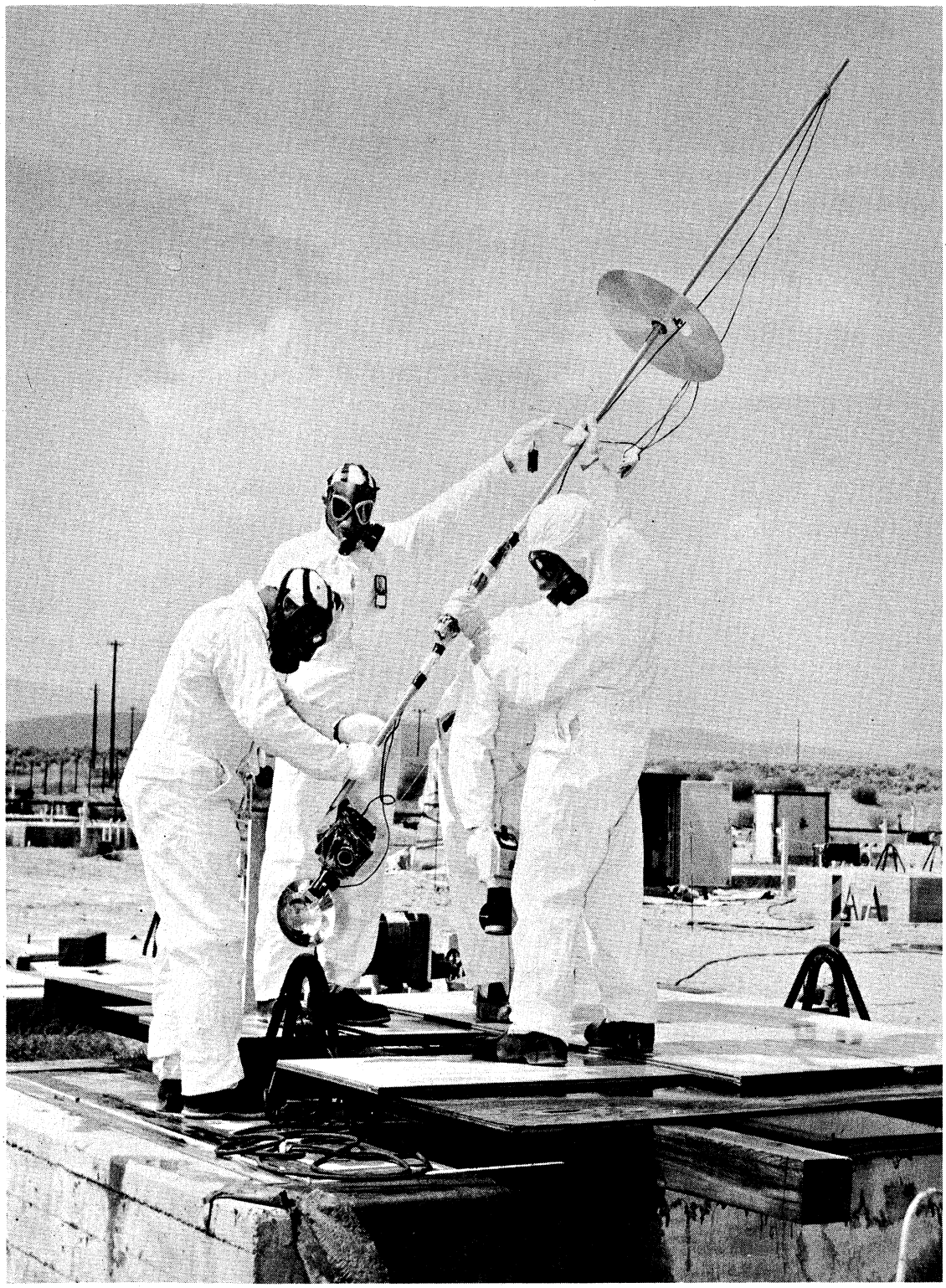

7.21 Photographic inspection of underground tank used for storage of waste fission products at Hanford. (Courtesy of General Electric Co.)

Experiment No. 7

Measurement of Per Cent Moisture by Neutron Slowing Down

Discussion

A calibration curve for the per cent moisture present in sand is to be obtained by measurement of the thermal flux of neutrons.

Neutrons from neutron (α,n) sources and from thermal neutron reactors are born at energies of several Mev lose their energy in collision with other nuclei until they are in thermal equilibrium (0.25 ev) at which time they wander around the medium until they are absorbed or leak out.

The source of high energy neutrons in this experiment is from the (α,n) reaction on Beryllium -- the source of alpha particles being Pu. The detector, or the absorber, is a $B^{10}F_3$ tube (the B^{10} has a 1/v cross section for thermal neutrons -- see reference 2) and detects via the ionization produced in the (n,α) reaction on B^{10}.

A hydrogen nucleus has the same mass a neutron which permits maximum transfer of energy on collision. Therefore, neutrons will require fewer collisions with hydrogen of the water than with silicon or oxygen of the sand (see question 4) to reach the thermal region and be counted with the $B^{10}F_3$ tube. The count rate from neutrons scattered in a bed of wet sand will be dependent on the number of hydrogen nuclei per unit volume which in turn is proportional to the number of neutrons that reach the thermal energy region -- this is the neutron slowing down density - q. (See Ref. 2 p.57-60.)

For a point source of neutrons in an infinite medium 9 obeys the equation

$$q(r) = \frac{e^{-r^2/4\tau}}{(4\pi\tau)^{3/2}}$$

where r is the distance from the source to the detector and τ is the Fermi Age

$$\tau = \int_{E_T}^{E_o} \frac{D\,dE}{\epsilon\Sigma_s E}$$

If hydrogen is taken as the only moderator and the scattering cross section, σ_s, is considered constant, then

$$\tau = \frac{\ln E_o/E_r}{N^2\sigma_s{}^2}$$

where N is the number of hydrogen nuclei per unit volume.

thus,

$$q \approx N^3 \sigma_s^3 \frac{[\ln (E_t/E_o)]^{3/2}}{(4\pi)^{3/2}} e^{-r^2 N^2 \sigma_s^2 \ln E_r/E_o}$$

for which small r gives a cubic dependence on N.

Procedure (J. Sickles)

The equipment to be used in this experiment consists of a 1 curie Pu-Be source and the following detection equipment: B^{10} tube, pre-amplifier linear amplifier and scaler. A block diagram of the neutron moisture gage is shown in Fig. 7.22.

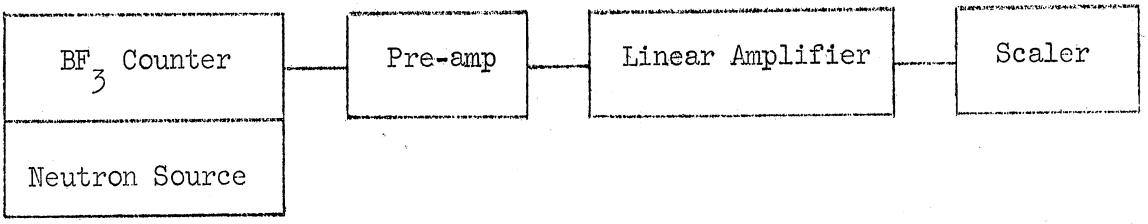

Fig. 7.22

1. Set the scaler voltage to that recommended for the particular $B F_3$ tube you are using, i.e. 1450 volts for the $B F_3$ tube at 20 mm pressure. Also set the internal voltage of the scaler at 0.75 volts and adjust the discriminator setting of the linear amplifier to a value which eliminates amplifier noise but not neutron pulses. An oscilloscope may be used for this purpose but in this experiment a discriminator setting of 10 will likely suffice.

2. Measure the initial moisture weight per cent of the sand and then determine a calibration curve of moisture weight per cent vs count rate by taking count rates at intervals of about 3 per cent until saturation is reached. Use counting times of at least two minutes and establish a σ by taking three measurements at each point. (See Ref. 2). Caution: Leave the $B F_3$ tube in the probe only when measurements are being made. This will prolong the life of the tube.

3. Test the effect of geometry by placing the probe at several different locations in the bucket. Does the count rate vary significantly? If so, why?

4. Use your calibration curve to measure the moisture weight per cent in an unknown sample.

References

1. Murray, R.L. "Nuclear Reactor Physics," Prentice-Hall, 1957

2. Price, "Nuclear Radiation Detection," McGraw-Hill, 1958
($B^{10}F_3$ tubes and assiciated counting system)

3. BNL-325--Cross Sections for Nuclei ("Barn" Book)

Questions

1. How well does the shape of the counting rate curve compare with that predicted by the above theory? Explain any discrepancies.

1.b. What is the "mean-free-path" of the neutrons at this value of percent moisture? (Consider only the hydrogen.) (See Ref. 1.)

2. Explain why the counting rate stays relatively constant below this value.

3. Show that the $B^{10}F_3$ counter truly measures the thermal flux. (See Ref. 2.)

4. On the average, how many collisions does it take for the neutron to get from 10 Mev to .1 ev in (a) hydrogen,(b) oxygen, (c) silicon. (See Ref. 1, p. 36-37.)

5. Sketch the cross section curves for hydrogen, silicon, and oxygen.

6. Obtain equations 1-4 above.

Appendix for Experiment No. 7

Outline of Neutron Fundamentals

1. Possible existence suggested in 1920.

2. Studies in 1932 by Curie-Joliets of secondary radiation produced by alphas on Beryllium. Believed to be new type of electromagnetic radiation. Could not explain ejection of protons from paraffin by new radiation. Protons had a range of 40 cm in air, equivalent to 5 Mev which would require 55 Mev photons.

(Wrong Eq.) $_4Be^9 + {}_2He^4 + E \rightarrow {}_6C^{13*} \rightarrow {}_6C^{13} + h\nu$

Where E_1 = KE of α particle.

$$9.01503 \text{ amu} + 4.00388 \text{ amu} + 5 \text{ Mev} \rightarrow 13.00751 + h\nu \quad (0.00536 \text{ amu})$$

1 amu = 931.2 Mev. $\therefore$ 5 Mev = .00536 amu

By balance of energy plus mass: $\Delta E = \Delta m\, c^2$

$h\nu$ = 0.01676 amu = 15.6 Mev available. (Not enough for 55 Mev photon.)

3. Neutron existance verified by Chadwick in 1932. He showed that radiation could not be electromagnetic unless energy of radiation was considered dependent upon nature of target nucleus.

Example

Protons from paraffin ~ 5.7 Mev., need 55 Mev. γs
Protons from nitrogen ~ 1.2 Mev., need 90 Mev. γs

(Photon E must increase with mass of recoil atom). Difficulties disappear if radiation treated as particles of mass 1 and 0 charge

$$_4Be^9 + _2He^4 \rightarrow _6C^{13*} \rightarrow _6C^{12} + _0n^1 + Q$$

(Correct Equation).

4. α-n Reactions

$$_3Li^7 + _2He^4 \rightarrow _5B^{11*} \rightarrow _5B^{10} + _0n^1 + Q$$

$$_4Be^9 + _2He^4 \rightarrow _6C^{13*} \rightarrow _6C^{12} + _0n^1 + Q$$

$$_5B^{11} + _2He^4 \rightarrow _7N^{15*} \rightarrow _7N^{14} + _0n^1 + Q$$

$$_7N^{14} + _2He^4 \rightarrow _9F^{18*} \rightarrow _9F^{17} + _0n^1 + Q$$

$$_9F^{19} + _2He^4 \rightarrow _{11}Na^{23*} \rightarrow _{11}Na^{22} + _0n^1 + Q$$

$$_{13}Al^{27} + _2He^4 \rightarrow _{15}P^{31*} \rightarrow _{15}P^{30} + _0n^1 + Q$$

$$_zXa^A + _2He^4 \rightarrow _{(z+2)}Y^{(A+4)*} \rightarrow _{(z+2)}Y^{(A+3)} + _0n^1 + Q$$

Q = Quanta (= 2.7, 4.47 + 6.7 Mev γ's for Be reaction.)

5. Chadwick's Demonstration Apparatus

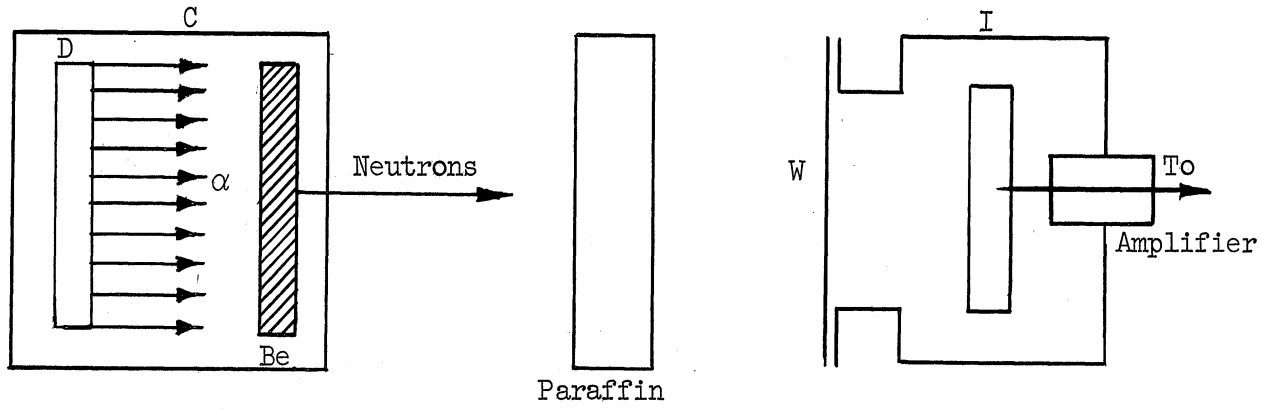

C = Evac Chamber

D = Po α Source

Be = Beryllium Plate

I = Ionization Chamber

W = Window

6. Thermal Neutrons

Neutrons in temperature equilibrium with their surroundings do not have a fixed speed but a distribution of speed that is accurately characterized by the gas equation of Maxwell

$$n(v) = n_o \left[4\pi \left(\frac{m}{2\pi KT}\right)^{2/3} \right] v^2 e^{-mv^2/2Kt}$$

where n_o is the number of neutrons per cubic centimeter

K (Boltzmann constant) = 1.38×10^{-16} ergs/°K

T is the temperature of the medium °K

For room temperature, T = 293°K, the distribution looks as shown on the next page.

The most probable speed is given by the peak of the curve and can be found

)y setting $\frac{dn}{dv} = 0$. This speed turns out to be $v_p = \sqrt{\frac{2KT}{m}} = 2200$ m/sec.

'or neutrons in a medium characterized by T = 293°K. A more useful quantity des-

:ribing the speed distribution is the average speed, $\bar{v}$

$$\bar{v} = \frac{\int_0^\infty vn\,(v)\,dv}{\int_0^\infty n\,(v)\,dv} = \frac{2}{\sqrt{\pi}}\,vp$$

ıd for neutrons at T = 290, $\bar{v}$ = 2482 meters/sec

)nsider hydrogen atom in heavy water at 25° C

Most probable vel, v_p = 2200 m/sec

.E. = 1/2 Mv^2 = 1/2 (1.66 x 10^{-24} gm/atom) (2.2 x 10^5 cm/sec)^2 = 4.0 (10^{-14}) Ergs

(Ergs) = m (gms.) (C, cm/sec)^2

where C = Vel. of light = 2.99790 $(10)^{10}$ cm/sec

$\frac{0\ (10^{-14})\ \text{ergs}}{6\ (10^{-6})\ \text{erg/ Mev}}$ = 0.025 ev. = Energy of thermal neutron

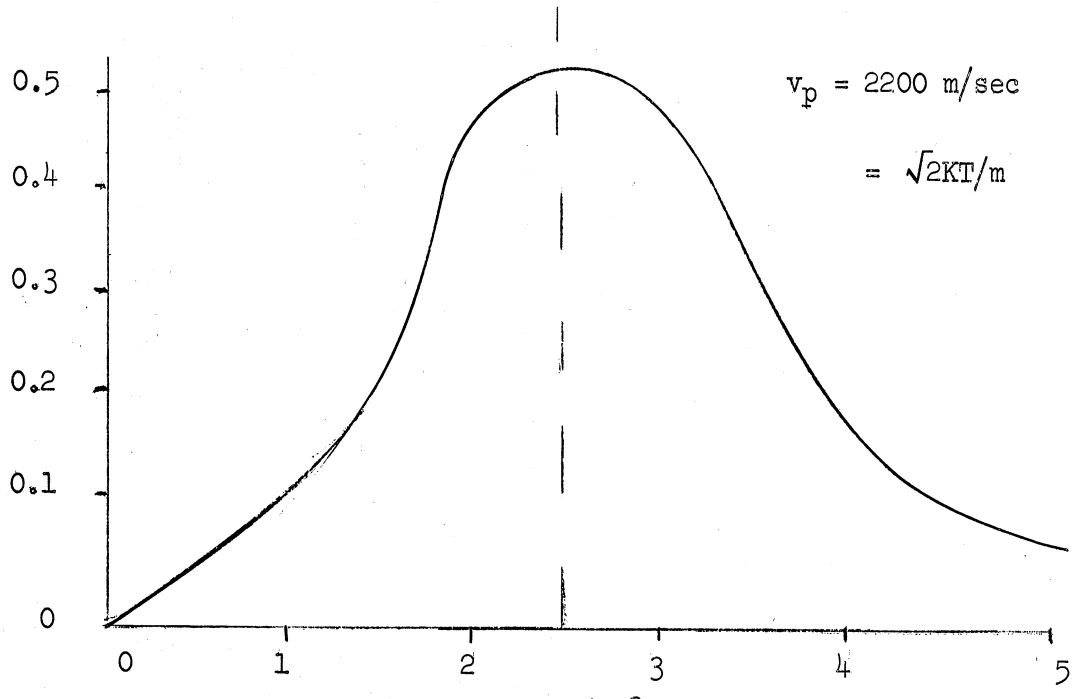

Maxwellian Distribution of Neutrons at 25° C

E_p = Energy corresponding to most prob. Vel. = 1/2 m v_p^2 = KT

K = Boltzmann's constant = 1.38 (10^{-16}) erg/°

$$K = \left| \frac{\text{R, ideal gas constant/mole}}{\text{Na, number of particles/mole}} \right|$$

v_p (25° C) = 2 (1.38) (10^{-16}) /(1.66 x 10^{-24}) = 2.2 (10^5) cm/sec

7. Neutron Cross Sections

Cross section is measure of probability of a process

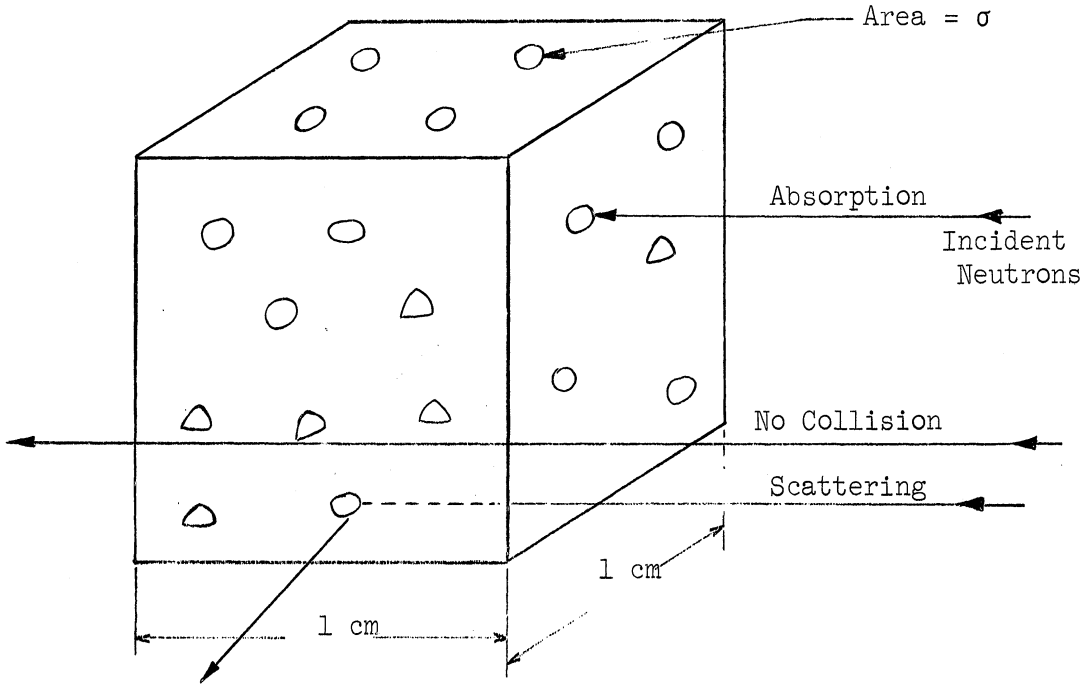

Consider cube 1 cm x 1 cm x 1 cm

Based on geometry, probability of collision

$$\frac{\text{Target Area}}{\text{Total Area}} = \frac{N\sigma}{1}$$ where N = no. atoms/unit vol.

σ = target area/atom

Geometry concept is approximate with thermal neutrons

Example:

Diameter of atomic nucleus $\approx 10^{-12}$cm

Area of atomic nucleus $\approx 10^{-24}$ cm^2

Experimental cross section of $U^{235} = 650\ (10^{-24})$ cm^2

Experimental values are used. Holloway and Baker (Los Alamos) suggests Barn as unit: 1 Barn = 10^{-24} cm^2

Thermal Neutron Microscopic Cross-Section, σ, Barns

Isotope	σ_s	σ_a	σ_f
H	38	0.33	
Be	7	0.01	
B	4	750.	
C	4.8	.0045	
Fe	11	2.43	
Cd	7	2400.	
Xe^{135}	4.3	3.5×10^6	
U (nat)	8.2	7.42	3.92
U^{235}	8.2	650.	459.
U^{238}	8.2	2.80	0.
Pu^{239}		1025.	664.

σ Total = σ scatter + σ absorption + σ fission

Absorption cross sections depend upon neutron energy in two ways:

(1) 1/v dependence

(2) resonance

$\sigma a = (\sigma_a)_o \left(\frac{v_o}{v}\right)$ where v_o = 2200 M/sec for 0.025 ev neuts.

Neutron Cross-Sections Cont.

Examples of Velocity Dependence

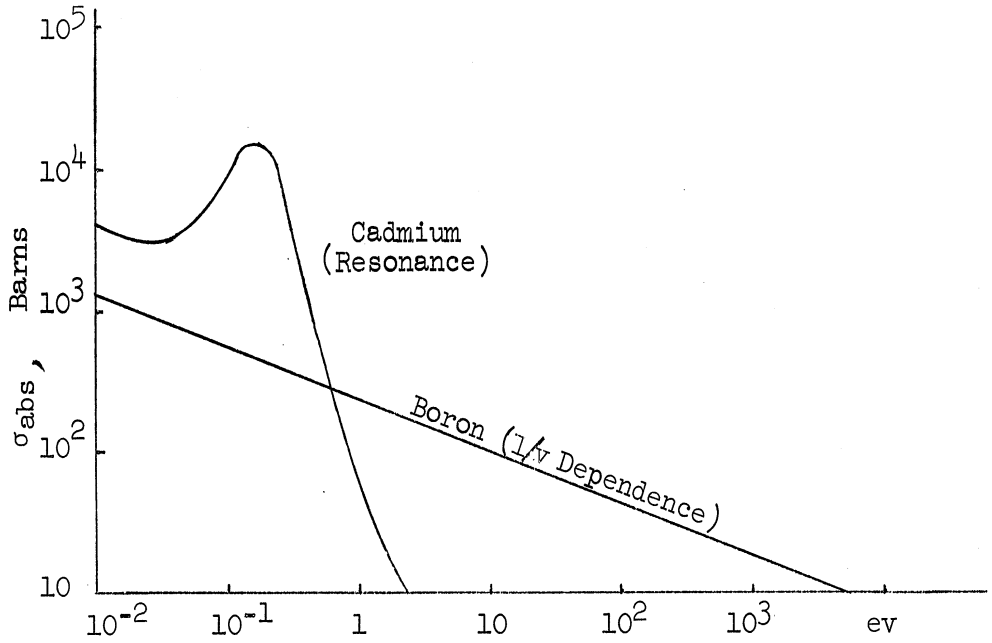

Macroscopic cross sections, Σ

$\Sigma = N\sigma$

Example calculation of N for carbon

Atomic wt. carbon = 12.01 GM/GM mole

Density = 1.65 GM/ CC

1 GM mole contains 6.023 (10^{23}) atoms

$$N = \frac{1.65 \text{ GM/CM3 } (6.023)\ (10^{23}) \text{ atoms/GM mole}}{12.01 \text{ GM/GM mole}}$$

$= 0.0827\ (10^{24})$ atoms/CM3

Calculation of Σ for Boron: $N = pNa/M = 2.5\ (6.023)(10^{23})/10.82 = \frac{0.139(10^{24})}{cm^3}$

$$\Sigma_a + N\sigma_a = \frac{0.139(10^{24})}{cm^3} \quad (750)\ (10^{-24})\ cm^2 = 104\ cm^{-1}$$

Neutron Mean Free Path

Consider target thickness dx

Neutron flux ϕ = nv, Σ_s = scatter cross section

$$\phi = \phi_o e^{-\Sigma_s x} = \text{number particles}$$

$$d\phi = \phi_o \Sigma_s e^{-\Sigma_s x} dx = \text{number scattered}$$

Average distance before collision = $\bar{x}$

$$\lambda_s = \bar{x} = \frac{\int x d\phi}{\int d\phi} = \frac{\int_o^\infty x \phi_o \Sigma_s e^{-\Sigma_s x} dx}{\int_o^\infty \phi_o \Sigma_s e^{-\Sigma_s x} dx} = \frac{1}{\Sigma_s} = \text{mean free path}$$

λ_s = average distance a single particle travels between collisions

Example: Compute λ_s for C

$$\sigma_s = 4.8\ (10^{-24})\ CM^2$$

$$N = 0.0827\ (10)^{24}$$

$$\lambda_s = \frac{1}{\Sigma_s} = \frac{1}{N\sigma_s} = \frac{1}{.0827\ (10^{24})(4.8)(10^{-24})} = 2.5\ CM$$

9. Neutron Energy Loss on Collision

Head-on Collision:

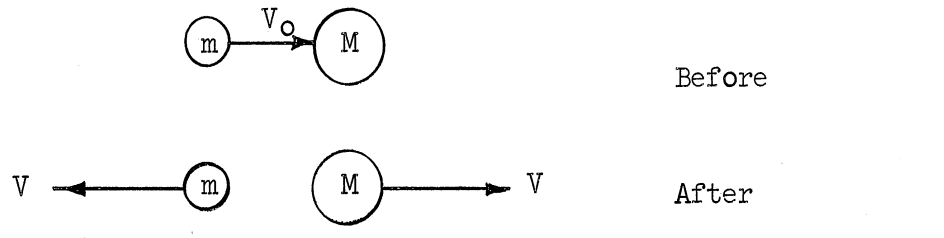

Glancing Collision:

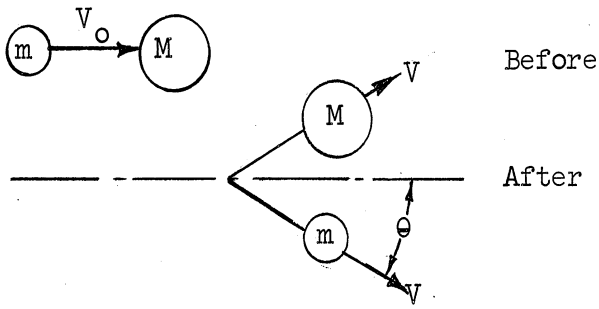

i.e. Source = Leakage + Absorption
Now if $q(E,\underline{r})$ is in introduced as the number of neutrons crossing energy E per unit volume per unit time then

$$S(E)\,dE = q(E + dE,\underline{r}) - q(E,\underline{r}) = \frac{\partial q(E,\underline{r})\,dE}{\partial E}$$

and our balance equation becomes

$$-D\nabla^2\phi + \Sigma_a\phi = \frac{\partial q}{\partial a} \quad \text{(Age equation in reactor theory)}$$

Above the thermal energy region $\Sigma_a \simeq 0$ and also in this region $\phi = \frac{q}{\epsilon\Sigma_s E}$ as can be seen by the following argument.

The number of collisions required to cross the energy interval dE with average change in ln E of ϵ is

$$\frac{d\ln E}{\epsilon} = \frac{dE}{E\epsilon}$$

The number of collisions per unit time in this interval is $\Sigma_s(E)\,\phi(E)$ Thus, $\Sigma_s\phi\epsilon E$ is the number that emerges from the interval per unit time and if there is no absorption, this quantity is equal to q the slowing down density. We have

$$\phi(E) = \frac{q}{\epsilon\Sigma_s E}$$

Note that this gives a 1/E dependence of flux on energy

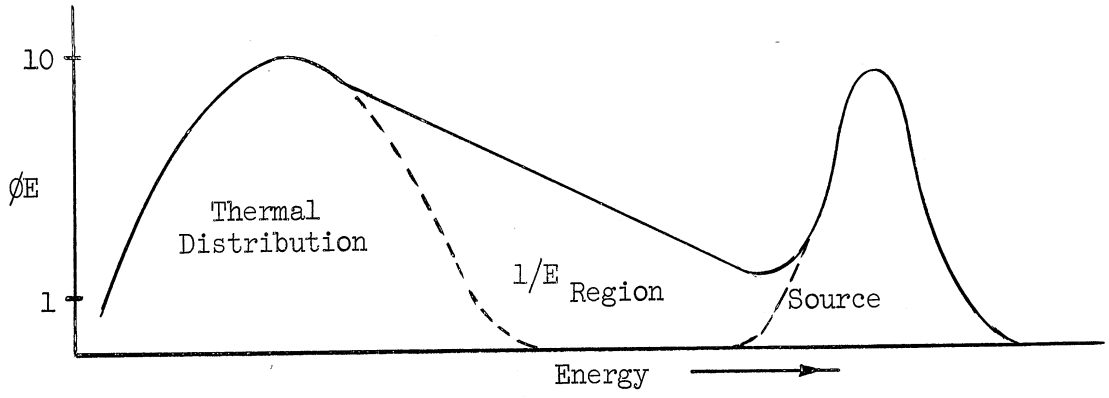

With the equation $\phi(E) = \frac{q}{\epsilon \Sigma_s E}$ our balance relation becomes

$$\frac{-D}{\epsilon \Sigma_s E} \nabla^2 q = \frac{\partial q}{\partial E}$$

And if the variables are changed so that $d\tau = \frac{-D}{\epsilon \Sigma_s} \frac{dE}{E}$

We then obtain $\nabla^2 q = \partial q / \partial \tau$ [Fermi Age Equation no absorption]. Which, mathematically, is the same as the heat equation. If we have a point source of neutrons in an infinite medium, then by substitution $q(r,\tau)$ can be seen to obey the equation

$$q(r,\tau) = \frac{q_o e^{-r^2/4\tau}}{(4\pi\tau)\ 3/2} \qquad \left[\begin{array}{l}\text{Slowing down density} \\ \text{from a point source.}\end{array}\right]$$

If the mean squared distance $< r^2(\tau)>$

$$< r^2(\tau) > = \frac{\int_0^\infty r^2\, q(\tau,r)\, dV}{\int_0^\infty q(\tau,r)\, dV}$$

to reach a certain age τ is computed, it is found that

$$< r^2(\tau) > = 6\tau$$

or τ is one sixth the mean square distance from birth at energy E_o to energy E.

$$\tau = -\int_{E_o}^{E} \frac{D}{\epsilon \Sigma_s E}\, dE = \int_{E}^{E_o} \frac{D}{\epsilon \Sigma_s} \frac{dE}{E}$$

Similarly if the balance relation for thermal neutrons

$$(\nabla^2 \phi - \frac{\Sigma_u}{D} \phi = 0) \quad \text{is solved for a point source}$$

ϕ becomes

$$\phi = \frac{\phi_o \, e^{-\sqrt{\frac{\Sigma_a}{D}}\, r}}{4\pi \, Dr}$$

and if $< r^2 >$, the mean squared distance that a neutron travels from its source to absorption, it is found that

$$< r^2 > = \frac{\int_0^\infty r^2 \Sigma_a \, \phi \cdot r^2 \, dr}{\int_0^\infty \Sigma_a \, \phi \cdot r^2 \, dr} = 6 \frac{D}{\Sigma_a}$$

or if we call $\sqrt{D/\Sigma_a}$ the diffusion length then L^2 is one sixth the mean squared distance to capture.

Scattering mean free path

$$\lambda_s = \frac{1}{\Sigma_s}$$

$$L_f = C \, \lambda_s = \ln \frac{(E_f/E_t)}{\epsilon \, \Sigma_s \, (avg)} \qquad \text{(But } \Sigma_s \text{ varies with E)}$$

In spite of scatter neutrons advance from origin. The average cosine of angle Θ is a measure of advance. Thus, we can define "transport mean free path" $= \lambda_t$

$$\lambda_t = \frac{\lambda_s}{1 - \cos \Theta} \, , \quad \Sigma_t = \frac{1}{\lambda_t}$$

$$\cos \Theta = \frac{2}{3 \, M} \, , \qquad L_f^2 = \frac{\lambda_t + \lambda_s \, C}{3}$$

$$\tau = L_f^2 = \int_{E_t}^{E_o} \frac{\lambda t}{3\Sigma_s} \frac{dE}{\epsilon E}$$

Average distance thermal neuts move before absorption is called "thermal diffusion length" = L

$$L = \sqrt{\frac{\lambda t \ \lambda a}{3}} = \sqrt{\frac{1}{\Sigma_t \ \Sigma_a}}$$

12. Neutron Shielding

A reactor core during operation. Fission of U^{235} produces an average of 2.5 neutrons/fission with the following spectrum

$$S(E)\,dE = \sqrt{2/\pi e}\ \text{SINH}\ \sqrt{2E}\ e^{-E}\,dE$$

where S(E) = No. neuts/fission neut in energy range from E to E + dE for high energy neuts (E = 2 to 12 Mev). Above equation reduces to :

$$S(E)\,dE = 3.3\ e^{-0.72E}\,dE$$

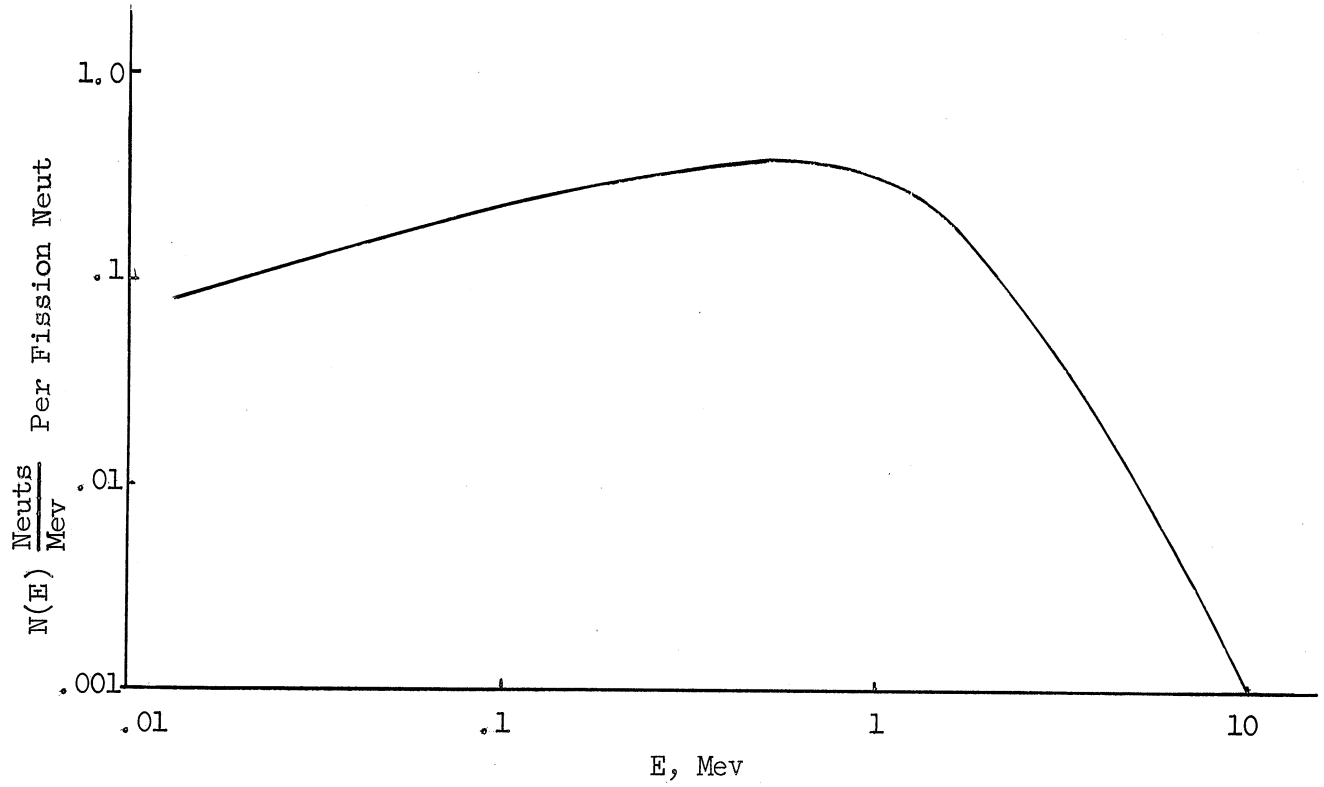

Ideally, a reactor shield would be composed of those materials, in such amounts and distributions, that would reduce the levels of neutron flux, primary gamma flux, and secondary gamma flux to just less than safe tolerances at the outer reaches of the shield. Usually other considerations (in particular space, weight, cost, or structural strength) prohibit the use of such an optimum design. In such cases, one of these three fluxes will predominate. This particular one, say, for example, primary gamma flux, then becomes the limiting factor on the overall shield thickness; i.e., if the shield is thick enough to reduce the primary gamma flux sufficiently, all other radiations will be more than adequately attenuated. Unfortunately, the discovery of any such possible predominance must generally await the performance of all or some of the calculations described below.

1. Neutron Attenuation.—The neutrons produced in a reactor are distributed in energy about a mean of approximately 2 mev; for shielding design purposes, their maximum energy can be considered as 14 mev. The neutron flux is reduced by the process of neutron capture, i.e., a neutron passing sufficiently close to a nucleus, forming a new (compound) nucleus. However, the probability of such a capture occurring (for most nuclei) is very small unless the energy of the neutron is approximately thermal (i.e., a few hundredths of an electron volt). Thus, the majority of the neutrons must first lose energy before they can be captured.

This energy degradation is accomplished by the process of scattering, both inelastic and elastic. A neutron cannot experience an inelastic collision unless its energy is greater than or equal to the energy corresponding to the first excited state of the nucleus with which it interacts. This threshold may be as low as 0.5 mev for elements of moderate or high mass numbers, but for light elements it is several mev. In fact, hydrogen is incapable of causing inelastic scattering at any energy. Therefore, in general, if a scattering collision occurs below 1 mev it will probably be elastic. On the other hand, inelastic scattering becomes increasingly probable as neutron energy increases.

The process of elastic scattering of high-energy neutrons does not contribute materially to the reduction of the high-energy neutron flux. The energy lost by a neutron in an elastic collision is dependent upon the mass number of the interacting nucleus and the angle through which the neutron is scattered. For a given scattering angle, the fraction of the neutron energy transferred to the nucleus increases as the mass number decreases. However, at high neutron energies the scattering cross section of an element of low mass number is quite small, since the scattering cross section at high energy $= 2\pi r^2 = (2\pi)\,(1.5 \times 10^{-13} \times A^{1/3})^2 = 1.415 \times 10^{-25} \times A^{2/3}$.

Although at high neutron energies about one-half of the total scattering cross section of an element of high mass number represents elastic scattering, the scattering angle and loss in energy are both quite small.

Hence, neutrons whose energies are in excess of 2 mev can best be degraded in energy by inelastic-scattering collision with nuclei of high mass number. A single such collision reduces the neutron energy to approximately 1 mev (the cross section being about one-half the total cross section of the heavy element).

At neutron energies from 1 mev down to just above thermal, elastic scattering by hydrogen constitutes the most effective mechanism to attenuate neutrons. As noted above, inelastic-scattering cross sections are either zero or quite small in this energy range. Elastic scattering by hydrogen produces a greater degradation in neutron energy than by any other element. In addition, the scattering process is more nearly isotropic; this has the effect of lengthening the effective shield path of a given shield thickness.

Thermal neutrons (those with energies of the order of magnitude of the average energy of the nuclei through which they are diffusing) are easily removed by capture in any of several elements which possess high thermal-capture cross sections. Of course, most of the elements in the shield can capture higher-energy neutrons; but, with the exception of certain narrow resonance regions, the corresponding cross sectionsare very low in comparison to thermal cross sections. Many of these capture processes are (n,γ) reactions, some producing single gamma photons with energies in excess of 7 mev. This potential source of secondary gammas can be reduced by employing materials such as boron-10. Boron-10 has a large (n,α) cross section. Although some of the liberated energy does appear as a gamma photon, its energy is only 0.5 mev.

In summary, fast neutrons are best attenuated by materials of high density through inelastic scattering. Unfortunately, secondary gamma production accompanies this interaction so that materials for this purpose are placed close to the reactor core to allow shielding of these gamma rays. Usually one or more of the following elements are used for this purpose: tantalum, tungsten, thorium, lead, iron, or barium. Iron, having high structural strength, can be incorporated as part of the supporting structure of the shield. Where compactness is of chief concern, denser materials, such as lead, are preferable.

Intermediate-energy neutrons are most effectively attenuated by elastic scattering by light nuclei, which, for reasons of cost, limits the available material to one element, hydrogen (either as water, hydrogenous waxes, or plastics).

Thermal neutrons require materials which have high thermal-neutron capture cross sections, such as boron-10, and which do not yield hard-capture gammas. Usually, this can be included as an impurity or alloy.

As can be seen from the above discussion, the analysis of the neutron-attenuation processes is important not only from the standpoint of the reduction of neutron flux to safe levels but also as a means of estimating the distribution and strength of secondary gamma sources throughout the reactor, associated components, shielding, etc.

2. Gamma-Ray Attenuation.—Attenuation processes for gamma radiation have been discussed in detail in the previous section dealing with the gamma-radiation source. (See Chap. 4.)

13. Attenuation Calculations

1. Fast-Neutron Attenuation.—As can be seen from the above discussion, an exact analysis of fast-neutron attenuation in a reactor shield would entail a rather complex mathematical model requiring a prodigious amount of numerical computation. The present scarcity of experimental data has made it impossible to construct a theory containing only those elements which are physically most important. However, steps in this direction have been made, notably by Albert and Welton.*

As previously noted, a considerable amount of hydrogen must be included in the shield to attenuate intermediate-energy neutrons. In a practical shield, collision with hydrogen usually has nearly the effect of absorption (insofar as required thickness is concerned). Qualitatively, this is true because of the degradation in energy which accompanies the collision, combined with the rapid increase of the hydrogen cross section as the neutron energy decreases. A small fraction of the initial collisions with hydrogen will give rise to neutrons having very nearly the source energy and almost their original directions. These neutrons will cause the spatial distribution of neutron flux to depart slightly from the exponential form which would be valid if these first collisions with hydrogen were, in fact, capture processes.

Likewise, high-energy neutrons which are inelastically scattered by an oxygen or a heavy nucleus may be assumed to be removed, since, as noted previously, its reduced energy will be something like 1 mev, the cross section of hydrogen at this energy being sufficiently high to insure rapid absorption.

Similarly, at low energies isotropic elastic scattering is quite probable. Such collisions effectively change the direction of the scattered neutrons so that these neutrons give a small contribution at the outside of the shield.

a. Effective Removal Cross Section.

On the basis of the above arguments and certain experimental evidence, a so-called "effective removal cross section" is defined. If a shield is composed of at least 50% by volume of water, the remainder consisting mostly of

* Albert, R. D., and Welton, T. A., Atomic Power Division Report, WAPD-15, Westinghouse Electric Corporation, 1950. (Classified)

heavier materials, it was found that the fast-neutron level generally decreases nearly exponentially through the shield. Thus, except for perturbations in the neighborhood of interfaces, the flux obeys an equation of the type

$$\text{neutron flux} = \text{constant} \times e^{-\Sigma x} ;$$

or, for a point source,

$$\text{flux} = \frac{\text{constant}}{4\pi r^2} e^{-\Sigma x} , \qquad (2.13)$$

where

x = shield thickness,
r = distance from source to point x, and
Σ = a constant.

The constant, $\Sigma \equiv \Sigma_R$, is called the "effective removal cross section." Table 2.4 contains values of Σ_R for fission neutrons for a number of materials which have been measured recently at ORNL. An approximation of

$$\Sigma_R/\rho = 0.085\, A^{-1/3} ,$$

where ρ is density and A is atomic weight, is quite good for atomic weights above 10.

TABLE 2.4

EFFECTIVE REMOVAL CROSS SECTIONS FOR FISSION NEUTRONS **

Material*	Cross section,† barns/atom	Material	Cross section,† barns/molecule
Aluminum	1.31	C_7F_{16}	26.3
(Boron)	0.97	C_2F_3Cl	6.6
Beryllium	1.07	CH_2	2.8
Bismuth	3.49	B_4C	4.3
Carbon	0.81	$C_{30}H_{62}$	80.0
(Chlorine)	1.2	D_2O	2.8
Copper	2.04		
(Fluorine)	1.29		
Iron	1.98		
Lithium	1.01		
Nickel	1.89		
(Oxygen)	0.99		
Lead	3.5		
Tungsten	2.5		

*The effective removal cross sections for the materials in parentheses were derived from analysis of compounds containing these elements.

†These removal cross sections are for a source of neutrons with a fission spectrum.

** Blizard, E. P., "Nuclear Radiation Shielding," Annual Review of Nuclear Science, 1955.

The exact relationship for the attenuation of a beam of fission neutrons of unit source strength can be given in the following way* If S (E) dE gives the fraction of fission neutrons at E in range dE, then the number at a distance x from a plane monodirectional fission source having 1 fission/cm^2-sec penetrating through a mixture of water with other substances is

$$N_o(x) = ve^{-\Sigma \mu_{ri} x} \int_o^\infty S(E)\, e^{-\mu_H(E)\, x} dE$$

where μ_{ri} is the macroscopic removal cross section for the ith component of the mixture of water with other materials not containing hydrogen or oxygen. These macroscopic cross sections are related to the microscopic cross sections by

$$\mu_H = \frac{.602\ \theta\ \sigma_H}{9} \qquad \mu_{ri} = \frac{.602\ \theta_i\ \rho_i}{A_i}\ \sigma_{ri}$$

$$\mu_o = \frac{.602\ \theta\ \sigma r0}{18}$$

where the σ's are in barns, θ is the volume fraction of water in the mixture, θ_i the volume fraction of the other materials, ρ_i and A_i their densities and atomic weights.

An approximate solution to this equation can be developed by assuming that from 2 to 12 Mev σ_H is well approximated by

$$\sigma_H = \frac{5.13}{(E^{0.725})}$$

the fission spectrum by

$$vs(E) = 3.3E^{-.72E}$$

the integrand $S(E)\ e^{-u_H x}$ at large distances is a sharply peaked function of E which leads to the prediction that the maximum of the integrand occurs at an energy

$$E_o = 0.541\ (\theta x)^{0.58}\ \text{Mev.}$$

with a full width at half maximum of

$$\Delta E = 1.55\ (\theta x)^{0.29}\ \text{Mev.}$$

thus to carry out the integration, the integrand is represented as a Gaussian, centered at the peak energy

$$S(E)\ e^{-u_H x} = C\ e^{-(E-E_o)^2}$$

The constants are determined by sitting the function in the neighborhood of the peak. The final result by this "saddle point" method is

$$N_o(x) = 5.4\ (\theta x)^{0.29}\ e^{-\Sigma u\ x}\ e^{-0.928\ (\theta x)^{0.58}}$$

* Goldstein, Herbert, "The Attenuation of Gamma Rays and Neutrons in Reactor Shields," USAEC, May 1, 1957.

b. Saddle-Point Method. *

For purposes of shielding calculations an approximate method (the so-called "saddle-point method") has been derived to estimate the attenuation of the fast-neutron flux by a thick-slab shield. Only the results of the derivation are presented here.

The peak energy E_o of the neutron spectrum at a distance x centimeters from the source is

$$E_o = 0.541\ (\theta x)^{0.58} , \qquad (2.14)$$

where θ is the volume fraction of water in the shield and E_o is energy (mev).

The half-width, ΔE (spectrum width at one-half maximum value), of the spectrum at x centimeters from the source, is given by

$$\Delta E = 1.55\ (\theta x)^{0.29} . \qquad (2.15)$$

Finally, the neutron flux, N(x), at x centimeters from an infinite-plane source emitting 2.5 neutrons/cm^2-sec in a parallel beam is given by

$$N(x) = 5.4\ (\theta x)^{0.29}\ e^{-\theta\Sigma_o x}\ e^{-(1-\theta)\Sigma_r x}\ e^{-0.928\ (\theta x)^{0.58}} \qquad (2.16)$$

where Σ_o is the macroscopic oxygen-scattering cross section and Σ_r is the macroscopic scattering cross section of the heavy elements in the shield.

While the above method is based upon a homogeneous distribution of materials in the shield, laminated shields can also be treated in this manner. In such cases the flux obtained at the outer edge of a given lamina is treated as a source at the inner face of the subsequent lamina.

2. Thermal-Neutron Flux Distribution.—As previously mentioned, a shield which adequately attenuates fast neutrons and gamma photons will generally be more than sufficient as an absorber of thermal neutrons. However, capture gammas, activation, and heating effects may require an accounting of the thermal-neutron flux distribution.

A definite phenomenological theory similar to the fast-removal theory is not available. Generally speaking, the thermal flux can be estimated by suitable bulk-shielding experiments.

3. Geometrical Effects in Fast-Neutron Attenuation.—

* Wigner, E. P., and Young, G., Rept. MonP-283, Oak Ridge National Laboratory, (Classified)

For a point source the geometrical factor $1/4\pi r^2$ is all that is needed.

a. Thermal Neutrons, Ideal Cases

(1) For thick slab of shield

$$\phi = \phi_o \, e^{-x/L}$$

where ϕ_o = initial flux, $\frac{\text{neuts}}{\text{CM}^2\text{-sec}}$

L = diffusion length, CM

x = thickness of shield, CM

Example $\phi_o = 10^{10}$ neuts/CM^2-sec

shield = water

L = 2.88 CM

x = 2.88 CM

$$\phi = 10^{10} \, e^{-28.8/2.88} = \frac{10^{10}}{e^{10}} = 3.69^{10} = 4.65 \, (10^5)$$

(a) Point source in infinite shield

$$\phi = \frac{3n_o}{4\pi\lambda_t r} \, e^{-r/L}$$

where:

n_o = thermal neutron emission

λ_t = transport mean free path

Note r in neutron eq. is to first power rather than square as for gammas because of diffusion by scatter in the case of neutrons rather than straight line travel as for gamma photons.

$$j = -\frac{\lambda t}{3} \left(\frac{d\phi}{dr}\right)$$

where j = neutron current (flow across unit surface)

(3) Point source in a finite sphere, radius R

$$\phi = \frac{3n_o}{4\pi\ \lambda_t r} \cdot \left(\frac{\text{SINH } (R-r)/L}{\text{SINH } R/L}\right)$$

$$j_R = \frac{n_o}{4\pi RL\ (\text{SINH } R/L)} \approx \frac{n_o}{2\pi RL}\ e^{-R/L}$$

Example: Point source $n_o = 10^6$ neuts/sec

$R = 4$ ft. = 61 CM

shield = water

find neutrons escaping

$$n = 4\pi R^2 j$$

$$\approx n_o \frac{2R\ e^{-R/L}}{L} = 10^6 \frac{122}{2.88}\ e^{-61/2.88} = 0.027$$

(4) Attenuation in material where $\sigma_a \gg \sigma_s$

(Example, cadmium and boron)

$$\phi = \phi_o\ e^{-Kx} \qquad \text{where } K = \Sigma_a$$

c. Shielding Calculations for Thermal Neuts Using Neutron Leakage Factors

take keff = $1 = k_\infty\ \tau\ L_t$

then $(k_\infty\ \tau - 1)$ = thermal neuts escaping core per k_∞ fast neut

$$\left(= \frac{1}{L_t} - 1\right)$$

$$= K^2L^2$$

$$\frac{\text{leakage}}{\text{fission neut}} = \frac{K^2L^2}{k_\infty}$$

$$\text{No. fission neuts} = P(\text{watts})\ c\ \frac{\text{fissions}}{\text{watt-sec}}\ \nu\ \frac{\text{neuts}}{\text{fission}}$$

$$\text{total neut leakage} = \frac{K^2}{K_\infty L^2}\ (Pc\ \nu)$$

Example

Calculate leakage of thermal neuts from graphite-moderated thermal reactor:

Power = 1 MW, k = 1.10, R = 250 CM, f = 0.9

$$K^2 = \left(\frac{\pi}{R}\right)^2 = \left(\frac{\pi}{250}\right)^2$$

$$L^2 = L_o^2\,(1-f) = 50^2(1-.9) = 250$$

$$\frac{K^2L^2}{k_\infty} = \frac{\pi^2(250)}{(1.1)250^2} = \frac{0.0362 \text{ neuts}}{\text{fission neut}}$$

$$\text{No. fission neuts} = 10^6 \text{ watts } \left(\frac{3 \times 10 \quad \text{fissions}}{\text{watt-sec}}\right)^{2.5}$$

$$= 7.5\,(10^{16})\ \frac{\text{neuts}}{\text{sec}}$$

$$\text{total leakage} = 0.0362 \times 7.5\,(10^{16})$$

$$= 2.7\,(10^{15})\ \frac{\text{neuts}}{\text{sec}}$$

d. Fast Neutron Shielding Calculations Using Leakage Factors

Cross sections for fast neuts are small and are close to those predicted by the nuclear radius, r

$$r = 1.4\,(10^{-13})\ A^{1/3}\ \text{CM}$$

Example: for lead A = 207

$$\text{Approx. cross section} = \pi\, r^2$$

$$= \pi(1.4)^2\,(10^{-13})^2\,(207)^{2/3}\ \text{CM}$$

$$= 2.2 \text{ barns}$$

(measured value = 3.5 barns)

Approx. shield thickness required to reduce fast neutrons to thermal energy is given by:

$$q = \frac{n_o \, e^{-(r^2/4\tau^2)}}{(4\pi\tau)^{3/2}}$$

where q = No. neuts that become thermal/sec in unit vol. at distance r from point source of n_o fast neuts

τ = Fermi Age or distance from fission to thermal energy

Using the relation $\int r^2 \, q \, dv / \int q \, dv$

Gives:

$$\bar{r}^2 = 6 \, \tau^2$$

where $\bar{r}^2$ = avg. square of r^2

Neutron Slowing Down Distributions in Water and Graphite

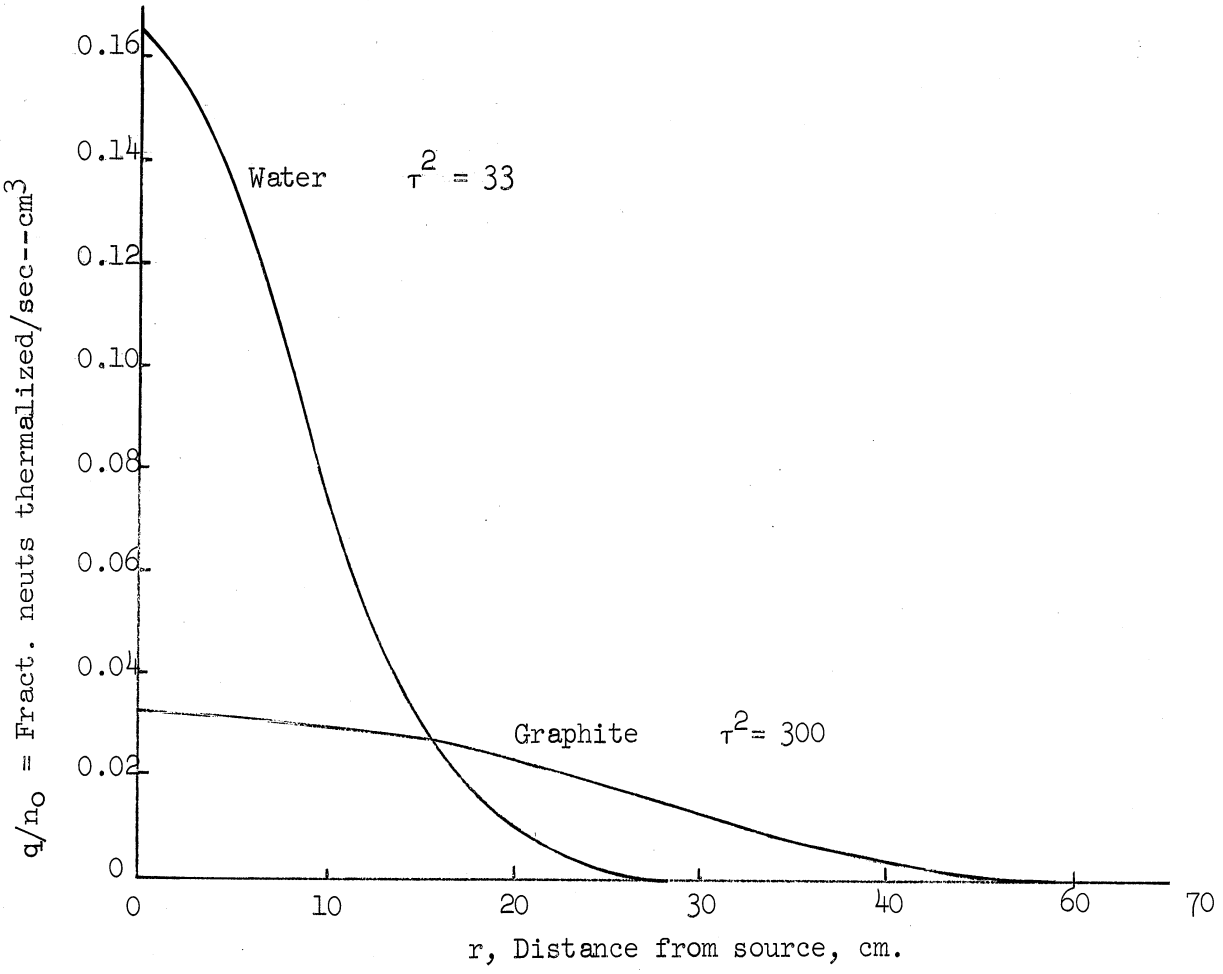

e. Use of Relaxation lengths in flux calculations for fast neutrons.

$$\phi = \phi_o \, e^{-x/\lambda}$$

where λ = effective relation length

= 11 cm for ordinary concrete (p = 2.0-2.5)

= 7 cm for hi-density concrete ($=\sim 3.5$)

= 4.2 cm for water

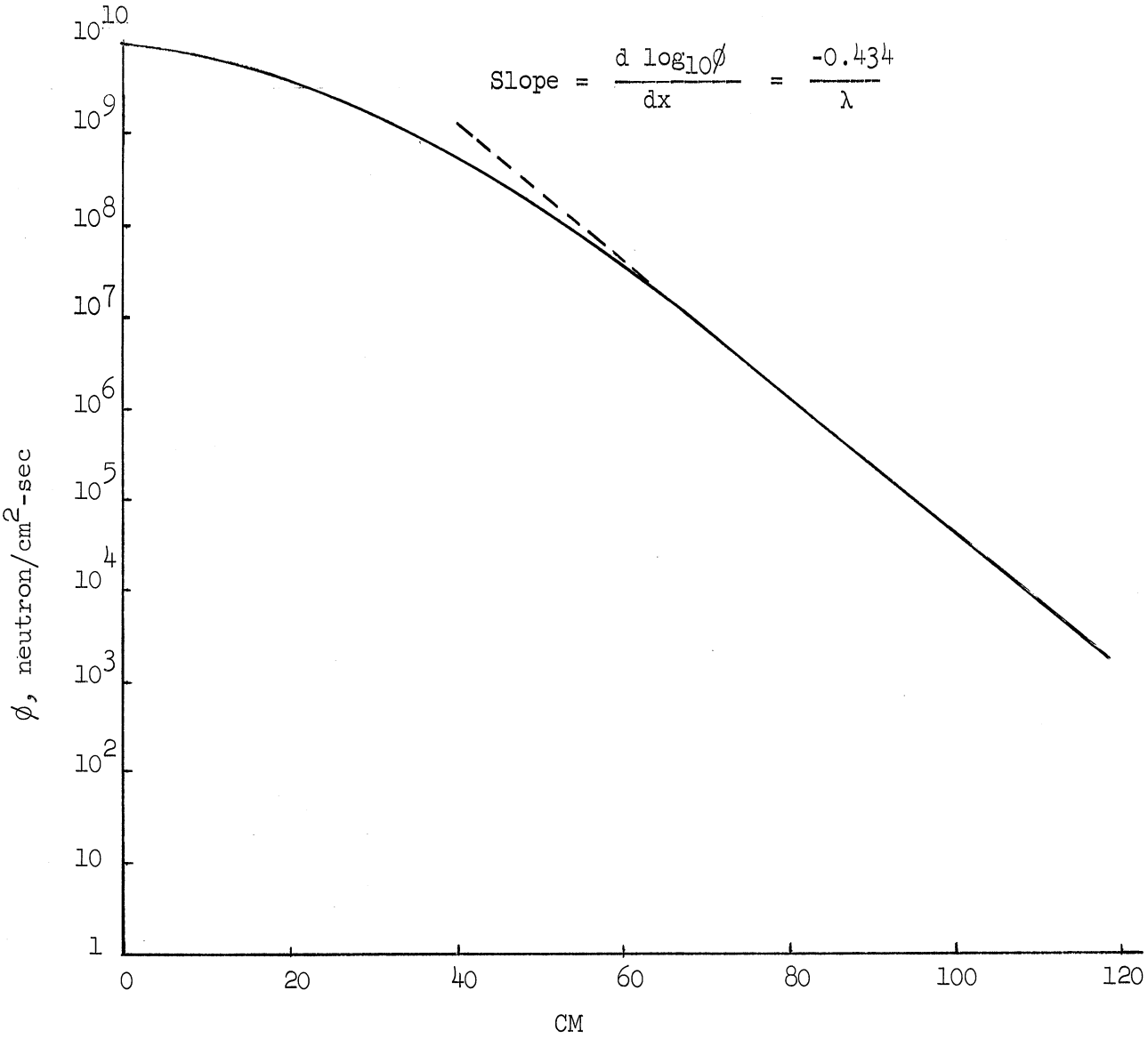

After fast neutrons travel some distance from origin their attenuation approximates a straight line on semilog paper as shown on p. 7.25. The slope can be used to determine λ, the relaxation length. Flux reductions for outer shields can then be estimated in a manner similar to use of 1/10 values in gamma shiedls.

Example: Fast neutron flux = $10^{11}/CM^2$-sec

shield thickness = 6 ft.

shield material = hi-density concrete, λ = 7 CM

$$x = 6 \times 12 \times 2.54 = 183 \text{ CM}$$

$$\phi = \phi_o \, e^{-x/\lambda} = 10^{11} \, e^{-(183/7)} = 0.5 \, \frac{\text{neut}}{CM^2\text{-sec}}$$

$$\left(\text{tolerance} = \frac{22 \text{ neuts}}{CM^2\text{-sec}}\right) \quad (2 \text{ Mev})$$

Problem: A homogeneous reactor, 40 CM dia., has a fast neutron flux at the surface of 2.5×10^{11} neuts/CM^2-sec. A reflector of water 10 CM thickness is used around the spherical core followed by a shield of high-density concrete 150 CM thick. Consider reactor as a point source (producing 2.5×10^{11} flux at 20 CM radius) and calculate flux at outside of concrete shield. (Concrete contains 15 wt. % H_2O, ρ = 3.5.)

1. By relaxation length method

   λ = 4.2 CM for water reflector

   λ = 7.0 CM for concrete shield

2. By saddle point method using σ_o

   for oxygen = 0.9 barns, σ_r for elements in shield = 2.0 barns; avg. atomic weight of heavy elements in shield = 120

$$\phi = \frac{(5.4 \, \theta x^{0.29}) \, (e^{-.928(\theta x)^{0.58}}) \, (e^{-\theta \Sigma_o x}) \, (e^{-(1-\theta)\Sigma_r x})}{r_2^2 / r_1^2}$$

(For point source in spherical geometry emitting 2.5 neuts/sec.)

Solution to problem

1.

$$\phi = 2.5 \times 10^{11} \left(e^{-10/4.2}\right) \left(e^{-150/7}\right)$$

$$= 2.5 \left(10^{11}\right) \frac{e^{-2.38}}{(30/20)^2} \quad \frac{e^{-21.42}}{(180/30)^2} = 2.5 \left(10^{11}\right)(4.13)(10^{2})(1.37)(10^{-11})$$

$$= 0.141 \text{ neut/Cm}^2\text{-sec}$$

2. a. water attenuation

$$\theta = 1$$

$$\Sigma_o = \frac{0.9 \left(10^{-24}\right)\text{CM}^2}{\text{atom}} \quad \frac{6.023 \times 10^{23} \text{ atoms/CM mole (1 GM)}}{18 \text{ GM/GM mole} \qquad (\text{CM}^3)}$$

$$= 0.03 \text{ CM}^{-1}$$

$$\frac{\phi_a}{\phi_o} = \frac{5.4 \text{ (1)}(10 \cdot 29 e^{-.928(1)(10)^{.58}} e^{-(1)(0.03)(10)}}{(30\text{CM}/20 \text{ CM})^2}$$

$$= 5.4 \text{ (1.906) } e^{-3.62} e^{-0.3} = 4.57 \text{ (0.296)(.792)}$$

$$= 0.010$$

b. concrete attenuation

$$\phi = 3.5 \text{ (0.15)} = 0.525, \ \theta\text{-1} = .475$$

$$\Sigma_o = 0.03 \text{ CM}^{-1}$$

$$\Sigma_r = \frac{2.0 \text{ (3.5)}(6.023)(10^{-1})}{120} = 0.035 \text{ CM}^{-1}$$

$$\frac{\phi_b}{\phi_o} = \frac{5.4 \text{ (.525)}(150)^{.29}}{180^2/30^2} \left(e^{-.928(.525 \times 150)^{.58}}\right)\left(e^{-.525(.03)(150)}\right)\left(e^{-.475(.035)(150)}\right)$$

$$= 0.337 \text{ (.823 x } 10^{-5})(.095)(0.9827) = 2.09 \times 10^{-8}$$

$$\phi = 2.5 \left(10^{11}\right)(0.01)(2.09)(10^{-8}) = 52 \text{ neuts/CM}^2\text{-sec}$$

(Note: Increasing water content of concrete reduces flux.)

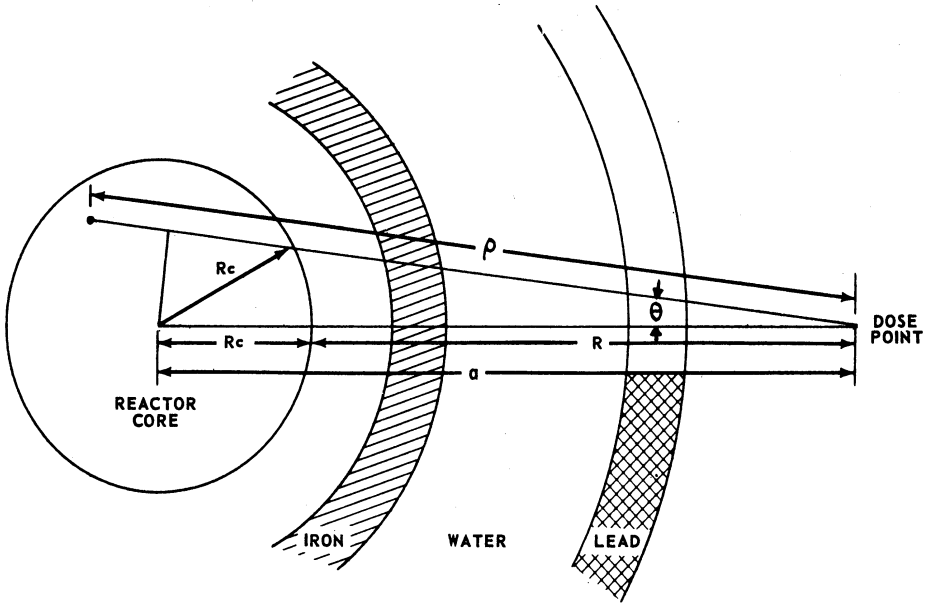

Geometry of spherical core and shield.*

If the core and shield are shown with a uniform power distribution (p watts/cm^3) in the core, the uncollided fast flux at distance R centimeters beyond the surface of the core is

$$\phi_u(R) = 2\pi(7.75)(10)^{10} P \int_{\sqrt{1-(R_c/a)^2}}^{1} d\mu \int_{a\mu - \sqrt{a^2\mu^2 - b_c}}^{a\mu + \sqrt{a^2\mu^2 - b_c}} \rho^2 d\rho\, G(\Sigma_c\rho_c) G(\Sigma_s\rho_s), \quad (2.17)$$

where

$7.75 \times 10^{10} P(\text{watts}) = \text{fission neutrons/cm}^3\text{-sec}$,

$a = R + R_c$,

$b_c = a^2 - R_c$,

$\mu = \cos\theta$,

$G(\Sigma\rho)$ = the point-source attenuation kernel,

$G(\Sigma_c\rho_c)$ = the point-source attenuation kernel for the core, and

$G(\Sigma_s\rho_s)$ = the point-source attenuation kernel for the shield.

There are two possible choices for $G(\Sigma\rho)$: Equation 2.14or an exponential fit to an experimentally determined distribution. The latter will have the form

$$G(\Sigma\rho) = \frac{1}{4\pi\rho^2} \sum_{i=1}^{N} A_i\, e^{-\Sigma_i\rho} \quad . \quad (2.18)$$

If the volume fractions of materials other than water are f_c and f_s in the core and the shield, respectively, Equation 2.19 reduces to

* Rockwell, Theodore, III, "Reactor Shielding Design Manual", TID-7004, March 1956

$$\phi_u(R) = 3.875(10)^{10} \frac{P}{2} \left(\frac{R_c}{R_c + R}\right)^2 \sum_{i=1}^{N} \frac{A_i}{f_c(\Sigma_{mc} - \Sigma_{ic}) + \Sigma_{ic}}$$

$$\cdot \exp\left\{-\left[f_s(\Sigma_{ms} - \Sigma_{is}) + \Sigma_{is}\right] R\right\}$$

$$\cdot \left(1 - \exp\left\{-2\left[f_c(\Sigma_{mc} - \Sigma_{ic}) + \Sigma_{ic}\right] R_c\right\}\right) , \qquad (2.19)$$

where

$\rho_c = \rho - \rho_s$ = the distance from unit-source volume to surface of sphere along line between unit source and the point R,

$\rho_s = a\mu - \sqrt{a^2\mu^2 - b_c}$ = the distance in shield along line between unit-source volume and point R,

Σ_{mc} = the effective removal cross section for the nonhydrogenous materials in the core (cm^{-1}), and

Σ_{ms} = similarly, for the shield.

b. Cylindrical Core and Shield. *

If cylindrical coordinates are used (see Fig. 2.4), the uncollided flux at distance R centimeters beyond the surface of the core is

$$\phi = \frac{1}{2\pi} \int_{\psi=0}^{\pi} \int_{r=0}^{R_c} \int_{z} \frac{s(r,z)\, r\, d\psi\, dr\, dz}{\rho^2} G(R) , \qquad (2.20)$$

where

$\rho^2 = z^2 + a^2 + r^2 - 2ar \cos\psi$,

ψ = the azimuthal angle with respect to the transverse axis of the cylinder, and

a = the distance from the axis of the cylinder to the point at which the flux is being calculated.

* Rockwell, Theodore, III, "Reactor Shielding Design Manual," TID-7004, March 1956

7.8 Experiment No. 8

Germination and Growth of Irradiated Seeds and Sprout Inhibition in Tubers

Discussion

Authorities differ widely in their opinion on the use of ionizing radiation to affect the germination and growth of plant seeds. In an article by Kuzin (1) four different methods of irradiating treatments were tried with varying degrees of success.

1. irradiation before sowing
2. soaking of seeds in solutions containing natural and artificial radioactive substances
3. treatment of the soil with radioactive substances serving as micro-fertilizers
4. continuous irradiation of growing crops with radiation

Kuzin claims that irradiation of seeds prior to sowing offers the greatest advantages as compared to the other methods of treatment.

Its chief merits are:

1. Irradiation can be performed in specially equipped places
2. Irradiation of the seeds can be completed in a selected finite time.
3. Complete absence of radioactivity both in the sowing material and in the yeild.

Also, the acceleration of the initial stages of germination is important since it may influence the yield in arid districts as well as those where the sowing period is limited.

Observations at the University of Michigan have indicated some of the effects of radiation on seeds and tubers (see Chap. 9 of "Radiation Uses in Industry and Science").

In studies in production of mutants, seed walnuts were irradiated at various dosages from 0 to 50,000 rad, labeled, placed on a mat of sawdust and covered with several layers of damp burlap to hasten germination. Inspections were made twice weekly to check germination progress and to dampen the walnuts and burlap. The following table summarizes the early observations on germination of walnuts.

Observations on the Germination of Irradiated Walnuts

Number stratified, Mar. 27	Dosage, Krad	Germinations, May 24	Germinations total, July 3	Number growing, Aug. 8	Aug. 22
50	0	3	7	5	5
50	1	2	4	4	3
50	5	3	6	6	6
50	10	2	8	7	7
50	20	2	10	9	9
50	30	2	16	12	10
50	40	3	16	3	1
50	50	3	18	1	0

In student experiments at the Fission Products Laboratory radish seeds were irradiated at various doses and planted in a small plot of ground outside the laboratory. Figure 7.24 shows the experimental radish bed. Reading from right to left the radiation dosages were 0, 400 rad, 1,000 rad, 5,000 rad, 10,000 rad, 50,000 rad. Typical plant specimens were removed when the plants were four weeks old and are shown in Fig. 7.25. These experiments were inconclusive because of lack of sufficient control of the variables, but limited data indicated that a dose of 1,000 rad appeared to produce the most vigorous plants. These and other observations indicated a two-fold effect of radiation: (1) interference with cell division at doses of 5000 rad and greater, as indicated by inhibition of continued growth of sprouts; (2) stimulation of growth hormones as shown by more rapid sprouting of irradiated onions and hormone studies on potatoes. However, if the radiation dose is kept sufficiently low, it is believed that stimulation of growth may be effected without significant interference with cell division.

In the Russian studies the most beneficial dosages usually ranged from 300 to 1000 roentgens.

Rye seeds given a dose of 750 rad, produced roots having a diameter of 393 μ for nonirradiated rye seeds used for control purposes. This

observation is theoretically important because the increase in root diameter is due not to the growing size of the cells, but to the increase

In student experiments at the Fission Products Laboratory radish seeds were irradiated at various doses and planted in a small plot of ground outside the laboratory. Figure 7.24 shows the experimental radish bed. Reading from right to left the radiation dosages were 0, 400 rad, 1,000 rad, 5,000 rad, 10,000 rad, 50,000 rad. Typical plant specimens were removed when the plants were four weeks old and are shown in Fig. 7.25. These experiments were inconclusive because of lack of sufficient control of the variables, but limited data indicated that a dose of 1,000 rad appeared to produce the most vigorous plants. These and other observations indicated a two-fold effect of radiation: (1) interference with cell division at doses of 5000 rad and greater, as indicated by inhibition of continued growth of sprouts; (2) stimulation of growth hormones as shown by more rapid sprouting of irradiated onions and hormone studies on potatoes. However, if the radiation dose is kept sufficiently low, it is believed that stimulation of growth may be effected without significant interference with cell division.

In the Russian studies the most beneficial dosages usually ranged from 300 to 1000 roentgens.

Rye seeds given a dose of 750 rad, produced roots having a diameter of 393 μ on the 3rd day of development as compared to 304 " for nonirradiated rye seeds used for control purposes. This observation is theoretically important because the increase in root diameter is due not to the growing size of the cells, but to the increase in their number. For example, the number of cells in the subepidermal layer of shoot roots was 68 for the rye seeds given 750-rad dose as compared to 40 for the control rye seeds given 0-rad dose. The root length on the 4th day of development was 52.2 mm for the 750-rad rye seeds as compared to 43.5 mm for the control.

Similar results on stimulation of plant growth have been observed with other species. On the 5th day of development radish, pea, and cucumber shoots from seeds given an X-ray dose of 500 rad had shoot length of 72.2, 61.2, and 89.5 mm, respectively; whereas the respective untreated seeds had shoot lengths of 50.0, 53.6, and 82.6 mm, respectively.

Yields per unit field area were also increased. In the case of radishes grown in a greenhouse a dosage of 1000 rad gave a 30 per cent increase in total weight of tuber yield as compared to the controls. Field grown radishes from seeds receiving the same dosage gave a 40 per cent increase as a result of irradiation. Cabbage seeds given a dosage of 1000 rad produced plants that ripened earlier than the control and gave a 19 per cent increase in yield per area. The harvest yield of peas given an X-radiation dose of 350 rad produced 10 per cent more pea seeds per plant. Furthermore, the weight of 1000 pea seeds was 16 per cent greater for the yield from irradiated plants than from the controls. The irradiation of soaked pea seeds with Co^{60} gamma radiation gave up to 50 per cent increase in weight of peas per plant and up to 24 per cent increase in the vegatation mass as compared to untreated controls. Irradiation of rye seeds (750 to 1000 rad resulted in 21 to 22 per cent increase in the weight of 1000

harvest grains.

Low doses of ionizing radiation (5,000 to 20,000 rad) have been used to prevent the sprouting of tubers and bulbs during storage. Figures 7.26 and 7.27 show irradiated and nonirradiated potatoes and onions respectively stored for a few months after irradiation.

Onions and potatoes seem to respond differently to irradiation. During initial storage both irradiated and control onions developed small sprouts. In the case of the White Pearl onions the irradiated onions sprouted first. In all cases sprouts on irradiated onions grew only a short distance (about 1/2 to 1 1/2 in.) and then withered and died. On the control onions, sprouts continued to grow up to 6 to 8 in. All irradiated onions remained dry and firm (but lost some crispness) whether or not they had sprouted; control onions became moist and soft.

The contrast in appearance of the control and irradiated Bermuda onions is shown in Fig. 7.27. This photograph shows the long sprouts of the control onions protruding several inches and no sprouts on the irradiated onions.

Tests of the irradiated onions after storage indicate some loss in crispness and some loss in pungency. Brownell et al. concluded that a 7-krep dosage of gamma radiation may not completely prevent initial sprouting, but it inhibits the continued growth of sprouts, keeping the onion more firm and increasing storage life.

Studies of Potato Irradiation in Europe

Studies on irradiated potatoes have been underway in Russia since 1955. Extensive investigations have been made on the chemistry, odor, taste, and cooking qualities. On the basis of these tests the USSR Chief of Public Health Inspection authorized the use of potatoes given a dose of 10,000 rads for human consumption. A large capacity radiation facility has been constructed and the process is in use.

Norwegian studies indicated that radiation doses as high as 16,000 rads could be used on potatoes. Similar studies in France indicated that doses higher than 10,000 rads increase spoilage and that doses of about 7500 rads are to be preferred. In 1959 Vidal of France commented that "For short term storage doses of 5000 to 6000 rads are sufficient but for long term storage (12 months or longer) it is necessary to use doses of 7500 to 10,000 rads."

Burton and de Jong of England reported extensive studies on irradiated Ware variety potatoes. They stated "The effect of irradiation (high level) is thus to stop sprouting completely but not to prolong storage indefinitely...Irradiation at a low level--say 5000 rads--either does not induce harmful side-effects or does not induce them so soon but it may not always stop sprouting completely. The irradiation dose should be the minimum which will give com-

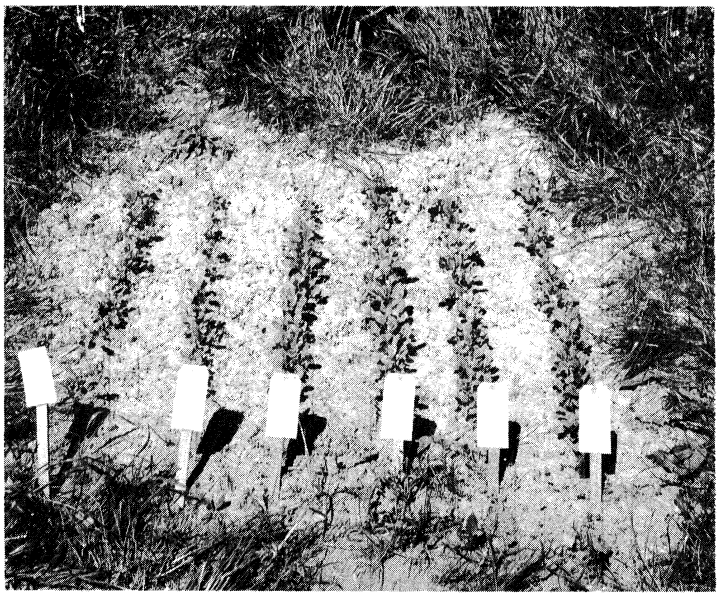

7.24 Plot of growing radishes from irradiated seeds (reading right to left, control, 400, 1000, 5,000, 10,000 and 50,000 rad).

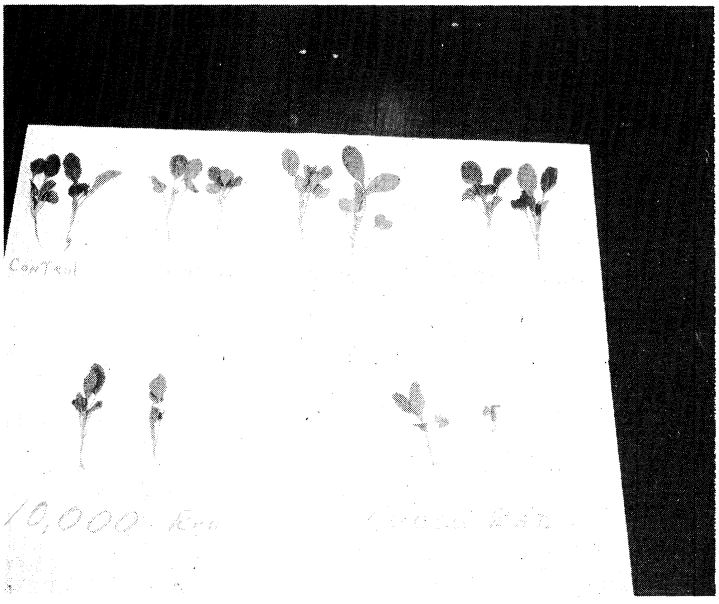

7.25 Typical radish plants from irradiated seeds. (Top row left to right, control, 400, 500, 1,000 rad; bottom row 10,000 and 50,000 rad.)

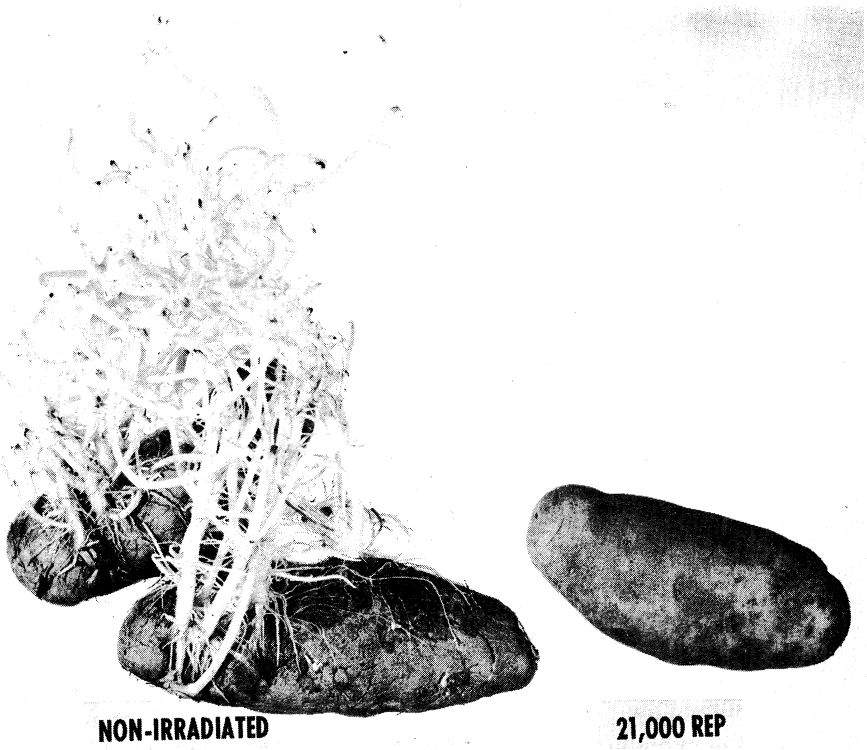

Fig. 7.26 Irradiated and nonirradiated potatoes (irradiated in May and stored four months before photographing).

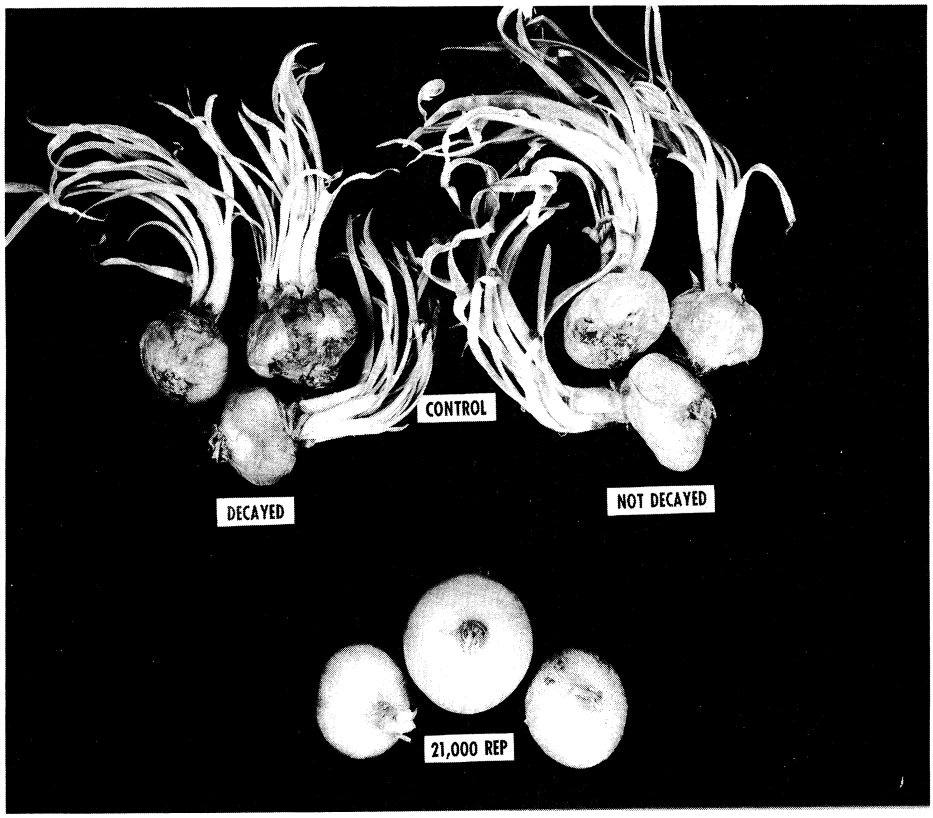

Fig. 7.27 Irradiated and nonirradiated onions (irradiated in May and stored four months before photographing).

mercially acceptable sprout suppression--certainly less than 10,000 rads."

American studies have shown that the permissible dose varies appreciably with variety, length of storage before irradiation, and storage conditions. This may explain some of the differences in doses recommended by European investigators.

Procedure

a. Sprouting inhibition

Immediately after harvest tubers, bulbs, and other root crops have a period of dormancy during which sprouting does not occur whether irradiated or not. Therefore, in demonstrating sprout inhibition by irradiation, root crops should be used that have been in storage for a sufficient period of time for sprouting to be imminent. Autumn harvested potatoes stored until spring and onions stored for about three months are usually satisfactory. Sweet potatoes, carrots, beets, and turnips showing small sprouts may be used. If the tubers have small sprouts, the buds or sprouts may be brushed off so that none remain. The tubers may be divided into a number of similar groups and radiation doses given each group in increments of about 5,000 rads. After irradiation, the tubers should be stored and observed for evidence of sprouting and/or rotting. At the first sign of development of rot the tuber involved should be disposed of to avoid spread of spoilage organisms. Onions will keep best when stored at temperatures not below 50 degrees F. and humidities not above 70%. Potatoes store well at refrigerator temperatures of about 35 to 40 degrees F. and humidities of 90%.

b. Seed germination

Most workers in radiation biology agree that limited doses of radiation are beneficial in stimulation of the germination of seeds particularly seeds that sometimes show poor germination. For experimental purposes a variety of seeds may be selected and irradiated at doses in the range used by Kutzin (200-2,000 rad). A few larger doses (10,000, 50,000, 100,000 rad) may be used to demonstrate harmful effects of excessive irradiation. Extensive data on germination alone may be obtained by placing small seeds between dampened pieces of blotting paper. The larger seeds and nuts may be placed in dampened sawdust, peat moss, or vermiculite. The seeds should be kept moist until germination is complete. Germination tests alone do not indicate whether or not better growth and better yields are possible as evidenced by the early death of the irradiated walnut seeds receiving 40 and 50 krad doses (see table). These seeds germinated well but died shortly after germination. To obtain data on growth and yield the irradiated and control seeds must be planted in suitable containers for hot house studies or in suitable plots of ground outside. Many variables are involved which has resulted in wide differences in the reports of various investigators as to the benefits of an irradiation treatment on crop yields.

7.9 Experiment No. 9 Food Irradiation

Discussion

1. Radiosterilization--Many studies have been conducted in various laboratories using various doses of ionizing radiation for food preservation. The initial studies were in most cases directed toward the use of "sterilizing" doses in the range of 2-5 megarad. Preliminary studies indicated that sterilizing doses of radiation produce undesirable changes in most foods, particularly in the odor and flavor of meats and dairy products.

Many investigators in various laboratories are studying the problem and satisfactory solutions have been found for certain food items. Radiosterilization which permits long-term storage at room temperature is the ultimate goal of much research being conducted in this field. However, it presents more problems than the use of lesser dosages of radiation which would not completely sterilize.

2. High-Radiopasteurization--Limited studies have been made at the University of Michigan using a "high-radiopasteurization" dose of gamma radiation of about 1 megarad. This dose is not sufficient to sterilize completely, but is sufficient to preserve food. Thus, this process could not be used where the possibility of growth of Clostridium botulinum exists. Destruction of the spores of this organism is the first requisite in successful thermal processing of canned foods. However, if the danger of botulism is avoided by control of pH or oxygen level and temperature, a dose of 1 megarad would be sufficient to preserve food from spoilage by vegetative microorganisms, mold, yeasts, etc.

In limited tests, smoked fish (salmon and chub) packaged in 2-mil heatsealed polyethylene bags and given a radiation dose of 1 and 0.8 megarad, respectively, "kept" at room temperature for several months. The irradiated salmon and chub were considered to have very good flavor immediately after irradiation and the flavor was still good after storage for one month at room temperature. After 3-mo. storage at room temperature, the salmon developed a slightly rancid taste. Packages of salmon that received 1-megarad dosages and eventually spoiled did so as a result of mold growth.

Fig. 7.28 shows a photograph of the irradiated salmon and control after storage for nine days at room temperature. The samples of salmon were removed from the polyethylene bags for photographying. Note the development of mold on the control sample. Mold of this type first appeared after storage for about three days, whereas no mold growth appeared on the irradiated salmon. Fig. 7.29 shows a plot of the original salmon samples and, although only a few samples were used in this limited study, the curves are indicative of subsequent data obtained with larger numbers of samples

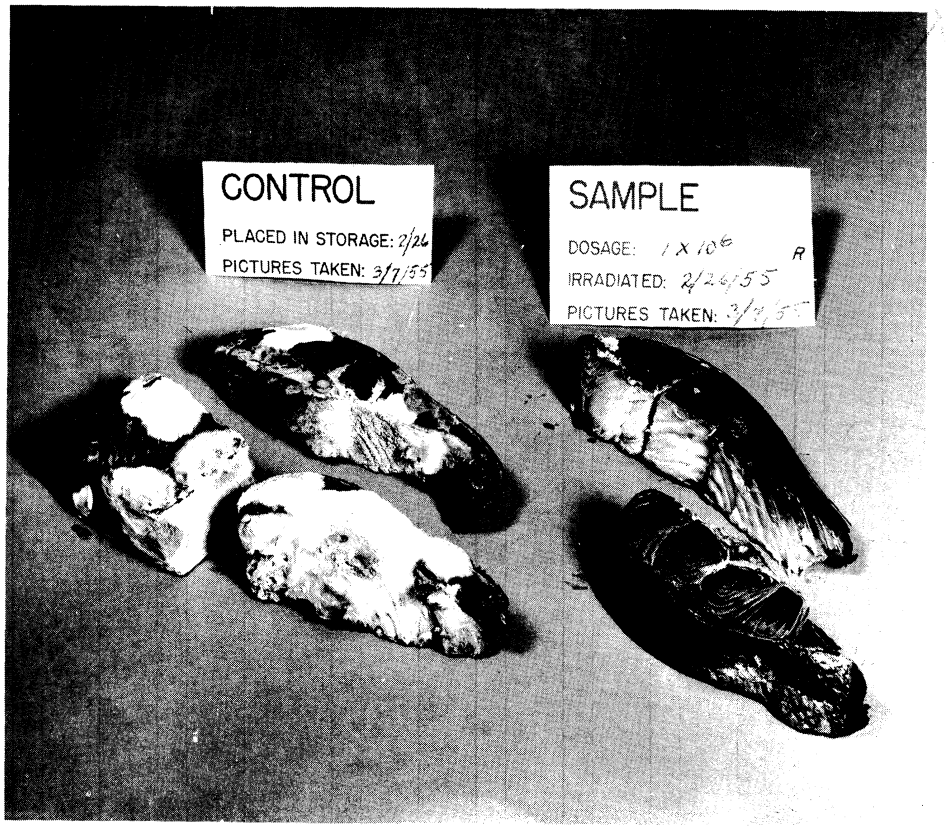

Fig. 7.28 Sample of Irradiated and Nonirradiated Smoked Salmon after Removal from Sealed Polyethylene Bags.

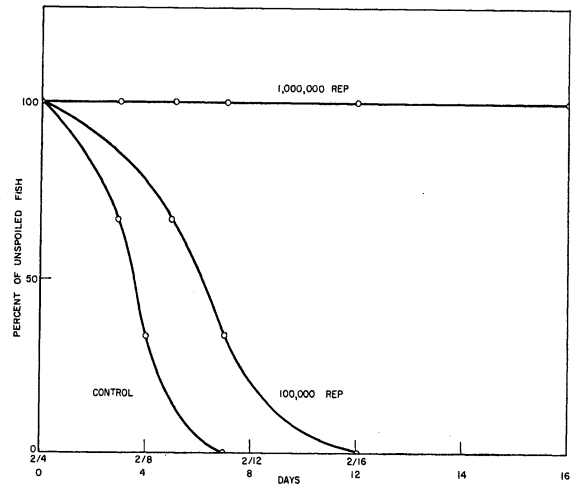

Fig. 7.29 Irradiated smoked salmon data. Salmon was stored at room temperature.

3. Radiopasteurization---A dose of radiation less than that required for sterilization and in the range of about 100,000 rad might be termed a radiopasteurization dose in that, like thermopasteurization, most but not all of the microorganisms are destroyed. Radiopasteurizating doses equal to 2-5% of sterilizing doses can be used to reduce the population of microorganisms 90-99% without producing undesirable changes in the food. Such a radiopasteurization treatment could be used to extend the refrigerator shelf-life of perishable foods which might make possible new methods of handling.

A new method of wholesaling fresh meat has been proposed for consideration by some of the larger packing houses and some of the larger retailers of fresh meat. This proposed new method consists of preparing packaged standard cuts of fresh meat, packaged fresh ground meat, packages of cut chicken, etc., in retail-size portions at the packing house rather than at the retail meat market, and of radiopasteurizing the packaged meat at the packing house by using a dose of about 100,000 rad prior to shipping to the retailer. The extension of the refrigerator shelf-life of fresh meat by radiopasteurization should make this new method feasible. A number of advantages might be realized by the consumer, the retailer, and the packing house as a result of using this new method of wholesaling meat and radiopasteurization.

Since microorganisms play a major role in the spoilage of meat and meat products, their storage life at refrigerator temperatures should be increased by keeping the microbial flora at a minimum. Rigid satitation practices by meat packers and meat processing plants have done much to increase the storage life of meats, but the subsequent exposure of meat to air and contaminated surfaces makes the control of the microbial population a difficult problem.

Radiation dosages needed to inactivate vegetative forms of microorganisms are much lower than those required for bacterial spores. Decreasing the vegetative microbial flora sufficiently to prolong the storage life of meat at refrigerator temperatures should require a much smaller dose of gamma radiation than is required for sterilization and destruction of spores.

In some tests at the University of Michigan grams of fresh lean ground steak were aseptically transferred to flasks containing sterile glass beads and sand. Prior to irradiation the meat was inoculated with 1 ml of a suspension of a psychrophilic gram-positive bacterium originally isolated from spoiled ground beef. This organism grew readily at a temperature of 4° C. An uninoculated control sample was kept to establish the meat's normal population

Table 1 shows the microbial counts on the meat immediately after irradiation. No significant differences in counts are apparent up to a dosage of 40,000 rep. Table II shows counts per gram of meat after subsequent storage at 4° C. The data are plotted on semi-logarithmic paper in Fig. 7.30 as total counts per gram.

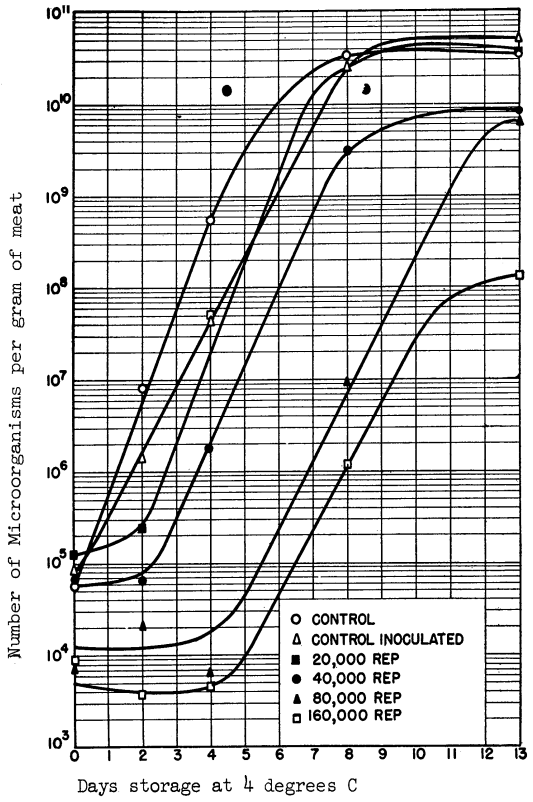

Fig. 7.30 Growth of microorganisms in irradiated meat

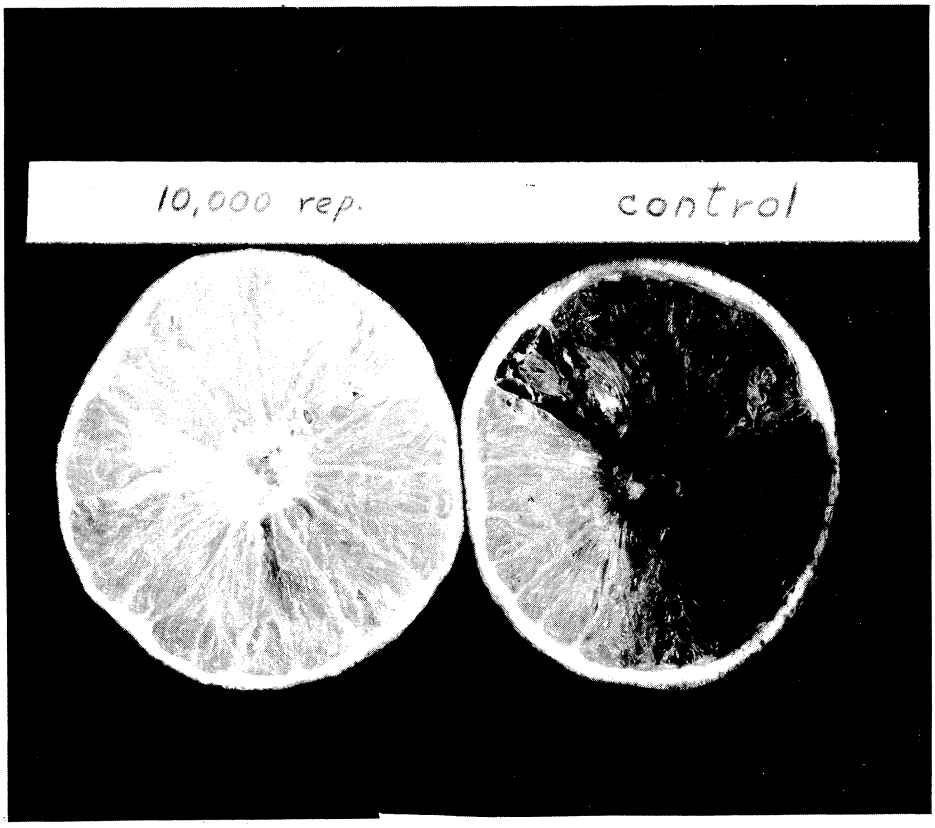

Fig. 7.31 Irradiated (left) and nonirradiated (right) grapefruit previously infested with eggs of the Mexican fruit fly after development of mature larval stage. Note secondary damage from mold in the control fruit.

TABLE I-EFFECT OF GAMMA RADIATION

ON AEROBIC MICROBIAL FLORA OR GROUND BEEF INOCULATED WITH 3.2×10^4 PSYCHROPHILIC BACTERIA PER GRAM

Sample	Microorganisms Per Gram	% Survivors
Control	8.0×10^4	100.0
20,000 rep	1.4×10^5	100.0
40,000 rep	6.8×10^4	85.0
80,000 rep	7.5×10^3	9.0
160,000 rep	9.5×10^3	12.0

TABLE II-EFFECT OF SUBLETHAL DOSES OF GAMMA RADIATION

ON THE AEROBIC MICROFLORA OF GROUND BEEF AFTER STORAGE AT 4° C

Sample	Number of Microorganisms per Gram of Meat After Indicated Number of Days of Storage at 4° C				
	0	2	4	8	13
Control	5.5×10^4	8.0×10^6	5.5×10^8	3.3×10^{10}	2.8×10^{10}
Control Inoculated	8.0×10^4	1.5×10^6	4.3×10^7	2.5×10^{10}	4.5×10^{10}
20,000 rep	1.3×10^5	2.2×10^5	5.0×10^7	---	2.8×10^{10}
40,000 rep	6.8×10^4	6.5×10^4	1.8×10^6	3.0×10^9	8.3×10^9
80,000 rep	7.5×10^3	2.0×10^4	6.3×10^3	9.3×10^6	6.5×10^9
160,000 rep	9.5×10^3	2.8×10^3	4.3×10^3	1.2×10^6	1.3×10^8

No detectable differences in either color or odor were noted in the samples immediately after irradiation. After five days of storage, both the inoculated and uninoculated controls had a pronounced putrid odor. Initiation of spoilage in the sample receiving a radiation does of 20,000 rep was indicated by a slight off-odor. After 13 days of storage, all the irradiated samples except that which received a dose of only 20,000 rep were still free of off-odors and there was no indication of spoilage.

4. Low Radiopasteurization--A still lesser dosage of radiation or 10,000-25,000 rad termed low radiopasteurization might be used for some other types of food processing. Such low-radiopasteurization doses will not destroy a sufficient quantity of the population of vegetative microorganisms found in fresh foods, such as meat, to affect appreciably the storage life at either refrigerator or room temperatures. This range of radiation, however, has the least influence on flavor and color and would be the most economical to employ because of the high radiation capacities possible at such low dosages.

Such a dosage might be used for the treatment of potatoes and onions for sprout inhibition, for grain, cereal products, and fruit (See Fig. 7.31) for insect control, to break the cycle of trichinosis in pork, to control tapeworm from beef, pork, and fish, and to control a number of other diseases caused by parasites. The irradiation of potatoes and wheat, as well as other grains, is considered to be feasible on a mass scale from the viewpoint of both engineering and economics. Because of the tremendous quantities of these staple foods, the application of radiation would be on a large scale.

Procedure

The experimental demonstration in a precise manner of the preservative effect of radiation on various foods is complex since it involves the determination of populations of microorganisms, molds, and yeasts, that might cause food spoilage. Such studies can only be performed with precision in a laboratory equipped for studies in bacteriology. Also, the evaluation of the quality of irradiated food is best investigated by the use of skilled pannels and a statistical number of evaluations.

However, for purposes of demonstration a number of simple experiments may be performed. Dairy products and meats are particularly susceptible to flavor, odor, and/or color changes as a result of irradiation. In one experimental demonstration of flavor changes induced by irradiation replicate samples of pasteurized milk, American process cheese, butter and a cooked meat product may be given radiation doses of 0, 50,000, 100,000, 200,000, and 400,000 rads. After irradiation the flavor, odor, and appearance of the samples receiving the various dosages should be compared to the control sample (0 dosage). Most individuals report a threshold for off-flavor in irradiated milk at about 50,000 rads. Irradiated butter and other fats have a similar off-flavor threshold, but the rancid flavor of irradiated fats may be removed in many cases by heating

the fat after irradiation. Recooking meat after irradiation also is beneficial to the flavor of this product.

To demonstrate the preservative effect of radiation from spoilage by microorganisms fresh bread slices may be packaged in polyethylene bags, heat sealed and given radiation doses of 0, 200,000, 400,000 and 800,000 rads and stored for several weeks at room temperature. The control (0 dose) usually molds in about one week at room temperature. The sample receiving 200,000 rad may not show mold growth for several weeks. Samples receiving 400,000 or higher doses may not mold during storage for months.

Fresh strawberries and lemons may be used to show the use of radiation for the prevention of mold growth on the surface of the fruit. In this experiment, boxes of strawberries may be given 0, 50,000, 100,000, and 200,000 rad doses of radiation and then stored in the refrigerator. After one week or less of storage, the nonirradiated strawberries may mold, whereas the irradiated fruit may be stored two to three times as long before mold appears. Similar observations can be expected with treated lemons stored at room temperature except that the time for mold development may be longer. The unspoiled irradiated bread and fruit also may be tasted for evidence of flavor change.

7.10 Experiment No. 10 Effects of Radiation on Chemical Reactions

by N. C. Kothary

The use of electromagnetic radiations to induce and accelerate chemical reactions has been known for several decades. However, in the past this phenomenon was limited to the use of ultraviolet light which was recognized as the chief component of sunlight effective in promotion of chemical reactions. The rapid growth of the use of radiosotopes and nuclear radiations has stimulated interest in the effect of other types of radiation on chemical reactions.

There are several advantages associated with use of radiation for promotion of chemical reactions. Certain reactions can be induced which are not possible otherwise. Certain other reactions normally require a very high temperature or catalyst which could be eliminated or the requirements could be reduced to more convenient values by use of radiation.

Discussion

In the present experiment the study is limited to use of cobalt-60 gamma radiation in synthesis of polysulfones.

Radiation Chemistry:

Gamma radiation in the energy range used does not induce radioactivity. The major primary effect is the liberation of a number of electrons as a result of absorption of radiation by matter. These electrons may lose their energy by exciting or ionizing molecules along their paths. The subsequent roles played by the excited and ionized molecules in producing the final chemical change is not understood completely. In many chemical systems however, it is shown quite conclusively that the reactions are typical of free radicals which are uncharged molecules with unpaired electrons. These radicals are produced by the eventual decomposition of excited or ionized molecules and free electrons, and are usually extremely reactive.

Certain chemical reactions are of the chain type and suffer a loss in free energy due to the chemical change. In such a case the initiation of a single chemical reaction by radiation may result in cleavage and formation of a large number of chemical bonds. This results in a highly efficient use of radiation energy. This is an important factor because of the high cost of this form of energy. Radiation induced polymerization is a chain reaction giving high yields and the products obtained may show high purity because of the absence of catalyst.

There are certain peculiarities of radiation induced chemical reactions which proceed by radical mechanisms:

1. The reaction is sensitive to the presence of oxygen which reacts with the free radicals.

2. The reaction is also sensitive to slight amounts of impurities which may act as radical scavengers.

3. Reactions in the condensed phase will differ from those in gaseous phase. An important effect known as Frank-Rabinowitch "cage" effect states that if two entities are formed due to radiation and are unequal in size, the larger fragment has a smaller probability of leaving the "cage" of surrounding molecules, before reacting further.

4. Another effect known as "sponge effect" explains the greater stability of benzene or other aromatic structures as due to the larger number of energy levels of the phenyl group. The absorbed energy could be dissipated throughout the molecule in such a case, rather than cause a chemical change.

5. The rate of polymerization is most often proportional to the square root of the intensity ($I^{0.5}$) of radiation. This dependence is typical of many radical polymerizations where the termination step occurs by the combination or disproportionation of two growing chains.

In most of the work the yield of a chemical reaction initiated by radiation is usually expressed by what is known as "G" value. This is defined as the number of molecules converted per 100 ev absorbed.

Synthesis of Polysulfones:

Bray[1] has studied the copolymerization of sulfur dioxide with olefins. The resulting polysulfone is a thermoplastic resin having many physical properties similar to those of some commercial plastics. He has suggested the following steps for the reaction.

1. Production of Compton electrons.

2. Ionization and excitation of molecules by Compton electrons.

3. Neutralization of ionized molecules by thermalized electrons producing excited molecules.

4. Decomposition of excited molecules to free radicals.

5. Propagation and termination of free radicals in the copolymerization reactions.

Barb[2] has studied the copolymerization of styrene with sulfor dioxide initiated by ultraviolet light. He found that in general the polymer was composed of two molecules of styrene to one of sulfur dioxide and the following

structure is indicated. Yemin at the University of Michigan is now studying this reaction using gamma radiation instead of ultraviolet light.
The copolymer formula is:

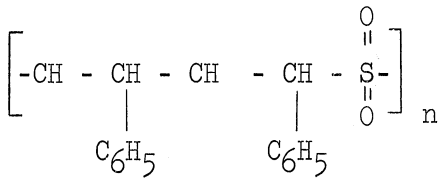

Procedure

(1) Purification of Reactants

As mentioned in the discussion, and indicated for the experiment on dosimetry using ferrous sulfate, small amounts of impurities in the reaction system are not desirable. Hence, the reactants used should be of reagent grade and purified further if possible and found necessary.

The styrene used for the reaction is reagent grade styrene supplied by Eastman-Kodak Company and purified further by distillation in a nitrogen atmosphere under reduced pressure. This is also necessary as commercially available styrene contains an inhibitor which is added to prevent polymerization under normal storage conditions. The sulfur dioxide used is Matheson reagent grade and is purified further during the loading procedure used.

(2) Loading of Reactants

A heavy walled pyrex vial is used as the reaction vessel. It is constructed from heavy walled 14 mm pyrex tubing with one end sealed and the other drawn out to a constricted neck and 7 mm open tube. The use of heavy walled tube is necessary as the reactants develop super-atmospheric pressure at room temperature. (See Fig. 7.32.)

The vials are cleaned with chromic acid cleaning solution and rinsed with distilled water and reagent grade acetone and finally dried at 120 degrees C. After weighing the vial, a known volume of styrene is introduced by siphoning from the distillate receiver. The vial is weighed again to find out the exact weight of styrene used.

It is then attached to the vacuum system. (See Fig. 7.33.) The vacuum system is a glass manifold with inlet valves for reactants, manometer and the vacuum pump. The whole system is evacuated for some time after immersing the vial with styrene in dry ice. At this temperature (-79 degrees C.) the vapor pressure of styrene is negligible and thus, negligible losses occur. After evacuating the system of residual gases to a pressure of 10^{-1} mm, the sulfur dioxide valve is opened and the reactant is condensed in the vial. Again the reactant is measured by volume and weighed later to check the exact amount.

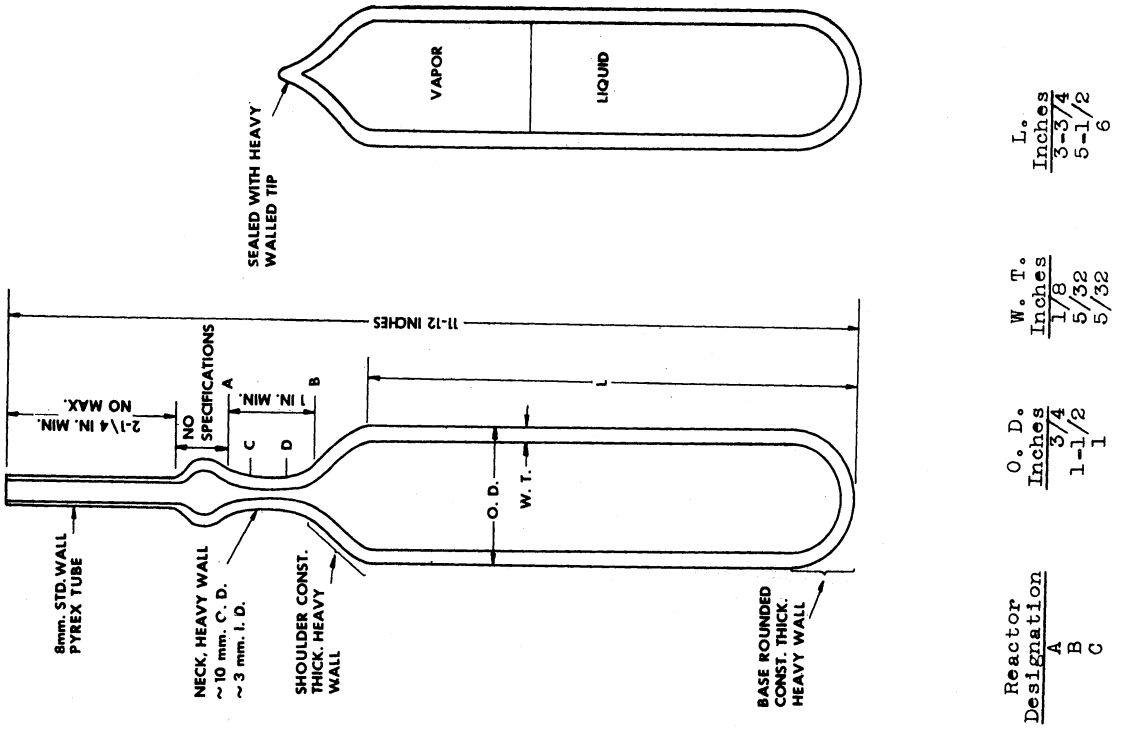

Fig. 7.32 Drawing and specifications for pyrex heavy walled glass reactors

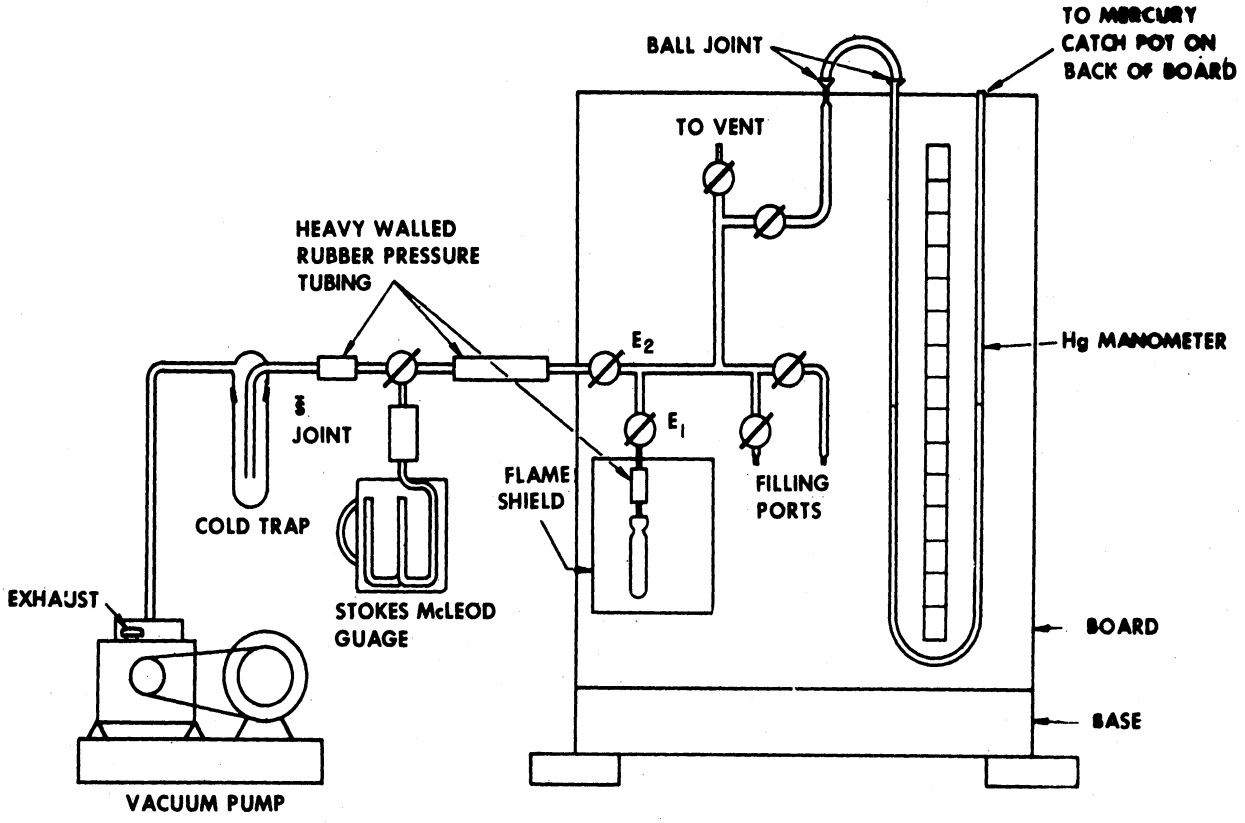

Fig. 7.33 Drawing of the stainless steel reactor no. E used in the room temperature runs

After the loading is completed, the vial is sealed off at the neck with a torch. The open tube end of the vial is saved for subsequent weight measurements.

(3) Irradiation of Vials

The vial is placed in a Dewar flask containing a constant temperature bath (0 degrees C. provided by ice in water) in the center well for 6 hours. The radiation intensity and total dose should be noted from previous experiments.

(4) Recovery of Product

After irradiation, the vial is cooled and opened by scratching the vial near the neck and touching one end of the scratch with the molten end of a pyrex glass rod.

It should be noted that improper opening of the vial may result in shattering and explosion of tube, and release of poisonous sulfur dioxide. The whole operation should be conducted in a fume hood.

The contents of the vials are allowed to thaw and are poured while still cold into 200 cc of methanol containing hydroquinone. Methanol is used as solvent for the monomer. The polymer formed due to reaction is not soluble and precipitates out. The hydroquinone (a free radical scavenger) is added to stop any reaction which might proceed as a post irradiation effect.

The solution is filtered through a Buchner funnel and precipite recovered on a preweighed Whatman #42 filter. The filter and the precipitate are dried and weighed, to determine the amount of polymer formed.

Questions

1. Determine the percent yield of the reaction and the "G" value for the same.

2. Briefly discuss the significance of various factors that might be considered in determining the economic feasibility of a chemical reaction promoted by radiation.

References

1. Bray, B.G. "The Effect of Gamma Radiation in Several Polysulfone Reaction" Ph. D. Dissertation, University of Michigan, Ann Arbor, 1957

2. Barb, W.C., Proc. Roy. Soc. London, A-212: 177092 (1952)

3. Kothary, N.C., and Yemin, L. "The Effect of Gamma Radiation on Several Reactions of Unsaturated Organic Compounds", Engin. Research Institute, University of Michigan, Ann Arbor, 1957

7.11 Experiment No. 11

Glass Dosimetry-Cobalt Type

Discussion

Ferrous-ferric (5-50 Krad) and the cupric-cuprous (10 Mrad) dosimetry require a certain degree of operator technique to produce consistent results. There are inherent problems assiciated with any form of liquid dosimeter that are avoided by the use of solids for dosimetry such as cobalt glass (Bausch & Lomb F - 0621. This method of dosimetry provides a relatively simple and positive means of measuring doses in the region of 10^4 to 10^6 rad.

Under irradiation the cobalt glass and other dosimetry glasses such as silver activated phosphate glass develop color centers which result in an increase in the absorption spectrum between 3,000 Å and 5,000 Å. However, the optical density of the silver activated phosphate glass is less stable with them than the cobalt glass. At high doses there is some fading and also a noticeable fall-off in the curve of dose vs absorption coefficient. This indicates there is a saturation of the color centers occurring. Higher temperatures will hasten fading of the high dose samples. (See Chapter 3 for additional information.) Figure 7.32 shows a plot of optical density vs dose for Bausch & Lomb cobalt glass. Table 7. lists Bausch and Lomb specifications and prices for cobalt glass, silver phosphate glass and accessories.

Table 7.

Specifications for Bausch & Lomb Cobalt Glass

and Silver Activated Phosphate Glass and Accessories

Catalog No.	Description	Price Each
33-99	Cobalt dosimeter glass, 15mm x 6mm x 1.5mm, faces polished, edges rough grind...	$ .30
33-99	Silver-activated phosphate glass, 15mm x 6mm x 1.5mm, faces polished, edges rough grind...	.40
33-66-02	B & L Microdosimeter Reader, 10-10,000 rads, for 60 cycle, 155 volt A.C., including directions for use, plastic dust cover, and one pair Microdosimeter Rod tweezers...	1,490.00

Table 7. Cont.

Catalog No.	Description	Price Each
33-66-20	B&L Microdosimeter Rods, package of 100, silver-activated phosphate glass, 6mm long, 1mm diameter, ground and polished both ends, (rods furnished with nomial diameter of .99 or 1.01 mm ± .01mm)...	44.00*
33-66-00	B&L Microdosimeter Low "Z" Rods, package of 100, special silver-activated phosphate glass 6mm long, 1mm diameter, ground and polished both ends, (rods furnished with nomial diameter of .99 or 1.01mm ± .01mm)...	44.00
33-29-40-02	Spectronic 20 Colorimeter, 340-650mu for 60 cycle 115 volt A.C., 1/2" test tube adapter, directions for use and plastic dust cover...	255.00
33-29-10	Constant voltage transformer (for unusual voltage fluctuations)...	40.00
33-29-23	Holder, for cobalt dosimeter glass, fits standard 1/2" test tube adapter...	15.00
33-99	Filter, 0.9 sptical density...	2.50
33-33-68	Extra 6-volt lamp...	2.20
	*25% quantity discount on 10 packages or more. 33-1/3% quantity discount on 100 packages or more. 45% quantity discount on 200 packages or more.	

Procedure

After irradiating the 15mm x 6mm x 1.5mm cobalt glass in known fields for doses between 10^4 and 5×10^6 rads, the change in optical density of the glass is measured on the Beckman DU spectrophotometer at a wave length of 340 mu and a slit width of .4mm. After waiting for a week, measure the optical densities of the samples a second time and follow this with another measurement after an hour of anneafing at 150 degrees C. An attempt at erasing the color centers should then be made at 500 degrees C.

Questions

1. From the log-log plot of dose versus optical density what can be said about its functional relationship?

2. From the results on the annecling and the attempt at erasing the color centers, give an explanation of the mechanism of annealing and erasing.

References

1. Chapter 3 of "Radioisotope Technology"by L. E. Brownell, University if Michigan.

2. Kreidl & Blair, "A System of Meya roentgen Glass Dosimetry," Nucleonics 14, No. 1, January 1956

3. Davidson, Goldblith & Proctor, "Glass Dosimetry," Nucleonics 14, No. 1, January 1956

4. Kreidl and Blair, "Recent Developments in Glass Dosimetry," Nucleonics 14, No. 3, March 1956

Chapter 8

Nuclear Radiation Detection and Measurement

By Geza L. Gyorey
and Philip R. Pluta

8.1 Discussion

This chapter is designed to acquaint the student with the basic instruments and methods used in nuclear engineering for the detection and measurement of nuclear radiation, and also, to acquaint the student with the basic standards for protection against radiation. The experiments which are performed involve the use of radioactive materials of a variety of types and activities. The use of radioactive materials involves some dangers which are very slight as long as certain precautions are observed. If precautions are not observed, the danger increases by orders of magnitude. For this reason, the rules which are set forth below are enforced most rigorously in the Nuclear Measurements Laboratory. Disregard of these rules may result in the loss of privilege to use this laboratory.

The reason for the establishment and strict enforcement of these rules is partly a concern for the safety of the individual student and a desire to instill good working habits. To a great extent, the reason is a concern for the safety of the public, including other persons working in the vicinity of the laboratory.

The following reference material is required reading for students in this course:

Code of Federal Regulations,
Title 10 - Atomic Energy,
Chapter I - Atomic Energy Commission,
Part 20 - Standards for Protection Against Radiation, including amendments published through January, 1961

Film badges (or pocket chambers) must be worn in this laboratory at all times. The film badges may not be worn in other laboratories without the direct permission of the instructor.

8.2 General Laboratory Procedures

In all work always avoid exposing yourself and others to a higher radiation dose than absolutely necessary. Be aware of the radiation field

intensity in which you are working. Always have a survey meter ready when removing a high level source from its shield, and do not leave a high level source unshielded unnecessarily.

Do not handle sources of higher than a few microcuries of activity without the direct permission of the instructer. If you suspect that a source might have broken open resulting in radioactive contamination, speak to the instructor at once.

If you are not sure of what you are doing, stop and think.

Do not smoke, eat, or drink in the laboratory. Radioactive materials may be ingested this way.

Be very careful when working with high voltage supplies, the shock they deliver may be dangerous.

Keep the laboratory neat and orderly. This promotes safety to a great extent.

Cardinal Rule: Check your hands and shoes for possible radioactive contamination when leaving the laboratory. If you detect any activity, do not leave, call the instructor.

The material in this chapter covers the subject of nuclear radiation detection and measurement in an introductory fashion. Intensive periods of lecture, group discussion and experimentation, including a thoughtful writeup of each new technique learned are necessary to transform a novice into a confident practitioner of the art. The material presented here would serve as part of the helpful background material which might be read. The questions at the end of the chapter are typical of some of the problems which should be understood before the equipment can be used with insight.

8.3 List of Recommended Equipment

Frequently, questions are asked about the prices of the pieces of equipment used, and also about the total cost of the equipment in a nuclear measurements laboratory well equipped for teaching purposes. The subsequent list is intended to answer some of these questions.

It is felt that this amount of equipment is quite adequate for a laboratory designed to accomodate, at one time, eight to twelve students working in four groups. The equipment was selected with those experiments in mind which are outlined in this chapter. From a study of the experiments

one might observe that it is quite possible to get along with considerably less equipment than the list shows. This observation is quite correct as long as all the equipment works properly at the same time, or if it is possible to repair the equipment between laboratory sessions, which is not generally true.

The prices listed were taken from 1960-61 catalogs, and they pertain to high quality equipment which, in the opinion of this instructor, will excellently fulfill the requirements of a graduate level laboratory. For top quality research equipment one should expect to pay more, and conversely, lower quality equipment is available at lower prices than those indicated.

Quantity	Description	Unit Cost	Total Cost
1	Laboratory monitor, giving audible signal, equipped with very thin window Geiger tube.	370	370
1	Geiger type portable survey meter	300	300
1	Juno survey meter	325	325
1	Radector survey meter	300	300
1	Cutie Pie survey meter	300	300
1	Slow-fast neutron survey meter	700	700
20	Self reading, neutron and gamma sensitive pocket dosimeters	45	900
1	Charger for pocket dosimeters	50	50
2	Electroscopes	125	250
1	Large air equivalent ionization chamber	100	100
1	Electrometer for ionization chamber	400	400
3	End window Geiger tubes	60	180
3	Geiger tube mounts and shields	200	600

Quantity	Description	Unit Cost	Total Cost
2	Windowless flow counters	200	1000
2	Gas cylinders with pressure regulators	100	200
2	BF_3 counter tubes	125	250
2	Scintillation probes with preamplifiers	400	800
2	Scintillation probes with cathode followers	400	800
2	NaI well type crystals 1 3/4" x 2" high	300	600
1	NaI solid crystal 1 3/4" x 2" high	250	250
2	Beta scintillation crystals	120	240
2	Alpha scintillation crystals	70	140
2	Scintillation counter shields	750	1500
7	Scalers with preset timers and 2500 volt high voltage supplies	950	6650
2	Cathode follower preamplifiers	110	220
2	Linear amplifiers with integral discriminators	500	1000
2	1500 v super stable high voltage supplies	470	940
2	Non-overloading amplifiers with single channel pulse height analyzers	900	1800
2	Count rate meters	525	1050
2	Pulse generators	300	600
2	Cathode ray oscilloscopes	1250	2500
2	5 to 50 millicurie level gamma sources	150	300
1	Lead shield for gamma sources	100	100

Quantity	Descriptions	Unit Cost	Total Cost
1	1 curie Pu-Be neutron source with shield	525	525
18	Small alpha, beta, and gamma sources	20	360
	Assorted foils		100
50	Lead bricks	6	300
	Miscellaneous equipment, such as spare tubes, tools, voltmeters, absorbers, source preparation kits, cables, connectors, instrument racks and cabinets, etc.		3000
	TOTAL		$30,000

8.4 Introduction to Theory of Instrumentation

"Nuclear Radiation Detection" by Price is the basic text used in this laboratory course and will be covered, in more or less detail, in its entirety. Other texts which will be referred to often are "The Atomic Nucleus" by Evans and "Vacuum Tube and Semiconductor Electronics" by Millman.

We are concerned with the detection of particles of interest to nuclear engineering research and development. These particles are emitted from a nuclear reactor and from naturally and artificially induced radioactive substances. Every fissioning reactor liberates neutrons, beta particles, gamma/rays and alpha particles. Radioactive substances emit neutrons, betas, gammas and alphas, also. Of lesser importance to our studies are other particles such as protons, deuterons, positive electrons or positrons, neutrinos and the host of particles of a more transient nature such as the mesons, etc.

The basis of detecting these particles is through their interaction with matter and the measurement of the disturbance caused by their interaction in the form of a current flow, voltage drop, voltage pulse, darkening of a photographic plate, change in color of a substance or its physical properties, etc.

In the laboratory, we shall be most concerned with electrical methods. Charged particles are the easiest to detect electronically, since they create ionization, i.e. ion pairs, in the media through which they pass through interaction of the coulomb fields. As the particle produces ionization, its energy decreases until it no longer can supply the required ionization energy. For an alpha particle, classical theory of radiation interaction can quite accurately predict, $\pm$15%, the rate of loss of energy as a function of distance travelled, x, in the media. The result of such analysis (a derivation is given at the end of this section) is,

$$-\frac{dE}{dx} = \frac{4\pi z^2 e^4 ZNB}{mv^2}$$

where E is the instantaneous energy of the alpha associated with its kinetic energy, $1/2\ mv^2$, z e is the charge on the alpha (z = 2), Z is the atomic number of the media atom, N is the concentration of media atoms and B, depending on v and Z in a logarithmic manner, is (see Evans for relativistic formulation for B) known as the "stopping number". From the equation, the rate of energy loss depends directly on the number of media electrons per atom, the atomic concentration and inversely on α energy. The number of ion pairs produced per unit path length of the α is known as specific ionization. An estimate of the total number of ion pairs formed can be made if the energy required to produce one ion pair in the media and the initial particle energy is known. For example, the energy required to produce an ion pair in a gas has been measured for air $\hat{=}$ 35 ev and for helium $\hat{=}$ 31 ev. Thus, a 3.5 Mev α produces about 10^5 ion pairs in air.

Sufficient numbers of ion pairs are created by α particles to produce a measurable quantity of charge. Because of the massive size of the α its path is relatively straight as it loses energy in the media.

Electrons are also easily detected because of their charge of -e. Electrons lose energy primarily by inelastic collision and secondarily by radiative loss. The rate of energy loss due to inelastic collision is given qualitatively by the equation for α energy loss, however, the stopping number is approximately constant for electron energies less than 1 Mev. The radiative loss occurs when the electron is in the Coulomb field of an atom and is accelerated due to its small mass. From classical theory, a charged particle emits electromagnetic radiation when subjected to an acceleration. For β energies less than 5 Mev the radiation effect is not of major importance. Notice that since $-\frac{dE}{dx}$ is proportional to z^2/E the electron will travel a greater distance in the media than an α

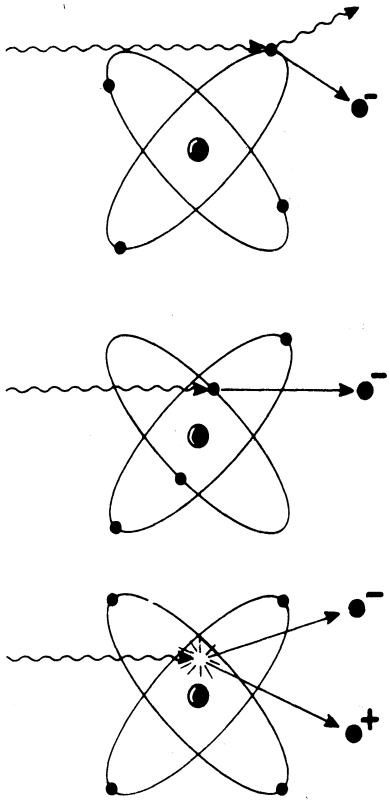

Figure 8.1. Principal Gamma Ray Interactions.

before dissipating its energy.

Gamma rays interact with matter in three important ways, photoelectric, Compton scatter, and pair production, See Figure 8.1. In the photoelectric effect, the γ loses its entire energy to the atom which then transfers this energy to an inner electron which is ejected. The kinetic energy of the ejected electron is equal to the energy of the γ minus the binding energy of the orbital electron. Compton scatter describes the interaction between a γ and an electron. The γ transfers only part of its energy to the electron. The amount of energy transferred depends on the angle between the direction of the struck electron and the incident γ path, and the incident γ energy. For a 180° recoil interaction, maximum energy is transferred. Klein and Nishina have calculated the differential scattering cross section for this interaction quantum mechanically and found it to be proportional to $\frac{NZ}{h\nu} = \frac{NZ}{E}$. In pair production a high energy γ, $E > 2\ m_o c^2 > 1.02$ Mev, is converted in the presence of a nucleus to a beta and a positron. For intermediate energies $0.5 < E < 5$ Mev the Compton effect is predominant.

Since neutrons are uncharged, measurement is usually made indirectly. The neutrons interact with matter to produce detectable radiation. Two such systems easily envisioned are a thermal fission detector and a thermal boron detector. In the fission chamber the neutrons cause fission and the resulting charged particles are detected by their ionization. In a boron detector, one has the (n, α) reaction

$$B^{10} + n \longrightarrow \alpha + Li^{7}$$

where the ionization due to the α and Li is measured.

8.5 Derivation of Charged Particle Energy Loss in Matter

A derivation of the energy loss of a charged, massive particle moving through matter, is included to give insight to a widely quoted result. Consider Figure 8.2,

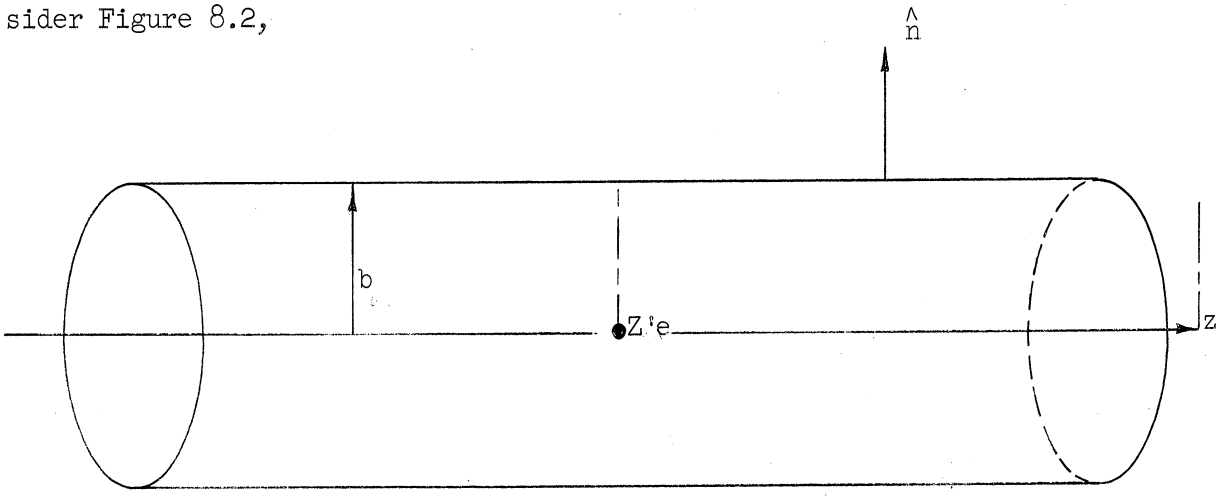

Figure 8.2. Geometry for energy loss derivation

For the electric field in an ∞ cylinder of radius b, with charge Z'e inside, on the axis, recall Maxwell's equation:

$$\underline{V} \cdot \underline{D} = \rho = \frac{Z'e}{\pi b^2 z} \qquad \text{(rationalized mks)}$$

$$\int_{\text{volume}} \underline{V} \cdot \underline{D}\, dv = \rho \int_{\text{volume}} dv = Z'e$$

by Green's theorem, convert to a surface integral,

$$\int_{\text{volume}} (\underline{V} \cdot \underline{D})\, dv = \int_{\text{surface}} \underline{D} \cdot \hat{\underline{n}}\, ds$$

$$Z'e = \int_{\text{surface}} E_o E_n\, (2\pi b)\, dz$$

Where $\underline{D} = \mathcal{E}\, \underline{E}$ and E_n is the normal component of the field

$$\int_{\infty}^{\infty} E_n(z)\, dz = \frac{Z'e}{E\, 2\pi b}$$

$$\int_{-\infty}^{\infty} E_n(t)\, dt = \int_{-\infty}^{\infty} E_n \frac{dz}{V} = \frac{Z'e}{E\, 2\pi b v}$$

where V is the speed of the charged particle.

The normal impulse given to an electron in db about b is simply

$$\int_{-\infty}^{\infty} F_n(t)\, dt = \int_{-\infty}^{\infty} e\, E_n(t)\, dt = \text{impulse}$$

The impulse is defined as the change in momentum of the electron, $\therefore$, assuming the electron to be initially at rest, the total energy transfer to the electron is

$$\frac{p^2}{2\,m_o} = \frac{(\text{Impulse})^2}{2\,m_o} = \frac{1}{2\,m_o}\left[\frac{Z'e^2}{\mathcal{E}2\pi bV}\right]^2$$

where m, is the electron rest mass.

Consider a collection of uniformly distributed electrons with concentration = NZ electrons/m^3, N being the atomic conc. and Z the atomic no. of the media. The differential no. of electrons per unit length in a shell bounded by b + bd and b is,

$$\left[\pi(b + db)^2 - \pi\, b^2\right] NZ = 2\pi b\, NZ\, db$$

The total energy loss by the charged particle to the electrons in a volume between $b_{min.}$ and $b_{max.}$ is simply,

$$-\frac{dE}{dx} = \int_{b\ min.}^{b\ max.} \left[\frac{Z'e^2}{\mathcal{E}2\pi bV}\right]^2 \frac{2\pi b\, NZ\, db}{2\,m_o}$$

$$-\frac{dE}{dx} = \frac{Z'^2\, e^4\, NZ}{4\pi\mathcal{E}^2\, m_o V^2} \ln\left(\frac{b_{max.}}{b_{min.}}\right)$$

putting in the form of the previously quoted result, let $Z' \rightarrow z$, and since Price's result is in Gaussian or c.g.s. units note the extra factor $4\pi\mathcal{E}^2$ due to the mks, and let

$$\ln \frac{b_{max.}}{b_{min.}} \longrightarrow B$$

8.6 Ionization Chambers

Alpha and beta particles and gamma rays interact with matter to produce free electrons and positively charged ions. In the presence of an electric field, the electrons are forced toward the anode and the positive ions to the cathode. When the interaction takes place in the gas phase, the majority of recombination events between electrons and ions producing a neutral atom take place in the immediate vicinity of the electrode surfaces where the concentration of atoms is greater than in the gas. In general, a measuring system must be set up which detects the effect of the ions collected at the electrodes, either in the form of an electric current, voltage pulse or reduction in charge.

8.7 Mean Level Chamber

A mean level chamber measures the electric current directly, see Figure 8.3, or the integrated effect of a current by means of a change in the amount of charge stored on a capacitor. In an ionization chamber, the maximum charge collected is equal to that created by the incident radiation, the primary ionization, in the absence of recombination. Gas multiplication, i.e., the ratio of collected ionization to primary ionization, is less than or equal to unity, as opposed to multiplications of 10^2 to 10^{10} for proportional and Geiger-Muller chambers, respectively (discussed more fully later). As a result, the total charge collected for each ionizing particle is very small. Leakage currents in the insulator between the electrodes must be minimized. Leakage occurs primarily on the surface of the insulator and is reduced by the manufacturer in a variety of ways.

Guard rings are used in the chamber to help eliminate field distortion due to ion collection on the insulator, to define the active collection volume and to reduce leakage currents. Guard rings are kept at approximately the same potential as the collecting electrode (the output of the collecting electrode goes to the measuring circuit).

A typical mean level ionization chamber useful as a laboratory survey meter is shown in Figure 8.4.

Instead of measuring the mean current directly, the chamber can be used as a current integrating capacitor, $\Delta V = \frac{1}{C}\int i\,dt$, i.e., the change in the voltage between electrodes can be used to infer the charge collected. This type of chamber is used primarily as a personnel radiation monitor.

The Lauritsen chamber (Figure 8.5) has a built-in microscope to view the amount of deflection of a quartz fiber which decreases as the charge on the electrode decreases. A pocket dosimeter is shown in Figure 8.6. It is inconvenient to have a chamber large enough so that all the "associated corpuscular emission" resulting from the incident radiation is collected. This complication can be neatly avoided by using either an air wall or an air-equivalent wall chamber. These chambers compensate for the ion pairs that are produced outside the collecting region by having the "walls" of the collecting volume made of air, or a substance whose atomic number is equivalent to air, about 8. In this fashion, ideally, the same amount of ion pairs enter the sensitive volume from the walls as are produced outside this volume. The walls of a standard air wall chamber are defined by guard rings. Bakelite and other plastics are usually used as construction material

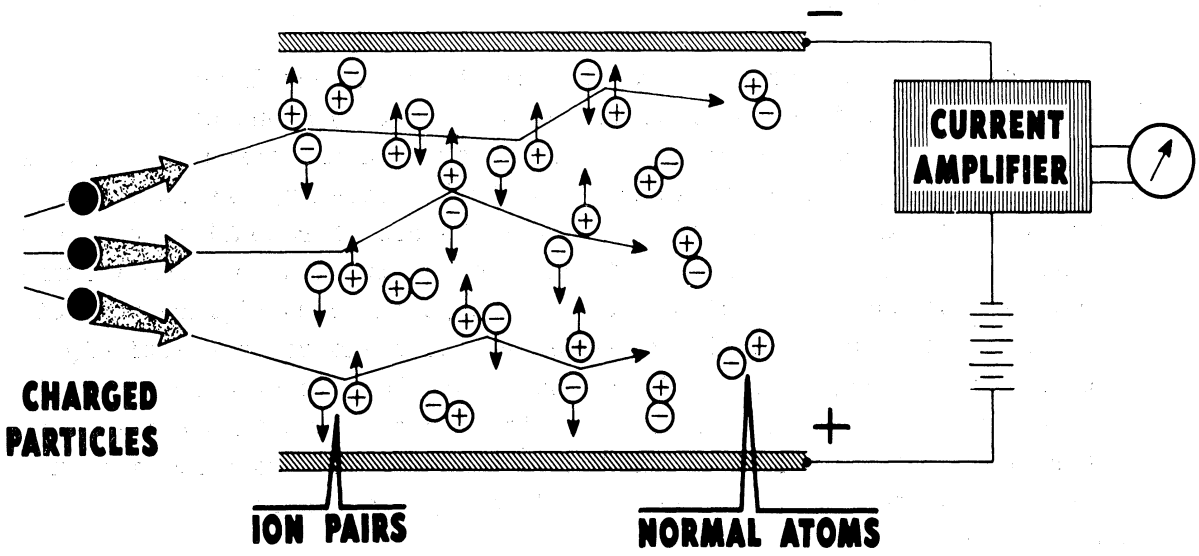

. INCOMING PARTICLES IONIZE ATOMS
. ELECTRODES ATTRACT IONS
. ARRIVAL OF IONS CONSTITUTES CURRENT
. CURRENT IS MEASURE OF PARTICLES

Figure 8.3. Ionization Current.

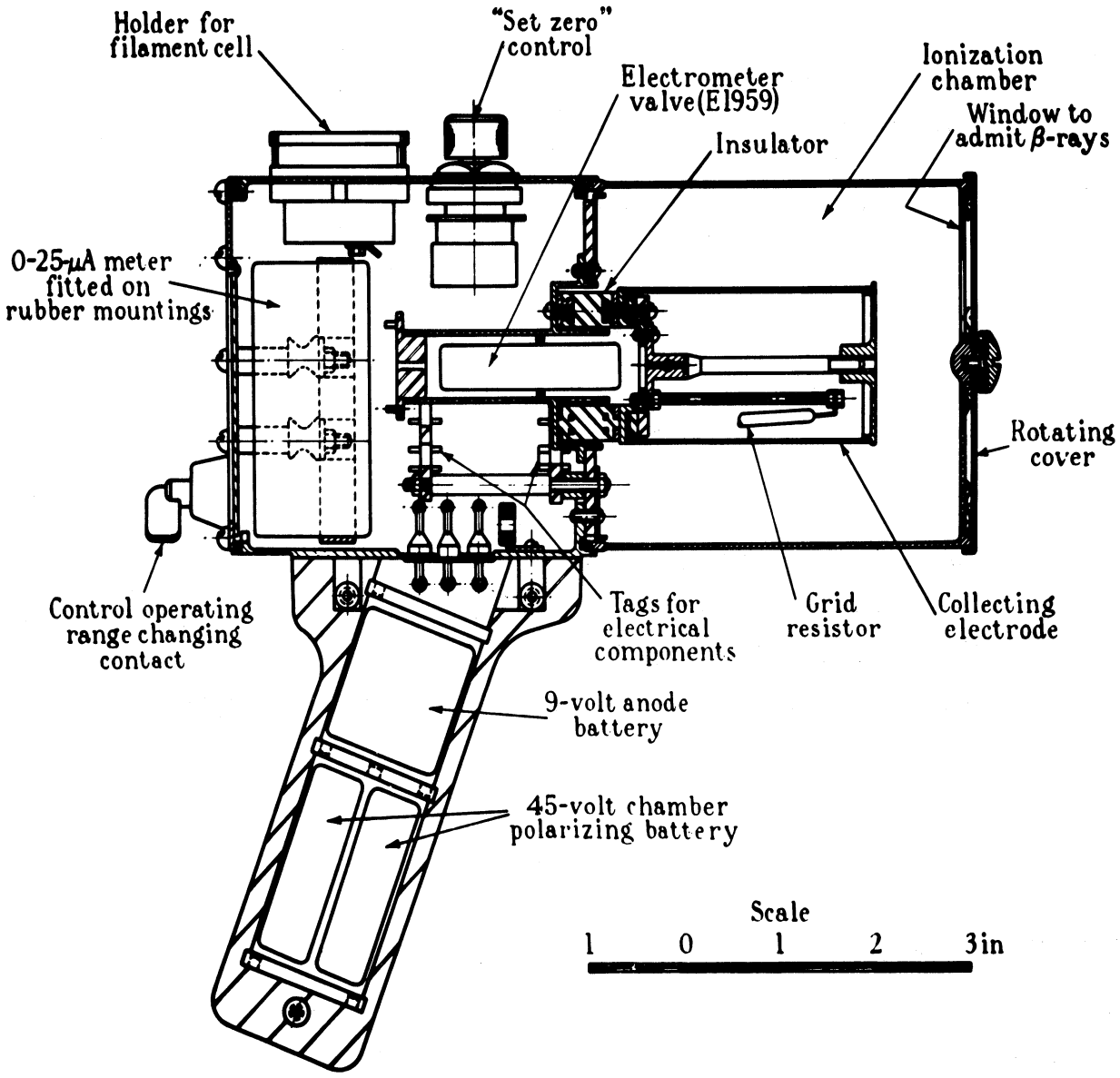

Figure 8.4. Typical Ionization Survey Meter. (Courtesy of Atomic Energy Research Establishment)

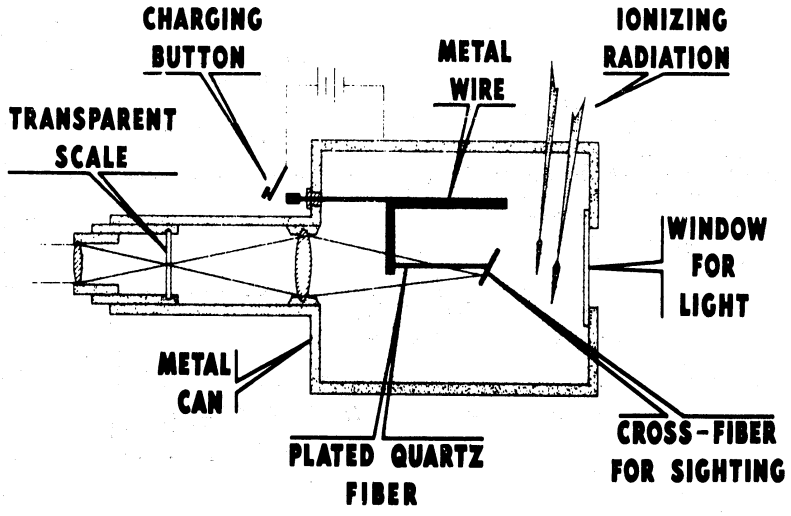

. CHARGE BENDS FIBER FROM WIRE
. IONS PRODUCED IN GAS BY RADIATION
. IONS MOVE TO WIRE AND REDUCE CHARGE
. AMOUNT OR RATE OF IONIZATION OBSERVED WITH TELESCOPE

Figure 8.5. The Lauritsen Electroscope.

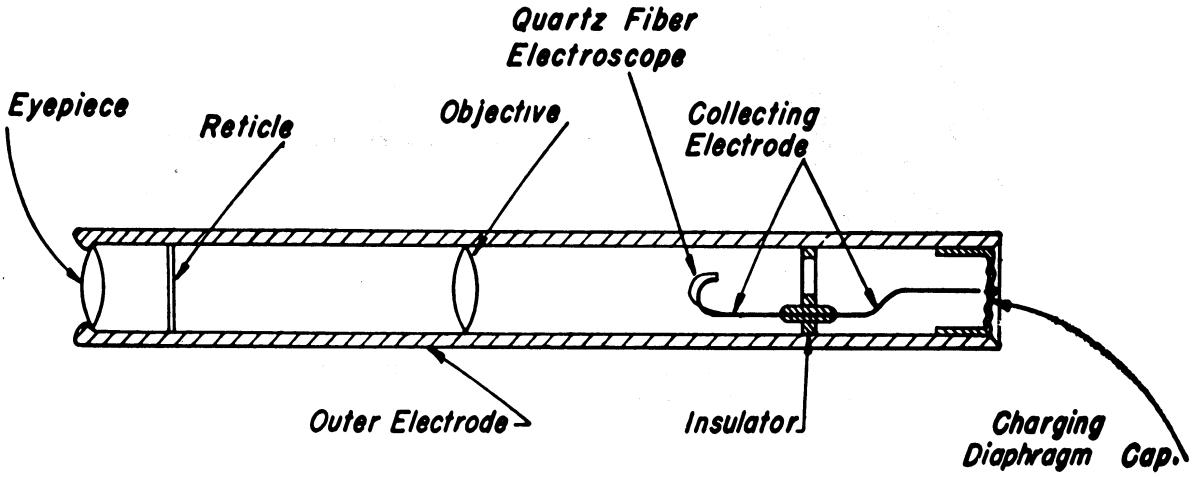

Figure 8.6. Pocket Dosimeter.

in the walls of an air-equivalent chamber The inner surface of the plastic is coated with carbon to make it an electrode. Usually a standard known source such as radium is used to calibrate an ionization chamber. The radium is packaged to ensure that only γ may impinge on the chamber. The γ energy spectrum from radium and its decay products are well known, and by an extension of the arguments given in a previous chapter on dosimetry, the theoretical dose in roentgens produced in the chamber can be calculated.

8.8 Pulse Ionization Chambers

The measurement of individual voltage pulses requires an understanding of the dependence of the electrode voltage on the system parameters and the manner in which the voltage pulse reaches the electrodes by induced charge build up. It is useful to define two quantities in an attempt to formulate a theoretical equation describing the motion of the charged particles in the sensitive volume. The mobility, μ, is $\left|\frac{vP}{\mathcal{E}}\right|$ where v is the average charged particle drift velocity due to the electric field $\mathcal{E}$ and P is the gas pressure. The mobility is different for each different kind of charged particle, depending on the chamber gas and the mean free path of an ion in the gas. Massive positive ions have much smaller mobilities than electrons. As the gas pressure is increased, the mean free paths decrease giving a reduced drift velocity as implied in the definition. The diffusion coefficient, D, is defined in a manner similar to reactor engineering, e.g., for negative particles, $\left|\underline{J}_- / \underline{V}\, n_-\right|$ where $\underline{J}_-$ is the current per unit area due to a gradient in the negative particles whose concentration is n_-.

To gain an appreciation for the behavior of the charged particles in the chamber, write a balance equation for the positive and negative particles. Write the balance equation for electrons, realizing that the positive ion equation is similar with the exception of signs. Consider a differential element of volume in the gas, Adx. The net rate of change of electrons is determined by the rate of recombination, leakage current due to a gradient, the current due to the field, and the rate electrons are created by either primary ionization or gas multiplication. Consider one dimension for simplicity. The balance on negative charge in the x direction is (See next page for Figure 8.7)

$$e \frac{\partial n}{\partial t} Adx = I_x A + S\, Adx - R\, Adx - I_{x+dx} A$$

where S is the volumetric rate of creation in dV and R is the volumetric rate of recombination.

Figure 8.7. Diagram for Charged Particles in Ionization Chamber.

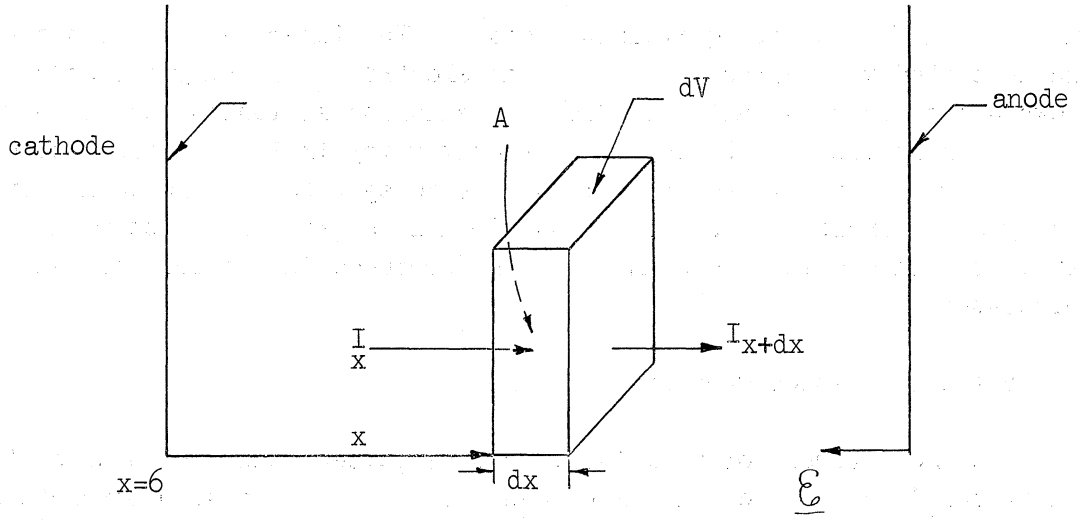

$$I_x = - D\, e \frac{\partial n}{\partial x} + v_x\, n\, e$$

(the minus sign because electrons flow down the concentration gradient)

$$I_{x+dx} = I_x + \frac{\partial}{\partial x}(I_x)\, dx$$

or,

$$e \frac{\partial n}{\partial t} = S - R + e \left[\frac{\partial D_-}{\partial x} \frac{\partial n}{\partial x} + D_- \frac{\partial^2 n}{\partial x^2}\right]$$

$$- \frac{e}{P} \left[\frac{\partial \mu_-}{\partial x} (\mathcal{E}_x n) + \mu_- \frac{\partial}{\partial x} (\mathcal{E}_x n)\right]$$

where $v_x = \frac{\mu_- \mathcal{E}_x}{P}$. Usually it is assumed that $\frac{\partial D_-}{\partial x} = \frac{\partial \mu_-}{\partial x} = 0$, giving in generalized coordinates,

$$e \frac{\partial n}{\partial t} = S - R + e\, \underline{D}\, \nabla^2 n - \left(\frac{e\mu_-}{P}\right) \underline{\nabla} \cdot (\underline{\mathcal{E}} n)$$

The form of the recombination term is usually arrived at empirically, e.g., away from the electrode surfaces R is often represented by, Constant x (conc. of electrons) x (conc. of positive ions). The balance equation has not been solved analytically in a manageable form for the general case. Price gives approximate expressions (pg 72, 73) which estimate the fractional loss in the saturation current (all charge collected) due to recombination and due to diffusion for certain conditions at mean level, but nothing for pulse operation.

There are two main conditions required for an ionization chamber to count individual pulses, rather than a mean level current. The voltage pulse height must be separable from a low level background, and the system

must be fast enough to differentiate between individual successive pulses. To estimate the energy absorbed in the chamber gas, it is necessary to have a known relationship between the size of the pulse and the number of ion pairs formed. The time required for the pulse to build up to peak voltage and decay is important, also. Because the positive ions are generally more massive than the negative ions (usually electrons), it takes them longer to migrate to the cathode (on the order of a millisecond) whereas the electron transit is usually measured in microseconds.

The following simple example may illustrate a few points. Consider a parallel plate chamber operating at 200 volts with a plate separation of 2 cm. Let a positive ion having a mass of 8 amu. and an electron be created in the center of the collecting volume. Recall,

$$\mu = vP/\mathcal{E}$$

In air, the mobilities are approximately

$$\mu_- = 10^6 \left(\frac{\text{cm}}{\text{sec.}} \right) \left(\frac{\text{mm of Hg}}{} \right) \Big/ \frac{\text{volt}}{\text{cm}}$$

$$\mu_+ = 1070 \quad " \qquad\qquad "$$

giving,

$$v_- = 1.3 \times 10^5 \text{ cm/sec}$$

$$v_+ = 1.4 \times 10^2 \text{ cm/sec}$$

Thus, the transit times are $t_{f-} = 7.7 \times 10^{-6}$ seconds and $t_{f+} = 7.2 \times 10^{-3}$ seconds. These collection times on the order of a microsecond and millisecond are quite representative for most ionization chambers. A discussion is given in the next section concerning the calculation of induced charge and voltage pulse forms as seen by the amplifier.

On the basis of what has been shown above, one can conclude that any ionization pulse chamber whose operation depends on measuring the effects of the positive and negative ions, the so called ion pulse chamber, must be restricted to low count rates, on the order of 100 per second because of the long time required for the positive ion to reach the cathode. This limitation can be overcome by making the RC time constant of the system longer than t_{f-} and shorter than t_{f+}, making the voltage pulse output less dependent on the induced charge of the positive ions. This type of chamber is the commonly known variety and is called an electron pulse chamber.

8.9 Input Voltage Pulse Forms to a Counting Circuit Caused by the Production of Ion Pairs Between Two Electrodes

The electrostatic potential is a scalar point function. The potential at a point, P, which is at distances r_i from charges q_i, due to q_i is

$$V(P) = \frac{1}{K} \sum_{i=1}^{n} q_i/r_i$$

where K is the dielectric constant and n is the total number of charges.

The mutual energy of any system of charges can be found from the definition of the electrostatic potential. For a charge q_j,

$$W_j = q_j V_j = \frac{q_j}{K} \sum_{i=1}^{n} q_i/r_{ij} \ , \ i \neq j$$

where V_j is the potential at the position q_j due to the charges q_i. The work to put all the charges in place is simply

$$W = \frac{1}{2K} \sum_{i=1}^{n} \sum_{j=1}^{n} q_i \, q_j/r_{ij} \ , \ i \neq j$$

the factor 1/2 takes account of the fact that the j^{th} charge is brought into the field of the i^{th} charge and the i^{th} charge is brought into the field of the j^{th} charge in the summation. Since V_j is the potential where q_j is located, this may be written

$$W = \frac{1}{2} \sum_{j=1}^{n} q_j V_j$$

If all the charge is on one conductor, at a potential V_o and the sum of the charge is Q,

$$W_{conductor} = \frac{1}{2} \sum_{cond.} q_j V_j = \frac{1}{2} Q V_o$$

But $C = Q/V_o$, therefore, $W_{cond.} = 1/2 \, CV_o^2$, which is the energy of a charged conductor. For a capacitor whose plates are at V_1 and V_2 with charge Q and -Q, respectively,

$$W = \frac{1}{2} \left[Q V_1 - Q V_2 \right] = \frac{1}{2} Q \left[V_1 - V_2 \right]$$

and for a condenser, $Q = C(V_1 - V_2)$

$$W = \frac{1}{2} C \left[V_1 - V_2\right]^2$$

Consider charges q_1, q_2, ... q_n at positions where the existing potentials due to the other charges are V_1, V_2, ... V_n, and a new set of charges, at the same positions, q_1', q_2', ... q_n' causing analogous potentials V_1', V_2', ... V_n'. By definition,

$$V_j = \frac{1}{K} \sum_{i=}^{n} q_j / r_{ij} \ , \ i \neq j$$

and

$$V_j = \frac{1}{K} \sum_{i=1}^{n} q_i' / r_{ij} \ , \ i \neq j$$

Multiply V_j by q_j' and V_j' by q_j and sum over j,

$$\sum_{j=1}^{n} V_j \, q_j' = \sum_{i=1}^{n} \sum_{j=1}^{n} q_j \, q_j' / r_{ij} \ ; \ \sum_{j=1}^{n} V_j' \, q_j = \sum_{i=1}^{n} \sum_{j=1}^{n} q_j \, q_j' / r_{ij}$$

Since j and i are just summation indices, it is clear that

$$\sum_{j=1}^{n} V_j \, q_j' = \sum_{j=1}^{n} V_j' \, q_j$$

This is the Green reciprocation theorem. This theorem can be extended to n conductors of potentials V_j carrying charges q_j by combining the points of equal potential into a single term.

Now consider a charge, q, in the vicinity of a conductor connected to a sink or source of electrons, such as ground or a battery. The charged particle produces a potential at the position of the conductor. A positive charge raises the effective potential of the conductor. Current flows from higher to lower potential, i.e., electrons flow from lower to higher potential. Thus, the effect of the charge on the conductor is to raise its potential and cause electrons to flow to it. These additional electrons may be classified as an induced charge. Thus, a positive particle induces a negative charge on a conductor and a negative particle induces a positive charge. If a charged particle is placed in the middle of two conductors, the net effect on the potential drop between the conductors is zero, since both potentials are changed in equal amounts.

However, as the particle gets closer to a particular conductor, the net effect is no longer zero, since the potential change is not identical, as is shown below.

As a special case, consider two grounded conductors with a charge q at some point, P, between them. An induced charge will appear on the conductors. We can find the induced charge Q on either of the conductors, if the potential, Vp' is known, to which the point P would be raised, q being absent, by raising the conductor to a potential V', using the reciprocity theorem. Recall,

$$\sum_{j=1}^{n} V_j' \, q_j = \sum_{j=1}^{n} V_j \, q_j'$$

Giving,

$$V_1 \, q_1' + V_2 \, q_2' = V_1' \, q_1 + V_2 \, q_2$$

For the sake of clarity, let $q = q_1$ and $Q = q_2$, then $V_1 = V_p'$, and $V_2 = 0$ (since the conductors are grounded, giving a zero potential when $Q = 0$). Similarly, let $0 = q_1'$ and $Q' = q_2'$ with $V_p' = V_1'$ and $V' = V_2'$, then we have

$$V_p' \, q + V'Q = V_p(0) + 0(Q') = 0$$

or,

$$Q = -V_p' \, q/V'$$

Realize Q can be induced on either conductor. The total charge induced on both conductors is equal to the negative of q when one conductor encloses the other,

$$-q = Q_a + Q_b.$$

In the absence of a charge, q_1', between the conductors, a and b, at conductor voltages of V_a' and V_b', let the potential at P be V_p'. Using the reciprocity theorem, for grounded conductors ($V_1 = V_2 = 0$), gives

$$Q_a V_a' + Q_b V_b' + q \, V_p' = 0$$

Substituting for Q_b in terms of Q_a and q gives

$$Q_a = (V_b' - V_p')q/(V_a' - V_b')$$

and

$$Q_b = (V_a' - V_p')q/(V_b' - V_a')$$

V_p' is just the potential distribution in the space charge free region between two electrodes. For parallel plate electrodes

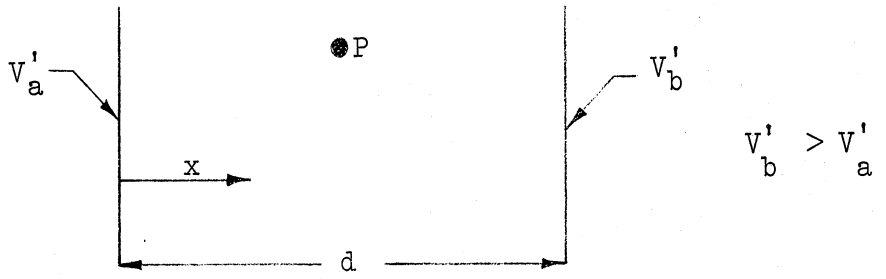

Figure 8.8. Charged Particle Between Two Electrodes

The potential between the conductors is given by the Poisson equation

$$\frac{d^2V'}{dx^2} = 0 \; ; \; V' = A\,x + B$$

when

$$x = 0 \; , \; V' = V_a' ; \quad x = d, \; V' = V_b'$$

therefore,

$$V'(x) = \frac{V_b' - V_a'}{d}\, x + V_a' = V_p'(x)$$

Substituting,

$$Q_a = \left(\frac{x - d}{d}\right) q$$

and

$$Q_b = -q - Q_a = -\frac{x}{d}\, q$$

For a cylindrical electrode arrangement, the field is in the form,

$$\mathcal{E}(\wedge) = (V_b' - V_a') \; / \; r \; \ell n\left(\frac{r_2}{r_1}\right)$$

where r_2 and r_1 are the inner radius of the chamber and the outer radius of the anode, respectively, gives, for $V_b' > V_a'$,

$$\int_{V_b'}^{V_p'} dV' = V' - V' = \frac{V_b' - V_a'}{\ell n\left(\frac{r_2}{r_1}\right)} \int_{r_1}^{r} \frac{dr}{r}$$

or

$$V_b' - V_p' = \frac{V_b' - V_a'}{\ell n\,(r_2/r_1)}\; \ell n\,(r/r_1)$$

$$Q_b = - \ell n \left(\frac{r_2}{r}\right) q / \ell n \ (r_2/r_1)$$

$$Q_a = - q - Q_b = - \ell n \left(\frac{r_1}{r}\right) q / \ell n \ (r_1/r_2)$$

In practice, both electrodes are not grounded. The argument used to justify the application of these results to finding pulse forms is plausible, i.e., the voltage change on the grounded or collecting electrode is small since the capacitance of the system (sum of chamber and input circuit capacitance), C, is large and for the other electrode (held at a minus potential in steady state) the effect of the induced charge is superimposed on the steady state charge and therefore may be treated separately.

As a function of time, the voltage to the input circuit due to the net charge induced by positive and negative particles on the COLLECTING electrode, Q(t), since current flows in the opposite direction of electrons, the voltage of the collecting electrode drops, is,

$$V(t) = - Q(t)/C$$

Let $- Q_+ (t)$ be the induced charge due to positive particles and $-Q_-(t)$ due to negative particles. The net induced charge is $Q(t) = -Q_+(t) - Q_-(t)$,

$$V(t) = [Q_+(t) + Q_-(t)]/C$$

When the negative particles reach the collecting electrode, $Q(t) = +Nq = -Ne$ where N is the number of pairs created per incident radiation particle. When the positive particles are collected on the other electrode, $Q_+ (t) = 0$, due to cancellation with the induced negative charge. Thus, from $t = t_-$ to t_+

$$V(t) = [Q_+(t) - Ne]/C$$

i.e.,

$$V(t > t_+) = - \frac{Ne}{C}$$

The voltage pulse to the input circuit is determined by the induced charge on the collecting electrode. For the parallel plate chamber shown above, where the collecting electrode is at V_b,

$$V(t) = \frac{1}{C} \left[\frac{x_+}{d} Ne - \frac{x_-}{d} Ne\right]$$

For the cylindrical chamber, with the collecting electrode at the center, using Q_b,

$$V(t) = \frac{1}{C}\left[\ell n\left(\frac{r_2}{r_+}\right) Ne/\ell n\left(\frac{r_2}{r_1}\right) - \ell n\left(\frac{r_2}{r_-}\right) Ne/\ell n\left(\frac{r_2}{r_1}\right)\right]$$

The position, x or r, as a function of time is found by solving the balance equation on positive and negative charge given in a previous section.

For an electron chamber, i.e., $t_- < RC \leq t_+$ and

$$x_+ = x_o - v_+ t \ , \ x_- = x_o + v_- t$$

or

$$r_+ = r_o + v_+ t \ , \ r_- = r_o - v_- t$$

where the subscript zero refers to the creation location and v is the speed of the particle as a function of time, we can neglect the effect of the velocity of the positive ion on the pulse from ($v_+ t \ll x_o$ or r_o) giving

$$V(t) = - Ne\ v_-\ t/Cd$$

and,

$$V(t) = \frac{-Ne\ \ell n\ (r_o/r_-)}{C\ \ell n\ (r_2/r_1)}$$

8.10 Experiment On the Use of Ionization Chambers

Procedure

Before attempting to use an instrument, please read the appropriate sections of the instruction manual of that instrument.

1. Check the calibration of all the survey meters in the laboratory with the radium source of known strength. If you find that some of them should be recalibrated, please call this to the attention of the instructor.

2. Using the same source, calibrate one of the Lauritsen and one of the Landsverk electroscopes. Determine whether their scale readings are linear. Determine also whether the instruments are directional.

3. Determine a safe working distance from the cobalt-60 source. Determine the effective source strength of this source in millicuries. Calculate

the effective strength of this source at the time of its purchase.

4. Charge a few of the Victoreen and a few of the self-reading pocket chambers. Expose them in a known radiation field for a known length of time so that they accumulate a radiation dosage of about 50 mr. Compare their readings with the calculated results.

5. Compute the expected relationship between the radiation dose rate and the meter reading for the G.E. air equivalent ionization chamber used with an appropriate electrometer. Decide on which of the two sources mentioned previously you want to work with. Make measurements with the chamber for at least two different source-to-chamber distances. Use a collecting voltage of 135 volts. Compare your data with the calculated results. At the smallest of the source-to-chamber distances take readings also for collecting voltages of 90 and 180 volts. Note and explain any variation in the results. At the largest of the distances connect one of the guard rings directly to the collecting electrode, and compare the resulting reading with that obtained when the guard rings were connected properly. Explain the difference using a schematic circuit diagram of the apparatus. Determine how much of this difference is due to ionization near the end of the chamber and how much of it to leakage through the insulation. Measure roughly the time constant of the apparatus.

Please include in your report your calculation of the relationship between source strength and dose rate for radium and cobalt 60. Explain what is meant by an air-equivalent ionization chamber.

8.11 Proportional Chambers

Proportional counters are similar in principle to the ionization chamber and the Geiger-Muller counter, in that all three operate on the principle of gaseous ionization. In general, the proportional counter operates at a higher voltage than an ionization chamber. By using a fine wire as the collecting electrode, it is shown below that electrons gain sufficient kinetic energy from the field to cause secondary ionization, et. in the immediate vicinity of the anode, see Figure 8.9. Over a limited voltage range, the proportional voltage region, gas multiplication is independent of the amount of primary ionization. With large gas multiplication, a preamplifier is not required. The multiplication depends primarily on the magnitude of the electric field. Since this dependence is very sensitive to small fluctuations in the collector voltage, the proportional counter is of little value as a mean level chamber, and is used almost exclusively as a pulse chamber. As a pulse

chamber there is a discrimination between incident particles which produce different amounts of primary ionization, because of the constant gas multiplication. For example, a proportional chamber can be used to differentiate between incident α, β and γ, see Figure 8.10.

If most of the gas multiplication takes place in the immediate vicinity of the anode wire, the total charge produced is almost independent of where the primary ionization originated in the chamber. The above may be verified as follows: To compute the field, assume that the charge density is zero between the electrodes, then

$$\underline{\nabla} \cdot \underline{\nabla} V = 0$$

Using the boundary conditions that $V = V_o$ at $r = r_1$ (cylindrical coordinates, $r = 0$ at the center of the anode) and the inner surface of the cathode is at r_2, recall that $\mathcal{E}_n = - \partial V/\partial r$. Assume angular symmetry

$$r \frac{d^2V}{dr^2} + \frac{dV}{dr} = r \frac{d\mathcal{E}}{dr} + \mathcal{E} = 0$$

$$\frac{d\mathcal{E}}{\mathcal{E}} = - \frac{dr}{r}$$

$$\mathcal{E} = K/r$$

$$\int_{V_o}^{o} dV = -K \int_{r_1}^{r_2} \frac{dr}{r} \; ; \; K = \frac{V_o}{\ell n \left(\frac{r_2}{r_1} \right)}$$

giving,

$$\mathcal{E} = V_o/[r \; \ell n(\tfrac{r_2}{r_1})]$$

Quantitatively, one asks at what space position in the chamber will an electron have gained enough energy to create an ion pair. In air, this takes about 35 ev. An electron has an interaction on the average every mean free path. Since the interaction is primarily with the orbital electrons of the neutral gas molecules, it is reasonable to assume that the energy transfer in the form of thermal excitation is large enough to prevent the creation of a secondary electron, unless enough energy to create a pair is gained during a single mean free path. The mean free path for electrons in air is about 2×10^{-4} cm. at 1 atm. Let $r_1 = 0.001$ inches, $r_2 = 1$ inch, $V_o = 500$ volts. The field required to

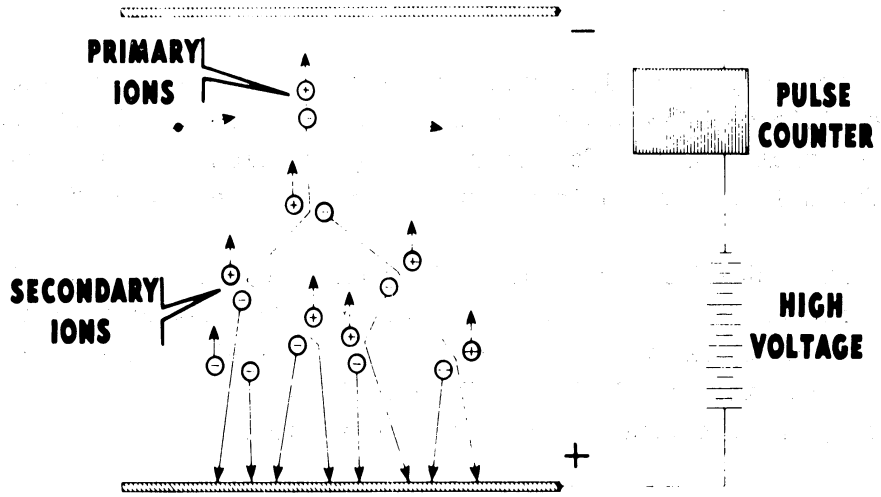

. ELECTRONS RECEIVE ENOUGH ENERGY TO IONIZE
. AVALANCHE OF SECONDARIES
· CURRENT MULTIPLIED BY 1.000 TO 1.000.000

Figure 8.9. Simplified Representation of Gas Multiplication.

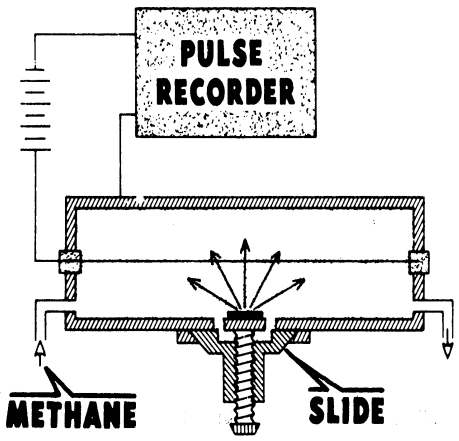

GAS-FLOW TYPE

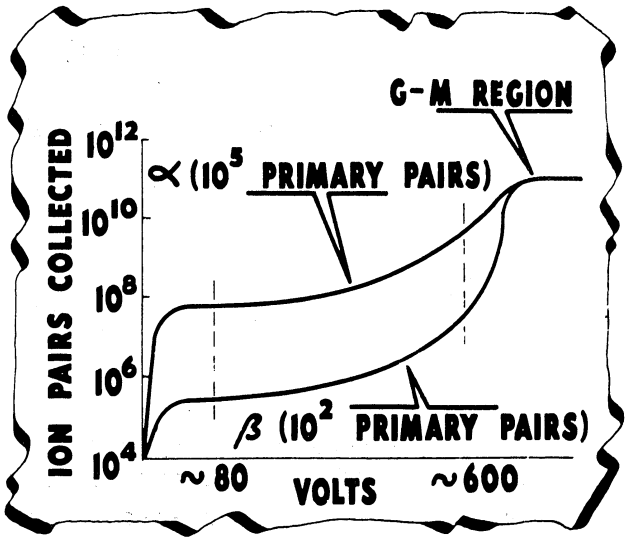

. PULSES PROPORTIONAL TO IONIZING POWER
. RECORDER CAN BE SET FOR PULSE SIZE RANGE
. CAN COUNT α'S IN LARGE FLUX OF β'S
. NO WINDOW TO STOP PARTICLES

Figure 8.10. A Gas Flow Proportional Counter.

create a pair is just $\left(\frac{35.2}{2 \times 10^{-4}} \right) = 17.6 \times 10^4$ volts/cm. This field occurs in the chamber at $r = 500/(17.6\ 10^4) \ln 10^3$ or, $r = 4.1 \times 10^{-4}$ cm but r_1 is 2.5×10^{-3} cm, so must either up the voltage or lower the gas pressure, thereby increasing the mean free path, to get multiplication. Suppose the voltage were raised to a very high 2×10^3 volts, find $r = 1.6 \times 10^{-3}$ cm, which still won't give multiplication. Hopefully, the above has illustrated why proportional (and Geiger Muller) counters are almost always operated at reduced pressures. If instead the chamber had been at 500 volts and 10 cm of Hg,

$$\mathcal{E}_\varphi = 35.2/[2 \times 10^{-4} \left(\frac{76}{10} \right)] = 2.3 \times 10^4 \text{ volts/cm},$$

and $r = 3.1 \times 10^{-3}$ cm.

It has been found by experiment that the gas multiplication is less sensitive to small voltage changes if a polyatomic gas is added in small amounts to the chamber gas. It is thought that the polyatomic gas reduces photoemission by absorbing the electromagnetic radiation.

For pulse work, the details of the pulse time behavior are important. Since most of the ion pairs are created next to the anode, there are a large number of localized positive ions surrounding the anode after each avalanche. The electrons are collected quickly because of their higher mobility and proximity to the anode. The positive ion sheath around the anode moves relatively slowly toward the cathode. By having the input time constant less than the positive ion collection time and greater than the electron collection time, fast pulses are produced whose heights are proportional to the primary ionization. Price plots the pulse form in Figure 5.4 as a function of the ratio of system time constant to the collection time of the positive ions. It should be noted that quite high resolving times are possible because the ion sheath is localized, i.e., another avalance can occur at a different position along the wire after a previous pulse has passed the discriminator level, and be counted, in spite of the fact that the ion sheath of the previous pulse is making a localized field distortion. For highest accuracy in measuring pulse amplitudes, pulse pile up must be avoided, limiting the count to a maximum on the order of 10^4 to 10^5 per sec., depending on chamber characteristics.

Proportional counters are used widely for α particles. Because of the short range of the α, it is convenient to be able to put the sample inside the detector, right in the chamber gas. Because it is often convenient to use a different or a purer gas than the usual laboratory air, most proportional counters are made as gas flow counters. In the gas flow counter, the chamber gas is purged of laboratory air after a sample

is introduced by means of a special regulated gas supply which feeds the chamber. After the chamber has been purged, the flow of gas is reduced to a bubble per second or less to insure that the chamber gas will not change as a result of high level count rate operation, and minimize the effects of a leak.

Because of the discriminator in the counting system, proportional counters have extremely small background noise levels when used to detect α or β. The counting rate as a function of counter voltage has a characteristic plateau. For a given multiplication, particles with the largest specific ionization are first to pass the discriminator, e.g., α before β. Since α's are almost monoenergetic, and β's have an energy distribution, it is to be expected that the β plateau have the greater slope. Typical count rate as voltage curves are shown in Figure 8.11 for α and β emitters.

Chambers in which the sample emits radiation which subtends an angle of 2π radians in the chamber gas are known as "2π" counters.

There are considerations such as backscatter and self absorption which require attention when the sample is placed in the chamber and one desires to measure or calculate the absolute rate of disintegration. In backscatter, radiation which is emitted originally in a direction which would exclude it from the active chamber volume suffers a number of scattering events such that its direction is changed and it does produce a measureable pulse. Self absorption simply refers to the count loss due to absorption of radiation by the sample itself. Price covers these details quite adequately.

8.12 A Note on Gas Multiplication (See Figure 8.9)

Consider N electrons with sufficient energy to produce an ion pair. Let the probability that this electron produce a pair be ϵ. As a first approximation, assume that ϵ is independent of the electron energy, i.e., the only requirement is that the electron has the capability of producing one pair, but as it gains energy in the field it may produce one pair after another. Let us follow the creation process for n generations. Start with N, these produce $N\epsilon$, giving a total of $N + N\epsilon$; these produce $(N + N\epsilon)\epsilon$ or a total of $N + 2N\epsilon + N\epsilon^2$, and so on for n generations giving a total of

$$N + nN\epsilon + nN\epsilon^2 + \ldots + nN\epsilon^{n-1} + N\epsilon^n$$

Let M_1 be the total number of electrons produced per incident radiation particle.

$$M_1 = N[1 + n (\sum_{i=1}^{n} \epsilon^i)]$$

Recall,

$$\frac{1}{1 - \epsilon} \simeq 1 + \epsilon + \epsilon^2 + \ldots + \epsilon^n$$

for $\epsilon \rightarrow 0$ and $n \rightarrow \infty$, $\therefore$,

$$M_1 = N [1 + n (-1 + 1/1-\epsilon)].$$

The gas multiplication usually referred to, in the absence of photoemission, is M_1/N, and is most often determined empirically. There are some additional counts introduced because of the interaction of the electromagnetic radiation associated with the production of the secondary, tertiary, etc. electrons with the neutral gas atoms and principally the walls of the electrodes. Electrons are ejected into the chamber gas due to photoelectric effect interaction of this radiation. These electrons, caused by photoemission, initiate new gas multiplication. Since it is desirable to maintain proportionality between the energy deposited in the gas by incident radiation and the chamber output pulse size, an organic gas is usually added to suppress this effect.

8.13 Experiment on the Use of the Proportional Counter

Use the windowless flow counter in this experiment. Please avoid initiating a continuous discharge, or introducing air into the counting volume. Before starting the experiment, read the appropriate instruction manuals, and see whether the pieces of equipment are connected correctly.

1) Determine the count rate versus voltage characteristics of the counter using a thorium foil. Explain the meaning of your results. Use the oscilloscope to observe the behavior of the pulses as the voltage is varied. Determine the voltage at which some of the pulses cease to be proportional to the initial ionization.

2) Obtain a count rate versus voltage curve for background. Note the magnitudes of the background count rates in the alpha and beta plateau regions. Explain why there is a background count in spite of the fact that no alphas or betas can pass through the shield surrounding the counting volume.

3) Cover the thorium foil with some material which is just thick enough to absorb all the alphas. Obtain the count rate versus voltage curve for the covered source. Compare this with the one obtained without the cover. Comment on the similarities and differences.

4) Obtain a count rate versus voltage curve using a source emitting betas but no alphas, such as cobalt 60. Compare this with the curve obtained using the covered thorium source. Comment on the similarities and differences. Explain how a plateau in the proportional region differs from a Geiger plateau; discuss pulse height variation and the cause of the positive slope of the plateau.

8.14 Geiger-Muller Chamber

The Geiger-Muller, GM, chamber is the simplest to understand and the easiest to use of the gaseous ionization chambers. The GM is just an extension of the proportional counter concept to higher gas multiplication, using a higher collection voltage. The gas multiplication at these higher voltages is so great that the primary avalanche produces a cascade of daughter avalanches by photoemission which are continued until the positive ion sheath which surrounds the entire anode reduces the field below that required for gas multiplication to continue. At an even higher voltage, the chamber is reduced to uselessness because of the essentially continuous discharge caused by photoemission.

Since the size of an output pulse on the GM plateau is on the order of a volt, very little external equipment is necessary to count pulses. Thus, the GM tube is a low cost detector, as well as rugged, see Figure 8.12. The GM is versatile in the sense that an incident, α, β or γ, etc. all produce the same size output pulse, once gas multiplication has begun. Since only one ion pair is required to initiate a discharge in the absence of recombination, GM is useless for energy resolution, or pulse analysis

The GM tube can be used for count rates almost as high as in a proportional counter. The same equations may be used to describe the pulse time characteristics and ion transit time with the understanding that the massive collection of positive ions near the anode in the GM will tend to modify these reuslts due to the greater field distortion. As in the proportional chamber, the time constant of the input circuit has a value between the collection times of electrons and positive ions for maximum resolution.

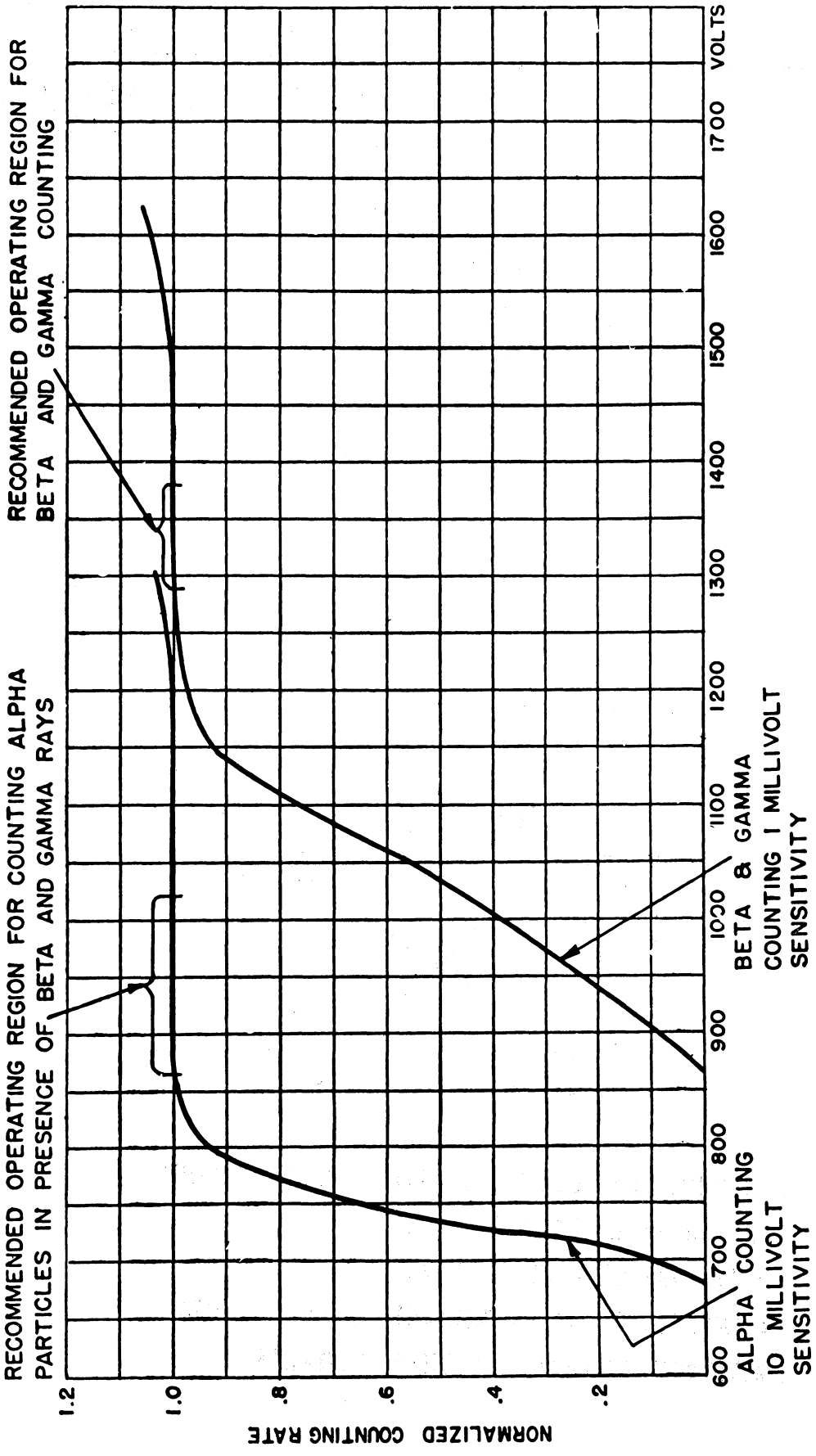

Figure 8.11. Proportional Counter Characteristic Curves for an Alpha, and a Beta or Gamma Emitter. (Courtesy of Tracerlab Inc.)

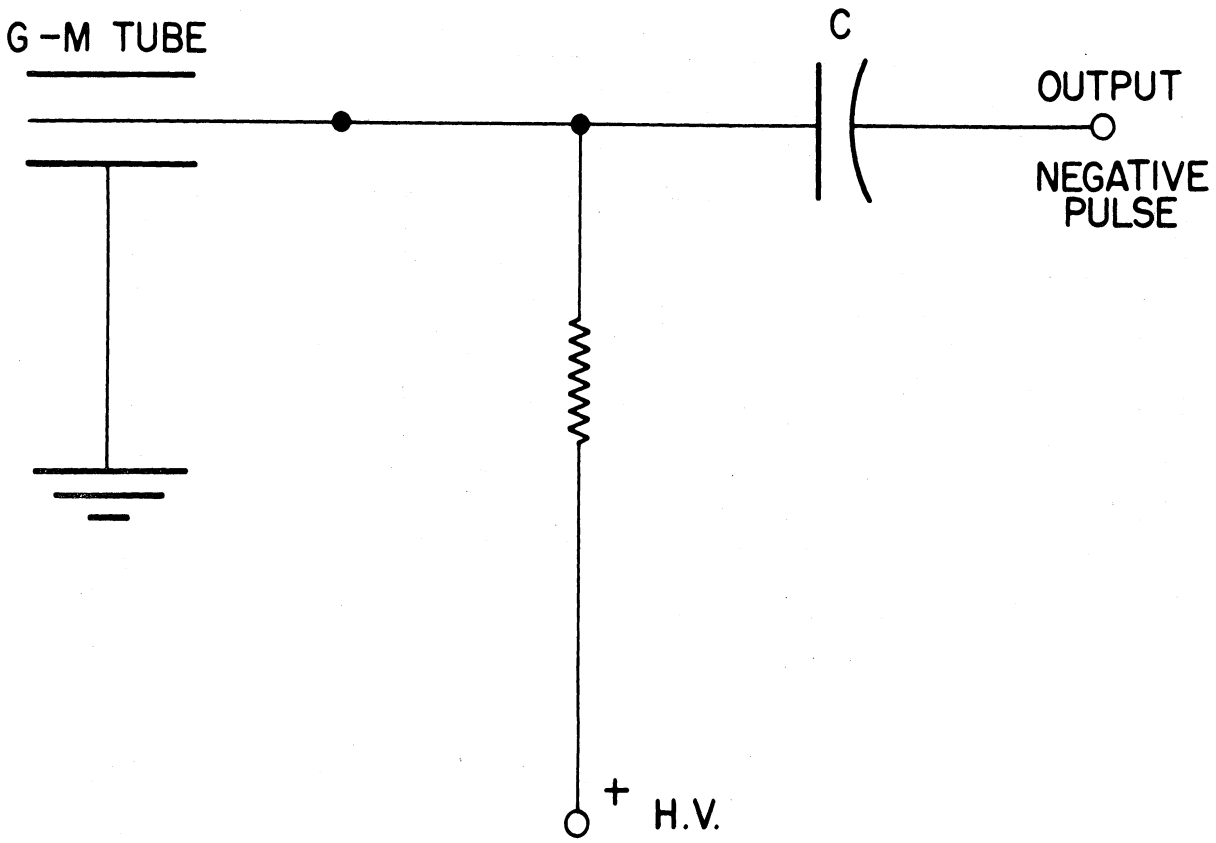

Figure 8.12. Basic Circuit for Geiger Muller Chamber.

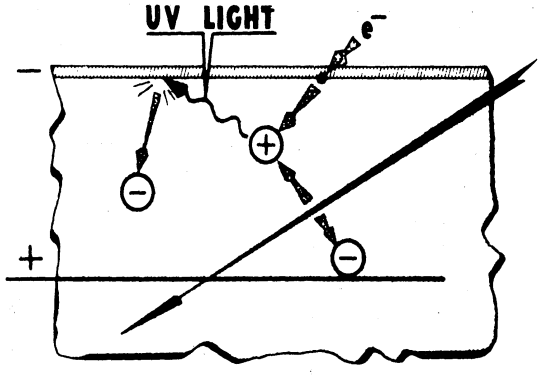

. POSITIVE ION DRAWS ELECTRON FROM CATHODE
. ION BECOMES EXCITED ATOM
. ATOM RADIATES IN ULTRAVIOLET
. LIGHT EJECTS PHOTOELECTRON FROM CATHODE
. ELECTRON INITIATES FURTHER CASCADES

Figure 8.13. Need for Quenching in a GM Tube.

GM counters require quenching, see Figure 8.13. That the energy difference between a positive ion reaching the cathode and the work function of the cathode is sufficient to cause the emission of an electron or a photoelectron into the chamber gas to produce another avalanche is well established. The idea of quenching this behavior by mixing gas molecules with higher work functions in the chamber gas was the next logical step, see Figure 8.14. In the organically quenched tubes, after the positive charge is transferred to the organic molecule, the excess energy is used to dissociate the molecule when it reaches the cathode. The molecule can be used only once to transfer the charge since the dissociation is not a reversible process. This difficulty is avoided by using halogen quenched tubes in which recombination does take place.

Because the ion sheath surrounds the entire anode, thereby reducing the field, for a certain fraction of the time after an avalanche has stopped, another avalanche can not be initiate because the field has not had a chance to build up to the necessary strength. The time during which the chamber is insensitive to incident radiation, as passed by the counter discriminator set for the GM plateau voltage, is known as the GM dead time. Any primary ionization during the dead time is not counted. The dead time sets the inherent lower limit at which the GM can resolve individual pulses. The dead time depends on the magnitude and space and time distribution of the ion sheath. The dead time is slightly different for every pulse counted in single tube because of statistical fluctuations in these quantities. The characteristics of the voltage amplifier used will influence the effective pulse resolution of the system. The resolving time usually refers to the time which the system, the GM and associated pulse amplification and detection equipment, requires to distinguish between two successive pulses. The resolving time is always greater than the dead time, by definition. The form of the pulse from the GM was considered in a previous section.

When GM tubes are used for absolute particle counting, e.g., to determine the activity of a radioactive sample, it is necessary to correct the measured count for all losses. For a given counting geometry it is necessary to make corrections for the number of particles which don't produce a measureable pulse having reached the sensitive chamber volume, backscatter into this volume, self absorption in the media between the surface of the source and this volume including the walls of the GM tube, dead time or resolving time losses, and the number of multiple counts not produced by the types of particles being measured which originate from the source such as background, and spurious photoemission counts. The

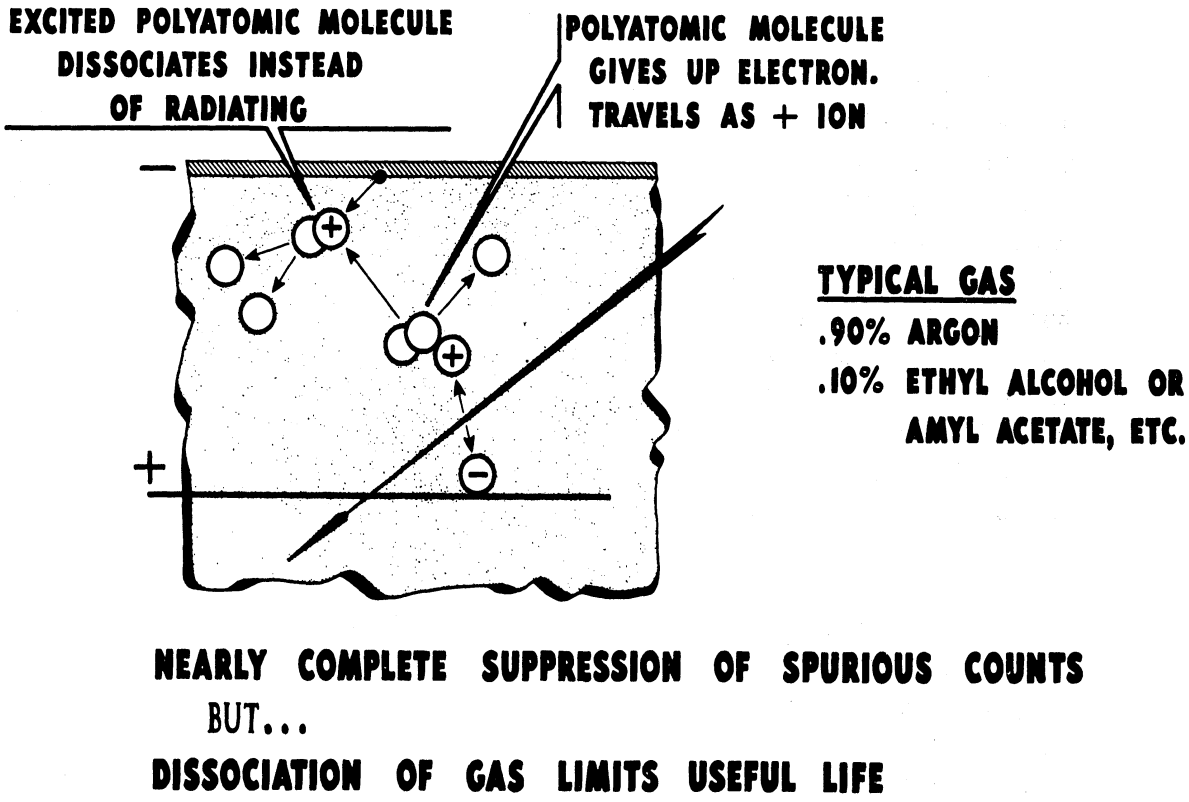

Figure 8.14. Action of Quenching Gas in GM Tube.

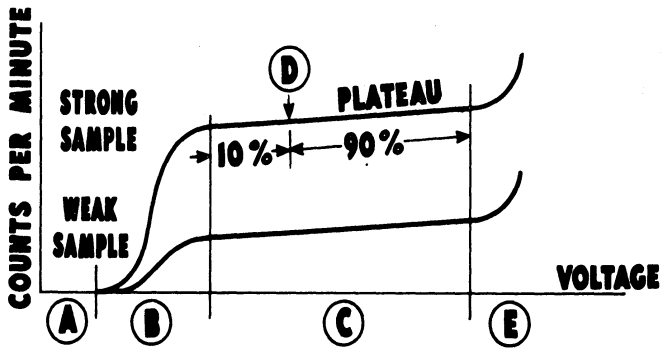

(A) NO PULSES LARGE ENOUGH FOR RECORDER

(B) AVALANCHES GROW LARGER WITH VOLTAGE
NUMBER OF RECORDER PULSES INCREASES

(C) ALL PARTICLES TRIGGER MAXIMUM AVALANCHE
ALL PULSES RECORDED

(D) OPTIMUM SETTING FOR OPERATING VOLTAGE
HIGHER VOLTAGE GIVES SHORTER TUBE LIFE

(E) SPURIOUS DISCHARGES LEAD TO BREAKDOWN

Figure 8.15. GM Characteristic Plateau Curves.

straightforward account by Price is self-explanatory as are the bulk of examples of tube types used for different applications.

A typical characteristic curve of a GM chamber is given in Figure 8.15.

8.15 Experiment On the Use of the G.M. Chamber

Procedure

Please exercise due caution in working with Geiger-Muller tubes and the associated electronic equipment. The end windows of the tubes are very fragile, do not let anything come into contact with them. The high voltages used present a shock hazard. Turn off the high voltage supply while connecting the equipment. Excessive voltage can damage the tubes. Before turning on the high voltage supply, turn the voltage adjustment down as far as it will go. Increase the voltage slowly and only while the scaler is counting.

1. Determine the count rate versus voltage characteristics of an end window tube using any convenient source. Determine the useful length of the plateau, and pick an operating voltage. Explain why the plateau has a positive slope, and justify the selection of your operating voltage.
2. Familiarize yourself with the cathode ray oscilloscope. Observe the pulses coming from the GM tube. Plot pulse height versus applied high voltage in the plateau region. At the operating voltage, estimate the dead time of the tube, the resolving (dead) time of the counting system, and the recovery time of the tube. Compute the counting rates at which the dead time (or coincidence) losses are about 1%, 5%, and 10%. Observe and comment on the variation in resolving time with changes in applied high voltage in the plateau region.
3. Determine the dead time of your counting apparatus by the two-source method. Use the Tl-204 split sources and the inactive dummies. Position the sources in such a way that the counting losses are between 5% and 10% when the sources are counted simultaneously. The following procedure is recommended.
   a) Count the sources simultaneously for 15 minutes.
   b) Replace source 1 by dummy 1 without touching source 2. Count for 10 minutes.
   c) Replace source 2 by dummy 2 without touching dummy 1. Count for 5 minutes.
   d) Replace dummy 1 by source 1. Count for 10 minutes.

Calculate the dead time. Compare this with the results of the measurements with the oscilloscope.

4. Observe the effect of operating voltage on the resolving time of the system and explain.

8.16 Statistics

We attempt to determine certain aspects of nuclear decay phenomena by measuring emitted radiation. The inherent laws governing the nuclear processes are statistical in nature. The distribution functions which describe the statistical fluctuations are known. The most useful distributions in our work are the Poisson, Normal or Gaussian and Interval functions. For a thorough study of statistics read Cramer's Mathematical Methods of Statistics (Princeton University Press).

8.17 Poisson Distribution

The Poisson distribution is a special case of the Binomial distribution which is applicable when the mean life of the emitting sample is long compared to the experimental observation time, and there are sufficient identical, independently acting atoms to allow significant data. In more general terms, a Poisson distribution should be expected from a random process in which the probability of an event happening is small and independent of time. The probability that an observation will result in x counts over a time interval for which the true mean count is m is given by

$$P_x = \frac{m^x e^{-m}}{x!}$$

(read especially Chapters 26, 27, and 28 of Evans and 3 of Price). Note that P_x is not a continuous function, since x is restricted to integer values. A representative histogram of a Poisson distribution can be given, see Figure 8.16.

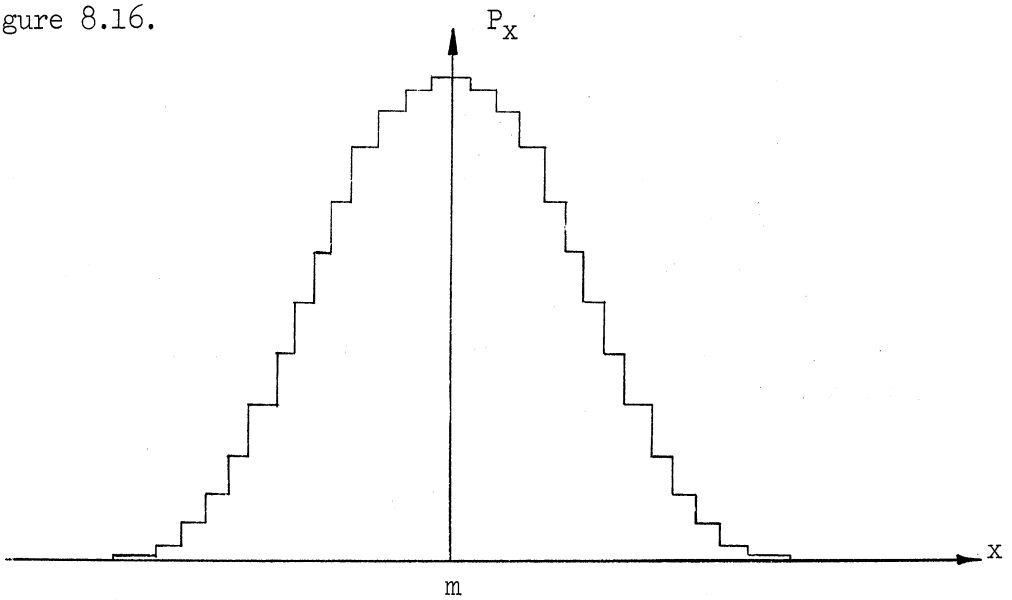

Figure 8.16. Poisson Distribution.

The distribution is not symmetrical, but is skewed toward $x < m$. The assymmetry increases as $x \to 0$. The Poisson distribution describes most nuclear radiation decay events for the listed assumptions, and may be used when only a relatively small amount of data is available.

For any distribution, a measure of the spread in the data about the mean is given by the standard deviation, σ.

$$\sigma^2 = \sum_{\text{all } x} (x-m)^2 P_x = \text{the variance}$$

For Poisson,

$$\sigma^2 = \sum_{x=0}^{\infty} \frac{(x-m)^2 m^x e^{-m}}{x!}$$

or

$$\sigma = \sqrt{m}$$

As will be shown under the Normal distribution, about 68% of the observations should fall in the region $m \pm \sigma$. In a practical calculation, with N finite observations, the mean, $\bar{x}$, is given by,

$$\bar{x} = \frac{1}{N} \sum_{i=1}^{N} x_i$$

and

$$\sigma^2_{\text{sample}} = \frac{1}{N-1} \sum_{i=1}^{N} (x_i - \bar{x})^2$$

From the theory of errors, it is known in general that the distribution of mean values tends to be more nearly Normal than the distribution from which the means were calculated. Thus, it is shown that the mean found by repeating the entire experiment would fall within $x \pm \sigma_{\bar{x}}$ about 68% of the time, where $\sigma_{\bar{x}} = \sigma/\sqrt{N}$.

Normal Distribution

The Normal distribution is an approximation to the Binomial distribution for a large number of observations and a constant average value. The probability that x will lie between x and $x + dx$ is given by,

$$dP_x = \frac{1}{\sigma\sqrt{2\pi}} e^{-(x-m)^2/2\sigma} dx$$

Note that σ is independent of m, whereas in the Poisson, $\sigma = \sqrt{m}$. The normal distribution lends itself nicely to analysis and gives an exact interpretation to σ. As the Poisson, the Normal is normalized to unity,

$$\int_{-\infty}^{\infty} dP_x = 1$$

This distribution is not restricted to integer values of x, and for large N, is essentially continuous, and symmetrical. From the analytic distribution it may be shown that tangents to the curve at the points of maximum slope intersect the x axis at $m \pm 2\sigma$, also, the half width at half maximum is given by $\sqrt{2\ell n2}\ \sigma$. Thus, σ may be found from the data in graphical form or from the variance. By direct integration of dP_x it can be shown that 68% of the observations fall within $m \pm \sigma$.

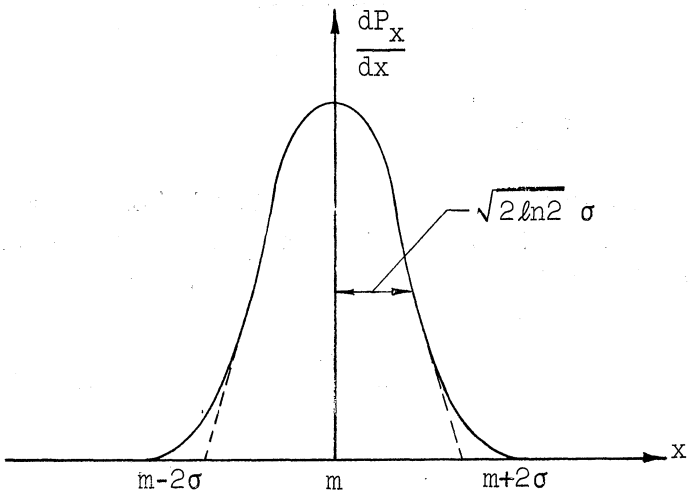

Figure 8.17. The Normal Distribution

For a process governed by Poisson, the analytic Normal and Poisson distributions become identical as $N \rightarrow \infty$ for mean values greater than approximately ten.

Given a population (complete set of data) whose mean, m, and variance are known, the sample (smaller amount of data) mean, $\bar{x}$, has $\left(\frac{\sigma^2}{N}\right)$ as variance. For the sample, the variance of the variance is given by $\sigma^2/2N$. These results are true for all values of N for a Normal distribution, but depend on knowing the true population m and σ. This distinction must be noted and any analysis of 1 or 2 data points must take account of this fact.

One can check on the probability that the given sample mean is representative of the population mean by using the student t distribution where,

$$t = (\bar{x} - m)\sqrt{N} \ / \ \sigma_{sample}$$

and t follows the distribution,

$$dP = dt \,/\sqrt{F}\, B\left(\frac{1}{2}, \frac{F}{2}\right)\left(1 + \frac{t^2}{F}\right)^{\frac{1}{2}(F+1)}$$

B representing a Gamma variate and F the number of degrees of freedom (see below). By integration of this distribution, significance limits can be obtained as was done, for example, with the Normal in determining the value for σ, etc. The t distribution can also be used to decide whether 2 sample means differ significantly or whether they can be assumed to be from the same population.

8.18. Interval Distribution

The interval distribution describes the probability that the time interval from t to t + dt between random events which have a constant mean rate, a, and a Poisson distribution is given by

$$DP_t = a\, e^{-at}\, dt$$

The number of intervals falling between t_1 and t_2, n, is

$$n = Na \int_{t_1}^{t_2} e^{-at}\, dt = N[e^{-at_1} - e^{-at_2}]$$

where N is the total number of intervals between t = 0 and ∞. The average interval is just $\bar{t} = 1/a$. Letting $t_2 \to \infty$, the probability that an interval is longer than $\bar{t}$ is

$$\frac{n}{N} = e^{-1} = 0.37.$$

Thus, 63% of the intervals are less than $\bar{t}$, an important consideration in estimating counting losses due to counter dead time.

8.19 Checking Equipment Using Count Rate Data

Since the nuclear phenomena being studied follow the statistical distribution law, we expect the results of a measurement to follow the same law, neglecting counter losses. If there is no spread in the data, something is wrong. If there is considerably more spread than the law predicts, something is wrong. The initial data taken in every experiment should be analyzed to see if it falls within the range of acceptability from a statistical standpoint. The Chi-squared test is one of

the most decisive in determining whether or not the data follows a particular distribution. Consider the quantity,

$$Q^2 = \frac{1}{\bar{N}x} \sum_{i=1}^{n} (x_1 - \bar{x})^2 = \frac{\sigma^2}{\bar{x}} \left(\frac{N - 1}{N} \right)$$

For a true Poisson, $N \to \infty$, $\sigma^2 = m$, $\therefore$, $Q^2 = 1$. For data which is not Poisson, or if an insufficient amount of data is used, the calculated $Q^2 \neq 1$. It is difficult to tell the amount by which Q^2 can vary from unity and still represent acceptable data. To establish an acceptable spread from the mean in a counting experiment, chi, χ, was defined as follows,

$$\chi^2 = \sum_{i} [(\text{observed} - \text{expected})^2/\text{expected}];$$

where the summation is over the number of discrete counts recorded in a fixed time interval. Applying this to a Poisson distribution in which a total of M time intervals were considered, the expected number of observations of a count, x, is given by,

$$L_x = M P_x$$

and the observed number of time intervals in which x counts were recorded is ℓ_x, giving,

$$\chi^2 = \sum_{i} [(\ell_x - L_x)^2 L_x]_i$$

Theoretical studies have shown that the approximation to the true chi value (∞ amount of data) using a finite amount of data is acceptable if there are at least 5 discrete counts each having been recorded at least 5 times. If there are fewer than 5 discrete counts then there must be more than 5 intervals in which such counts are recorded.

Define the number of degrees of freedom, F, which is the number of independent ways in which the series of discrete counts may differ from the expected series. The maximum degrees of freedom are i. For the Poisson described above, two degrees of freedom are used up, first, the total number of events (to calculate the mean used in P_x), giving $F = i - 2$.

The random variable, W, possesses a X^2 distribution if the probability that W takes a value in $d\omega$ about ω is given by

$$P_F \, d\omega = \left[\left(\omega^{\frac{F}{2} - 1} \right) \Big/ \left(2^{\frac{F}{2}} \, \Gamma \left(\frac{F}{2} \right) \right) \right] e^{-\omega/2} \, d\omega$$

$\omega > 0$, where F is the number of degrees of freedom. $\int_0^\infty P_F \, d\omega = 1$. For this distribution, the mean = F, and the variance = 2F. As F increases, the distribution approaches the Normal, if the Normal standard deviation is replaced by $\sqrt{2F}$ and the mean by F. For $F > 30$, the X^2 distribution can be replaced by the Normal as a good approximation.

In selecting N items from a population, the value of each of the N variables may range over all values in the population, naturally. The χ^2 distribution can be used to test how well a sample distribution agrees with a population distribution. Let $x_1, x_2, \ldots x_N$ (N = total number of data points taken, whether or not the same) be a sample of values of χ and let the range of χ be divided into r class intervals, $Y_1 \leq x < Y_2$, $Y_2 \leq x < Y_3$, $\ldots$ $Y_r \leq x \leq Y_{r+1}$. Let the number of values of x_i from the sample falling into these intervals be $f_1, f_2, \ldots f_r$, respectively. Let the relative frequencies in these same intervals expected in the population distribution be $g_1, g_2, \ldots g_r$ so that the number of values expected in each interval from a sample of N points are $f_1' = Ng_1$, $f_2' = Ng_2$, $\ldots$ $f_r' = Ng_r$, respectively. Now,

$$\chi^2 = \sum_{i=1}^{r} [f_i - f_i']^2 / f_i'$$

It has been shown that for a large enough N, $\chi^2 \longrightarrow \omega$. This limiting distribution is independent of the population distribution. Usually, require each $f_i \geq 10$ for this approximation of "large enough N" to be acceptable. Thus, the chi-squared test compares the sample χ^2 to a theoretical distribution of χ^2 which is independent of the type of population distribution from which the sample is taken. The theoretical χ^2 distribution can be integrated to obtain significance limits on χ^2. The results of such integrations are shown on page 776 of Evans in terms of the number of degrees of freedom and the calculated χ^2 with the probability, P, that larger deviations from the theoretical population distribution would be observed in the next series of data taken from the same population. The significance limits set on P of 0.98 and 0.05 are arbitrarily set to establish whether or not the data is statistically acceptable.

8.20 Degrees of Freedom

The number of degrees of freedom, F, measures the extent to which f_i are known in advance to agree with f_i'. In all cases the sample size and the number of population values used are equal. Thus if r - 1 of the f_i' are given, the remaining f_i' can be calculated, therefore, F = r - 1. This is the value of F to use when the population distribution is prescribed and the χ^2 is used to test whether f_i is consistent. When the population distribution is determined by fitting some distribution to the sample, i.e., when the sample and population distributions are made consistent by means of their means, variance, moments, etc., for each such parameter, a degree of freedom is lost. For b of such parameters, F = r - 1 - b.

8.21 Test of Fit of Sample to Poisson

For a sample of positive integers, $x_1, x_2, \ldots x_N$ from a population known to be Poisson with an unknown parameter, λ, proceed as follows: Divide the integers i into r intervals, where the first interval contains the integers $0 \leq i < C_1$, the second, $C_1 \leq i < C_2$, ... $C_{k-1} \leq i < C_k$, the r^{th}, $C_{r-1} \leq i < \infty$.[1] Let the sample frequency of occurrence of values x_j in the k^{th} interval be v_k. For Poisson, the probability that x = 1 is

$$P_i = \frac{\lambda^i}{i} e^{-\lambda}$$

The population frequency of occurrence of values in the k^{th} interval is $\omega_k = \sum NP_i$, where the sum runs from $i = C_{k-1}$ to $C_k - 1$. Thus,

$$\chi^2 = \sum_{k=1}^{r} (v_k - \omega_k)^2/\omega_k$$

The minimum χ^2 is assumed if $\lambda = \bar{x} = \frac{1}{N} \sum_{j=1}^{N} x_j$. The approximation involved in setting $\chi^2 = \sum_{k=1}^{r} (x_k - \bar{x})^2/\bar{x}$ as done in Price should be understood.

8.22 Several Simultaneous Statistical Fluctuations

Consider simultaneous, independent random fluctuations, such as a nuclear disintegration and background noise due to stray radiation. Let x, y, z, .. be the average number of particles from the independent sources per unit time producing a, b, c, .. specific effects per particle which are detected. The average detection rate is

$$u = ax + by + cz + ..$$

For the Poisson distribution, it can be shown that the variance of a single observation of u is given by

$$\sigma^2 = a^2x + b^2y + c^2z + \ldots$$

For example, if one records 100 α particles, each producing 10^5 ion pairs and 10^4 β producing 10^3 ion pairs in an ionization chamber, $u = 2 \times 10^7$ and $\sigma = \sqrt{10^{12} + 10^{10}} = 1.005 \times 10^6$ showing that the α contributes 99.5% of the fluctuation. If a second chamber records only 100 α's per unit time and its output subtracts from the first, $c = -10^5$ and $z = 100$, giving $u = 10^7$ and $\sigma = 1.4 \times 10^6$, or the fluctuation is greater than for the uncompensated chamber. For a Geiger tube, where every incident particle results in one voltage pulse, $a = b = 1.0$.

In general, when any number of random statistical quantities which are combined by addition or subtraction, the result can be given as,

$$(\bar{a} + \sigma_{\bar{a}}) \pm (\bar{b} \pm \sigma_{\bar{b}}) + \ldots = (a \pm b + \ldots) \pm (\sigma_{\bar{a}}^2 + \sigma_{\bar{b}}^2 + ..)^{1/2}$$

$$= \bar{\psi} \pm \sigma_{\bar{\psi}}$$

For example, to determine the difference between (source + background), $(\bar{v} \pm \sigma_{\bar{v}})$ and background, $(\bar{u} \pm \sigma_{\bar{u}})$ count, the best estimate is given by,

$$(\bar{s} \pm \sigma)_{\text{source}} = (\bar{v} - \bar{u}) \pm (\sigma_{\bar{v}}^2 + \sigma_{\bar{u}}^2)^{1/2}$$

If the difference between two means is twice the larger σ of the two, there can be little doubt that the means represent different quantities. This is especially important when measuring a signal which is not much larger than the background. A typical example would be an ionization chamber with a background of 5 α's and 50 β's per unit time, giving $\sigma = \sqrt{a^2x + b^2y} = 2.2 \times 10^5$ ion pairs. Using the above definition for significant data, the smallest numbers of β's which can be detected is $2\sigma/c = z$, $z = 2(2.2 \times 10^5)/10^3 = 450$ β/unit time. Realize that the mean signal to noise ratio is a useless quantity ... the fluctuations in the signal and the noise must be given. It is one thing to report the results as $\varphi = 631.6938$ and quite another to report $\varphi = 632 \pm 54$. Never give a result without some measure of the spread in the data. In particular, I recommend that you read Chapters 26, 27 and 28 in Evans for a more detailed presentation of most of the work covered in this paper.

To multiply or divide independent results, we have,

$$(\bar{a} \pm \sigma_{\bar{a}}) \times (\bar{b} \pm \sigma_{\bar{b}}) \times (\ldots) = \bar{a} \times \bar{b} \ldots \pm \bar{a} \times \bar{b} \times \ldots \sqrt{\left(\frac{\sigma_{\bar{a}}}{\bar{a}}\right)^2 + \left(\frac{\sigma_{\bar{b}}}{\bar{b}}\right)^2}$$

and,

$$\frac{(\bar{a} \pm \sigma_{\bar{a}})}{(\bar{b} \pm \sigma_{\bar{b}})} \quad \frac{\bar{a}}{\bar{b}} \pm \frac{\bar{a}}{\bar{b}} \sqrt{\left(\frac{\sigma_{\bar{a}}}{\bar{a}}\right)^2 + \left(\frac{\sigma_{\bar{b}}}{\bar{b}}\right)^2}$$

These results may be applied again to the usual counting experiment to show the importance of proper background and source counting times in taking good data. Let the average background rate be b for a time t_b and b+s be the rate with a source and background for a time t_s. The background can be expressed as $(bt_b \pm \sqrt{bt_b})/t_b$ and the source and background as $([s+b]t_s \pm \sqrt{(s+b)t_s})/t_s$, giving the net count rate due to the source alone as $s \pm \sqrt{\frac{s}{t_s} + \frac{b}{t_s} + \frac{b}{t_b}}$ and depending on the relative magnitude of s and b, one can choose a reasonable t_s and t_b. If $b \ll s$, then want $t_s > t_b$. If $b \gg s$, then for $s \pm \sqrt{\frac{s}{t_s} + b\left(\frac{t_s + t_b}{t_s\, t_b}\right)}$ require $(t_s + t_b) \ll t_s t_b$, etc. For a fixed counting time, $t_s + t_b$ = constant, Price suggests a minimum in the standard deviation is obtained by setting $d\sigma_s/dt = 0$, i.e.,

$$-2\sigma_s\, d\sigma_s = [(s+b)/t_s^2]\, dt_s + (b/t_b^2)\, dt_b = 0, \text{ but } dt_s/dt_b = -1$$

giving

$$(s+b)/b = (t_s/t_b)^2$$

for minimum standard deviation.

8.23 Counting Loss Due to Chamber Dead Time

In the interval distribution, it was shown that the fraction of time intervals associated with events which occur between time t_1 and t_2 is $n = N(e^{-at_1} - e^{-at_2})$, where a is the count rate and N the total number of intervals for all times. Consider a chamber which requires a minimum time, ϵ, between events, whether or not these events are recorded, before it can record the next event. The fraction of the number of intervals which are separated by times less than or equal to ϵ is just $(1-e^{-a\epsilon})$. The observed number of counts is the true count (no. of intervals) minus losses due to the chamber resolving time,

$$n = N - N(1-e^{-N\epsilon/T}) = Ne^{-N\epsilon/T}$$

where the true count rate is N/T. The observed count rate is then,

$$r_n = R_N \, e^{-R_N \epsilon} \ .$$

This type of chamber is referred to as 'paralyzable' since the count goes to zero as the number of events goes to infinity.

The other extreme chamber type can record only events which take place after a time ϵ, after an event has occurred in the chamber. Events which occur between the count time and count time plus ϵ do not affect the chamber in any way, and are the only events which are not recorded. The fraction of the time during which the chamber is insensitive during a total counting time T is $n\epsilon/T$. Thus, the fraction of the true count which is being observed must be $n/N = (T-n\epsilon)/T$, giving $N = Tn/(T-n\epsilon)$. The true count rate and the observed rate are,

$$R_N = r_n/(1 - r_n\epsilon) \qquad , \qquad r_n = R_N/(1 + R_N\epsilon) \ .$$

Thus, as $N \rightarrow \infty$, $R_N \rightarrow \infty$ and $r_n \longrightarrow 1/\epsilon$. The fact that this counter retains a finite count has resulted in the descriptive label, 'non-paralyzable'. We shall be using counters or rather chambers of both these types. The counter resolving time usually may be found from an oscilloscope trace directly, or by comparing the statistics from a counting experiment using the standard two source method at low count rates.

8.24 Experiment on the Statistics of Counting

Counter Plateau

Use the well counter and end window GM tube and any convenient source. Determine the count rate versus applied voltage curve in voltage steps of 25 volts. Determine the useful length of the plateau and its slope.

Statistics

Dead time

By observation of the pulseform from the GM on the oscilloscope screen read directly the values of the dead and recovery times. Calculate the dead time from the split source data of a previous experiment. Compare with the CRO results. Calculate the statistical deviations for the measured count rates and modify the counting times used to determine the dead time for a better result.

Prove that the time for counting with two sources should be $\sqrt{2}$ longer than for either one source count if both sources have equal strength and background can be ignored.

Calculate the standard deviation of the calculated dead time (hint, see pg 49 of Experimental Nucleonics by Bleuler and Goldsmith).

Fluctuations at low counting rates

Count background 30 times for an interval of 30 seconds. Let n be the counts per interval, and N be the number of trials. Determine the average number of counts per interval and the standard deviation. Derive a formula for the standard deviation of this series of measurements in terms of the counting rate and the time interval used, and the mean. Compute the variance of the data using the standard expression involving the mean, the individual counts and the number of trials. Discuss the significance of this second moment quantity as relates to our measurements. Compare the theoretical and experimental standard deviations as found by the above. Discuss the reasons for the observed difference.

Determine the number of counts n_i for which the absolute value of deviation from the mean exceeds 0.67, and 1, 1.6, and 2 times the standard deviation. Compare with the theoretical probabilities. Is such a comparison meaningful? Are the results you found experimentally reasonable?

Fluctuations at High Counting Rates

Repeat the procedure and calculations for a source giving about 5,000 cpm. Count for 10 intervals of 2 minutes each, or a more optimum time if you can determine it. Introduce dead time corrections only in the final results, not in the individual counts. Compare the percentage error of the higher and low count rates with theory and discuss.

Poisson's distribution

Count background for 100 intervals of 5 seconds each.

Determine the number of intervals during which n=0, 1, 2, ... counts were observed. Calculate the average number of counts. Compute the probabilities from the Poisson using the experimentally determined mean. Plot the experimental and theoretical probability distributions as a function of n. Discuss and explain any differences.

Do a chi-squared analysis of some of your interesting data (high, low or both types of count rate). Discuss results.

Considerations

1. Show that for radioactive decay the standard deviation can be expressed as the square root of the mean. Make very clear the assumptions and limitations placed on the physical model to arrive at such a result.

2. It is desired to make a measurement of the counting rate due to a given source in a shielded GM tube enclosure. A 1 minute count with and without the source resulted in 790 and 33 counts respectively. What would be the optimum counting schedule with and without the sample, and what would be the accuracy of the results if the total available time is one hour?

3. What is the difference between a sample and population mean? When only a limited amount of data is available, what restrictions does this place on your statistical analysis of the results?

4. Is one justified in using precisely defined quantities for a Normal distribution in the analysis of Poisson data? Discuss.

5. Does the chi-squared test have any value or worth over the more standard means of analyzing data?

8.25 Scintillation Detectors

The scintillation detector utilizes two well known phenomena to count incident particles and analyze their energies. The interaction of radiation particles with certain substances results in the emission of electromagnetic radiation. This radiation has an energy which is suitable for the production of energetic electrons by the photoelectric effect. These electrons can be increased in number by means of a special electronic tube, the "photomultiplier tube", until they exist in sufficient quantity to be readily counted. If the number of primary electrons released from a "photocathode" by the electromagnetic radiation are proportional to the energy dissipated in the scintillation material by the impinging radiation, and if the percentage increase in the number of electrons in the photomultiplier tube is independent of the number of primary photoelectrons, and if the entire process of absorption and photomultiplication takes place in a short time, say less than a microsecond, it is clear that the energy distribution in the impinging radiation radiation can be deduced. The above remarks summarize the manner in which a scintillation detector works. The details of the production of the electromagnetic radiation and the multitude of different substances which can be used as scintillators, or synonomously, which can produce light energy from molecular excitation and ionization, the collection of this light in the most efficient manner, etc.,

etc., should not hide these basic concepts. Scintillators can be used to detect most particles and in fact are so sensitive they were used to measure the presence and confirm the existence of the neutrino.

Scintillators can be classified as solid or liquid, organic or inorganic, and in terms of sensitivity to different types of radiation, i.e., the fraction of the incident energy absorbed, efficiency in converting absorbed energy to useful light energy, and decay time of the emitted radiation, or the length of time after the radiation has been absorbed during which the substance emits 68% of the total light energy. There are many substances and combinations of substances which are scintillators, but only a relatively few have useful characteristics for nuclear radiation detection applications. Fortunately, there are some materials which have excellent properties. Some of the more common substances which are used here are anthracene crystal, sodium iodide crystal, zinc sulphide crystal and terphenyl.

8.26 Scintillation Mechanism

For gamma detection, sodium iodide with a small amount of thallium as an impurity is often used. A simple explanation of the mechanism which causes the scintillation can be postulated. Quantum mechanics has shown that the electrons in a solid can be classified according to their energy level. The electrons are permitted to exist only in discrete energy intervals or bands. In a solid, most electrons are normally in the valence band. These electrons can not move freely throughout the crystal. At a higher energy level, there is the conduction band of the solid. Electrons in the conduction band are free to move about. The understanding of these bands has led to the explanation of a variety of physical phenomena associated with solids, e.g., the solid state detector to be described in a future lecture. In a perfect crystal, due to the discreteness of nature, electrons can exist either in the valence or in the conduction bands but not between. In an imperfect crystal and/or one contaminated with impurities in small amounts, such as NaI(Tl), discrete energy levels exist between these bands. The incident radiation imparts some of its energy to electrons in the valence band. These electrons can only go to the intermediate levels or the conduction band. Since the valence band represente a lower energy, more stable state, the excited electrons eventually return to the valence band and emit the difference in energy between the state they left and the state to which they have gone in the form of electromagnetic radiation. The only change of states which produce radiation appropriate for the photoelectric effect are between the impurity levels and valence band. These transitions occur in NaI(Tl) with a decay time of 2.5×10^{-7} seconds. Since the incident particle loses its energy to the crystal in less than 10^{-6} seconds,

the electrons emitted from the photocathode can be considered as having been formed all at the same time, as the result of the one incident particle. Unless the count rate is greater than 10^6 per second there is little possibility of pulse pile up at the output of the photomultiplier tube. The crystal is transparent to the electromagnetic radiation produced since it does not have enough energy to lift an electron from the valence band back up to the same impurity level.

In organic solids the idea is somewhat the same but no impurities are needed. The electrons are transferred to a higher vibrational energy state in which a part of the energy is dissipated by thermal excitation. Eventually a certain fraction of these electrons, in dropping down to the more stable vibrational energy states, will emit radiation with theproper wavelength for photoemission. The decay time for this possibility is 2.7×10^{-9} seconds for anthracene.

The mechanism for luminescence in organic liquids is not well known. However, for inorganic gases such as xenon and helium, as the excited atoms or ions return to their ground states high frequency radiation in the ultraviolet is emitted with a decay time of about 10^{-9} seconds or less. Because no lower energy radiation is emitted relatively few photoelectrons are produced, but the fast decay time is cause for considerable research on this type scintillator. Probably the most easy to produce and obtain in quantity are the organic liquids, since it has been found that reagent organics are satisfactory scintillators.

Experiment has shown that the amplitude of the photomultiplier output pulse is almost linear with the incident nuclear particle energy for energies of interest in this laboratory. Price gives the results of such experiments up to energies of 15 plus Mev. for a variety of particles (Fig. 7-4, 7-5). It has been found that $ZnS(A_g)$ with a decay time of 10^{-5} seconds is excellent for alphas and many organics for β's. For a particular energy spectrum, one should check the literature to find the best scintillator for a given application.

In mounting the scintillator on the photomultiplier tube it is obvious that all external light should be prevented from reaching the photocathode. Also, the interface between the scintillator and the photocathode is important because of the light which is reflected back into the scintillator because of the different indices of refraction of the two media. Light striking the interface making an angle, θ, with the normal to the surface will be totally reflected above the critical angle, $\theta = \sin^{-1}(n_2/n_1)$, where n, is the index of the scintillator. Air makes a very poor interface because its index is so low, giving a small critical angle. If it is inconvenient

to have the scintillator physically close to the photocathode, it has been shown practical to use light "pipes", sometimes as long as a foot or two, to serve as a guide for the light.

There is always a distribution in the output of the photomultiplier tube due to the statistics of all the processes involved and the tube itself. The resolution of the output of the tube for a constant energy radiation particle impinging on the scintillator can be defined in any number of ways. Price uses the definition that the resolution is the ratio of the square of the mean voltage pulse amplitude to the difference of the mean of the square and the square of the mean.

For gamma counting, the scintillator efficiency is defined as the fraction of γ's absorbed in the scintillator. For a point source on the axis of the scintillator, the intrinsic efficiency is defined as the $\frac{1}{\Omega_o} \int_{\Omega_o} (1 - e^{-\mu x}) \, dr$ where Ω_o is the source solid angle subtended by the surface of the scintillator nearest the source, note x is the straight through distance the gamma travels inside the scintillator. For convenience the intrinsic efficiency is usually plotted as a function of γ energy for a given shape of the scintillator volume with the source distance from its surface as a parameter. This efficiency is required if one desires to make an absolute determination of the source activity.

The upper limit in counting is usually set by the resolving time of the scaler, about 2×10^{-6} seconds.

To analyze a continuous distribution of incident energies or to investigate system resolution, it is convenient to use a channel analyzer. The analyzer is simply a piece of equipment which accepts only pulses between preset limits, ΔE, when used as a differential analyzer and only accepts pulses above a preset limit, E_d, when used as an integral analyzer. On differential, the width of the voltage spread accepted is set by the "window" of the analyzer, ΔE. The differential analyzer gives the number of pulses in a given energy (voltage) interval, ΔE, above a base voltage denoted by $E_{dial} = E_d$, which is continuously adjustable by the operator.

8.27 Analysis of Gamma Ray Pulse Distribution (Jointly with W. Smith).

The units of E_d are not important, (for our equipment $0 \leq E_d \leq 1000$ units, $0 \leq 80$ volts) as long as a relationship can be established to determine the energies of the gammas interacting in the scintillation crystal.

A representative block diagram of the equipment is given in Figure 8.18. Details on the scintillation crystal and photomultplier are shown in Figures 8.19 and 8.20. Figure 8.21 is a typical well scintillation counter found in most detection laboratories.

The abscissa of a differential curve is usually given in E_d units and the ordinate in counts per unit time per window. The pulses in ΔE are initiated in the crystal by energy transferred to the crystal by electrons (details given below). The electrons are produced by the interaction of x and gamma rays with the crystal. These photons interact in three principle ways as indicated earlier. Consider the effect of each type of interaction on the observed differential spectrum.

In a photoelectric absorption, the photon disappears and an electron of kinetic energy

$$E_k = h\nu - w$$

is emitted, w being the binding energy of the electron. The electron will lose all its energy in the crystal, and the X-ray emitted by the atoms returning to the ground state are soft, and therefore totally absorbed. Thus, the pulse will correspond precisely to the energy of the gamma ray. The pulses due to photoelectric effect will not be all equal, but will spread around the value E_γ forming a peak, as shown in Figure 8-22. This distribution of the pulse size is due to many reasons, such as the random nature of the interactions in the crystal, the variation of the amount of light reaching the photocathode, the non-uniform response of the photosensitive surface to uniform-size light pulses and the statistical variations in the phototube multiplication.

In Compton scattering, part of the energy of the photon is transferred to an electron, and a secondary photon of energy

$$h\nu' = \frac{E_\gamma}{1 + \frac{E_\gamma}{mc^2}(1 - \cos\theta)}$$

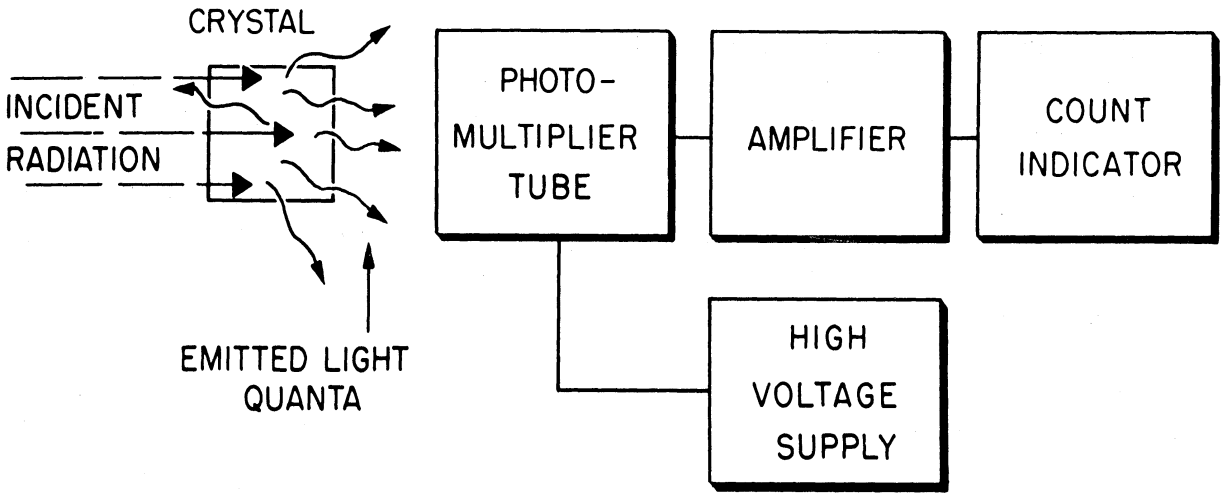

Figure 8.18. Representative block diagram for scintillation counter.

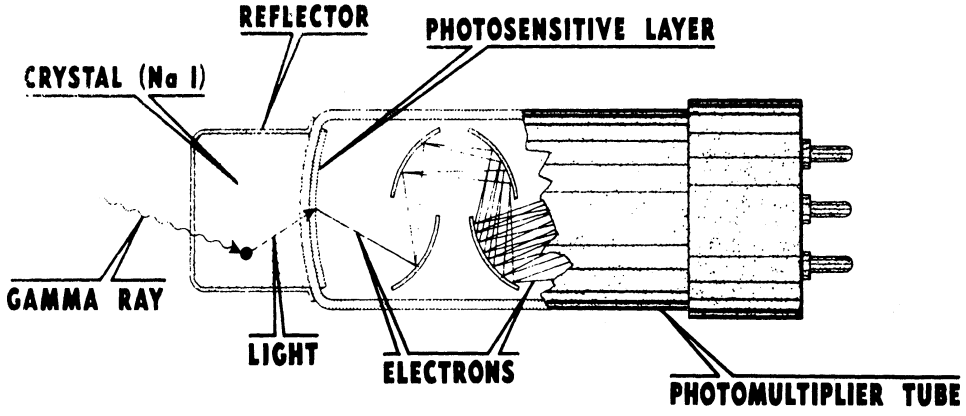

TOTAL LIGHT TO TUBE NEARLY PROPORTIONAL TO GAMMA RAY ENERGY

IF 1 ELECTRON EJECTS 5 FROM A DYNODE, 11 DYNODES RESULT IN 5^{11}

OR

ABOUT 50 MILLION ELECTRONS OUTPUT

Figure 8.19. Scintillation Counter.

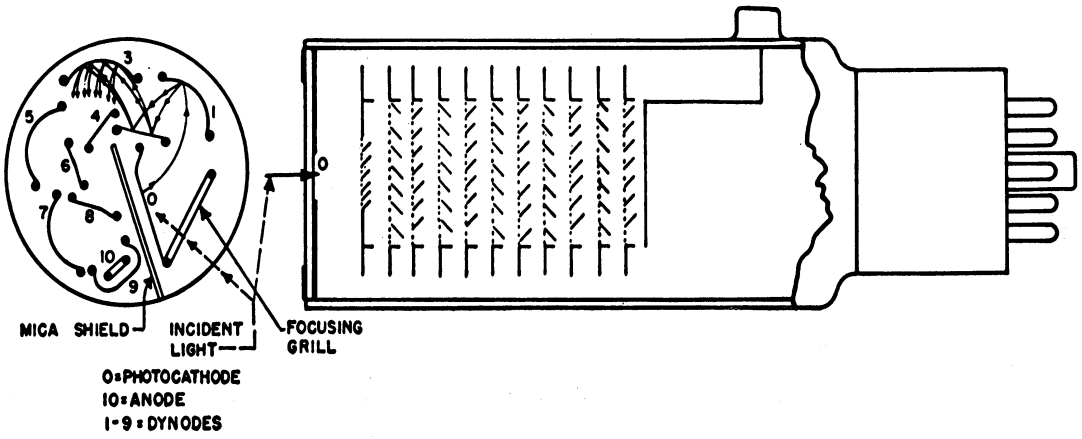

Figure 8-20. Detail on Two Types of Photo-multiplier Tubes. (Courtesy Tracerlab, Inc.)

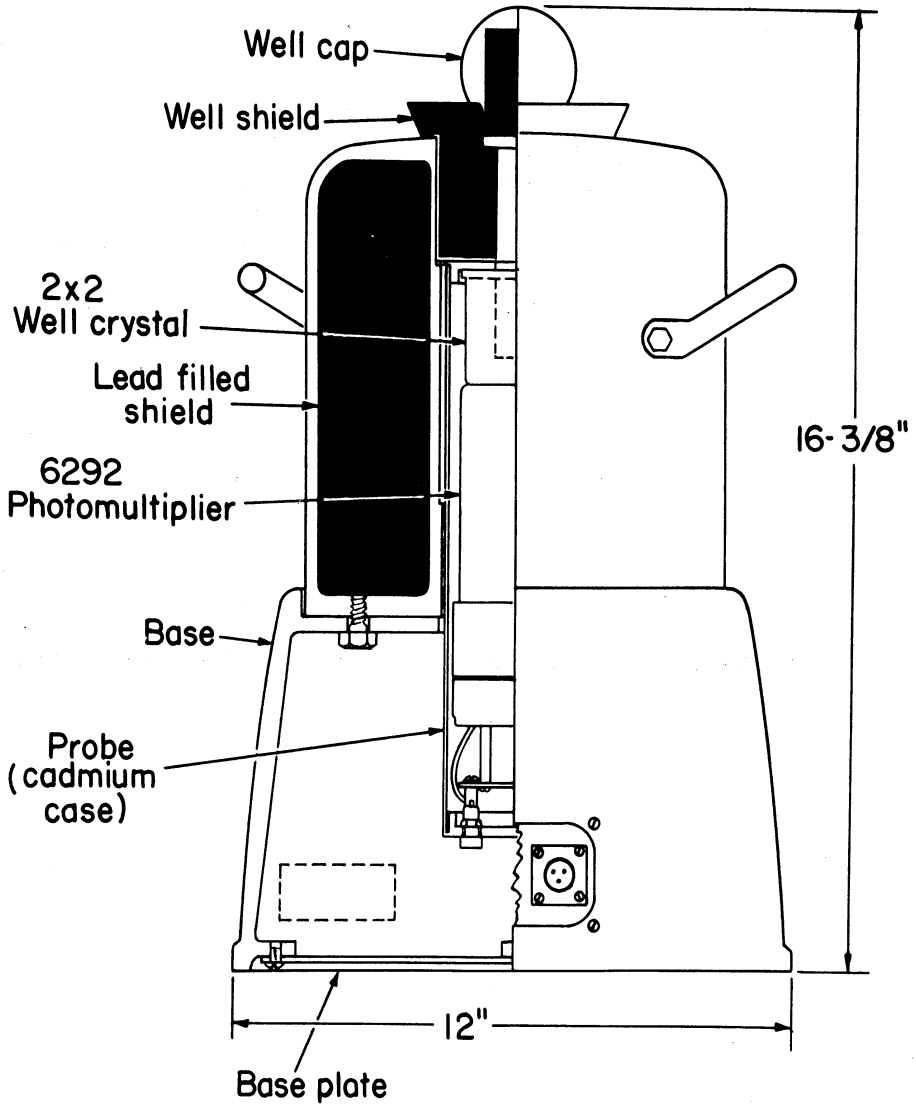

Figure 8.21. Typical well counter. (Courtesy RCL Inc.)

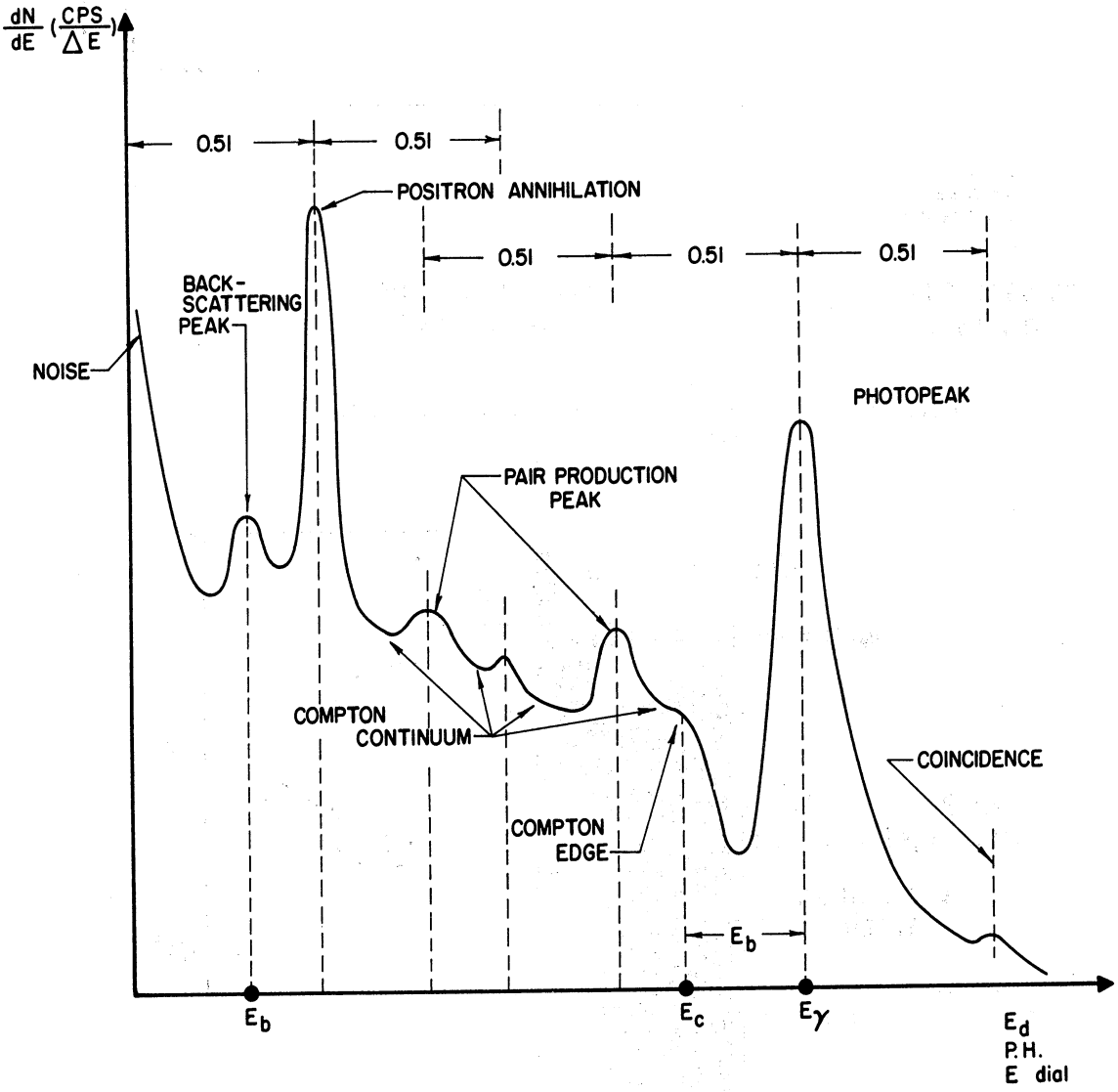

Figure 8-22. Idealized differential curve for monoenergetic gammas

is ejected at an angle θ. The Klein-Nishina formula describes how the probability of scattering varies with θ, and indicates that more forward scattered electrons and back-scattered photons are produced than of any other energy. If we assume for one moment that all gamma interactions are Compton scattering and further, that the secondary photons always escape the crystal, the pulse size distribution would be as indicated, with a maximum number of electrons going in the forward direction. Actually, the scattered photons will suffer further interactions, and will be partially or totally absorbed, and the pulses resulting from Compton interactions will have a continuous distribution ranging from zero to the maximum energy that can be transferred to the electron.

The energy of the backscattered photon for $\theta = 180°$ is

$$E_b = \frac{E_\gamma}{1 + \frac{2E_\gamma}{mc^2}}$$

The electron maximum energy is then:

$$E_c = E_\gamma - E_b = \frac{E_\gamma}{1 + \frac{mc^2}{2E_\gamma}}$$

which defines the so called Compton edge. It must be observed that in principle the photon scattered with energy E_b could suffer another interaction. However, if the values of E_c and E_b are calculated for the current range of primary gamma energies, we get:

E	E_b	E_c
0.5	0.169	0.331
1.0	0.203	0.797
5.0	0.242	4.756

showing that the range of variation of E_b is limited to a region where the photoelectric effect is predominant. Then, if the backscattered photon is absorbed, the total primary energy would have been absorbed, and the pulse size will be under the photopeak. In most of the case, however, the secondary photon will escape the crystal, since it is directed outwards, and therefore very few counts will be noticed between E_c and the photopeak, giving origin to a characteristic valley in the differential curve. The spreading of the pulses around E_c is due to the same causes listed above.

Pair production can occur only when the energy of the primary gamma is above 1.02 Mev. The energy E_γ of the photon is used to create the pair and to impart kinetic energy to the positron and the electron. This kinetic energy will be absorbed in the crystal, and finally the positron will annihilate with one electron of the medium. Two photons of 0.51 Mev appear in opposite directions and three cases are possible: 1) if both photons are absorbed, then the total gamma energy E_γ has been absorbed in the phosphor, and the pulse will fall under the photopeak; 2) if one of the photons escapes, the total energy deposited in the crystal is:

$$E_a = E_\gamma - 0.51$$

and a peak will appear at that point; and 3) if both 0.51 Mev photons escapes the crystal - and the probability for that is considerably smaller, since they are ejected in opposite directions - the energy absorbed in the crystal is:

$$E_a = E_\gamma - 1.02$$

and a second and smaller pair production peak will appear superimposed to the Compton continuum.

It must be noticed that although several interactions can take place successively, the total time is short compared with the decay time of the crystal, so all of them will yield a single pulse.

Other peaks of interest are usually present in the differential curves, although they are not due to direct interaction of the primary gamma with the crystal. If the scintillation detector is surrounded by a lead shield, many of the gammas will be back-scattered towards the crystal, where by photoeffect they will produce a peak at energy E_b. Even without a shield, this peak could be noticeable if the crystal is close to any other object, since back-scattering is predominant in Compton effect.

If the source emits a positron, it will annihilate after losing its kinetic energy, creating two photons of 0.51 Mev moving in opposite directions. One of

them will almost always reach the crystal and will show in the differential curve as a peak at 0.51 Mev. This photopeak is rather large, because the cross-section for photoelectric effect increases with decreasing energy. The second 0.51 Mev photon will or will not reach the crystal, depending upon the geometry (well type crystal, solid crystal) and the place where the annihilation occurs. If it does reach the crystal, a smaller peak will show at 1.02 Mev.

It can also happen that one of the primary gammas, with energy E_γ, will suffer a pair production interaction in the shield. The positron of this pair will annihilate also in the shield, but then only one of the two 0.51 Mev photons can hit the crystal, since the other one will go in the opposite direction. In that case, then, only a 0.51 Mev peak will be observed.

Finally, when we have two gammas of different energies, as for example in the case of Figure 8.22, the primary of energy E_γ and the 0.51 Mev gamma from positron annihilation, it can happen that both will hit the phosphor at the same time, adding up their respective pulses to produce a coincidence peak at energy $E_\gamma + 0.51$.

8.28 Details on the Conversion of Gamma Energy to a Measureable Pulse from the Phototube (Jointly with J. Trombka)

The light emission spectrum for pure NaI is essentially the same as the absorption spectrum and is well below the visible range. To enhance recombination and to provide a "wave shifter" thallium impurity centers are added, which have the effect of providing intermediate energy levels in the forbidden band. The emission spectrum of Tl in NaI is lower than its absorption spectrum and provides a scintillation with wavelength in the visible region. This emission spectrum and the absolute conversion efficiency of the crystal ionization excitation into light emission is denoted by the conversion efficiency symbol $C_{n\cdot p}(\lambda)^2$. The total light energy produced, starting with the initial excitation energy of the electron, E_e is

$$E_\ell = E_e \int_0^\infty C_{np}(\lambda)\, d\lambda = E_e C_{np} \qquad (1)$$

and has the following spectral shape (from Price).

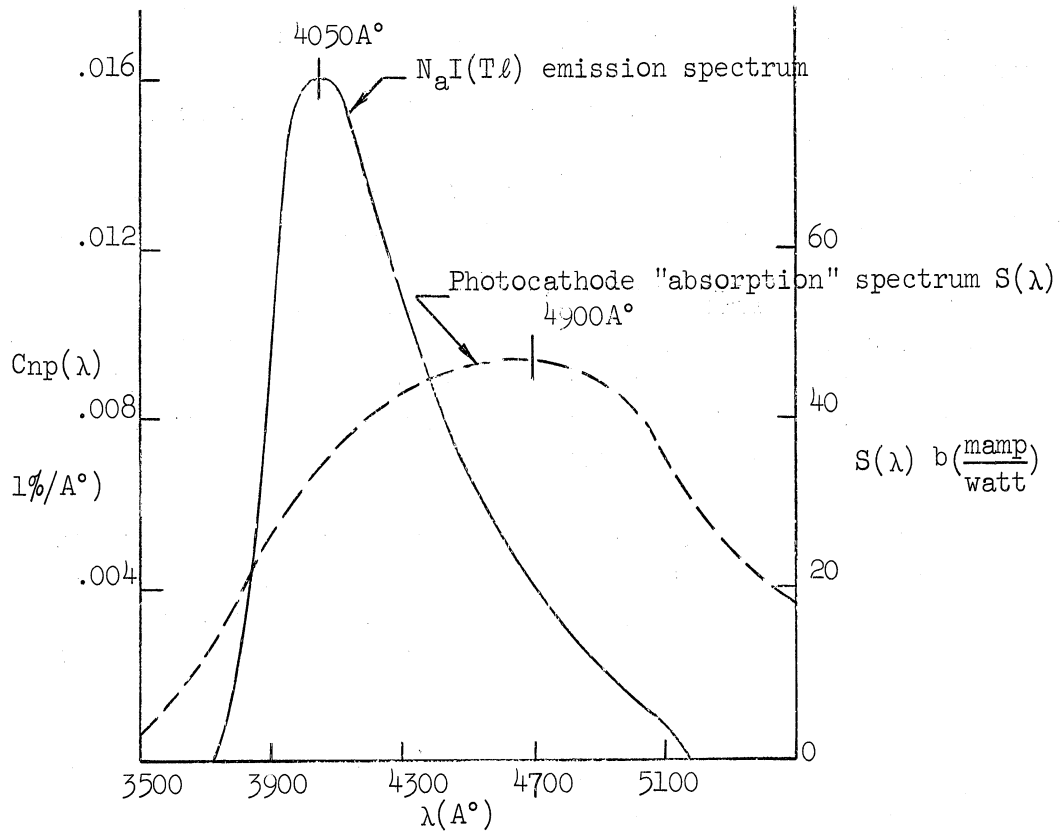

Figure 8.23. Conversion Efficiency $C_{np}(\lambda)$ and Spectral Sensitivity $S(\lambda)$ of Type S-11 Photocathodes.

The total area under this spectrum curve is roughly 550A° (0.016%/A°) $\approx$ 8%. The conversion efficiency C_{np} is dimensionless.

8.29 Conversion of Light Energy to Photo-electrons and Subsequent Multiplication

If we place an end-window photocathode ($SbCs_3$) surface in optical contact with the crystal, the fraction of photon energy which strikes this surface will be E_ℓ ($T_\rho \cdot F_p$) where T_ρ is the transparency of the crystal and of the phototube optical seal, and F_p is the non-escape probability. For a well reflected crystal both should be nearly unity. A fraction of this energy will be absorbed in the photocathode, giving rise to a number of low energy photoelectrons released inside the phototube. The efficiency of this conversion from photons to electrons depends on the absorption spectrum of $SbCs_3$ and on the electronic stopping power of the photocathode and is measured by the sensitivity factor, $S(\lambda)$, shown also in Figure 8.23. $S(\lambda)$ is measured in units of amperes/watt and has a maximum of 0.056 amps/watt at 4900A°. This can be redefined in terms of the number of photoelectrons per ev of incident light

$$S(\lambda) = \frac{dq/dt}{dE/dt}\left(\frac{amp}{watt}\right) = \frac{dq}{dE}\left(\frac{Coulombs}{Joule}\right) \Rightarrow \frac{dn_e}{dE}\left(\frac{electron}{ev}\right)$$

Hence

$$\frac{dn_e}{dE} = S(\lambda), \qquad dn_e = S(\lambda)\, dE$$

From (1) above,

$$dE = dE_\ell = E_e C_{np}(\lambda)\, d\lambda,$$

so

$$dn_e = E_e C_{np}(\lambda)\, S(\lambda)\, d\lambda \cdot T_p \cdot F_p$$

or the NUMBER OF PHOTOELECTRONS EJECTED = n_e
and depends on the overlap of the spectra of Figure 8.23.

$$n_e = E_e \int_0^\infty C_{np}(\lambda)\, S(\lambda)\, d\lambda \cdot T_p F_p \qquad (2)$$

If we now define F_c as the fraction of such electrons striking the first dynode and if the subsequent phototube multiplication is M, the total charge produced at the phototube output, due to a single original γ event is $q = n_e \cdot e \cdot M \cdot F_c$ where e is electronic charge, or

$$q = E_e\,(T_p F_p F_c)\, M \cdot e \int_0^\infty C_{np}(\lambda)\, S(\lambda)\, d\lambda \qquad (3)$$

If this charge collects on the input capacity of an amplifier without leakage losses, the resultant voltage pulse will have the maximum value

$$V_{in} = E_e(T_p F_p F_c)\, \frac{e}{C_{in}}\, M \int_0^\infty C(\lambda)\, S(\lambda)\, d\lambda$$

(As "typical" example, if $(T_p F_p F_c) \simeq 0.5$, $M \simeq 5 \times 10^4$, $C_{in} \approx 25\mu\mu f$ then for a photopeak pulse from Cs^{137} ($E_e = E_\gamma = 0.661$ Mev)

$$V_{in} \simeq \frac{(.66)(5\times 10^4)(.5)(.002 \times 10^6)(1.6 \times 10^{-19})}{25 \times 10^{-12}} = 0.2 \text{ volts} \qquad (4)$$

8.30 Pulse Height vs. Energy

The interaction time for any of the three gamma interaction processes mentioned above is much shorter than the decay time of the scintillations in the crystal. Therefore, one gamma ray upon suffering an interaction or multiple interactions will produce only one pulse of photons. It is very important to observe that the number of photons in a given pulse will be proportional to the energy lost to the crystal as kinetic energy of electrons. Further, there is a linear relationship between the number of photons striking the photocathode and the electronic charge appearing at the output of the multiplier phototube. Thus charge will appear as a voltage pulse across the amplifier input capacitance. The pulse height in volts observed at this point will then be proportional to the ionization produced by the gamma ray in the crystal.

Thus, the number of pulses per unit time at the phototube output is equal to the number of gamma photons interacting with the crystal per unit time; while the magnitude of each pulse is proportional to the ionization produced whithin the crystal by a given gamma ray.

8.31 Energy Resolution

Finite Width of Photopeak

The events producing pulses in the photopeak have a spread in apparent energy even though they represent full capture of the γ energy ($E_{\gamma Total} = E_e$). This is because there are statistical factors in the system which give a probability distribution in pulse height. Some of these factors are CORRECTABLE such as those associated with light collection optics. Every effort must be made to bring T_p, F_p as close to unity as possible. Some factors are INHERENT in the technique and set a severe bound to energy resolving power of the technique. If we define resolution as the full width at half maximum of the photopeak

$$R = \frac{2|E_o - E_{1/2}|}{E_o} \qquad (5)$$

it will be found that the smallest value obtainable for the Cs peak is $\sim 6\%$ (which for mediocre optics it may be 10 to 15%). This inherent limit is energy dependent and is due mainly to (a) statistical fluctuation in the number of electrons from the photocathode as given by Equation 2 and (b) to statistical fluctuation in phototube multiplication M. These two statistics must be "folded into" each other to determine the overall probability distribution.

The statistical variation in n_e is truly Gaussian in nature and one can define the probability that an incoming particle of energy E_o will give a burst of photoelectrons of a number corresponding to some energy E_1 as

$$P_1 = \frac{n_e(E_1)}{n_e(E_o)} = e^{-\frac{|E_1 - E_o|^2}{a^2}} \tag{6}$$

The statistical nature of M is complex and not truly Gaussian. We will assume it to be approximately so, so that we can define the probability that the phototube multiplication of these $n_e(E_1)$ will be of a magnitude corresponding to a pulse of energy E_2 as

$$P_2 = \frac{M(E_2)}{M(E_1)} = e^{-\frac{|E_2 - E_1|^2}{b^2}} \tag{7}$$

The probability of obtaining a pulse height corresponding to an APPARENT ENERGY E_2, originating from a pulse of true energy E_o will be the product of $P_1 \cdot P_2$ summed over all possible values of E_1 (or $E_1 - E_o$); the pulse heights will then have the value, from (3), (6), (7),

$$q = C \cdot \int n_e(E_1)\, M(E_2)\, dE_1$$

$$= C n_e(E_o)\, M(E_1) \int P_1 P_2\, dE_1$$

$$= C \bar{n}_e(E_o)\, \bar{M} \int P_1 P_2\, dE_1$$

Letting $\epsilon = (E_2 - E_o)$, and $\chi = (E_1 - E_o)$

$$q(\epsilon) = C \bar{n}_e \bar{M} \int_{-\infty}^{+\infty} e^{-\frac{\chi^2}{a^2}} e^{-\frac{(\epsilon-\chi)^2}{b^2}}\, d\chi \tag{8}$$

Integration of this expression will lead to the distribution function

$$q(\epsilon) = C \bar{n}_e \bar{M}\, e^{-\epsilon^2/2\sigma^2} \tag{9}$$

where $2\sigma^2 = a^2 + b^2$; σ^2 is the dispersion (σ = the standard deviation) of the distribution and a^2, b^2 are the dispersions of the photoelectrons' production rate and subsequent multiplication rate, respectively. It is shown in Nucleonics (10, 51 (1952) that the dispersion of the multiplication is a complex function of dynode multiplications, but photoelectron dispersion is just proportional to n_e, the count rate:

$$\sigma_n^2 = \frac{a^2}{2} \simeq \bar{n}_e = C_1 E_o$$

$$\sigma_m^2 = \frac{b^2}{2} \simeq \bar{n}_e f(M) = C_2 E_o$$

so

$$\sigma^2 = C_3 E_o \qquad (10)$$

Now from (5), (9), (10)

$$R = \frac{2\epsilon_{1/2}}{E_o}$$

$$\epsilon_{1/2} = \sqrt{2 \ln 2}\, \sigma \qquad (10a)$$

so

$$R(E_o) = 2\sqrt{2 \ln 2}\, \frac{\sigma}{E_o} = \frac{2.36\sigma}{E_o}$$

and

$$R(E_o) = 2.36(C_3)^{1/2} \cdot \frac{1}{\sqrt{E_o}} \qquad (11)$$

Hence a 10% resolution system for the Cs^{137} peak (E_o = .661Me) should exhibit a value for the .41 Mev γ from Au^{198} of 10% $(.661/.411)^{1/2}$ = 12.7%.

Integral of Photopeak

$$N_p = \int_{-\infty}^{+\infty} N(\epsilon)\, d\epsilon = 2\int_{0}^{\infty} N(E_o)\, e^{-\frac{\epsilon^2}{2\sigma^2}} d\epsilon = N(0)\sqrt{2\pi\sigma^2} \qquad (12)$$

where N_p is the total number of counts under the photopeak and N(0) is the maximum count per unit width.

8.32 Detection Efficiencies

We now look at the problem of the detection efficiencies. In the following discussion we will not consider pair production. The analysis of course can be extended to include this process. The cross sections of interest therefore will be those for photoelectric absorption and for Compton scattering.

Consider the case of a monoenergetic point source. We assume that there is no scattering from surrounding source materials

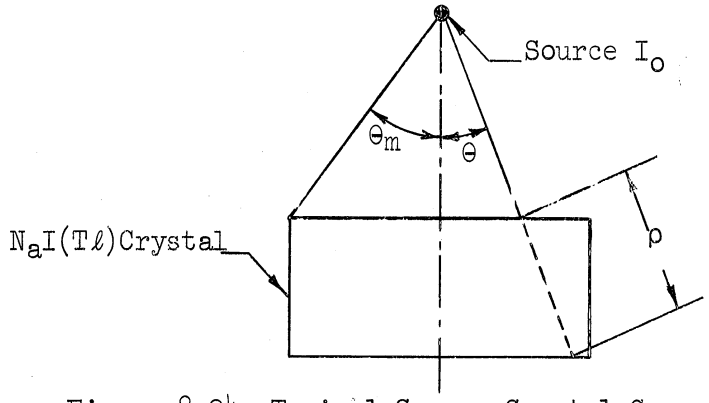

Figure 8.24. Typical Source-Crystal Geometry.

If I_o gamma rays per unit time are emitted from the source, then $I_o\Omega/4\pi$ will be the number of gamma rays incident upon the top surface of the detector (where $d\Omega = 2\pi \sin\Theta d\Theta$ and by integration for $\Theta = 0$ to $\Theta = \Theta_m$, $\Omega = 2\pi(1 - \cos\Theta_m)$. Define the total intrinsic efficiency, ϵ_{Ti} as the probability per unit solid angle that the gamma ray suffers a first collision, then

$$N_T = I_o \frac{\Omega}{4\pi} \epsilon_{Ti} \qquad (13)$$

where N_T is the number of gamma rays emitted from the source which suffers first collision in the crystal.

Since one pulse will appear for every primary collision, and since only the pulse height is effected by the type or number of interactions for a given gamma ray, the number of pulses per unit time detected, independent of pulse height, will equal N_T. Therefore, if we add up all the pulses produced per unit time under the pulse height spectrum, we obtain the number of primary interactions occurring per unit time. If A_T be the total area under the pulse height spectrum, then

$$A_T = N_T = I_o \frac{\Omega}{4\pi} \epsilon_{Ti} \qquad (14)$$

If we consider any interaction in which a gamma loses energy, and this energy eventually is converted to scintillations by absorption, then μ can be defined as the linear absorption cross section for first interactions due to photoelectric and Compton interactions. Then with respect to Figure 8.24, $e^{-\mu\rho}$ will be the non-interaction probability along the path ρ within the crystal, and $(1 - e^{-\mu\rho})$ will be the probability of suffering a first interaction along ρ. Then

$$\epsilon_{Ta} = \int_0^{\theta_m} (1 - e^{-\mu\rho(\theta)}) \frac{d\Omega}{4\pi} \equiv \text{Total absolute efficiency} \qquad (15)$$

is the probability that if a gamma ray is emitted from the source, it will interact in the crystal. The integration is carried out over the solid angle subtended by the source and top of the crystal.

Then we define

$$\epsilon_{Ti} = \frac{\epsilon_{Ta}}{\frac{\Omega}{4\pi}} \equiv \text{Total intrinsic efficiency} \qquad (16)$$

which is the fraction of those gamma incident on the crystal face which interact with the crystal. Both integrations are carried out over the solid angle described above. This then is the efficiency ϵ_{Ti} shown in Equation (13). This efficiency has been studied as a function of source detector distances for a number of energies and for several crystal sizes.

In terms of the analysis, it is usually simpler to study the area under the photopeak only. This area can be determined much more precisely than the total area. There are two major reasons for the difficulty in obtaining the total area. First, it is rather difficult to eliminate all scattering effects due to the surrounding materials. These will appear as pulses in the Compton continuum. Secondly, pulse height analyzers cannot detect all pulses down to zero pulse height, for below certain pulse height levels, the equipment noise and the thermal noise of the phototube completely interfere with the detection. We, therefore, consider

$A_p \equiv$ the area under the photopeak

$\epsilon_{pi} \equiv$ the intrinsic peak efficiency

or, ϵ_{pi} is the fraction of those gammas striking the crystal face which are totally absorbed.

If both sides of (14) are divided by $\frac{A_T}{A_p}$ we obtain

$$A_p = I_o \frac{\Omega}{4\pi} \epsilon_{pi}$$

where

$$\epsilon_{pi} = \frac{A_p}{A_T} \epsilon_{Ti} = P_T \epsilon_{Ti} \qquad (17)$$

P_T is the peak to total ratio A_p/A_T.

The total number of absorptions in the photopeak may be obtained from Equation 12. (When using a pulse height analyzer to measure these pulse height spectra - histograms rather than true differential spectra are obtained because the analyzer measures all pulses in a finite ΔE increment about E. Therefore N(o) of Equation 12 will equal $A_{max}/\Delta E$ where A_{max} is the experimentally determined maximum of the photopeak in the measured pulse height distribution. Thus

$$A_p = N_p = \frac{A_{max}}{\Delta E} \sqrt{2\pi\sigma^2}$$

where σ and ΔE are measured in the same units (e.g., either pulse height or energy) and σ is determined from Equation 10a.) Then, using the known geometry of the source-crystal assembly and the tabulated values of efficiencies, that fraction of the gammas emitted by the source which is totally absorbed in the crystal and appears in the photopeak is obtained. Hence, the source strength may be absolutely determined.

8.33 Experiment Using a Scintillation Counter

Please use extreme caution in working with photomultiplier tubes so that they will not be damaged by excessive voltage, by exposure to light while high voltage is applied or by breakage.

Use the G.E. scintillation counter for parts 1 through 6, and the RCL well type counter for rest of the experiment.

1) Obtain the count rate versus voltage curve with no source and no scintillator in order to find out where tube noise begins to produce counts and to check the light tightness of the detector.

2) Repeat the procedure with the ZnS screen in place, but no source.

3) Obtain the count rate versus voltage curve using thorium foil and the ZnS screen.

4) Show that you were counting alpha particles by covering the thorium with a suitable absorber. The thorium, together with its disintegration products, emits betas as well as alphas. The efficiency of ZnS in converting ionization enery into light is the same for alphas and betas. With these points in mind, explain why you were counting primarily alphas with the ZnS scintillator.

5) Obtain the count rate versus voltage curve with the anthracene crystal and no source.

6) Repeat the procedure using the bismuth 210 (RaE) source, and then the carbon 14 source. Compare these two curves, and explain why they do not have the same shape.

7) Obtain the gamma background count rate versus voltage curve with the well type counter.

8) Obtain the characteristic curves for cobalt 60, cesium 137, and cobalt 57. Comment on the similarities and explain the differences.

9) Decide on an operating voltage for the cobalt 60 source. At this voltage, count the background and the source as the scaler input sensitivity is varied. Calculate the ratio of the background count rate to the count rate due to cobalt at each sensitivity setting. Explain why this ratio may vary with sensitivity.

8.34 Experiment on Scintillation Spectrometry

Use a scintillation counter with a single channel pulse height analyzer in this experiment. Please note that the super stable high voltage supply can deliver a lethal electric shock.

It is recommended that you use 1000 volts for thephotomultiplier tube. The tube may require a positive or a negative high voltage, depending on whether the photocatode or the collector anode is held at ground potential. It is recommended that you use an amplifier gain value such that the cesium 137 peak occurs at an E dial setting of about 350.

1) Both the E and ΔE dials of the single channel analyzer are divided into one thousand divisions. One division on the E dial, however, corresponds to many divisions on the ΔE dial; that is, the graduation of the ΔE dial is much finer than that of the E dial. Determine experimentally what percentage of the maximum E dial setting is equivalent to the maximum ΔE dial setting. This figure is called the maximum window width. For complete checking of the ΔE dial, one must ensure that the window width is not dependent on the E dial setting, and that the ΔE dial is linear. These checks can be performed simply by using a pulse generator.

2) The next step is the calibration of the E dial; that is, the determination of the proportionality factor between E dial setting and energy. With an approximately 1% window width, locate the full-energy peaks of cobalt 60, cesium 137, and cobalt 57. Draw the E dial calibration curve, and decide whether it is linear and whether zero setting corresponds to zero pulse height; if not, please call this to the attention of the instructor.

3) Determine the complete pulse height distribution curves for cobalt 60, sodium 22, cesium 137, and cobalt 57. Please note that you need the background pulse height distribution to do this. Use a 1% window, and take data at as many E dial settings as necessary to determine the shapes of the curves. When drawing the curves, graduate the horizontal scale in both E dial and energy units.

Point out and explain the characteristics of the obtained curves. Identify all peaks; give two reasons why the full energy peak corresponding to the lower energy gamma of cobalt 60 is higher than that of the higher energy gamma, in spite of the fact that equal numbers of these two gamma are emitted. Compare the sodium 22 spectrum obtained with an unshielded solid crystal with that obtained with a shielded well type crystal. Point out and explain the differences in the locations and the relative magnitudes of the peaks.

Determine the energy resolution of your equipment for cesium 137 and cobalt 57 gammas in terms of the absolute width and the percentage full width of the photopeak at half of the maximum value. Explain the reason for the difference in resolution associated with the two isotopes.

Please describe how you would determine the activity (in gammas emitted per unit time) of a source, given that the intrinsic peak efficiency of your crystal for the particular geometry used and the particular gamma energy of the source is ϵ.

8.35 Neutron Detection

Because neutrons are uncharged, their passage through matter does not create ion pairs. For our purposes, any neutron induced reaction which has either charged particles or gamma rays as a reaction product is potentially useful. The cross sections for neutron reactions are generally energy dependent. By measuring the effects of the products of the neutron interaction, one can not infer both the neutron flux and the neutron energies, since they are independent. In most measurements there are a spectrum of neutron energies. Energy bands can be selected from this spectrum mechanically using time of flight, crystal spectrometry or absorption techniques. Or, if the spectrum is known, e.g., Maxwell-Boltzmann, the count rate can be related to the incident flux.

The most common gaseous chambers employ boron 10 or fissionable material. The solid boron or fissionable material is coated on the inner walls of the chamber. In the thermal neutron-boron reaction an alpha is produced and charged fission products as well as lighter particles in the neutron-fissionable material reaction. By proper design, these charged particles produce ion pairs in a convenient chamber gas. Since boron exists in the gas phase in the form of BF_3, the chamber can be filled with this gas to accomplish the desired result of neutron detection. Because of the high specific ionization associated with α_s and the massive fission products, these chambers can be used easily for pulse detection. Boron lined chambers usually have a plateau with a greater slope than BF_3 tubes because of the variation in the α energy lost in the solid as opposed to most of the α energy being dissipated in the BF_3 gas. Fission chambers have the greatest slope in the count rate vs. discriminator voltage with chamber voltage as a parameter, because of the large fluctuations in primary ionization produced by the fission fragments, whose range is very small. The fission chamber must be operated as an ionization or proportional chamber to discriminate between the fission fragments and the background of α, β, and γ.

Fast neutrons are usually measured through the intermediate step of an (n,p) scattering reaction, i.e., the neutron scatters with either a hydrogen or a hydrogen containing molecule and an energetic recoil proton is produced. The ionization produced by the proton is measured.

A very common method of measuring neutron flux levels in a reactor, when a minimum flux perturbation is required, is the use of small pieces of metallic foil. The neutrons produce reaction products in the foil which are radioactive. When the foil has become sufficiently radioactive to give good counting statistics, the decay radiation is measured by standard means. If the energy distribution of the neutrons striking the foil is known the flux corresponding to the measured foil count rate can be calculated. It is clear that this method can only give

integrated neutron flux levels. Gold and idium are common foils for flux measurements. By enclosing the foil in a material with a large resonance cross section over a certain energy interval it is possible to restrict the energy spread of the neutrons entering the foil. Cadmium, which has negligible absorption for energies greater than about 0.5 ev and a very large cross section at lower energies, is often used to shield the foil from thermal neutrons. By measuring the foil activation with and without the cadmium shield, one can get a direct measure of the thermal neutron flux. The often quoted "cadmium ratio" simply refers to the ratio of the activation without to that with the cadmium present. The cadmium ratio is greater than or equal to one in a "thermal" reactor. A little thought should give the characteristics which an ideal foil would have with regard to cross section, type and energy of radioactivity and decay time. Dalton, at this university, has recently written a thesis on the flux depression inside thin foils which gives theoretical predictions of the neutron flux in excellent agreement with experiment.

Scintillation techniques can be used for neutron detection by utilizing the products of a neutron reaction to form ion pairs in the scintillation material. In high density scintillators, compensation for induced background pulses is often difficult. There are a host of development problems. New scintillators and designs are being worked on at this time.

Other means of measuring the products of a neutron interaction can be envisioned and are used in one form or another. For example, the recoil proton path can be captured on a photographic type emulsion, or the heat of reaction can be measured by the thermoelectric effect, or the amount of evolved gas can be measured, etc., etc.

In working with neutron sources it is important to keep personnel dose rates below the permissible levels. Figure 8.25 gives the maximum permissible neutron fluxes as a function of neutron energies.

8.36 Experiment on Neutron Detection Using BF_3 Tubes

Use a BF_3 detector for this experiment. In order to avoid electrical shock, please turn off the high voltage when handling the detector.

The main objects of this experiment are the determination of an operating point, in terms of amplifier gain, discriminator setting, and high voltage, at which neutrons can be counted in the presence of gamma radiation; and the measurement of neutron fluxes. Use the cathode ray oscilloscope throughout this experiment.

Basis: 14×10^6 neutrons per square centimeter equivalent to a dose of 1 rem. (See Federal Register Title 10, Chapter 1, Part 20: Standards for Protection Against Radiation.)

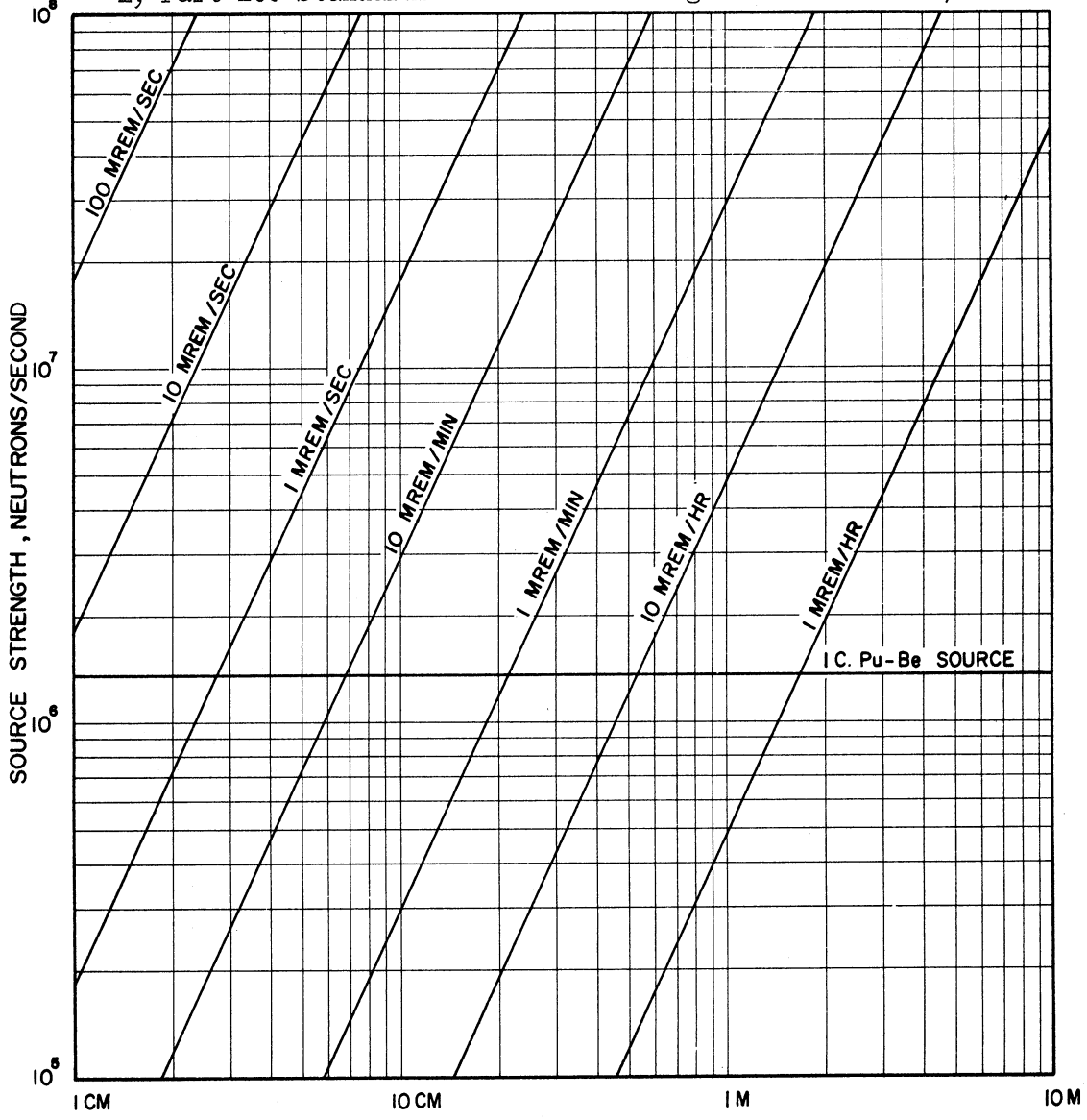

Fig. 8.25 Radiation dose rates due to an unshielded point isotopic source of fast (10 to 30 Mev) neutrons.

Prepared by
G.L. Gyorey

1) If the gain is too high, the amplifier will be overloaded by the larger pulses and will be rendered inoperative for a short time. The optimum gain is the one for which only a few counts are registered at a discriminator setting of 100. To find this value, set the gain to its maximum value, use the high voltage setting recommended by the manufacturer of the detector, and start counting neutrons. Reduce the gain until the desired value is reached. Ask the instructor to remove the neutron source.

2) Using the gain setting just determined, turn off the high voltage and set the discriminator to its lower limit. The counts should now be due to noise. Determine the discriminator setting at which the count rate due to noise becomes negligible.

3) Turn on the high voltage and expose your detector to a gamma field of a few mr/hr. The count rate should now be due to the gamma radiation. Determine the count rate versus discriminator setting characteristics of your apparatus for gamma radiation. Remove the gamma source.

4) Expose the detector to radiation from a source emitting mainly neutrons, placing both the source and the detector into a block of paraffin. Obtain the count rate versus discriminator setting characteristics, and compare it to the one obtained for gamma radiation. Decide what discriminator settings you would use for detecting neutrons in the presence of gamma radiation and for counting neutrons when no appreciable gamma field is present. If the two values are not the same, use the latter for the rest of the experiment.

5) Obtain the count rate versus voltage curve, and determine wheather the high voltage value that has been used is a desirable one. If not, please bring this to the attention of the instructor.

6) Determine what fraction of your counting rate is due to thermal neutrons by taking counts with and without a cadmium shield, which absorbs practically all of the thermal neutrons around the detector. From your count rates in the paraffin block and outside the paraffin shield, calculate the thermal neutron fluxes at these two points. Calculate also the radiation dose rates at these points due to thermal neutrons, given that exposure to a thermal neutron flux of 670 neutrons/sec/cm^2 is equivalent to 2.5 mrem/hr.

8.37 Thermal Neutron Flux Measurements in a Nuclear Reactor Using Activation Techniques

The activation method of neutron flux measurement makes use of the production of radioactive nuclei by the absorption of neutrons in a detecting material. The radioactive nuclei so produced decay with the emission of nuclear

radiation and can thus be detected. The most widely used detecting materials are indium and gold in the form of foils or wires.

The rate of production, R, of the radioactive nuclei depends on the absorption cross section of the detecting material and on the neutron flux in the following manner:

$$R = N_D \int_0^\infty \sigma_a (E)\, \phi (E)\, dE$$

where N_D is the number of nuclei in the detector, σ_a the absorption cross-section, ϕ the neutron flux, and E the neutron energy.

A rough plot of σ_a for low energies (in general) is given below in Figure 8.26

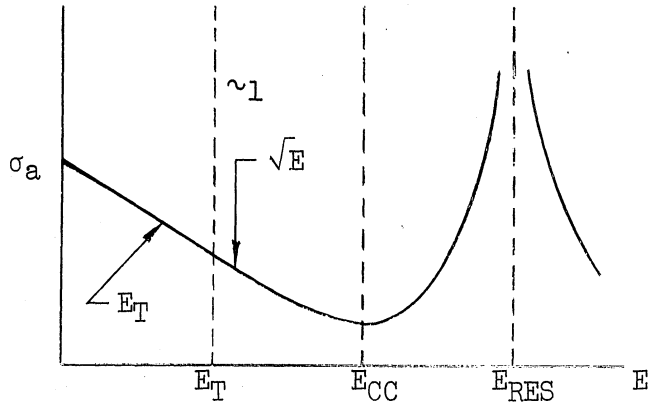

E_{RES} for In: 1.44 ev
Au: 5 ev
Co: 120 ev

Figure 8.26 Typical Neutron Absorption Cross Section σ_a vs. Energy, E.

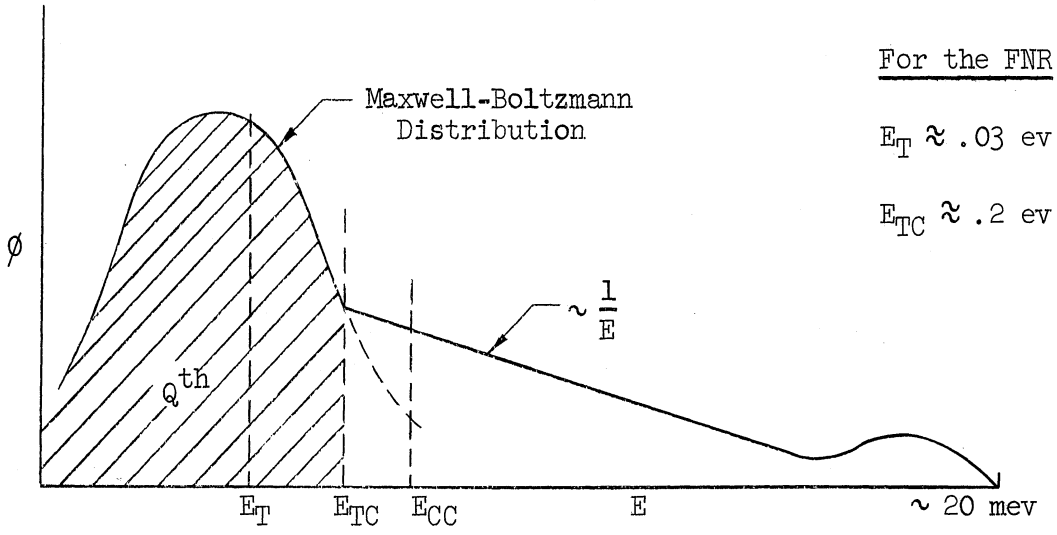

For the FNR

$E_T \approx .03$ ev

$E_{TC} \approx .2$ ev

Figure 8.27 Neutron Flux, ϕ,v,x, Energy, E

Here E_T is the most probable energy of the thermal neutrons, E_{TC} is the thermal cutoff energy, and E_{CC} will be discussed below.

We may now write

$$R = N_D \left[C_M \sigma_{E_T} \phi_{th} + \int_{E_{TC}}^{\infty} \sigma_a (E) \phi (E) dE \right]$$

where C_M is a factor which is applied to σ_{E_T} so that $C_M \sigma_{E_T}$ gives the average cross section for the thermal flux. In order to measure ϕ_{th}, one must somehow differentiate between the quantities of radioactive nuclei produced by slow and fast neutrons. This can be done by first making measurements with a cover placed over the detecting material. This will screen out one of the two neutron groups. A material for which σ_a varies as shown below is needed.

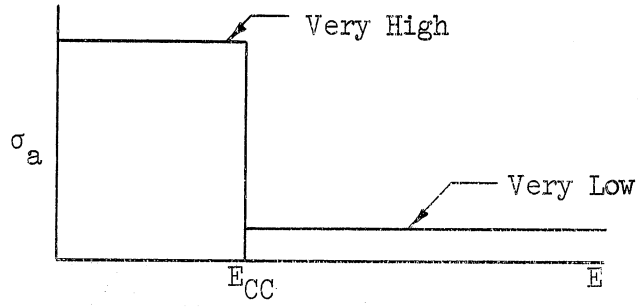

Figure 8.28 Idealized Absorption Coefficient vs. Energy for Screening Slow from Fast Neutrons.

Here E_{CC} is the cutoff energy. We would like to have $E_{CC} \approx E_{TC}$. A rough plot of σ_a for cadmium is shown below

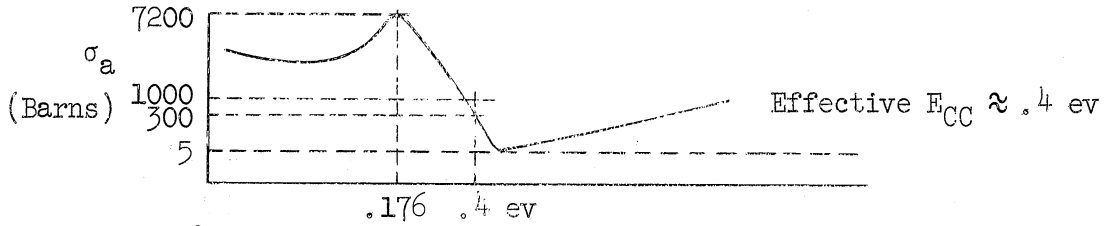

Figure 8.29 Approximate Absorption Coefficient for Cadmium.

Now if we assume that no neutrons with $E < E_{CC}$ get through the cover, and that all neutrons with $E > E_{CC}$ go through it, we have:

$$R_C = N_D \int_{E_{CC}}^{\infty} \sigma_a (E) \phi (E) dE$$

With a bare detector, that is, with no cover, we have

$$R_b = N_D \left[C_M \sigma_{E_T} \phi_{th} + \int_{E_{TC}}^{E_{CC}} \sigma_a (E) \phi (E) dE + \int_{E_{CC}}^{\infty} \sigma_a (E) \phi (E) dE \right]$$

R_b/R_c is called the cadmium ratio.
Taking the difference of the two rates:

$$R_b - R_c = N_D \left[C_M \sigma_{E_T} \phi_{th} + \int_{E_{TC}}^{E_{CC}} \sigma_a (E) \phi (E) dE \right]$$

Let us now look at the integral term. For the energy $E_{TC} < E < E_{CC}$ let $\sigma_a(E) \approx \sigma_o/\sqrt{E}$ and $\phi(E) \approx \phi_0/E$, where σ_0 and ϕ_0 are appropriate constants. We now may write:

$$\int_{E_{TC}}^{E_{CC}} \frac{\sigma_0}{\sqrt{E}} \frac{\sigma_0}{E} dE = \sigma_0 \phi_0 \int_{E_{TC}}^{E_{CC}} E^{-3/2} dE$$

$$= \sigma_0 \phi_0 \left[-2E^{-1/2} \right]_{E_{TC}}^{E_{CC}} = 2\sigma_0\phi_0 \left[\frac{1}{\sqrt{E_{TC}}} - \frac{1}{\sqrt{E_{CC}}} \right]$$

But $\sigma_{th} = \frac{\sigma_0}{\sqrt{.025}}$, so that $\sigma_0 = \sqrt{.025}\ \sigma_{th}$
where σ_{th} is the value of $\sigma_a(E)$ at .025 ev.

Also, $\sigma_{E_T} = \frac{\sqrt{.025}}{\sqrt{E_T}}\ \sigma_{th}$, so that

$$R_b - R_c = N_D \left[C_M \sqrt{\frac{.025}{E_T}}\ \sigma_{th} \phi_{th} + 2\sqrt{.025}\ \sigma_{th} \phi_0 \left(\frac{1}{\sqrt{E_{TC}}} - \frac{1}{\sqrt{E_{CC}}} \right) \right]$$

If we define $\bar{\sigma}_{th} = C_M \sigma_{E_T} = C_M \sqrt{\frac{.025}{E_T}}\ \sigma_{th}$, we get

$$R_b - R_c = N_D \left[\bar{\sigma}_{th} \phi_{th} + \frac{2}{C_M} \sqrt{E_T}\ \sigma_{th} \phi_0 \left(\frac{1}{\sqrt{E_{TC}}} - \frac{1}{\sqrt{E_{CC}}} \right) \right]$$

So that finally we may write

$$R_b - R_c = N_D \bar{\sigma}_{th} (\phi_{th} + k \phi_0)$$

where k is a constant. For example, for $E_T = .03$ ev, $E_{TC} = .2$ ev, $E_{CC} = .4$ ev. $C_M = \sqrt{\pi/4}$,

Correction Factors:

~ 1/.845 for .75" dia. 5 mil In.
~ 1/.84 for 1.5" dia. 5 mil In.
~ 1/.86 for 1.5" dia. 5 mil Au.

REFERENCES:

1. Deutsch, R. W., "Computing Three-Group Constants for Neutron Diffusion," Nucleonics, Vol. 15, No. 1 (1957).

2. Dayton, I. E., and Pettus, W. G., "Effective Cadmium Cutoff Energy," Nucleonics, Vol. 15, No. 12 (1957).

3. Tittle, C. W., "Slow Neutron Detection by Foils" I and II, Nucleonics, Vol. 8, No. 6 and Vol. 9, No. 1 (1951).

4. Martin, D. H., "Correction Factors for Cd-Covered Foil Measurements," Nucleonics, Vol. 13, No. 3 (1955).

5. Gallagher, T. L., "Foil Depression Factors for Indium Discs Detectors," Nuclear Science and Engineering, Vol. 3, No. 1 (1958).

6. Klema, E. D., and Ritchie, R. H., "Thermal Neutron Flux Measurements in Graphite Using Gold and Indium Foils," Phys. Rev., 87, 167 (1952).

7. J. L. Shapiro et al, "Initial Calibration of the Ford Nuclear Reactor," MMPP 110-1, April, 1958.

8.38 Experiment on Neutron Detection by Induced Activity

You will be given a number of foils which have been exposed to neutrons in a subcritical nuclear reactor assembly. You will also be given the following data: the time of insertion and withdrawal of the foils, the weights of the foils, and their relative positions during irradiation.

By measuring the activity of the foils and making use of the supplied data, compute the relative magnitudes of the neutron flux at the points where the foils were exposed, and plot the logarithm of some quantity directly proportional to the neutron flux against position. Please state clearly what quantity you are plotting. The plot should show the standard deviations associated with the quantities which are plotted.

$$k = .258$$

Now if $\phi_{th} \gg k\,\phi_0$, and it usually is, we may take

$$R_b - R_c \approx N_D\,\bar{\sigma}_{th}\,\phi_{th}$$

One should, however, distinguish between the thermal flux and the subcadmium flux at least in principle. Reference 1 discusses the determination of E_T and E_{TC}, and reference 2 the determination of the effective E_{CC}.

Up to this point we have dealt with the rates of the production of the radioactive nuclei. Now we must relate this quantity to one that we can measure. The quantity that we measure is the rate of disintegration of the radiocative nuclei at the time of measurement, which is some time after the removal of the detector from the neutron flux.

The buildup of the radioactive nuclei during irradiation is described by the equation

$$\frac{dN_R}{dt} = R - \lambda N_R$$

If $N_R\ (t = 0) = 0$:

$$N_R = \frac{R}{\lambda}\left(1 - e^{-\lambda t}\right)$$

Here t is the time of irradiation, R the rate of production of the radioactive nuclei, N_R the number of such nuclei, and λ their decay constant. The rate of disintegration A during irradiation is

$$A = \lambda N_R = R\left(1 - e^{-\lambda t}\right)$$

As $t \to \infty$, $A \to R$, the so called saturated activity A_∞.

$$A_\infty = R = \frac{A}{1 - e^{-\lambda t}}$$

After removing the detector from the neutron flux at $t = t_1$, A will fall exponentially:

$$A = A(t_1)\, e^{-\lambda(t-t_1)} = A(t_1)\, e^{\lambda t_1}\, e^{-\lambda t}$$

The time behavior of A is sketched below:

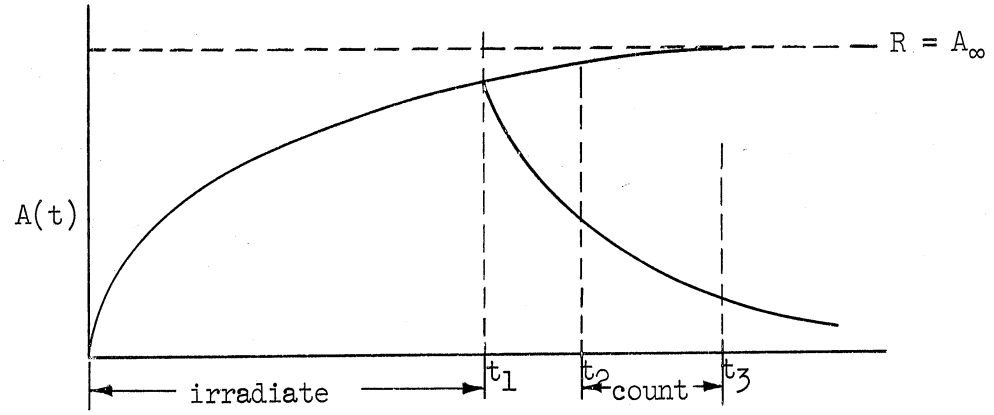

Figure 8.30 Detector Foil Activity During Irradiation and Counting.

Counting the decaying nuclei with counting efficiency f from t_2 to t_3, the number of counts, C, is:

$$C = f \int_{t_2}^{t_3} A(t\,)\, e^{\lambda t_1}\, e^{-\lambda t}\, dt + \text{background}$$

$$= fA(t_1)\, e^{\lambda t_1} \left[-\frac{1}{\lambda} e^{-\lambda t} \right]_{t_2}^{t_3} + \text{background}$$

$$= fA(t_1)\, e^{\lambda t_1}\, \frac{1}{\lambda} (e^{-\lambda t_2} - e^{-\lambda t_3}) + \text{background}$$

but $A(t_1) = R(1 - e^{-\lambda t_1})$,
and if we define $C_{corrected} \equiv C$ - background,
then

$$C_{corrected} = f\, R\, \frac{1}{\lambda} (e^{\lambda t_1} - 1)(e^{-\lambda t_2} - e^{-\lambda t_3})$$

so that

$$R = \frac{C_{corr}/f}{\frac{1}{\lambda} (e^{\lambda t_1} - 1)(e^{-\lambda t_2} - e^{-\lambda t_3})}$$

The analysis up to this point has neglected the following facts:

1) Some neutrons with $E < E_{CC}$ pass through the Cd cover.

2) The Cd cover stops some of the neutrons with $E > E_{CC}$.

3) The presence of the dector with its relatively high absorption cross section depresses the neutron flux.

4) The detector has a finite thickness, and therefore the inner volume elements are shielded by the outer ones, that is, the activity per unit volume is uniform. A detailed discussion of the above factors is beyond the scope of this paper. Only an indication of the results of some experimental investigat.ons will be shown. References 3 through 6 should be consuled for further information.

The first two effects mentioned above can be investigated by irradiating detectors with different thicknesses of Cd cover. A typical plot of A_∞ vs. Cd cover thickness.

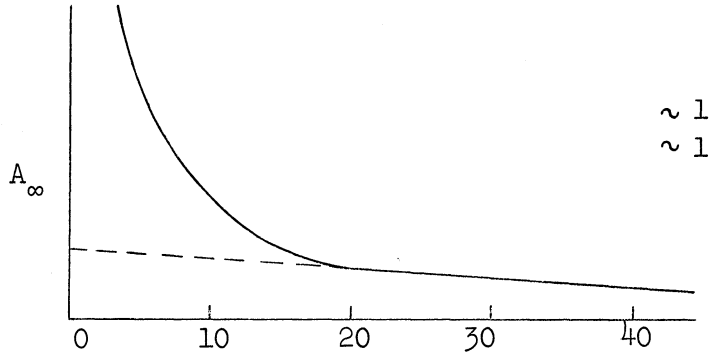

Correction Factors:

$\sim$ 1.1 for 5 mil In, 40 mil Cd
$\sim$ 1.02 for 5 mil Au, 40 mil Cd

Figure 8.31 Detector Foil Activity vs. Cadmium Cover Thickness.

The shape of the curve depends on several factors, such as the material and dimensions of the detector, the medium in which the measurements are made, and the Cd ratio. The steep slope at and below 10 mils of Cd thickness shows that more than a negligible number of sub-Cd neutrons reach the detector. More than about 20 mils of seems to reduce this leakage enought so that only a small slope remains indicating the absorption of the epi-Cd neutrons by simply extrapolating the slope to zero Cd cover thickness.

Effects 3 and 4 can be investigated by irradiating detectors of different thicknesses, plotting the activity per unit thickness against detector thickness, d, and again extrapolating to zero thickness. The slope of such a curve will depend on the detector material and dimensions, and the medium in which the measurements are made. A typical plot is shown below

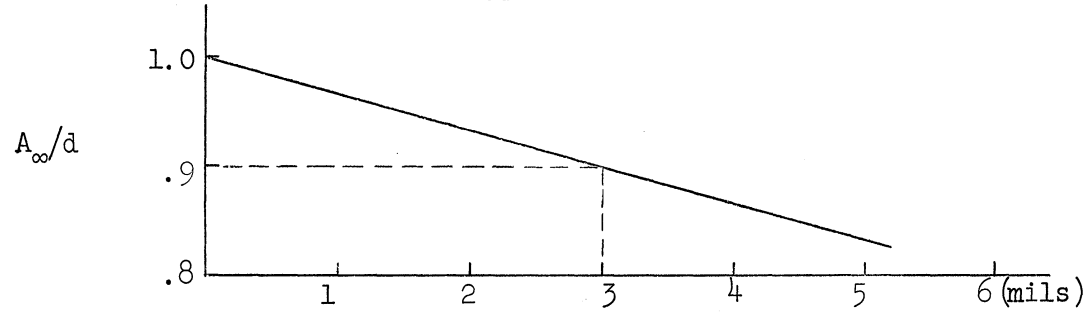

Figure 8.32 Detector Activity, Per Unit Thickness vs. Detector Thickness.

8.39 Fundamentals of Junction-Type Solid State Ionization Detector (Jointly with G. Brown)

Rapid progress has been made in solid state detector technology since McKay[1] first measured alpha particles with a p-n junction in 1951. Detectors are now available which are suitable for the measurement of charged particles and gamma radiation. Although the principles of operation are well known to semiconductor physicists, many workers have not had the opportunity to obtain more than just a descriptive understanding of the solid state detectors.

The relations obtained in this section for barrier layer depth and electrostatic potential, as a function of reverse bias, apply to both the p-n junction and surface barrier detectors. In addition to specific references in this paper, references 4 to 7 should provide helpful information for further study. Conventional notation[2] is used wherever possible. Because this detector is not considered by Price, considerable mathematical detail will be given.

8.40 Junction Detector

Consider a crystal of a group IV element, such as silicon, with a very small amount of group III impurity such as boron homogeneously distributed in the lattice. The group III atoms act as electron acceptors in order to satisfy the bond requirements of the surrounding group IV lattice elements. The positions in the crystal from which these electrons migrate are positively charged relative to the negatively charged group III lattice position. Since the group III atoms are fixed in the lattice, most of an electric current would be carried by positively charged "holes", moving through the crystal. When the majority of the charge carriers are holes, the crystal is p-type. If the impurity had been group V, such as arsenic, an electron would be available to the lattice from this donor impurity, because of the low dissociation energy, resulting in a positively charged ion in the lattice and most of the current carried by negative electrons. When the majority of the charge carriers are electrons, the crystal is n-type. The silicon p-n junction detector is made by diffusing a group V element into a silicon crystal with a group III impurity. The transition region in the crystal is described by the distribution of the equilibrium concentrations of electrons, holes and ionized impurities. The n and p type portions of the crystal have low resistivity compared to the transition region. When an external voltage is applied, essentially all the potential difference takes place across the transition region. Since the width of this region is usually less than 10^{-2}cm, high electric fields are developed. When an ionizing particle enters this region and produces electron hole pairs, i.e., raises electrons from the valence band to the conduction band, the electrons and holes are swept across the barrier in opposite directions by the electric field. The resulting induced charge gives a measurable voltage pulse in the external circuit.

8.41 Fermi Statistics

The probability, f(E), that a quantum state of energy E is occupied by an electron at equilibrium is,

$$f(E) = 1/[e^{(E-E_F)/kT} + 1] \tag{1}$$

and is known as the Fermi distribution function.[2] The Fermi energy level, E_F, can be given physical significance as the half occupancy energy since $f(E) < 0.5$ for $E > E_F$. (1) is valid for particles which obey the Pauli principle. The probability of non-occupancy of a quantum state is 1-f(E), or equivalently, is the probability of occupancy by a hole.

The concentration of allowed energy levels in the conduction band which lie in the energy interval dE about E is given by

$$D_c(E)\,dE = \frac{N_c}{kT\sqrt{\pi}} \left(\frac{E-E_c}{kT}\right)^{1/2} dE \tag{2}$$

where E_c is the electron energy at the lower edge of the conduction band and N_c is the effective density of states in the conduction band. Explicitly,

$$N_c = 2\left(\frac{2\pi\, m_n\, kT}{n^2}\right)^{3/2} \tag{3}$$

The concentration of electrons in the conduction band is given by

$$n = 2\int_{E_c}^{\infty} D_c(E)\, f(E)\, dE \tag{4}$$

The factor of 2 accounts for the spin degeneracy for each energy level. Assuming that $E_F < |E_c - 3kT|$ gives $f(E) \underline{\sim} \exp[(E_F - E)/kT]$. The solution of (4) is

$$n \underline{\simeq} N_c \exp[(E_F - E_c)/kT] \tag{5}$$

The concentration of allowed energy levels in the valence band in dE about E is analogously given by

$$D_v(E)\,dE = \frac{N_v}{kT\sqrt{\pi}}\left(\frac{E_v-E}{kT}\right)^{1/2} dE \qquad (6)$$

where $N_v = 2\left(\frac{2\pi m_p kT}{h^2}\right)^{3/2}$ is the effective density of states in the valence band, and m_p is the effective mass of the hole at the uppermost energy of the valence band, E_v. Similarly to (4), the concentration of holes in the valence band is given by

$$p = 2\int_{-\infty}^{E_v} D_v(E)\,[1 - f(E)]\,dE$$

with the solution

$$p \simeq N_v \exp\,[(E_v-E_F)\,kT] \qquad . \qquad (7)$$

For an intrinsic semiconductor, $n = n_i = p = p_i$. Equating (5) and (7) and solving for the Fermi level in an intrinsic semiconductor,

$$E_F = \frac{(E_v+E_c)}{2} + \frac{3}{4}\,kT\,\ell n\,\frac{m_p}{m_n} \qquad . \qquad (8)$$

At thermal equilibrium, $np = n_i^2$. Thus, from (5) and (7),

$$n_i = \sqrt{N_c V_v}\quad \exp\,[-(E_c-E_v)/2kT] \qquad (9)$$

It is shown[2] that $f(E_D)$, the probability that a donor energy level be occupied by an electron, is

$$f(E_D) = 1/[\,\frac{1}{2}\exp\,\{(E_D-E_F)/kT\} + 1]$$

where E_D is the electron energy at the donor level. If the concentration of donors is n_D at E_D, $n_D f(E_D)$ are neutral and $n_D[1 - f(E_D)]$ are positively charged and a corresponding number of electrons are raised to the conduction band. For the condition $(E_D - 3kT) > E_F$, $n_D \simeq n_{D+}$, i.e., the impurities are totally ionized.

For an acceptor impurity,

$$f(E_A) = 1/[\,2 \exp\{(E_A-E_F)/kT\} + 1] \qquad (10)$$

If n_A is the total acceptor concentration, $n_A f(E_A) = n_{A^-}$ will be occupied by an electron from the valence band, leaving a corresponding concentration of holes in the valence band. For $(E_A + 3kT) < E_F$, $n_A \simeq n_{A^-}$.

8.42 Effect of Impurity Concentration Change and Bias on the Fermi Level

In a region where the space charge density, ρ, is zero, the condition of electric neutrality is given by

$$n_{D^+} - n_{A^-} = n - p \simeq n_D - n_A \qquad (11)$$

Substituting for n and p from (5) and (7),

$$n_D - n_A = N_c \exp[(E_F-E_c)/kT] - N_v \exp[(E_v-E_F)/kT] \qquad (12)$$

When $n_D \gg n_A$, the Fermi level on the donor side of the junction can be found directly from (12),

$$E_{F_n} = E_c - kT\, \ell n\, (N_c/n_D) \qquad (13)$$

When $n_D \ll n_A$, on the acceptor side,

$$E_{F_p} = E_v + kT\, \ell n\, (N_v/n_A) \qquad (14)$$

When $n_D = n_A$,

$$E_F = \frac{(E_v+E_c)}{2} + \frac{kT}{2}\, \ell n\, (N_v/N_c) \qquad (15)$$

Note that (15) is almost identical with (8) which described E_F in an intrinsic semiconductor. Since N_v and N_c are on the order of $10^{19}cm^{-3}$ at 300°K and the impurities are on the order of $10^{21}cm^{-3}$ and less, it is possible for $E_F < E_c$.

Consider the effect of an externally applied potential or bias, V_o. Using a reverse bias, i.e., the n side of the junction is made more positive with respect to the p side, the Fermi level is displaced by an amount eV_o,

since thermal equilibrium has been destroyed. As a first approximation, it can be assumed that the spatial forms of n and p are not changed, in other words, that the applied voltage can be superimposed on the internally developed space charge potential.

8.43 Depletion Depth and Barrier Capacitance

The ratio of the depletion depth to the range of an ionizing particle gives an estimate of the fraction of its energy transferred to the crystal. Since linearity between incident particle energy and detector pulse output is desirable, the depletion depth for a given detector should be known. By relating the internal detector potential to this depth theoretically, the depth can be found by a simple measurement. Alternatively, if a known energy is deposited, and the output pulse observed, the depth can be found from the capacitance per unit area.

Consider a p-n junction geometry for which the space charge is zero on the p side at $x \leq -x_p$, $n_{D^+} = n_{A^-}$ at $x = 0$ and the space charge is zero on the n side at $x \geq x_n$. In general, n_{D^+} will depend on the method used to make the diffused junction and the degree of perfection of the crystal. Ideally, $n_D(x) = n_D(-x_p)\ \mathrm{erfc}\ (x/2\sqrt{Dt})$, where D is the diffusion coefficient for impurity atoms in the crystal at some chosen temperature for a diffusion time, t. This distribution falls off sharply with x and makes an analytic solution of the potential problem unattainable. The junction is defined at the position in the crystal where $n_{D^+} = n_{A^-}$. The Fermi level is constant, however, throughout the entire crystal when no external bias is applied.

From (5) and (7) the distributions for electrons and holes on either side of the junction are known,

$$\begin{aligned} n_n(x) &= N_c \exp\left[(E_F - E_{cn}(x))/kT\right] \\ p_n(x) &= N_v \exp\left[(E_{vn}(x) - E_F)/kT\right] \\ p_p(x) &= N_v \exp\left[(E_{vp}(x) - E_F)/kT\right] \\ n_p(x) &= N_c \exp\left[(E_F - E_{cp}(x))/kT\right] \end{aligned} \tag{16}$$

Since $n \simeq n_D$ for $x > x_n$, $n_D \gg n_i$ and $p \simeq n_A$ for $x < -x_p$, $n_A \gg n_i$, i.e., outside the depletion region,

$$n(x \geq x_n) \simeq n_D \simeq N_c \exp\left[(E_{cn} - E_F)/kT\right] \tag{17}$$

and

$$p(x \leq -x_p) \simeq n_A \simeq N_v \exp\left[(E_{vp} - E_F)/kT\right]$$

Substituting for N_c and N_v from (17) into (16) and replacing $E_{cn}(x)$ and $E_{cp}(x)$ by $E_c(x)$, and $E_{vn}(x)$ and $E_{vp}(x)$ by $E_v(x)$ gives,

$$\begin{aligned} n(x) &= n_D \exp\left[(E_{cn}-E_c(x))/kT\right] \\ p(x) &= n_A \exp\left[(E_c(x)-E_{cp})/kT\right] \end{aligned} \tag{18}$$

since $E_v(x) - E_{vp} = E_c(x) - E_{cp}$.

The crystal energy levels can be replaced by the electrostatic potential, since $E = -eV$ giving,

$$\begin{aligned} n(x) &= n_D \exp\left[e(V(x) - V_D)/kT\right] \\ p(x) &= n_A \exp\left[-eV(x)/kT\right] \end{aligned} \tag{19}$$

where $V(x < -x_\rho) = 0$ and $V(x > x_n) = V_D$. The potential drop across the depletion region is found from (19) by solving the ratio $p(x < -x_p)/p(x > x_p) = p_n/p_p = \exp\left[eV_D/kT\right]$ for V_D. Using $p_p \simeq n_A$, $p_n \simeq n_i^2/n_D$ gives

$$V_D = \frac{kT}{e} \ell n \left(n_A n_D/n_i^2\right) \quad , \tag{20}$$

The space charge density is given in general by

$$\rho(x) = e[p(x) - n(x) + n_{D+}(x) - n_{A-}(x)] \tag{21}$$

Assuming the permittivity of the junction region is constant, the one dimensional electrostatic potential is obtained by solving the Poisson equation,

$$\frac{d^2V}{dx^2} = - \rho(x)/\epsilon \tag{22}$$

For convenience, assume $n_{D+}(x)$ is a constant, n_{D+} for $0 < x \leq x_n$, and more reasonably that $n_{A-}(x)$ is constant for $-x_p \leq x < 0$, and $n_{D+} = n_{A-} = 0$, otherwise. Combining (19), (21) and (22),

$$\frac{d^2V}{dx^2} = \frac{e}{\epsilon}\left[n_{D+}\left\{e^{e(V(x)-V_D)/kT} - 1\right\} - n_{A-}\left\{e^{-\frac{eV(x)}{kT}} - 1\right\}\right] \tag{23}$$

where $n_{D+} = 0$ for $x < 0$, and $n_{A-} = 0$ for $x > 0$. Multiplying (23) by dV/dx and integrating over x, gives

$$\left(\frac{dV}{dx}\right)^2 = \frac{2en_{D+}}{\epsilon}\left[\frac{kT}{e}\left(1 - e^{e(V-V_D)/kT}\right) + V(x) - V_D\right] \tag{24}$$

For $0 < x < x_n$, and

$$\left(\frac{dV}{dx}\right)^2 = \frac{2en_{A^-}}{\epsilon}\left[\frac{kT}{e}\left(-1 + e^{-eV/kT}\right) + V(x)\right] \qquad (25)$$

For $-x_p < x < 0$.
Equating (24) and (25) at $x = 0$ and rearranging gives,

$$V(0)\,[n_{D^+} - n_{A^-}] - \frac{kT}{e}\,[n_{D^+} \exp\{e(V(0) - V_D)/kT\} \qquad (26)$$

$$+ \left(n_A -\right)\exp\{-eV(0)/kT\} = n_{D^+} V_D - \frac{kT}{e}\,[n_{D^+} + n_{A^-}]$$

which is useful for determining $V(0)$.

The electric field, $E_x = \frac{-dV}{dx}$, is known for the entire depletion region from (24) and (25). However, because (24) and (25) are non-linear, no closed solution for $V(x)$ has been found. Making a further approximation[3], let

$$\rho(x) = e[n_{A^-} - n_{D^+}] \qquad (27)$$

where $n_{A^-} = 0$ for $x > 0$ and $n_{D^+} = 0$ for $x < 0$.

The solution of (27) proceeds straightforwardly. Using the boundary conditions that

$$V(-x_p) = 0,\ \left.\frac{dV}{dx}\right|_{-x_p} = 0,\ V(x_n) = V_D \text{ and } \left.\frac{dV}{dx}\right|_{x_n} = 0$$

gives

$$\left.\begin{aligned} E_x(x) &= +\frac{en_A}{\epsilon}\,(x + x_p) \\ V(x) &= \frac{en_{A^-}}{2\epsilon}\,(x + x_p)^2 \end{aligned}\right\} -x_p < x < 0 \qquad (28)$$

and

$$\left.\begin{aligned} E_x(x) &= -\frac{en_{D^+}}{\epsilon}\,(x_n - x) \\ V(x) &= V_D - \frac{en_{D^+}}{2\epsilon}\,(x_n - x)^2 \end{aligned}\right\} 0 < x < x_n$$

The maximum field, at x = 0, is

$$E_{max} = \frac{en_A x_p}{\epsilon} = \frac{en_D x_n}{\epsilon} \tag{29}$$

and, also, from (28) at x = 0

$$V_D = \frac{e}{2\epsilon}\left(n_D x_n^2 + n_A x_p^2\right) \tag{30}$$

The condition of electric neutrality is, $n_A x_p = n_D x_n$, i.e.,

$$\int_{-\infty}^{\infty} \rho(x)\, dx = 0 \tag{31}$$

Solving (30) and (31) for the depletion widths, $n_D \gg n_A$,

$$\begin{aligned} x_p &\simeq \left(2\epsilon V_D/en_A\right)^{1/2} \\ x_n &\simeq \left(2\epsilon V_D n_A/en_D^2\right)^{1/2} \end{aligned} \tag{32}$$

The barrier capacity per unit area, C is given by

$$C = \frac{\epsilon}{x_p + x_n} \simeq \frac{\epsilon}{x_p} \simeq \left(e\epsilon n_A/2V_D\right)^{1/2} \tag{33}$$

Another impurity distribution which partially fits empirical results in the graded junction,

$$\rho(x) = a\, x$$

where a is

$$a = \frac{n_D(x_n) - n_A(x_n)}{x_n} = \frac{n_D(-x_p) - n_A(-x_p)}{-x_p}$$

The solutions are

$$\left.\begin{aligned} E_x &= \frac{ea}{2\epsilon}\left(x^2 - x_p^2\right) \\ V(x) &= \frac{ea}{2\epsilon}\left(-\frac{x^3}{3} + x_p^2\, x + \frac{2}{3} x_p^3\right) \end{aligned}\right\} -x_p \leq x < 0 \tag{34}$$

and, $E_x = \frac{ea}{2\epsilon}(x^2 - x_n^2)$

$$V(x) = -\frac{ea}{2\epsilon}\left(\frac{x^3}{3} - x_n^2 x + \frac{2}{3}x_p^3\right) + V_D \quad \left.\right\} \; 0 < x \leq x_n \tag{35}$$

At $x = 0$, $V_D = \frac{ea}{3\epsilon}[x_n^3 + x_p^3]$

For electric neutrality

$$\int_{-x_p}^{x_n} axdx = 0 \tag{36}$$

giving $x_p = x_n$. From (35)

$$x_n = \left(\frac{3\epsilon V_D}{ea}\right)^{1/3} \tag{37}$$

and,

$$c = \frac{\epsilon}{2x_n} = \left[\frac{\epsilon^2 ea}{24 V_D}\right]^{1/2} \tag{38}$$

These models predict a slope in $\ell n\, c_D$ vs $\ell n\, V_D$ of -1/2 and -1/3. Experimentally, these are representative values, giving some credence to their usefulness.

8.44 Balance Equation and Pulse Output

The equation which describes the position of the electrons and holes produced by ionizing radiation in the depletion region is common to many branches of science[2,3].

$$\nabla \cdot \underline{J} = -\frac{\partial \rho}{\partial t} \quad . \tag{39}$$

$\underline{J}$ is the total current,

$$J = e\underline{E}[n\mu_n + p\mu_n] + e[D_n \nabla_n - D_p \nabla_p] \tag{40}$$

and μ_n is the electron mobility, D_n is the diffusion coefficient for electrons, etc.

The approximate location and time of creation of ion pairs can be estimated. Depending on the degree of approximation, (39) can be solved either in closed form or by machine iteritive procedures.

The charge induced on the electrodes by the electrons and holes is known. The voltage pulse form to the scaler or analyzer can be calculated as a simple RC circuit.

To get an appreciation of the magnitudes of the various quantities associated with these detectors, consider a particular p-n silicon junction detector.

8.45 Range of α Particle in Silicon

The range of an alpha particle in silicon can be estimated within 15 per cent by the Bragg-Kleeman rule,

$$R_\alpha^{Si} = 3.2 \times 10^{-4} \times \frac{\sqrt{A_{Si}}}{\rho_{Si}} \times R_\alpha^{air}$$

The range in air of a 5.3 Mev P_o^{210} α-particle is approximately $R_\alpha^{air} \simeq 3.9$ cm . For silicon, A = 28 and $\rho_{Si} = 2.33$ gm/cm^3. Thus

$$R_\alpha^{Si} \simeq \frac{(3.2 \times 10^{-4})(\sqrt{28})(3.9)}{(2.33)}$$

$$\simeq 29.1 \times 10^{-4} \text{ cm} = 29.1 \ \mu\text{m}.$$

Now, for the detector under consideration,

$$d_a \simeq 93 \ \mu\text{m}$$

$$d_d \simeq .09 \ \mu\text{m}$$

Including the junction depth ($\simeq$ 1μm), the depletion region extends approximately 94 μm into the detector. Thus, a P_o^{210} α particle will lose all its energy in the depletion region.

The amount of ionization produced in the detector is proportional to the incident α-energy, as long as $R_\alpha^{Si} < d_a$. If $R_\alpha^{Si} > d_a$, ionization occurs outside of the depletion region. These e-h pairs may diffuse back into the depletion region and be collected. However, most of these e-h pairs recombine before this occurs.

At what alpha energy would non-linearity be expected to occur? The answer to this question, of course, is that energy where the range in silicon exceeds the depletion depth. Using the Bragg-Kleeman relation R_α^{air} is determined by substituting $R_\alpha^{Si} = 94$ μm.

$$R_\alpha^{air} \simeq \frac{R_\alpha^{Si}\ \rho_{Si}}{(3.2 \times 10^{-4})\sqrt{A_{Si}}} \simeq 13.18 \text{ cm.}$$

From Price (page 8) the energy of an α particle corresponding to a range in air of 13.2 cm is 11.4 Mev. Thus, with a reverse bias of 100v, non-linearity would be expected to occur for α particles whose incident energy is > 11.4 Mev. Of course, increasing the reverse bias would extend this energy limit.

8.46 Energy Loss by Incident α-Particle

A charged particle moving through material loses most of its energy by ionization. The energy loss per unit path is given by the relativistic relation derived in an earlier part of this chapter,

$$\frac{-dE}{dx} = \frac{4\pi e^4 z^2 NZ}{m_o v^2} \ln \frac{2m_o v^2}{J}$$

where: z = +2 or +1 for alpha particle
N = 0.50×10^{23} atom/cm^3 for silicon
Z = 14 for silicon
m_o = 9.11×10^{-28} gm = rest mass of electron
J = ionization potential ≃ .4 ev
v = velocity of charged particle .

After the alpha particle slows down to a speed approximately equal to the speed of an orbital electron of a helium atom, the alpha picks up an orbital electron $He^{++} + e \rightarrow He^{+}$.

8.47 Limiting Energy of Ionization (E_i)

When the energy of an incident α is reduced to some value E_i (called limiting energy of ionization), atomic displacement replaces ionization as being the predominate method for losing energy.

The energy degradation formula may be rewritten as

$$\frac{-dE}{dx} = \frac{k}{\alpha} \ln \frac{\alpha}{J}$$

where: $k = 8\pi 4z^2 NZ$
$\alpha = 2m_o v^2$

By setting the first derivative of the above with respect to α equal to zero, it can be shown that -dE/dx reaches a maximum at some alpha energy

$$\frac{d}{dx}\left[\frac{1}{\alpha}\ln\frac{\alpha}{J}\right] = 0$$

$$\frac{1}{\alpha}\frac{d\ln\alpha/J}{d\alpha} + \ln\alpha/J\,\frac{d(1/\alpha)}{d\alpha} = 0$$

$$\frac{1}{\alpha}\frac{\ln(\alpha/J)}{d\alpha} + \ln a/J\,(-1/\alpha^2) = 0$$

$$\ln\alpha/J = \alpha\frac{d\ln\alpha/J}{d\alpha} = \alpha\frac{1}{\alpha/J}\frac{d(\alpha/J)}{d\alpha} = 1$$

$$\alpha/J = e = 2.71$$

$$\alpha = 2m_o v^2 = 2.71\,J$$

The energy of the incoming α-particle is $E = 1/2\ m_\alpha v^2$. Thus $2m_o v^2 = 2m_o\frac{2E}{m_\alpha} = 2.71\,J$ or

$$E_m^{\,2} = \left(\frac{2.71}{4}\right)\cdot J\left(\frac{m_\alpha}{m_o}\right) = \text{energy at which maximum dE/dx occurs.}$$

Also, as $2m_o v^2 \to J$ the energy degradation formula approaches zero.

$$\frac{-dE}{dx} = \frac{k}{\alpha}\ln\frac{\alpha}{J} \to 0 \quad \text{as } \alpha \to J$$

$$\alpha/J = 1$$

$$2m_o v^2 = J$$

Substituting $\ln v^2 = 2E/m_\alpha$,

$$E_F = \frac{1}{4}\cdot\frac{m_\alpha}{m_o}\cdot J$$

which is the energy at which ionization is no longer predominate. Most ionization occurs around the maximum point, which is near the end of the α range.

8.48 Time Required for α to Complete Ionization

In order to get an idea of the length of time required for an α particle to ionize completely, the alpha range R_α^{Si} is divided by the initial velocity of the α and then by the velocity where atomic displacement predominates. The time for ionization will lie in these limits. The initial velocity v_o of a 5 Mev α particle is

$$v_o = \frac{2E_\alpha}{m_\alpha} = \frac{2 \times (5 \times 10^6)(1.602 \times 10^{12} \text{ gm cm}^2/\text{sec})}{6.69 \times 10^{-24} \text{gm}}$$

$$= 1.55 \times 10^9 \text{ cm/sec} = 1.55 \times 10^7 \text{ m/sec.}$$

The energy at which atomic displacement becomes predominate is $E_F = \frac{1}{4} \frac{m_\alpha}{m_o} J$.

$$v_F = \frac{1}{2} \frac{m_\alpha}{m_\alpha m_o} J = \frac{.5 \times .4 \text{ ev} \times 1.602 \times 10^{-12}}{9.11 \times 10^{-28}} = \sqrt{3.52 \times 10^{-16}}$$

$$= 1.88 \times 10^{+8} \text{ cm/sec} = 1.88 \times 10^6 \text{ m/sec.}$$

The minimum time is given by

$$\tau_{min} = \frac{29.1 \times 10^{-6} \text{ m}}{1.55 \times 10^7 \text{m/sec}} = 18.8 \times 10^{-13} \simeq 1.9 \times 10^{-12} \text{ sec.}$$

Similarly, τ_{max} is

$$\tau_{max} = \frac{29.1 \times 10^{-6} \text{ m}}{1.88 \times 10^6 \text{m/sec}} = 15.5 \times 10^{-12} = 1.6 \times 10^{-11} \text{ sec}$$

Thus, the time to complete ionization is less than 1.6×10^{-11} sec and more than 1.9×10^{-12} sec.

8.49 Estimation of Charge Collection Time and Charge Collected

Neglecting diffusion currents, and assuming a constant average electric field in the depletion region, the total current density is given by

$$J = e \mu_n n \xi + e p \mu_p \xi$$

Let V = volume of depletion region, A = cross sectional area and d = deplation depth. The total current is given by

$$I = AJ = e \frac{N}{V} \mu_n \xi A + \frac{P}{V} \mu_p \xi A$$

The charge collected in time Δt is

$$\Delta Q = I \Delta t = e \Delta t \left(\frac{N}{d} \mu_n \xi + \frac{P}{d} \mu_p \xi \right)$$

Now, $v_n = \mu_n \xi$ and $v_p = \mu_p \xi$

thus, $\Delta x_n = \frac{\Delta x_n}{\Delta t} \Delta t = v_n \Delta t = \mu_n \xi \Delta t$

and $\Delta x_p = \frac{\Delta x_p}{\Delta t} \Delta t = v_p \Delta t = \mu_p \xi \Delta t$

The total charge collected is

$$\Delta Q = Ne \frac{(\Delta x_n + \Delta x_p)}{d} .$$

If all electrons and holes reach the electrodes, $\Delta x_n = x_n$ and $\Delta x_p = x_p$ and

$$\Delta Q = Ne \frac{(x_n + x_p)}{d} = Ne ,$$

since $x_n + x_p = d$, where x_n is the distance from the point of e-h formation to the p electrode and x_p is the distance to the n electrode. If the e-h pairs do not reach the plate, the following inequality holds

$$Q = \frac{Ne(\Delta x + \Delta x_p)}{d} < Ne$$

The maximum time required for an electron to induce all its charge is determined in the following manner. Assume the e-h pair is formed just inside the p electrode. The electron will migrate to the n electrode under the effect of the electric field. The time for an electron to do this gives an indication of how fast the charge is collected (this is a lower limit). Let the electric field be $\xi_{av} = 10^5$ v/cm, and the electron mobility be $\mu_n = 1300$ cm^2/V sec. Then the average velocity of the electron is $v_n = \mu_n \xi_{av} = 1.3 \times 10^8$ cm/sec. The time to travel the width of the depletion region $d \simeq 93 \times 10^{-4}$ cm is

$$\tau = \frac{93 \times 10^{-4} \text{ cm}}{1.3 \times 10^8 \text{ cm/sec}} = 72 \times 10^{-12} \simeq 7 \times 10^{-11} \text{ sec.}$$

8.50 Estimation of Voltage Output of the Detector

Assume the following:

1. Detector biased 100 v negative.

2. Barrier layer capacitance $C_d = .2\,65\ \mu\mu f/mm^2 \times 2\ mm^2 = .5\,3\ \mu\mu f.$

3. Incident P_o^{210} α particle ($E_o = 5.3$ Mev) loses all energy in depletion region.

4. $3.6 \pm .3$ ev/e-h pair = Energy of Ionization.

5. Input capacitance of electronic system = 60 $\mu\mu f = C_a$

The output pulse is given by

$$V_{out} = \frac{\Delta Q}{(C_d + C_a)}$$

$$\Delta Q = Ne = \frac{5.3 \times 10^6 \text{ ev}}{3.6 \text{ ev/e-h pr.}} \times (1.602 \times 10^{-19} \text{coulomb}) = 2.36 \times 10^{-13} \text{ coulomb}$$

$$C = C_d + C_a = (.27 + 60)\ \mu\mu f = 60.3\ \mu\mu f$$

$$V_{out} = \frac{2.36 \times 10^{-13} \text{ coulomb}}{60.3\ \mu\mu f} = .039 \times 10^{-1} \text{ volt} = 3.9 \text{ mv.}$$

Thus, the expected pulse voltage would be less than 4 mv.

BIBLIOGRAPHY

1. McKay, K. G., "Phys. Rev.," 84, 829 (1951).

2. Spenke, E., Electronic Semiconductors, McGraw-Hill, Inc. New York, 1958.

3. Smith, R. A., Semiconductors, Cambridge University Press, London, 1959.

4. Mayer, J. W. and B. R. Gossick, "Rev. Sci. Instru.," 27, 407 (1956).

5. Walter, F. J., J. W. Doobs, L. L. Roberts, and H. W. Wright, ORNL 58-11-99 (1958).

6. McKenzie, J. M. and D. A. Bromley, "Phys. Rev. Letters," 2, 303 (1959).

7. Friedland, S. S. and J. W. Mayer, "Nucleonics," 18, No. 2, 54 (1960).

8.51 Experiment on Alpha Particle Detection Using the P-N Junction

Purpose

To obtain differential pulse height spectrums for Po^{210} alphas using the P-N junction detector under several different external biasing conditions. To obtain from the above, energy resolution as a function of bias, pulse height as a function of bias and detector voltage output.

To determine the gain characteristics of the transistorized preamplifier and its input noise signal.

Incident alpha particles lose their energy in the detector predominantly by ionization producing electron hole pairs. Strong electron and hole concentration gradients exist in the junction region which result in a changing space charge density and its attendant electric field. Due to this strong electric field ($\sim 10^5$ v/cm) holes migrate to the p-type material and the electrons to the n-type material resulting in a collection of charge which along with the junction barrier capacitance and input capacitance to the amplifying system produces a voltage pulse on the order of millivolts. The charge collection time is known to be less than 3.5×10^{-9} sec.

List of Equipment

1 m curie Po^{210} alpha source ($T_{1/2}$ = 138 d, E = 5.3 Mev)
Hughes P-N junction detector
Transistorized pre-amplifier (Rise time = 0.2μs, Gain = 45)
Linear Amplifier (T_R = 0.2 μ sec)
Single channel differential analyzer
High voltage power supply
Scaler counter
Pulse height generator (0.2 μ sec T or less, millivolt range)
Cathode ray oscilloscope (at least 0.2 μ sec rise time)

It should be noted that the display of the signal voltage pulse is limited by the electronics. It would be desirable to have electronics which approach 10^{-9} sec rise time or less.

Procedure

1. Using the P^{210} α source (1 mc, 5.38 mev) and the detector-preamp-amp-dif. anl. system, obtain differential spectrums

for several detector reverse biases (0 to 180 v DC) i.e., for a given window width, obtain count rate for various E_{dial} settings about the peak count rate.

Plot relative pulse height vs. count rate for each of the different biases

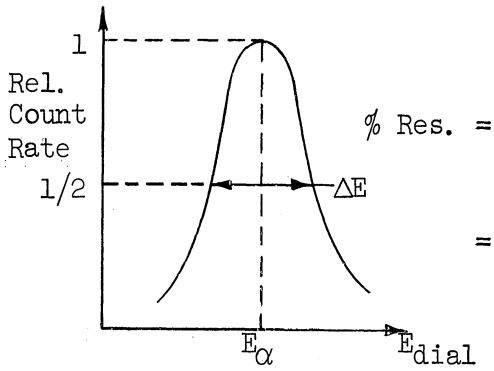

$$\% \text{ Res.} = \frac{100\% \times \text{full width at 1/2 max pulse height}}{\text{Energy under maximum P.H.}}$$

$$= \frac{\Delta E}{E_\alpha} \times 100\%$$

Figure 8.33 Relative Count Rate vs. E Dial.

Compute the energy resolution for each of the different biases. Plot resolution vs. detector bias.

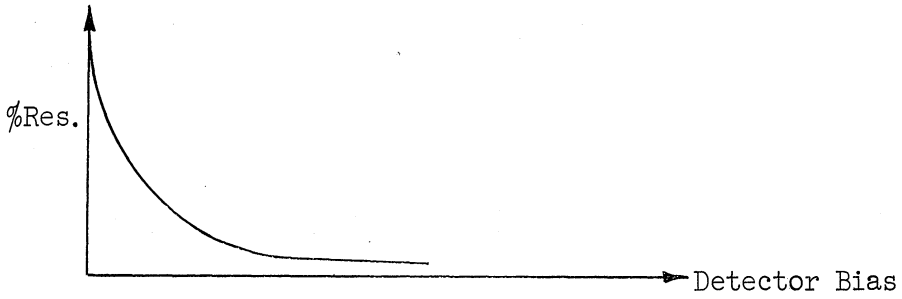

Figure 8.34 Percent Resolution vs. Detector Bias.

From the E_α's given from above curves, plot detector bias vs. pulse height at E_α

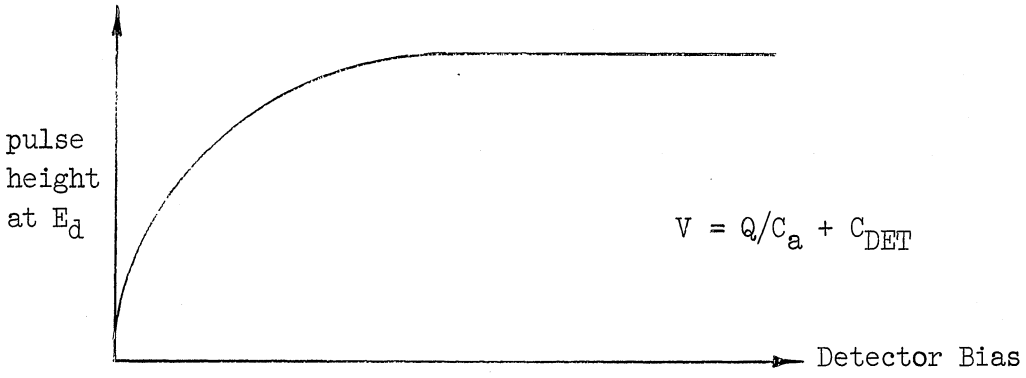

Figure 8.35 Pulse Height at E_α vs. Detector Bias.

2. Determine the input noise to the detector-preamp-amplifier system utilizing the CRO

$$\text{System Input Noise} = \frac{\text{Voltage Out of Amplifier}}{(\text{Gain of Preamp})(\text{Gain of Amp})}$$

3. Determine the voltage output from the detector and thus, the input signal to noise ratio.

$$\text{Detector Output Voltage} = \frac{\text{Signal Pulse Voltage Out of Amp}}{(\text{Gain of Preamp})\ (\text{Gain of Amp})}$$

$$\text{Signal to Noise Ratio} = \frac{\text{Detector Output Voltage}}{\text{System Input Noise}}$$

8.52 Questions

The following questions are representative of those used in exams covering the topics considered in this chapter. Your background should be broadened by outside reading until this type of question, which stresses qualitative understanding of the equipment and the processes involved, is no challenge.

8.53 Ionization Chambers

1. Given mean level ionization chamber which has been calibrated using a radium source of 5 curies:

   (a). Discuss the problems involved, qualitatively, in determining the strength of any radioactive material in curies using this calibrated instrument.

   (b). Using formulae if necessary, describe carefully the specific method you would use to convert the measurement of the radioactive material using the calibrated instrument to the exact strength in curies.

2. Consider the following statement in connection with ionization chambers.
   "Very large chambers are not practical, and therefore an air equivalent wall is used to increase the sensitive volume of the chamber and to increase its efficiency. The wall is made of materials with about the same average atomic mass as that of air. The thickness of the wall must be less than the range of the ions which are formed inside the wall so that these ions can get to the collecting electrode and produce discharges. Discuss any inaccuracies.

3. An ionization chamber and a G-M counter are operating properly with positive high voltages or their center wires and their shells grounded. Would you expect them to operate properly if one would change the

sign of the voltages impressed upon the center wires? Please give reasons for your answer.

4. You are given the task of designing an air-equivalent ionization chamber. In selecting the wall thickness, what considerations will govern your decision?

8.54 GM-Proportional Counters

1. A radiation survey is to be made of the gamma field in a radiation laboratory. Using a Geiger-Muller type survey instrument, Mr. X performs this task by reading the mr/hr figures indicated by the meter of the instrument.

   Under what conditions, if any, are the results of this survey meaningful? Please state fully the reasons for your answer.

2. What determines the resolving time of the GM counting system?

3. What determines the resolving time of the proportional counting system?

4. (a) Discuss qualitatively the basic concepts required to develop the theoretical form of the voltage pulse from a GM tube.

   (b) Discuss the relative magnitudes of the migration times of the positive and negatively charged particles, t_+ and t_-, respectively, in a pulse ionization chambers. Be specific in considering (1) air equivalent type chamber, (2) proportional chambers and (3) GM tubes.

   (c) Draw a representative pulse for a GM tube when the time constant, RC, is (1) $RC < t_-$, (2) $t_- < RC \ll t_+$, and (3) $t_+ < RC$.

5. For a GM tube:

   (a) Draw the voltage pulse forms as seen with a CRO to determine dead time, resolving time and recovery time. Indicate on your figure how these times would be measured.

   (b) Draw the voltage on the collecting electrode as a function of time corresponding to the figure in part a. Explain.

   (c) Draw the resolving time of the GM as a function of anode voltage. Explain the behavior you have shown physically.

6. (a) In the gas flow proportional counter, what specific characteristics of the gas are desirable?

(b) Is a quenching gas necessary, as in the GM tube? Explain.

(c) What effect does the gas pressure have on the overall multiplication? What considerations would effect the operating gas pressure of a chamber which you had the responsibility to design?

8.55 Statistics

1. Given: A radioactive source whose disintegrations satisfy a Poisson population description, and a GM counting setup.

(a) Considering the low efficiency of the GM system for detecting gammas, justify the use of a Poisson distribution when analyzing the sample data.

(b) Discuss the effect of the source gamma energy spectrum on the analysis of this sample data

(c) Discuss the effect of geometry and source activity on this analysis.

2. Prove or disprove that the sample mean is known with less uncertainty when the data is taken in 10 separate, equal time intervals, T, rather than in one interval, 10T.

3. Prove or disprove that the variance of the data is identical for both methods of data taking in part (d), when the total counts recorded are identical.

4. (a) What is the difference between sample and population data?

(b) Are statistical quantities such as standard deviation derived from sample data information?

5. Please state the physical requirements, and only those physical requirements, which have to be satisfied in order that one may apply the following statistical laws to radioactive decay.

(a) Poisson's distribution

(b) Gaussian distribution

Do not use mathematical symbols and inequalities, and do not make your statements redundant.

6. You take two successive one minute counts of a radioactive material. The first yields 10,000 count, the second 9,500; please comment very briefly on these results.

7. Student A counts a source for 10 minutes. Student B counts a similar source for 10 one minute intervals. Student A remarks to B: "Since both of us obtained about the same total number of counts and therefore our results have about the same standard deviation, you certainly wasted a lot of time taking your data in ten pieces, and by resetting and restarting your scaler." Please discuss this statement.

8.56 Scintillation Spectrometry

1. You are given the task of determining the absolute activity of a small amount of radioactive material of the order of one microcurie, which emits only monoenergetic gamma radiation of about one Mev energy. No calibrated standard of this material is available.

   (a) By means of a detailed block diagram, show the pieces of equipment you need. Your diagram should show a separate block for each function to be performed, that is, you might have to show several blocks for pieces of equipment built on the same chassis. Carefully label all blocks and interconnections. Describe fully the function of all blocks and interconnections.

   (b) Describe fully the measurements you would make with this equipment on the radioactive material.

   (c) Describe fully how you would use the results of your measurements to compute the activity of the material. If information in addition to your experimental results is needed, please state clearly what this information is.

2. Given: a monoenergetic γ source and a shielded well type NaI(Tl) crystal and a single channel analyzer setup operated in differential.

   (a) Explain the reason for the presence of a backscatter peak and its corresponding energy.

   (b) What is the effect of the size of the crystal on the relative height and width of this peak? Explain.

(c) Explain the decrease in count rate to the right of the Compton edge.

(d) Physically explain the observed photopeak resolution of 10%.

(e) How is the photopeak resolution affected by the size of the crystal? Explain.

3. For a source with an equal number of gammas per unit energy and a continuous energy distribution up to a cut-off of 1.02 Mev, draw a representative curve of count rate vs. E_{dial} (where E_{dial} should be plotted in equivalent gamma energy) for a NaI(Tl) well crystal on INTEGRAL. Explain the behavior.

4. Repeat part c for DIFFERENTIAL. (Cont'd.)

5. What differences should one expect to see in the differential spectrum for a given gamma source between a well and a crystal scintillation counter. Explain fully.

6. What is the Compton edge? What is its significance in analyzing a differential spectrum from a mixed gamma source?

7. Consider a gamma of energy E, E > 1.02 Mev, impinging on a NaI(Tl) crystal. In pair production, the kinetic energy of each of the two betas formed is (E - 1.02)/2. When the positron recombines with an electron (assumed at rest) the kinetic energy of either of the resulting gammas (moving in opposite directions) is just (E - 1.02)/2 + 0.51 = E/2. Assume the resulting gammas can lose all their energy in the crystal, or one or both can escape entirely, the pair production photopeaks should occur at E - E/2 and E - 2(E/2) = 0 rather than at E - 0.51 and E - 1.02 as commonly claimed. Please make a critical analysis of the above remarks, being sure to explain any points of disagreement, if any.

8.57 Neutron Detection

(a) What is meant by the optimal or correct settings for the anode voltage and the discriminator and the amplifier gain?

(b) Draw on the same graph representative curves of count rate vs. discriminator setting for: 1. the optimal anode voltage, 2. a higher voltage, and 3. a lower voltage. Explain this behavior.

(c) Draw representative curves of count rate vs. anode voltage with 3 discriminator settings as parameter on the same graph. Use

the correct discriminator setting for the optimal anode voltage and a higher and a lower discriminator setting. Explain this behavior.

(d) Can the CRO be used to find the correct discriminator setting if the optimal anode voltage is known? Explain.

(e) Can the CRO be used to find the optimal anode voltage if the proper discriminator setting is known? Explain.

(f) Can the CRO be used to find the proper settings for both discriminator and anode voltage given a BF_3 tube about which no characteristics are known? Explain.

(g) Define the efficiency of a BF_3 tube for neutron detection. What is the order of magnitude of this efficiency? Why?

(h) Why are the neutron induced pulses from the BF_3 tube not of uniform height?

(i) In the BF_3 experiment, the importance of keeping the field at a low (e.g. less than 1000r/hr) value was emphasized. How could you design a gaseous BF_3 tube which reduces the effect of gammas on tube operating characteristics while maintaining the same neutron sensitivity? Explain.

8.58 Foils

1. In the foil activation experiment, we speak of a saturation activity. Explain this term physically.

2. Is it necessary to know the saturated activity to calculate the relative flux? Explain.

3. How could you use the foils to find absolute flux levels?

4. What characteristics does an ideal foil have?

5. What considerations determine the counting equipment you would use to measure the radiation given off by the foils?

8.59 Solid State Detector

1. What effect does an increase in reverse bias have on the space charge

density, the electric field, depletion depth, barrier capacitance and output pulse from an α particle? (Be specific, give equations and sketches to explain).

2. Suppose the reverse bias is removed from the detector while the detector is still connected to the electronics. Will it still be possible to detect incident alpha particles? Explain.

3. What effect does extending the high frequency range seen by the electronics have on the observed alpha voltage pulse?

4. Why does the pulse height vs. alpha particle energy curve become non-linear?

5. If the junction were formed 12 microns beneath the surface, what effect would this have on the pulse height vs. alpha particle energy curve?

6. Why is the solid state detector more effective than a crystal detector with an externally applied electric field?

7. Is there any advantage to having a detector with a resistivity of 100,000 ohm-cm rather than the 300 ohm-cm detector used to take the data in this laboratory?

8. In the solid state detector experiment, the pulse at the amplifier output was observed to reach a saturation value at a reverse bias of about 30 volts. Why?

9. Why is the observed pulse rise time about one microsecond?

10. Why is the detector light sensitive but not effective in measuring our beta sources (0.1 μc).

8.60 General

1. Given a current ionization chamber calibrated against a known radium source in mr/hr. What effects must be considered when using this chamber to measure the STRENGTH of an unknown gamma source. Be specific, using equations.

2. Given a calibrated Geiger-Mueller chamber, instead of a current ionization chamber, reanswer (1).

3. Given: a source that emits α, β, and γ

   (a) What equipment would you use to count these particles, under the restriction that the counts due to each type of particle be resolveable? Draw a block diagram(s) of the proposed system(s).

   (b) How could absolute counting be done using the equipment of part a?

4. Comment on the relative merits of an end window GM counter and a well type NaI scintillation counter for determining the activities of neutron activated materials, such as indium-116 and gold-198, which emit both betas and gammas. Consider such points as counter efficiency, background, and effect of foil thickness.

5. Please describe fully the physical phenomena which account for the rise in the output current, or count rate, with increased voltage in the plateau regions of the following instruments:

   a) Ionization chamber
   b) Proportional counter
   c) Geiger counter
   d) Scintillation counter (on integral count)

6. (a) Explain the difference between the "total absorption coefficient" and the "true energy absorption coefficient" for gamma radiation.

   (b) Which of the above mentioned coefficients would you expect to obtain by measuring the attenuation of a narrow beam of gammas? Please explain why.

   (c) Which one of the above mentioned coefficients would you use in calculating the radiation dose rate in roentgens per unit time at a certain distance from a given radiation source? Please explain why.

7. Develop and explain clearly the theory of the two source method of resolving time measurement. State the approximations involved and state approximately what the counting rates should be for best results. Do not restrict your discussion to one type of detector.

8. Recommend a type of instrument to de each of the following jobs. Explain in detail your reasons.

(a) Conduct tracer analysis using a gamma emitting isotope.

(b) Monitor the radiation level in the open air after an atomic attack.

(c) Measure exposure dose at a few feet from a 20 mc unknown gamma source.

(d) Measure exposure dose at a few feet from a 20 mc Co-60 gamma source.

(e) Monitor continuously the effluent gases from ventilation waste stacks from a laboratory using many different kinds of radioactive materials.

8.61 Calculational Problems

1. Given a known point source of C curies:

(a) SYMBOLICALLY, develop the formalism for computing the whole body dose in REM which you would receive standing ten feet from the exposed source. Define all SYMBOLS CLEARLY, giving UNITS. State ASSUMPTIONS.

(b) At a distance for which your survey meter is on scale, SYMBOLICALLY relate the instrument reading in mr/hr (calibrated with a RADIUM source) to the actual air dose rate at the location of the meter caused by the hot source to which you are exposed.

(c) At this distance, SYMBOLICALLY, develop a GENERAL relation expressing the dose rate which your body receives on the basis of the measured meter reading.

(d) If the instrument in part b had been a Geiger Mueller rather than a mean level type, please reanswer part b.

(e) For the GM meter, reanswer part c.

2. Develop a GENERAL expression relating the strength of a point gamma source in curies to the dose rate, r/hr, at a distance d cm. in air. Define all terms used. Do not restrict to one gamma per disintegration, nor to one gamma energy.

(a) Write an integral expression for the rate with which neutrons interact with a BF_3 gas tube for a given geometry. Define all terms used. State any important assumptions clearly.

3. One of the men under your supervision in a radiation laboratory accidentally swallows some radioactive material. Upon investigation you find that this particular isotope emits gamma radiation only, becomes evenly distributed in the body and is eliminated from the body in an approximately linear manner in about 100 hours. The material undergoes 3.72×10^{11} disintegrations per hour, emitting a 0.625 Mev ($=10^{-6}$ erg) gamma per disintegration, with a half life of 2.2 years. About half of the gamma energy is absorbed in the body.

   (a) Compute the total radiation dose in REM units that this man will receive from this material.

   (b) Decide on the period of time this man should spend away from his regular job where he receives 2.5 millirems per hour on the average.

   (c) One of the other men under your supervision remarks: "It would have been much better if the material this fellow swallowed had been an alpha emitter instead of a gamma emitter. The alphas, due to their small penetrating power, would cause much less damage than the gammas." Please comment on this remark.

4. Derive an expression for the dose rate, D, in mr/hr, at a distance d (cm) from a point source of strength S (curies). Define all conversion factors required SYMBOLICALLY, being SPECIFIC on the UNITS of all symbols used.

5. Radium gives off a variety of gammas per alpha disintegration. Qualitatively, how is this effect exhibited in the expression derived in 4, given S curies of radium?

6. Show SYMBOLICALLY the procedure which you would follow to arrive at the present strength of a Co60 source, given the dose rate D in mr/hr at a distance, X cm at a prior time, T, such as March 20, 1952. Define any additional symbols required in your analysis as needed.